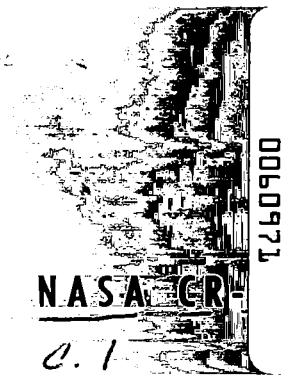

NASA CONTRACTOR REPORT

NASA CR-1907

SNAP-8 ELECTRICAL GENERATING SYSTEM DEVELOPMENT PROGRAM

Prepared by
AEROJET-GENERAL CORPORATION
Azusa, Calif. 91702
for Lewis Research Center

NATIONAL AERONAUTICS AND SPACE ADMINISTRATION • WASHINGTON, D. C. • NOVEMBER 1971

1. Report No.	2. Government Accession No.	3. Recipient's Catalog No.
NASA CR-1907		

4. Title and Subtitle	5. Report Date
SNAP-8 ELECTRICAL GENERATING SYSTEM DEVELOPMENT PROGRAM	November 1971
	6. Performing Organization Code
7. Author(s)	8. Performing Organization Report No.
	10. Work Unit No.
9. Performing Organization Name and Address Aerojet - General Corporation 1100 West Hollyvale Street Azusa, California 91702	11. Contract or Grant No. NAS3-13458; NAS5-417
	13. Type of Report and Period Covered Contractor Report, 1960-71
12. Sponsoring Agency Name and Address National Aeronautics and Space Administration Washington, D.C. 20546	14. Sponsoring Agency Code

15. *Supplementary Notes*

Project Manager, Martin J. Saari, Space Power Systems Division,
NASA Lewis Research Center, Cleveland, Ohio

16. Abstract

The SNAP-8 program has developed the technology base for one class of multikilowatt dynamic space power systems. Electrical power is generated by a turbine-alternator in a mercury Rankine-cycle loop to which heat is transferred and removed by means of sodium-potassium eutectic alloy subsystems. Final system overall criteria include a five-year operating life, restartability, man rating, and deliverable power in the 90 kWe range. The basic technology has been demonstrated by more than 400,000 hours of major component endurance testing and numerous startup and shutdown cycles. A test system, comprised of developed components, delivered up to 35 kWe for a period exceeding 12,000 hours. The SNAP-8 system baseline is considered to have achieved a level of technology suitable for final application development for long-term multikilowatt space missions.

17. Key Words (Suggested by Author(s))	18. Distribution Statement
Multikilowatt dynamic space power system Turbine alternator Mercury-Rankine cycle Sodium-potassium eutectic alloy (NaK)	Unclassified - unlimited

19. Security Classif. (of this report)	20. Security Classif. (of this page)	21. No. of Pages	22. Price*
Unclassified	Unclassified	467	$6.00

* For sale by the National Technical Information Service, Springfield, Virginia 22151

CONTENTS

TABLES

FIGURES

SUMMARY

The SNAP-8 program has developed the technology base for one class of multikilowatt dynamic space power system. The final SNAP-8 system overall criteria includes a five-year operating life, restartability, man rating, and deliverable power in the 90-kWe range. Electrical power is generated by a turbine-alternator in a mercury Rankine-cycle loop to which heat is transferred and removed by means of sodium-potassium eutectic alloy subsystems.

The predominant amount of SNAP-8 development effort was directed toward establishing a 35-kWe system. The major system components have been designed, fabricated, and tested under steady-state, transient, off-design, and environmental conditions. The components include the turbine-alternator, pumps, mercury boiler, mercury condenser, and electrical control system. Requirements have been specified, preliminary designs prepared, and partial development testing performed for other components including valves, reservoirs, and heat exchangers. System analysis and design provided the information that was used to establish component functional and physical characteristics as well as system and compoment test requirements, and established the compatibility of the SNAP-8 power conversion system and nuclear system during startup, shutdown, and steady-state operation. Designs for possible mission-applicable system configurations have been prepared. A system state point and required component modifications have been defined for a 90-kWe SNAP-8 consistent with proven component capabilities.

The validity of the basic technology developed on the program has demonstrated by more than 400,000 hours of major component endurance testing at design conditions, and by numerous planned startup and shutdown cycles. Component material barrier problems have been resolved including selection of boiler containment and turbine structural materials for high-temperature and high-pressure mercury. A test system comprised of SNAP-8 developed components delivered up to 35 kWe for a period exceeding 12,000 hours. The reference system start sequence was demonstrated by successful test system bootstrap startups. Based on the technology established and the demonstrated component performance, SNAP-8 systems producing up to 120 kWe of net output power with a 20% overall system efficiency have been defined for operation with a 600 kWt heat source.

As a result, the SNAP-8 system baseline is considered to have achieved a level of technology suitable for final application development for long-term multikilowatt space missions.

1.0 INTRODUCTION

1.1 OVERVIEW OF THE SNAP-8 PROGRAM

At the inception of the SNAP-8 program, the U.S. space effort was in the midst of a rapid expansion. Space power systems were projected for use in deep-space instrumented probes and electrical power requirements were projected at levels above the capabilities of systems then available. As one approach to meeting the anticipated space power needs, the decision was made to develop and extend mercury Rankine-cycle power plant technology for eventual space-mission applications. At the initiation of the SNAP-8 project in May 1960, mercury Rankine-cycle space power technology was embodied in the SNAP-2 system which had a two-loop mercury Rankine-cycle power system coupled with a reactor. The net power output from SNAP-2 was 3 kWe; the SNAP-8 initial requirement, at this time, was for 30 kWe. The ten-fold extrapolation in system net power output rapidly led to changes which brought mercury Rankine-cycle power system technology from the SNAP-2 power level to the present SNAP-8 capability for multikilowatt applications.

One of the significant changes was to employ a compact mercury condenser in conjunction with a liquid metal heat rejection loop rather than to extrapolate the condensing radiator design used for SNAP-2. The basic system output power level was increased to 35 kWe when the compact condenser, liquid metal heat rejection loop approach was adopted.

The present SNAP-8 capability has evolved from a single start, instrument-rated SNAP-8 system operating at 35-kWe output with 10,000 hour life, to a restartable man-rated system operating at 90-kWe output with five-year life. The SNAP-8 electrical generating system consists of a nuclear system, power conversion system, and flight radiator system. Heat is transferred to the mercury loop from the nuclear heat source by means of sodium-potassium eutectic alloy (NaK) subsystems. Heat is rejected from the mercury loop to another NaK subsystem which, in turn, radiates the system waste heat to space. The heat source is required to produce power at levels up to 600 thermal kilowatts, depending upon the system electrical power output.

To establish the present SNAP-8 technology, extensive efforts were directed toward system analysis and design; component design, development, fabrication, and testing; materials evaluation; and design and erection of suitable test facilities. As the overall national space program became more clearly defined, consideration of lunar landings, space stations, space bases, as well as deep-space probes had an impact on potential SNAP-8 mission profiles and therefore system design. Consequently, in parallel with the development of the technology required for component design, a continual review and updating of component and system requirements was maintained by system analysis and design efforts. As a result, component designs and design approaches have been proven for major liquid-metal Rankine-cycle power system components including the mercury-vapor driven alternator, mercury pump, mercury boiler, mercury condenser, NaK pumps, valves, coolant-system pumps, instrumentation,

and electrical controls. Over 400,000 component test hours have been accumulated including more than 12,000 hours of system test operations. During this time, all material barrier problems were resolved establishing the feasibility of operating SNAP-8 systems for the long lifetimes specified.

System and component modifications have been defined for a system capable of producing up to 90-kWe output at an overall efficiency of 15%. Many existing components can be used in their basic form for the various power systems in the 35-to-90 kWe range. A product improvement program initiated from the 90-kWe system baseline would lead to a SNAP-8 system capable of producing 120 kWe at an overall system efficiency of 20% when provided with a 600 kWt heat source, without the need to introduce new technologies. Based on corroboration of designs through testing and validation of systems and component analytical models, SNAP-8 technology has been brought to readiness for mission application.

1.2 OBJECTIVES OF FINAL REPORT

This SNAP-8 final report has been prepared with the following objectives:

(1) To define the development status of SNAP-8 system and components at the completion of the current phase of activity.

(2) To record the detailed technology developed in the various program disciplines; namely, systems analysis and design, component design, materials engineering, and test operations; and to record the significant program achievements.

(3) To identify the technology developed on the SNAP-8 program which would be of consequence for other governmental and industrial projects.

(4) To preserve the status of SNAP-8 technology in a manner enabling continuation of development of mercury Rankine-cycle power systems for space missions.

In summary, this report presents the development status of the 90-kWe and 35-kWe SNAP-8 systems and the components designed and/or developed for these systems. Contained within the report are the significant design criteria and requirements, steps in the development, and an evaluation of performance characteristics for all components and the overall system functions which were under the cognizance of the Aerojet-General Corporation.

1.3 ORGANIZATION OF FINAL REPORT

The SNAP-8 program final report describes the 90-kWe and 35-kWe systems and component design and operational characteristics. Each major component is described in a separate section discussing function, description, development background and performance characteristics. The 90-kWe system is considered to be the baseline for subsequent development of mercury Rankine-cycle space power systems; however, the 90-kWe system is an extension of the technology developed for the earlier 35-kWe system. All component development,

performance demonstration, and endurance testing was accomplished with components designed for the 35-kWe system. Therefore, a detailed description of the 35-kWe system is presented to provide a proper background for the 90-kWe system design and analysis.

References are listed at the end of the report. Each reference is available from the National Aeronautics and Space Administration Scientific Technical Information Facility, P.O. Box 33, College Park, Maryland 20740. Data from the Aerojet technical files for the SNAP-8 program will be stored in archives at the NASA Lewis Research Center, Cleveland, Ohio.

2.0 SNAP-8 PROGRAM DEVELOPMENT

2.1 PRESENT STATUS

In its original concept, the SNAP-8 electrical generating system was a two-loop Rankine-cycle unit with a nuclear reactor heat source providing 30 kW of 1000 Hz electrical power for 10,000 hours for instrument-rated (unmanned) space missions (including power for electrical propulsion). This concept evolved to the latest system design for a multiple-loop Rankine-cycle system providing 90 kW of 400 Hz electrical power for up to five years for either man-rated or instrument-rated space missions, or operation in a ground test facility. The original concept was based on providing 30 kW of electrical power when supplied with 300 kW of thermal power from a nuclear reactor heat source. The reactor was designed to provide 600 kWt so that, by combining two power conversion systems, a total net electrical output of 60 kW would be available. A basic change in system concept from the original two-loop unit to a multiple loop system, incorporating a compact mercury condenser and liquid metal heat rejection loop, was accompanied by a change to 35 kW of 400 Hz electrical power. The latest system design could provide 90 kW of useful electrical power when supplied with the full 600 kW of thermal power available from the nuclear reactor.

This latest system was in the preliminary design stage at the time of program termination and represents an improvement in the capability and performance of the SNAP-8 system for potential use in a wider range of more demanding space applications. This system is an outgrowth of one designed to provide 35 kW of useful electrical power which represented the major design, development, and test efforts expended on the overall SNAP-8 program. The 90-kWe system design had reached a point where system state-point conditions and major component requirements had been defined, the general system configuration and component arrangement had been determined, piping layouts had been initiated in preparation for hydraulic and stress analyses, plans were being formulated for a combined nuclear system/power conversion system test at the NASA Plum Brook Space Power Facility, and a mockup frame (suitable for use in the combined systems test) had been fabricated. Many of the major components to be incorporated in the 90-kWe system are either identical to, or minor modifications of, components proven during the development of the SNAP-8 35-kWe system. The most notable exception is the turbine assembly which requires a new design, but one that is based on the mercury turbine technology developed on the SNAP-8 program.

The SNAP-8 system, as presently conceived, could provide 90 kW of 400 Hz useful electrical power when 600 kW of thermal power are provided with a heat source nominal outlet temperature of 1220°F. The system can be utilized for either man-rated or instrument-rated space missions, and can operate unattended, continuously for periods up to five years. The 90-kWe system design provides a base point for planners of future space missions from which to evaluate electrical power availability against power requirements; furthermore, it provides a technology base for reactivation of the development of multi-kilowatt mercury Rankine-cycle space power systems.

2.2 EVOLUTION OF THE MULTIPLE-LOOP SYSTEM

2.2.1 Two-Loop System

The SNAP-8 development program, started in May 1960, was based on an initial concept for a simple two-loop system as shown in Figure 2-1. The initial system concept consisted of a primary loop in which the reactor coolant fluid was circulated by a motor-driven centrifugal pump through the reactor to a boiler. The second (Rankine-cycle) loop consisted of a boiler which utilized heat from the primary loop to boil and superheat mercury, a turbine to convert thermal to mechanical power, a tube-and-fin condensing radiator, and a jet-centrifugal mercury pump to circulate the working fluid. One of the major features of the system was the power drive assembly which included the turbine, alternator, and mercury pump mounted on a common shaft with mercury-lubricated thrust and journal bearings. The electrical power generated by the alternator was distributed internally to operate the power conversion system electrical components, and to the vehicle load with any excess electrical power being dissipated in a parasitic load resistor located in the primary loop.

Analysis, design, fabrication, and initial testing of components for the two-loop system proceeded to the point where design and operational difficulties were becoming apparent. The primary difficulties were associated with the power drive assembly where: (1) thermal distortion and external loads caused rubbing between the turbine and turbine case, (2) operational difficulties with the mercury-lubricated journal and thrust bearings resulted in bearing failures and abrupt turbine stoppages, and (3) evidence of seal leakage became apparent. In addition, problems associated with corrosion and erosion of the mercury and NaK containment materials were uncovered.

In view of these difficulties and potential problems with stable operation of an extended condensing radiator during vehicle maneuvers, a major reassessment of program objectives and accomplishments was undertaken during the latter part of 1962. The reassessment resulted in an extensive redirection of the overall SNAP-8 program with emphasis on reliable operation for 10,000 hours and greater assurance of successful development by adopting component designs more closely associated with the existing state-of-the-art.

2.2.2 Four-Loop, 35 kWe, Instrument-Rated System

The program reassessment culminated in the definition of a revised system with four basic fluid loops and new component requirements based on state-of-the-art technology. A simplified flow schematic for the four-loop system is shown in Figure 2-2 from which a number of the system and component changes are readily apparent. The addition of the heat rejection loop was made necessary by the adoption of a compact mercury condenser to eliminate potential problems associated with variations in gravitational and acceleration forces. All pumps were driven by separate motors to facilitate independent development and testing. The turbine and alternator were separable and connected by a flexible coupling with each assembly mounted on its own bearings.

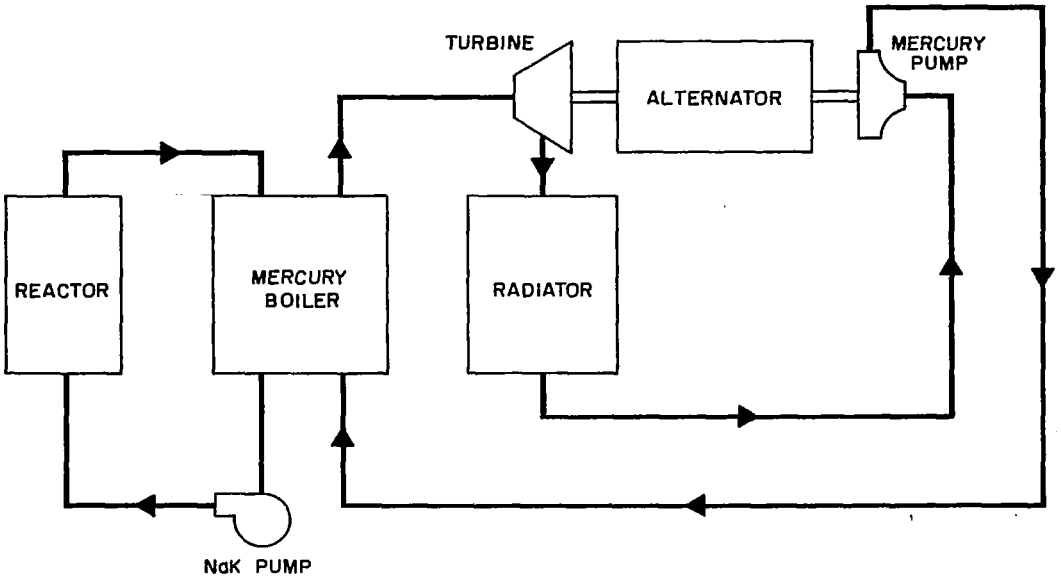

Figure 2-1 Two-Loop SNAP-8 Power Conversion System Schematic

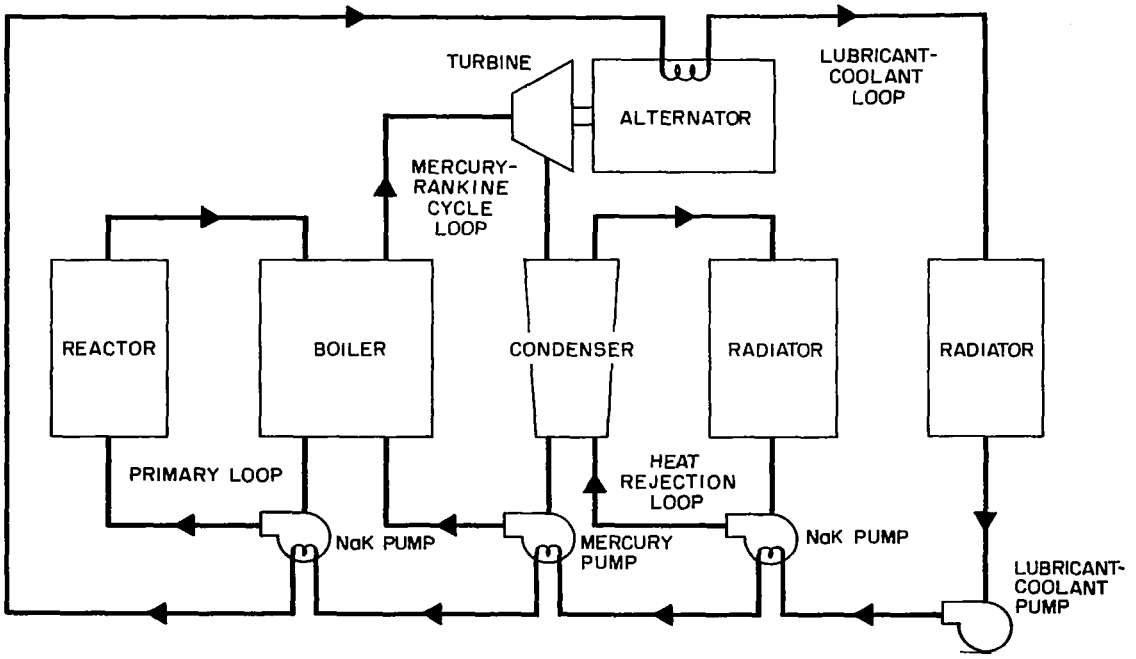

Figure 2-2 Four-Loop SNAP-8 Power Conversion System Schematic

Initially, bearings for all rotating components were to be state-of-the-art rolling contact, oil lubricated types. The only exception was the NaK pump for which NaK-lubricated journal bearings were adopted. A lubricant-coolant loop was incorporated to provide the circulation system for the bearing lubricant and to provide a low-temperature coolant and heat rejection system for temperature-limited electrical components. This lubricant-coolant loop also provided cooling for the alternator and pump motors, eliminating the need to develop high-temperature electrical insulation systems for these components.

The output power requirements were changed to provide a net output of 35 kW of 400-Hz, 208-Vac (line-to-line voltage) electrical power. The 400-Hz power was selected to permit the use of more standardized aerospace state-of-the-art electrical equipment and design practices.

General system requirements remained relatively unchanged; specifically, the system was to operate unattended for 10,000 hours in a shadow-shielded,* instrument-rated configuration and was to be capable of one automatic startup in a space (zero-g) environment. Design priority was placed on reliability, performance, and weight, in that order.

The program development efforts emphasized the analysis, design, and fabrication of the four-loop system components, test loops, and breadboard test systems. Several test facilities were planned and built for both component and system testing including the following:

- A low-power loop for evaluating the effects of mercury-vapor corrosion and erosion on various materials
- Two rated-power loops for performance and endurance testing of components (primarily the boiler, turbine-alternator, and condenser) and subsystems
- Liquid mercury loops for performance and endurance testing of mercury pumps and other components associated with the liquid portion of the mercury loop
- Liquid NaK loops for performance and endurance testing of NaK pumps and minor NaK loop components
- Seal test rigs for evaluating mercury and lubricant-coolant fluid dynamic seals, molecular pump and visco pump designs, and measuring leakage rates

---

* Although the nuclear reactor emits radiation omnidirectionally, it is necessary to protect only system components for an instrument-rated mission. Consequently, a nuclear radiation shield is interposed between the nuclear system and the balance of the electrical generating system. In effect, the nonnuclear sections are located within the "shadow" of the nuclear shield, hence, the term "shadow shield" introduced above. Any point in space not within the shield shadow is exposed to reactor radiation.

- An electrical component test facility for evaluating alternator performance, speed control system capabilities, and other electrical component characteristics

- Small-scale test loops (located at Aerojet Nucleonics Co., San Ramon, Calif.) for investigating boiler tube configurations and materials compatibility with working fluids

- System test loops for performance and endurance testing of components and complete power conversion systems.

These test facilities played important roles in the development of SNAP-8 components and subsystems by providing performance and endurance data. Equally important, operating procedures were developed and many design and operating problems were uncovered during various test phases. However, the system test loops were never fully utilized for their intended purposes. The introduction of the SNAP-8 phaseout program in late 1964 resulted in a sharp curtailment of development and test activities. Fabrication of a second system test facility was halted, and operations in the initial systems test loop were curtailed and eventually halted before a breadboard system was fabricated. Instead, the rated-power loop facility was modified and upgraded to a complete breadboard system and remained as the only SNAP-8 system test facility at Aerojet until the final termination of the SNAP-8 program.

During the phaseout program, a significant amount of component and breadboard system testing was accomplished which improved confidence in the feasibility of the system concept. Performance potential and mission application studies, separately funded by NASA, indicated greater potential usage for space power systems with power levels of the magnitude projected for SNAP-8. These studies also indicated the desirability of incorporating system changes which would help to meet newly defined long-range goals for SNAP-8.

2.2.3 35 kWe Man-Rated System

An important aspect of the newly defined goals was a system that was both instrument-rated and man-rated. The main impacts of man-rating the system were as follows:

- Necessity to protect the crew from reactor nuclear radiation

- Necessity to protect the crew from NaK-activated gamma radiation

- Consideration of crew access for maintenance

- Consideration of system restartability

- Consideration of system redundancy and associated switchover to provide greater system reliability.

Crew protection dictated a major change in configuration and shield design. The reactor, which had been at the "top" (in relation to the gravity vector) in the instrument-rated system, was moved to the "bottom" to place the reactor as far from the manned core of a space station as possible. In addition, studies for a lunar base application showed that it would be desirable to have the reactor "down," that is, on the lunar surface where it could be more readily shielded. The changes in position and the relative locations of the various portions of the system are illustrated in Figure 2-3. A typical concept for the 35-kWe system in a flight configuration is shown in Figure 2-4, and in a typical ground test configuration with a nonnuclear heat source in Figure 2-5.

The shielding method which resulted was an extension of the shadow-shield concept. Since the activated reactor coolant gamma levels were well above human tolerance, all reactor NaK components and piping were located near the instrument-rated shadow shield. This included the boiler, NaK pumps, expansion reservoir, and auxiliary heat exchanger. A second shadow-shield (the biological shield) was installed between the reactor coolant loop and the rest of the power conversion system to reduce the gamma and neutron radiation from the reactor primary loop to man-rated levels. This man-rated configuration could be modified for instrument-rated missions by removing the biological shield.

Consideration of a man-rated SNAP-8 system for space missions led to the reactivation of SNAP-8 activities in late 1966. The revised program placed increased emphasis on the definition and design of a power conversion system to be used in ground prototype system testing with both nonnuclear and nuclear heat sources. This effort formed the basis for system configuration studies and designs for both flight- and ground-test applications.

2.2.4 4-pi* Shielded Man-Rated 35-kWe System

As the preliminary design of the 35-kWe shadow-shielded system neared completion, several additional mission-related factors appeared. First, by definition, a shadow-shielded nuclear system provides personnel protection only within the envelope of the shadow. A shadow-shielded system would unduly affect earth-orbiting missions by restricting access to the electrical generator system for crew recycling and system and component replacement. For a lunar base, the reactor would have to be located below the lunar surface, this could require an unreasonable amount of excavation or additional shielding to permit personnel to operate at ground level near the system. It was decided to incorporate 4-pi shielding with the nuclear system to permit the SNAP-8 system to better accommodate these potential manned missions. A concept for the 35-kWe system with test support 4-pi shielding for a combined nuclear system/power conversion system test is shown in Figure 2-6.

---

* 4-pi shielding refers to shielding which completely surrounds a nuclear source (a sphere in space subtends a solid angle of 4-pi steradians about its origin).

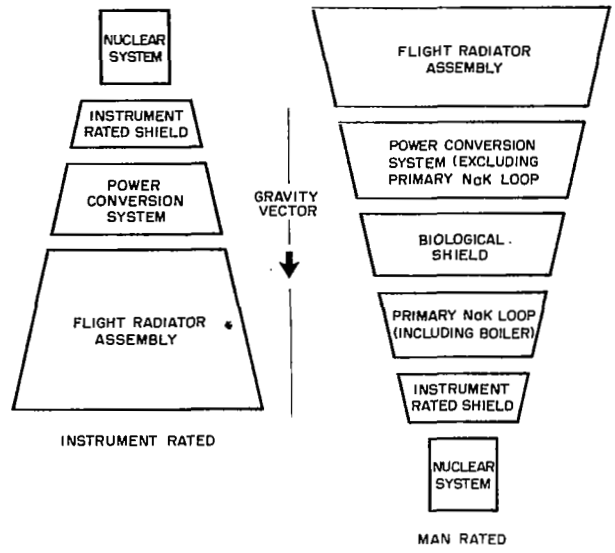

Figure 2-3 Diagram Showing Modifications Made to Convert the SNAP-8 System from an Instrument-Rated to a Man-Rated System

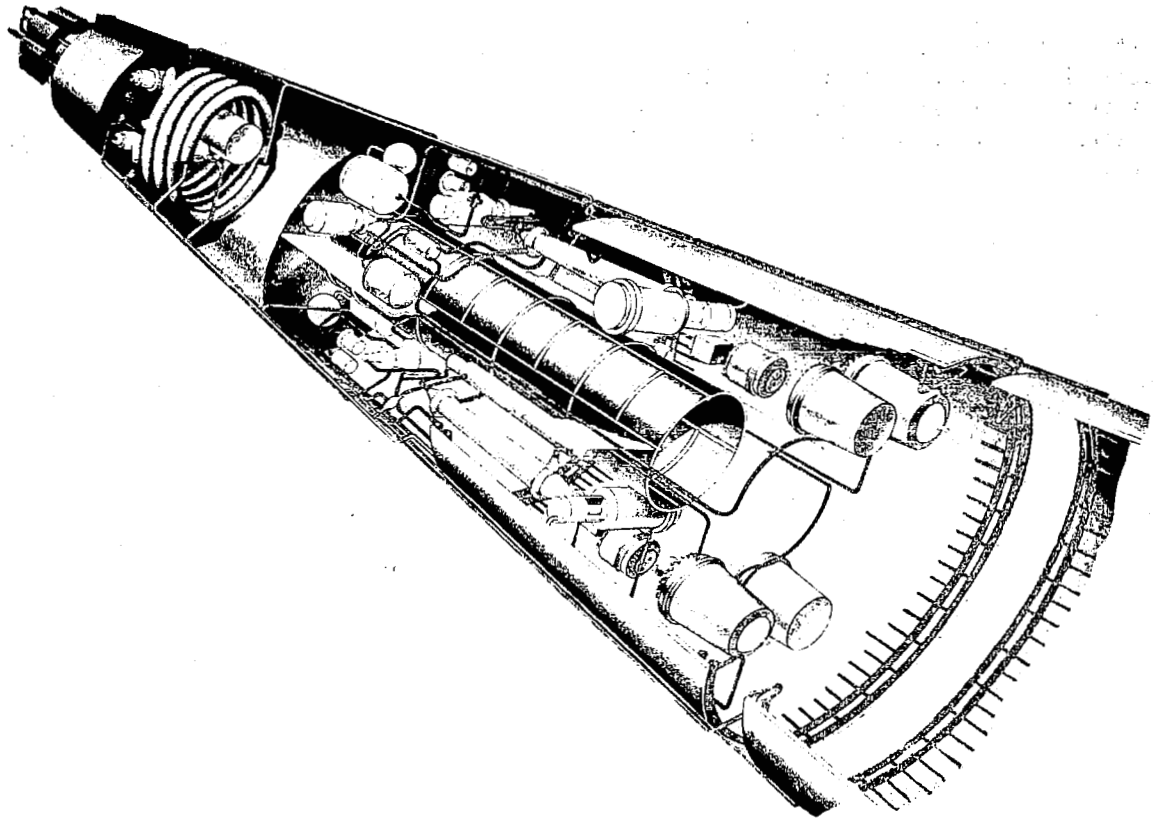

Figure 2-4 Possible Flight Configuration for a 35-kWe Man-Rated System

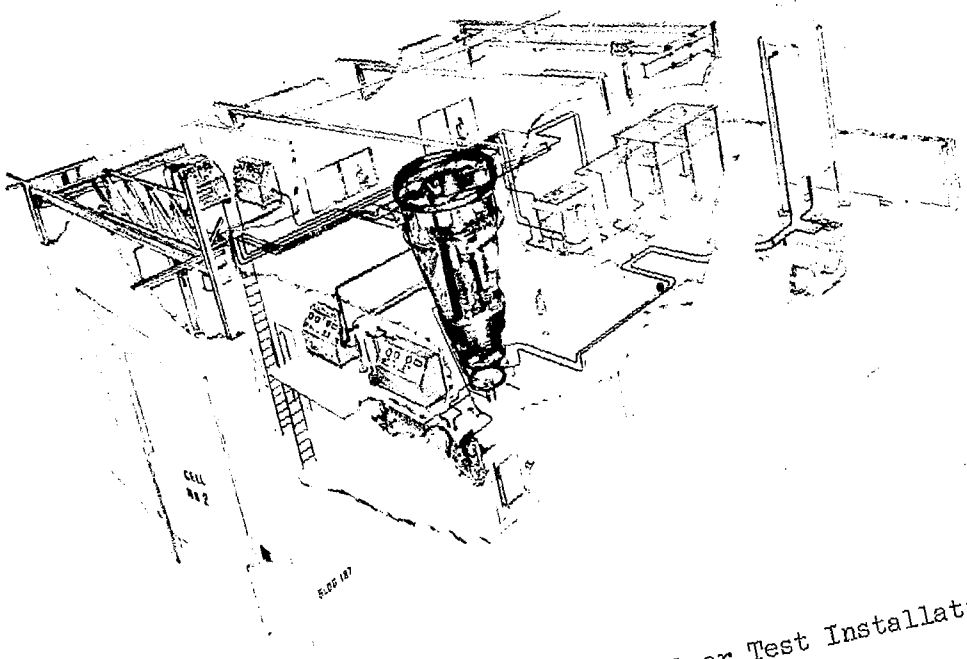

Figure 2-5 SNAP-8 System Nonnuclear Test Installation

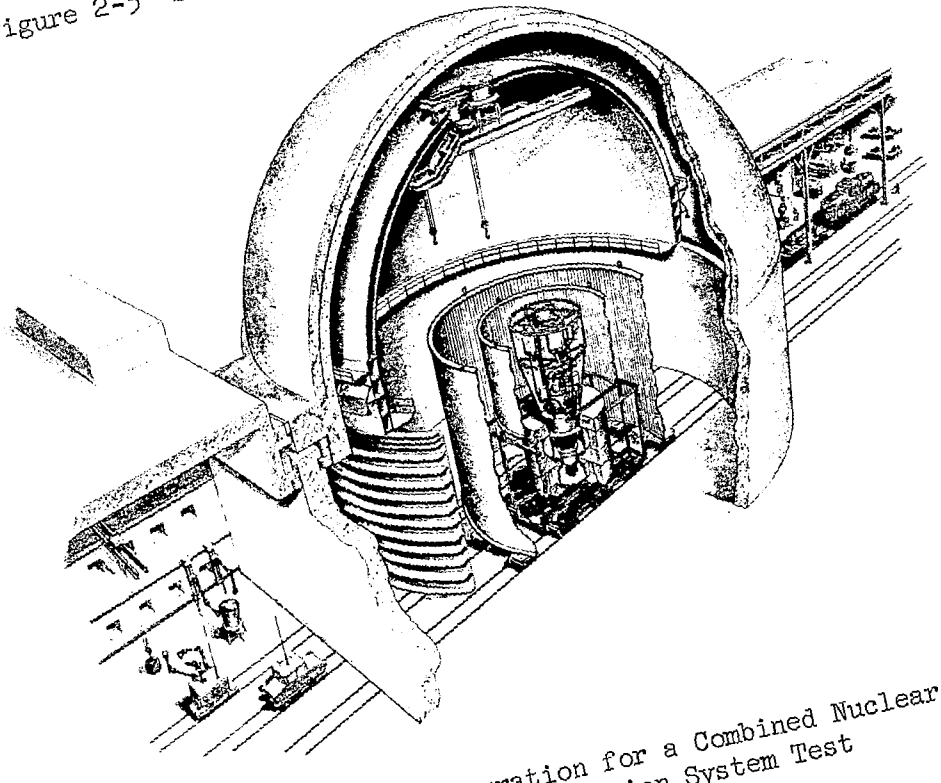

figuration for a Combined Nuclear System/
ersion System Test

The size (and, therefore, weight) of the 4-pi shield (Figure 2-7) is significantly affected by the height of the gallery section (the section of the electrical generating system located between the instrument-rated shield and the biological shield seen in Figure 2-3). Since the boilers in the gallery were the main contributors to gallery height, an attempt was made to reduce the gallery section height by removing the boilers from the gallery and introducing a NaK loop (referred to as the intermediate loop) between the reactor coolant loop and the mercury loop. An intermediate loop heat exchanger was located in the gallery section, and the boilers were relocated to the main section above the biological shield.

While the intermediate loop was under consideration, the nominal allowable reactor outlet temperature was reduced from 1300°F to about 1200°F. This change meant that a new overall system state point had to be established. A significant increase in turbine output power was required to maintain the net electrical output of 35 kW. The solution was to modify the turbine design to accommodate a lower exhaust pressure (from the previously established value of 14 psia) and to take advantage of the higher turbine efficiency available by operating at the higher volume flows associated with lower turbine inlet pressure and temperature. From the studies conducted to determine new state-point conditions, it became evident that a substantial increase in net electrical output was achievable. The increase in usable power was consistant with apparent increasing space power demands. A man-rated system with increased net electrical output, an intermediate loop, and redundant components and power conversion systems evolved from the performance and design studies.

2.2.5 4-pi Shielded, Man-Rated, 90-kWe System

The final phase of the SNAP-8 development program was to consider ways to significantly increase overall system performance and efficiency. These improvements would better align the system capabilities with the power level and operating requirements emerging from the phase B space station/space base studies currently in process. Since the key element of the electrical generating system is the turbine-alternator, emphasis was placed on improving this component. By decreasing the turbine back pressure to 2.5 psia and by redesigning the turbine, system output was increased to 90 kWe. Decreasing the turbine back pressure to 2.5 psia results in increased radiator weight and area. However, the weight associated with a 4-pi shield requires the use of a larger booster vehicle for space missions so that the increases in radiator weight and area become secondary factors. The turbine-alternator was modified to incorporate a straddle-mounted, dual-path, reaction turbine with five stages on each path, and with an alternator (identical to the alternator developed for the 35-kWe system) attached to each end of the turbine by means of a quill shaft. Bearings and seals associated with the turbine-alternator are of the same design as those used for the 35-kWe system. The overall power conversion system configuration for a combined systems ground test is shown in Figure 2-8. This configuration is for a nonredundant power conversion system concept. A fully redundant system design was initiated but not fully implemented at the time of the program termination.

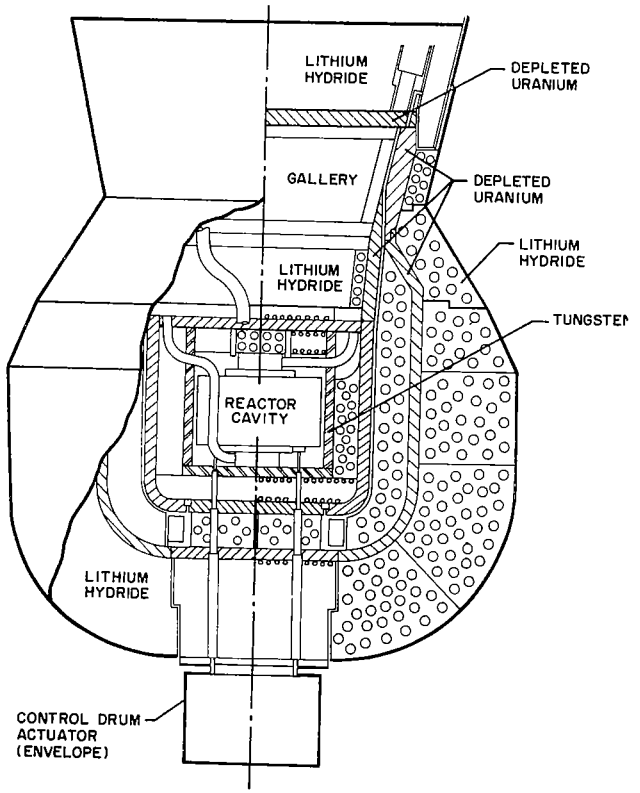

Figure 2-7 Reactor 4-pi Shield Concept Flight Configuration

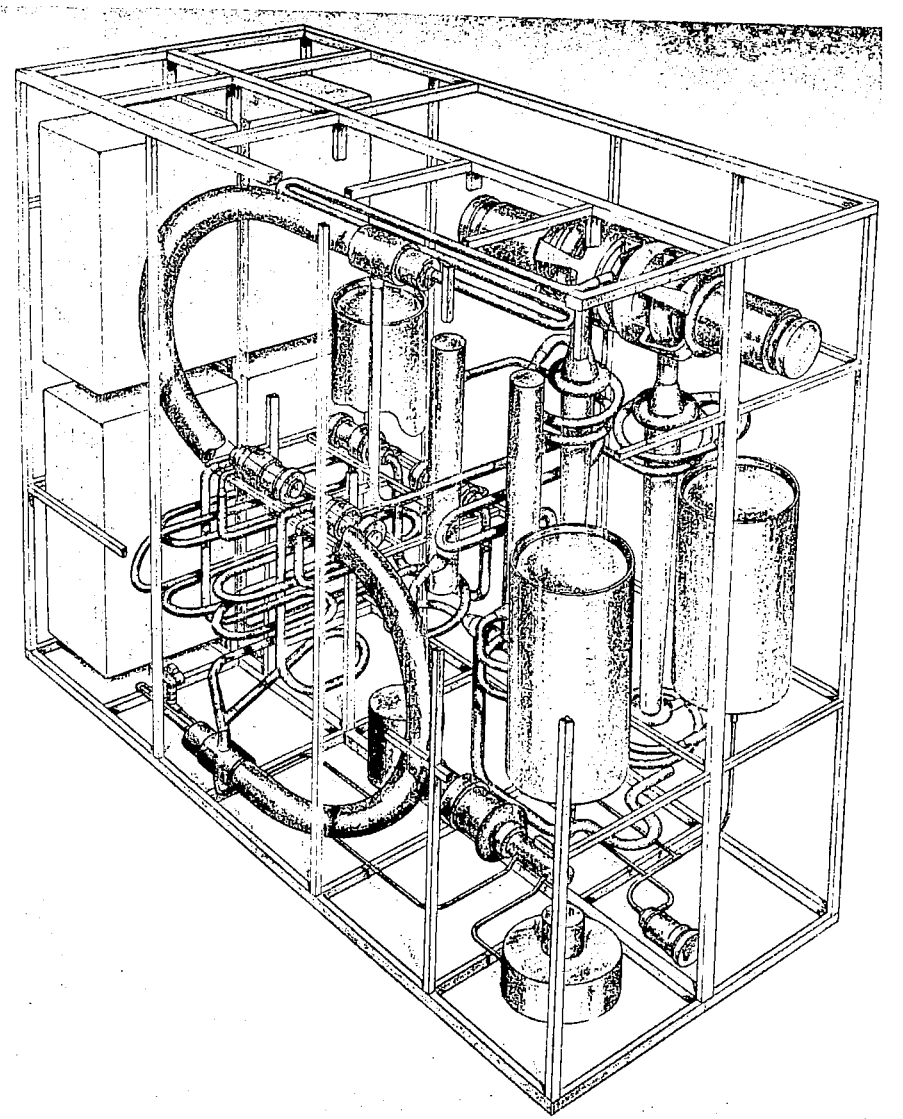

Figure 2-8 90-kWe Power Conversion System for Ground Testing

3.0 SYSTEM DEFINITION

3.1 SYSTEM DESCRIPTION

The SNAP-8 nuclear electrical generating system includes four main subsystems: a nuclear system to provide thermal power, a power conversion system to convert thermal to electrical power, a radiator to remove excess or waste heat from a Rankine cycle, and an organic-fluid loop to cool and lubricate specific components. A simplified schematic showing the relationship of the loops and the major components for the 90 kWe system concept appears in Figure 3-1.

The overall system may be further categorized into a number of individual and interrelated fluid loops. For the latest system planned for development, the following apply:

- A reactor primary loop which receives heat from the nuclear reactor
- An intermediate loop which transfers heat from the reactor primary loop to the mercury Rankine-cycle loop
- A mercury Rankine-cycle loop which converts heat to mechanical power
- A heat rejection loop which removes excess or waste heat from the Rankine-cycle loop
- An auxiliary NaK cooling loop, actually a branch of the heat rejection loop, which cools specific components, removes heat generated in the reactor shield, and removes reactor heat under certain system operating modes
- An organic-fluid lubricant-coolant loop which cools and lubricates specific components.

3.1.1 90-kWe System

The latest system considered for development and testing in the NASA Plum Brook Space Power Facility would provide a nominal net electrical power output of 90 kW. Design and definition of the 90-kW system were not completed; but, since this was one of the final project goals, and since significant progress was made toward a final design definition, this system is discussed here.

While the SNAP-8 system is intended for eventual application to manned space missions, the system configuration planned for use in ground tests combines the power conversion system with a reactor heat source and a ground test radiator for waste heat rejection. Many features associated

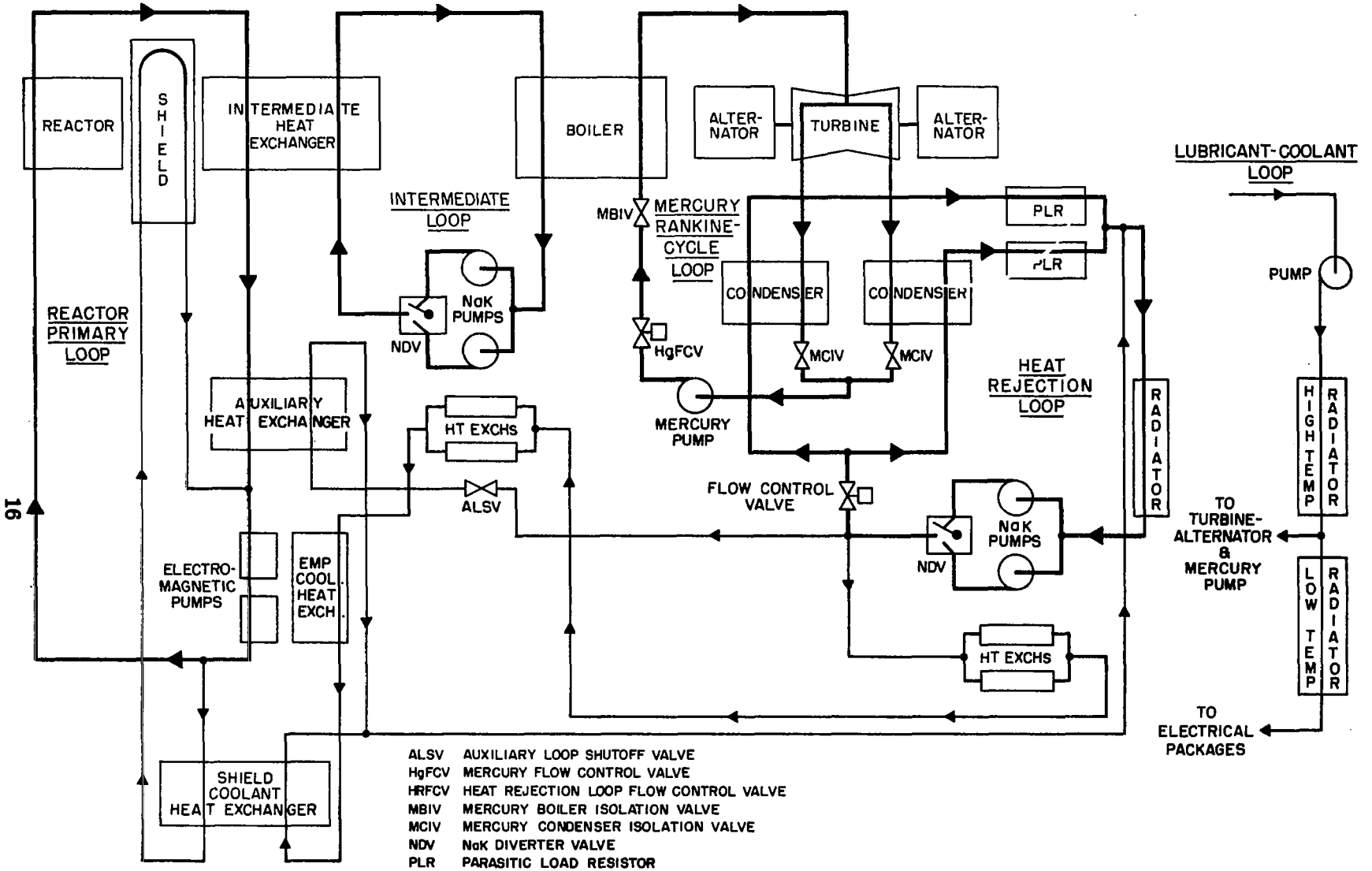

Figure 3-1 90-kWe Electrical Generating System Schematic

with a manned space application are included in the design. Component redundancy is incorporated (or provisions are made for incorporation at a later date) and considerations for operation of future systems in reduced gravity have been taken into account in the design, wherever practical.

The functions of the various system loops and the components contained therein are described below.

3.1.1.1 Reactor Primary Loop

The reactor primary loop (RPL) transfers heat generated by the reactor to the power conversion system using NaK* as the working fluid. The RPL consists of a main heat-transfer loop with a branch loop to cool the reactor radiation shield. The main RPL loop consists of the SNAP-8 "reference" reactor, an intermediate heat exchanger which transfers heat from the RPL to the intermediate loop, an auxiliary heat exchanger which transfers heat from the RPL to the heat rejection loop (HRL) during startup and shutdown, an electromagnetic pump system employing redundant pumps, a fluid expansion reservoir, and associated piping.

The RPL shield cooling branch circuit uses a fraction of the NaK flow circulated by the electromagnetic pump system to remove heat generated by thermalizing neutrons and gamma rays in the nuclear system 4-pi shield. NaK is circulated through passages within the reactor shield and through a heat exchanger which transfers the heat to the HRL.

3.1.1.2 Intermediate Loop

The intermediate loop (IL) uses NaK to transfer heat from the RPL to the boiler in the mercury Rankine-cycle loop. The IL consists of a boiler, two NaK pumps, a NaK diverter valve, an expansion reservoir, interconnecting piping, and connecting lines to the tube side of the intermediate heat exchanger. Of the two NaK pumps in the IL, one circulates the working fluid, and the other is a redundant standby unit. The NaK diverter valve, located at the outlet of the pumps, prevents NaK backflow through the idle pump while directing the fluid flow from the operating pump through the remainder of the loop. All components of the intermediate loop are contained within the power conversion system structure.

3.1.1.3 Mercury Rankine-Cycle Loop

The Rankine-cycle loop, with mercury as the working fluid, is the main energy conversion loop of the system and consists of a turbine, dual alternators, two condensers, a liquid mercury pump, a liquid mercury flow control valve, three solenoid-operated shutoff valves, the mercury containment tubes of the boiler, and interconnecting piping.

---

*NaK: a eutectic mixture of sodium and potassium (22% Na - 78% K)

Heat is transferred from the intermediate loop NaK which circulates through the shell side of the boiler. As the mercury passes through the boiler, it is preheated to saturation conditions, boiled to produce vapor, and superheated. The superheated vapor is directed through the turbine where the thermal energy is converted to mechanical power and to electrical power by the alternators coupled directly to the turbine shaft. The "wet" mercury vapor leaving the turbine flows to the condenser where it is condensed and subcooled. The heat produced by condensation and subcooling is transferred to the HRL NaK circulating through the shell side of the condenser. The subcooled mercury flows to the mercury pump where the fluid pressure is increased to meet the required boiler inlet conditions. The rate of mercury flow through the loop is controlled by the position of the variable-area orifice in the motor-driven flow control valve.

Ancillary to the mercury Rankine-cycle loop is the mercury injection and recharge subsystem which consists of a mercury reservoir, two solenoid-operated shutoff valves, and a solenoid-operated four-way reservoir actuator valve. This subsystem injects mercury at a controlled rate into the Rankine-cycle loop during startup, removes the working fluid from the loop during shutdown, and controls the mercury inventory in the condenser during system operation to maintain proper condensing conditions. All components of the Rankine-cycle loop are contained within the power conversion system structure.

3.1.1.4 Heat Rejection Loop

NaK in the heat rejection loop (HRL) removes excess, or waste, system heat primarily from the mercury loop. The waste heat will be rejected from a radiator to space in mission applications and from a radiator to a cold wall in ground tests. The HRL consists of a radiator, two NaK pumps, a NaK diverter valve, an expansion reservoir, a motor-driven flow control valve, two parasitic load resistors, interconnecting piping, and connecting lines to the shell side of the condensers. The two NaK pumps and the NaK diverter valve are used in the same manner as described for the similar components in the intermediate loop. The motor-driven flow control valve is used only during startup and shutdown to control the NaK flow to the condenser to maintain proper condensing pressures. The parasitic load resistors dissipate (in the form of heat) electrical power in excess of the power used to operate the system or to meet mission demands. The components of the heat rejection loop, except the radiator, are contained within the power conversion system structure.

3.1.1.5 Auxiliary NaK Cooling Loop

The auxiliary NaK cooling loop, a branch of the heat rejection loop, uses a fraction of the flow circulated by the HRL NaK pump to cool the HRL pumps, the IL pumps, and the RPL electromagnetic pumps, to remove heat from the heat exchanger in the shield-cooling branch of the RPL; and to remove heat from the auxiliary heat exchanger during startup and shutdown. The auxiliary loop consists primarily of interconnecting piping to the tube sides of the various heat exchangers and cooling coils of the components within the loop flow circuit, and a solenoid-operated shutoff valve which stops the flow to the auxiliary heat exchanger after system startup has been completed.

3.1.1.6 Lubricant-Coolant Loop

The lubricant-coolant loop uses an organic fluid* to perform three functions:

- Lubricate bearings in the turbine, alternator, and mercury pump.
- Cool components which must operate at temperatures below the HRL NaK temperature.
- Provide pressure to operate the mercury injection and recharge system.

A schematic of the lubricant-coolant loop is shown in Figure 3-2. The loop consists of a pump, an expansion reservoir, a high-temperature radiator, a low-temperature radiator, six solenoid shutoff valves, and interconnecting piping to the various components which must be lubricated and cooled. Lubricant is supplied to the turbine, alternator, and mercury pump bearings. The solenoid shutoff valves are sequenced open during startup and sequenced closed during shutdown to assure proper timing of lubricant flow to the bearings. Coolant from the lubricant-coolant high-temperature radiator is supplied to the turbine-alternator space seal heat exchangers, the alternator housings, the mercury pump space seal heat exchanger, and the mercury pump motor housing. A fraction of the flow leaving the high-temperature radiator is directed to the low-temperature radiator which further reduces the fluid temperature and cools the electrical assembly packages. An additional low-temperature electrical package, the programmer, will also be cooled by the fluid from the low-temperature radiator for mission applications; but, for a ground test system, the programmer will be located in the control room and will not require cooling. All components of the lubricant-coolant loop, except the radiators, will be contained within, or mounted on, the power conversion system structure.

3.1.1.7 Electrical System

The electrical system performs several functions during system operation, and interfaces with the nuclear system controls and with the test facility or mission vehicle. A block diagram of the electrical controls and

---

*The SNAP-8 lubricant-coolant fluid must meet a number of requirements in terms of working characteristics; these are: thermal stability, nuclear radiation stability, high heat-transfer coefficient, high specific heat, suitable viscosity at 200 to 400°F, noncorrosive to common engineering materials, good lubricity, and low vapor pressure. Polyphenyl ether (Shell Mix 4P3E) was selected as the best of the available fluids to meet these requirements mainly because of its ability to withstand nuclear radiation. This fluid falls into the class of polynuclear aromatics which are known to be the most radiation resistant, thermally and oxidatively stable fluids currently available. The properties of this fluid and the methods for controlling composition to avoid the formation of undesirable precipitates are discussed in References 1 and 2.

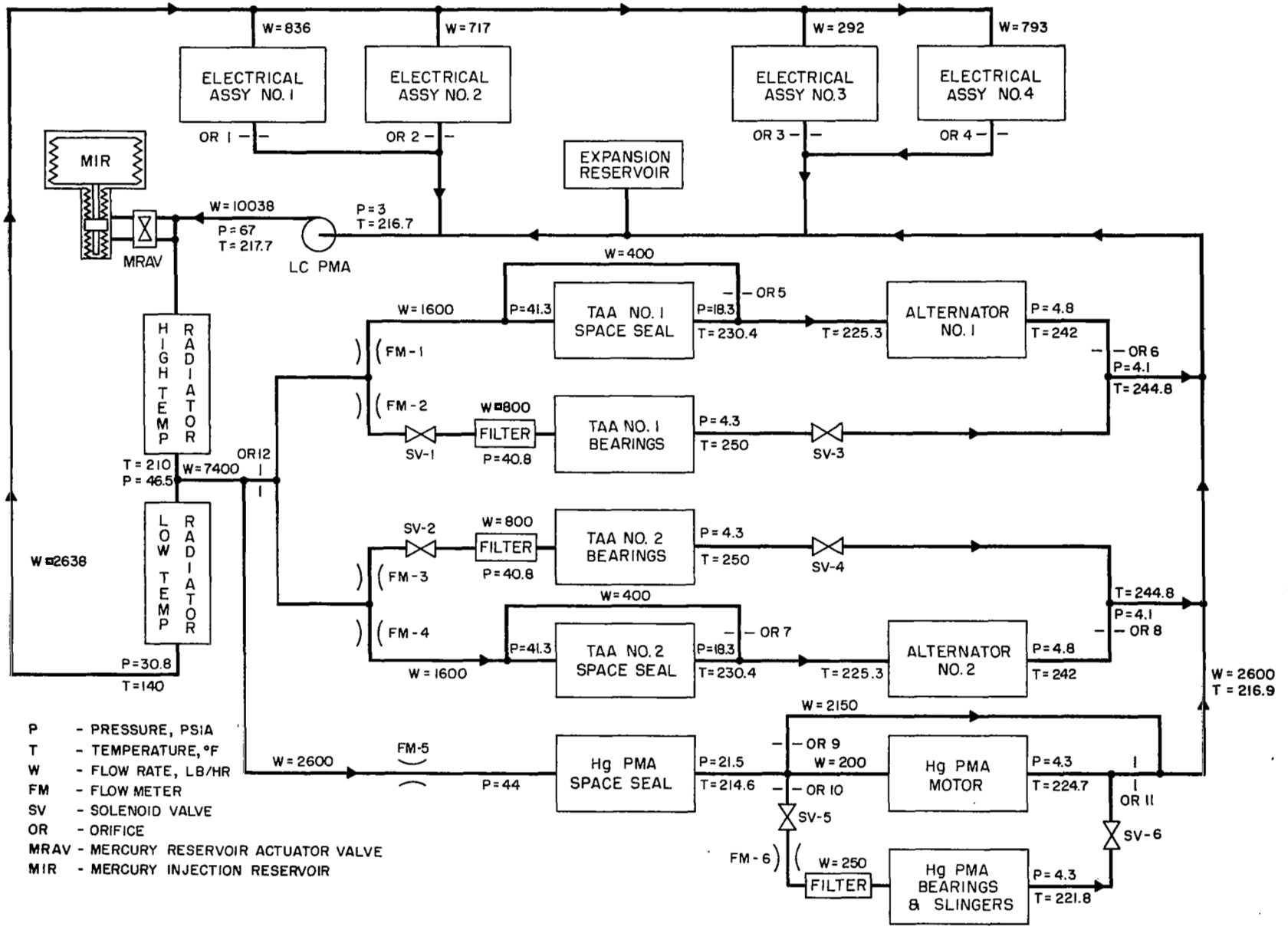

Figure 3-2 90-kWe System Lubricant-Coolant Loop Schematic

components appears in Figure 3-3. The individual electrical component functions and requirements are presented in Section 6.0 of this report. In general, the electrical system provides the following:

- Control functions to permit the sequenced process of system startup, shutdown, and emergency shutdown.
- Control of the turbine-alternator speed to maintain the alternator frequency and voltage within the specified limits.
- A protective system which receives instrumentation signals and initiates appropriate actions when the signals are not within specified limits.
- A power distribution system to supply the electrical power required by the electrical components and the demands of the vehicle loads.

a. Control Functions.- The major control functions for the sequence, interaction, and timing of the various events required for startup, steady-state operation, and shutdown are controlled by the programmer. The timing of the various events is adjustable to permit modification of the sequences without major rework. In addition, the ability to respond to external command signals, including overrides, has been incorporated to increase the versatility and reliability of the unit. Since the first 90-kWe system was planned for testing in the Space Power Facility, the programmer would be located in the facility control room to provide ready access of adjustments and modifications if required.

During steady-state operation, the alternator frequency and voltage are maintained within specified limits by the speed control system and the voltage regulator-exciter. The dual alternator arrangement and the desirability of using equipment developed for a system with lower net electrical power capability requires the use of two speed control systems, two voltage regulators, two parasitic load resistors, two power factor correction assemblies, and load compensation equipment to permit synchronizing and paralleling of the alternator outputs.

The electrical controls system initiates the programmed automatic shutdown sequences when emergency or potential emergency situations are indicated by sensor signals. In addition, an electrical protective system provides for the following situations which may occur during steady-state operation:

- When the alternator voltage drops below 95% rated voltage any time after startup or prior to initiation of a shutdown, an emergency shutdown of the power conversion system and nuclear system is initiated.
- When an alternator voltage unbalance occurs, the vehicle load breaker is cycled to verify that the source of the unbalance is in the power conversion system. If so, an emergency shutdown is initiated.

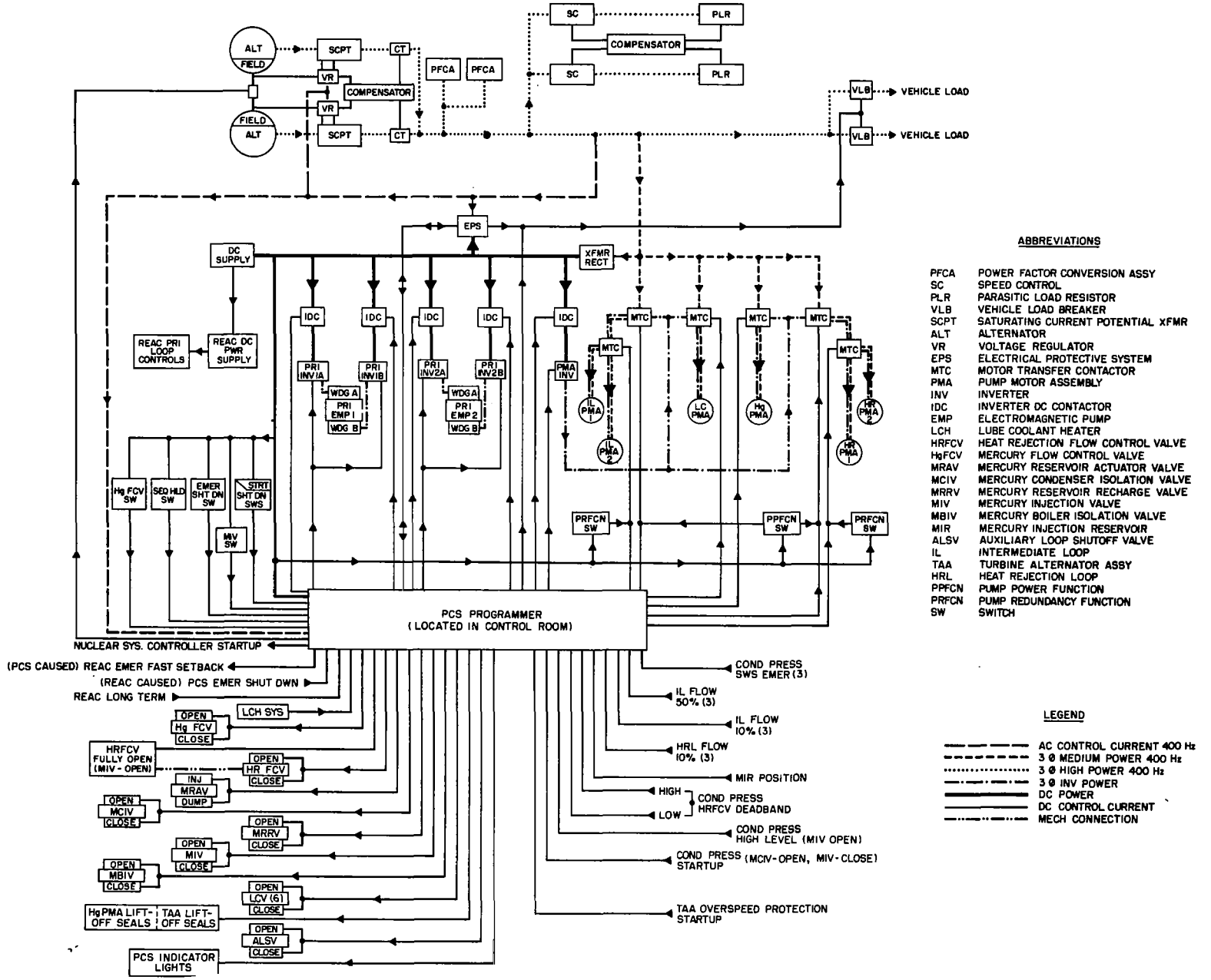

Figure 3-3 Electrical System Diagram for the 90-kWe Power Conversion System

b. Power Supply and Distribution.- The power supply for the electrical system is a silver-zinc battery which provides 30 Vdc to operate the programmer and to perform the programmed functions during startup and shutdown. These functions include (1) actuation of valves, relays, and contactors, (2) providing alternator field flashing and saturable reactor bias current, and (3) providing power for the nuclear controls. The battery will also provide both 30 and 60 Vdc to operate the pump inverter and 60 Vdc to operate the reactor primary loop electromagnetic pump inverters during startup and shutdown. A battery charging system provides a fast charge following system startup and a continuous trickle charge during steady-state operation to ensure the availability of adequate battery power for shutdown and a subsequent restart.

Electrical power is distributed through an electrical harness. The harness is a series of electrical cables with high-temperature insulation; steel-braided flexible conduit will be used in areas requiring additional protection from operating and handling environments. Cable routing will be along nonremovable members of the power conversion system frame. Connectors at the components and terminal boards will be a combination lug and weld type to facilitate initial wiring and checkout and final welding to terminal posts prior to system operation.

c. Modular Packages.- The electrical subassemblies and components are grouped into four modules with the individual subassemblies and components arranged as shown in Figure 3-4. The components are grouped to facilitate routing of interconnecting cables and attachment of the subassemblies and components to a single heat sink for cooling by the lubricant-coolant fluid. Each module will contain a terminal board to which all components are connected and from which all external connections are made. The modules are enclosed in nonsealing protective covers for accessibility to the individual components.

3.1.2 35-kWe System

The SNAP-8 system development has progressed through a number of major changes in both application and performance goals. The system evolved from a relatively simple two-loop system designed to produce a net electrical output of 30 kWe in a zero-g environment while in the near-earth orbit. The system was required to start only once, while in orbit, and was to be used only for instrument-rated missions. The nuclear radiation shielding for this application was to be sufficient to protect instrumentation and electronic equipment. System performance and mission application changes have resulted in configuration changes first to a 35-kWe system and finally to the 90-kWe system described above.

As the system evolved, a major system configuration, design, and performance definition was completed for the 35-kWe system which has been the basis for subsequent system definitions and estimates of the effects of transient operating conditions on the system and major components. This system was designed to meet the major requirements shown in Table 3-I. The 35-kWe system is shown in Figure 3-5 in a configuration for a manned space mission. Major design, performance, and transient studies and tests were completed resulting in a significant overall system development phase which merits detailed discussion.

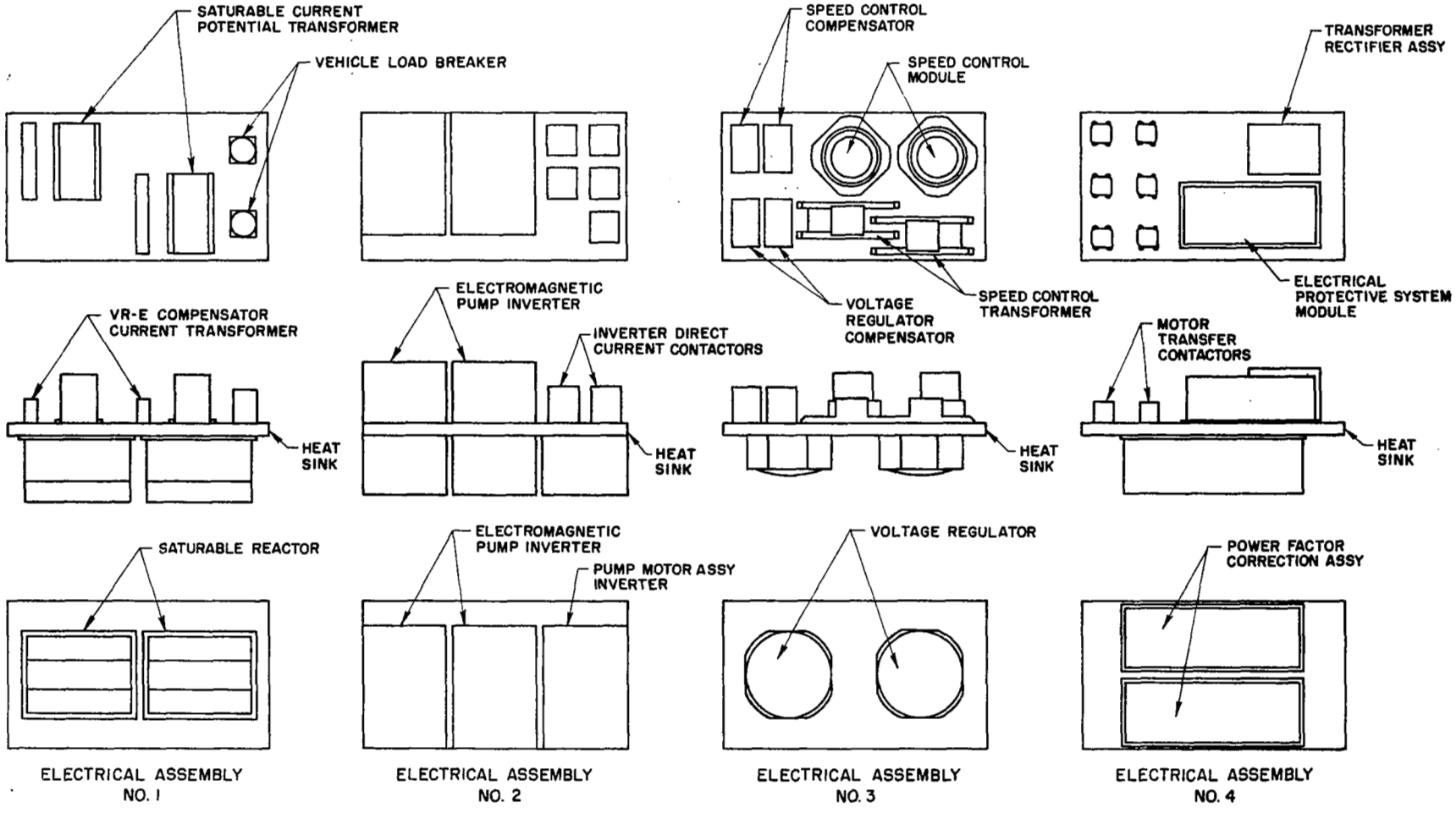

Figure 3-4 90 kWe System Electrical Component Assembly Arrangement

TABLE 3-I MAJOR REQUIREMENTS - 35-kWe SYSTEM

Note: The system meeting these requirements is applicable to instrument-rated, man-rated, and ground-test installations.

Net electrical output	35 kWe (min.)
Vehicle load power factor	0.85 (lagging)
Voltage (rms, line to line)	208 Vac, $\pm$ 5%
Frequency	400 Hz, $\pm$ 1%
Operating life (continuous)	10,000 hr
Reactor power	600 kWt (max.)
Reactor outlet temperature (steady-state range)	1280 to 1330°F
Environment	
Gravitational field (operating)	0 to 1 g
Radiation	
PCS (integrated dose for 10^4 hr)	
Fast neutrons (0.1 MeV or greater)	5×10^{12} nvt
Gamma rays	5×10^7 rads (c)
Solid-state electronics (integrated dose for 10^4 hr)	
Fast neutrons (0.1 MeV or greater)	10^{11} nvt
Gamma rays	10^6 rads (c)
Acceleration (system not operating)	
Longitudinal axis	$\pm$ 6 g
Transverse axis	2 g
Restart capability	
Number of automatic restarts without servicing	20
Gravitational field	0 to 1 g
Envelope requirements	(See Section 3.3 of this report)

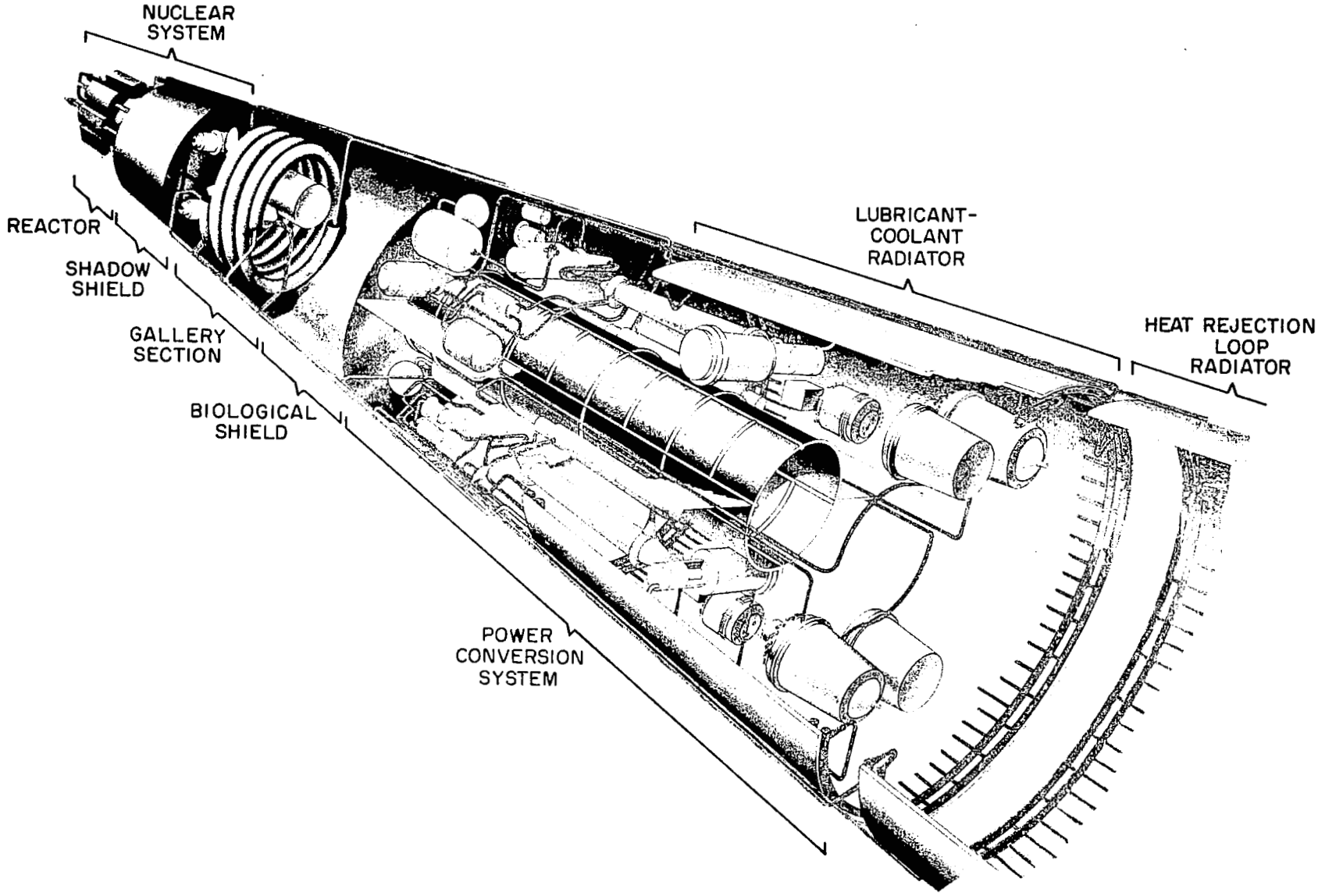

Figure 3-5 35-kWe Electrical Generating System for Manned Space Missions

The 35-kWe system includes four main subsystems: a nuclear system to provide thermal power, a power conversion system to convert thermal to electrical power, a radiator system to remove waste heat from a Rankine cycle, and an organic-fluid loop to cool and lubricate specific components.

The system can also be described as a number of individual, interrelated loops which have functions similar to those described for the 90-kWe system. The major differences between the 90- and 35-kWe systems in regard to loop functions is that (1) the 35-kWe system does not employ an intermediate loop, (2) the lubricant-coolant loop provides cooling for the NaK pump motors, and (3) the 35-kWe system employs redundant power conversion systems to provide increased reliability for man-rated applications. The redundant power conversion system concept implies the use of two independent mercury Rankine-cycle loops, heat rejection loops, lubricant-coolant loops, and electrical subsystems. The redundant power conversion systems are incorporated into the overall system by providing two boilers, in series, in the primary loop. A simplified schematic, Figure 3-6, shows the location of the two boilers in the primary loop and the relationship of the remaining loops for one of the redundant power conversion systems.

3.1.2.1 Individual Loop Functions

The functions of the various fluid loops or the differences from similar loops in the 90-kWe system are described below:

a. Primary NaK Loop.- The primary NaK loop (PNL), with NaK as the working fluid, transfers heat from the reactor to the boiler in the mercury Rankine-cycle loop. The PNL consists of the reactor, two boilers, two NaK pumps, a NaK diverter valve, an expansion reservoir, two auxiliary heat exchangers, and interconnecting piping. The two NaK pumps are connected in parallel in the PNL; one circulates the working fluid, and the other is a standby unit. The NaK diverter valve, located at the output of the pumps, prevents NaK backflow through the idle pump while directing the fluid flow from the operating pump through the remainder of the loop. The shell sides of two boilers are connected in series in the PNL to provide for transfer of reactor heat to either of the two (one of which is a redundant standby unit). Similarly, two auxiliary heat exchangers are contained in the PNL to transfer reactor heat to either heat rejection loop during startup and shutdown. The components of the primary loop, except the reactor, are contained in the gallery section of the system shown in Figure 3-5, that is, between the nuclear system shadow shield and the biological shield.

b. Mercury Rankine-Cycle Loop.- The Rankine-cycle loop performs the same function as that described for the 90-kWe system. However, the following differences exist in the component complement: a single-path impulse turbine with one alternator, one condenser, and two solenoid operated shutoff valves.

c. Heat Rejection Loop.- The function of the heat rejection loop in the 35-kWe system is similar to that in the 90-kWe system with the following differences in component complement: a single NaK pump is used so that a NaK diverter valve is not required, and only one parasitic load resistor is needed.

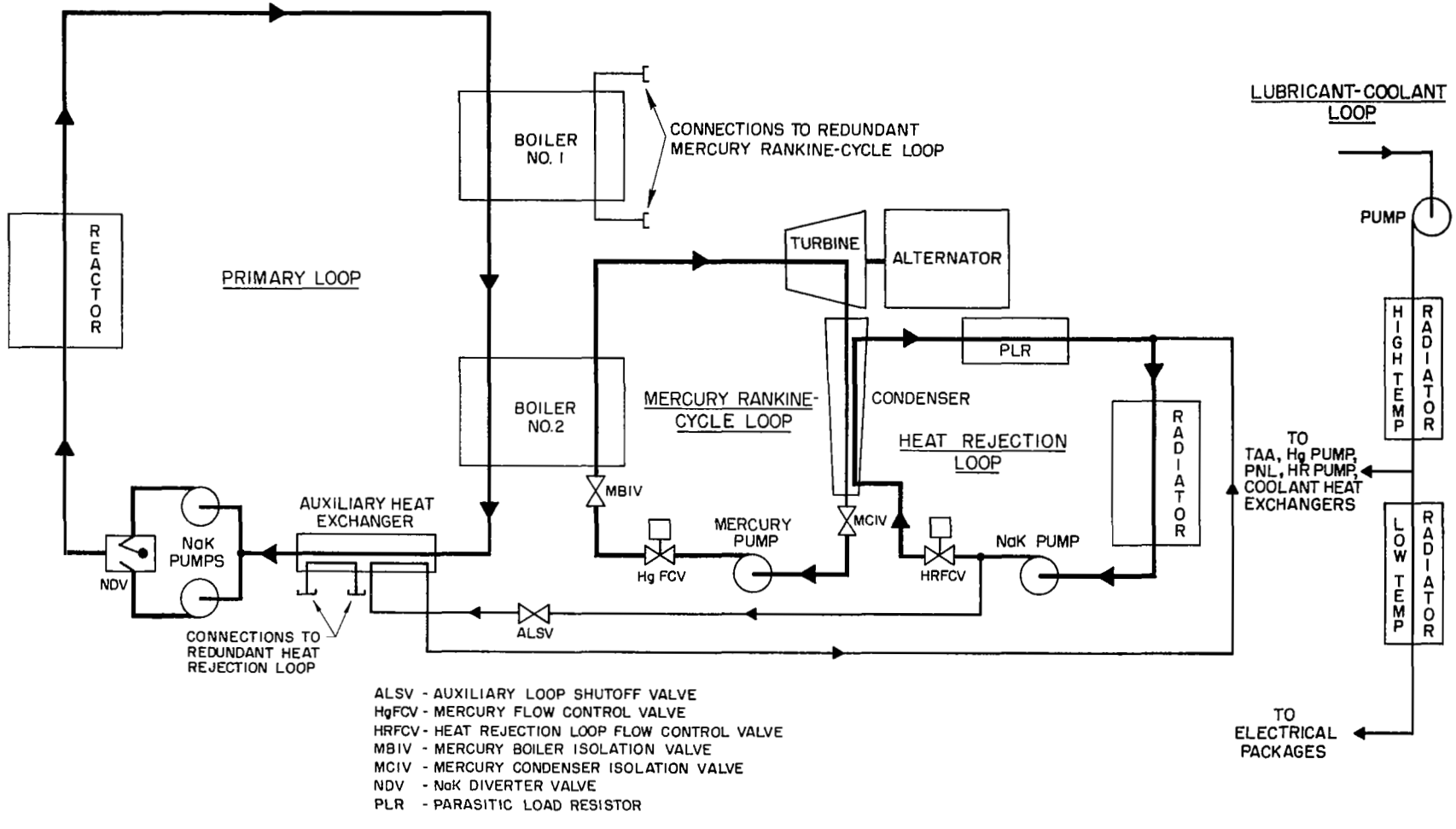

Figure 3-6 35-kWe Electrical Generating System Schematic

d. Auxiliary NaK Loop.- The auxiliary NaK loop, a branch of the heat rejection loop as for the 90-kWe system, uses a portion of the flow to remove heat from the PNL by means of the auxiliary heat exchanger during startup and shutdown. The auxiliary loop does not provide coolant for the NaK pumps as in the 90-kWe system, and is therefore simpler.

e. Lubricant-Coolant Loop.- The lubricant-coolant loop performs the same functions as those described for the 90-kWe system, and also cools the NaK pumps in the primary and heat rejection loops. In addition the electrical components for the 35-kWe system were packaged in high-temperature ($\approx 210^{\circ}F$) and low-temperature ($\approx 140^{\circ}F$) groups. Grouping the electrical components in this manner permitted a reduction in the size of the lubricant-coolant radiators.

A schematic of the lubricant-coolant loop is shown in Figure 3-7. Lubricant is supplied to the turbine, alternator, and mercury-pump bearings. Coolant, from the high-temperature radiator, is supplied to the following: turbine-alternator space seal heat exchanger, alternator housing, mercury-pump motor, mercury-pump space seal heat exchanger, primary and heat rejection loop NaK-pump cooling heat exchangers and high-temperature electrical packages. A fraction of the flow leaving the high-temperature radiator is directed to the low-temperature radiator which reduces the fluid temperature and is used to cool the low-temperature electrical controls package and the programmer. The programmer to be used for ground tests in the Space Power Facility would be located in the facility control room and therefore would not be cooled by the lubricant-coolant system.

3.1.2.2 Electrical System

The electrical system performs functions similar to those described for the 90-kWe system. However, since only one alternator is required and the system does not include an intermediate loop, the amount of electrical equipment and the programmer sequencing functions are reduced. The electrical controls and components are presented in block diagram form in Figure 3-8.

During steady-state operation, alternator frequency and voltage are maintained within specified limits by the speed control system and the voltage regulator-exciter. Power factor correction provides a unity power factor at the alternator when rated output is produced thereby achieving maximum alternator efficiency at rated conditions. The electrical controls system will respond to external commands or sensor signals indicating potential emergency situations by initiating automatic shutdown procedures.

The electrical system power supply is a silver-zinc battery which provides 30 Vdc to operate the programmer and to perform the various programmed functions that occur during startup and shutdown. The battery will also provide both 30- and 60-Vdc power to the pump motor inverter during startup and shutdown. A battery charging system provides a fast charge following system startup and a continuous trickle charge during steady-state operation to ensure availability of sufficient battery power for shutdown and a subsequent restart.

Electrical power distribution is provided by an electrical harness with connectors and terminal boards as described for the 90-kWe system.

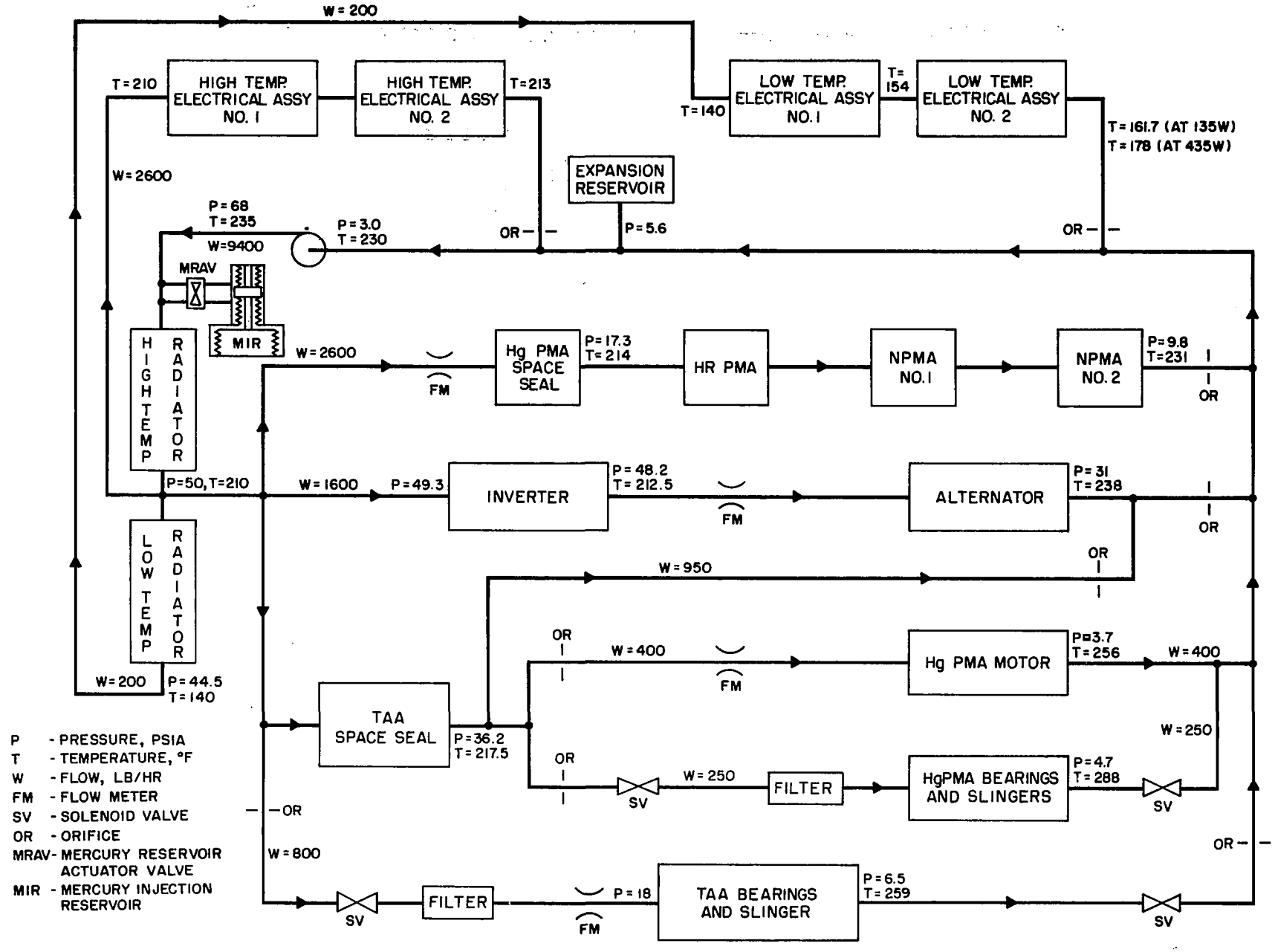

Figure 3-7 35-kWe System Lubricant Coolant Loop Schematic

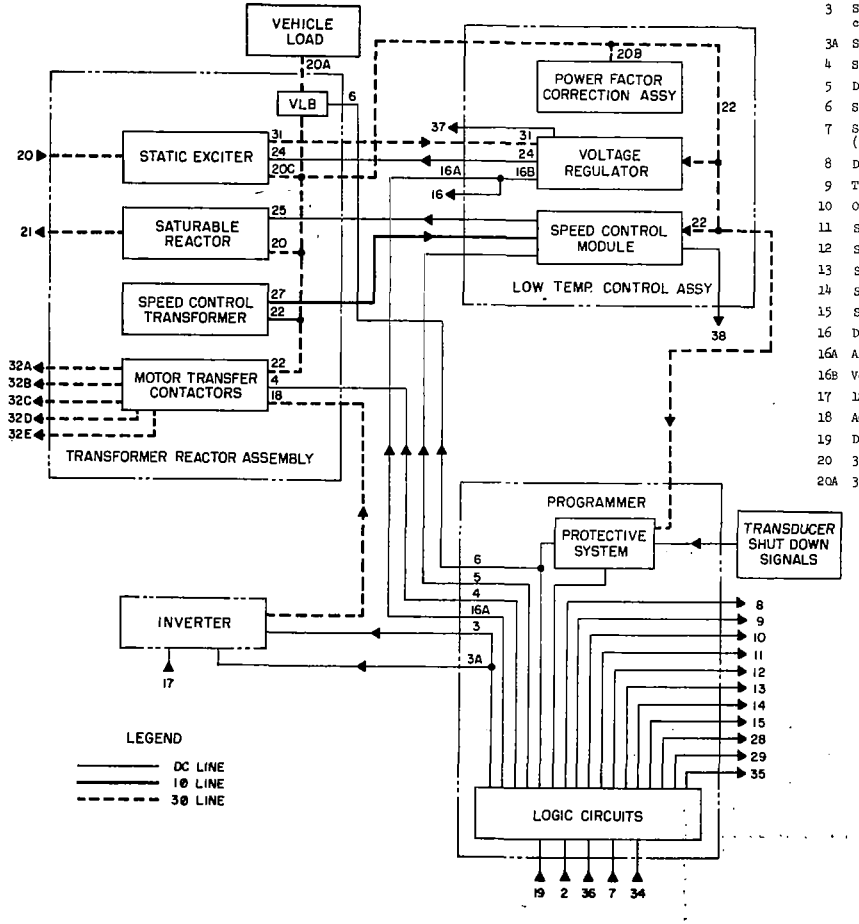

LINE/SIGNAL IDENTIFICATION

1	Deleted
2	Signal for startup sequence
3	Signal for inverter high-low tap changing contactor inverter shunt field control
3A	Signal to close contactor to start inverter
4	Signal to operate motor transfer contactor
5	DC bias circuit for speed control
6	Signal to control vehicle load breaker
7	Signal to start sequence for mercury injection (external signal)
8	DC power to nuclear reactor
9	To be determined
10	Open and close signal for FCV
11	Solenoid valve control } mercury pump
12	Solenoid valve control } bearing lubricant
13	Solenoid valve control } turbine-alternator
14	Solenoid valve control } bearing lubricant
15	Solenoid valve control, auxiliary loop
16	DC current for alternator field
16A	Alternator flashing current
16B	Voltage regulator DC current for alternator field
17	120 VDC power for inverter
18	AC output of inverter
19	DC power to programmer
20	3 phase, 4 wire alternator output:
20A	3 phase, 4 wire to vehicle load
20B	3 phase, 3 wire to power factor correction assembly
20C	3 phase, 3 wire to saturable reactor
21	3 phase, 2 wire to parasitic load
22	Low power, 3 phase, 4 wire alternator output
23	Deleted
24	DC control for static exciter control winding
25	DC control for saturable reactor
26	Deleted
27	AC power for speed control amplifier
28	MIV control
29	MRV control
30	Deleted
31	AC power for speed control amplifier
32	PMA power
32A	PML PMA No. 1
32B	L/C PMA
32C	PML PMA No. 2
32D	Hg PMA
32E	HRL PMA
33	Deleted
34	Normal shutdown signal
35	LCH power
36	TSE signal for PMA checkout
37	Voltage set point adjust
38	Frequency set point adjust

Figure 3-8 Electrical System Diagram for the 35-kWe Power Conversion System

The electrical subassemblies and components are grouped into four separate packages with the individual subassemblies and components arranged as shown in Figure 3-9. Two of the packages are cooled by fluid from the low-temperature radiator, and two by fluid from the high-temperature radiator. The relative location of the electrical packages in the lubricant coolant loop is shown in Figure 3-7.

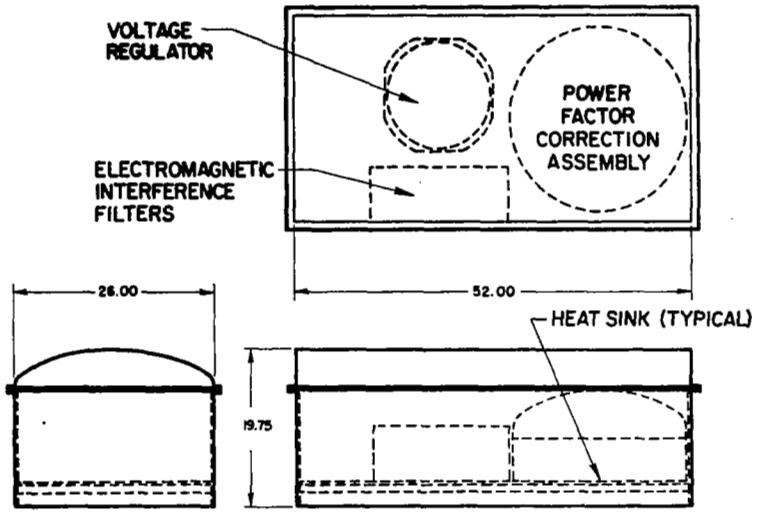

LOW TEMPERATURE ELECTRICAL ASSEMBLY NO. 1

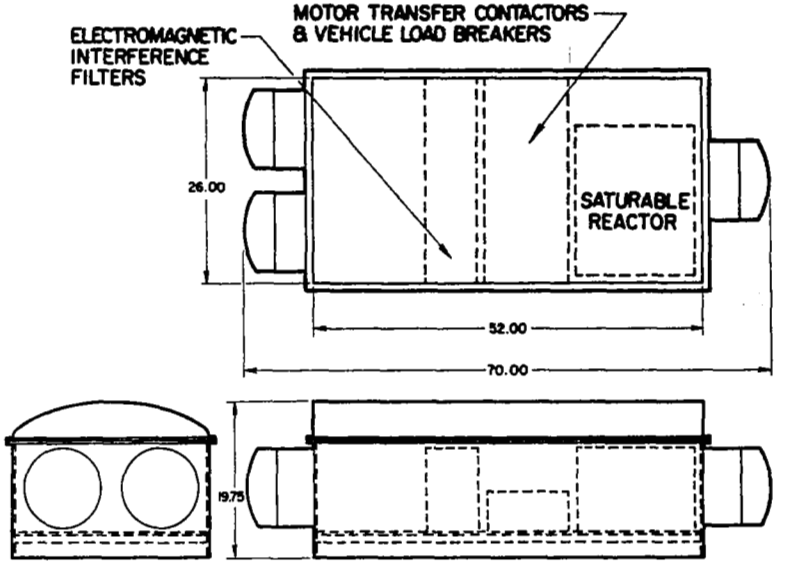

HIGH TEMPERATURE ELECTRICAL ASSEMBLY NO. 1

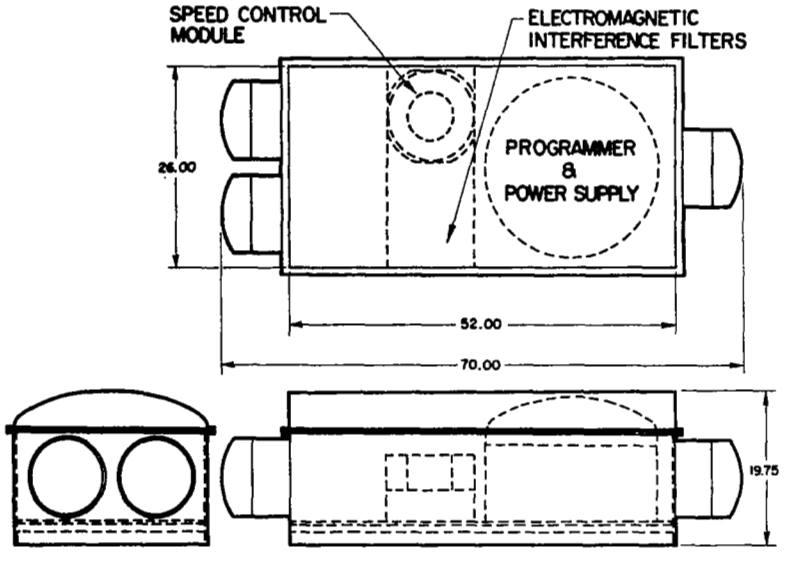

LOW TEMPERATURE ELECTRICAL ASSEMBLY NO. 2

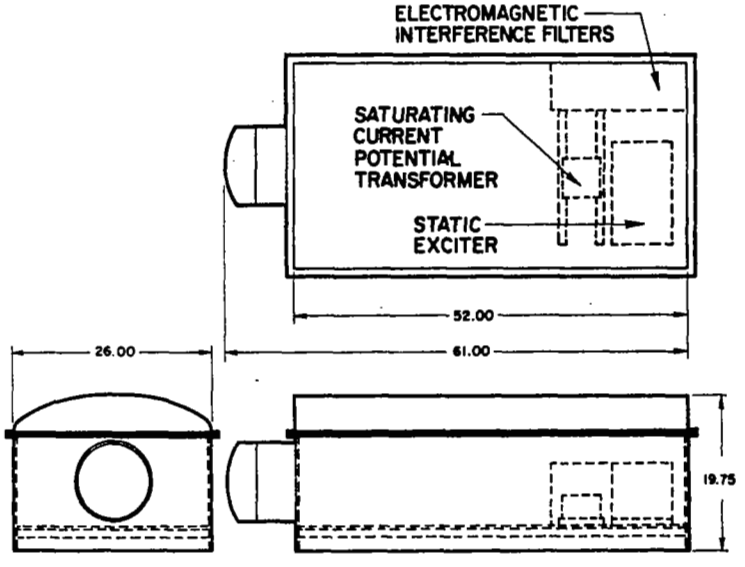

HIGH TEMPERATURE ELECTRICAL ASSEMBLY NO. 2

Figure 3-9 35-kWe System Electrical Component Assembly Arrangement

3.2 STATE-POINT DEFINITION

3.2.1 90-kWe System

The system state-point or steady-state operating conditions are based on a number of performance requirements and design criteria. In addition, limitations may be imposed which restrict the selection of design alternatives and performance capabilities. This is true of the present SNAP-8 system which has evolved through a continuing progression of changes and improvements associated with component performance, overall system performance, operating conditions, and envelope dimensions. One of the major restrictions throughout the SNAP-8 development program has been a continuing desire to limit the number and extent of component changes and redesigns to ensure maximum utilization of existing designs and hardware. This restriction has resulted in limitations on performance and on simplicity of overall system design. Studies have been conducted which indicate that, with modifications to several components, a SNAP-8 system having a net output of 120 kWe and a system efficiency of 20% could be produced. The results of the studies are presented in Reference 3, and the component modifications defined therein are all within the technology developed on the SNAP-8 program.

The 90-kWe system represents the latest effort to improve and upgrade the performance and mission capability of the SNAP-8 system. The primary objective for establishing the 90-kWe system was to define a system with maximum net electrical output which involved a minimum number of component changes. The major factors which limit net electrical output are: maximum available reactor power, maximum allowable reactor outlet temperature, boiling stability, mercury pump suction pressure requirements, and power conversion system efficiency. The effects of these factors are described below:

- The reactor outlet temperature, boiler stability and mercury pump suction pressure requirement determine the Rankine-cycle efficiency in the following manner: the reactor outlet temperature determines turbine inlet enthalpy, boiler stability determines boiling pressure by the minimum pinch-point temperature difference criteria, and the mercury pump suction pressure requirement determines the condenser pressure and, therefore, the turbine outlet isentropic enthalpy.

- The available reactor power limits the mercury flow rate.

- The available power is determined by the mercury flow rate and the Rankine-cycle efficiency.

- The net electrical output is determined by the available power and the power conversion system efficiency which includes the turbine efficiency and system losses (pumping power requirements, electrical system losses, and heat losses).

The steady-state, long-term operating limits for the advanced reactor*, as defined by the nuclear system contractor, are:

- Maximum power: 600 kWt
- Outlet temperature control band: 1210 to 1235°F

The objective to limit the number of component changes restricts the ability to utilize the available reactor power most efficiently. However, the largest single increase in overall system performance can be obtained by improving turbine efficiency. Significant improvements in turbine efficiency can be obtained by employing a reaction turbine rather than the impulse type as developed for previous SNAP-8 systems. A reaction turbine requires full admission which implies a high mercury vapor volume flow. A high volume flow can be obtained by increasing mercury flow or reducing turbine inlet pressure. Since the available reactor power limits mercury flow, the turbine inlet pressure must be reduced. In conjunction with lower turbine inlet pressure, the turbine exhaust pressure must also be low in order to maintain a high enthalpy difference and pressure ratio. (The turbine exhaust pressure limit is a function of condenser performance which is discussed in the following paragraph.) A reaction turbine becomes feasible for a high-output power system since two alternators of existing design can be used in conjunction with a dual-opposed reaction turbine. The dual-opposed turbine configuration has the additional advantage of cancelling the high axial-thrust bearing loads associated with reaction turbines.

The dual-opposed reaction turbine configuration permits the use of two condensers of existing design thereby allowing operation at reduced pressures and mercury flows compared to the original design conditions. The condenser performance characteristics for operation at the 90-kWe system conditions were obtained by evaluating system test results of operation at reduced condensing pressures and mercury flows, as shown in Figures 3-10 and 3-11. These data were used to devise a mathematical model to predict performance at condensing pressures and mercury flows lower than values obtained during the tests. The development and use of the mathematical model is discussed in detail in Reference 4. From the information shown in Figure 3-10, it is evident that, at mercury flows on the order of 8000 lb/hr, condensing pressures less than 2.5 psia cannot be obtained regardless of the NaK flow or NaK inlet temperature. Mercury flows on the order of 7000 lb/hr were expected for each condenser to be used in conjunction with the dual reaction turbine; therefore, a turbine exhaust pressure of 2.5 psia was chosen for the state-point condition.

* The advanced reactor is the latest compact reactor design for space power systems being developed by Atomics International under contract to the AEC.

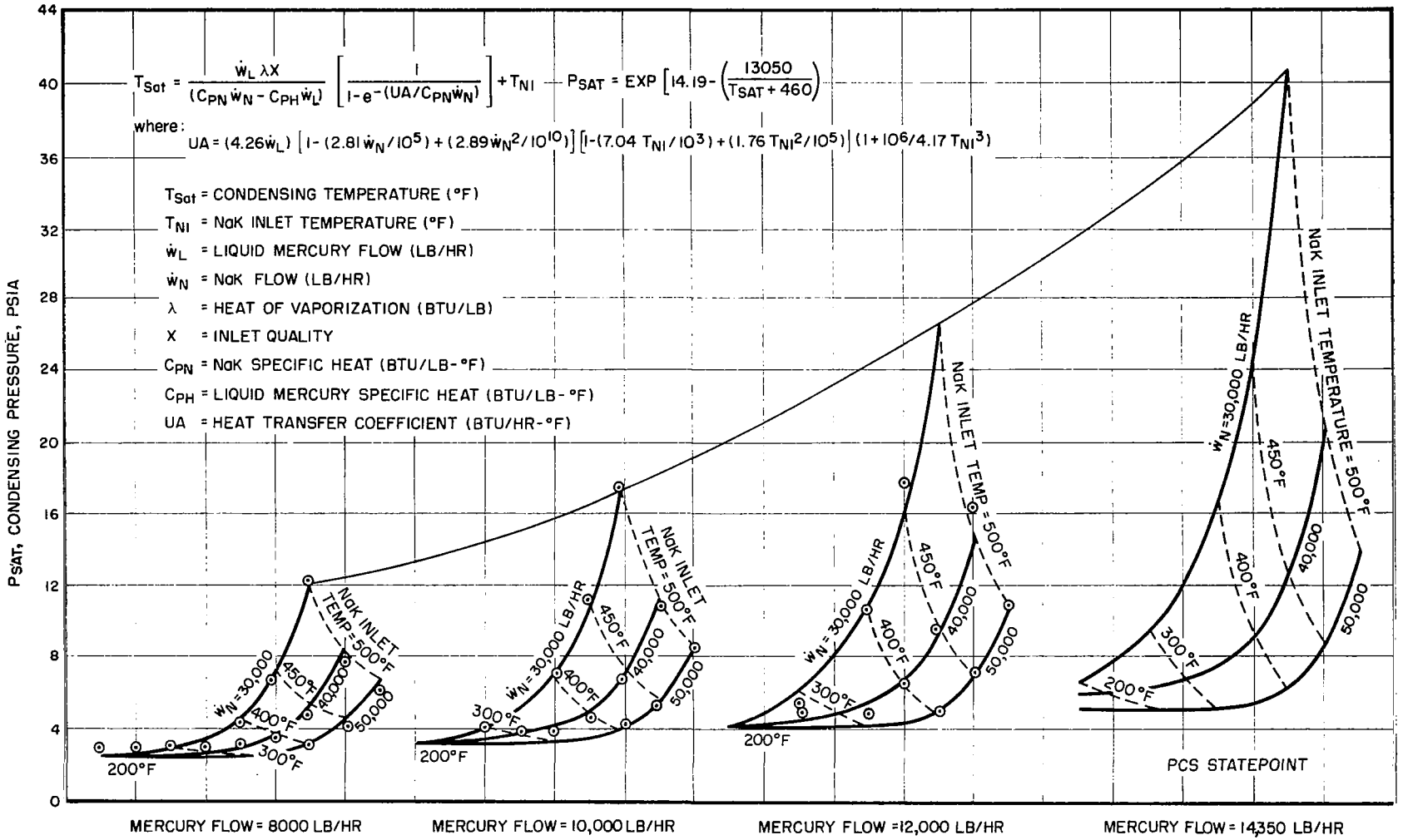

Figure 3-10 - Condenser Test Performance Characteristics - Condensing Pressure as a Function of Mercury Flow, NaK Flow, and NaK Inlet Temperature

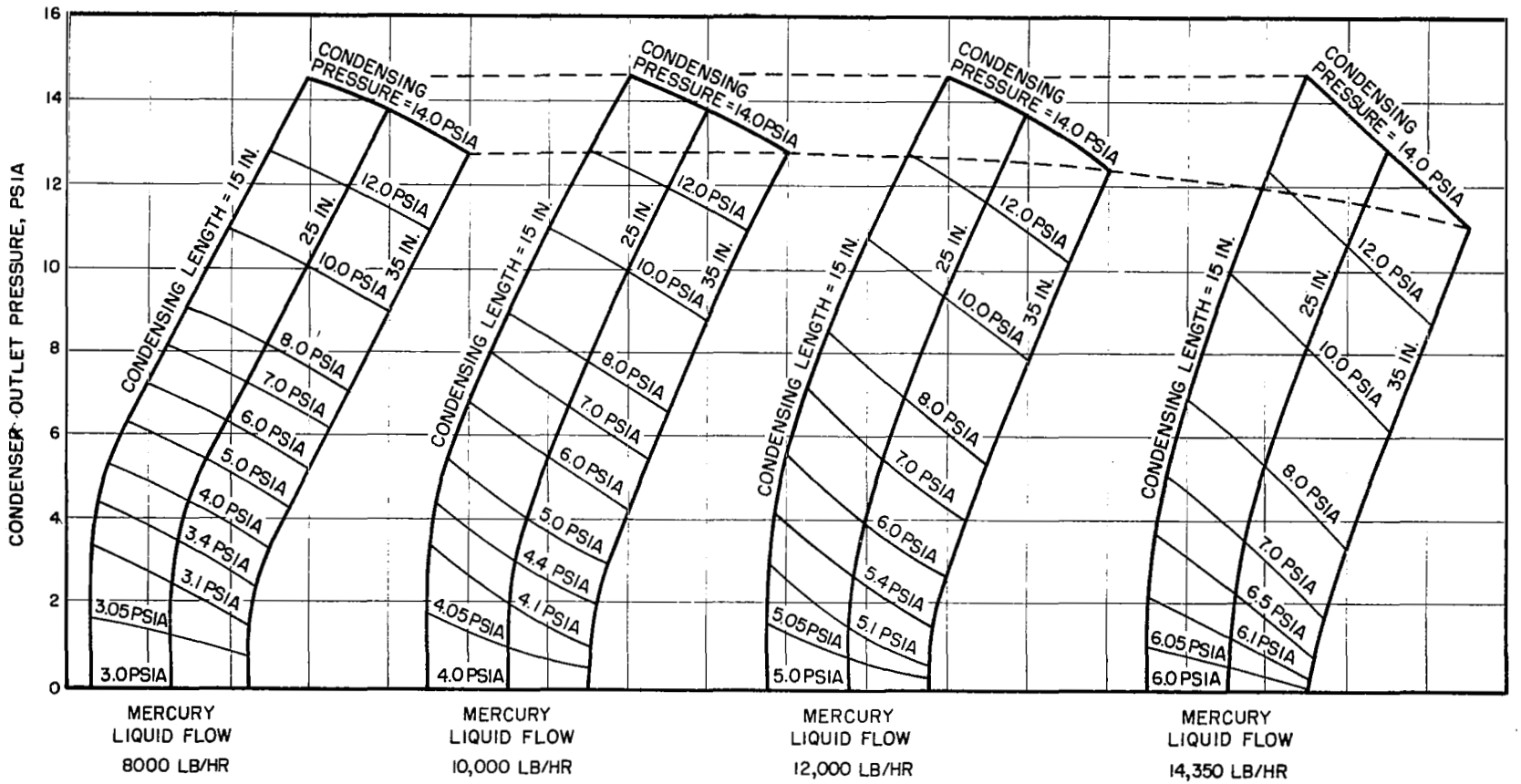

Figure 3-11 - Condenser Test Performance Characteristics - Condenser Outlet Pressure as a Function of Mercury Flow, Condensing Length, and condensing Pressure

The performance characteristics of developed components were obtained by evaluating the results of extensive testing. Alternator performance is presented in Figure 3-12. NaK pump and mercury pump performance is presented in Figures 3-13 through 3-15. The pump performance characteristics were used to evaluate the relationship between desired flows, available pump pressure rise, and system loop pressure drop. Since relatively high NaK flow rates are desirable (on the order of 60,000 lb/hr) it was found necessary to use 3.0-inch OD tubing in the NaK loops to assure that the pump pressure rise would be sufficient to meet the loop pressure drop characteristics.

Performance characteristics for components associated with the reactor power loop must be defined before the system state-point can be established. These components - the intermediate heat exchanger, the nuclear system shield cooling heat exchanger, and the reactor power loop electromagnetic pump system - have not been developed; so, performance characteristics were obtained from preliminary studies. One such study for the intermediate heat exchanger indicated that a 600-kWt NaK-to-NaK heat exchanger could be designed to operate with a 20°F terminal temperature difference. Preliminary information from the nuclear system contractor indicated that the shield coolant heat exchanger should be designed to transfer a 20-kWt heat load at nominal operating conditions. Preliminary information obtained from NASA's Lewis Research Center indicated that an ac electromagnetic pump with an efficiency of 10% could be designed for the flow rate and pressure rise required in the reactor primary loop, and that the electrical power conversion equipment required to operate the electromagnetic pump would have an 80% efficiency.

The major performance criteria and limitations are shown in Table 3-II. These criteria (in conjunction with the component performance characteristics determined from test results and evaluations, and performance characteristics determined from preliminary studies for components to be developed) form the basis for the definition of the state-point conditions. The final state-point conditions selected for the 90 kWe system are shown on Figure 3-16, and represent the design-point conditions for the system and various components. The values shown on Figure 3-16 are for system operation at beginning of life and with the temperature of the NaK leaving the reactor at the value corresponding to the lower end of the nuclear system deadband control. The design point is chosen with the reactor operating at the lower end of the nuclear system deadband control since this condition corresponds to the lowest NaK temperature entering the boiler; this, in turn, defines the minimum pinch-point temperature difference for boiler operation. The significance of pinch-point temperature difference on boiler operation is discussed in Section 5.5.

With the system operating at the design-point conditions, as shown in Figure 3-16, the net electrical output is 92.8 kWe which satisfies the requirement for a minimum output of 90 kWe. The +2.8 kWe above the minimum requirement provides a margin for system and component degradation over the operating life of the system.

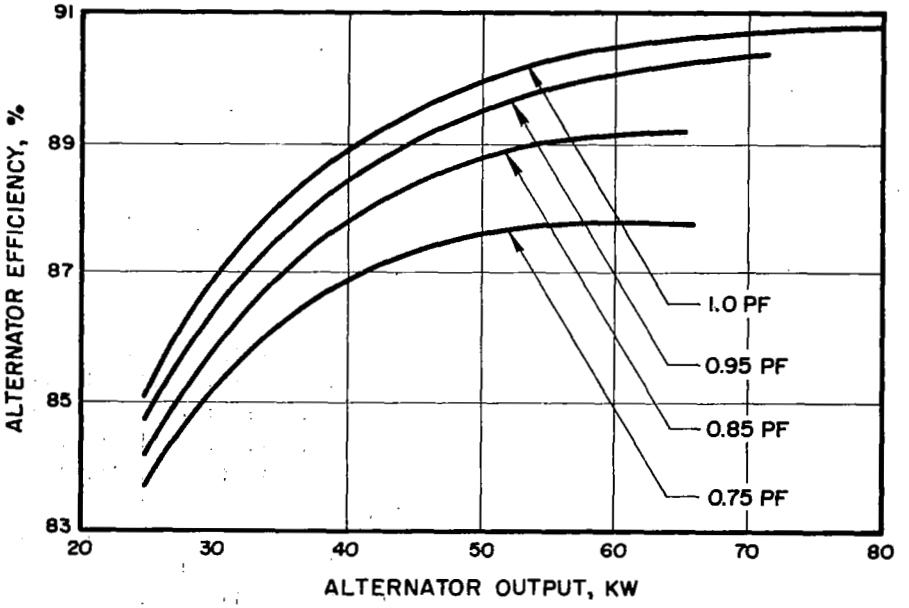

Figure 3-12 - Alternator Efficiency as a Function of Load and Power Factor

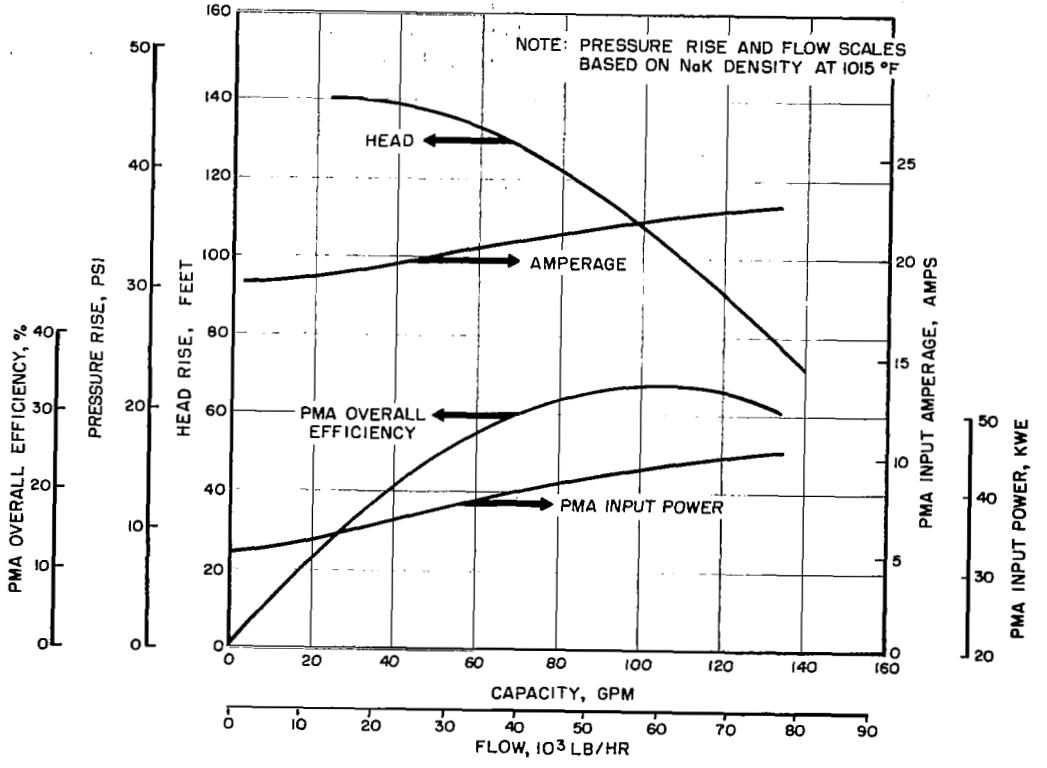

Figure 3-13 - Intermediate Loop NaK Pump Performance Characteristics

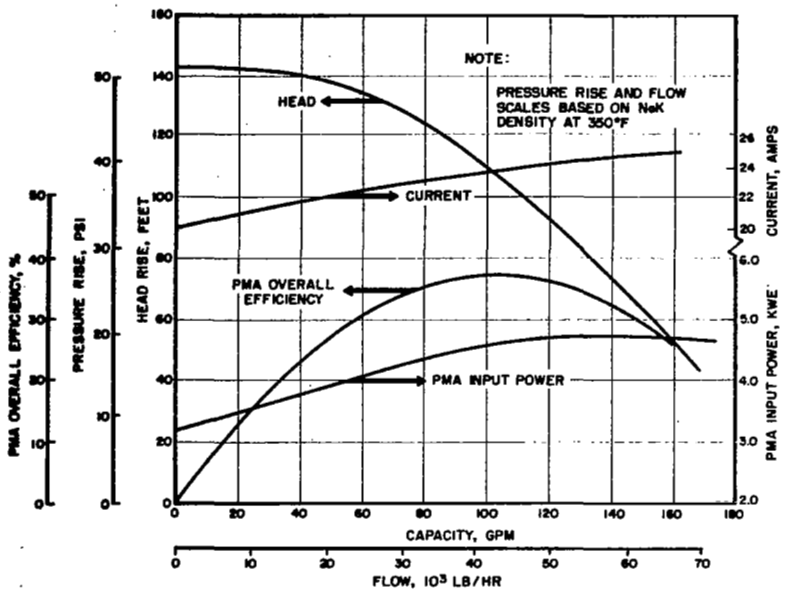

Figure 3-14 - Heat Rejection Loop NaK Pump Performance Characteristics

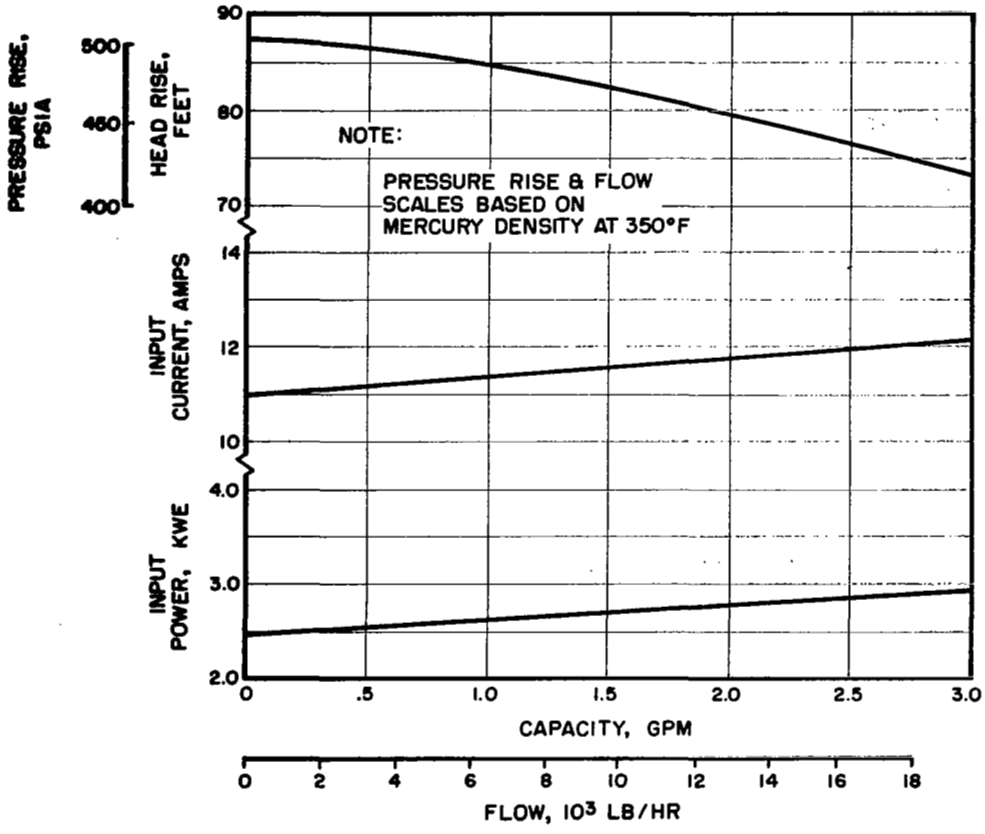

Figure 3-15 - Mercury Pump Performance Characteristics

TABLE 3-II - POWER CONVERSION SYSTEM PERFORMANCE CRITERIA
90-KWE SYSTEM

System	
Power Delivered to Vehicle Load	90 kWe (min.)
Reactor Power Level	600 kWt (max.)
Boiler NaK Inlet Temperature	1200°F (nominal)
Reactor Primary Loop	
Intermediate Heat Exchanger Terminal Temp. Diff.	20°F
RM Pump System Overall Efficiency	8%
Reactor Shield Cooling Heat Loss	20 kWt
Components	
Turbine (New design)	
Efficiency	78%
Exhaust pressure	2.5 psia
Boiler (Redesign)	
Number of mercury tubes	12
Pressure drop	32
Pinch point ΔT	38°F
All other components, use existing designs	

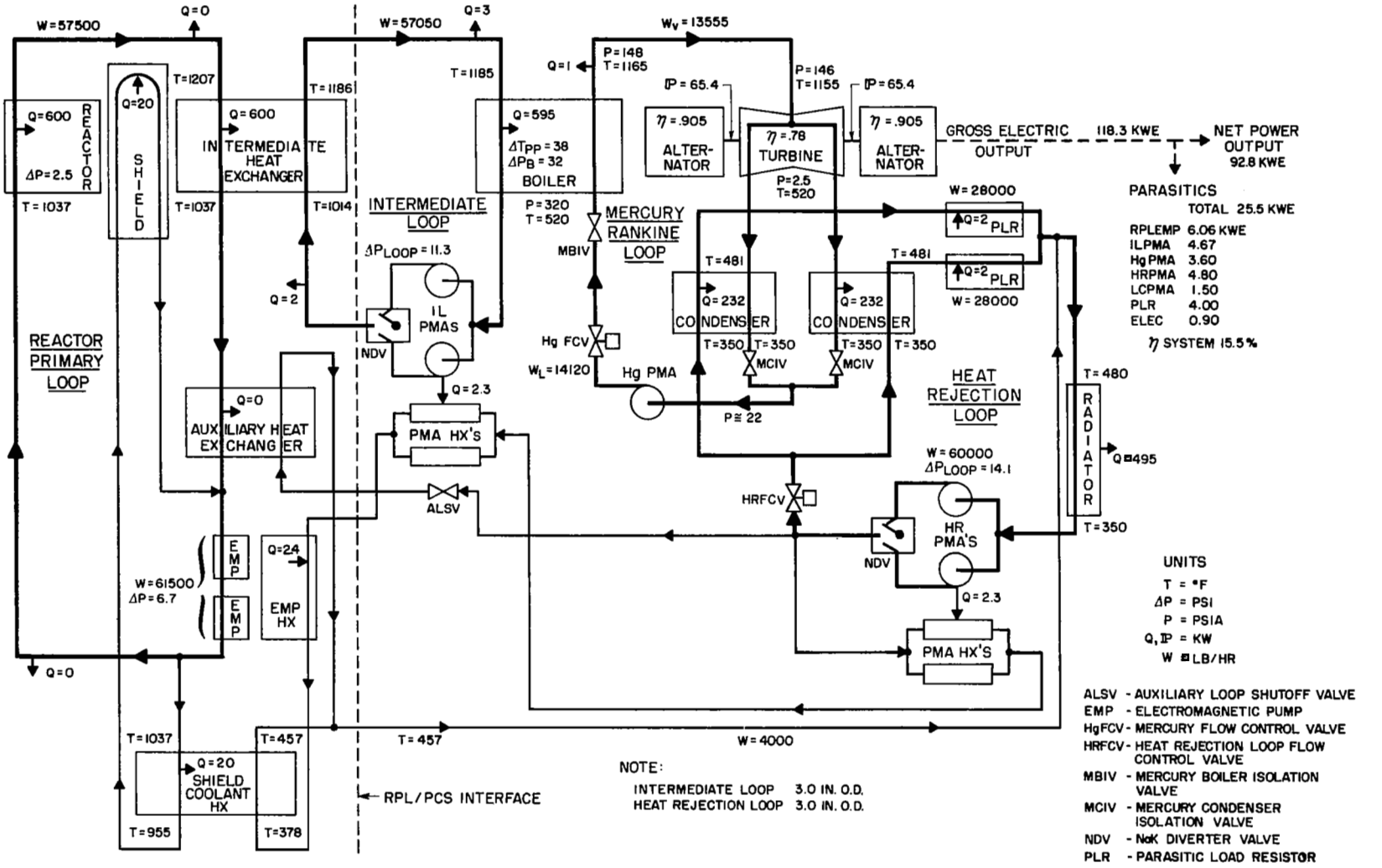

Figure 3-16 State-Point Diagram for 90-kWe Power Conversion System (Design-Point Conditions: Reactor Outlet Temperature at Lower End of Deadband Control)

As a corollary to the design-point conditions, the state-point conditions occurring when the NaK temperature at the reactor outlet corresponds to the upper value of the nuclear system control deadband is also of significance. During normal system operation, the NaK temperature leaving the reactor will slowly drift between the nuclear system deadband control limits. The resulting change in NaK temperature to the boiler will produce changes in mercury flow rate and, therefore, changes in gross electrical output.

Although state-point conditions have not been calculated for the 90-kWe system with the higher reactor outlet and boiler inlet NaK temperatures, they are sufficiently important that the expected result should be described. As the NaK temperature to the boiler increases, the mercury-side pressure drop will increase thereby reducing mercury flow and producing a decrease in gross electrical output. An estimate based on results obtained from previous studies of SNAP-8 system indicates that a reduction on the order of 1-kWe in gross electrical power will occur when the reactor outlet NaK temperature reaches the upper limit of the nuclear system deadband control. This slight change in electrical output will still permit the system to produce the required 90-kWe *minimum* net electrical output.

3.2.2 35-kWe System

The system design state point and steady-state operating conditions are based primarily on overall requirements defined by the NASA Specification 417-1. Additional requirements and limitations have been imposed by the nuclear system contractor and by component performance characteristics defined during the development program. The 35-kWe system - a major step in the overall SNAP-8 development program - is based on a concept which is compatible with both man-rated and instrument-rated missions. The principal features of this concept are (1) shielding of the radioactive portions of the primary loop to allow access to the remainder of the power conversion system, (2) a nonoperating redundant power conversion system (except for the primary loop), and (3) a unit based on current component designs, including the S8DR reactor* design. The significant S8DR reactor limitations for steady-state operations are:

- Maximum power: 600 kWt
- Outlet temperature control band: 1288 to 1330°F

In addition, an envelope of operating conditions was defined, as shown in Figure 3-17, which relates reactor power and reactor coolant temperature rise and, therefore, coolant flow. The reactor may be operated at any condition on or below the limit labelled "line of equal stress" as shown in Figure 3-17.

*S8DR reactor: SNAP-8 development reactor built by Atomics International under contract to the AEC.

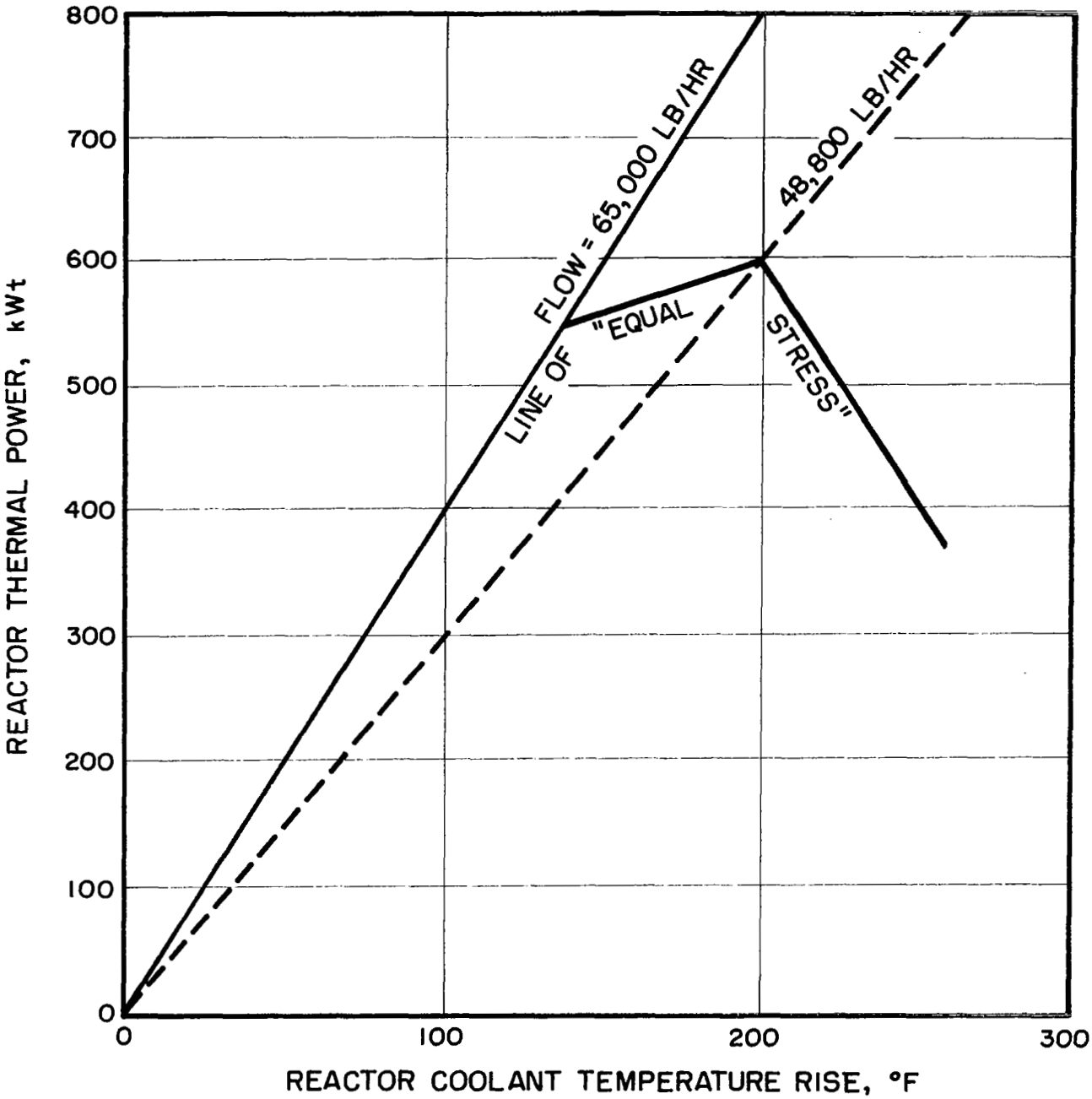

ASSUMPTIONS:

(1) CONSTANT OUTLET TEMPERATURE (BETWEEN 1200°F AND 1330°F)

(2) MAXIMUM EXPECTED HYDROGEN LEAKAGE

Figure 3-17 Envelope of Allowable Reactor Operating Conditions (Power as a Function of Coolant Temperature Rise)

The same major factors described for the 90-kWe system limit the net electrical output of the 35-kWe system. However, the 35-kWe system requirements are sufficiently different so that state-point conditions are determined in a different manner. The major objective was to define a system which would produce a net electrical output of 35 kW for 10,000 hours. Therefore, mercury flow is not limited by available reactor power but is determined by the Rankine-cycle and power conversion system efficiencies. The Rankine-cycle efficiency is determined by the reactor outlet temperature, boiler stability, and condenser pressure. The condenser pressure is determined primarily by the mercury pump suction pressure requirement. The system is required to operate in a zero-g environment with a mercury pump jet pump of existing design for which a suction pressure of approximately 10 psia must be provided. The mercury pump suction pressure requirement, in combination with line pressure losses and condenser pressure drop, resulted in a condenser pressure (turbine back pressure) of 14.0 psia. The power conversion system efficiency is determined primarily from the turbine efficiency and pump power requirements. For the 35 kWe system, the ground rule to utilize existing, developed components implied the use of the impulse turbine with a single alternator and NaK and mercury pumps of existing designs.

Definition of state-point conditions is a continuing process during the development of a system, particularly when component and system test results permit more complete characterization of component performance, interactions of components within a system, or indicate performance characteristics different from early predictions. Therefore, after the basic system and component arrangement were defined, a computer program was developed to permit calculations of state-point conditions for several types of system studies, such as the following:

- Update state point as component performance characteristics are determined by test.
- Determine off-design conditions over a wide range of operating conditions.
- Determine effects on overall system conditions of component performance changes defined by test results.
- Optimize operating conditions for the system and components.
- Examine potential performance limitations and isolate areas where changes can produce maximum improvements.
- Revise state-point conditions and component performance characteristics as system performance requirements are changed.

The basic calculation scheme, required input data, output information, and the initial functional relationships are described in Reference 5. The basic system and component performance relationships used in the development of and initial studies conducted with the computer program are contained in Reference 6. The computer program, identified as SCAN (SNAP-8 Cycle ANalysis), was used to define state-point and off-design conditions for the 35-kWe system.

Component performance characteristics and associated functional relationships used in the SCAN program were modified as component and system test data were obtained and as supplementary studies were completed. Performance characteristic curves for the primary loop NaK pump, the heat rejection loop NaK pump, the mercury pump, the lubricant-coolant loop pump, and the alternator are all contained in Reference 6. The boiler characteristics were simulated primarily by a simplified empirical relationship between pressure drop, mercury flow, and pinch-point temperature difference which was derived from component test data. The significance of pinch-point temperature difference in defining boiler performance is discussed in Section 5-5.

At steady state, the condenser operates close to design conditions in the 35-kWe system. Therefore, the condenser characteristics could be based on established heat-balance and heat-transfer relationships with critical constants determined from test results. The primary condenser performance relationship is as shown on Figure 3-11.

The validity of the condenser relationship was established during component and system tests. The test results were used primarily to determine the overall heat-transfer coefficient under various combinations of temperature, NaK and mercury flows, and available condensing area.

The detailed performance characteristics of the radiator assembly, consisting of the heat rejection loop radiator and the high- and low-temperature lubricant-coolant radiators, are not necessarily required to establish overall system design-point conditions. However, interface conditions must be established which are compatible with the system, with feasible radiator design configurations, and within the established envelope limitations. In addition, more detailed radiator characteristics must be established to define proper system off-design characteristics. Therefore, studies were conducted to establish conceptual designs for the heat rejection loop radiator and the high-temperature lubricant-coolant radiator to facilitate off-design performance studies and to establish an acceptable radiator assembly configuration. Parametric studies were conducted with tube size, fin width, tube length, armor thickness, and general configuration as variables. The general configurations were limited to cylindrical, conical, and combinations of cylindrical and conical which would meet the envelope criteria. Typical results of the studies conducted for the heat rejection loop radiator are shown in Figure 3-18 which contains plots of radiator area, weight, and pressure drop for various combinations of tube size, fin thickness, and number of tubes. Typical tube, fin, and armor dimensions are also shown in Figure 3-18. The general radiator system characteristics selected for the 35 kWe system are shown in Table 3-III.

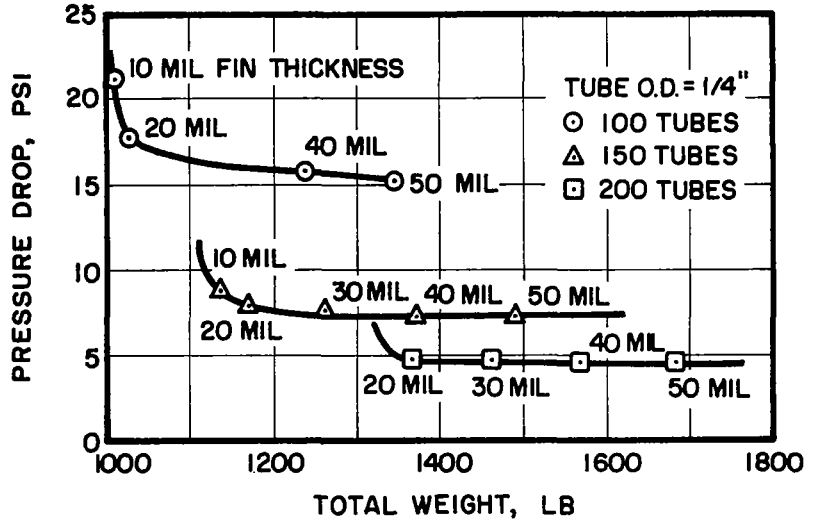

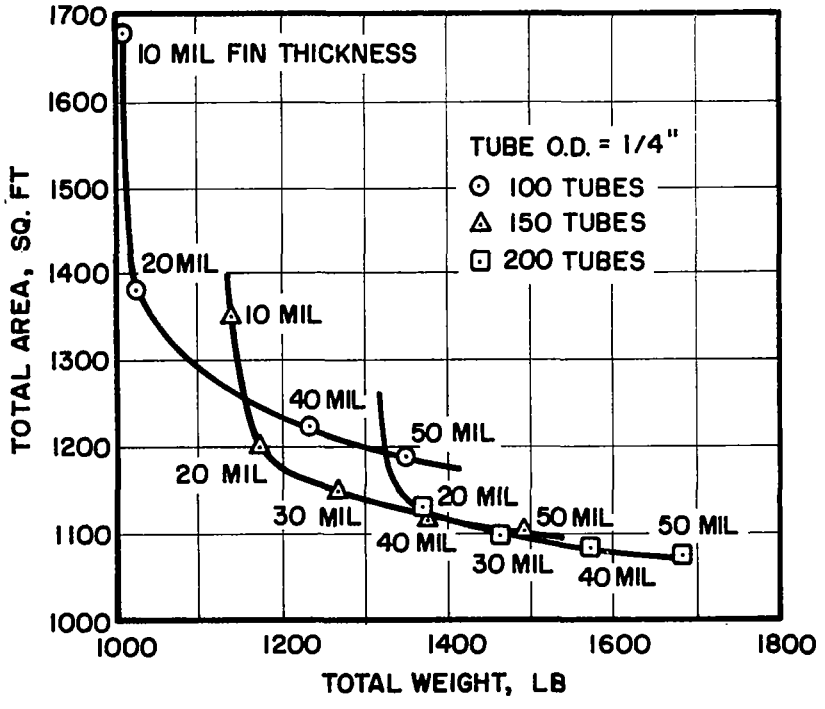

FIN-TUBE CONFIGURATION

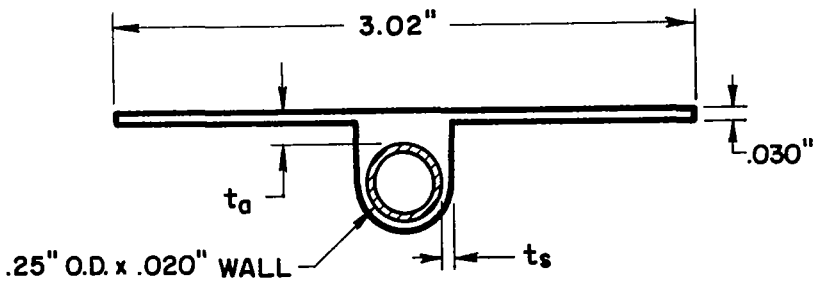

t_a = .160" (VULNERABLE AREA ARMOR THICKNESS)

t_s = .040" (SIDE WALL ARMOR THICKNESS)

Figure 3-18 35-kWe System Heat Rejection Loop Radiator Characteristics and Fin-Tube Configuration

TABLE 3-III - GENERAL RADIATOR CHARACTERISTICS FOR 35-KWE SYSTEM

		HRL Radiator	L/C Radiator (High Temp.)	L/C Radiator (Low Temp.)
Selected Area	(ft^2)	1150	335	144
Selected Weight	(lb)	1265	330	150
Selected Height	(ft)	30.4	10.4	3.8
Radiator ΔP	(psi)	7.5	12	-
Fluid Inventory	(lb)	103	38	~15

OVERALL RADIATOR ASSEMBLY CHARACTERISTICS

Total Area	(ft^2)	1630
Total Weight	(lb)	1745
Total Height	(ft)	44.6
Total Fluid Inventory	(lb)	155

The final-35-kWe state-point conditions, obtained from the SCAN computer program results, are shown in Figure 3-19. The values shown are for the design point; i.e., at the beginning of life, with the reactor outlet NaK temperature at the lower value of the nuclear system control deadband, and operation in a zero-g environment. The net electrical output at this condition is 37 kWe, indicating a 2-kWe margin for degradation effects over the operating life. The arrangement of the radiator assembly configuration relative to the overall system envelope is also shown in Figure 3-19.

The state-point conditions prevailing when the NaK temperature at the reactor outlet corresponds to the upper value of the nuclear system control deadband are considered to be corollaries to the design point. The state-point conditions at the nuclear system upper deadband control temperature are presented in Figure 3-20. Note that the net electrical output at this condition is 37 kWe, the same as for the design-point operating condition.

The fact that the net electrical output is the same at both the upper and lower values of the nuclear system temperature control deadband is a result, primarily, of the boiler and condenser off-design operating characteristics. When the NaK temperature into the boiler increases from the lower deadband control value (1280°F) to the upper deadband control value (1330°F), the boiler pressure drop increases causing a reduction in mercury flow. The reduced flow results in lower condenser temperatures and, therefore, reduced condensing pressure and turbine exit pressure. The overall result is that the total energy available to the turbine is essentially unchanged, thereby causing no change in net electrical output. The component characteristics which permit the system to operate in a manner resulting in no change in electrical output must be considered unique to the particular component designs and operating conditions involved. Normally, changes in operating conditions result in changes in net electrical output; but in the case of the 35-kWe system, the changes were small enough to have no practical effect on overall system performance.

The system operating characteristics were verified by tests of a breadboard system with a nonnuclear heat source and an air-cooled radiator heat rejection system; all other components were of the type planned for use in the flight configuration. The results of these tests generally confirmed the conclusion that essentially no change in net electrical output is obtained for reactor outlet temperature changes between the limits of the nuclear system control deadband.

POWER DISTRIBUTION

Turbine shaft power	63.5 KW
Alternator efficiency	91.5 %
Alternator gross output power	58.0 KW
Parasitic load total	21.0 KW
PNL PMA	4.7
Hg PMA	3.5
HRL PMA	4.6
L/C PMA	1.4
PLR	5.5
Control System	1.3
Net output power	37.0 KW

HEAT RADIATED BY L/C RADIATOR

Turbine	5.25 KW
Alternator	4.20 KW
L/C PMA	1.40 KW
Hg PMA	3.14 KW
HRL PMA	2.25 KW
#1 PNL PMA	2.12 KW
#2 PNL PMA (standby)	0.12 KW
TRA	0.59 KW
	19.08 KW

DESCRIPTIVE FEATURES

Turbine aerodynamic efficiency - 55.7%
Turbine inlet pressure - 248 psia
Turbine exhaust pressure - 13.4 psia
NaK PMAs: 5800 rpm induction motors, both NaK loops
Nak PMAs: Cooled by L/C fluid
Hg PMA with motor scavenger
Tube-in-tube boiler (7 Hg tubes)
Tube-in-shell condenser (73 Hg tubes)
SNAP reactor
Parasitic load resistor (PLR) in HRL
Saturable reactor-magnetic amplifier speed control
Radiator NaK T - 175°F

PERFORMANCE SUMMARY

Net reactor input to PCS	528 KWT
Net electrical output	37 KWE
Overall system efficiency	7.0 %
HRL radiator	
Area	1150 ft^2
Heat rejected	437 KWT
L/C radiator	
Area	335 ft^2
Heat rejected	19.08 KWT
L/C low temp. radiator	
Area	144 ft^2
Total radiator area	1629 ft^2
ECS weight, less shield	10,450 lbs
PCS frame	1600
Components	5340
Radiators & supports	2720
Nuclear system	790

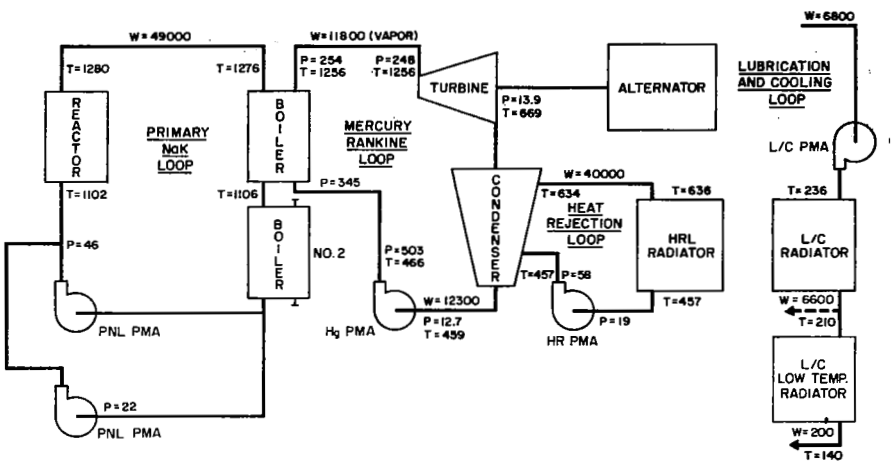

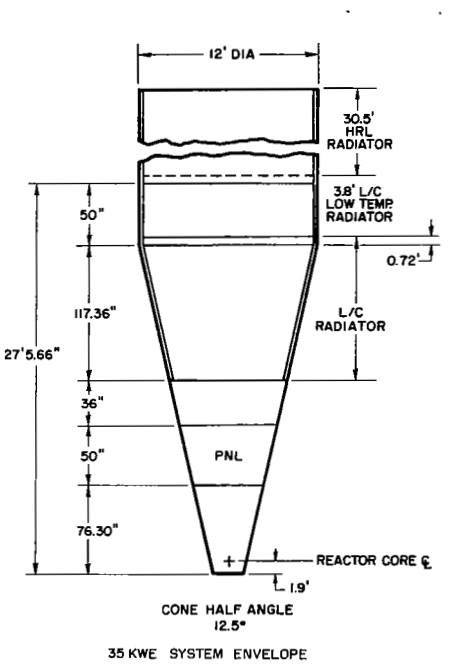

Figure 3-19 State-Point Diagram for 35-kWe Power Conversion System (Design-Point Conditions: Reactor Outlet Temperature at Lower End of Deadband Control, and Zero-g Environment)

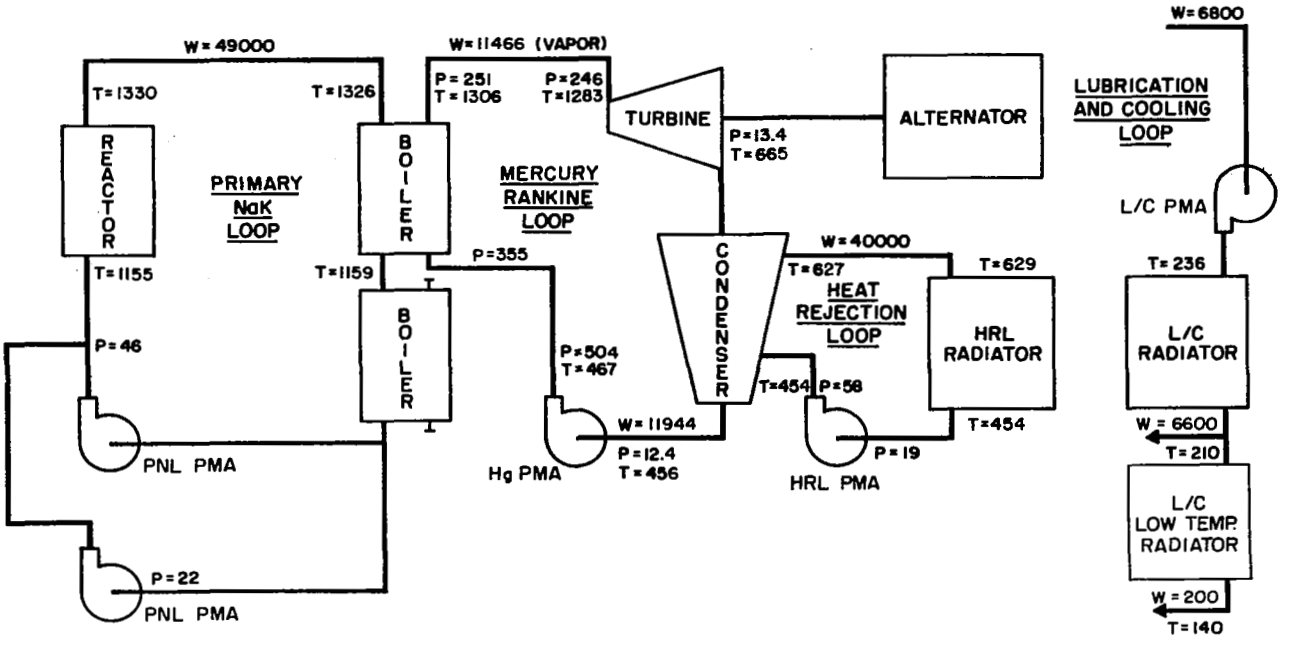

POWER DISTRIBUTION

Turbine shaft power	63.9 KW
Alternator efficiency	90.9 %
Alternator gross output power	58.0 KW
Parasitic load total	21.0 KW
PNL PMA	4.7
Hg PMA	3.5
HRL PMA	4.6
L/C PMA	1.4
PLR	5.5
Control System	1.3
Net output power	37.0 KW

HEAT RADIATED BY L/C RADIATOR

Turbine	5.25 KW
Alternator	4.20 KW
L/C PMA	1.40 KW
Hg PMA	3.14 KW
HRL PMA	2.25 KW
#1 PNL PMA	2.12 KW
#2 PNL PMA (standby)	0.12 KW
TRA	0.59 KW
	19.08 KW

DESCRIPTIVE FEATURES

Turbine aerodynamic efficiency - 55.6%
Turbine inlet pressure - 248 psia
Turbine exhaust pressure - 13.9 psia
NaK PMAs: 5800 rpm induction motors, both NaK loops
NaK PMAs: Cooled by L/C fluid
Hg PMA with motor scavenger
Tube-in-tube boiler (7 Hg tubes)
Tube-in-shell condenser (73 Hg tubes)
S8DS reactor
Parasitic load resistor (PLR) in HRL
Saturable reator-magnetic amplifier speed control
Radiator NaK ΔT - 179°F

PERFORMANCE SUMMARY

Net reactor input to PCS	537 KWT
Net electrical output	37 KWE
Overall system efficiency	6.9 %

Figure 3-20 State-Point Diagram for 35-kWe Power Conversion System (Off-Design Condition: Reactor Outlet Temperature at Upper End of Deadband Control, and Zero-g Environment)

3.3 SYSTEM DESIGN

3.3.1 General Criteria

Design criteria were established which applied to the man-rated 35- and 90-kWe configuration concepts. The results of analyses which formed the basis for some of these criteria and design studies for which the criteria were used in defining an interim system are presented in Reference 7. These criteria are examined in detail below.

3.3.1.1 System Redundancy

To increase the reliability of a man-rated system and to increase its flexibility, system and component redundancy were employed where necessary. Tradeoff studies indicated the proper mode of redundancy where it was not readily apparent. Redundancy was considered for the following electrical generating system elements:

- Power conversion systems
- NaK pumps
- Boilers
- Radiators
- Electrical systems
- Instrumentation
- Reservoirs and Valves

a. Power Conversion Systems.- The basic redundancy approach was to have two independent mercury Rankine-cycle power conversion systems with independent heat rejection, lubricant-coolant, and electrical subsystems. Two power conversion systems were selected to provide an electrical generating system of minimum weight and space which would provide continuous power (except during system switchover) and which could take advantage of crew availability to replace malfunctioning components.

The impact of a man-rated system appears here since redundancy with component replacement would not be plausible with an instrument-rated system. Further, the selection of dual power conversion systems with one on standby sets the framework within which the balance of the redundancy concepts are established.

b. NaK Pumps.- Personnel access to the NaK loop containing the reactor is not possible while the system is operating because of high temperature, high gamma radiation levels in the NaK, and the radiation levels between the instrument and biological shields, or in the volume enclosed by a 4-pi shield. Since component replacement is not possible in this section, dual pumps were decided upon for the reactor coolant loop.

The intermediate loop had two boilers in series (and, hence, a single intermediate loop) to provide redundancy as described above. Since there would be no way to replace a malfunctioning NaK pump in the intermediate loop and simultaneously maintain system operation, two NaK pumps were provided.

c. Boilers.- It was decided that a boiler would be provided for each power conversion system (the operating system and the redundant system). The alternative would be to have one boiler with switching capability on the mercury side to each of the two mercury Rankine-cycle loops. This design was not selected because it was felt that the unreliability of the required 1300°F mercury vapor valve would compromise the system operation. Further, even if a leakproof valve were developed, any failure of the boiler that allowed the mercury inventory to mix with NaK would result in loss of both power conversion systems since the mercury inventory would be shared by the two systems. The boiler double-containment concept discussed below (3.3.1.1, i) would prevent mixing of the flowing NaK and mercury. However, leakage between the static NaK chamber and mercury would still result in contamination of both power conversion systems. For these reasons, the decision was made to use two boilers with each boiler servicing a separate power conversion system. The boilers were coupled on the NaK side (primary NaK loop of the 35-kWe system and intermediate loop side of the 90-kWe system).

The boilers were connected in series (relative to NaK flow) because parallel connection would have required valves which would have decreased the overall system reliability. With the boilers in series, the pressure drop in the NaK loop increases, but no valving is required. It was decided that the pressure drop penalty (about 3 psid) was preferable to the addition of four NaK valves to the system.

d. Radiators.- A reliability analysis (reported in Section II-A of Reference 7) was performed to determine which would be preferable: a single heat rejection loop with a single tube radiator, or two completely independent heat rejection loops servicing each of the two mercury Rankine-cycle systems with a dual tube radiator (shared fin design). This study indicated that, for high component reliability (over .98) and high system reliability (over .97), the dual-tube radiator is preferable.

e. Electrical System.- A reference approach was selected for the dual power conversion system electrical equipment and programmers. The options considered were as follows:

- A single set of electrical equipment in combination with one and two programmers (with and without interchangeability for the two power conversion systems)
- Two sets of electrical equipment in combination with one and two programmers (with and without interchangeability for the power conversion systems)

- Two sets of electrical equipment (with and without interchangeability for the power conversion systems) in combination with one and two programmers (with and without interchangeability for the power conversion systems).

The selected configuration was one programmer and one set of electrical equipment for each power conversion system with interchangeability between electrical systems and the power conversion systems. This choice from the options considered was based on the excessive amount of switch gear (control transfer contacts, valve transfer contacts, emergency shutdown transfer contacts, control diodes and valve diodes) required for the other cases.

f. Instrumentation.- A two-fold redundancy was used in the instrumentation system. First, in the emergency shutdown system, a "two-out-of-three" voting logic circuit approach was used. This meant that at least two out of three measurements must confirm that a design point has been exceeded before the shutdown could be initiated. Second, redundant instrumentation was provided where the loss of one instrument would not permit steady-state performance analysis during a combined system test.

g. Reservoirs.- In certain situations, duplicating components does not provide effective redundancy, and in these cases other measures were taken. All loop expansion reservoirs, for example, were of a bellows sealed design with a passive pressurization system consisting of a captured gas volume. Since failure of the expansion reservoir bellows would lead to loss of system inventory and pump cavitation, all reservoirs were provided with redundant bellows; i.e., no single bellows failure would prevent the reservoir from performing its function in the system.

h. Double Acting Solenoid Valves.- To avoid continuous operation of the system isolation solenoid valves (located in lubricant-coolant system, heat rejection loop, auxiliary loop, and mercury injection system), all solenoid valves were bistable and mechanically latched in one of the two normal operating positions until actuated.

i. Double Containment.- Because a reactor coolant leak could have serious consequences to personnel located above the biological shield, a concept of redundancy was selected for components which presented a potential for cross-leakage between the reactor coolant loop and other loops; for example, the boiler in the 35-kWe configuration, the auxiliary loop heat exchanger, and intermediate heat exchanger. The design ground rule established required double containment of these components. As used here, double containment is defined as component construction such that no single structural failure can result in intermixing of flowing fluids through the component. In general, this was implemented by providing a static NaK zone between the active fluid passages in the heat exchangers.

3.3.1.2 System Maintainability

The power conversion system was designed so that all components are replaceable without requiring the either removal of other components or disconnecting of piping and electrical harness not directly mating with the component to be replaced. Access for maintenance depended on the electrical

generating system configuration. For the case of the 35-kWe system with a conical envelope, access was through a four-foot access core along the system centerline. In the case of the rectangular 90-kWe system, access was from front, back, and top of the unit. Allowance was made at the component/piping interface for three component removals and rewelds. In addition, adequate space was provided for semi-automatic welding and brazing equipment. Although flanged joints would enhance maintainability, mechanical joints are unacceptable from the standpoint of reliability. Therefore, connections in liquid metal loops are of an all-welded design. System structural members which would have to be moved to permit access for component replacement were bolted in place. Structural mounts were designed so that identical components could be replaced without changing or replacing the mount.

In general, however, the power conversion system was designed to require no routine maintenance, repair, or service; the concept of maintenance, as applied to the electrical generating system, was limited to one of component replacement.

3.3.1.3 Piping Design Approach

At the high temperatures associated with the SNAP-8 system, provision must be made for the thermal expansion of the piping between components. There are several ways to do this. By taking advantage of the piping configuration between components, it is possible to reduce the pipe stress and component end loading to acceptable levels. By arranging the components so that the interface points of contiguous components are located as closely as possible in as many coordinate axes as possible, the flexibility requirements are reduced. The disadvantages of using the connecting piping itself to absorb thermal growth is that, compared to other component mating methods, the length of piping required results in greater pressure losses (hence, increased pump power), increased pipe insulation and fluid inventory weight, additional pipe supports, and increased expansion reservoir capacity. On the other hand, the reliability of the system is high since the quality control for piping can be extremely good and component supports are simplified since components can be treated as anchor points for the piping.

Another way to allow for thermal expansion is to insert expansion joints in the piping between components. Several methods could apply. First, a single bellows can be used to absorb the thermal movement of the section of pipe between components. An unrestrained bellows, however, will impose a pressure thrust on the piping and hence the component interface due to the unbalanced pressure between the bellows convolutions and external environment. If the piping between the components is not in a straight line, bending moments will be imposed on the bellows which are undesirable. Second, a pressure-compensating bellows can be used to eliminate the pressure thrust generated by an unrestrained bellows. These are usually large and complex making quality control even more difficult. In addition, they are not drainable and would trap quantities of liquid metal creating a possible corrosion problem as well as test loop handling problem. Third, a gimbal bellows design can be employed.

In this case, several bellows are used in the line segment between components. The bellows are internally or externally restrained by means of tie-rods so that no pressure thrust is transmitted to the lines. The thermal movement of the line is accommodated by flexing of the bellows. This method, however, would require two or three bellows between every two components in the system. The decision was made not to use bellows in the SNAP-8 piping system because of the difficulty in procuring uniformly fabricated bellows with predictable characteristics.

One other way to control thermal expansion would be to support the components in a manner that would allow them to move to meet line growth demands. This approach was taken in the W-1 test facility at the Lewis Research Center. For the SNAP-8 engine, however, it was decided that this would result in relatively complex supports (e.g., slides and rollers) which were not adaptable to flight systems.

As a result, the piping system was designed to take advantage of piping flexibility to provide a system which would be highly reliable and adaptable to the demands of an evolving system arrangement.

3.3.1.4 Environmental Requirements

The overall requirements for the SNAP-8 electrical generating systems are specified in NASA Specification No. 417-1. The environmental requirements for the SNAP-8 system are given in NASA Specification No. 417-2, Revision C. Both specifications pertain to the SNAP-8 system as a whole and to the various subsystems and individual components. Because neither the system envelope nor the mission/system interface and system/booster interface requirements have been defined, it is premature to apply either environmental design criteria or environmental test requirements to the power conversion system. The design approach taken was to maintain the flight environmental requirements for the components individually, but to limit the system environmental requirements to those encountered in ground testing and handling.

The environmental design criteria for the SNAP-8 power conversion system components are delineated in NASA Specifications 417-1 and 417-2, Revision C. Specific exposure data are presented for the terrestrial, space, and lunar natural environments as well as the induced environments expected during transportation, launch, lunar landing, and system operation. Induced and natural environments exist simultaneously in real time, and the design criteria include the combined loading effects.

The natural terrestrial environments are based on conditions experienced in coastal areas of the United States; in particular, the Atlantic Missile Range. These conditions apply to the components during handling, installation, or flight readiness for a period of up to six weeks. The specific requirements include the extremes and typical values of conditions for humidity, sand, dust, fungus, salt fog, temperature, wind, rain, explosive atmosphere, and magnetic field.

The conditions of natural space and lunar surface environments apply to the components prior to and during startup, operation, and shut-down in space for a minimum of five years. Design values are presented for the component exposures to external pressure, magnetic field, and a variety of radiation sources. Included in the radiation sources are values for earth radiation, cosmic and solar high-energy particles, and constants for black-body radiation of solar and galactic origin.

The induced environments of terrestrial origin are based on conditions experienced in packaging, handling, transportation, and storage. Specific handling and storage requirements for components are defined in individual component specifications. The system handling and storage requirements are given in NASA Specification No. 417-2, Revision C.

The launch and/or lunar landing phases of induced environments are applicable to the components installed in the launch vehicle. The components are filled with service fluids but not operating. The specific design requirements include the range and typical values of vibration, shock (15-g peak), acoustic noise and linear acceleration ($\pm$ 5-g longitudinal and $\pm$ 1.25-g perpendicular).

The induced environments of space and/or lunar surface origin apply to the components under both operating and nonoperating conditions. The design requirements include vibration frequencies and levels, maneuvering accelerations, and reactor-induced radiation. The maximum total integrated radiation, including direct, scattered, and secondary radiation from all nuclear sources, will be one of the following limits depending on the location of the specific component in the structure: Level 1 defines the design criteria for solid-state control electronics, Level 2 for mechanical and electromechanical components, and Level 3 for components located within the gallery between a dual shadow-shield and/or a 4-pi shield,

- Fast neutrons (0.1 MeV or greater) total integrated dose in five years:

  Level 1 = 1×10^{11} nvt

  Level 2 = 5×10^{12} nvt

  Level 3 = 1×10^{17} nvt

- Gamma rays, total integrated dose in five years:

  Level 1 = 1×10^{6} rads (c)

  Level 2 = 5×10^{7} rads (c)

  Level 3 = 1×10^{9} rads (c)

A major contribution to the system gamma dose rate results from activation of the reactor coolant. The sodium constituent of NaK becomes the primary gamma source, although potassium contributes to the NaK dose rate also. The NaK gamma dose level is comparable to the reactor gamma dose rate after attenuation by the instrument shield.

3.3.1.5 Materials Engineering

At the start of the SNAP-8 program, it was acknowledged that mercury loop construction materials would be subject to corrosion and mass-transfer attack by mercury at system operating conditions. Consequently, testing was directed toward the selection of suitable mercury containment materials. Solubility tests were made using specimens of various candidate construction materials. In 1962 capsules of selected materials were tested under thermal gradient conditions between 1025 and 1250°F for periods of 500 to 10,000 hours. Results of this program were reported in References 1, 8, and 9. A mercury corrosion loop was established which further evaluated the effects of mercury corrosion under simulated system operating conditions at 1/19th scale. These tests are described in Reference 10. In 1969, after 8700 hours of operation, the 35-kWe power conversion system was temporarily shut down and a thorough evaluation of mass transfer throughout the mercury loop was made. The results of this survey were reported in Reference 11.

The general result of these programs was that mercury corrosion and associated mass-transfer problems were solved by using the following materials to construct mercury loop elements: refractory metal (tantalum) for mercury containment in the boiler, 9 Chrome-1 Molybdenum steel alloys in the lower-temperature components (mercury pump and condenser tubes), S-816 cobalt alloy in the hot turbine parts, and Type 316 stainless steel for component interconnecting piping. The use of Type 316 stainless steel for piping was a basic criterion for the mercury loop design.

The extent of corrosive attack in sodium-potassium containment materials depends on the oxide level in the flowing NaK. Tests verified that stainless steel materials (316 series, 321 series, 347 series, 304 low carbon, 410 series) were completely satisfactory in NaK service, and life expectancies of five years can be postulated subject to one major condition: oxide levels must be maintained at low levels (20 to 25 ppm). SNAP-8 system goals were set at a 5-ppm level.

3.3.2 90-kWe System

3.3.2.1 Design Criteria

The overall power conversion system envelope was defined as a rectangular parallelepiped. The final outside dimensions of the envelope were 5 x 12 x 10 ft (height). This envelope was selected with the following objectives:

- To provide the maximum possible access for component maintenance
- To fit inside potential space shuttle vehicle envelopes.

The power conversion system was to be designed and fabricated at Aerojet and delivered to the NASA Space Power Facility at Plum Brook, Ohio. Here, the power conversion system would be mated with the reactor primary loop (including reactor and 4-pi shield), the heat rejection loop heat sink, and the lubricant-coolant loop heat sink for a combined system test. Initially, a nonnuclear heat source was to have been substituted for the reactor to permit system checkout.

The power conversion system was designed to the ground rule that the maximum environmental temperature would correspond to the lubricant-coolant radiator operating temperature. This eliminated the need for special provisions to protect system elements such as valve motors, instrumentation, and NaK pumps from the elevated temperatures which would result if the heat rejection loop radiator were to surround the power conversion system. To avoid placing undue restrictions on the test configuration, however, the power conversion system structure was to have been fabricated from stainless steel instead of a lower-service-temperature material (aluminum, for example) since auxiliary cooling could be provided for other elements if a heat rejection loop radiator were ultimately located around the power conversion system; but the frame could not readily be protected, and fabrication of a second frame would be unnecessarily costly and could delay the testing schedule.

The system design was based on nominal operating conditions associated with a 1200°F reactor outlet temperature; however, the ability to operate at the former system state point for a 1300°F reactor temperature was retained. This was reflected in the component requirements specification also.

The system was designed for an operating life of five years. Wherever practicable, existing component designs were used. Maintenance access was considered permissible from all planes except the bottom plane.

A mating flange was provided at the base of the power conversion system structure to permit the unit to be bolted to the reactor primary loop structure. All piping interfaces were designed as anchor points so that the power conversion system piping was independent of other electrical generating system and facility piping. The power conversion system was designed for a one-g vertical operating load, and two-g vertical and one-g lateral nonoperating loads.

The power conversion system test article would have been nonredundant with respect to total subsystems; however, component redundancies would have been incorporated.

3.3.2.2 Component Arrangement

The components listed in Table 3-IV are shown arranged for the combined system test unit in Figure 3-21. Component arrangement reflects the ground rule of using existing components where possible and emphasizes maintenance and component accessibility.

TABLE 3-IV SNAP-8 90 kWe POWER CONVERSION SYSTEM PARTS LIST

Item	Quantity
*Structure	1
*Boiler	1
Turbine Alternator Assembly	1
Condenser	2
Parasitic Load Resistor	2
Pump Motor Assembly, Heat Rejection Loop	2
Pump Motor Assembly, Intermediate Loop	2
Pump Motor Assembly, Mercury Loop	1
Pump Motor Assembly, L/C Loop	1
*Reservoir, Expansion, Heat Rejection Loop	1
*Reservoir, Expansion, Intermediate Loop	1
*Reservoir, Expansion, Boiler Static NaK	1
*Reservoir, Expansion, L/C Loop	1
Reservoir, Mercury Injection	1
*Valve, NaK Diverter, Heat Rejection Loop	1
*Valve, NaK Diverter, Intermediate Loop	1
Valve, Flow Control, Heat Rejection Loop	1
Valve, Flow Control, Mercury Flow	1
Valve, Shutoff, Mercury Loop	4
Valve, Shutoff, Heat Rejection Loop	1
Valve, Shutoff, L/C Loop	6
Heat Exchanger and Cold Trap, Heat Rejection Loop Pump Motor Assembly	2
Heat Exchanger and Cold Trap, Intermediate Loop Pump Motor Assembly	2
*Electrical Assembly No. 1	1
Transformer Current - VR-E Compensator	2
Transformer, Saturating Current-Potential	2
Breaker, Vehicle Load	2
Saturable Reactor	2
Valve Four-Way, L/C Loop	1

Item	Quantity
*Electrical Assembly No. 3A	1
Voltage Regulator	2
Speed Control Module	2
Transformer, Speed Control	2
Compensator, Speed Control	2
Compensator, Voltage Regulator	2
*Electrical Assembly No. 2	1
*Inverter, EM Pump	4
*Inverter, NaK Pump-Motor Assemblies	1
Contactor - Inverter DC	5
*Electrical Assembly No. 4B	1
Transformer Rectifier Assembly	1
*Contactor - Motor Transfer	6
Electrical Protective System Module	1
Power Factor Correction Assembly	2
Electrical Harness	1
*Electrical Controls Assembly, Nuclear System	1
Flowmeter, EM, Intermediate Loop	2
Flowmeter, Mercury Loop	1
Flowmeter, EM, Heat Rejection Loop	3
Flowmeters, Lube/Coolant Loop	5
Line Heaters, L/C	1 set

* Government Furnished Equipment

** Does not include reactor primary loop components, shielding, or radiator assembly

The turbine-alternator and condensers are close-coupled to minimize the pressure loss between the turbine exhaust and condensers since the system net electrical output decreases by about one kWe for every one psia of pressure increase in turbine back pressure. The turbine-alternator is oriented horizontally because it was designed to operate in this position relative to the local gravity vector. Similarly, the condenser operates with its longitudinal axis within five degrees of the environmental gravity vector.

The reservoirs are oriented so that the fluid inventory does not place side loads on the bellows; i.e., the certerline of the bellows is parallel to the local gravity vector.

The lubricant-coolant loop components are located near the components that are serviced by the lubricant-coolant circuit (mercury pump, turbine-alternator, mercury injection system, and electrical system). This results in minimum lubricant-coolant piping. The NaK pumps are cooled by heat rejection loop NaK.

The mercury pump is located below the condensers to maintain the required NPSH during system operation. The mercury pump is also located so that the suction pressure does not exceed $\sim$ 40 psia, the pump visco seal limit. The mercury injection reservoir is located adjacent to the mercury pump to help eliminate NPSH problems during startup and to facilitate mercury-loop dumping during a system shutdown.

The condenser mercury discharge valves are located close to the condensers so that the lines between the condensers and mercury pump are filled from the reservoir and do not have to be filled by condensing mercury on startup.

The boiler mercury outlet is located as close to the turbine inlet as possible to minimize stresses in the mercury vapor line due to thermal expansion, and to reduce the amount of heat required to bring the vapor line up to operating temperature during startup.

The NaK pumps are operated horizontally since they were tested in this position for more than 56,000 hours. However they were designed to operate in any attitude.

The two parasitic load resistors are located adjacent to the condensers since the heat rejection loop has parallel flow paths through each condenser/parasitic-load-resistor pair.

The electrical components are located as far from the nuclear radiation source as possible, and can be readily isolated thermally from the higher-temperature loop components and piping. The electrical configuration reflects the following ground rules:

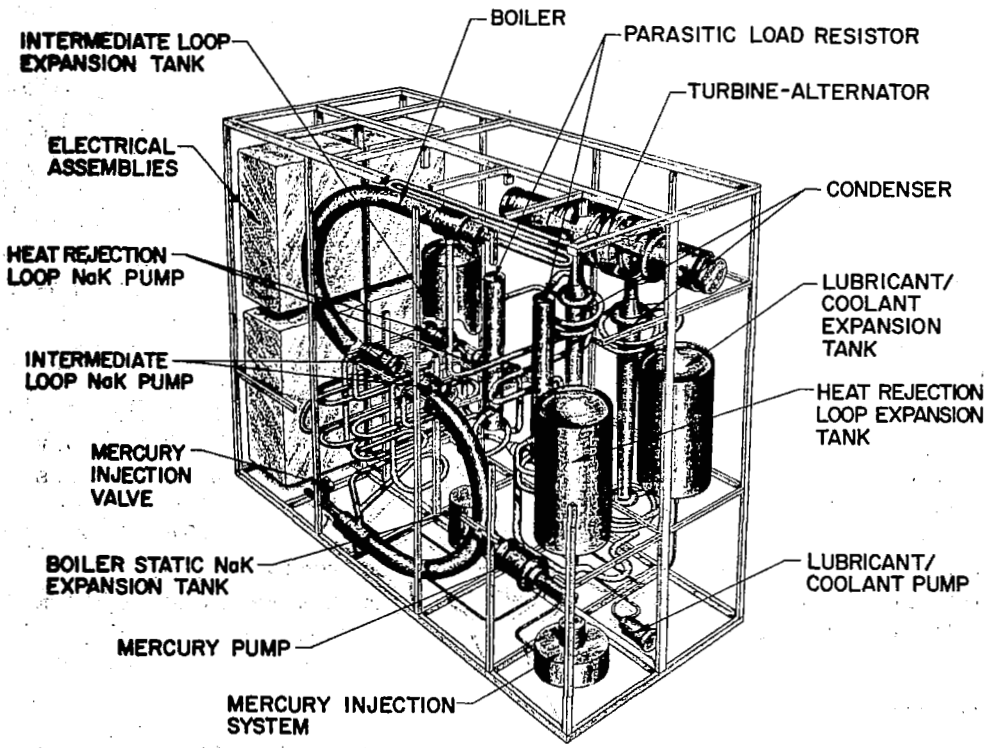

Figure 3-21 90-kWe Power Conversion System Arrangement for the Combined System Test

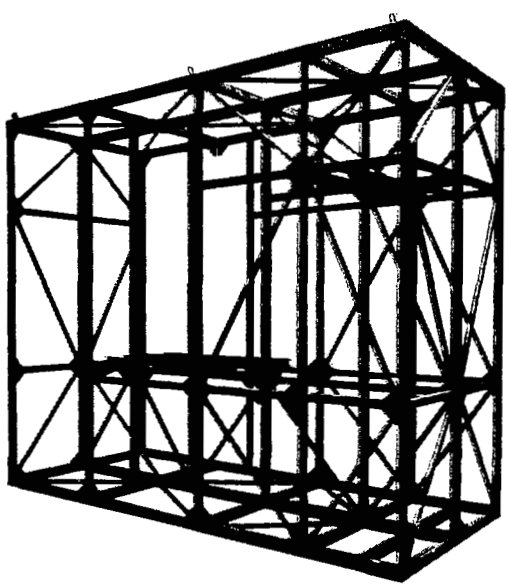

Figure 3-22 Power Conversion System Frame Assembly

- Start programmer elements are not part of the electrical assemblies, but will be located in the control room during the combined system test.

- Electromagnetic interference filters will not be included in the electrical assemblies for the power conversion system, but there is some space available for incorporation if desired.

- Space for static inverters (needed for rotating and electromagnetic pumps) has been provided in the assemblies.

- The electrical assemblies consist of a cold plate with a vented protective cover fastened to the base plate. To aid in system assembly and subsequent diagnostics, the protective covers are removable, whereas the individual terminal strips remain attached to the base plate.

The planar S-shaped boiler was selected from several candidate configurations because it provided the most compact power conversion system with good access for component maintainability.

3.3.2.3 Structural Design

The power conversion system frame, shown in Figure 3-22, is based on a truss concept. The center plane and supporting end faces form the basic structure. These members are welded since they do not have to be removed for component maintenance or initial installation. The top plane of the central "I" section is supported by columns in the front and rear face of the structure. For analysis, it was assumed that the structure would be supported at the exterior columns for ground tests leaving the central area unsupported. The structure was also designed so that the complete power conversion system could be lifted from the top plane (exclusive of the reactor primary loop).

Square and rectangular turbine members were used rather than round members to simplify joint design and component mounting. Furthermore, a square member is lighter than a round member of given stiffness and envelope dimension. Structural member sizes were based on the results of a comprehensive computer-solution stress analysis. Analyses were completed for vertical and lateral frame loading. Diagonal members were inserted in the top, bottom, end, center and outside faces to limit frame deflection under lateral loading and to stiffen the frame against vertical deflection due to the method of support (because the external supports are located at the outer periphery, the center plane tends to deflect downward relative to the outer structure). No members cross between the center and outer faces except for the two beams at the turbine-alternator support. This provides maximum space for piping, components, and the associated supports. Columns and diagonals in the outer faces are removable where required to facilitate system assembly and component replacement.

Stainless steel was selected as the structural material. Aluminum, carbon steel, and stainless steel were considered (see Figure 3-23). Aluminum was eliminated for the following reasons.

- Use of aluminum would preclude installation of the heat rejection loop radiator around the power conversion system during system test. At 600°F, aluminum has poor strength characteristics.
- The overall cost of fabricating an aluminum structure would exceed the cost of a steel structure despite the lower material costs (this is because a large aluminum structure would require use of special fixtures and heat treatment to eliminate distortions during fabrication).
- For similar deflection allowances, an aluminum frame would weigh about 100 pounds less than a steel frame.
- In the event of a mercury leak, the aluminum structural strength could be drastically reduced.

Stainless steel was selected over carbon steel for the following reasons:

- The material cost advantage of carbon steel is diminished by the costs associated with providing surface protection against environmental corrosion.
- Virtually no difference in weight.
- The long-term yield strength of carbon steel decreases rapidly above 400°F.
- Thermally-insulated mounting brackets for the boiler and other high-temperature components and piping are not required when stainless steel is used.

The power conversion system component weights are itemized in Table 3-V (the weights of the radiators have not been included).

Figure 3-23 Yield Strength vs Temperature for Power System Candidate Structural Materials

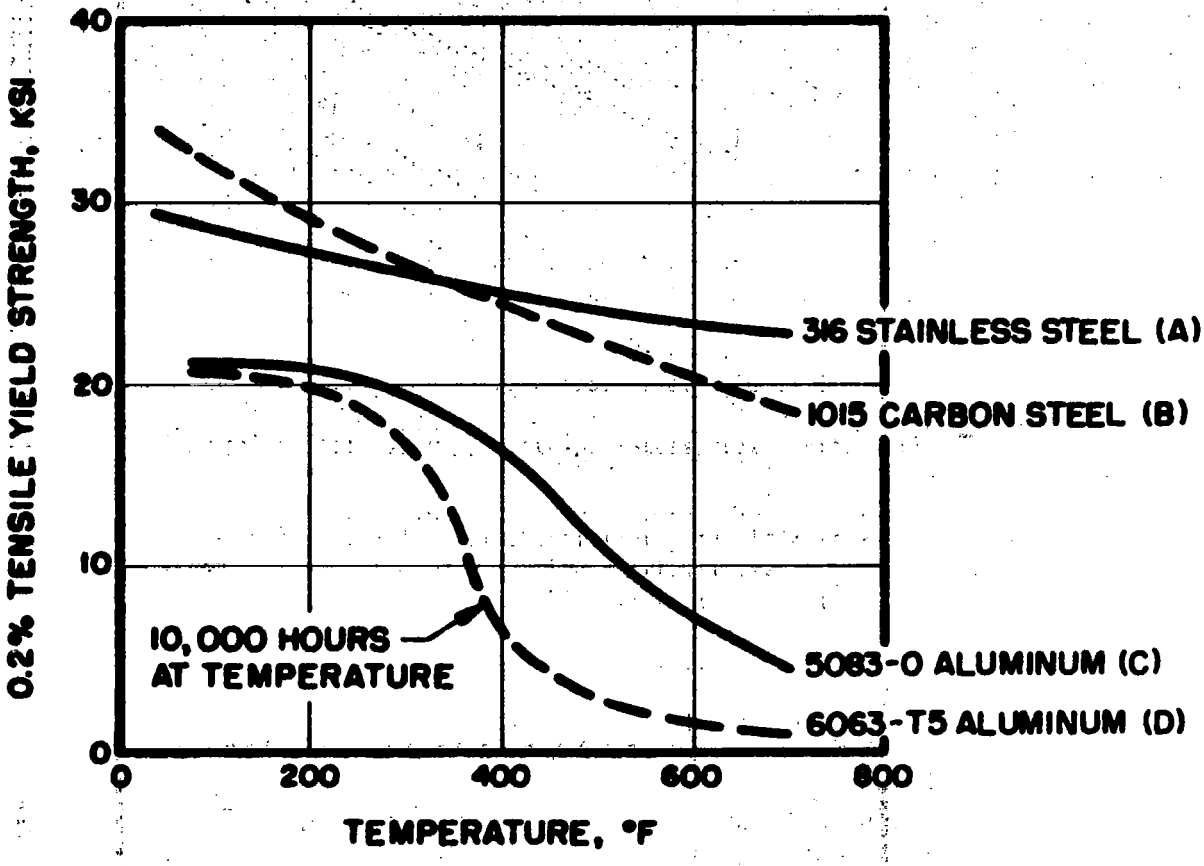

REFERENCES:

(A) ASTM STP 124
(B) ASTM STP 180
(C) AL STD AND DATA AL ASSOCIATION, 1969
(D) KAISER AL DATA

TABLE 3-V COMPONENT WEIGHTS FOR 90-KWE POWER CONVERSION SYSTEM *

Component	Weight (lb)
NaK Pump, Intermediate Loop (2)	324
NaK Diverter Valve, Intermediate Loop	12
Boiler, dry	833
Reservoir, Intermediate Loop	142
NaK Pump Heat Exchanger, Intermediate Loop (4)	80
Boiler Reservoir	40
Mercury Pump	200
Mercury Flow Control Valve	8
Turbine-Alternator, 12 Stage (2 Alternators)	1,572
Condenser, dry (2)	187
Double-Acting Solenoid Valve (4)	27
Mercury Injection System Reservoir	200
NaK Pump, Heat Rejection Loop (2)	324
NaK Pump Heat Exchanger, Heat Rejection Loop (2)	40
NaK Diverter Valve, Heat Rejection Loop	12
NaK Flow Control Valve, Heat Rejection Loop	25
Parasitic Load Resistor, dry (2)	160
Heat Rejection Loop Reservoir	142
Lubricant-Coolant Pump	26
Lubricant-Coolant Reservoir	142
Harness	463
Electrical Assemblies	1,860
Additional Electrical Components	536
Frame	1,484
Piping	828
Insulation	300
Fluid Inventories	
Mercury	470
NaK - Intermediate Loop	485
NaK - Heat Rejection Loop	390
Polyphenylether - Lubricant-Coolant Loop	200
	11,512 **

* Numbers in parentheses indicate number of units. Weight given is for total units.

** Does not include reactor primary loop components, shielding or radiator assembly.

3.3.2.4 Component Support Designs

a. Boiler.- The boiler mounting concept is presented in Figure 3-24. A study was made to identify a mounting method which would minimize stresses in the boiler caused by the boiler weight and the restraint of thermal movement of the boiler at operating temperatures. A detailed stress analysis was performed for the various concepts studied. The results of this study led to the arrangement shown, with the boiler anchored at the mercury-vapor outlet end and pinned at the NaK outlet end with several intermediate supports to distribute the gravity load. The mercury-vapor outlet end was anchored to prevent transmission of loads from the boiler to the turbine inlet housing. Because of the stiffness of the boiler shell, the loads transmitted to the end points, with the resulting stresses, were excessive. To limit these stresses, the approach finally selected was to "spring" the cold boiler so that it operated in a virtually stressless condition at temperature.

b. Turbine-Alternator/Condenser.- The turbine-alternator/condenser mounting concept is shown in Figure 3-25, which also shows the mounting bracketry. The mounting system must be able to accommodate the following factors:

- Axial expansion of the turbine housing between the condenser and the turbine center line
- Vertical expansion between the condenser and the turbine center line
- Condenser radial expansion
- Condenser gravity loading
- Piping loads at the condenser piping interfaces
- Vapor line loads imposed on the turbine
- Frame deflections
- Turbine-alternator gravity loading.

The design approach selected uses a formed bellows between the turbine exhaust and condenser inlet to isolate the turbine exhaust mainfold from the loads imposed directly or indirectly by the factors listed above. Each bellows is restrained with two tie rods to prevent a large pressure thrust from being imposed upon the turbine exhaust manifold. This pressure thrust would result only if a condenser overpressure condition occurred during testing since the nominal operating pressure is low. The bellows are deflected during assembly so that they are unstressed during system operation. Since the temperature (600°F) and pressure (2.5 psia) are low and the deflections are small, a formed bellows affords adequate reliability (a similar unit operated for more than 10,000 hours in the 35-kWe system test loop).

The various brackets seen on the exploded assembly, Figure 3-25, function as follows:

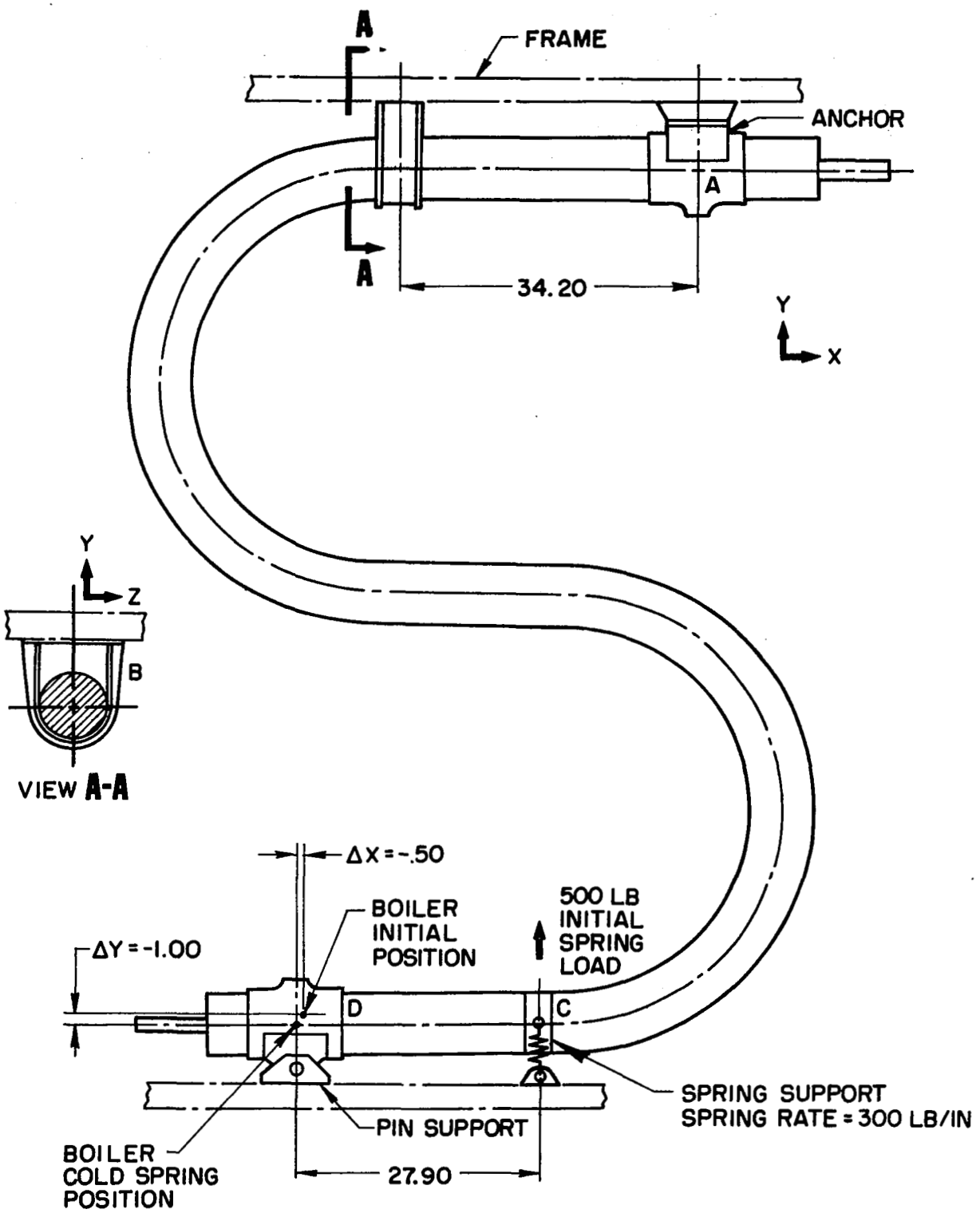

Figure 3-24 Boiler Mounting Concept

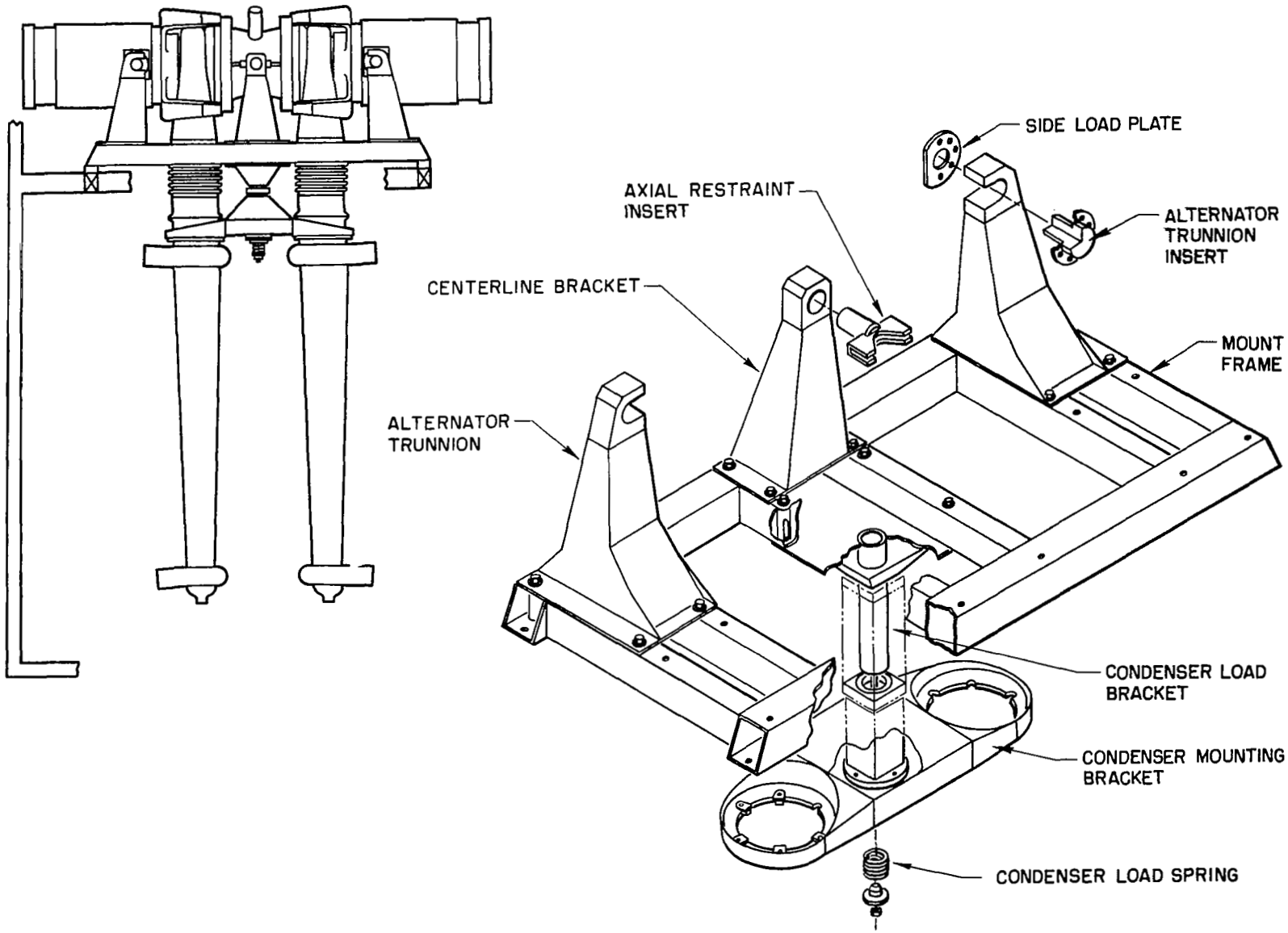

Figure 3-25 Turbine-Alternator/Condenser Mounting Concept.

The alternators are supported by trunnion mounts into which are fitted the trunnion inserts located on the alternator housing. The trunnion supports are slotted to accommodate the turbine axial expansion. These four brackets sustain the turbine-alternator vertical loading.

The two center-line brackets position the turbine-alternator so that the center of the unit does not move in the turbine shaft axial direction. These brackets are slotted vertically so that they take no vertical load and cannot cause bending of the turbine housing.

The two condensers are bolted to a common condenser mounting bracket which can move vertically on the condenser load-bracket shaft. This allows the condensers to move downward to accommodate the vertical expansion of the turbine exhaust manifold. It also transmits the condenser/piping interface loads to the mounting frame which is bolted to the system structure. The only loads which can reach the turbine exhaust manifold are the vertical forces acting on the condenser and loads produced by the angular displacement of the bellows. These vertical forces are due to the weight of the condenser and the vertical component of the piping interface loads, and are transmitted to the turbine exhaust manifold through the bellows tie rods. The condenser load spring is adjusted to balance the vertical forces so that the net vertical force approximates zero.

Other designs considered all presented design and fabrication complexities that the bellows approach eliminated.

c. Reservoirs.- A common mounting design was used for all system reservoirs. Basically, each reservoir is connected to a support ring at the top and bottom skirt of the unit by means of a flat spring so that normal growth of the reservoir can be accommodated by deflection of the spring. The spring at the top of the unit is a square U shape that can absorb the axial growth of the unit. The thermal growth is away from the bottom of the unit so that the reservoir does not load the connecting pipe. The intent was to prepare a design which did not depend on moving or sliding parts in a vacuum in order to function.

d. Pumps.- The pumps (NaK, mercury, and lubricant-coolant) were bolted to brackets attached to the power conversion system or to the frame itself. Slotted holes provided for thermal growth of the pump and motor housings.

e. Parasitic Load Resistors.- Each parasitic load resistor was bolted to a bracket using the lugs located on the unit near its center of gravity. The bracket in turn is bolted to the frame. The mounting bracket is split so that the parasitic load resistor can be installed or removed without removing the bracket. A second support provided at one end of each resistor acts as a stop. Between the two supports, bending moments introduced at the component interface are translated into forces acting on the brackets.

3.3.2.5 Piping Requirements

a. Piping Arrangement.- The piping arrangement for the power conversion system is shown in Figure 3-21. The main flow piping in the intermediate and heat rejection loops is 3-inch OD x 0.083-inch wall 316 stainless steel, with the exception of the piping near the NaK pumps. The NaK pumps have 2-inch OD x 0.065-inch wall suction and discharge connections (also of 316 stainless steel). The heat rejection loop piping, to and from the facility heat sink, is anchored at the frame interface for several reasons. First, this decouples the heat rejection loop piping from the facility piping which is an advantage since greater facility piping loads can be imposed on the frame than on the power conversion system components. Second, as a consequence of the above, the pressure losses in the lines to the heat rejection loop heat sink can be decreased by using larger diameter piping than is used in the system. The piping to the reactor primary loop will also be anchored to decouple the power conversion system from the reactor primary loop.

The lubricant-coolant piping, which consists of low-temperature small-diameter tubing, is anchored at the power conversion system structure periphery.

Pressure losses for the intermediate and heat rejection loops are given in Figure 3-26. Loop piping sizes were derived by matching the NaK pump head rise with the system flow losses under transient and steady-state conditions.

Pressure losses in the mercury loop are also shown on Figure 3-26. The loop piping sizes were determined using the following guidelines:

- The mercury vapor line has a minimum pressure drop compatible with the component and piping stress limitations.
- The mercury pump suction line must not restrict the pump NPSH requirement of 10 psia, nor will it permit pressures in excess of 40 psia during ground tests.
- The mercury pump discharge line must maintain minimum volume within the head rise limitations of the pump.

The lubricant-coolant loop piping is sized for minimum system volume compatible with the component flow requirements. Two overriding design criteria were (1) the lubricant-coolant pump NPSH requirement of 1.8 psia, and (2) the back pressure requirement of 2 to 5 psia to the bearings of the mercury pump and turbine-alternator. The overall system pressure drop is not considered to be a problem because the performance of the lubricant-coolant pump is adequate for the current requirements.

b. Piping Stress Analysis.- Piping for the intermediate, mercury, and heat rejection loops was analyzed for thermal stresses at the system operating temperatures. In addition, the piping interface loads were calculated for one gravity assuming unsupported piping. The allowable rotating

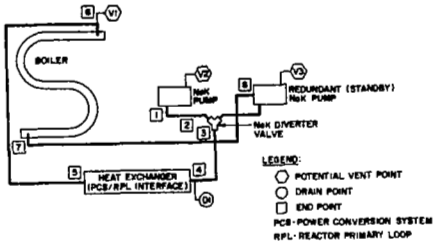

INTERMEDIATE LOOP COMPONENTS		ΔP (PSID) AT 57,020 LB/HR
END POINTS	DESCRIPTION	STATE-POINT VALUES
1-2	LINE - NaK PUMP TO NaK DIVERTER VALVE	0.85
2-3	NaK DIVERTER VALVE	1.00
3-4	LINE - NaK DIVERTER VALVE TO PCS/RPL INTERFACE	0.80
4-5	RPL HEAT EXCHANGER AND PIPING IN RPL	2.50
5-6	LINE - PCS/RPL INTERFACE TO BOILER	1.20
6-7	BOILER	2.50
7-8	LINE - BOILER TO NaK PUMP	2.39
NOTE: CALCULATED ΔP TOTAL - 11.24		TOTAL ΔP
NaK PUMP PRESSURE RISE - 18.10		LOOP - 11.24
MARGIN (ΔP) - 6.86		LINES - 5.24

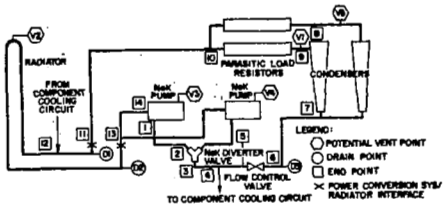

HEAT REJECTION LOOP COMPONENTS		ΔP (PSID) AT 60,000 LB/HR PUMP FLOW
END POINTS	DESCRIPTION	STATE-POINT VALUES
1-2	LINE - NaK PUMP TO NaK DIVERTER VALVE	.80
2-3	NaK DIVERTER VALVE	1.11
3-5	LINE - NaK DIVERTER VALVE TO FLOW CONTROL VALVE	.33
5-6	FLOW CONTROL VALVE	1.00
6-7	LINE - FLOW CONTROL VALVE TO CONDENSER	.15
7-8	CONDENSER	1.74
8-9	LINE - CONDENSER TO PARASITIC LOAD RESISTOR	.07
9-10	PARASITIC LOAD RESISTOR	.25
10-11	LINE - PARASITIC LOAD RESISTOR TO PCS INTERFACE	.88
11-13	LINE TO RADIATOR, RADIATOR, LINE FROM RADIATOR	6.12
13-14	LINE - PCS INTERFACE TO HEAT REJECTION PUMP	1.46
4-12	COMPONENT COOLING CIRCUIT	11.08
NOTE: ΔP TOTAL - 13.94		TOTAL ΔP
NaK PUMP PRESSURE RISE - 24.0		LOOP - 13.94
MARGIN (ΔP) - 10.06		LINES - 3.72

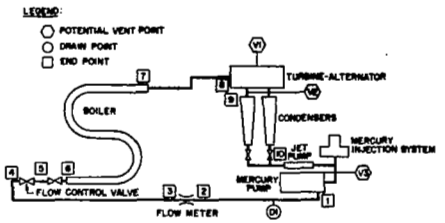

LOOP COMPONENTS		LOOP FLOW AT - 13,555 LB/HR VAPOR 14,120 LB/HR LIQUID
INTERFACE POINTS	DESCRIPTION	STATE-POINT VALUES
		ΔP (PSID)
2-3	FLOW METER	10.0
4-5	FLOW CONTROL VALVE - .50 OD TUBE - .75 OD TUBE	189.8 169.6
7-8	VAPOR LINE	2.08
		PRESSURE (PSIA)
1	MERCURY PUMP DISCHARGE	503.5
6	BOILER INLET (LIQUID)	320.0
7	BOILER OUTLET (VAPOR)	148.0
8	TURBINE INLET	145.9
9	TURBINE OUTLET	2.5
10	JET PUMP INLET	22.0
NOTE: MERCURY PUMP PRESSURE RISE - 481.5		

Intermediate Loop

Heat Rejection Loop

Mercury Rankine-Cycle Loop

Figure 3-26 90-kWe System Loop Pressure Loss Schedules

machinery interface loads are based upon existing configuration control drawings for these components. It was assumed that static components which have not been designed or are being modified can withstand interface loads comparable to loads that the connecting piping can accept. Some general results of the piping stress analyses are as follows:

(1) To minimize stresses in the intermediate loop NaK-pump suction lines and in the mercury vapor line, the boiler is mounted using a combination of anchors, pinned supports, spring support, and initial cold springing of the boiler itself.

(2) Some lines do not require intermediate supports in the one-g environment.

(3) The intermediate loop and heat rejection loop lines to and from the radiator are anchored at the power conversion system frame interface with the facility piping.

(4) The NaK diverter valves are considered part of the piping and are not supported independently.

(5) The boiler is considered anchored at the mercury-vapor outlet end to minimize the length of the mercury vapor line. The mercury-vapor line is as short as possible to minimize the boiler/turbine inlet line pressure loss and the possibility of mercury vapor condensation during system startup.

c. Insulation System.- A study was made to select the insulation method to be used for the power conversion system. Various kinds - such as Min-K, reflective insulation, super insulation, and vermiculite - were considered. The criteria which influenced the selection were:

- Cost
- Ease of application and reusability
- Resistance to nuclear radiation damage
- Compatibility with NaK and mercury
- Restraint on pipe movement
- Adaptability to piping configuration changes
- Weight and volume required
- Chloride content (per MIL-I-24244)
- Stability in a hard vacuum.

In addition, it was decided that the surface temperature of the insulation could be high enough so that personnel working on the loop would require asbestos gloves. To minimize insulation weight and volume, the insulation was sized for operation in a vacuum despite the fact that operation in air during checkout would be required. Since the normal operating mode is in vacuum this was the reference environment.

The material that best met the design criteria was Min-K* insulation which can be used in blanket and tape form with a stainless steel foil jacket around the outside.

In summary, vermiculite was not acceptable because of its high chloride content; super insulation is excessively costly and fragile; reflective insulation is excessively bulky, heavy, and cannot be readily changed to accommodate piping modifications. Since the manufacturer usually designs the latter insulation system, design data are proprietary making this method very difficult to study.

3.3.2.6 Electrical System

The electrical system appears in the block diagram in Figure 3-3. The various electrical components are located in protective housings and perform the functions described below.

a. Electrical Assemblies.- The low-temperature electrical assemblies provide an actively cooled heatsink to maintain the components at a stable temperature using 140°F lubricant-coolant fluid. This fluid is cooled by a separate, external heatsink (a low-temperature radiator or TSE equivalent). The following functions are performed by the components in the low-temperature electrical assemblies:

- The voltage regulator provides a control signal proportional to the frequency of the alternator output to the static exciter to regulate the alternator output voltage at the nominal system output value.

- The speed control module operates in conjunction with the saturable reactor and parasitic load resistor to regulate the steady-state frequency of the alternator.

- The power factor correction assembly corrects the power factor of the system and vehicle load demand on the alternator from lagging to approximately unity (when the vehicle load is at design conditions). The purpose is to increase alternator efficiency and hence available real-power output.

---

*Min-K insulation is manufactured by Johns-Manville Aerospace Products

- The electrical protective system protects the electrical system from internal (power conversion system) and external (vehicle load) faults. Any fault in the vehicle load is isolated from the power conversion system by opening the vehicle load breaker. An internal fault causes the power conversion system to shut down following a programmed sequence of events. The electrical sensors associated with the protective system operate from the electrical signal they sense and do not require additional power sources. Internal faults are distinguished from external faults by a time delay in the protective system which allows the system time to recover from an external fault after the vehicle load breaker has opened, and before action is taken to shut down the system.

- The inverter converts dc to ac power to start and operate the pumps during the period preceding and subsequent to alternator operation (startup, shutdown, and nuclear system decay heat removal).

- The inverter for the electromagnetic pump converts dc to ac power to start and operate the electromagnetic pumps during all phases of operation. During startup, shutdown, and nuclear system decay heat removal, the inverter input power is provided by a dc power supply; during steady-state operation, the power input is provided by a transformer-rectifier which receives its power from the alternator.

- The transformer rectifier converts 400 Hz alternator output to dc power which is input to the electromagnetic pump inverters.

- The inverter dc contactors are actuated by a signal from the programmer and cause electrical energy to be transmitted to the pump inverters. A latching design assures that no electrical input is required to maintain them in an open or closed position.

- The motor transfer contactors are actuated by a signal from the programmer and performs two functions: (1) cause the electrical input to the rotating pumps to be switched to the inverter, or (2) select the NaK pump which is to operate (redundant NaK pumps are installed in both the intermediate and heat rejection loops). When the actuating power is removed, the MTCs automatically transfer the pumps from the inverter output back to the alternator output. For shutdown, the programmer actuates the MTCs to transfer the pumps back to the inverter output power for decay heat removal.

- The saturable reactor controls the power delivered to the parasitic load resistor from the alternator in order to maintain nominal turbine speed.

- The speed control transformer assembly provides power to the speed control module.

- The saturating current potential transformer, in conjunction with the voltage regulator, provides alternator field current to control the alternator output voltage.

- The vehicle load breaker connects and disconnects the alternator to the vehicle load. A latching design assures that no electrical input is required to maintain it in open or closed position.

b. Parasitic Load Resistor.- This device functions in conjunction with the speed control system by acting as a variable electrical load on the alternator after the turbine speed enters the steady-state control range of the speed control system. For normal operation, the speed control system regulates the power dissipated in the parasitic load resistor to equal the difference between the electrical output generated by the alternator and the vehicle load demands together with the power required to operate the system components. In this way, the unit maintains a constant electrical load on the alternator so that the system state-point conditions are independent of the vehicle load. The parasitic load resistor is immersed in the heat rejection loop fluid, and rejects to the fluid as waste heat the electrical power absorbed.

c. Control Console.- The combined system test facility control console was designed to provide the following:

(1) System and component diagnostic instrumentation readout devices

(2) A power conversion system alarm panel

(3) A panel to permit remote manual control of the programmer and to initiate startup and shutdown. During steady-state operations, the manual control panel permits:

- Adjustment of the mercury flow through the flow control valve

- Interruption and reinitiation of the protective system vehicle load breaker reclosing cycle

- Adjustment of frequency and voltage

(4) A control panel for remote manual control of each pump at inverter output frequencies

(5) A startup-shutdown monitor with manual control capabilities. This monitor includes:

- An event recorder which indicates the startup or shutdown sequence status
- A clock which indicates total elapsed time from initiation of startup or shutdown
- An interval timer which indicates elapsed time of selected startup and shutdown subsequences
- A "hold sequence" switch which stops the startup or shutdown sequence at any point, except as follows: It shall not be possible to manually "hold" the startup sequence (or equivalent shutdown period), from the time that the boiler isolation valve is opened until 90% of the first mercury flow plateau time period elapses. The startup (or shutdown) sequence shall continue from the point of the "hold" when the "resume sequence" switch is actuated.

d. Programmer.- The programmer controls all functions of the power conversion system including sequencing on start, shutdown, and restart. It provides for internal and external fault protection by the use of the protective system. The programmer would be located in the facility control room for the combined system test at Plum Brook.

3.3.2.7 Interface Requirements

The regions of the power conversion system frame which have been assigned for mechanical, electrical, and instrumentation interfaces are shown on Figure 3-27. The power conversion system facility mechanical interfaces are located along one face of the frame to simplify mating with facility test support equipment. The loop vacuum/vent and fill-drain interfaces are located at the top and bottom, respectively, of the frame for ground tests.

The interfaces between the electrical harness and the power conversion system, and between the electrical harness and the facility will be governed by the following guidelines:

- Routing will be determined on a full-scale mockup with particular attention paid to thermal environment.
- Harness cable will be routed in bundles and clamped to nonremovable frame elements.
- Conductors will be welded to the terminals.
- Conductor insulation will be designed for a vacuum environment.

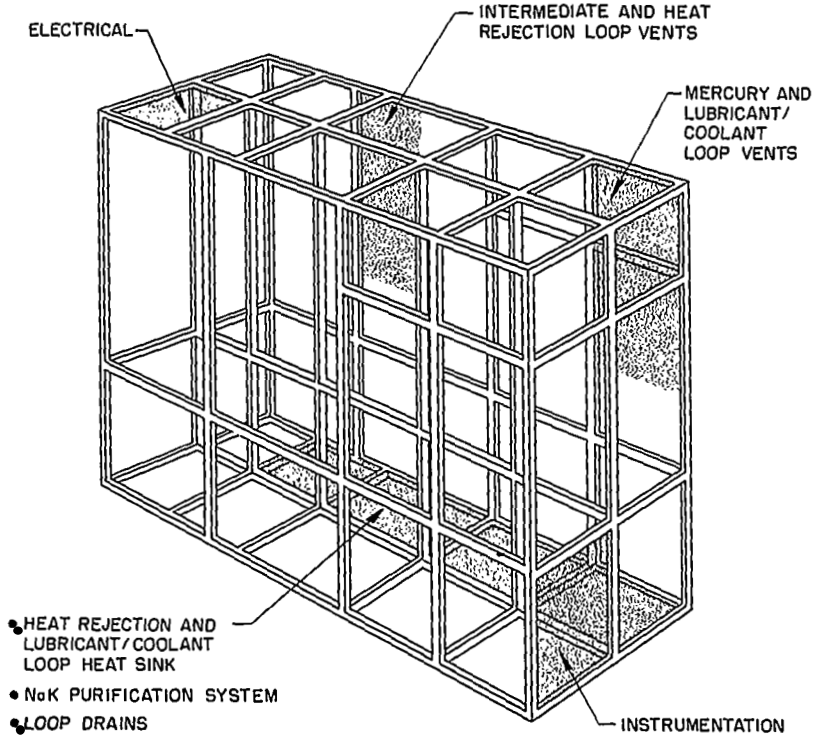

Figure 3-27 Power Conversion System/ Facility Interface Zones

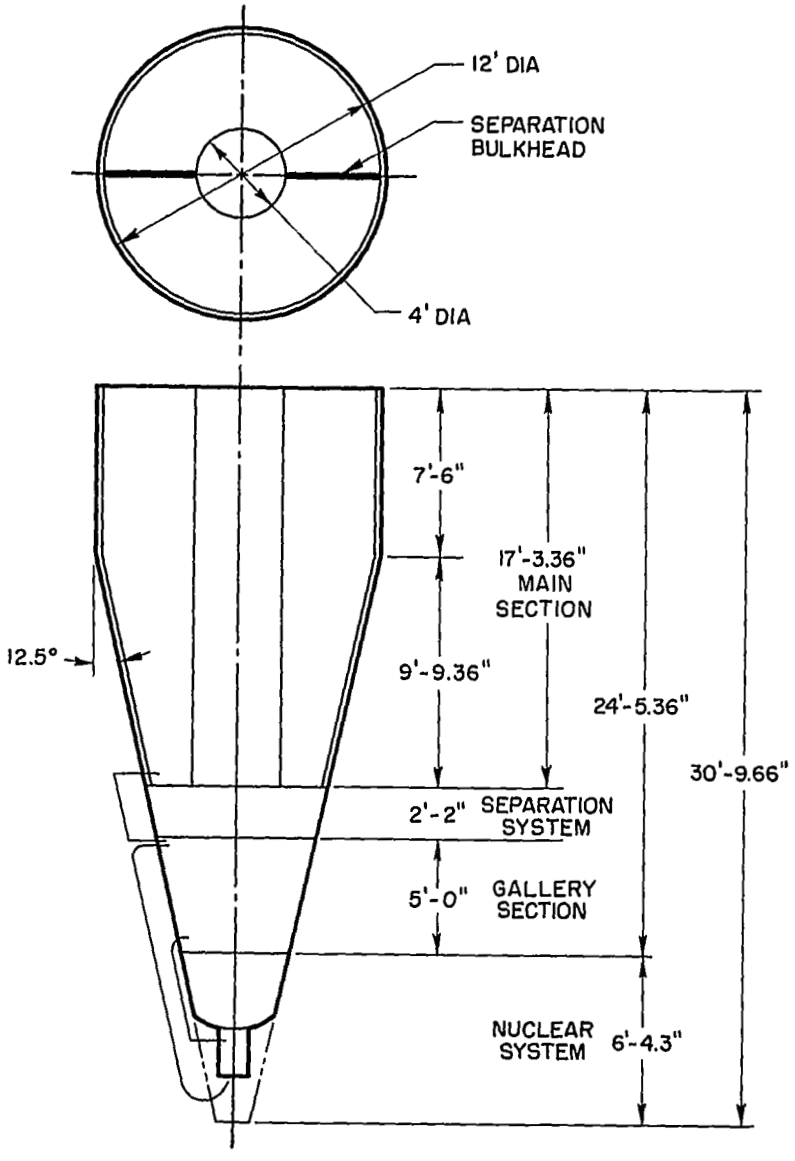

Figure 3-28 35-kWe System Envelope

The instrumentation harness interfaces will follow guidelines similar to those used for the electrical harness. In addition, appropriate routing and shielding will be incorporated to minimize electrical interference.

3.3.3 35-kWe System

3.3.3.1 System Configuration

The 35-kWe SNAP-8 envelope, shown in Figure 3-28, is a combined truncated cone and cylinder divided into the following four main assemblies:

- The nuclear system containing the reactor and nuclear shield
- The gallery section containing the power conversion system radioactive components
- The separation section containing the biological shield
- The main section containing the remainder of the power conversion system components and the system controls. This section is divided axially into two compartments of equal size which are completely independent (no piping or components cross from one compartment to the second).

A four-foot-diameter access cylinder through the center of the main section frame accommodates initial component installation and subsequent maintenance, since the main section would be surrounded with a radiator and would not be accessible from the outside.

Accessibility to the gallery section components for initial assembly is by means of removable frame members. After the system becomes operative, the NaK is radioactive and the gallery section is not accessible.

The main section was designed to be compatible with a heat rejection loop radiator around the outside. The gallery was designed to be surrounded by a 4-pi shield.

The 35-kWe system flow schematic appears as Figure 3-29.

3.3.3.2 Component Arrangement and Mounting

Figure 3-5 (page 3-12) presents the overall 35-kWe SNAP-8 component arrangement for the dual power conversion system configuration for manned missions. The components are listed in Table 3-VI.

The boilers, auxiliary heat exchangers, primary loop NaK pumps, and the primary NaK loop expansion reservoir are mounted in the gallery section to minimize and centralize the volume containing radioactive materials. This configuration permits the use of shadow radiation shielding as opposed to larger and heavier individual component shielding.

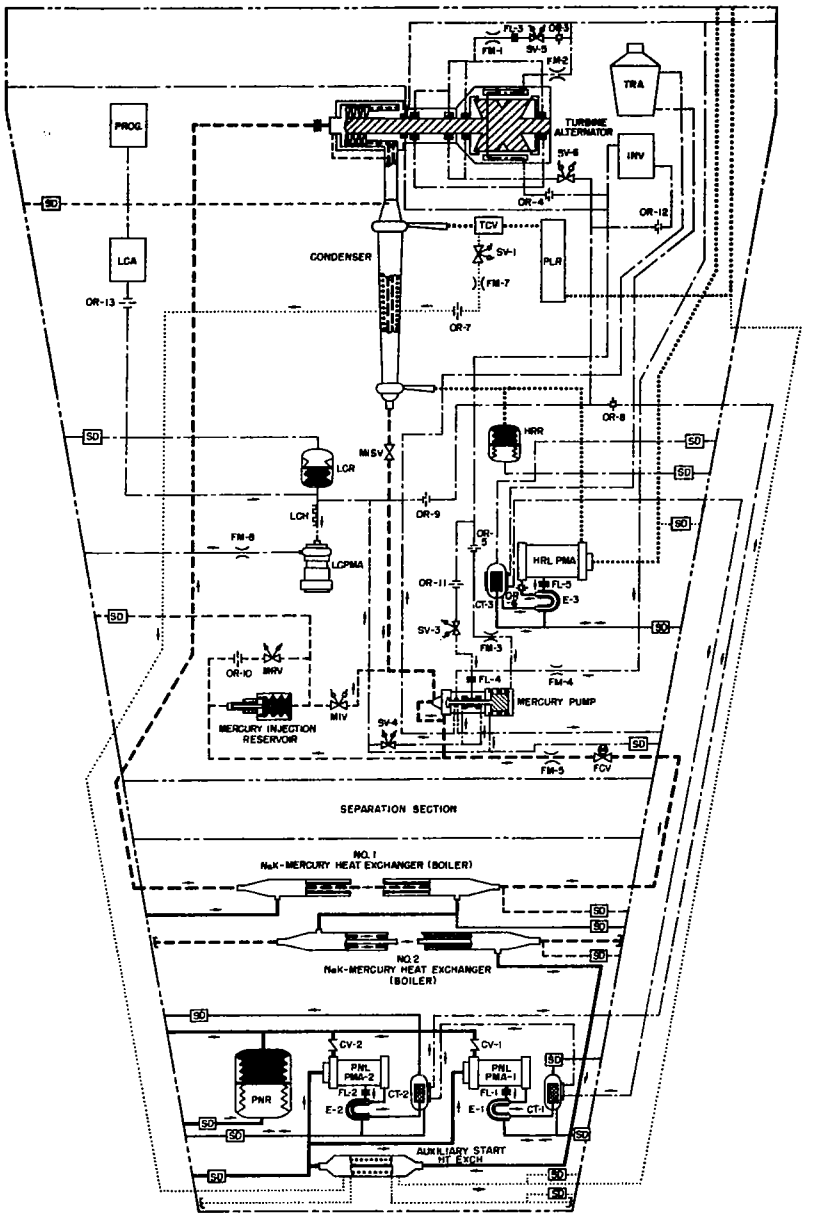

SYSTEM/COMPONENT LEGEND

PNL	PRIMARY NaK LOOP
NMHX-1	NaK - MERCURY HEAT EXCHANGER (BOILER)
NMHX-2	NaK - MERCURY HEAT EXCHANGER (BOILER)
ASHX	AUXILIARY START HEAT EXCHANGER
PNL PMA-1	PUMP MOTOR ASSEMBLY - PNL
PNL PMA-2	PUMP MOTOR ASSEMBLY - PNL
CT-1	COLD TRAP - PNL PMA-1
CT-2	COLD TRAP - PNL PMA-2
E-1	ECONOMIZER - PNL PMA-1
E-2	ECONOMIZER - PNL PMA-2
OR-1	DELETED
OR-2	DELETED
FL-1	FILTER - PNL PMA-1
FL-2	FILTER - PNL PMA-2
PNR	EXPANSION RESERVOIR - PNL
CV-1	CHECK VALVE - PNL
CV-2	CHECK VALVE - PNL
HgL	MERCURY LOOP
TAA	TURBINE ALTERNATOR ASSEMBLY
SV-5	SHUTOFF VALVE - TAA
SV-6	SHUTOFF VALVE - TAA
FM-1	FLOWMETER - TAA
FM-2	FLOWMETER - TAA
OR-3	ORIFICE - TAA
OR-4	ORIFICE - TAA
FL-3	FILTER - TAA
COND	CONDENSER
Hg PMA	PUMP MOTOR ASSEMBLY - Hg
SV-3	SHUTOFF VALVE - Hg PMA
SV-4	SHUTOFF VALVE - Hg PMA
FM-3	FLOWMETER - Hg PMA
FM-4	FLOWMETER - Hg PMA
OR-9	ORIFICE - Hg PMA
OR-11	ORIFICE - Hg PMA
FL-4	FILTER - Hg PMA
MIS	MERCURY INJECTION SYSTEM
MIR	MERCURY INJECTION RESERVOIR
MIV	INJECTION VALVE - MIS
MRV	RECHARGE VALVE - MIS
OR-10	ORIFICE - MIS
MCV	CONDENSER ISOLATION VALVE - MIS
FM-9	FLOWMETER - HgL
FCV	FLOW CONTROL VALVE - HgL
HRL	HEAT REJECTION LOOP
TCV	TEMPERATURE CONTROL VALVE - HRL
PLR	PARASITIC LOAD RESISTOR
HRR	EXPANSION RESERVOIR - HRL
HRL PMA	PUMP MOTOR ASSEMBLY - HRL
CT-3	COLD TRAP - HRL PMA
E-3	ECONOMIZER - HRL PMA
OR-6	ORIFICE - HRL PMA
FL-5	FILTER - HRL PMA
SV-1	SHUTOFF VALVE - HRL
FM-7	FLOWMETER - TO ASHX
OR-7	ORIFICE - TO ASHX
LCL	LUBRICATION AND COOLANT LOOP
LCH	LUBRICANT AND COOLANT HEATER
LCR	EXPANSION RESERVOIR - LCL
OR-8	ORIFICE - LCL
OR-13	ORIFICE - LCL
L/C PMA	PUMP MOTOR ASSEMBLY - LCL
OR-9	ORIFICE - LCL
FM-6	FLOWMETER - LCL
TRA	TRANSFORMER REACTOR ASSEMBLY
OR-15	ORIFICE - TRA
TSE	TEST SUPPORT EQUIPMENT
NaK	SODIUM-POTASSIUM
Hg	MERCURY
LCA	LOW TEMPERATURE CONTROL ASSEMBLY
PROG	PROGRAMMER
SO	SHUTOFF DEVICE
	LUBRICATION/COOLANT LINE
	PNL (NaK) LINE
	NRL (NaK) LINE
	HGL (MERCURY) LINE
	ORIFICE
	FLOWMETER
	FILTER
	SOLENOID VALVE, DOUBLE ACTING
	VALVE, MOTOR OPERATED
	SOLENOID VALVE
	DIRECTION OF FLOW
	LINE HEATER

Figure 3-29 35-kWe Power Conversion System Flow Diagram

TABLE 3-VI COMPONENTS IN SNAP-8 35-KWE DUAL POWER CONVERSION SYSTEM

Component		Quantity
NaK Pump		4
Boiler		2
Start Loop Heat Exchanger		2
Primary NaK Loop Expansion Reservoir		1
Primary NaK Loop Check Valve		1
Mercury Pump		2
Mercury Flow Control Valve		2
Turbine Assembly		2
Condenser		2
Mercury Injection System		2
Heat Rejection Loop Flow Control Valve		2
Parasitic Load Resistor		2
Auxiliary Start Loop Shutoff Valve		2
Heat Rejection Loop Expansion Reservoir		2
Lubricant-Coolant Pump		2
Lubricant-Coolant Expansion Reservoir		2
Lubricant-Coolant Shutoff Valves		8
Mercury Condenser Isolation Valve		2
Mercury Boiler Isolation Valve		2
Alternator		
High-Temperature Electrical Assembly	1	2
	2	2
Low-Temperature Electrical Assembly	1	2
	2	2
Inverter		2
Programmer		2

The gallery-section height was minimized by coaxially mounting the two boilers, two auxiliary heat exchangers, and the expansion reservoir. Effectively, the boilers and auxiliary heat exchangers acted as pipe runs from the gallery interface to the NaK pump suction line interface. The reservoir was located inside the boiler coil. The boiler/reservoir combination was insulated as a unit with a two-inch thick blanket of Min-K insulation around the periphery, across the top of the reservoir and across the bottom of the auxiliary heat exchanger. The reason for this was to create a constant-temperature definable environment for the reservoir.

To simplify the reservoir pressurization system, a captured-gas inventory in the reservoir was used to provide the operating pressure. The temperature of captured gas inventory with no regulator will follow the environmental temperature. The pressure "window" in the primary NaK loop is set by a maximum inlet pressure of 35 psia to the reactor and 20 psia to the NaK pump suction. Thus, the reservoir pressure was initially set to permit pump operation at startup frequencies without cavitation. As the loop heated up, the reservoir pressure rose to the normal operating value so that, by the time the pump accelerated to its nominal operating point, the loop pressure was properly set. An analysis established the steady-state gallery temperature profile and the primary loop reservoir transient response of the system during startup; the results are shown in Figures 3-30 and 3-31.

Figure 3-32 shows the effect of increased gallery height on biological shield weight. This assumes that the biological shield thickness is a constant so that increasing the gallery height moves the biological shield up the cone (see Figure 3-28) increasing its diameter and hence weight. The reference for this curve is the shield for the 50-inch gallery. The gallery target height was initially 50 inches.

The NaK pumps are mounted 180 degrees apart to facilitate component mounting as well as the routing and hydraulic characteristics of the interconnecting piping.

The component locations in the main frame section are based on the same guidelines used for the 90-kWe system components. In the 35-kWe system, the electrical assemblies are located as remote from the nuclear source as possible. The corresponding components of the dual power conversion systems are mounted 180 degrees apart thereby containing one set of power conversion system components in each vertical half-section of the frame. This arrangement also permits the use of duplicate component mounting brackets and interconnecting piping.

The following criteria were used in the design of the mounting provisions for the components:

- Three basic sections - bolted together
- $\pm$ 6-g longitudinal acceleration
- one-g lateral acceleration
- design for two sets of power conversion system components

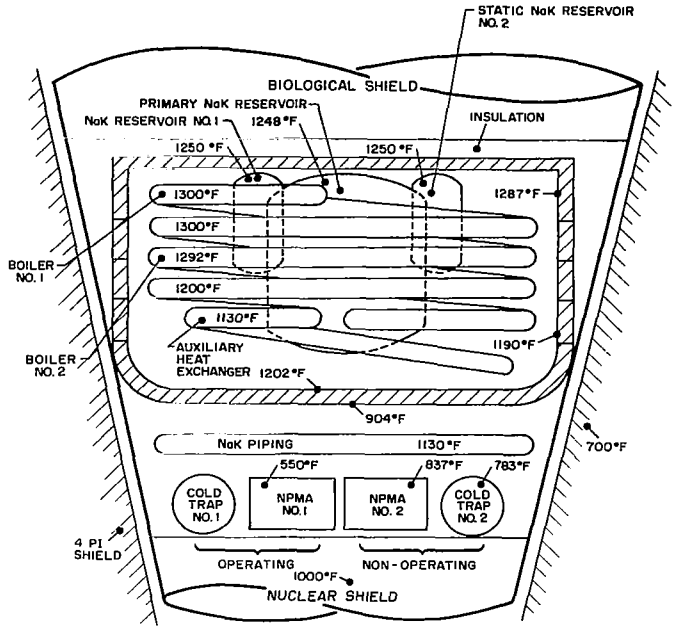

Figure 3-30 Gallery Section Thermal Map

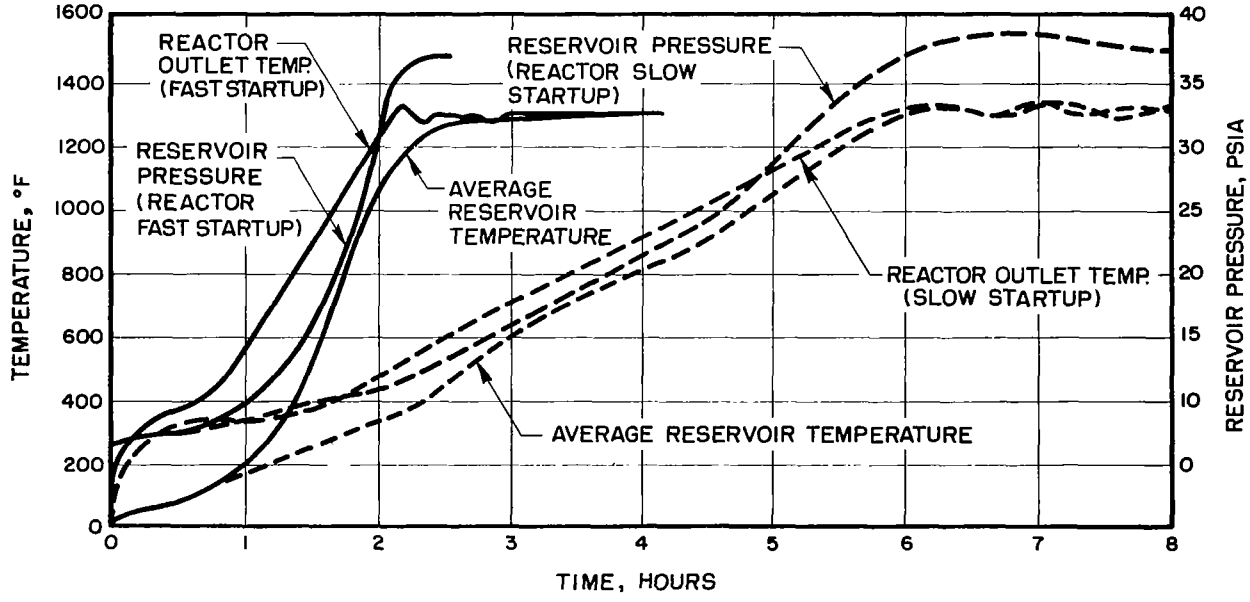

Figure 3-31 Primary NaK Loop Reservoir Response During System Startup

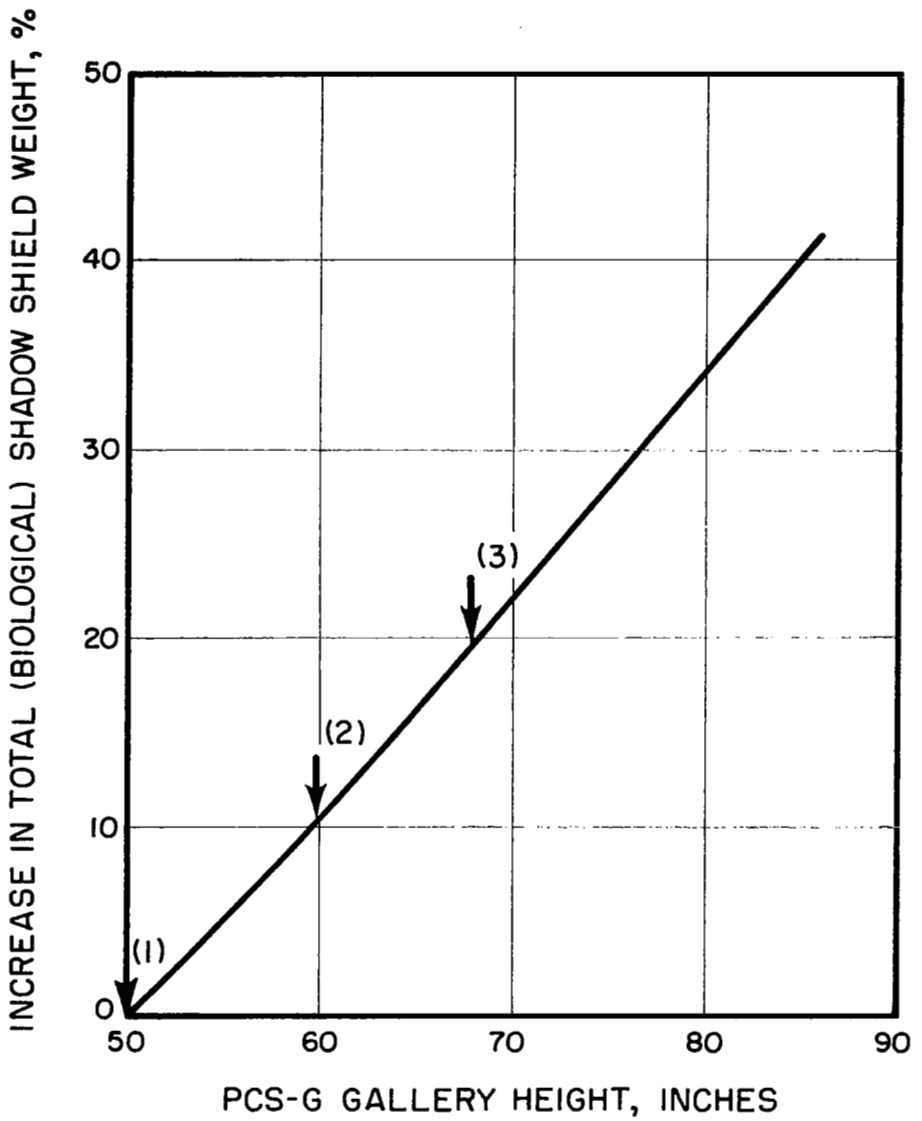

SHIELD WEIGHT
2" THK TUNGSTEN DISCS (2)

(1) CORRESPONDS TO 18' BOILER - 20,500 LB (REF)
(2) CORRESPONDS TO 31' BOILER - 22,700 LB
(3) CORRESPONDS TO 36' BOILER - 24,600 LB

Figure 3-32 Shadow Shield Weight (%) Increase as a Function of Gallery Height

- Components removable from 4-ft access tunnel, which can be a structural member
- Mounting to external frame columns is prohibited
- Two-inch annular region reserved for radiator
- Vacuum and high-temperature environment
- Factor of safety = 1.10 based on yield stress
- Two-year shelf life
- Five-year operating life

Some general component mounting features should be noted. The placement of all component mounts followed the ground rule that component replacement shall not necessitate the removal of any other component or the disconnection of any fluid piping not connected to the component being replaced. Original concepts of track and swing-out types of mounting were discarded in favor of simpler rigid supports and additional piping to provide adequate space for component replacements. None of the components in the main frame section was mounted to the external frame since the frame members were reserved for attachment of the radiators. Stainless steel mesh was incorporated in some of the mounts to permit component thermal growth and to support the component under handling loads.

3.3.3.3 Structural Design

The primary members of the gallery and main section frames are stainless steel rectangular tubing (Figure 3-33). The selection considerations for the frame members are the same as those stated for the 90-kWe system frame.

To demonstrate adequate volume based on member sizes for launch acceleration, the basic structure is designed to withstand a maximum gravity vector of $\pm$ 6 g's oriented along the longitudinal axis of the frame. Side loads of 1.5 g's are included in the frame requirements to accommodate ground handling. A detailed stress analysis verified design acceptability.

3.3.3.4 Piping Requirements

In general, the individual loop piping arrangement, guidelines, and limitations are the same as those stated for the 90-kWe system. The 35-kWe primary NaK loop contained the boiler, however, so that the mercury boiler and turbine were relatively remote. Piping stress analyses were performed for the individual fluid loops.

In summary the following conclusions are presented:

The individual pumps perform adequately, and meet their respective flow and pressure rise requirements at all speeds.

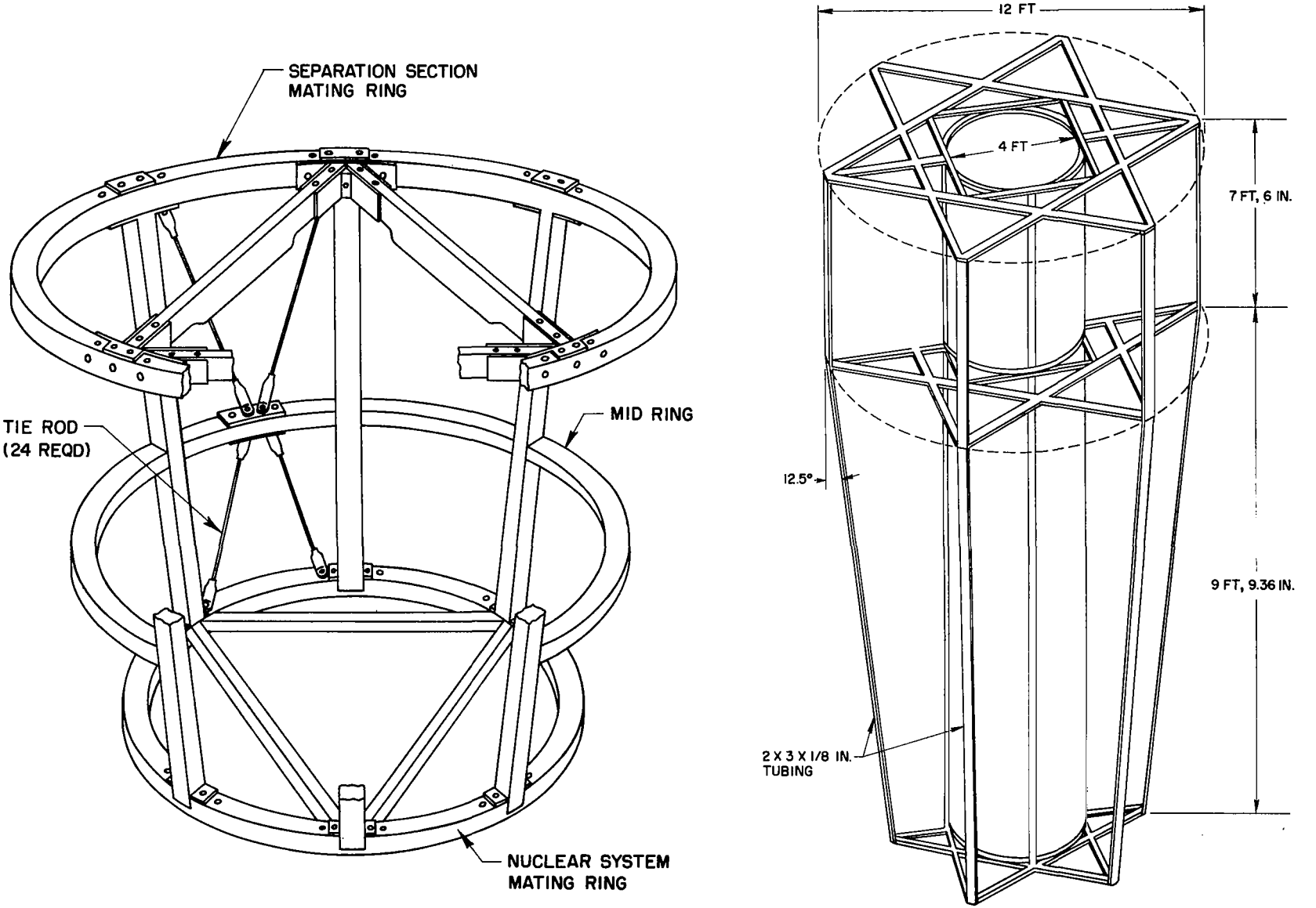

Gallery Section

Main Section

Figure 3-33 35-kWe Power Conversion System Frame

- The component/piping interface loads are all within tolerances.
- The piping stress levels are acceptable.
- The mercury vapor line requires preheating at startup (the auxiliary start loop return line is used to assist electric trace heaters).

3.3.3.5 Electrical and Instrumentation Requirements

The instrumentation and electrical subassemblies requirements conform to those for the 90-kWe system.

3.3.3.6 Interface Requirements

The system interfaces can be summarized as follows:

- The piping between the power conversion system and radiators is anchored at the frame.
- The piping between the gallery and power conversion system is not anchored. This permits greater line flexibility and specifically allows a minimum-length mercury vapor line.
- The radiators are terminated one foot above the bottom of the main section to provide an exit avenue for piping (drain lines, service lines, etc.) to the gallery.
- A two-inch envelope is left around the periphery of the main section to leave radiator space so that the configuration will not have to be changed later.
- The entire unit can be lifted from the top plane.
- All major subsections are designed to be bolted together.
- The main section/biological shield and the gallery/biological shield can be remotely disconnected; flanges are bolted together with detachable bolts and captive nuts (Figure 3-34).
- The intersection piping is designed for the use of remote parting and automatic rewelding tools.
- The main section frame can support the lubricant-coolant and heat rejection radiators and the lubricant-coolant cold walls in the combined system test (Figure 3-35).
- All service lines are designed to be isolated during the combined system test.

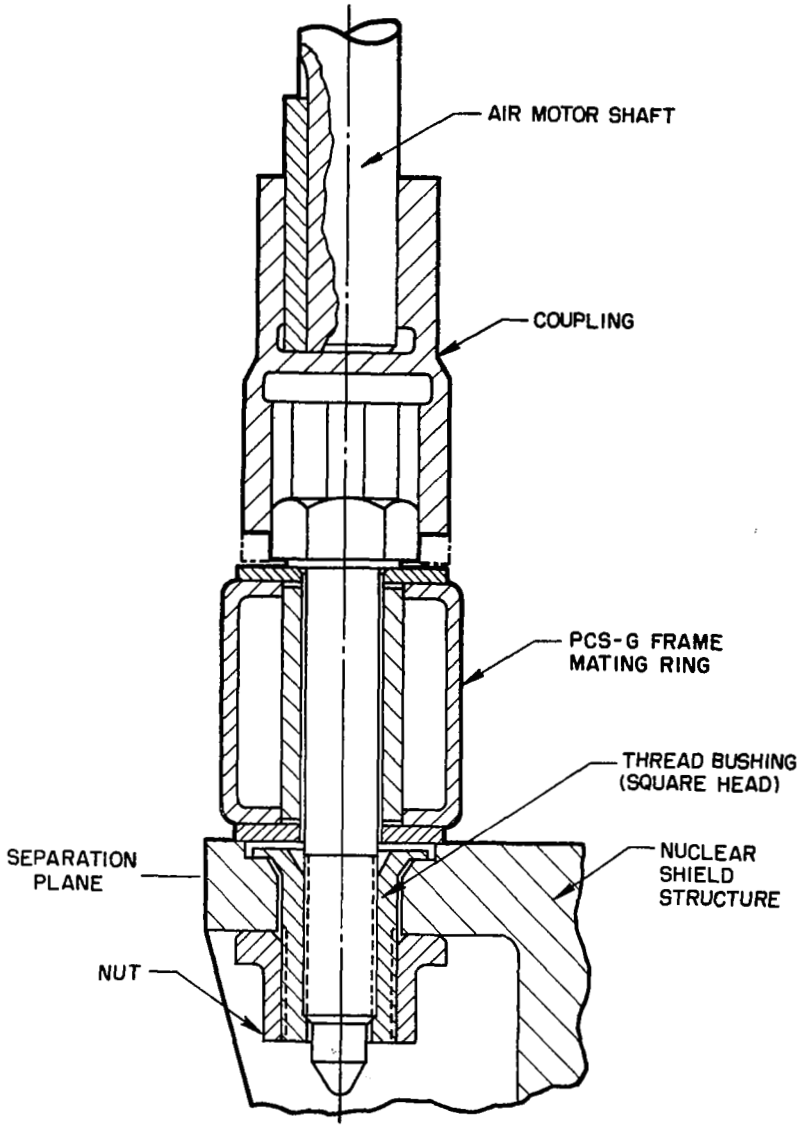

Figure 3-34 Remote Disconnect Bolting Concept

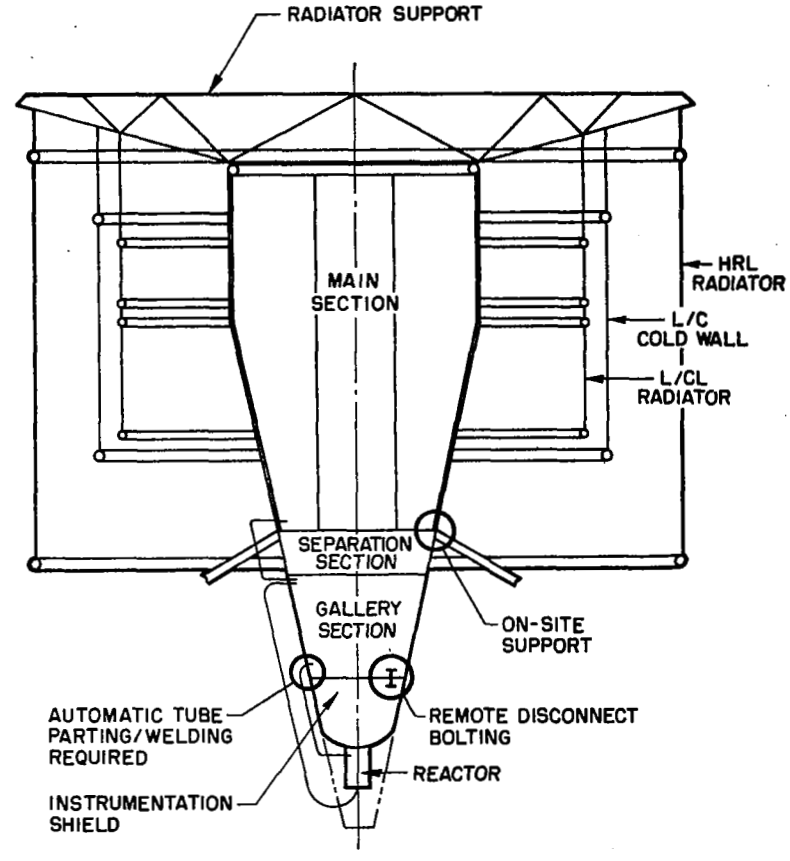

Figure 3-35 Combined System Test Facility Interfaces

3.3.3.7 Test Support Equipment

In conjunction with the 35-kWe system design, a study was made and a conceptual design prepared to define requirements for associated test support equipment (TSE). The TSE requirements were determined primarily for nuclear testing of the power conversion system at the NASA Space Power Facility. However, an approach was adpoted which would permit decoupling of the equipment from an operating system, and which would provide flexibility in the event of changes in the system concept and potential utilization in other facilities. The adoption of this approach resulted in the definition of three separate, transportable TSE carts.

The design and operation of each of the TSE carts are based on the following ground rules.

- The controls and instrumentation required for the operation of each cart are locally mounted and readily adaptable to remote operation.
- The cart components and frame materials are compatible with both vacuum and nuclear radiation environments.
- The cart frames are equipped with wheels, screw jacks, and choch brakes to provide mobility between stations and stability while in service.
- The cart interfaces are designed for maximum flexibility in the selection of the test facility and PCS subsystem that is to be serviced.

a. Pressure, Vent, and Vacuum (PVV) Cart.- The PVV cart supplies argon cover gas at pressures of 0 to 50 psig and a vacuum as low as 10^{-4} microns. The PVV cart is designed for use on any of the individual loops in the power conversion system and in conjunction with the TSE systems described below.

b. NaK Purification Cart.- The NaK purification cart circulates NaK at flow rates of 0 to 10 gpm. It can purify NaK to 5 ppm of oxygen or less, and provides a means of determining the oxygen content to levels below 5 ppm. Finally, the cart can heat the total NaK inventory of the purification cart and loops to approximately 1350°F.

c. Lubricant-Coolant Fluid Service Cart.- This cart circulates the service fluid, polyphenyl ether, at a flow rate of 6 gpm and heats the fluid to 300°F. The cart also filters solids to a residue of approximately 1 ppm or less and removes gases from the fluid.

3.4 FABRICATION AND ASSEMBLY

3.4.1 Full-Scale Mockups

The compact nature of the power conversion system led to the decision to fabricate a full-scale mockup of the power conversion system which would function as an engineering design aid and fabrication tool. Components used in the mockup were space SNAP-8 hardware or wooden component mockups. The major objectives of the mockup were as follows:

- Assist in the design of interconnecting piping and service lines. Mockup pipe runs were to be used as patterns for the final power conversion system piping.
- Develop the routing of the instrumentation and electrical harnesses.
- Develop the routing for the lubricant-coolant loop piping.
- Assist in the location and design of piping supports.
- Verify component installation sequences and techniques, and define critical areas or procedures.
- Evaluate component, frame member, and piping locations in terms of maintenance and replacement.
- Verify special tooling and equipment requirements.

3.4.1.1 Frame - 90-kWe Power Conversion System

The full-scale mockup frame for the 90-kWe power conversion system shown in Figure 3-36 was fabricated at Aerojet. The frame was fabricated from carbon steel and painted for environmental protection. The engine frame material was stainless steel; however, for the low-temperature-environment power conversion system ground test, it would have been possible to use the mockup frame as a test structure instead of fabricating a new frame. The mockup frame was fabricated to engine frame prints to derive maximum possible design and fabrication feedback.

3.4.1.2 Gallery Section - 35-kWe Power Conversion System

The ground test frame, piping, and component full-scale mockups were completed and are shown in Figure 3-37. Only instrumentation harnessing and some component mounts were required to complete the mockup of the gallery section. Flexible metal tubing was used to form the mockup boilers and piping. The flexible tubing was then rigidized using an epoxy resin so that it could be removed in sections to aid in the fabrication and assembly of the final test piping. Actual pump housings were used in the mockup; the remainder of the component mockups were fabricated from wood. The mockup was assembled in accordance with a preliminary draft of a gallery assembly procedure which would be updated based on the mockup experiences to become the engine gallery assembly specification.

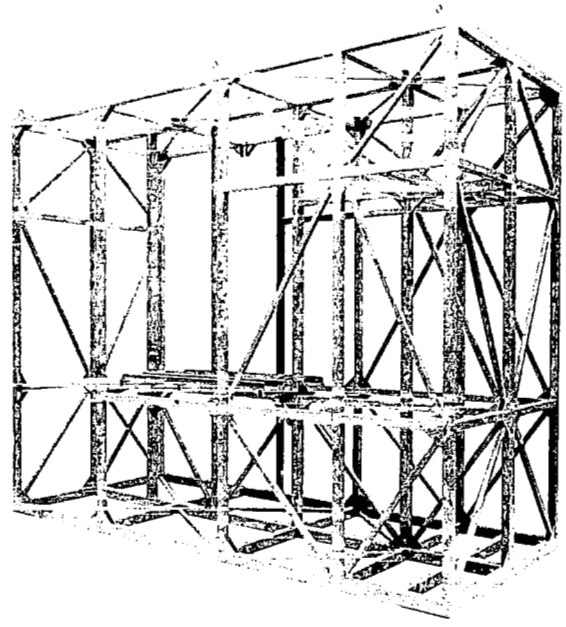

Figure 3-36 Full-Scale Frame Mockup - 90 kWe Power Conversion System

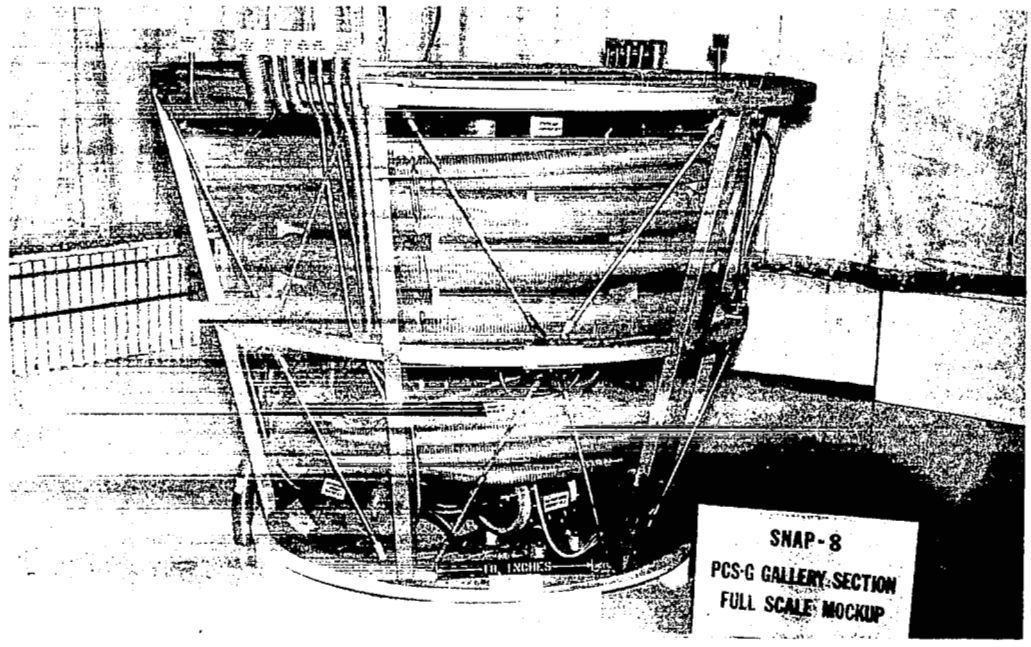

Figure 3-37 Full-Scale Gallery Section Mockup - 35-kWe Power Conversion Sy

3.4.2 Piping System Fabrication Investigations

3.4.2.1 Tubing Preparation

The dense packaging of the power conversion system components and piping and the requirement for system cleanliness led to the decision to use semiautomatic tube-cutting and weld-preparation tooling for some phases of fabrication and component replacement. Known tubing equipment manufacturing companies who might have the required tooling were surveyed. One company was identified as an organization that manufactured a standard line of portable, manual, and compact tools that could be used for tubing cutting, cleaning and deburring stainless steel tubing in sizes up to two inches in outside diameter.

3.4.2.2 Tubing Welding and Brazing

Investigations were undertaken to identify possible systems which would automatically weld and braze tubing. It was intended to use braze joints in the lubricant-coolant system and weld joints in the liquid-metal systems. Braze fittings are available which contain the braze alloy for the tube joint. The system is complemented by the tooling mentioned in section 3.4.2.1.

Hand butt-welding of tubing in SNAP-8 test systems occasionally resulted in excessive weld drop-through or weld spatter and lack of penetration. To maintain system cleanliness, repeatable welds, and increase the probability of successfully executing closure welds, automatic weld systems were investigated. In addition, compact designs were required to permit welding in the confined regions of the power conversion system.

4.0 SYSTEM OPERATION

4.1 90-KWE SYSTEM

4.1.1 Steady-State Operation

The steady-state design-point operating conditions for the 90-kWe system are described in Section 3.0 of this report. In addition to the design operating point, a number of off-design operating conditions occur which represent deviations from the design point, but which may still be considered steady-state operating points.

One of these conditions is operation with the reactor outlet NaK temperature at the upper limit of the nuclear system control deadband. The effect of this condition on the net electrical output is also discussed in Section 3.0.

The effect of sunlight and earth shadow for space missions in a near-earth orbit presents another such condition. As a vehicle moves from sun to shadow, the heat rejection radiator temperature decreases, lowering the condenser coolant temperature. This, of course, reduces the condenser operating pressure which means that the backpressure on the turbine is lower allowing an increase in turbine power and net electrical output.

The effect of reductions in vehicle load on system state-point conditions offers yet another condition. When a part of the vehicle load is removed from the system, the excess electrical output is absorbed by the parasitic load resistor where it is transferred as heat to the heat rejection loop. The effect is to raise the condenser coolant temperature which increases the turbine backpressure. This results in a reduction in system gross electrical output.

A final off-design steady-state operating point is due to the effects of reductions in condenser mercury inventory primarily as a result of turbine-alternator and mercury pump space seal losses during extended operating periods. Using a condenser of the existing design in the 90-kWe system means that the condenser will operate far from the original design point. Condenser mercury inventory losses cause appreciable reductions in mercury vapor pressure and a tendancy toward an unstable liquid-vapor interface in a zero-g environment. However, since the 90-kWe system in its present form was intended primarily as a ground test article in a one-g environment, the interface instability problem is not significant. The condenser would have to be redesigned if operation in a zero-g environment became a requirement.

4.1.2 Startup and Shutdown Modes

The 90-kWe test was designed primarily as a test article to start, operate at steady-state, and shutdown in a one-g environment in the NASA Space Power Facility at Plum Brook. Startup and shutdown procedures were formulated for this system based on the procedures developed for earlier SNAP-8 systems and the studies conducted to verify the acceptability of the transients produced during startup. Similar studies to verify the acceptability of startup and shutdown procedures for a 90-kWe system, or for a system with an intermediate loop and a nominal reactor outlet temperature of 1200°F*, have not been conducted. However, extensive startup- and shutdown-transient studies were conducted earlier in the development program for system with no intermediate loop and with a nominal reactor outlet temperature of 1300°F. The results of these earlier studies (combined with the facts that the reactor operating temperature is lower, and the intermediate loop attenuates temperature transients) indicate that the startup and shutdown procedures for the 90-kWe system will be acceptable. The details of some specific conditions and procedures, such as the initial NaK flow and ac frequency supplied to the pump drives at the beginning of startup, remain to be completed.

4.1.3 System Transients

The major transients to which the system is subjected are associated with startup and shutdown. The most severe transients occur during an emergency shutdown. Lesser transients, which may be considered as deviations from steady-state operation, occur as a result of vehicle load changes, and system and component degradations causing changes in parameters such as flows, pressures, fluid inventories, and heat transfer effectiveness.

An analysis of transients, using a computerized dynamic simulation of the system, is needed to adequately determine the effects of the various transients on the overall system and on individual, critical components. Earlier versions of SNAP-8 systems were simulated on computers, but these simulations were not updated to reflect the changes associated with the 90-kWe system. So, while the effects of the various transients on the system and components can only be estimated, the knowledge gained from the previous studies, combined with an assessment of the potential effects of changes in the system and components, provides a reasonable basis for these estimates.

The major criteria determining the acceptability of various system transients - particularly those associated with startup and shutdown - are related to limitations of the reactor, the mercury pump, and the turbine exhaust pressure.

The reactor limitations, defined by the nuclear system contractor, are primarily associated with maximum allowable rates of temperature change and maximum allowable temperature values. The limitations had been defined

---

* Most recent reactor coolant outlet temperature recommended by the nuclear system contractor.

for a specific reactor design with a nominal operating temperature of 1300°F. After the reactor limitations were established, design changes were incorporated and a nominal operating temperature close to 1200°F was recommended by the nuclear system contractor. Although the contractor indicated that some of the reactor limitations would be more restrictive as a result of the design changes and information obtained from test evaluations, revised reactor limitations have not been established.

The mercury pump limitation is primarily associated with suction pressure requirements during startup when condensing pressures are low. This limitation is not a significant factor for 90-kWe system operation in the ground test facility since elevation head becomes the predominant factor in determining pump inlet pressure. However, ground tests should demonstrate the validity of principles and acceptability of equipment associated with system operation in zero gravity. Consequently, studies of system transients must be conducted to determine the control conditions and hardware performance requirements needed to maintain adequate condenser and pump inlet pressures.

The turbine exhaust-pressure limitation is related primarily to the condenser operating conditions. The design must assure that condenser pressures during startup do not increase to the point where turbine acceleration is impeded or turbine deceleration is induced. Therefore, system transient studies must be conducted to determine just what controls and hardware requirements are needed to assure that the proper condenser pressure will be maintained.

Hardware requirements and proper control conditions had been established for earlier SNAP-8 systems. Experience with these systems make it reasonable to assume that similar equipment and procedures will adequately meet limitations which may be imposed on the 90-kWe system. However, new criteria and applicable limitations must be defined and transient studies conducted before the startup and shutdown procedures, proper control conditions. and hardware requirements can be established.

The hardware requirements and control conditions which must be established are primarily related to the mercury injection system functions and the operating characteristics of the heat rejection loop flow control valve which regulates condenser conditions during startup and shutdown. Concepts were generated for both the mercury injection system and the heat rejection loop flow control valve. The primary functions of the mercury injection system are (1) to introduce mercury into the Rankine-cycle loop, at controlled rates, during power conversion system startup, and (2) to act as a reservoir for the mercury inventory which is pumped from the Rankine-cycle loop during shutdown. A secondary function is to provide a means for adjusting the Rankine-cycle loop inventory during long periods of system operation

A schematic of the mercury injection system is shown in Figure 4-1. During power conversion system startup, mercury is injected into the loop at the mercury pump inlet, through the mercury injection valve, as the reservoir volume is decreased by the movement of the actuator piston. Pressure is applied to the actuator piston from the lubricant-coolant pump discharge.

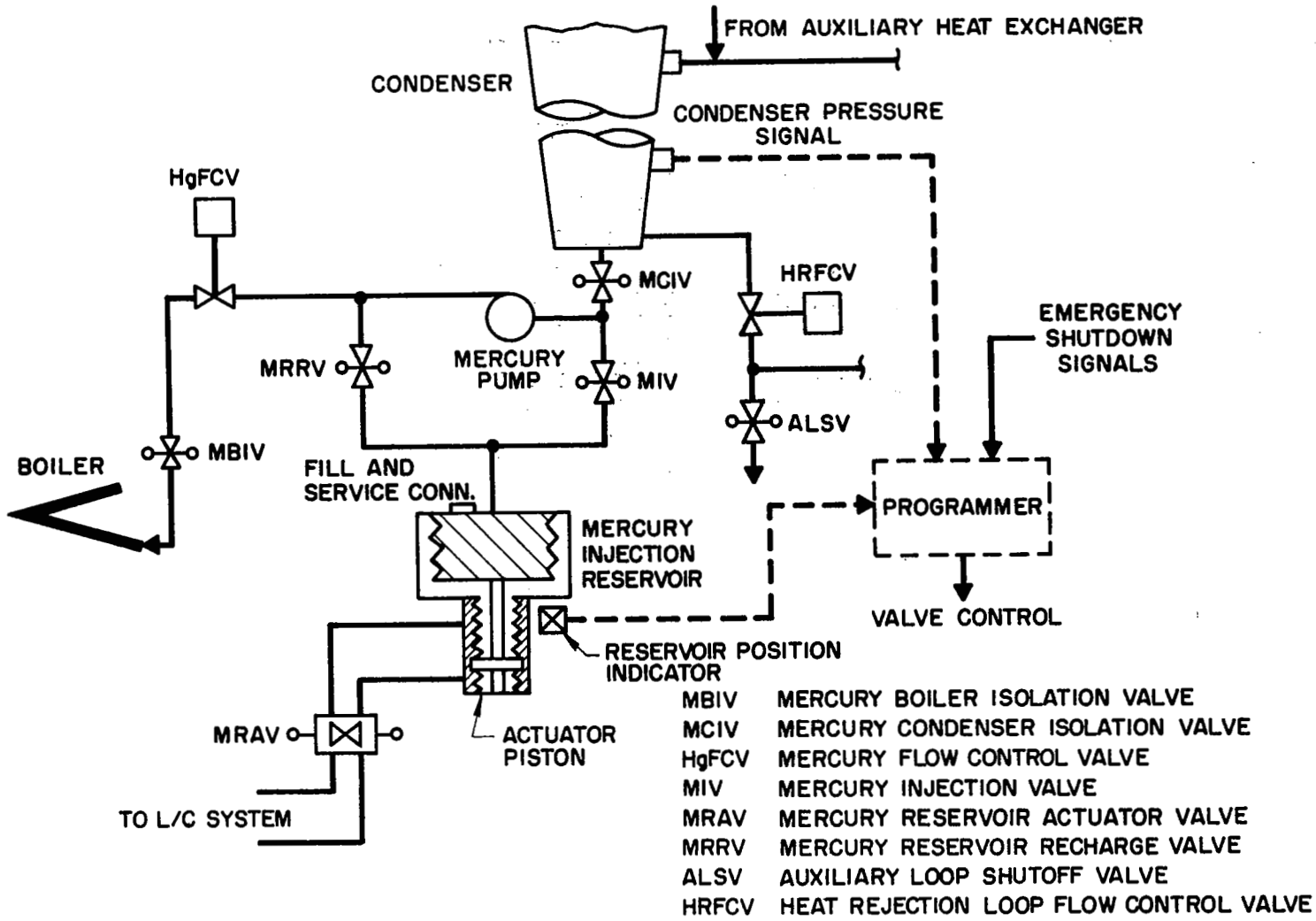

Figure 4-1 Low Pressure Mercury Injection and Restart System

The rate of mercury injection is controlled by the action of the mercury flow control valve. The mercury injection valve is closed when the reservoir position indicator shows that the proper loop inventory has been injected. The mercury condenser isolation valve is closed at the same time and the mercury pump then circulates mercury through the loop.

During a normal power conversion system shutdown, the mercury reservoir recharge valve is opened and the loop inventory is pumped back to the reservoir, at a low rate, by the mercury pump discharge pressure. The force exerted on the reservoir by the mercury pump pressure is greater than the force exerted on the actuator piston by the lubricant-coolant pump discharge thereby permitting the loop inventory to be returned to the reservoir.

During an emergency shutdown, the mercury reservoir actuator valve is actuated to the "dump" position. This action permits the lubricant-coolant pump discharge pressure to act on the side of the actuator piston which will move the reservoir bellows to rapidly increase the reservoir volume. At the same time the mercury boiler isolation valve is closed and the mercury injection valve is opened. As a result, the mercury reservoir becomes a very low-pressure sink and mercury inventory is returned to the reservoir by the differential pressure created by boil-off of residual boiler inventory and by the condenser pressure.

The motor-driven heat rejection loop flow control valve performs an important function during power conversion system startup and shutdown. The heat rejection loop flow control valve is signalled to move in a manner that will maintain the condenser pressure within a tolerance band around the steady-state operating value. A condenser pressure sensor actuates the valve motor in the proper direction. The condenser pressure is maintained at a level near the steady-state operating value to assure adequate mercury pump suction pressure and to prevent high condenser pressures which would tend to inhibit turbine acceleration or induce turbine deceleration. Therefore, during startup the valve increases heat rejection loop flow as mercury flow and condenser heat load are increased. During shutdown, the valve reduces the heat rejection loop flow as mercury flow and condenser heat load are decreased.

4.2 35-KWE SYSTEM

4.2.1 Steady-State Operation

The steady-state design-point operating conditions for the 35-kWe system are described in Section 3.0. Studies were conducted to determine the effects on net electrical output and system conditions of other steady-state operating conditions which represent perturbations from the design point.

The first condition is operation with the reactor outlet NaK temperature at the upper limit of the nuclear system control deadband. The effect of this condition on net electrical power is discussed in Section 3.0, and the resulting statepoint conditions are shown in Figure 4-2.

The effect of variations in sun and shade environments for space applications in a near-earth orbit is shown in Figure 4-3. As a result of the decrease in heat rejection loop radiator temperatures when moving from sun to shade, the condensing temperature is reduced approximately 25°F which results in a decrease in turbine exhaust pressure of approximately 2 psia. The increase in enthalpy available to the turbine produces an increase in net electrical output of 1.9 kW.

Reductions in vehicle load demands on the system increase radiator temperatures since the unused electrical power is dissipated in the parasitic load resistor located in the heat rejection loop. The effect of the most severe reduction in vehicle load demand (when the vehicle load is zero) is shown in Figure 4-4. The increased radiator temperatures cause an increase in turbine exit pressure, a reduction in enthalpy available to the turbine, and a decrease in gross electrical output of approximately 2 kW.

During long-term steady-state operation, some mercury leakage occurs from the mercury pump and turbine-alternator space seals. A conservative estimate (based on tests) indicates a total leakage of 10 lb over 10,000 hours of operation. The leakage is reflected as a loss in condenser inventory which increases the available condensing area causing a reduction in the condensing temperature and pressure. As a result, the net electrical output will increase slightly, approximately 0.1 kW, as shown in Figure 4-5.

The effects of the off-design operating conditions on the electrical output are summarized in Table 4-I.

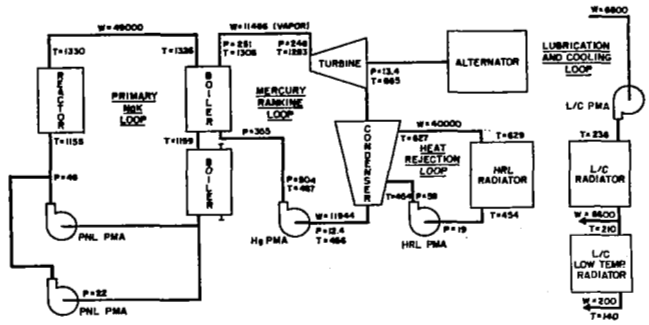

POWER DISTRIBUTION

Turbine shaft power	63.9 KW
Alternator efficiency	90.9 %
Alternator gross output power	58.0 KW
Parasitic load total	21.0 KW
PNL PMA	4.7
Hg PMA	3.5
HRL PMA	4.6
L/C PMA	1.4
PLR	5.5
Control System	1.3
Net output power	37.0 KW

HEAT RADIATED BY L/C RADIATOR

Turbine	5.25 KW
Alternator	4.20 KW
L/C PMA	1.40 KW
Hg PMA	3.14 KW
HRL PMA	2.25 KW
#1 PNL PMA	2.12 KW
#2 PNL PMA (standby)	0.12 KW
TRA	0.59 KW
	19.08 KW

DESCRIPTIVE FEATURES

Turbine aerodynamic efficiency - 55.6%
Turbine inlet pressure - 248 psia
Turbine exhaust pressure - 13.9 psia
NaK PMAs: 5800 rpm induction motors, both NaK loops
NaK PMAs:: Cooled by L/C fluid
Hg PMA with motor scavenger
Tube-in-tube boiler (7 Hg tubes)
Tube-in-shell condenser (73 Hg tubes)
SNAP reactor
Parasitic load resistor (PLR) in HRL
Saturable reactor-magnetic amplifier speed control
Radiator NaK ΔT - 179°F

PERFORMANCE SUMMARY

Net reactor input to PCS	537 KWT
Net electrical output	37 KWE
Overall system efficiency	6.9 %

Figure 4-2 State-Point Diagram for 35-kWe Power Conversion System (Off-Design Conditions: Reactor Outlet Temperature at Upper End of Deadband Control, and Zero-g Environment)

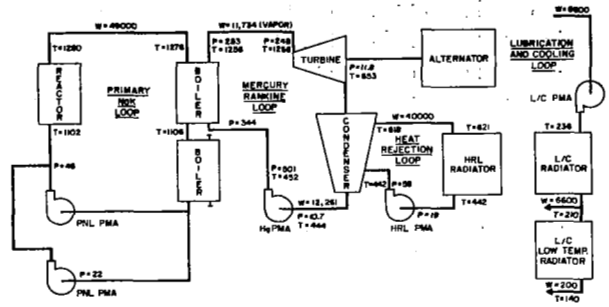

POWER DISTRIBUTION

Turbine shaft power	65.8 KW
Alternator efficiency	91.1 %
Alternator gross output power	59.9 KW
Parasitic load total	21.0 KW
PNL PMA	4.7
Hg PMA	3.5
HRL PMA	4.6
L/C PMA	1.4
PLR	5.5
Control system	1.3
Net output power	38.9 KW

HEAT RADIATED BY L/C RADIATOR

Turbine	5.25 KW
Alternator	4.20 KW
L/C PMA	1.40 KW
Hg PMA	3.14 KW
HRL PMA	2.25 KW
#1 PNL PMA	2.12 KW
#2 PNL PMA (standby)	0.12 KW
TRA	0.59 KW
	19.08 KW

PERFORMANCE SUMMARY

Net reactor input to PCS	537 KWT
Net electrical output	38.9 KWE
Overall system efficiency	7.2 %
Radiator NaK ΔT	179°F

DESCRIPTIVE FEATURES

Turbine aerodynamic efficiency - 55.9%
Turbine inlet pressure - 248 psia
Turbine exhaust pressure - 11.8 psia

Figure 4-3 State-Point Diagram for 35-kWe Power Conversion System (Off-Design Conditions: Reactor Outlet Temperature at Lower End of Deadband Control, and Shade Environment)

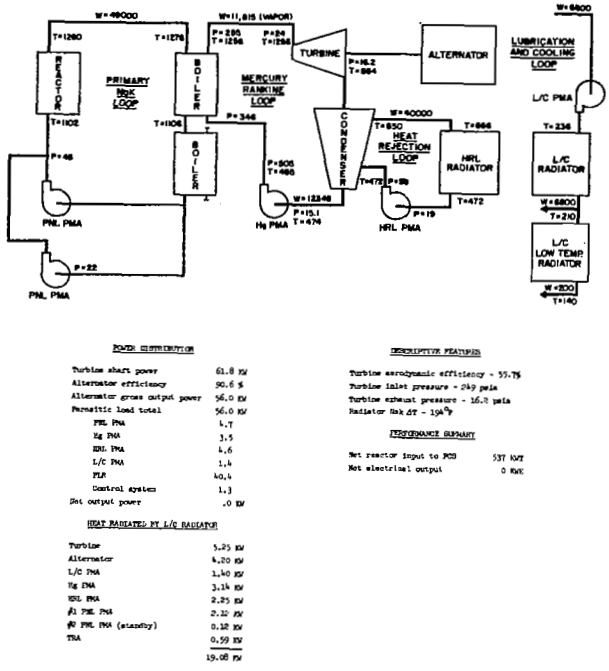

POWER DISTRIBUTION

Turbine shaft power	61.8 kW
Alternator efficiency	90.6 %
Alternator gross output power	56.0 kW
Parasitic load total	56.0 kW
PNL PMA	4.7
Hg PMA	3.5
HRL PMA	4.6
L/C PMA	1.4
PLR	40.4
Control system	1.3
Net output power	.0 kW

HEAT RADIATED BY L/C RADIATOR

Turbine	5.25 kW
Alternator	4.20 kW
L/C PMA	1.40 kW
Hg PMA	3.14 kW
HRL PMA	2.25 kW
#1 PNL PMA	2.12 kW
#2 PNL PMA (standby)	0.12 kW
TRA	0.59 kW
	19.08 kW

DESCRIPTIVE FEATURES

Turbine aerodynamic efficiency - 55.7%
Turbine inlet pressure - 249 psia
Turbine exhaust pressure - 16.8 psia
Radiator NaK ΔT - 194°F

PERFORMANCE SUMMARY

Net reactor input to PCS	537 kWt
Net electrical output	0 kWe

Figure 4-4 State-Point Diagram for 35-kWe Power Conversion System (Off-Design Conditions: Reactor Outlet Temperature at Lower End of Deadband Control, and No Vehicle Load)

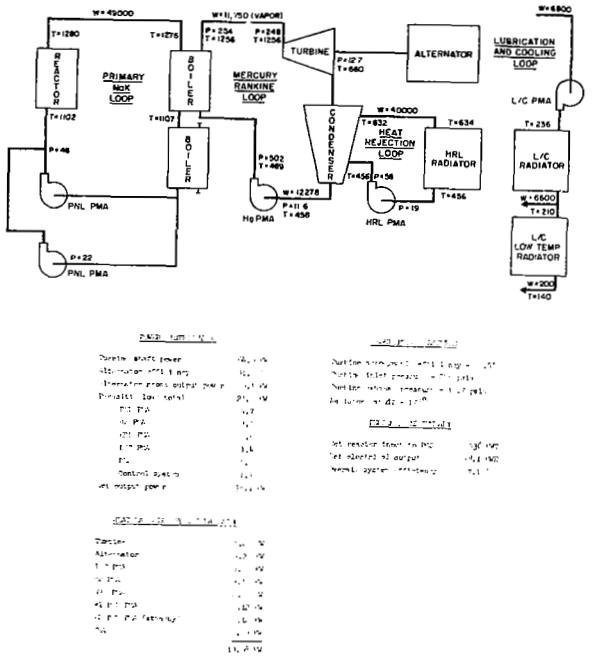

Figure 4-5 State-Point Diagram for 35-kWe Power Conversion System (Off-Design Conditions: Reactor Outlet Temperature at Lower End of Deadband Control, and 10-lb Reduction in Condenser Inventory)

TABLE 4-I. 35-KWE SYSTEM OFF-DESIGN OPERATING CONDITIONS

Operating Condition	Alternator Gross Output (kWe)	Net Electrical Output (kWe)
Shade	59.9	38.9
High Reactor Outlet Temperature	58.0	37.0
No Vehicle Load	56.0	0
10 lb. Mercury Inventory Loss	59.1	38.1
Design	58.0	37.0

4.2.2 Startup and Shutdown Modes

The SNAP-8 35-kWe system must start and shut down automatically in gravitational fields ranging from zero gravity to 1 g under differing initial conditions. The system must undergo an initial startup when the system fluids and components are "cold;" that is, at temperatures on the order of (but not below) 50°F. During this startup, the entire mercury inventory must be injected into the Rankine-cycle loop. The system must be capable of restarting automatically under temperature conditions similar to the initial startup, or under elevated temperature conditions resulting from a shutdown after system operation. During a system restart, the full loop inventory is not injected since the inventory located between the condenser outlet and boiler inlet isolation valves is not removed from the loop. Two types of shutdown are required. The first is a normal shutdown which is a gradual, controlled shutdown sequence required by predetermined test planning or in the event of minor system operating difficulties. The second is an emergency shutdown which is a rapid, controlled shutdown sequence resulting from indicated potential major system operating difficulties*. During a normal shutdown, the resulting system transients are gradual and within specified limits so that at least 20 such shutdowns can occur. During emergency shutdowns, however, the system transients are more severe so that only a very limited number are permitted. The primary purpose of the emergency shutdown is to limit the effects of potential major system operating difficulties and thereby maintain the integrity of the overall system.

* Potential major system operating difficulties include indication of loss of flow in the primary or heat rejection loops, turbine overspeed and underspeed, and condenser overpressure.

Extensive system dynamic studies were conducted to determine the proper startup and shutdown procedures for the 35-kWe system. These studies were also used to determine requirements for hardware and control components needed during startup and shutdown. The results of these studies are discussed in detail below. The detailed startup, normal shutdown, and emergency shutdown procedures were determined from the results of these system dynamic studies.

4.2.3 System Transients

4.2.3.1 Startup

During the development of the SNAP-8 system, the startup requirements were changed a number of times from an initial requirement for a single startup in space under zero-gravity conditions for an instrumented-rated system, to a multiple restart under zero to one gravity conditions for a man-rated system. To formulate system startup procedures which would result in acceptable transients for both the power conversion system and the nuclear system, dynamic studies were conducted using computer simulations of the system or significant portions of the system. Initial simulations for both the power conversion system and nuclear system were programmed on analog and hybrid computers, and studies were closely coordinated with Atomics International, the nuclear system contractor. Complementary studies were also conducted by Atomics International in which more detailed reactor simulations were used. The results of studies conducted by Atomics International are reported in References 12 and 13, and in various SNAP-8 reactor system progress reports prepared by Atomics International for the AEC.

Initial system startup studies were aimed primarily at defining procedures which would result in reactor temperature and power transients that would not exceed limitations established by the nuclear system contractor, and which would assure adequate net positive suction head for the mercury pump. The nuclear system limitations are shown in Table 4-II and Figure 4-6. The results of the studies conducted at Aerojet are presented in Reference 14, along with plots of typical system transients and preliminary requirements for hardware and control components associated with startup. The initial startup studies were conducted for a system required to start automatically only once and with no rigid shutdown requirements other than to scram the reactor. Therefore, some of the hardware and controls requirements generated from these studies, such as condenser temperature control valve, mercury injection system, and certain programmer functions, were of limited usefulness. However, the procedures developed from the studies kept system transients within the allowable limits and formed the basis for subsequent studies following changes in startup and shutdown requirements.

The change in requirements to a multiple startup and shutdown system for manned missions necessitated additional, expanded system dynamic studies. A digital computer simulation of the system was programmed and used to conduct studies for defining procedures and hardware requirements for a restartable system.

TABLE 4-II. SNAP-8 NUCLEAR SYSTEM OPERATING LIMITATIONS

Parameter	Minimum	Nominal	Maximum Steady	Maximum Transient
Thermal Power (kW)	NA	600	600*	675 (scram @ 750)
Outlet Temperature (^{o}F)	NA	1300	1330	1450 (scram @ 1400)
Inlet Temperature (^{o}F)	NA	1100	NA	1300
Core Temperature, ΔT (^{o}F)	--	200	NA	NA
NaK Flow (lb/hr)	(scram @ 10,800)	48,800	65,000	70,000
NaK Pressure in Reactor (psia): Operating	35		50	75
800-1300^{o}F	20		50	75
<800^{o}F	10		50	75
Rate of Change of NaK Temperature (^{o}F/min)	NA	NA	±150 (1 min or more)	(See Fig. 4-6)
Step Change in Temperature into Plenum (^{o}F)	NA	NA	NA	10
Number of Thermal Cycles, > 50^{o}F *	NA	NA	150	NA

* This limit does not include normal deadband cycling

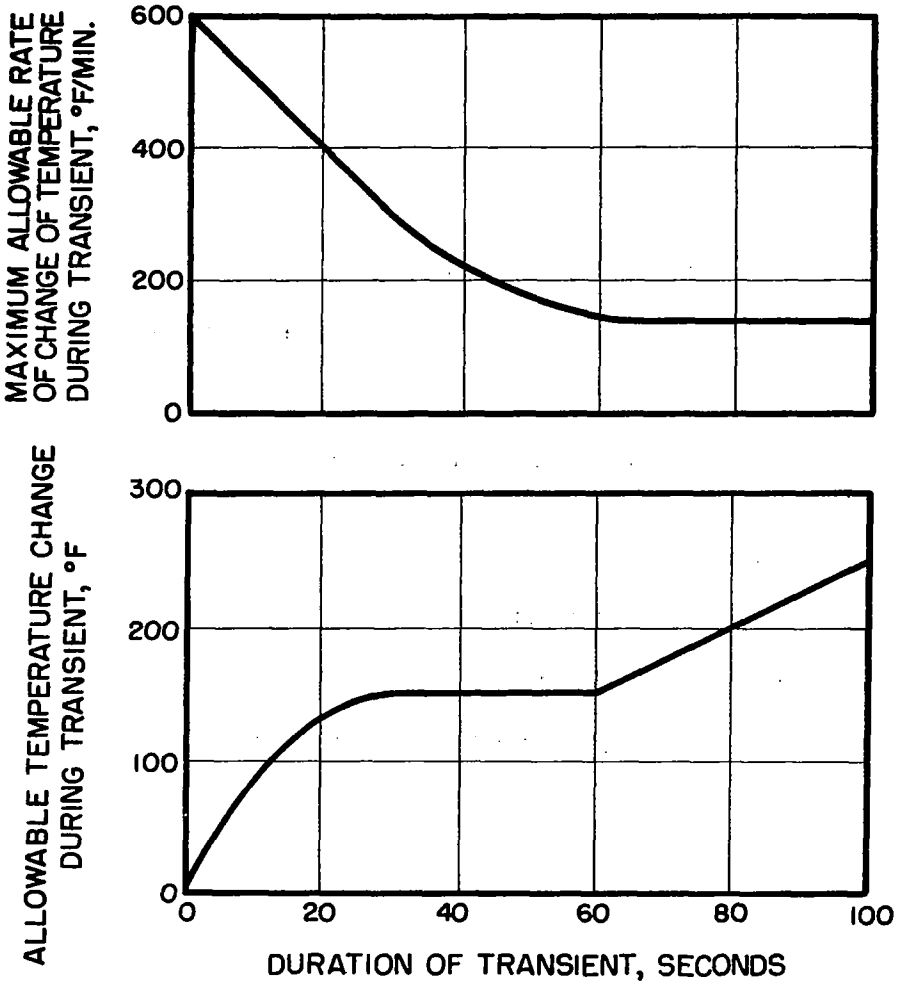

Figure 4-6 Allowable NaK Temperature Transients at Reactor Inlet and Outlet

The studies conducted to define a restartable system were based primarily on the following criteria:

- 20 starts without servicing
- 100 start cycles (servicing permissible)
- Both man-rated and instrument-rated concepts considered
- Zero- to 1-g operation
- Fully automatic startup and shutdown
- Restart after controlled and certain emergency shutdowns
- Comply with latest reactor constraints
- Utilize operating requirements and characteristics of existing hardware
- Utilize existing hardware where possible
- Restrict motion of mercury during launch and maneuver
- Contain mercury after shutdown
- Restart system to be readily adaptable for mercury inventory trim
- Boiler conditioned to permit self-sustained operation
- Turbine or vapor line preheat using mercury vapor not required
- Mercury loop evacuated and sealed prior to initial startup
- Power conversion system to be capable of more than one startup attempt
- Restart system design should not require flight verification test
- Suitable with redundant power conversion systems

The startup procedure developed for the restartable system was based on methods devised for earlier versions of the systems. The major steps in the startup process are:

(1) Flow is initiated in the primary and heat rejection loops at low levels. Pump power is provided by a battery-powered inverter. The reactor is started and brought up to nominal operating temperature at a low power level.

(2) After reactor transients have settled, the primary loop flow is increased to approximately 50% rated in preparation for power conversion system startup.

(3) The power conversion system is started by injecting mercury into the Rankine-cycle loop. The mercury flow is gradually increased and the turbine-alternator starts to accelerate.

(4) As the turbine-alternator accelerates and reaches approximately 50% rated speed, all pump motor loads are transferred from the inverter to the alternator. The turbine-alternator continues to accelerate thereby increasing the speed of the pumps and increasing flow rates in all loops until rated speed is obtained. This procedure is referred to as a "bootstrap" process.

(5) As the turbine-alternator reaches rated speed, the mercury flow is brought to a level at which sufficient electrical power is generated to operate all system pumps and controls. Mercury flow is maintained at this self-sustaining level until reactor transients have settled.

(6) The mercury flow is increased gradually to the rated value and net electrical output is increased until rated power is produced. Electrical power may then be supplied to the vehicle.

System and component transients determined for the startup procedures investigated were compared with acceptable values for various critical parameters. The most stringent limitations are those associated with the reactor, as shown in Table 4-II and Figure 4-6, so that the rate of change of reactor coolant temperature and reactor peak power are the most critical parameters. A typical startup transient for a situation in which mercury is injected at a rapid rate thereby producing the most severe reactor temperature and power transients, is shown in Figure 4-7. The 35-kWe system, designed with two power conversion systems for redundancy, incorporates two boilers in series in the primary NaK loop. Therefore, because of thermal and transport lags, the startup transients imposed on the reactor will be different, depending on which power conversion system (and therefore which boiler) is operated during startup. The reactor transients when operating the two different boilers on startup are compared in Figure 4-8. For this comparison, the programmed mercury injection into the two boilers was the same. The results show that injecting mercury into the boiler closest to the

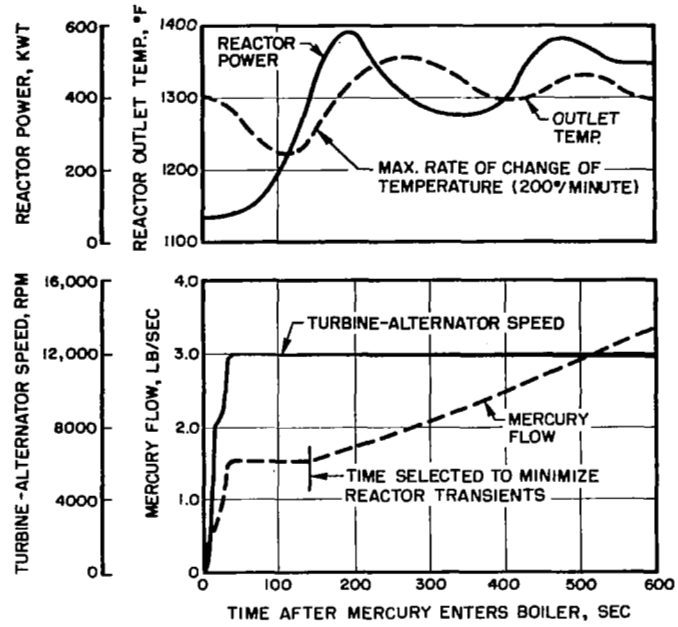

Figure 4-7 Typical Startup Transient for 35-kWe System with Rapid Initial Mercury Injection

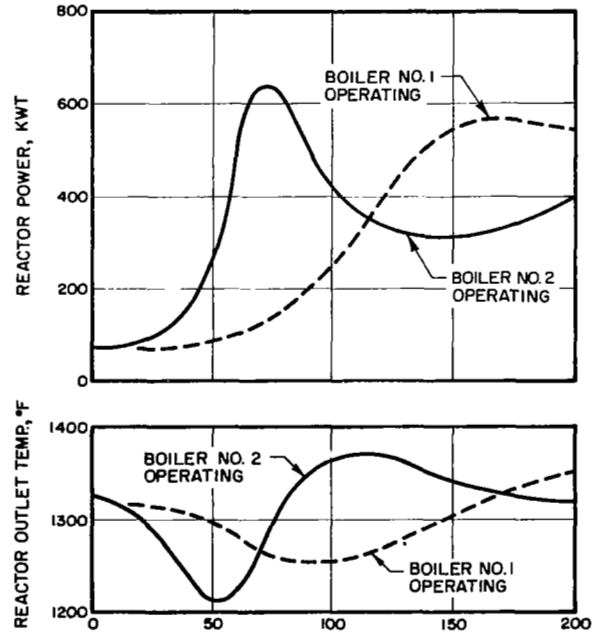

Figure 4-8 Comparison of Reactor Transients When Injecting Mercury Into the Two Boilers of the 35-kWe System

the reactor inlet produces the most severe transients. The startup transients imposed on the reactor are summarized in the table below which shows that acceptable values are obtained during startup with either boiler operating.

	Rate of Change of Reactor Temperature		Maximum Reactor Outlet Temp. (°F)		Peak Power (kWt)	
Unit	Allowed	Computed	Allowed	Computed	Allowed	Computed
Boiler 1	300°F/min in 30 sec	190°F/min in 30 sec				
	500°F/min in 5 sec	190°F/min in 5 sec	1375	1355	675	560
Boiler 2	300°F/min in 30 sec	250°F/min in 30 sec				
	500°F/min in 5 sec	395°F/min in 5 sec	1375	1368	675	640

The startup studies and resultant transients described above were based on reactor constants obtained from design studies and evaluation of early reactor test results as supplied by Atomics International. The results of subsequent tests with a reactor of modified design indicated that certain reactor constants had to be changed so that additional startup studies were required. The additional studies were expanded to include a set of conditions which would test the validity of the startup procedure and the control component characteristics to produce acceptable transients when extreme conditions are imposed on the system (i.e., when a combination of system conditions will produce transients which approach or tend to exceed the limits set for various critical parameters). The results of the computer runs made to test these limiting conditions are shown in Table 4-III, and are presented as margins of safety (i.e., a percentage of the maximum allowable value) for the critical parameters when the margin of safety is defined by the relationship:

$$\text{Margin of safety } (\%) = \frac{\text{maximum allowable value - computed value}}{\text{maximum allowable value}} \times 100$$

Therefore, a negative margin of safety indicates that an allowable value for a critical parameter has been exceeded. The results shown in Table 4-III indicate that the maximum allowable reactor temperature and the reactor peak power parameters are exceeded under certain conditions when the latest reactor constants were used in the computer simulation. These results indicate that some modifications to the startup procedure or reactor control characteristics may be required. Plots of the computed transients and a discussion of the results and analytical techniques used in this study are contained in Reference 15. The results of these startup studies formed the basis for a series of tests conducted by Aerojet in the 35-kWe system test loop and at the NASA/LeRC SNAP-8 system test facility. The results of the startup tests conducted by Aerojet are discussed in Section 4.3.3.

TABLE 4-III MARGINS OF SAFETY FOR CRITICAL SYSTEM PARAMETERS

Parameter	Maximum Allowable Value	Reactor Limit Test Boiler 2	Turbine-Alternator Limit Test Boiler 1	Condenser Limit Test Boiler 2
Reactor Inlet, $\dot{T}_5$ (1)	9.17°F/sec	+69%	+89%	+70%
Reactor Inlet, $\dot{T}_{30}$ (2)	5.0°F/sec	+50%	+82%	+54%
Reactor Outlet, $\dot{T}_5$	9.17°F/sec	+70%	+93%	+72%
Reactor Outlet, $\dot{T}_{30}$	5.0°F/sec	47%	+85%	+52%
Reactor Outlet Temperature	1375°F	-2%	+4%	-2%
Reactor Power	675 kW	-12%	+51%	-6%
Condenser Pressure	40 psia	+63%	+84%	+55%
Radiator Inlet	700°F	+14%	+20%	+4%
Mercury Pump Suction Specific Speed	14,700	+15%	+50%	+30%

(1) Maximum rate of change of temperature in a 5-second period

(2) Maximum rate of change of temperature in a 30-second period

Extensive system testing was conducted at the NASA-LeRC SNAP-8 test facility to investigate significant startup parameters. Two of the most significant investigated were the initial rate of increase of mercury flow during the turbine-alternator acceleration period, and the rate of increase of mercury flow up to the time when rated net electrical output is produced.

The initial rate of increase of mercury flow (the initial mercury flow ramp) is maintained until a flow level (the self-sustaining flow) is reached which will result in the generation of sufficient electrical power to operate all system pumps and electrical controls. The initial mercury flow ramp is a function of the mercury flow control valve characteristics and the acceleration characteristics of the turbine-alternator. The turbine-alternator acceleration characteristics are significant because the system pumps are transferred to the alternator output from the inverter when the alternator frequency exceeds the inverter frequency (approximately 50% of the rated alternator frequency). Once the pump motors have been transferred to the alternator output, the turbine-alternator will "bootstrap" to rated speed; that is, the mercury flow will increase due to increased mercury pump pressure resulting from increased pump speed. A range of initial mercury flow ramps exists which will result in acceptable system transients. The shortest initial mercury flow ramp (greatest rate of flow increase) is determined by the boiler mercury inlet pressure buildup and the resulting reactor temperature transients. The longest initial mercury flow ramp (slowest rate of flow increase) is determined by the capability to sustain the bootstrap process; that is, if mercury is introduced too slowly, the turbine-alternator will not produce sufficient power to continue acceleration after the pump motor loads have been transferred to the alternator output.

The results of startup tests conducted at the NASA-LeRC SNAP-8 test facility show that initial mercury flow ramps extending over time periods between 80 and 140 seconds are acceptable. Initial mercury flow ramps shorter than 80 seconds in duration are not desirable since they prohibit the use of an open-loop flow control and can result in unacceptable transients. Initial mercury flow ramps longer than 140 seconds in duration are not acceptable since marginal turbine-alternator acceleration occurs. A more detailed discussion of these tests and plots of the resulting transients are presented in Reference 16.

The rate of increase of mercury flow from the self-sustaining value to rated value is significant since the condenser pressure must be maintained close to the steady-state value during this period. If the condenser pressure becomes low, mercury pump suction pressure can be reduced to the point where cavitation can occur when operating in a zero-gravity environment. If the condenser pressure becomes high, the turbine back pressure can be increased to the point where output power is reduced and turbine deceleration can occur. Therefore, a mercury flow ramp must be provided which is gradual enough to permit the heat rejection loop flow control valve to make the necessary NaK flow adjustments to the condenser but does not unduly extend the startup period. The results of startup tests conducted at the NASA-LeRC SNAP-8 test facility show that good control of

mercury condenser pressure is attained when a mercury flow ramp time of 900 seconds is used. Satisfactory reactor temperature and power transients are obtained when mercury flow ramp times of 500 seconds or more are used. More detailed discussion of these tests and plots of the resulting transients are presented in Reference 17.

4.2.3.2 Normal Shutdown

The change in requirements to a multiple startup and shutdown system introduced the need for detailed studies of shutdown transients from which procedures, control requirements, and associated hardware requirements could be formulated. The shutdown transients investigated included not only those occurring as a result of power conversion system shutdown, but also those resulting from the nuclear system shutdown and the effects of the decay heat generated by the reactor.

The transients associated with the power conversion system shutdown portion of the overall system shutdown were investigated primarily with the aid of a digital computer program. The shutdown process generally resembles the startup process, but in reverse. The procedure basically involves controlled reduction of mercury flow by means of the mercury flow control valve. An idealized plot of mercury flow as a function of time is shown in Figure 4-9. The major steps in the process are:

(1) A gradual reduction in mercury flow to a value which will provide sufficient power to operate the system on the electrical output of the alternator. During this period, reactor power is reduced to an intermediate level and the reactor power and temperature transients produced are well within the limitations established by nuclear system contractor.

(2) A period of constant mercury flow, at a level to permit self-sustained system operation. This period, labelled as the "plateau" condition on Figure 4-9, allows for stabilization of the reactor power and temperature transients before additional, more severe transients are imposed.

(3) A rapid reduction in mercury flow to a low value adequate to maintain a condensing pressure high enough to permit returning most of the mercury loop inventory to the mercury reservoir. During this period, the turbine-alternator will decelerate to a speed at which the alternator frequency matches the frequency of the pump inverter and the pump electrical loads will be switched to the inverter thereby operating the system pumps at reduced speed.

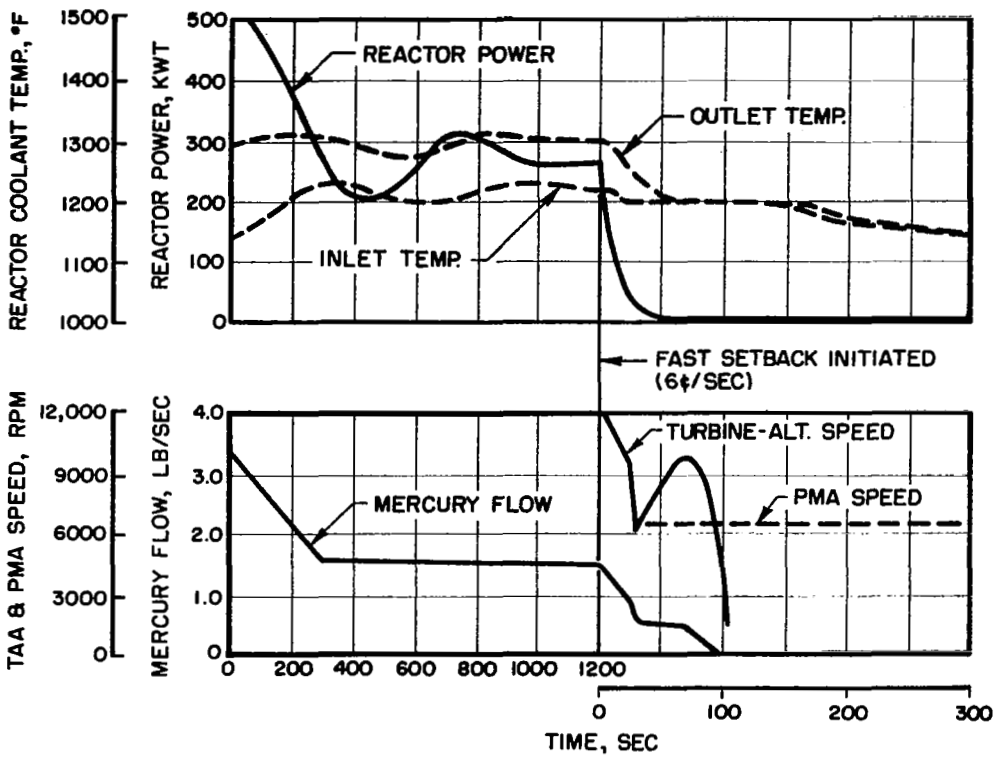

Figure 4-9 Idealized Mercury Flow Profile During Normal Shutdown

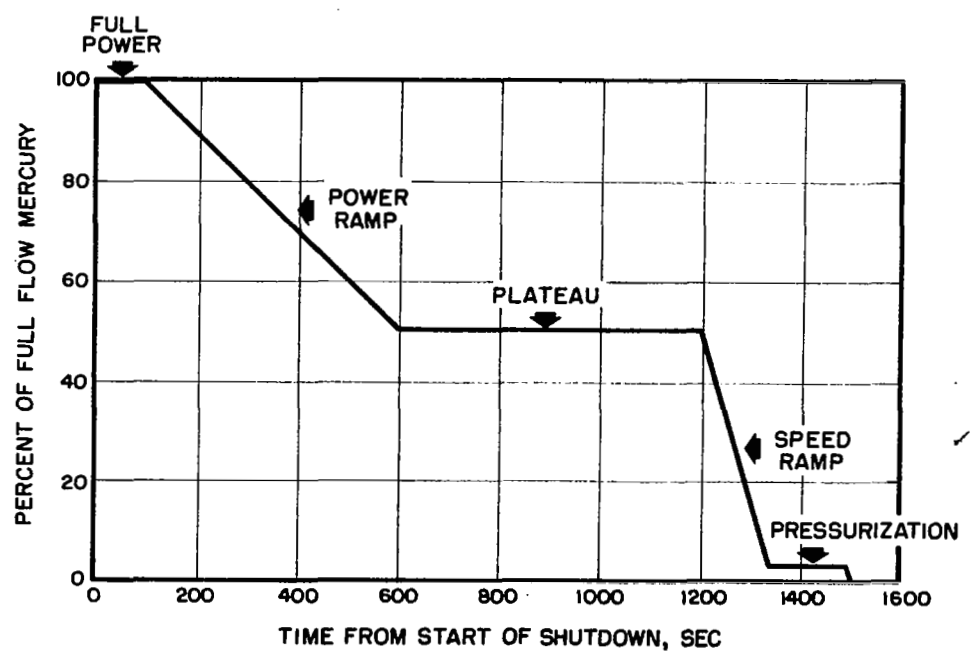

Figure 4-10 Typical Calculated Transients During Normal Shutdown

(4) A period of low mercury flow (3 to 5% rated flow) when the loop inventory is returned to the mercury reservoir. At the end of this period, the mercury flow control valve and mercury loop isolation valves are closed and the reactor is programmed on a "fast setback" mode.

(5) Primary and heat rejection loop flows are continued at low values for an extended period of time to remove the fission product decay heat generated in the reactor.

Typical shutdown transients obtained using a digital computer simulation are shown in Figure 4-10. The significant transients are those occurring during the first 1200 seconds when mercury flow and reactor power are gradually reduced and the reactor power and temperature transients are permitted to stabilize. The second portion of the transients shown in Figure 4-10, those after 1200 seconds, were superseded by later detailed studies.

Typical reactor and primary-loop transients obtained from this latter phase of shutdown are shown in Figure 4-11 for a simulation including the latest reactor constants obtained from the nuclear system contractor. The transients indicate that the maximum allowable reactor temperature is exceeded thereby requiring some modification of the shutdown procedure. Mercury-loop transients associated with this same shutdown period are shown in Figure 4-12 in which mercury flow to the boiler, turbine-alternator speed, and condenser conditions are plotted. The plot of condenser inventory indicates how the mercury loop inventory is returned to the mercury reservoir during this phase of shutdown. The plot of condenser inlet pressure indicates how pressure is maintained in the condenser at the very low mercury flows by the action of the heat rejection loop flow control valve.

Additional shutdown studies, particularly those associated with the reactor decay heat removal portion of system shutdown, were conducted with the aid of the digital computer program TAP (Thermal Analyzer Program) which provided a simplified simulation of the power conversion system and a more detailed simulation of the nuclear system. A description of TAP, a guide to the use of the program, and the simulation of several key elements used for the SNAP-8 system simulation are contained in Reference 18. The results of studies to determine flow requirements in the primary and heat rejection loops for removing reactor decay heat following the reactor "fast setback" shutdown period indicate that the primary loop and heat rejection loop NaK pumps should be operated at a frequency that provides approximately 20% rated flow in the primary loop. Flows of this magnitude must be maintained for a period of at least 1.5 hours to reduce reactor temperatures to acceptable values (on the order of 1000°F). Following this 1.5-hour period, the following possible courses of action exist:

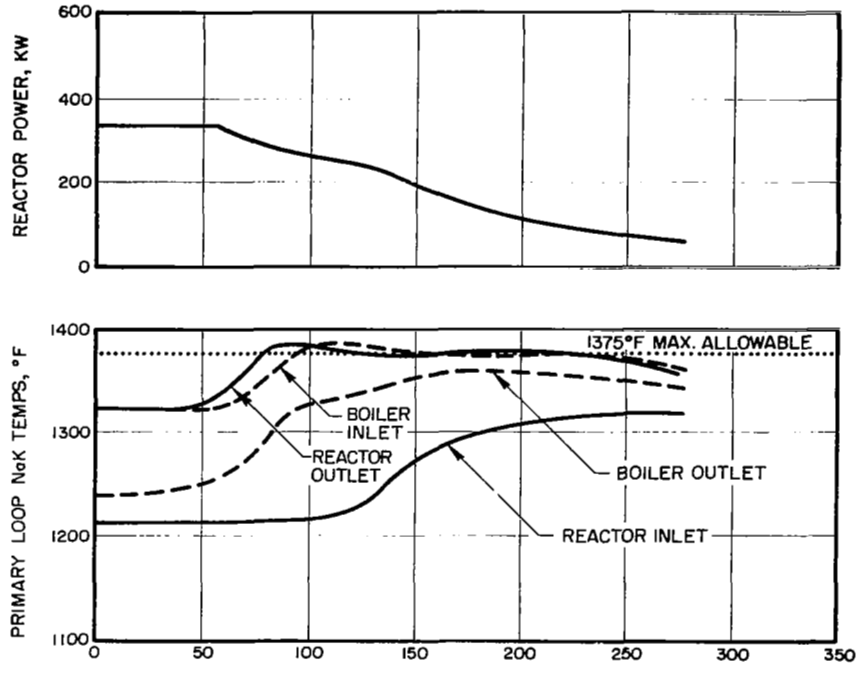

Figure 4-11 Calculated Primary Loop Transients Occurring During Final Phase of Normal Shutdown (Using Latest Reactor Test Constant)

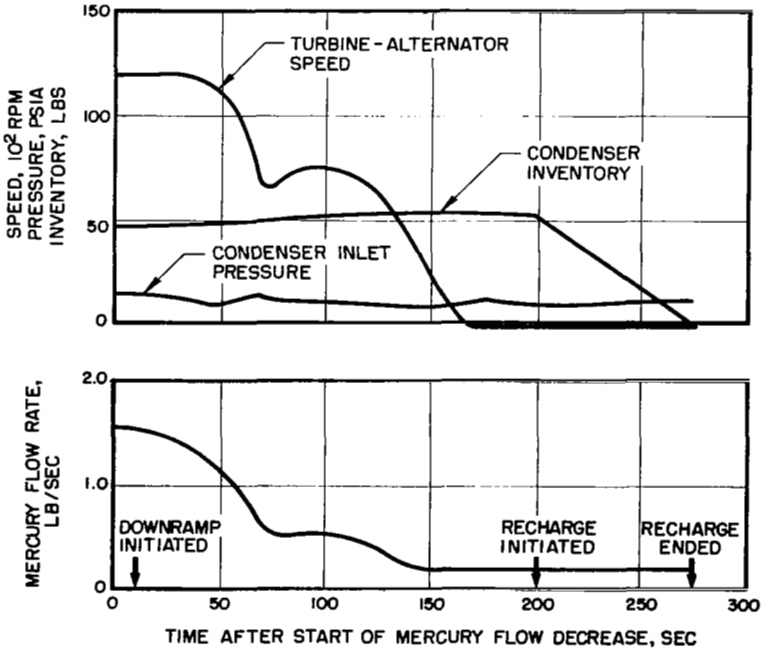

Figure 4-12 Calculated Mercury Rankine-Cycle Loop Transients Occurring During Final Phase of Normal Shutdown

(1) Continue operation of primary loop and heat rejection loop NaK pumps at a speed corresponding to approximately 20% rated flow for an additional, minimum time of 4.5 hours.

(2) Continue operation of the primary loop NaK pump only for an additional minimum time of seven hours.

The first will reduce reactor temperatures to a level substantially below the maximum 1100°F limit established by nuclear system contractor as a safe isothermal temperature for extended periods of time after shutdown. The second course of action will reduce reactor temperature initially to a level below the 1100°F isothermal temperature limit with a subsequent rise in temperature to approximately 1100°F after all pumping is stopped. Figure 4-13 shows the peak temperatures that will occur at the reactor inlet or outlet when all pumping is stopped at various times after the reactor "fast setback" has been completed.

An analysis of these actions was conducted with the assumption that the reactor would have a view of space or a cold wall for rejecting some heat by radiation. With the introduction of the 4-pi shielded configuration, the operation of the primary loop and heat rejection loop NaK pumps should be extended to assure adequate reactor cooldown. A system shutdown sequence was formulated which provides a conservative allowance for operation of the NaK pumps at reduced flows for a period of eight hours after reactor shutdown. Additional studies should be conducted to determine whether or not the period of pump operation could be shortened to reduce battery power requirements.

4.2.3.3 Emergency Shutdown

The requirements to provide a system with multiple startup and shutdown capabilities for use in a combined system test and manned-mission applications emphasized the need for studies to determine the severity of transients imposed by emergency situations, and to establish ways to reduce the transients by employing appropriate corrective actions. The scope of the emergency shutdown study was limited to those situations which could result in excessive reactor transients or produce conditions which may jeopardize the integrity of the system fluid loops or components.

A qualitative evaluation of potential emergency shutdown situations indicated that the most severe situations would occur if loss of flow occurred in either the primary loop or the heat rejection loop. Loss of flow in the primary loop eliminates the possibility of removing reactor heat either during a rapid shutdown or as a result of the decay heat generated by fission products. Loss of flow in the heat rejection loop eliminates the possibility of rejecting heat which is generated in the reactor or transferred to the mercury loop. Therefore, studies were conducted to determine transients primarily associated with the reactor as a result of loss of flow in either NaK loop. The most rapid rate of decrease of NaK flow occurs in conjunction with a NaK pump failure involving an impeller or rotor seizure.

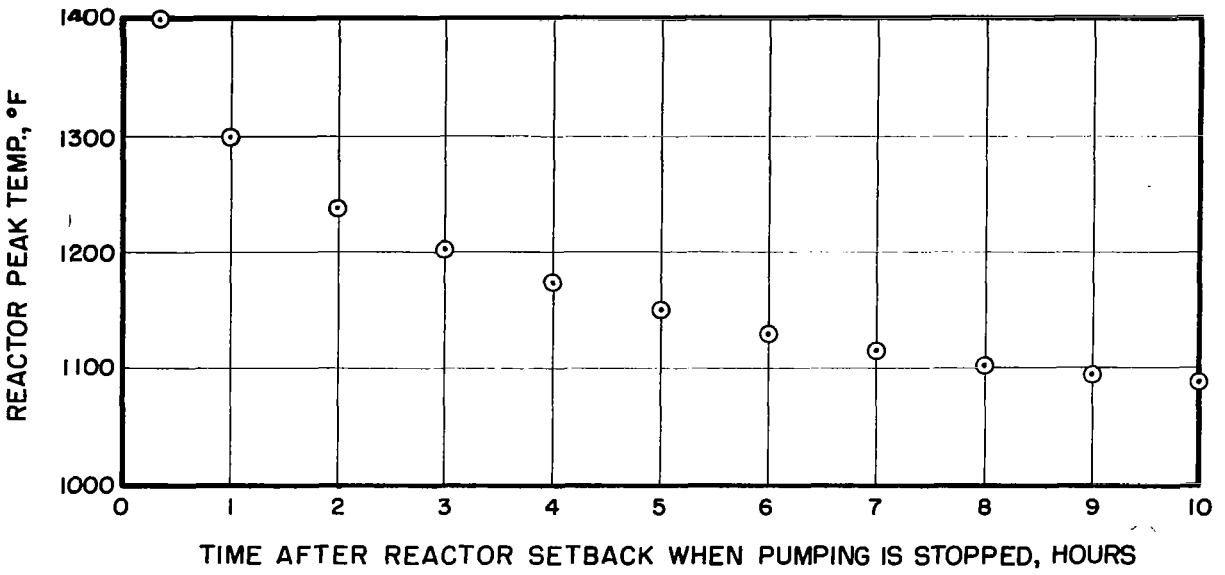

Figure 4-13 Peak NaK Temperatures at Reactor Inlet or Outlet Occurring After All Pumping is Stopped

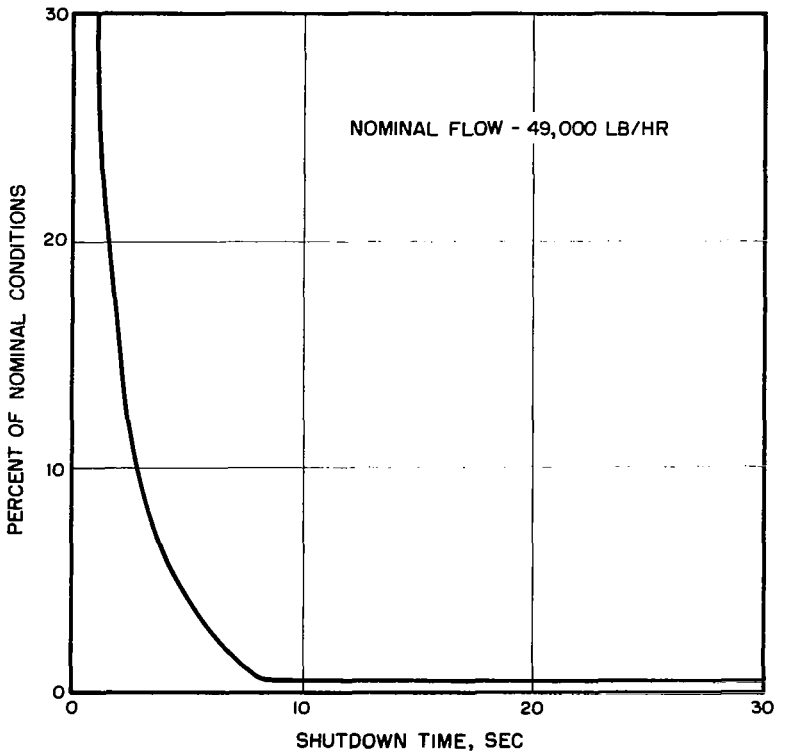

Figure 4-14 NaK Flow Decay Curve Resulting from Pump Stoppage

A NaK flow decay curve resulting from such an incident was obtained from test data and is shown in Figure 4-14. The flow decay curve was used in studies to determine transients involved in loss-of-flow incidents. The studies were conducted with the aid of the previously mentioned TAP digital computer program.

The initial results of studies to determine the effects of loss of primary loop flow showed that high rates of temperature changes (50°F/sec) in the reactor accompanied the rapid initial decrease in flow and that high maximum temperatures (>1650°F) will be produced at the reactor outlet. The longer the flow decrease persists without some corrective action being taken, the higher the maximum temperature at the reactor outlet will be. If loss of flow is detected, a reactor "fast setback" is initiated and the redundant NaK pump is started as a corrective action; the maximum temperature at the reactor outlet can be reduced to acceptable values (<1475°F). Typical results from this study are shown by the flow and temperature plots in Figure 4-15 which also shows the assumed flow decay curve.

Since the redundant NaK pump may not always be available for the corrective action, a more positive means of assuring NaK flow is to supply a backup pump with a reduced flow capability. Typical reactor temperature transients for a system employing this type of corrective method are shown in Figure 4-16. High initial rates of temperature change occur in the reactor, but the maximum temperature can be kept within allowable values if a backup pump with a flow capability about 20% of rated flow is used. This method has been recommended and is incorporated in the emergency shutdown procedure formulated for the system.

The studies conducted to determine the effects of loss of heat rejection loop flow were based on the assumption that, when a loss of flow is detected, the power conversion system would be shut down and the reactor started on a fast-setback mode. Two types of cases were studied for incidents involving loss of heat rejection loop flow. For the first type, it was assumed that the overall system would contain redundant power conversion systems so that flow could be initiated in the heat rejection loop of the redundant power conversion system at a level consistent with the low-frequency speed of the pump inverter (approximately 20% of rated flow). If the overall system did not contain a redundant power conversion system, a backup pump could be used to supply an equivalent flow. For the second type of flow-loss incident, it was assumed that no redundant power conversion system or heat rejection loop backup NaK pump would be available to supply flow following loss of flow. In both cases, it was assumed that a backup pump was available to supply approximately 20% flow in the primary loop following the power conversion system shutdown.

Reactor temperature transients resulting from these two cases are shown in Figure 4-17. Initial rapid rates of temperature change occur at the reactor outlet (50°F/sec) as a result of the primary loop flow decrease as the power conversion system is shut down and peak temperatures are

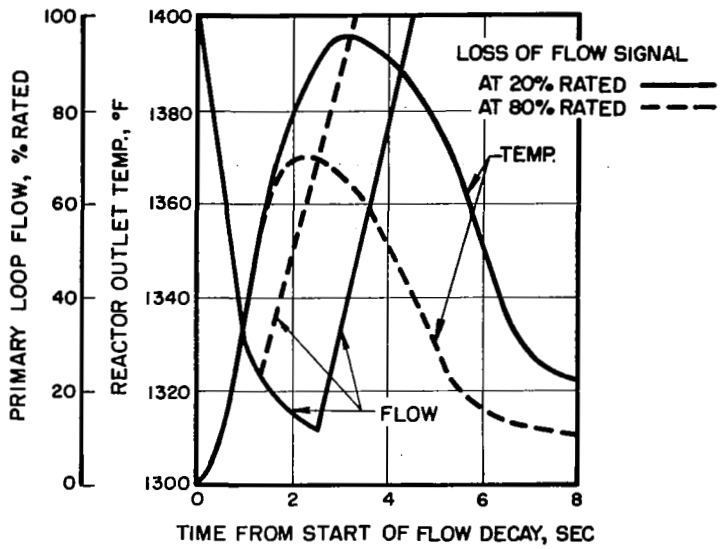

(1 SEC DELAY TO START OF ACCEL.)
(2 SEC PMA ACCEL. TIME)

Figure 4-15 Reactor Temperature Transients Resulting From Loss of Primary Loop Flow and Subsequent Starting of Redundant Pump

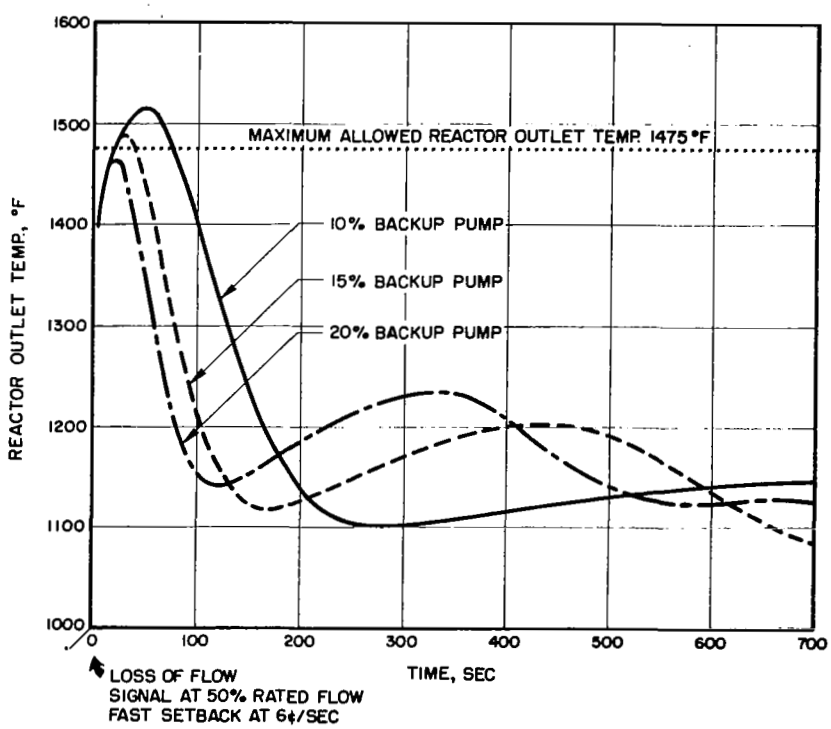

Figure 4-16 Reactor Temperature Transients Resulting From Loss of Primary Loop Flow and With Various Amounts of Backup Flow Capability

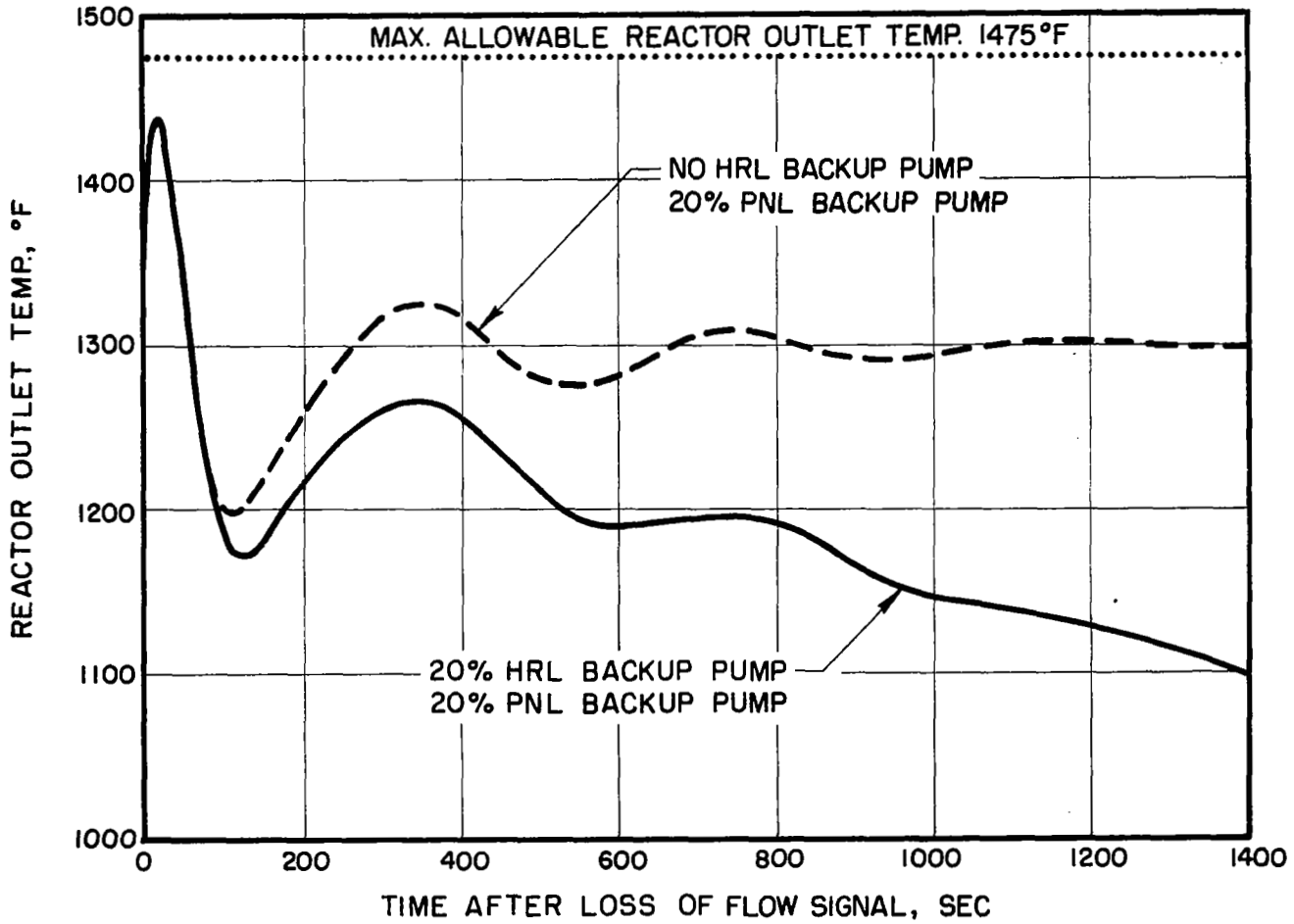

Figure 4-17 Reactor Temperature Transients Resulting From Loss of Heat Rejection Loop Flow, and with Various Amounts of Backup Flow Capability

limited to acceptable values by the primary loop backup NaK pump flow. For the case with no heat rejection loop backup pump, the reactor tends to become isothermal at temperatures around 1300°F, which is not desirable. For the case with heat rejection loop backup pumping, satisfactory reactor temperatures are maintained; that is, peak temperatures are less than 1475°F, and the reactor isothermal temperature is less than 1100°F. A shutdown procedure providing for a heat rejection loop backup pumping capability of approximately 20% of rated flow has been recommended.

A limited number of system shutdown tests was conducted at the NASA/LeRC SNAP-8 test facility including tests to simulate loss of heat rejection loop flow. The test results are discussed and plots of the system transients are presented in Reference 19. The results of these tests show that the system can be shut down rapidly without exceeding the reactor temperature limitations if primary-loop NaK flow can be maintained at a reduced level following shutdown of the power conversion system.

Other incidents (such as condenser overpressure, turbine-alternator overspeed, and alternator undervoltage) can also precipitate emergency shutdowns, but the emergency shutdown procedure is the same in all instances. Detailed studies of these other types of emergency situations were not conducted but would be included in more comprehensive safety studies which would be performed before initiating combined system tests. The safety studies would also include additional studies of the loss-of-flow incidents which would result in some refinements to the emergency shutdown procedure and equipment.

4.2.4 Restart System Component Studies

The system startup and shutdown studies conducted with the digital computer simulation were used to define hardware and control component requirements as well as to define the procedures and transients involved. Additional related studies, both qualitative and quantitative, were needed to adequately define the restart system component requirements. The restart system components consist of the mercury reservoir and actuating device, the mercury flow control valve, solenoid valves to direct the flow of mercury to and from the Rankine-cycle loop, and the heat rejection loop flow control valve to control condenser conditions.

A major item in the definition of the overall start system has been the mercury injection system which basically includes the mercury reservoir and the actuating method for expelling mercury from the reservoir. During the development of the SNAP-8 system, the mercury injection system has undergone a number of design iterations with the identification of the point for injecting mercury into the Rankine-cycle loop being a significant factor. The injection point may either be downstream of the mercury pump (thereby requiring a high-pressure system to inject mercury at pressures slightly greater than the pump discharge pressure), or upstream of the mercury pump (thereby requiring a low-pressure system to inject mercury at pressures sufficient to meet the pump suction pressure requirement.)

In the early stages of system development when a single startup was required, the relatively simple startup system shown in Figure 4-18 was devised which consisted of a regulated, gas-pressurized mercury reservoir. During injection, mercury flow to the boiler was metered at the proper rates by the mercury flow control valve. During injection, back-flow through the mercury pump was prevented by the check valve located at the pump discharge. When the loop inventory had been injected, the mercury pump circulated the flow through the loop and the valve at the pump discharge since pump pressure then becomes greater than the injection system pressure. A temperature control valve located at the condenser NaK outlet assured adequate mercury pump suction pressure when the pump is required to circulate the mercury. The temperature control valve regulated the flow of NaK coolant to the condenser thereby controlling condensing temperature and pressure which is the primary factor in determining mercury pump inlet pressure. Components for this system were used during tests conducted with the 35-kWe system at Aerojet.

Upgrading SNAP-8 to a man-rated system with the capability for multiple starts and shutdowns, including the ability to cope with emergency shutdown situations, required a reevaluation of the basic startup concept and components. The reevaluation took the form of qualitative and quantitative studies with several iterations performed to account for additional functions required of the restart system and changes in state-point conditions and system configuration.

Early restart system concepts, preliminary startup and shutdown procedures, and preliminary hardware requirements were devised for low-pressure injection systems with actuation provided by pump pressure generated by the lubricant-coolant and mercury pumps. A more comprehensive qualitative study was conducted to evaluate the relative merits of various concepts for both high- and low-pressure injection systems. The results of this study and detailed system transient studies were used to generate start-up and shutdown sequences and hardware requirements for a mercury-pump-pressurized, low-pressure restart system. During the transient studies conducted to define the requirements, it was determined that a valve more versatile and sensitive than the temperature control valve previously mentioned was needed to control NaK flow to the condenser during startup and shutdown. Therefore, preliminary requirements were established for a heat rejection loop flow control valve which could respond to signals from the programmer and from pressure transducers located at the mercury inlet to the condenser.

Interest was revived in high-pressure injection systems which could meet the restart requirements because of the interdependence of mercury flow and turbine-alternator acceleration during critical phases of the startup sequence with low-pressure injection systems. This interdependence presented some complications in defining the mercury flow control valve orifice characteristics for the period when turbine and pump speed increase from approximately 50% rated to full speed. A qualitative study of candidate

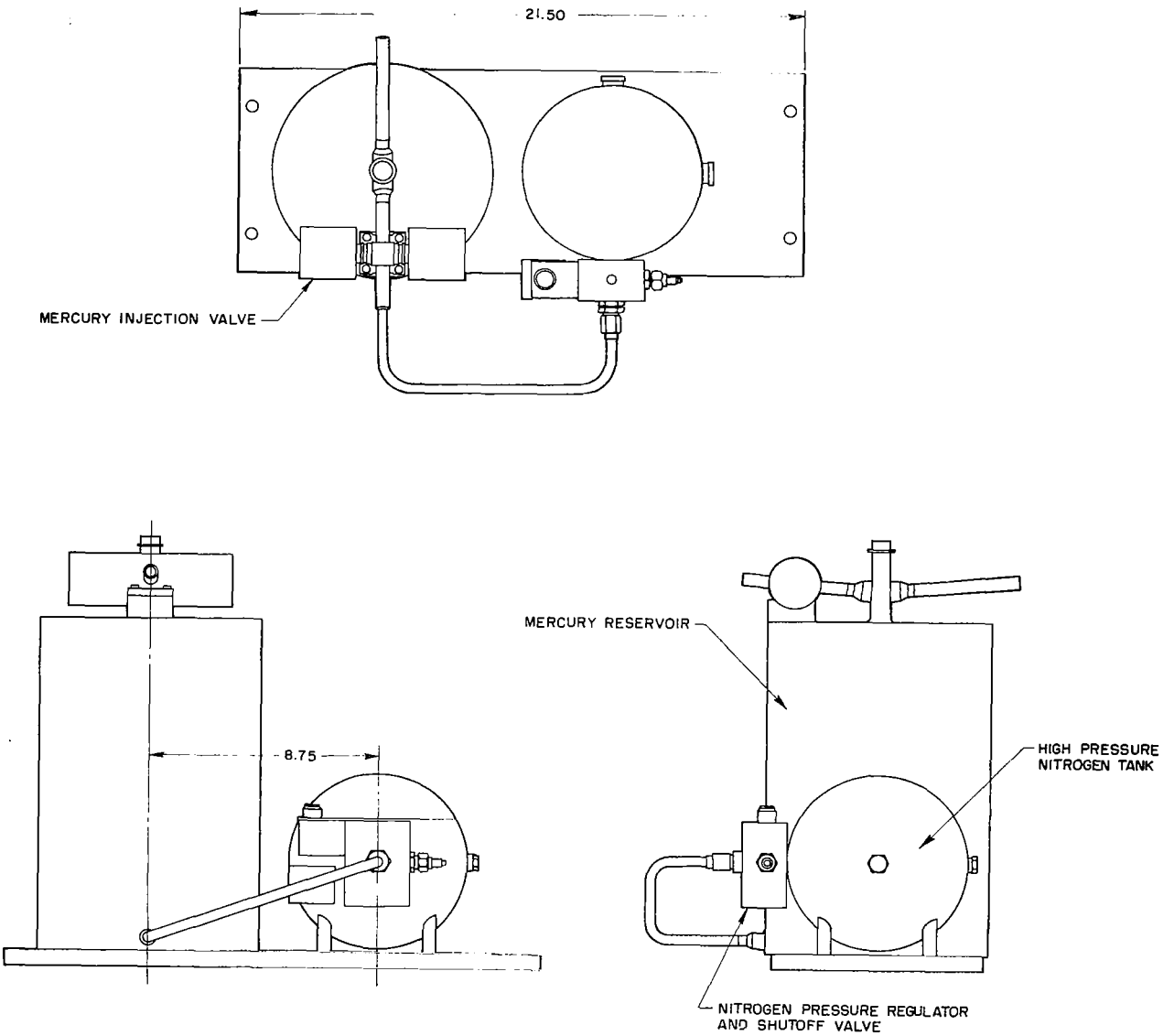

Figure 4-18 Single-Start, High-Pressure Mercury Injection System

high- and low-pressure injection systems was conducted. The results indicated that with a high-pressure injection system the mercury flow control valve characteristics could be more easily defined. Therefore, the startup and shutdown procedures and component requirements for a high-pressure injection system actuated by a separate pump-pressurized hydraulic fluid subsystem (as shown in Figure 4-19) were established.

As more information on startup transients was obtained from computer studies and test results from the 35-kWe system, it became evident that a feasible low-pressure injection system could be devised which would have advantages over a high-pressure system. An additional study of the relative merits of several candidate high- and low-pressure injection systems was conducted which included a detailed, quantitative analysis of the characteristics of the various systems and their capabilities to meet the numerous requirements of a system with restart capability. The results of the study were used (in conjunction with results obtained from 35-kWe system tests conducted at Aerojet and NASA-LeRC) to define the startup and shutdown procedures and component requirements adopted for the 35-kWe system. The procedures and component requirements for the system (as shown in Figure 4-1) formed the basis for the restart system component specifications.

The overall result was the definition of a feasible restart system, procedures, and components capable of meeting many diverse and stringent requirements. Many of the basic approaches to meeting the overall requirements and the component design principles involved should be applicable to other Rankine-cycle loop systems for ground or space power applications.

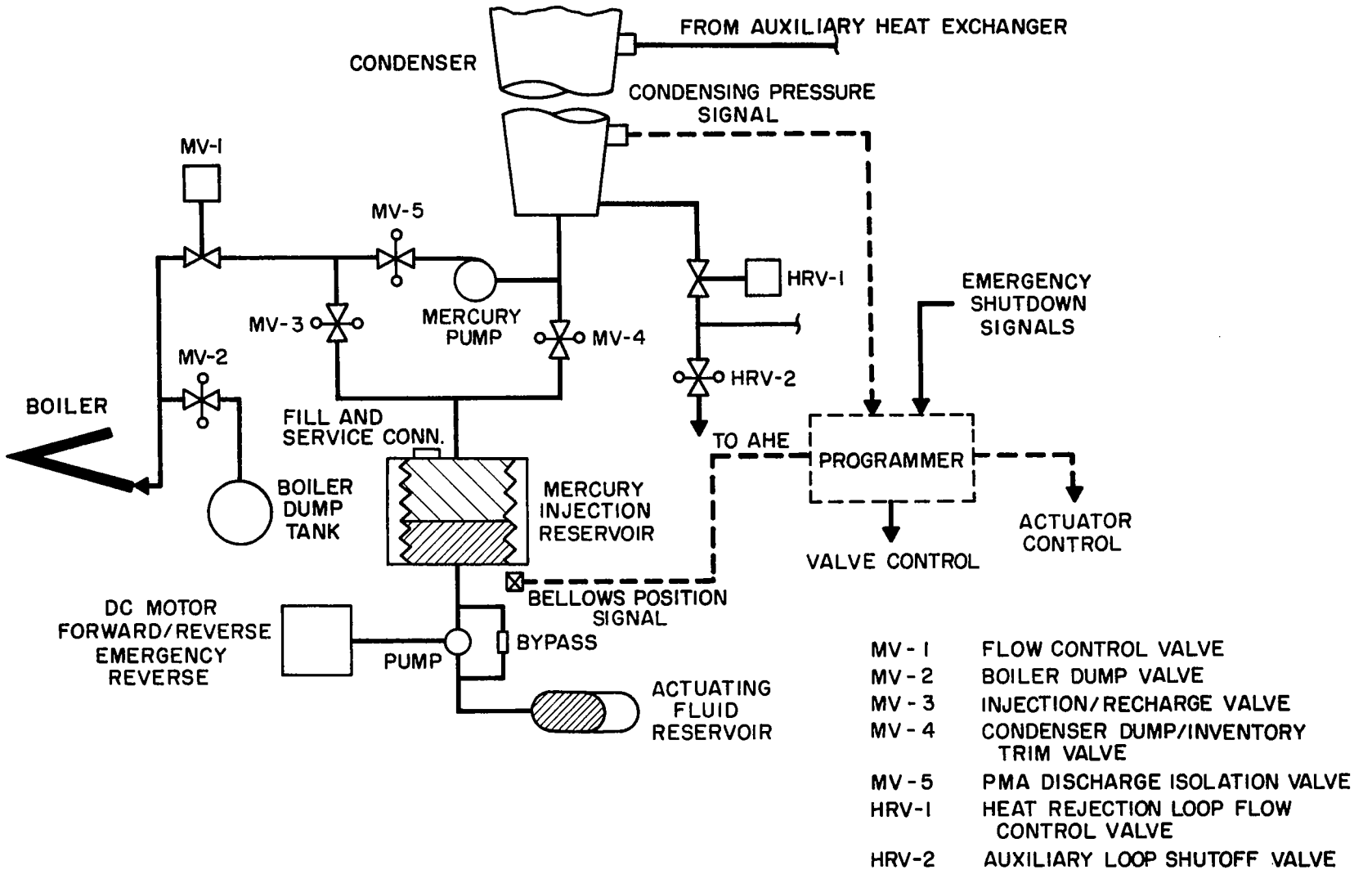

Figure 4-19 High-Pressure (Hydraulic-Pump Pressurized) Mercury Injection and Restart System

4.3 SNAP-8 SYSTEM TESTING

The objective of the SNAP-8 test program was to evaluate the performance and endurance potential of the components and system. Specific objectives were to observe interactions between the components and the system, to detect any life-related degradation or other reliability phenomena, to obtain basic off-design system performance data, and to investigate transients, including the demonstration of start and stop modes. These objectives were all successfully met.

The testing identified numerous areas of significant component and system interactions such as cause and effect relationships in boiling instability, system contamination, mercury inventory control, and transient operation. Endurance testing provided a measure of system reliability, and strengthened confidence in the integrity of the SNAP-8 power conversion system to operate continuously for more than 10,000 hours.[1] Performance mapping of the system identified the basic off-design performance of the components and system. The mapping defined the reactions of the system to disturbances that would be imposed by the reactor control system, sun-to-shade operation, radiator temperature variations, and mercury inventory variations.

The testing provided a physical demonstration of the feasibility of remote startup and operation of large liquid metal power conversion systems for space use. It also contributed to the knowledge of material properties, large liquid metal loop cleaning techniques, and liquid metal test facility design.

4.3.1 Test Facilities

Test programs were conducted at both NASA (Lewis Research Center) and Aerojet-General Corporation (Azusa Facility). The NASA testing was performed during the period 1965 through 1969 using a test facility known as W-1. The program consisted of three phases. The first phase (Reference 20) was a study of reactor transients. The facility contained a boiler and condenser; other components were simulated with test support equipment. The second phase (References 21 and 22) was a period of testing using a complete power conversion system. The principal objective was endurance testing using a double-containment, tantalum and stainless steel boiler. The third phase (References 19 and 23) studied startup and shutdown characteristics of the system. Shutdown sequences were performed which simulated both normal and emergency shutdown conditions.

At Aerojet, testing began in 1964 in a facility known as Rated Power Loop 2 (RPL-2). The facility had a complete mercury loop with test support equipment used in the NaK loops. The testing primarily studied boiler, turbine, and condenser performance.

During 1965, testing began on a complete 35-kWe system known as Power Conversion System 1 (PCS-1) (Reference 24). This system incorporated all of the SNAP-8 components with the exception of the reactor, radiator, and fluid reservoirs. System testing was conducted with gas heaters replacing the reactor, an air-cooled heat exchanger replacing the radiator, and gas-covered reservoirs replacing flight-type bellows reservoirs.

An overall view of the actual PCS-1 is not possible due to the interference of test cell walls and structure. Photographs of a scale model are used to give the best perspective of the test facility and system size and geometry. Figure 4-20 shows front and rear views of a 1/4-scale model of the facility and system. A schematic of the system is presented in Figure 4-21.

4.3.2 Endurance Testing

Endurance testing was always an objective in the test program, but it was not until 1968 that a true test of the power conversion system at Aerojet could be made. The components used in the power conversion system tests are listed below.

Boiler	Mercury Injection System
Condenser	Start Programmer
Mercury Pump	Inverter
Primary NaK Pump	Speed Control Module
Heat Rejection NaK Pump	Saturable Reactor
Lubricant-Coolant Pump	Voltage Regulator
Turbine Alternator	Static Exciter
Parasitic Load Resistor	Motor Transfer Contactor
Mercury Flow Control Valve	Speed Control Transformer
Lubricant-Coolant Valves	Stabilization Assembly
Mercury Isolation Valve	Protective System
Auxiliary Heat Exchanger	

As shown in Figure 4-22, the accrued operating time began to rise sharply in 1968. By the end of testing in 1970, the operating time of the power conversion system at Aerojet had reached a total of 13,400 hours.

Particularly noteworthy was an endurance test conducted on a single set of components. The objective was to have a specific power conversion system operate as long as possible without replacing any component. This approach allowed observation of any life-related system deficiencies or unexpected operating characteristics. The "single-set" test met, and exceeded, expectations. Originally, the objective was to operate 2500 hours with the single set of components. The test was terminated after 7300 hours of operation. The primary reason for terminating the test was to conduct an inspection of the turbine which had accumulated more than 10,000 test hours.

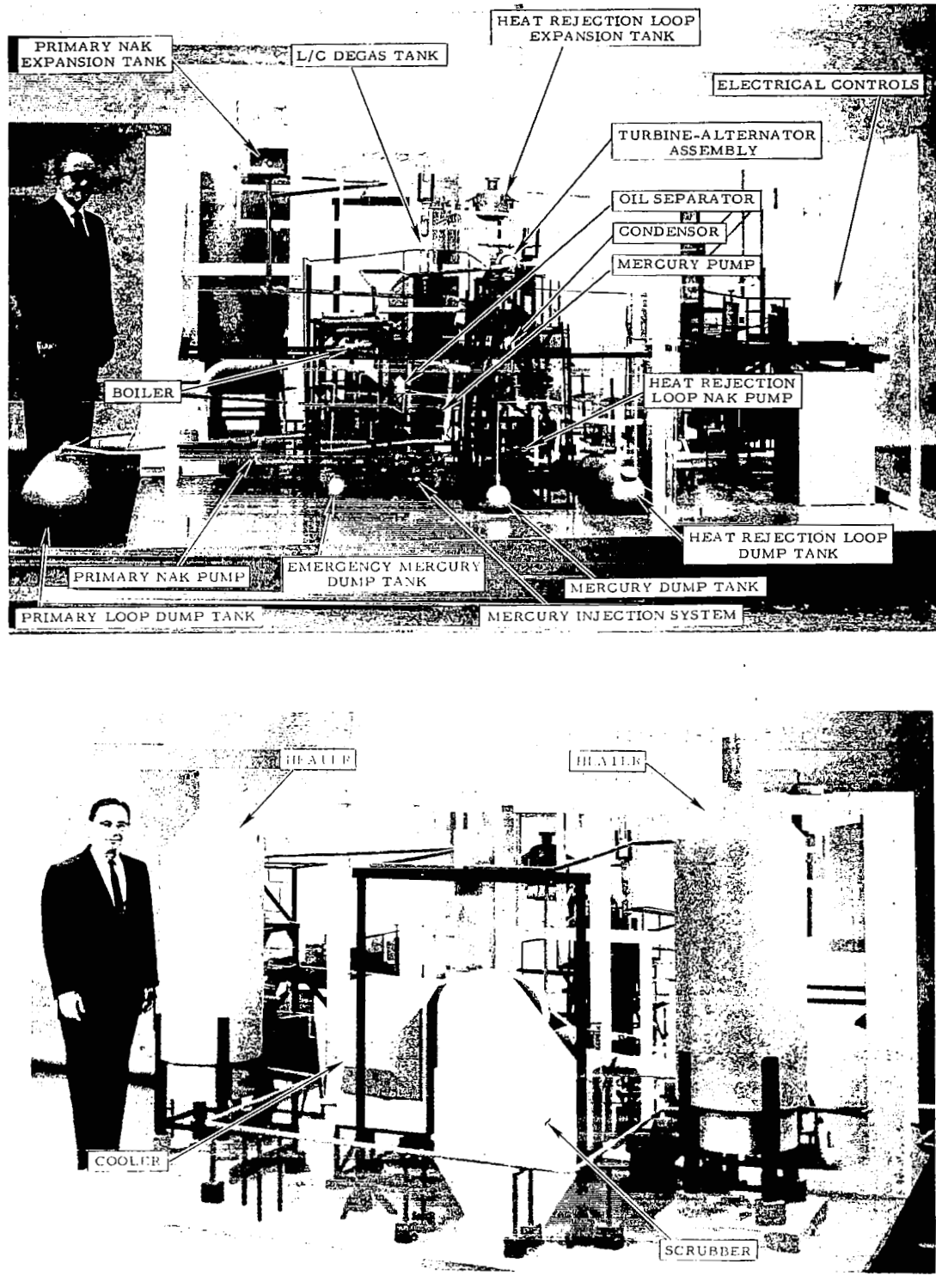

Figure 4-20 Power Conversion System Test Configuration: 1/4-Scale Model Front View (Top) and Rear View (Bottom)

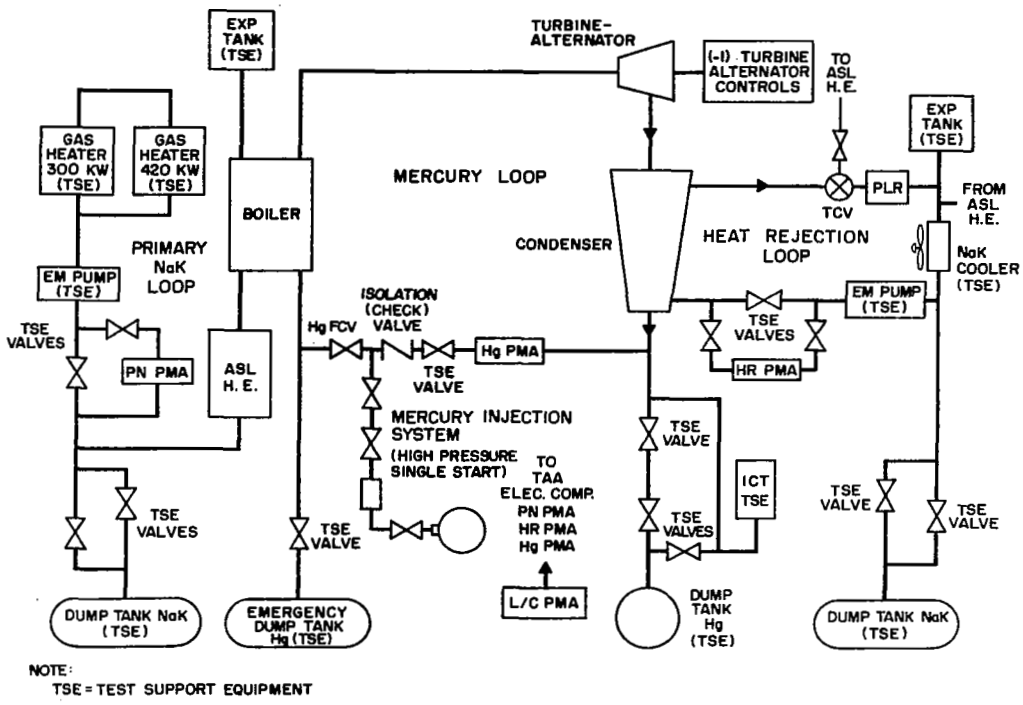

Figure 4-21 Power Conversion System 1 - Schematic Diagram

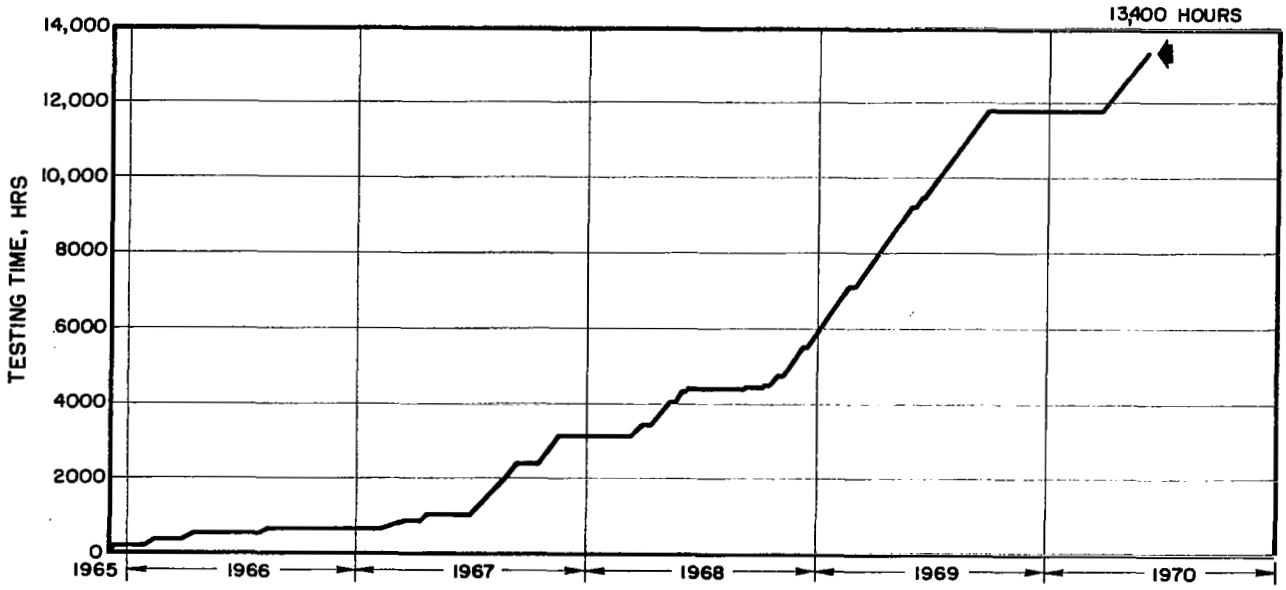

Figure 4-22 35-kWe System (PCS-1) Test Time

The single-set time was counted on the basis of the component with the least number of operating hours, in this case the mercury pump. Other components had significantly greater operating times; some passed the 10,000-hour mark, the original SNAP-8 life requirement. The operating times of the components at the 7300-hour, single-set point were:

Turbine-alternator	10,800 hours
Primary loop NaK pump	7,600
Heat rejection loop NaK pump	7,900
Mercury pump	7,300
Lubricant-coolant pump	12,700
Boiler	8,700
Condenser	13,200
Electrical controls	11,300

A special test was conducted during the single-set operation to determine the presence, and extent, of any long-term system transients. The system was adjusted to its design operating state and allowed to operate with absolutely no further adjustments being made. This procedure allowed the detection of any slow, otherwise unnoticeable, transients or system degradation. In all previous testing, the objective had been to obtain specific data on various components or some system characteristic, so manual adjustments to the system operating point were frequently made.

The "hands-off" operational mode was continued for 1400 hours. Although no large transients were observed, there were nevertheless, phenomena detected which otherwise would have been masked by normal data scatter and would have gone undetected. Over the 1400-hour period, the alternator output gradually decreased from 54.5 kw to 49.5 kw.

The power decrease was due to two factors: a decrease in mercury flow, and a turbine performance degradation. The decrease in mercury flow which was caused by an increase in boiler pressure drop accounted for 70% of the power decrease. An increase in boiler pressure drop is not unexpected and, in fact, is indicative of improved mercury wetting within the boiler and potentially better quality vapor. The change in boiler pressure drop and the resultant power loss was not a system problem. The system was equipped with a mercury flow control valve which could have readily adjusted for the change in boiler pressure drop. The flow-control-valve margin far exceeded the alteration required to compensate for the boiler pressure drop change. The hands off operation showed that some degree of mercury flow control valve adjustment would probably be necessary in a SNAP-8 application.

A turbine performance decline of approximately 2 percentage points in efficiency accounted for 30% of the power decrease. Turbine performance decline does not represent a hazard to system life potential; the turbine is considered capable of at least 20,000 hours of operation. Performance degradation is expected in a long-life system and was anticipated in the original

design. The SNAP-8 system design included a degradation allowance of 2 kWe which is sufficient to compensate for the observed turbine performance change.

Endurance testing provided a quantitative measure of the reliability of the SNAP-8 power conversion system. The components and system as a whole demonstrated a clear potential for at least a 10,000-hour life. Throughout endurance testing, the system was stable and gave no evidence of any life-limiting characteristics. The long-term transients which were observed were within the range for which compensation and allowance had been provided.

4.3.3 System Performance Evaluation

4.3.3.1 System-Component Interactions

Testing in PCS-1 resulted in acquisition of performance data for all of the components in a system configuration. The system and component interactions observed in the system tests are presented in detail in References 24, 25, and 26. Specific phenomena observed were:

- Quantity of unvaporized liquid droplets in the mercury vapor stream
- Effects of deconditioned boiler performance
- Pressure fluctuations generated by the boiler and the effect on system output
- Effects of partial loss of mercury inventory
- Pressure transients generated within the boiler during startup
- Degradation of turbine efficiency
- Effects of mass-transfer buildups on turbine performance
- Effects on the system of various types of component failures
- Effects of noncondensable gas in the system
- Condenser pressure instabilities
- Condenser choked flow phenomenon (References 4 and 26)
- Effects of rapid electrical load variations
- Speed control system perturbations
- Effects of mass transfer and gas accumulations on pump performance.

4.3.3.2 Transients Imposed by Operating Mode

The SNAP-8 system can experience numerous transients as a result of conditions associated with normal control functions of the mission. Extensive testing was performed to define the system reaction to these conditions. The following operational conditions, detailed test results of which are contained in References 24, 25, and 26, were studied during system testing:

- Boiler NaK temperature variations resulting from normal reactor control system perturbations
- Condenser NaK temperature variations resulting from missions having alternate sun-shade operation
- Mercury inventory variations resulting from space seal leakage or other causes of inventory loss
- Component and system heat load variations resulting from sun-shade effects on the coolant system
- Automatic system shutdowns caused by various system failures or mishaps.

4.3.3.3 Remote System Startup Demonstration

A significant phase of the SNAP-8 program was the development and demonstration of a method to start the system remotely in space. The basic ground rule was that the power conversion system must start reliably without imposing excessive thermal gradients on the reactor. In a sense, an optimum procedure exists, since the surest way to start the power conversion system is a rapid startup, whereas reactor reliability favors a slow startup. Extensive studies were conducted to develop a startup scheme which would be compatible with both the reactor and power conversion system. In 1968, a series of system startup tests was conducted to verify the results of the startup study program. The tests demonstrated the automatic remote startup capability of the SNAP-8 system.

Startup was divided into two separate phases: a reactor heatup phase, and a power conversion system startup phase. To simulate the reactor heatup phase, a dc inverter ran the lubricant-coolant pump and NaK pumps at about one-fourth speed. During this phase, the NaK loops were coupled by an auxiliary heat exchanger which provided a simulated heat sink for the reactor.

The first step in power conversion system startup was to increase the NaK and lubricant-coolant flows to about one-half rated value; this was done with the dc inverter. At this point, the mercury loop of the power conversion system was started. The mercury loop startup was a "bootstrap" operation. Mercury was injected into the boiler under pressure at a controlled rate to start rotation of the turbine-alternator and mercury pump which was electrically coupled to the alternator. When the turbine-alternator acceleration reached one-half speed, the NaK and lubricant-coolant pumps were transferred electrically to the alternator and all rotating components completed

acceleration to rated speed simultaneously with the turbine-alternator. As rated speed was approached, the electrical speed control system took over to control the speed and electrical output of the system.

The system startup scheme was first demonstrated with a SNAP-8 power conversion system under test at Aerojet. Similar but more extensive tests were subsequently conducted at NASA LeRC using an electric NaK heater as the reactor simulator. All startup tests required simulation of both the reactor and the radiator with appropriate heat exchangers. Future testing was planned at the NASA Plum Brook Space Power Facility to merge a power conversion system and a reactor to more accurately define the characteristics of a startup.

The primary results of a typical startup are shown in Figure 4-23. The data begin after the reactor heatup period and just before mercury injection; therefore, the pumps were all at one-half speed except for the mercury pump which accelerates with the turbine-alternator. The data show the mercury flow ramp, the turbine-alternator acceleration, the acceleration of all pumps together after one-half speed is reached by the turbine-alternator, the alternator output power, and boiler temperatures. Boiler outlet temperature is the critical parameter in the startup, as far as the reactor is concerned. The most severe transient the reactor experiences is during the relatively high initial mercury injection rate which accelerates the rotating components.

The tests demonstrated the validity of the SNAP-8 startup scheme. All thermal transients remained within limits specified by the reactor contractor. The success of the tests was a major step in the progress of the system toward an eventual space application. The testing at NASA LeRC also investigated system shutdown characteristics. Tests of shutdown sequences, reported in Reference 19, were performed which simulated both normal and emergency shutdown conditions. All transients remained within safe component limits.

4.3.3.4 Power Increase Potential

Throughout most of the SNAP-8 program, the goal was a net electrical output of 35 kW. Testing of the 35-kWe system occupied the majority of all testing. During the latter part of the program, design began on a modified version of SNAP-8 capable of a 90-kW net electrical output. The testing performed in 1970 centered around evaluation of the system at the elevated power-output condition.

The 90-kWe operating condition required a higher mercury flow and a lower condensing pressure. Testing was established to evaluate components at the conditions that would be experienced under the new conditions. The components in question were the turbine, alternator, boiler, and condenser. The turbine was known to be unsuited to the higher-power operation, so no test demonstration was attempted. The alternator was tested to its new requirement of 80 kVA and was found to be adequate, provided additional cooling was supplied.

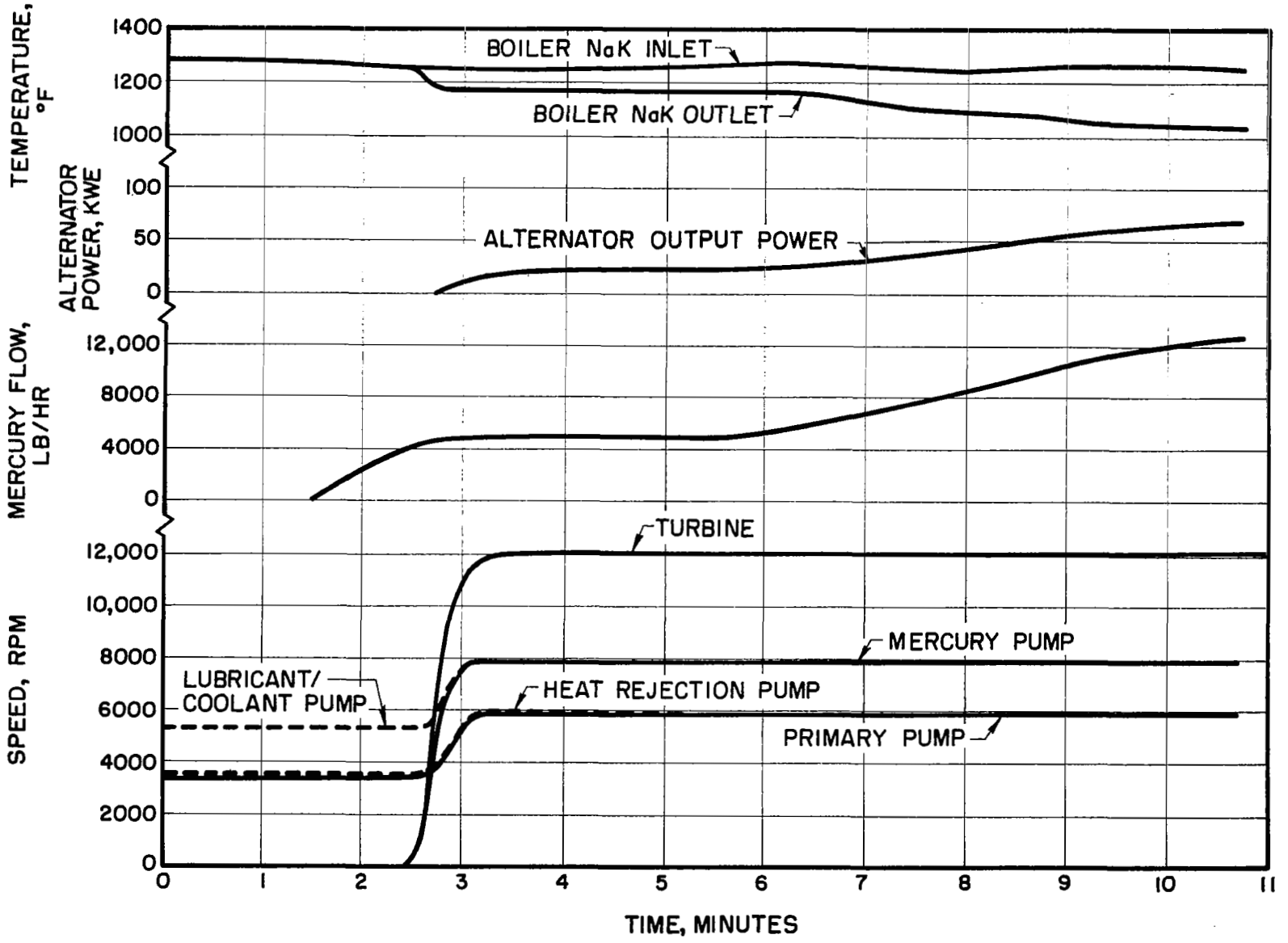

Figure 4-23 35-kWe System (PCS-1) Transients Occurring During Remote System Startup Demonstration

The boiler would also need to be redesigned. However, simulation of the new operating conditions was possible by using test parameters, but scaled on a per tube basis. The modified boiler design was substantiated by the tests.

The condenser was found to be unacceptable at the higher power level for a zero-g application. Although thermally acceptable, its pressure drop was excessive. The pressure drop could be reduced by maintaining a high mercury inventory level in the condenser, but this introduces interface stability problems. In a ground application, the condenser was satisfactory.

A detailed report of the testing is found in Reference 26.

4.3.4 Correlation of Test Results and Mathematical Models

Much of the SNAP-8 design and analysis was based upon mathematical models of the system. One of the objectives of system testing was to identify the degree of correlation between the mathematical models and actual system performance.

Two models were used in the program. The first defined the steady-state performance of the system. The model was used to predict the performance of the system when subjected to slow transients such as the NaK temperature variation caused by the reactor temperature control system. The computer program is known as SNAP-8 Cycle ANalysis (SCAN).

The second mathematical model predicted performance of the system during fast transients typical of system startup and shutdown. The model was programmed as a hybrid computer system simulation. Correlation between test and theory for each of these models is discussed below.

4.3.4.1 Correlation with the SCAN Computer Model

Extensive system testing was conducted to observe the effects on the system of various parameter perturbations. The NaK temperature variation is selected here as an example. The test consisted of changing the boiler NaK inlet temperature over the reactor deadband temperature range (1330 to 1280°F) with all other variables being allowed to vary without restraint.

The results of the test, together with SCAN predictions, are tabulated in Table 4-IV. The agreement between the test data and the SCAN data is good, giving considerable confidence in the ability of the model to predict the performance of future SNAP-8 system design. Test series investigating other typical system perturbations were equally successful.

4.3.4.2 Correlation with System Startup Computer Model

A direct comparison of the system startup mathematical model and test data is difficult. The reason is that the test facility did not use a reactor or a radiator. The functions of these components had to be simulated and an accurate simulation was not possible.

TABLE 4-IV SYSTEM RESPONSE TO REACTOR TEMPERATURE VARIATION FROM 1330 to 1280°F

Function	Test Data	SCAN Data
Heat Input to Boiler	1% increase	1% increase
Condensing Pressure	No noticeable change	0.1 psi increase
Turbine Inlet Temperature	30°F decrease	50°F decrease
Turbine Inlet Pressure	0.8 psi decrease	0.6 psi decrease
Boiler Mercury Outlet Pressure	0.8 psi decrease	0.5 psi decrease
Boiler Mercury Outlet Temperature	45°F decrease	45°F decrease
Heat Rejection	No noticeable change	0.2% increase
*Boiler Pinchpoint Temperature Difference	45°F decrease	45°F decrease
Condenser NaK Outlet Temperature	No noticeable change	No noticeable change
Alternator Output	0.5 kW decrease	0.3 kW decrease
Mercury Liquid Flow	100 lb/hr increase	100 lb/hr increase

*Minimum difference between NaK and Mercury Temperatures

However, the validity of the mathematical model was demonstrated. The model was used as a source of input data to conduct startup modes. Flow ramp rates, temperature simulations, inventory control, etc., were all based upon the predictions of the model. The fact that the startups were successfully accomplished is evidence of the validity of the model. Component accelerations, temperature gradients, and all other aspects of the startup, proceeded satisfactorily.

4.3.5 Projected Final Development Testing

The system testing conducted at Aerojet and NASA LeRC successfully demonstrated the performance and reliability of components and the integrity of system operational modes. However, several additional areas of valuable testing remain in order to have a fully developed nuclear powered electrical generating system.

The single most important additional test is a combined system test such as that originally planned to be conducted in the NASA Plum Brook Space Power Facility. The combined system test would include the power conversion system, the reactor and nuclear control system, a heat rejection system with the capability to simulate space conditions, and simulation of space vacuum conditions. In the combined system test, the complete spectrum of transient response would be investigated and evaluated. The transient response investigations would include those associated with the power conversion system, the nuclear system, and the interactions between the two, particularly the rapid transients occurring during startup and shutdown.

Additional testing, which could be included as part of the combined system test, would be conducted to investigate the following:

a. Hydrogen transport.- During the operation of a combined nuclear/power conversion system, hydrogen will escape from the reactor fuel elements and diffuse through the system. Hydrogen can effect system performance in several ways: react with containment materials and alter their mechanical or chemical properties; react with NaK to form a solid hydride and impair flow; accumulate in the mercury loop and affect condenser, boiler, or pump performance. Analytical studies have been made to establish the equilibrium distribution of hydrogen in the system. A computer program, designated as DCHT - Double Containment Boiler Hydrogen Transport Computer Program for SNAP-8 and described in Reference 28, was developed to calculate the anticipated hydrogen distribution. The analytical studies were supported by small-scale system loop tests in which hydrogen was injected into the primary NaK loop. Although the results were inconclusive, a tendency for hydrogen to accumulate in the mercury loop was indicated. A combined system test would permit the investigation of all potential problems associated with hydrogen diffusion and an evaluation of the effects on system performance.

b. Combined radiation and temperature effects.- The combined effects of radiation and temperature on the operation and performance of components should be evaluated. These effects should be evaluated particularly for components located in the high-radiation zone within the 4-pi shield.

c. Long-term degradation.- A more comprehensive evaluation of component and system degradation occurring during long-term endurance testing would define the possible degradation modes.

d. Mass Transfer.- Further investigations should be made to determine the effects of temperature and flow as they relate to the deposition and removal of mass-transfer products.

e. Mission adaptation tests.- Tests should be conducted to further define the effects of mission-imposed conditions on system performance and operation. The mission-imposed conditions include the proximity of the sun, sun-shade cycles, and system shutdown and restart requirements.

5.0 MECHANICAL COMPONENTS

5.1 TURBINE-ALTERNATOR

The SNAP-8 turbine-alternator converts the thermal energy of superheated mercury vapor into electrical energy for use within the SNAP-8 system and as useful electrical power to a mission vehicle. The turbine-alternator design for a 90-kWe system (identified as the Mark 70 design) consists of a dual five-stage split-flow reaction turbine. Two solid rotor, brushless, homopolar inductor-type alternators of proven design are used with one alternator attached to each end of the turbine shaft. The location of the turbine-alternator in the 90-kWe system is shown schematically in Figure 5-1. The turbine-alternator for the 35-kWe system (identified as the Mark 66 design) consists of a cantilevered four-stage axial-flow, impulse turbine coupled to a single alternator of the same design used for a 90-kWe system. All testing experience for turbine-alternators was achieved with the Mark 66 design. The location of the turbine-alternator for the 35-kWe system is shown schematically in Figure 5-2. The design features and operating characteristics for the turbine-alternators utilized in the two systems are presented below.

5.1.1 Mark 70 Turbine-Alternator

5.1.1.1 Development Background

Upgrading SNAP-8 to a 90-kWe system was done using the proven technology of the Mark 66 turbine (which had been successfully tested) and as much existing hardware as possible combined with an appropriate system state-point change. The major state-point change was to reduce the turbine back pressure from 14 psia (Mark 66 turbine) to a range of 2.0 to 2.5 psia. The increase in available energy across the turbine resulting from a reduction in back pressure was achievable with only a modest increase in flow rate over that required for the 35-kWe system. Combining the gain in available energy with a significant gain in turbine efficiency by using a reaction turbine, the net electrical output of the SNAP-8 system could be more than doubled which would, in turn, more than double the overall system efficiency. Studies of the SNAP-8 system with components optimized have shown that, for the same 600-kWt reactor power, an overall system efficiency of 20% can be achieved.

The system designed to produce higher output and overall efficiency was to use as much developed hardware and technology as possible. The exception to this was that the turbine assembly was to be redesigned as a reaction machine rather than the impulse type of turbine previously used. With this approach, the turbine efficiency could be increased from the 57% of the Mark 66 impulse to about 78% for the Mark 70 reaction machine.

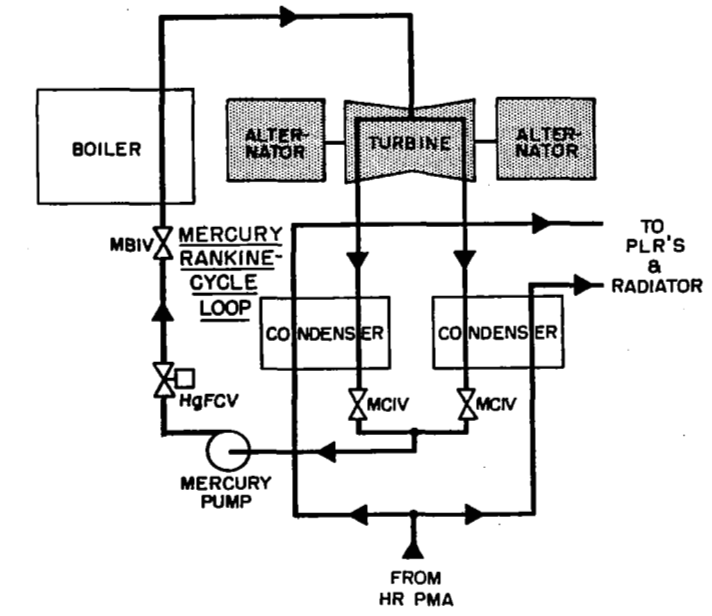

HgFCV MERCURY FLOW CONTROL VALVE
MBIV MERCURY BOILER ISOLATION VALVE
MCIV MERCURY CONDENSER ISOLATION VALVE

Figure 5-1 90-kWe System Schematic Showing Location of Mark 70 Turbine-Alternator

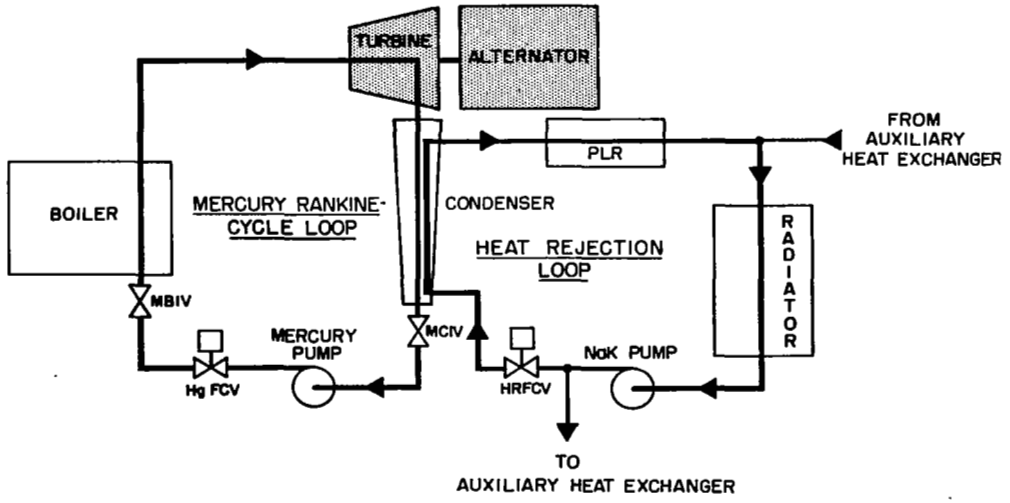

HgFCV - MERCURY FLOW CONTROL VALVE
HRFCV - HEAT REJECTION LOOP FLOW CONTROL VALVE
MBIV - MERCURY BOILER ISOLATION VALVE
MCIV - MERCURY CONDENSER ISOLATION VALVE

Figure 5-2 35-kWe System Schematic Showing Location of Mark 66 Turbine-Alternator

DUAL 6 STAGE AXIAL FLOW
SHOWN ABOVE CENTER

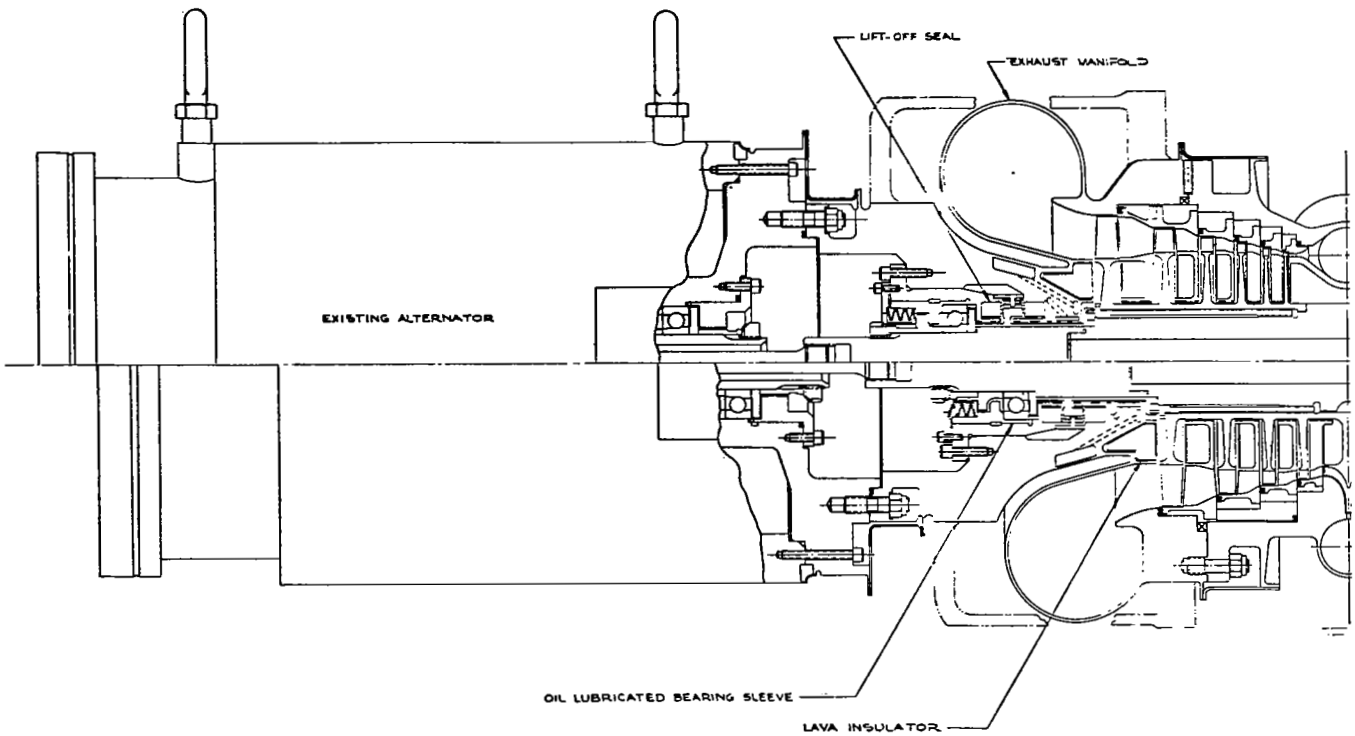

D[illegible] 5 STAGE DESIGN
([illegible]E AGE RADIAL INFLOW)

DESIGN
LINE

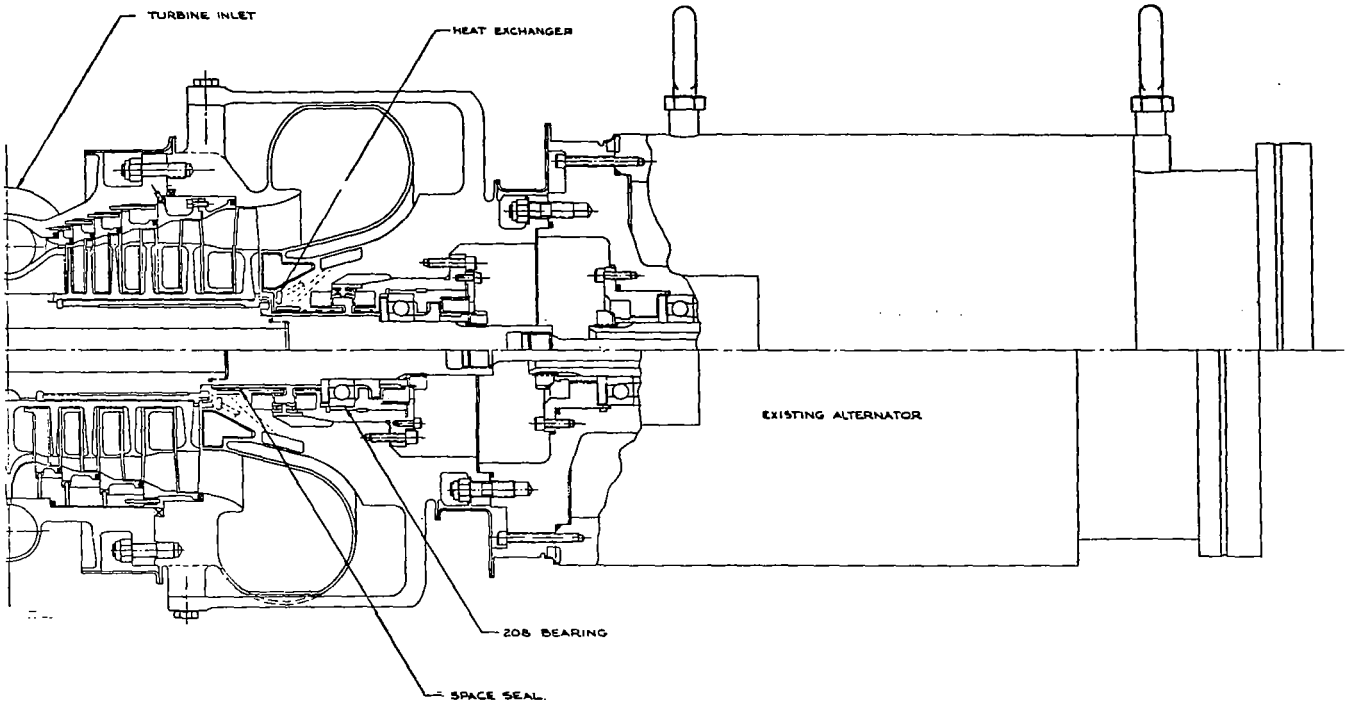

SHOWN BELOW CENTERLINE
4 STAGES AXIAL FLOW)

A reaction turbine and a higher system output level required a change in the turbine-alternator configuration. To preserve the bearing design of the Mark 66 turbine and still maintain a relatively low axial-thrust load, the reaction turbine was split into two opposed axial-flow reaction turbines on a single shaft to balance the axial thrust. This configuration incorporates two bearing and space seal arrangements having the design criteria that were proven in a 10,000-hour endurance test of the Mark 66 turbine. In addition, the two alternators driven by the turbine are located on opposite sides of the turbine with mechanical drive couplings similar to those previously used. The turbine-alternator configuration is as shown in Figure 5-3.

With two opposed alternators on a single shaft, one must rotate in a direction opposite to the present machine. Paralleling the output requires mechanical alignment to control load sharing and phase shifting. Other mechanical changes entail the simple replacement of right-hand parts with left-hand parts where the change in rotational direction so dictates (e.g., the visco seals and molecular pumps in the seal-to-space installation).

5.1.1.2 Turbine

The turbine consists of two five stage, opposed reaction turbines with the first stages being radial inflow and the remainder being axial flow. These mounted on a single shaft to minimize axial thrust loads. Introducing the turbine flow at the center of the assembly and splitting it in half cancels the axial thrust load. The design of this turbine is described in Reference 3.

The exhaust from each turbine flows directly to its own condenser where the flow paralleling is completed by jointly manifolding the two condensers. This arrangement preserves the use of a single mercury pump. Modification of the condenser inlet manifolds was required to achieve the design goal turbine back pressure of 2.0 to 2.5 psia.

The following state-point conditions were established for the reaction turbine.

Turbine mercury flow rate (total)	13,550 lb/hr
Turbine inlet pressure	146 psia
Turbine inlet temperature	1155°F
Turbine exhaust pressure	2.5 psia
Turbine exhaust temperature	520°F
Design goal efficiency (total-to-static)	78%

In addition to revised system state points, some restrictions were included to preserve the turbine technology and to assure the least development risk. Among these restrictions were a limiting tip speed of 450 fps to minimize turbine blade erosion, a minimum last-stage blade root diameter of 5.5 inches to allow sufficient room for the cooling ducts for the space seal which is similar to the Mark 66 design, and a requirement for the turbine rotor assembly to have a critical speed above the design speed.

The computer program used in the SNAP-8 turbine design was upgraded to include the effects of reaction and the latest applicable data on losses. Also included in the program was the ability to vary the different stage rotor diameters and work splits. This program was used for a parametric study of 5-, 6-, and 7-stage turbines, the stage-to-stage transition and flare problems, and the effect of shrouding some of the stages.

The effect of rotor tip clearance on turbine efficiency was also considered. This parameter was included because previous design approaches had included conservative mechanical integrity requirements, one of which was that the turbine must be capable of withstanding the thermal shock caused by super-heated mercury vapor when the turbine is at room temperature. Ruling out a turbine preheat cycle in the start sequence resulted in excessive rotor tip clearances on the order of 0.030 inch which penalized turbine performance. Since the system goal is to demonstrate high thermal efficiency, a design approach was adopted which allows maximized component performance with more reasonable design margins. With respect to the rotor tip clearances, either a turbine preheat cycle must be included or the rotor housings must be designed to "grow" faster than the rotors and blades during the startup thermal transient.

A turbine design with radial inflow on the first-stage was selected since it provided the best efficiency and mechanical design. The calculated efficiency for this design is in the range of 79.25 to 80%.

The conclusions from the preliminary design phase indicate that a turbine total-to-static design goal efficiency of 78% is attainable; however, the attainment of this efficiency depends primarily on the reduction of rotor tip clearances to the lowest practical values. Feasible design approaches exist to reduce rotor tip clearances and include shroud design considerations, modified system startup procedures, and a turbine preheat cycle.

5.1.2 Mark 66 Turbine-Alternator

The turbine-alternator Mark 66 design for the 35-kWe system is shown in a cutaway view in Figure 5-4 and as actual hardware in Figure 5-5.

The turbine in the Mark 63 SNAP-8 turbine-alternator (described in detail in Reference 28) had the following physical characteristics,

- Four axial stages:

  Stages 1 and 2, partial admission
  Stages 3 and 4, full admission

- Large radial rotor blade tip clearances

- Large nozzle vane/rotor blade overlap

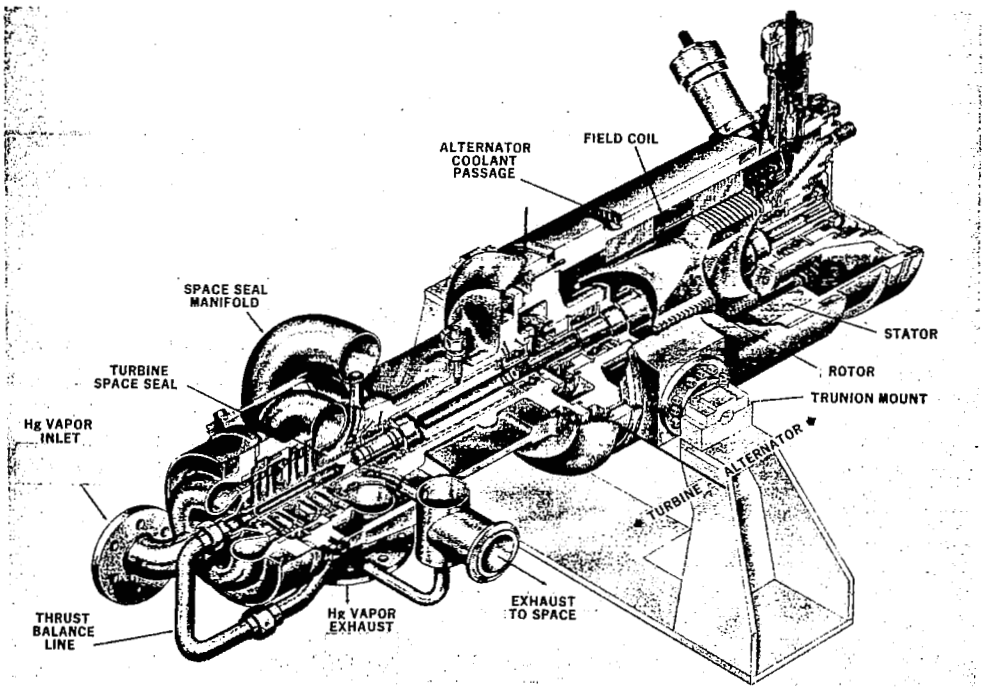

Figure 5-4 Mark 66 Turbine-Alternator Cutaway View

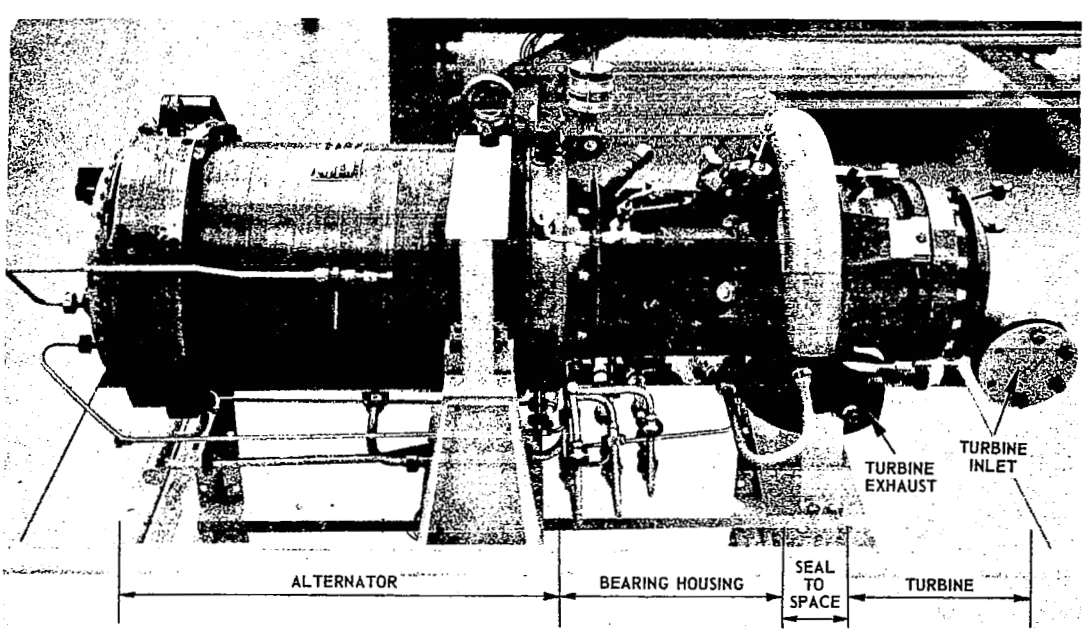

Figure 5-5 Mark 66 Turbine-Alternator

While the performance of most of the components in this unit was satisfactory, the turbine efficiency of 52.5% (based on test results of several units) was below the predicted level of 60%. In addition, the tests revealed a number of mechanical design deficiencies.

Examination of the system and component performances indicated that the most fruitful place to gain a significant performance improvement, with the least added complexity, was in the turbine, and design changes were made which led to the Mark 66 turbine.

The major changes were in the modification of aerodynamics for better flow control, a material change from Stellite 6B to S-816 for the turbine wheels and nozzles, and mechanical redesign for structural improvement. This is described in Reference 29. The reason for the material change was that Stellite 6B had shown a tendancy toward transformation and embrittlement in early testing. The transformation was from the relatively ductile face-centered cubic crystaline structure to the brittle haxagonal close packed form. This change was attributed to the temperature soak during operation.

5.1.2.1 Mark 66 Turbine Physical Description

The configuration of the turbine is characterized as follows:

- Four stages
- Impulse in each stage (as defined by zero pressure drop across the rotors)
- 12,000 rpm
- Dual-path partial admission in the first two stages (38% and 49% admission) and full admission in the last two.
- An overhung (cantilevered) assembly supported on two angular-contact ball bearings.

The nozzle areas of the two partial-admission stages are halved and spaced 180 degrees apart to avoid unbalanced torques on the bearings and to better distribute the heat input to the turbine housing.

The turbine case and inlet manifold housing are suspended by four arms extending from the bearing housing. The concentric location of the turbine case under thermal and mechanical loads is maintained by the four "cold-frame" support arms that are part of the bearing housing. These arms are tangentially and axially stiff, but radially flexible to accommodate thermal growth. Any tendency for the case to be eccentric is well constrained.

The turbine-blade tip clearances were set at a nominal 0.030 inch for the first two stages, and 0.025 and 0.020 inch in the third and fourth stages. The Mark 63 design had tip clearances of 0.040 inch in all stages.

Axial clearances between nozzles and wheels were set at a nominal 0.070 inch. An 0.50 inch clearance was used, however, between the second-stage wheel and the full-admission third-stage nozzle to minimize the transitional losses that occur in passing from a partial- to a full-admission stage.

Preloaded angular-contact ball bearings were used, and a space-seal system was interposed between the turbine exhaust end and the outborad turbine bearing.

To reduce bearing axial loads, the thrust load caused by unbalanced pressure forces on the shaft is counteracted by a balance labyrinth seal piston at the free end of the shaft.

a. Bearings, Slingers, and Lubrication.- The turbine assembly is supported by two angular-contact ball bearings, spring loaded in a back-to-back arrangement. The bearings are 208 size (40-mm bore) angular-contact ball bearings (ABEC, Class 7). The ball retainer is a lightweight, one-piece outer-land-guided type made of iron silicon bronze. Rings and balls are made of triple vacuum melt consumable electrode (CEVM) M-50 tool steel. The design and development of the ball bearings for the SNAP-8 turbine and alternator are described in Reference 30.

The bearings are lubricated by multiple-jet injection of an organic fluid (polyphenyl ether). Scavenging dynamic seals are used on both sides of each bearing to provide nonflooded bearing operation with the bearing cavity at the vapor pressure of the lubricant.

b. Seals to Space.- To use organic fluid for bearing lubrication, means must be provided to prevent the fluid from mixing with mercury where they occupy adjacent regions of the same shaft. Intercontamination of oil and mercury is avoided by venting a section of the rotating shaft to space and permitting a small controlled leakage of each fluid to the space vent cavity.

The seal combination developed for this application consists of a visco pump, slinger pump, and molecular pump in series located between the fourth-stage turbine wheel and the adjacent bearings. The visco pump and dynamic slinger elements develop stable liquid-vapor interfaces for both mercury and oil. The visco pump is surrounded by an organic-fluid heat exchanger which assures an adequate mercury temperature at the interface. The molecular pump provides the barrier to restrict the leakage to space of mercury molecules which evaporate from the interface.

The seal configuration is the result of a separate development program where extensive theoretical and experimental work was done. Testing during this program revealed that leakage rates of less than one pound per year can be expected. The design and development of this seal to space are covered in References 31 and 32.

c. Startup Seal.- The contact seals in the space vent cavity prevent the loss of liquid during startup and shutdown when the dynamic seals are inoperative. An auxiliary lift-off device disengages the contact seals after startup and prior to shutdown during ground test operations.

d. Materials.- Cavitation-erosion resistance to wet mercury vapor, creep data, and thermal expansion data were factors influencing the selection of turbine materials. All areas subjected to mercury vapor, wet or dry, at high velocities were made from S-816; these included turbine wheels, nozzles, labyrinth seals, and the turbine bolt. The inlet manifold assembly itself was forged Type 316 stainless steel. Material for the turbine case and bearing housing is cast Croloy 9M with the thin exhaust duct made from Type 410 stainless steel. Shaft material is AISI 4340 steel. The ball bearings are made from triple CEVM M-50 steel.

5.1.2.2 Mark 66 Turbine - Design Parameters

The design operating parameters for the turbine are as follows:

Turbine

Inlet temperature (^{o}F)	1,250
Inlet pressure (psia)	249
Mercury vapor flow (lb/hr)	11,800
Exit pressure (psia)	14.5
Speed (rpm)	12,000

Lubricant-Coolant System

Flow (lb/hr)	2400 $\pm$ 75
Inlet temperature (^{o}F)	210 $\pm$ 10
Inlet pressure (psia)	40 $\pm$ 2
Exit pressure (psia)	3.5

a. Thermal Mapping.- The steady-state thermal map of the Mark 66 turbine is shown in Figure 5-6. The calculated bearing outer race temperatures (269^{o}F for the alternator end and 249^{o}F for the turbine end) are consistent with the bearing outer race temperatures measured on units during 12,000 hours system testing. The wheel retaining bolt temperature varied from 1050^{o}F under the thrust balance seal to 460^{o}F at the threaded section. The temperature levels indicate that no condensation will form on the surfaces of the inlet duct, turbine case, nozzle shroud region, or on the first-, second-, or third-stage turbine disks. There is an indication that condensation will form on the fourth-stage wheel disk. At no point in the unit are the indicated temperature differentials great enough to cause excessive thermal stresses.

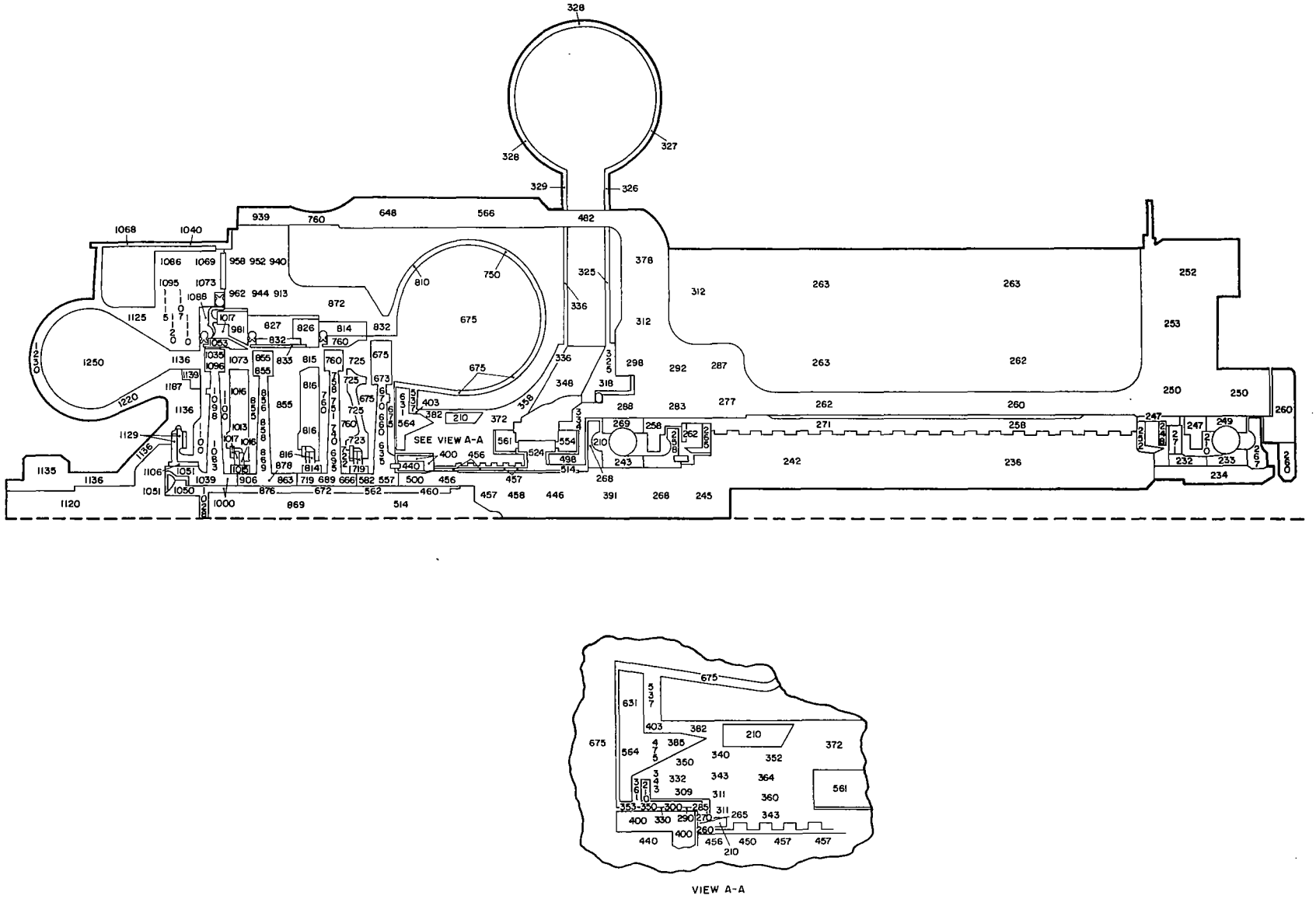

Figure 5-6 Steady-State Thermal Map of Mark 66 Turbine.

b. Dynamic and Vibration Analysis.- Three analyses of the vibrational characteristics of the turbine assembly were conducted.

The first analysis evaluated natural frequencies and structural integrity of the turbine wheel buckets. The turbine blades were calculated for conditions of resonance which could occur within the operating range of the turbine (i.e., up to 12,000 rpm). It was shown that the blade frequencies for all stages were well above the forcing function frequencies of the respective stages.

The second analysis was a parametric study of the turbine shaft whirl characteristics based on rotor-stator dynamics analyses. Particular attention was given to evaluating the rotor and housing displacements at the first-stage turbine wheel hub which is the point of greatest overhang. Effects of variations in bearing fits and bolt preload considering the stiffness of curvic coupling joints were also studied. Bearing reactions based on bearing-support maximum outer race clearance (allowing conical whirl) were evaluated and compared to the predicted bearing capacities for a 10,000-hour life with 99.5% reliability. The analyses indicated that the turbine shaft operating speed is sufficiently below the first critical speed. The latter is calculated to be 16,800 rpm for the rotor-stator model with a bearing spring rate of $.6 \times 10^6$ lb/inch. The second critical speed, which is primarily a housing mode, is calculated to be almost two times the nominal 12,000 rpm shaft speed.

The third analysis derived the axial vibration critical speeds of the SNAP-8 fourth- and second-stage turbine wheel disks. The analysis revealed that a minimum of 3x safety margin exists between the shaft operating speed and the critical speeds so that fatigue associated with wheel axial vibrations is not indicated. Some minor resonances were calculated at 16,200 rpm for the second stage and 16,900 rpm for the fourth-stage, with no expected ill effects. These three analyses are described in detail in Reference 33.

c. Stress Analysis.- The turbine parts which exhibited stress-failure modes in previous SNAP-8 turbines were the turbine wheels, nozzle assemblies, and inlet housing. The results of stress analyses for these components are discussed below.

Stress levels for the turbine wheels were calculated as follows:

	Stage			
	1	2	3	4
Maximum stress (psi):	9,354	8,525	19,883	10,432
Location :	@ ID	@ min. disk thickness	@ ID	@ ID
Minimum creep margin of safety :	0.91	1.11	-	-
Minimum yield margin of safety :	5.2	5.8	1.92	4.56

Vibratory stress levels were computed as follows:

- Root tensile stress (including a stress concentration factor of 2.0) due to rotation at 12,000 rpm:

Stage	Stress (ksi)
1	2.3
2	3.3
3	2.6
4	4.6

- Maximum gas bending stress (including a stress concentration factor of 1.54) at 12,000 rpm:

Stage	Stress (ksi)
1	1.1
2	1.58
3	0.48
4	0.87

This does not reflect the effects of impact associated with partial admission (which would give a maximum magnification of about 10) and resonant magnification.

The second-stage nozzle assembly was analyzed using the finite element method. The analysis considered thermal loading as well as normal pressure loading. The results indicated that the maximum elastic stresses (50,000 psi) occur in the second-stage nozzle diaphragm at 16 seconds after turbine startup, and are due mainly to the large thermal gradients through the thickness of the diaphragm. The subsequent maximum stress level of 10,000 psi due to the pressure difference of 75 psi across the diaphragm was essentially constant during the remainder of an operational cycle (until turbine shutdown). The results also showed an extremely conservative estimate of cyclic strain which indicated an expected life of 2700 cycles. More realistically, the maximum elastic stress level due to the thermal gradient at 16 seconds can be considered as a thermal shock occurring in an operational cycle of several hundred hours. Since the maximum elastic stress level is less than twice the yield strength, the stress-strain cycle will become elastic action (no further repeated plastic flow) after the first cycle.

The third-stage nozzle assembly was analyzed for steady-state operation as well as transient conditions that occur during startup. The maximum steady-state stress in the diaphragm was calculated to be 10,840 psi, and 31,500 psi (compressive) in the shroud. The thermal effects produced stresses as high as 63,000 psi which is significantly above the yield strength of 43,000 psi (at the appropriate temperature). The ultimate stress for this condition is 124,500 psi. Those relatively high stresses due to thermal

loading will result in plastic flow. The material used, S-816, has a ductility of approximately 15%; consequently, the plastic flow will lead to a reduction in the actual magnitude of the calculated stresses. Since these stresses are not excessively above the yield stress, and are well below the ultimate yield stress, risk of physical failure was considered remote and the part considered safe as designed.

The fourth-stage nozzle assembly has the smallest temperature and thermal gradients, and the resulting stress levels due to pressure differential and thermal loading are correspondingly low. The maximum calculated stress in the nozzle assembly of 14,920 psi (tensile, hoop) occurred in the shroud (yield of S-816 = 44,000 psi). The highest stress calculated in the diaphragm was 9000 psi (tensile). Both stresses resulted from the thermal loading.

The stress analysis for the turbine inlet housing was an axisymmetric case of a housing with a cross section remote from the first-stage nozzles. Both steady-state and transient conditions were analyzed. Each analysis was based on an axisymmetric case remote from the nozzle openings.

The steady-state condition occurs when the temperatures in the turbine housing have reached equilibrium. For analysis, the housing was assumed to be soaked at a uniform temperature of 1250°F. Thus, the only stresses present are those due to the pressures in the torus and downstream of the nozzle plate. The maximum stress calculated was 3675 psi and also below the stress of 7000 psi, which is required to produce one percent creep in 10,000 hours. Consequently, the turbine inlet housing was judged to be structurally adequate for steady-state operation.

An analysis of transient conditions indicated that some yielding would take place locally in the low-cycle fatigue regime. However, a conservative estimate indicated the part to be capable of withstanding at least 600 cycles compared to the required 100 cycles. This is described in Reference 34.

5.1.2.3 Mark 66 Turbine - Demonstrated Performance

a. Endurance Testing.- Initial endurance testing involved operation to 2500 hours. The performance has been evaluated for the Mark 66 turbine and turbine-alternator in the 35-kWe test facilities at Aerojet.

A turbine-alternator was operated for 2122 hours in the Aerojet facility before disassembly, inspection, and reinstallation. The initial performance of this unit at its design operating conditions was:

	Tested	35-kWe System Requirement
Turbine-alternator efficiency (%)	48.5	47.9
Turbine efficiency (%)	56.0	56.0
Power output (kWe)	58.0	57.9
Liquid carryover (%)	3.0	4.0 (maximum)

The Mark 66 turbine-alternator met the system requirements. This performance was measured, however, after the turbine had operated some 700 hours with an unconditioned boiler. The effects of mass transfer, which occurs most frequently with wet mercury operation, probably masked the true performance of the unit. Disassembly revealed large amounts of mass-transfer material deposited in the nozzle passages of each stage. The area reductions were considerable (2.7 to 15.5% of the original nozzle areas) and the true turbine efficiency and turbine-alternator power output (minus the effects of the mass-transfer deposits) was estimated to be at least 1.0 percentage point and 1.0 kW higher than measured. Subsequent cleaning, reinstallation, and testing confirmed the estimated effects of the mass-transfer products on performance. The turbine and turbine-alternator performance when reinstalled was as follows:

	Unit 5/3
Turbine-alternator efficiency (%)	49.5
Turbine efficiency (%)	57.5
Power output (kWe)	58.4

Operation of the same turbine-alternator in the 35-kWe system continued until a total of 10,823 hours of operation was reached. The major portion of this period was at steady-state operation. Various system and component tests took up the remainder of the time. During this period the unit accumulated 36 startup/shutdown cycles.

The performance of the turbine and turbine-alternator at design operating conditions during this period was not constant. A decline in turbine efficiency and alternator output was observed. The drop in efficiency of 2.1 percentage points and 2.25 kW in output occurred in four gradual steps after approximately 5600, 5200, 7000, and 8000 hours of operation. A detailed evaluation of the turbine performance after 7500 hours of operation is contained in Reference 35.

At 10,823 hours, the unit was disassembled and examined. A detailed description of the condition of the turbine and alternator following the endurance test is contained in Reference 36. The examination on disassembly indicated that only 0.5 percentage points of the 2.1-percentage-point loss could readily be accounted for by the condition of the unit. The following conclusions were drawn:

- The turbine-alternator was in very satisfactory condition, and showed no problems that would preclude further operation.
- Continued erosion of the turbine rotor blades occurred, limited mainly to the second and third stages. The degree of damage was not considered sufficient to affect the structural integrity of the blades and only slightly affect the blading performance.
- The only significant evidence of mass transfer appeared in the third-stage nozzle where flow area was reduced 7.5%. The deposit was considered a major contributor to the performance loss. Light deposits were found on the rotor blades of the first three stages.

- The rubbing evidence from thrust and interstage labyrinth seals indicated little or no further damage. An anomaly existed in the third-stage labyrinth where lands showed evidence of erosion and corrosion. The life of the turbine was in no way affected.

- Some minor cracks in the first-stage nozzle assembly (inlet housing) had propagated but were not considered structurally detrimental.

- The cavitation damage to the visco seal progressed from the level attained at 2122 hours of operation; however, the small increase in no way affected the structural integrity or the sealing capability of the part.

- The bearings of both turbine and alternator were in good condition and satisfactory for further extended use. They met the basic design objective of 10,000-hours. The bearings showed little service wear. No conclusions could be drawn concerning the fatigue life of these bearings since the design average life is more than 100,000 hours and no fatigue failure was expected during the testing program. Therefore, the absence of fatigue damage in a small sample with a relatively short operating time made a statistical life prediction difficult. The evidence indicated that bearing lubrication was satisfactory.

- A life estimate for the turbine indicated that, based on the evidence seen, the turbine should be capable of operating for a life of at least five years.

b. Transient Testing.- A turbine-alternator identical to that described above was tested in the 35-kWe system test facility at NASA-LeRc. This unit was tested for 157 hours and 135 start/stop cycles with no indication of any malfunction. This confirms the ability to survive the thermal shocks encountered during startup.

c. Vibration Test.- The turbine assembly has undergone shock and vibration testing at NASA-LeRC as part of a complete turbine-alternator. The tests covered sinusoidal vibration, random vibration, and shock in all three axes (x, y, z) as called for in NASA Spec. 417-2 (Rev. C, 1 June 1969). The power input levels are shown in Table 5-I. The turbine-alternator used in these tests was similar in configuration to the unit endurance tested in the SNAP-8 35-kWe system. A description of the test, together with details of the post-test disassembly and inspection is described in Reference 37.

The unit was examined at Aerojet following the vibration and shock test. The turbine-end bearing was in excellent condition except for several small patches of fretting corrosion and a large galled area on the outer surface of the outer ring. The inner raceway showed a superficial chatter pattern at ball-speed intervals with the normal contact angle. The alternator-end bearing was in good condition except for three galled areas on the outer

TABLE 5-I SUMMARY OF TURBINE-ALTERNATOR VIBRATION TESTS

Run Description	Run Number	Test Axis	Input Amplitude or G Level	Input Frequency	Sweep Speed	Run Duration	Maximum Responses			
							G Level	Frequency (Hz)	Axis	Location
			in. doub. ampl.	(Hz)	(oct/min)	(min)				
Fixture survey	1	Y	0.25 1G	5-9 9-2000	4	2.15	13	1600	Z	Trunion mount
Sinusoidal vibration	2	Y	0.25 1G	5-9 9-2000	4	2.15	17 38	190 1150	X&Z Z	Turbine shaft Alternator shaft
Sinusoidal vibration	3	Y	0.25 2G	5-13 13-2000	4	2.15	28 40 40	200- 230 1150	Y Z Z	Turbine shaft Alternator shaft
Random 13g rms overall	4	Y	+3 dB/octave $.4g^2$/Hz -6 dB/octave	20-100 100-600 600-2000		3 min	40-50	----	Y	Turbine and alternator shaft
Shock	5,6,7	+Y	15G			11 millisec				
Shock	8,9,10	-Y	15G			11 millisec				
Sinusoidal	11	Z	0.25 1G	5-9 9-2000	4	2.15	90 30	220 490	Z Z	Turbine shaft
Random 13g rms overall	12	Z	+3 dB/octave $.4g^2$/Hz -6 dB/octave	20-100 100-600 600-2000		3 min	50 20 80	220 500 ----	Z Z Z	Alternator shaft Alternator shaft
Shock	13,14,15	+Z	15G			11 millisec				
Shock	16,17,18	-Z	15G			11 millisec				
Sinusoidal	19	X	0.25 2G	5-13 13-100	6	1.5	28 28 25 28	375 1000 340 1450	X Z X Y	Turbine shaft Turbine shaft Alternator shaft Alternator shaft
Random 13g rms overall	20	X	+3 dB/octave $.4g^2$/Hz -6 dB/octave	20-100 100-600 600-2000		3 min	30- 40	---- ----	X	Turbine and alternator shaft
Shock	21,22,23	+X	15G			11 millisec				
Shock	24,25,26	-X	15G			11 millisec				

surface of the outer ring originating at the thrust face edge. The outer ring raceway showed a light ball vibration pattern at zero-degree contact angle with normal ball spacing between the patterns. Marks on the turbine wheel hubs indicated contact with the labyrinth seals located inside the nozzle diaphragm. This clearly showed the limit of the shaft deflection. This minor contact was apparently sufficient to dampen the vibration without serious impact effects.

5.1.2.4 Conclusions

The experience gained from extensively testing the Mark 66 impulse turbine has confirmed that the unit is capable of meeting the extended life of five years for the SNAP-8 system.

Applying this technology to the Mark 70 reaction turbine appears to present no major problems, and it is expected that the same reliability in operation could be achieved.

5.1.3 Alternator

The alternator was developed to meet the SNAP-8 power generating system requirements which included the ability to start and generate 60 kW of electrical power unattended in space for 10,000 hours.

5.1.3.1 Physical Description

The alternator configuration selected to meet these requirements was a solid rotor, brushless, homopolar inductor type operating at 12,000 rpm and producing 120/208-V, 3-phase alternating current power, with an output frequency of 400 Hz. The alternator is lubricated and cooled by a polyphenyl ether organic fluid. The electrical insulation system is an aromatic polyimide (ML) coupled with an epoxy resin compound. The reliability goal was 97.35% for 10,000 hours of continuous operation. The development of this alternator is described in Reference 38.

A cutaway view of the alternator, Figure 5-7, illustrates the trunnion mounting, flexible drive shaft, and other details.

The turbine and alternator housings are hermetically sealed. Each bolted joint is provided with a seal ring welded to the structure. Electrical connections are hermetically sealed with ceramic feed-through terminals. The alternator bearing system consists of two jet-lubricated spring-loaded divergent angular-contact bearings. The bearing cavity is scavenged by the seal system. Each seal consists of a disk slinger with a visco seal backup. The axial clearances are controlled by shimming at final assembly. The lubrication fluid is also used to remove the heat resulting from seal and rotor losses.

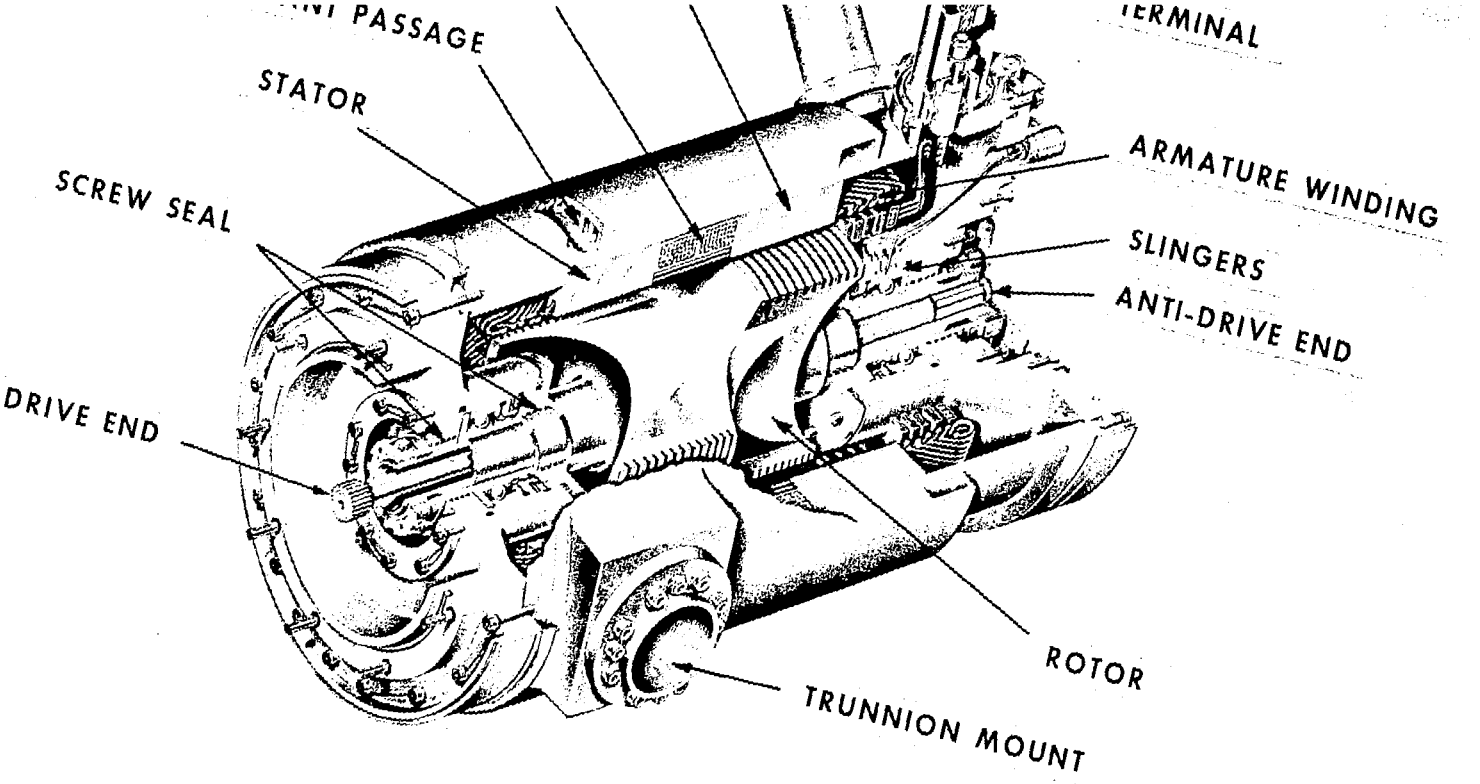

Figure 5-7 Alternator Cutaway View

5.1.3.2 Design Parameters

The alternator is a brushless solid rotor generator of the homopolar inductor type with a radial air gap. The field coil, which produces the direct-current working flux, is positioned between two identical sets of laminated cores. The electromagnetic circuit consists of the frame, which surrounds the core and field coil, the core sections, the radial air gaps, the solid rotor poles and the hub of the rotor.

The stator consists of two laminated core assemblies having a toroidal field coil between them and assembled in a common frame bore. A two-circuit design was chosen to minimize the radial bearing forces resulting from possible eccentricity between rotor and stator.

The rotor (Figure 5-8) was machined from an AISI 4620 steel forging to provide good strength and magnetic material properties. Slots were machined circumferentially in the rotor poles to reduce pole face losses.

The stator punchings are partially closed slots to reduce the pole face losses caused by flux pulsations in the air gap. The relatively large radial air gap of 0.060 inch decreases the radial bearing forces caused by eccentricity of the rotor and stator. A further effect of the large air gap is the need for a high magnetic potential between rotor and stator, leading to considerable leakage flux in the region between the rotor poles. This flux is limited by contouring the rotor between the four machined poles projecting from the hub to increase the effective depth of the rotor slot opposite the stator cores. The calculated flux and current densities at rated conditions are shown in Figure 5-9.

End-turn phase insulation was provided by wrapping 0.0105-inch ML glass between the involute of the armature coil and the extensions of the slot liners. Coil-side phase insulation was accomplished with 0.020-inch wall untreated braided-glass sleeving positioned on frog-legged coils prior to insertion. The sleeving provided sufficient separation between the coil sides, and was later impregnated with epoxy to provide added dielectric and coil support. A roof-shaped topstick was machined from polymer SP. This material has a polyimide chemical base and offers essentially the same properties as the ML family in a moldable solid form. Topsticks fabricated from this material provide high strength and ease of insertion.

Armature winding and insulation mechanical support, environmental protection, and corona resistance were achieved by vacuum impregnation with an epoxy varnish compound. The vacuum was applied to the windings after attachment of the phase connections and bus bar assemblies.

Solid connections were achieved by using TIG welding. Oxygen-free high-conductivity copper material was used for all flexible lead cables, bus bars, and field coil conductors. The intercoil connections were protected with a short section of untreated glass sleeving positioned over the joint, then filled with an epoxy compound to provide a bond. All other joints and joint areas were insulated by a double tape comprised of three thicknesses 0.0065-inch silicone-glass adhesive tape over the joint plus three layers of 0.005-inch

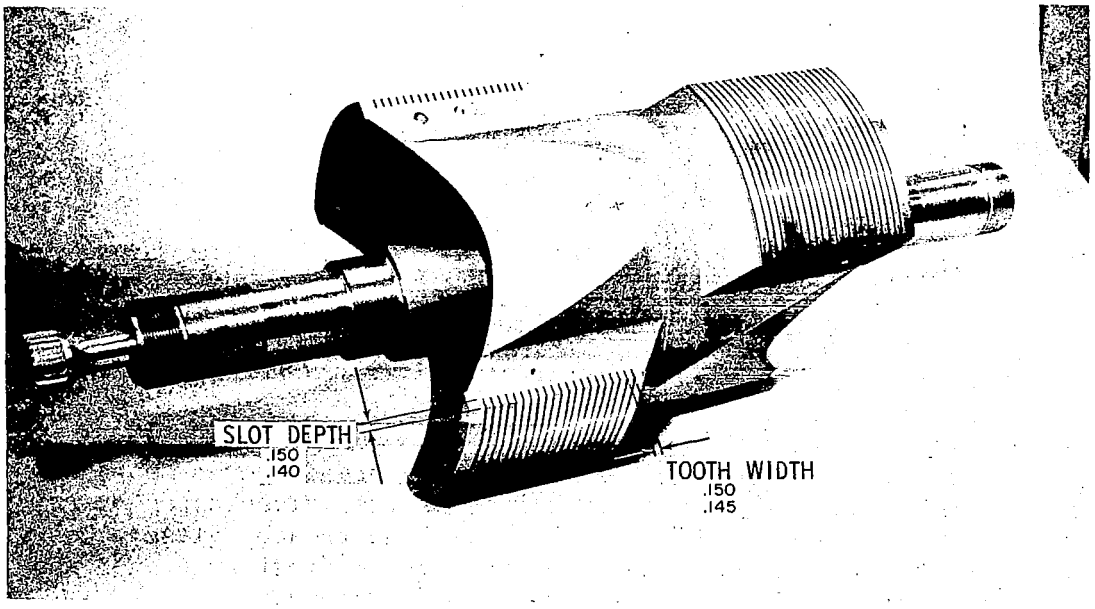

Figure 5-8 Rotor with Inner Shaft Assembled

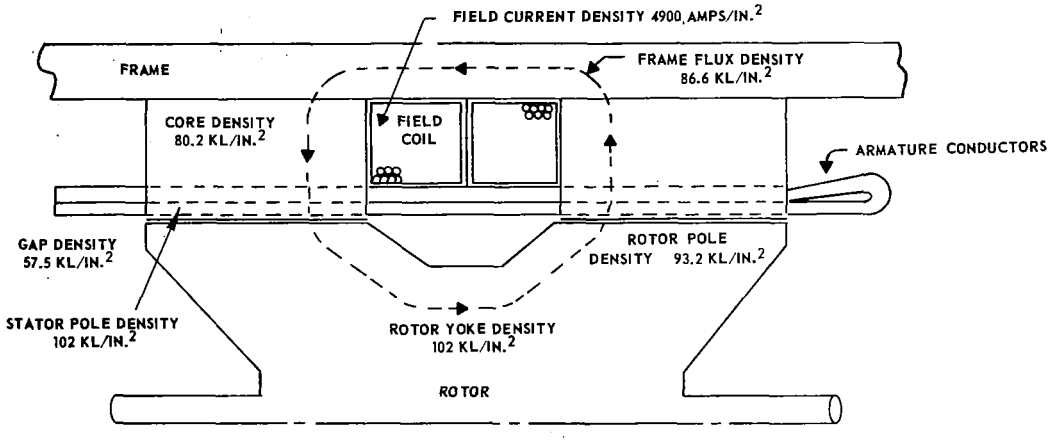

FLUX AND CURRENT DENSITY AT 80 KVA, 0.75 POWER FACTOR

ARM CONDUCTOR AREA	–	0.025675 IN.^{2}
FIELD CONDUCTOR AREA	–	0.00407 IN.^{2}
ARM CURRENT/CONDUCTOR	–	111.0 AMPS
FIELD CURRENT/CONDUCTOR	–	20.0 AMPS

Alternator Electromagnetics

Figure 5-9 Alternator Electromagnetics

desized glass tape. The tapes provided a strong dielectric joint. The phase connections consisted of a bus bar arrangement to provide numerous cross-overs and routing of the phase windings. The bars were positioned together to save space. Insulation was provided by placing a strip of 0.0105-inch ML glass on the bar at adjacent bus bar sides. Each insulation strip was taped in place and then the composite bars were taped together with desized 0.005-inch tape.

The insulation system was designed to meet the reliability and life requirements encountered in a space nuclear environment.

Contamination of the alternator cavity (and possible resulting change in vapor pressure at vacuum operation through out-gassing of adhesive in joint insulation tapes) was considered a disadvantage in the joint insulation method specified. This method consisted of three thicknesses (wraps) of 0.0065-inch silicone-glass thermosetting adhesive tape with an over-wrap of three thicknesses 0.005-inch untreated glass tape. A program was initiated to investigate other joint insulation methods and to establish the comparative performance by weight loss measurements at elevated operating temperatures. Seven methods tested included a combination of such materials as desized glass tapes over ML glass cloth and sleeving, Du Pont "H" film, and silicone treated glass adhesive tape. From these tests, it was concluded that the system first specified was the most stable and would result in least out-gassing effects.

The alternator cooling fluid is an organic polyphenyl ether. Hot fluid or vapors contacting conductors and insulation materials during alternator operation could result in damage by corrosion and chemical attack. Since data on the compatibility of the polyphenyl ether with the alternator materials were not available, a program was initiated to obtain the necessary information. The primary concern in the use of the fluid as a coolant was compatibility with alternator materials, and the dielectric effect in the alternator cavity. Tests conducted early in the program, simulating conditions and time contemplated in the machine, established that the hot polyphenyl ether did not cause deterioration of the insulating and conductor materials. The combined effects of oil mist, low vapor pressure, and radiation on the air dielectric effect were considered. It was postulated that, because of the low voltage levels, the combination would not produce corona or other effects detrimental to the reliability of the alternator. These conclusions were confirmed by insulation tests conducted at the Georgia Nuclear Laboratories.

Requirements considered of primary importance and the material selected to satisfy these requirements are described below. Twenty-six insulated conductors and insulating materials in simple combination specified for use in the alternator were studied in hot fluid and vapor at temperatures of 392 and 572 ^{o}F for periods up to 4000 hours. These tests demonstrated that all materials specified for use in the alternator were compatible with hot polyphenyl ether.

A thermal analysis of the alternator was performed during the design phase and the resulting major temperatures shown in Figure 5-10. The windings are cooled by introducing the coolant into the frame and passing it through axial slots in the outer edge of the frame. Preliminary investigations revealed that a laminar flow regime was required to limit the thermal resistance of the coolant and to keep the pressure drop low.

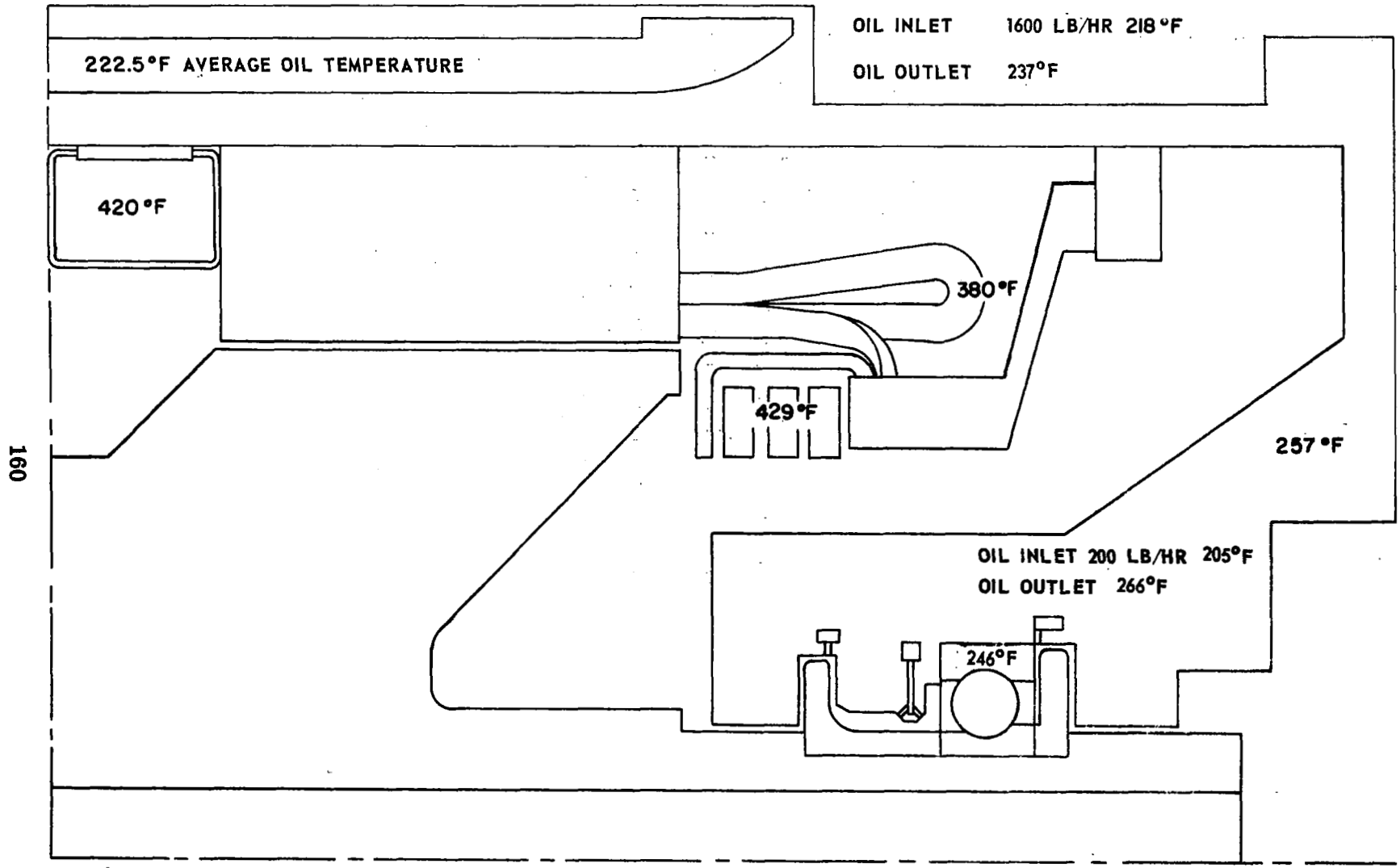

Figure 5-10 Alternator Thermal Map

Heat flows from the field coil to the copper enclosure of the coil, and then to the frame and coolant. The field coil within the frame was designed to ensure low thermal resistance contact under operating conditions with a vacuum in the generator cavity.

Stator core and armature copper heat losses flow through the stator cores to the frame and coolant. The stator core is assembled with an interference fit to minimize contact resistance. Some rotor pole face heat losses are radiated to the stator, then pass through the stator core and frame to the coolant. The remaining rotor heat losses and some radiation losses from the end turns to the end shields are removed by the bearing lubricant. The bearing and lubrication system is designed to remove heat from the shaft ends and heat generated by the seals and bearings.

The angular-contact ball bearing was selected as the best type for high-speed operation, long life, and high reliability. The design and development of the ball bearings for the SNAP-8 alternator is described in Reference 30. This type provides a maximum ball complement for increased bearing load capacity and high radial stiffness, and permits the use of a one-piece, lightweight ball separator. The low, nonthrust shoulder is on the inner ring, and the separator is piloted on both lands of the outer ring. This configuration provides full-width radial interface at the outer ring for the lubricant slingers, and keeps the balls away from the low shoulder at high speeds. With axial preloading, the bearing operates without internal looseness; this aids rotor dynamic balance and provides close running clearances for the dynamic slingers.

The 208 size (40-mm bore) light series, angular-contact ball bearing provides adequate load capacity.

The alternator rotor is straddle mounted between the two double-spring-loaded bearings in a back-to-back arrangement (i.e., with contact angles diverging toward shaft axis). The dual spring loading arrangement permits equal thrust capability in either direction.

The bearings are lubricated and cooled by four lubricant jets spraying on the inner ring. The bearing cavity is scavenged to prevent the bearings from running flooded.

The dynamic seal system used in the alternator to provide lubricant-coolant fluid containment is a plain slinger coupled to a screw seal. The slinger seal acts as a centrifugal separator. Since the pressure on both sides of the slinger is the vapor pressure of the saturated liquid, the slinger seals against a low pressure differential. Its main function is to form a stable interface between the vapor and the liquid, and to pump the liquid up to the return-line pressure. The function of the screw seal is to return drops of fluid escaping from the slinger liquid interface, back to the interface.

The frame was designed as a straight one-piece cylinder which permitted straightforward machining for the cooling passages, and also achieved the reliability and simplicity associated with one-piece construction. The frame is composed of a HY-80 alloy steel forged flange welded to a low-carbon,

seamless steel pipe frame shield. This provides the necessary strength in the trunnion support area and suitable magnetic properties in the frame.

The end shields are composites of Inconel X forged hubs welded to Type 304 stainless steel flanges.

5.1.3.2 Demonstrated Performance

a. Acceptance Tests.- The performance of a typical prototype alternator during acceptance testing is summarized in Table 5-II, 5-III, and 5-IV and Figure 5-11. The acceptance tests verify that the alternator meets the SNAP-8 requirements.

b. Turbine-Alternator Tests.- Since the alternator is part of a power conversion system which uses mercury vapor as the working fluid, the primary objective of the turbine-alternator tests was to evaluate all static and rotating components of the power conversion system as a unit rather than to specifically evaluate any one component. Electrical tests were made to determine speed control and voltage regulation characteristics under varying load conditions. Alternator electrical parameters were monitored along with winding and bearing temperatures, and lubricant flow, temperatures, and pressures. All operating parameters defined as SNAP-8 requirements were met.

The outboard screw seal seized during testing as a result of turbine over-speeds to approximately 19,000 rpm and 17,000 rpm on two alternators. The normal first critical speed with the bearings under the designed preload of 60 lb was 22,000 rpm. Examination of the bearings from the unit indicated that the bearings had operated without preload. Without the preload, the effective bearing stiffness is reduced and the rotor becomes unstable. Under these circumstances, the angular-contact bearings operate at virtually zero contact angle. The effective radial clearance was increased allowing the rotor to orbit and rub the stationary screw seals.

It was concluded that the malfunctions were caused by rotor instabilities due to loss of bearing preload, and operation at or near the first critical speed. The critical speed was lower than normal because the bearing stiffness had been reduced by loss of preload. The high amplitude expected under these conditions would cause rubbing and produce a wear pattern similar to the pattern actually observed.

Design modifications were made to reduce the tendency for the bearings to unload at speeds above design. The design modifications are discussed in Reference 30. Major features of the redesign were the replacement of the wavy springs with belleville spring washers, and the increase in length-to-diameter ratio for the sliding parts to reduce the possibility of the parts cocking. Redesigned parts were never procured or tested.

Four alternators were tested as part of complete turbine-alternator units in a power conversion system. Apart from the previously mentioned malfunctions, the performance was satisfactory and fulfilled the design requirements.

TABLE 5-II ALTERNATOR ELECTROMAGNETIC PERFORMANCE VERSUS SPECIFICATION LIMITS

Performance Item	Specification	Alternator Performance
Open circuit time constant (T'do)	0.60 sec. max. at steady-state temperature	0.57 sec. at 307°F
Short circuit ratio	0.25 min.	0.67
Short circuit capacity for 5 sec.	2 PU min.	2.94 PU (3 phase) 3.96 PU (1 phase)
Instantaneous voltage drop on sudden application of 2 PU impedance load	Voltage not to drop below 0.70 PU	Voltage dropped to 0.83 PU
Excitation	52 V max. 22 amps max.	43.3 V 19.6 amps
Wave form - total rms harmonic content (L-L at 1 PF)	7% max.	2.33%
Symmetry of construction (max. voltage difference between phases)	1 V max.	<1 V
Output voltage modulation	1% max.	0.14%
Efficiency, including field losses, at rated load, 0.75 PF	87% min.	87.8%
Field coil resistance	-	1.46 ohms
Stator phase resistance	-	.00583 ohms
Full load (80 kVa, .75 PF) excitation		
Voltage	52 V max.	42.0 V
Current	22 amps max.	18.9 amps
Loss breakdown		
Field I^2R (kW)	-	0.79
Stator I^2R (kW)	-	1.31
Bearing and seals (kW)	-	2.20
Core and stray load (kW)	-	4.00
Total kW	8.96 max.	8.30

TABLE 5-III COMPARISON OF SPECIFIED THERMAL REQUIREMENTS WITH TEST RESULTS

Item	Specification	Test	
Cooling Oil	Polyphenyl ether	Polyphenyl ether	
Flow (gpm)	2.84	2.84	
Inlet pressure (psia)	-	21.9	
temperature (^{o}F)	205	205	
Outlet pressure (psia)	-	8.3	
temperature (^{o}F)	-	230	
ΔP (psi)	14 max.	13.6	
		DE*	ADE**
Bearing			
Inlet flow (gpm)	0.35	0.338	0.320
pressure (psia)	20 $\pm$ 1	20.2	20.2
temperature (^{o}F)		196.0	198
Outlet flow - inborad (gpm)		0.155	0.138
flow - outboard (gpm)		0.175	0.176
pressure - inboard (psia)		6.7	6.5
pressure - outboard (psia)		6.7	6.7
temperature - inboard (^{o}F)		225.0	248
temperature - outboard (^{o}F)		259.0	258
Bearing cavity pressure (psia)		0.8	0.8
Winding Temperatures (^{o}F)			
Field coil average	-	307	
Field coil hot spot	392	324	
Stator winding end turn	392	367	
Stator winding 180^{o} bus bar	410	406	
Bearing temperature DE	300	244	
ADE	300	243	

* DE = Drive End
** ADE = Antidrive End

TABLE 5-IV ALTERNATOR PERFORMANCE SUMMARY

Parameter	Specification	Test
Cooling Oil Flow (gpm)	2.84	2.84
Cooling Oil Inlet Pressure (psia)	33	21.9
Cooling Oil Pressure Drop (psi)	13 max.	13.6
Cooling Oil Inlet Temperature (^{o}F)	200 - 210	205
Speed (rpm)	12,000	12,000
Output (kVa)	80	80
Power Factor	0.75 lagging	0.75 lagging
Voltage	120	120 - 120.1
Frequency (Hz)	400	400
Excitation Current (amps)	22 max.	19.1
Excitation Voltage	52 max.	41.9
Phase Unbalance (%)	1 max.	1

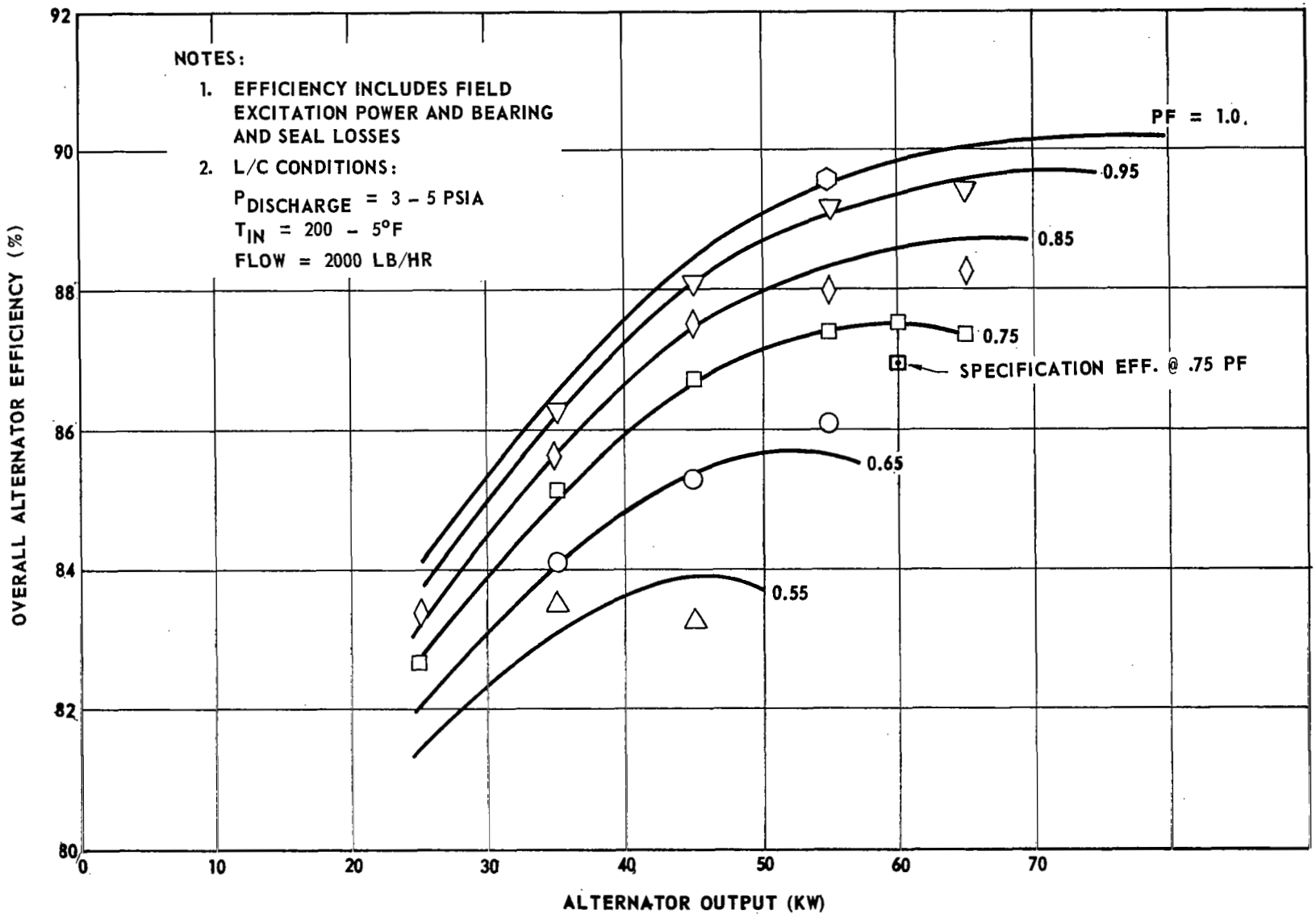

Figure 5-11 Alternator Efficiency Characteristics

The longest accumulated time on a single unit in the 35-kWe system test was in excess of 12,000 hours. The maximum number of startup and shutdown cycles on a single unit was 135.

Testing of a complete turbine-alternator in a mercury system was also conducted at NASA-LeRC in which a unit satisfactorily completed more than 1400 hours of continuous operation.

c. Endurance Tests.- An electrical component test facility was used for long-term testing to obtain endurance data for electrical components without the operational problems of a hot-mercury facility. The components tested include the alternator, the voltage regulator and static exciter, the speed control, and the saturable reactor. Operation was at rated load conditions.

The alternator performed satisfactorily during the initial 2500-hour endurance test. Inspection following disassembly revealed the alternator to be in good condition. The insulation had darkened and a few cracks were observed in the end-turn impregnating varnish. The insulation resistance of the stator winding-to-frame decreased from 9×10^9 ohms at the start of the test to 4.9×10^9 ohms at 2500 hours. The field-to-frame resistance decreased from 2×10^{11} ohms to 4.5×10^9 ohms over the same period. These lower values of insulation resistance indicated only minor electrical degradation which is typical of used alternators.

The alternator was reassembled, returned to the facility, and testing continued. A further 20,630 hours of satisfactory operation was achieved bringing the total accumulated time on one unit to more than 23,130 hours.

A detailed inspection of this alternator was made to determine whether or not life-limiting operating modes existed. It was ascertained that a loss of bearing preload had occurred in a similar manner to that experienced previously during turbine runaway operation in the 35-kWe system tests. However, all parts of the alternator were in excellent condition and a considerably extended life projection to at least five years was estimated. A detailed report of the condition of this alternator is contained in Reference 39.

d. Vibration and Shock Testing.- An alternator assembled to a turbine was tested to NASA specification 417-2, Rev. C. This is described in Reference 37. A detailed inspection of the alternator revealed some galling of the bearing outer rings in the housing bores, and a small leak in the alternator terminal ceramic-to-metal seal. The bearings showed almost imperceptible brinelling evidence and the alternator was judged to be able to pass the shock and vibration tests with only minor improvements.

5.1.3.3 Conclusions

The extensive testing of the alternator has confirmed its capability of exceeding the life objectives. Some minor modifications to improve the overall reliability are primarily concerned with the inherent weaknesses in the sliding elements of the bearing spring preload system.

A detailed description of a proposed design change is contained in Reference 30.

Also, in Reference 37, recommendations are made for eliminating the galling of the bearings and housings following vibration tests. This consists of providing a hardened housing surface for improved sliding compatibility with the bearing outer ring.

5.2 NaK PUMP

5.2.1 Development Background

The NaK pump was designed and developed to pump sodium-potassium liquid metal (eutectic NaK-78) in the heat transfer loops of the SNAP-8 nuclear space power system. For the 90-kWe system, NaK pumps are required in the intermediate loop and heat rejection loop as shown in Figure 5-12. For the 35-kWe system, NaK pump-motor assemblies are required in the primary loop and the heat rejection loop, as shown in Figure 5-13.

The NaK pump is shown in cross section in Figure 5-14. The design and development of the SNAP-8 NaK pump is described in detail in Reference 40.

5.2.1.1 Overall Design Philosophy

The NaK pump design was based primarily on the SNAP-8 system minimum life goal of 10,000 hours of unattended operation (with no maintenance) in space environment. This meant that the NaK pump had to be designed primarily for endurance.

The design requirements stressed that no NaK leakage could be tolerated. Canned motor construction and use of NaK-lubricated bearings in a hermetically sealed housing were, therefore, necessary.

Fluid in the primary loop of the 35-kWe system becomes radioactive as it passes through the reactor, and it is undesirable to introduce the radioactive fluid into the heat rejection loop. This eliminated the possibility of using a single pump to circulate NaK in the two loops or to use a single motor to drive two separate pumps.

Since the pump must supply its own cooling and lubrication, a cooling and purification system was included as part of the design. The optimum design is one which has the recirculation pump as part of the unit and a cooling and purification system external to the pump.

To facilitate pump development, some limited separate testing of subcomponents was done. Bearings were tested separately in oil, and an assembled pump was tested using water (which has hydraulic characteristics similar to NaK) as the working fluid.

5.2.1.2 Conceptual Design and Performance Requirements

A speed of 6000 rpm was selected based on the optimization of the pump and motor elements with electrical input power. The main pump is a single-stage, end-suction, double-volute, mixed-flow design with a semi-open impeller thrust-balanced axially with back vanes. Isolation of the 1100°F pump fluid from the 300°F motor fluid is achieved by a close-clearance annulus around the shaft between the pump and motor. The pump housing is supported mechanically by three pins mounted in support arms which extend from the motor housing. This feature isolates the hot pump housing from the relatively cool motor.

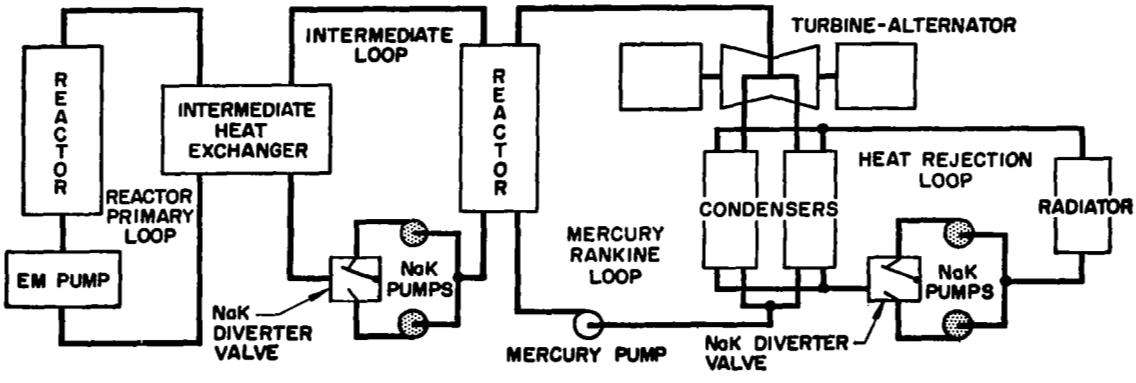

Figure 5-12 90-kWe System Diagram Showing Location of NaK Pumps

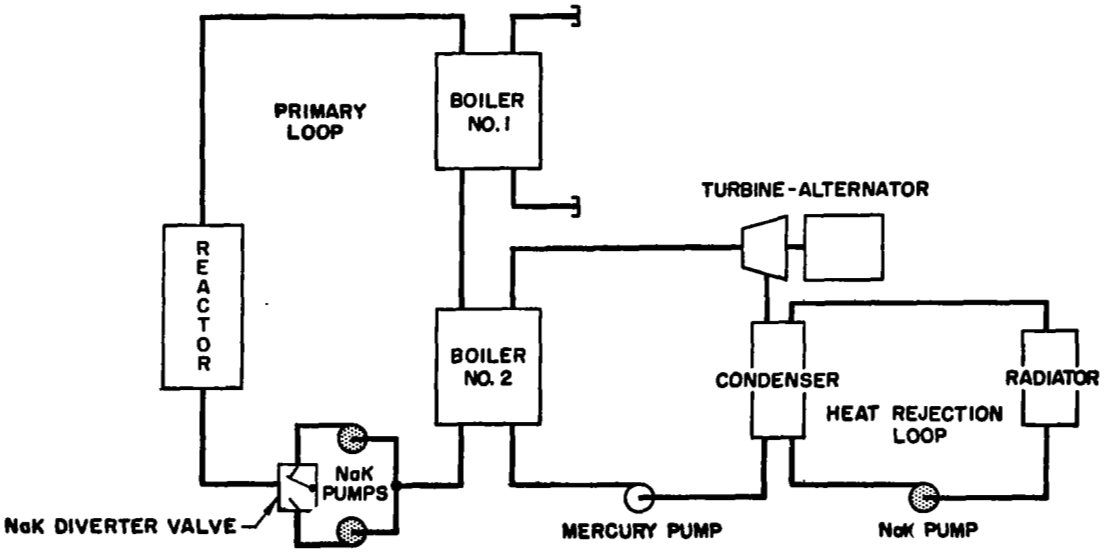

Figure 5-13 35-kWe System Diagram Showing Location of NaK Pumps

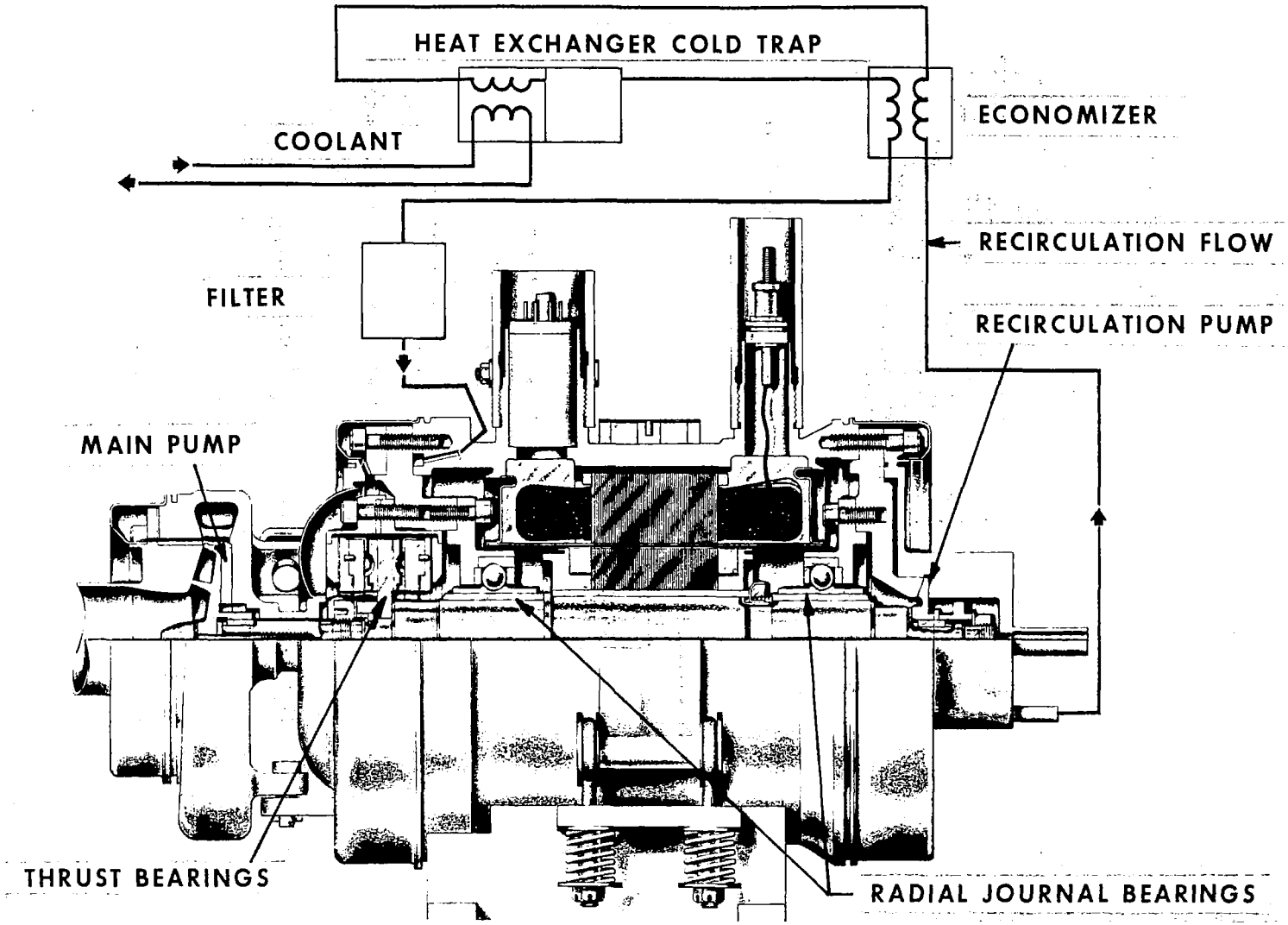

Figure 5-14 NaK Pump Cutaway View

The NaK in the motor cavity is cleaned, filtered, and cooled by a recirculation system driven by an open impeller, single stage, low speed recirculation pump located near the opposite end of the shaft from the main pump. Both impellers are keyed and bolted to the shaft. The main impeller bolt is designed to stretch under the torque load applied during assembly to maintain a preload under all differential thermal conditions.

The axial thrust bearing is located on the main pump side to control pump axial clearances due to shaft expansions. The thrust bearing is a tilting-pad hydrodynamic type.

The shaft is supported by two radial tilting-pad journal bearings, one on each side of the motor rotor. The design and development of the bearing system shaft used in the SNAP-8 NaK pump is described in more detail in Reference 41.

The motor is an 8-pole, squirrel cage, 3-phase, 208-V (L-L), 400-Hz, series-wound induction type hermetically sealed from the NaK. The stator incorporates a ceramic-fill insulation system. The three phases plus the neutral of the Y-connected stator are connected to individual ceramic hermetically sealed terminals.

5.2.2.1 Main Pump

The function of the main pump is to circulate NaK in the NaK loops of the SNAP-8 system. Hydraulic performance requirements for pumps in both loops is shown in Table 5-V, where the design values and test results are compared.

The pump design was based on standard pump criteria.

a. Impeller.- The impeller is a semi-open, mixed-flow, five-vaned centrifugal impeller with twenty-four 0.13-inch high, 90-degree radial back vanes for axial thrust balancing. Standard water-pump design practice was applicable since NaK and water are almost identical hydraulically. The semi-open design feature was chosen for the following reasons:

- Radial clearance was more critical than axial clearance.
- At the high temperature of 1300°F, no completely nongalling material of compatible coefficients of thermal expansion with the CRES 304 housing was available in NaK for wearing rings or other close-running parts.
- At the radial clearance required to avoid any possibility of rubbing, the amount of wearing-ring leakage would lower pump efficiency.
- In general, the semi-open impeller provides better clearances with less efficiency loss when handling thermal distoration associated with bimetal joints and axial and radial warpage.

TABLE 5-V - NaK PUMP PERFORMANCE DATA

Components and Parameters	HEAT REJECTION LOOP PUMP		PRIMARY LOOP PUMP	
	Calculated Design Data Based on In-Air Motor Test Results	Test Results	Calculated Design Data Based on In-Air Motor Test Results	Test Results
Pump, Centrifugal				
Flow, lb/hr	40,200	40,200	40,200	45,900
Inlet NaK Temp, °F	495	495	1,100	1,170
Flow, gpm	98.7	98.7	109.5	125
Inlet pressure, psia	15.0	15.0 (1)	28.6	30.8(1)
Pressure rise, psi	41.8	39.8	16.4	28.3
Head, ft	118	113	51.6	89
Outlet pressure, psia	56.8	54.8	45.0	59.1
Hydraulic power, kW	1.79	1.715	.78	1.54
Efficiency, %	63.8	68.5	69	64.2
Shaft input power, kW	2.81	2.51	1.14	2.39
Motor, Induction				
400 Hz, 3 Phase, 208 V (L-L)				
Electrical efficiency, %	72.5	75.5	68.4	74.4
Overall efficiency, %	60.7	54.6	47.3	53.
Input power, kW	4.60	4.60	2.37	4.52
Current amps	23.3	23.0	12.5	22.6
Pump Motor Assembly				
Overall pump efficiency, %	39.0	37.3	33.1	34.1
Summary of Losses				
Total electrical, watts	1,270	1,130	750	1,156
Total mechanical, watts	540	960	500	975
Total mechanical and electrical losses, watts	1,810	2,090	1,250	2,131

(1) System Requirements

Since low axial thrust on the thrust bearings was required to provide a design margin for the 10,000-hour life, an adjustable method of axial thrust balancing was desirable. Radial back vanes were used to provide load adjustments through vane trimming.

The impeller suction inlet is a free vortex incorporating an allowance for prerotation of 115% for improved efficiency. The impeller is keyed to the shaft and retained by a Hastelloy B bolt. The impeller back-vane clearance is adjusted by a parallel ground shaft end spacer.

b. Pump Housing.- The pump suction housing is a single-end suction housing without antirotation vanes. Shims are used to adjust the impeller front-vane clearance.

The pump discharge housing is a radial-flow double volute with an equal-side trapezoid impeller diffusion section flaring into a rectangular collector. The double volute reduces the radial shaft load from the impeller for off-design-capacity operation. To produce the hydraulic section of the discharge housing, two halves were machined and then welded. The discharge pump housing is made of 304 CRES forging stock.

The 0.040-inch radial shaft clearance annulus between the motor and main pump minimizes the NaK fluid interchange between the main loop and the NaK motor cavity which requires clean NaK for the bearings. Three load-support arms with slip-fit pins allow for the differential thermal growth between the 1300°F 304 CRES pump housing and a 300°F 9M* motor housing. These arms must carry the piping loads of 100-lb force and 600 pound-inches moment both in any direction simultaneously on the suction and discharge pipe pump interfaces. This feature also provides thermal isolation between the pump and motor.

5.2.2.2 Motor

The motor input power is furnished by the alternator. During reactor startup, with power supplied by a battery-powered inverter, the pump operates on 95-Hz, 19-V power, then switches to 220-Hz, 88-V power. The motor cavity is flooded with NaK necessitating a canned rotor and stator; the cans are 0.010-inch thick Inconel. More than half of the motor losses are associated with the "air gap," or magnetic gap area, so the recirculation system fluid was passed through the gap to remove this heat.

The motor design emphasized small operating torque margin to maintain a small motor diameter which minimizes hydraulic losses. The power required from the motor is shown in Table 5-V.

a. Stator.- The motor stator has 36 slots in a laminated 8-pole steel core, hand-wound with nickel-plated copper wire. The stator is completely sealed from the internal NaK and external pump atmosphere by a welded can. The stator cavity is back filled with dry nitrogen at 70°F and 14.8 psia. Figure 5-15

---

* 9Cr-1Mo

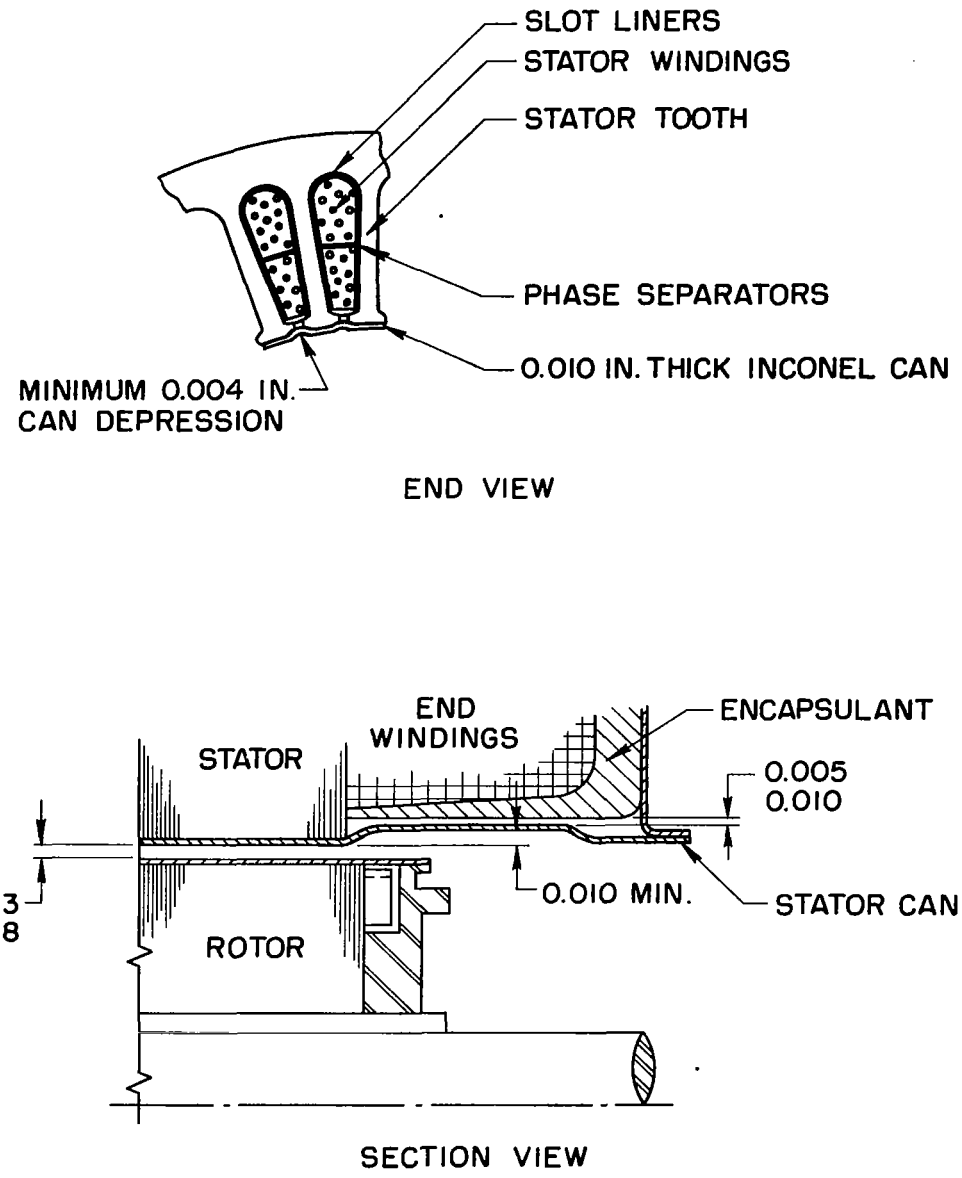

Figure 5-15 Stator Construction - NaK Pump

shows a cross section of the stator. The internal-to-external electrical leads, internally wye connected, penetrate the housing through sealed ceramic terminals. Eight sets of internal Chromel-Alumel thermocouples measuring the end turn, slot, and inside and outside core temperatures are brought out through two 8-pin ceramic connectors.

b. Insulation.- The stator construction employs an inorganic ceramic insulation system. Ceramic insulation provides superior resistance to the nuclear radiation present in the primary loop and the capability to operate indefinitely above 600°F (hot-spot temperature). The 600°F operating temperature allows the direct use of heat rejection loop NaK at 500°F for cooling. Aerojet had proven the insulation system prior to incorporation in the pump motor in a series of statorette tests. These conducted at 1000°F for 3200 hours produced no degradation of the insulation. The development of this insulation system is described in Reference 42. The design included slots liners and phase separators of glass-backed mica flakes, with the organic binders baked out prior to ceramic impregnation. Then the ceramic material, calcium aluminate, was vibrated into place and baked. The ceramic and glass cloth formed an insulation air gap to mechanically retain the wire in place. The inorganic ceramic does not deteriorate with temperature, but the thermal cycle expansion and contraction of the electrical wire on the ceramic presents the most likely mode of failure.

c. Stator Can.- The Inconel inside diameter cylinder (can) was hydraulically formed into the stator core and slots. Standard construction normally uses light shrink fits. Forming provided intimate surface-to-surface contact between the can and core teeth to provide support for the can. The dry nitrogen back fill in the stator provided the major heat path from the electrical winding to the motor-cavity NaK.

d. Rotor.- The rotor is a squirrel-cage design consisting of 46 semideep slotted laminations which are made of AISI M-22. Rotor conductor bars and end rings were made of oxygen-free electrical grade copper. The rotor was completely sealed by an Inconel can. The canning process consisted of a shrink fit 0.010-inch sleeve as the outside diameter and a much thicker sleeve on the inside diameter to end plates. The rotor assembly is shrunk onto the shaft.

5.2.2.3 Bearings

The axial and radial bearings support the loads applied to the NaK pump shaft. The bearing lubricant chosen was NaK in order to simplify the design. The most adverse fluid properties are at the highest expected operating temperature of 600°F. For reasonable pump critical speed, the radial bearing stiffness should be more than 18,000 lb/inch at operating speed (5900 rpm). Because of the thin NaK film and high operating temperatures, the bearing must be self-aligning. The starting problem and the low lubricant feed pressure available made the hydrodynamic type of bearing more desirable than the hydrostatic type. Because of its low viscosity, NaK as a lubricant presents two basic problems: load capacity, and stiffness. This is a result of the shaft mass which is to be subjected to acceleration forces. Fortunately, the low viscosity of NaK also leads to extremely low bearing power consumption and temperature rise which permits the use of relatively large bearing sizes. For

these reasons, preliminary design emphasis was placed upon load capacity and stiffness.

a. Thrust Bearings.- The thrust bearings have six self-aligning tilting-pads and are designed to operate with a 0 to 80-lb rated load. Each bearing pad is an individual plate which is free to pivot in a circumferential direction to provide a tapered lubricant film. The pad and thrust runner are made from Carboloy 44 alloy. Lubricant is normally fed to the center of the housing near the shaft and pumped through the bearings by centrifugal action. A small portion of the lubricant flows over the working bearing surfaces while the remainder passes through the spaces around the pads. The cone-shaped tungsten carbide rotating running plate provides a line contact surface for minimizing starting torque. The gimballed plate arrangement provides the required self-aligning feature.

For equally loaded pads, the minimum film thickness was calculated to be 0.0004 inch with a mean temperature rise in the film of 6.4°F. With maximum tolerances and deflections causing maximum load differences between the pads, the most heavily loaded pair of pads would have a calculated minimum film thickness of 0.00031 inch and a mean temperature rise in the fluid film of 10.7°F which is adequate for this application.

Two identical bearings are placed face-to-face operating on opposite sides of the same thrust plate to carry axial loads in either direction. By limiting the axial clearances, the shaft end play is controlled; the bearings are also preloaded and stabilized allowing for ground test operation or zero-g space conditions.

b. Radial Journal Bearings.- The journal bearings are hydrodynamic self-aligning tilting-pad bearings with four pads and designed to carry loads ranging from 0 to 50 lb. The specified minimum allowable film thickness was 0.0002 inch. The four pads are made of M-2 tool steel. The designed bearing radial clearance was 0.0008 to 0.0013 inch. By control of the running clearance, a slight bearing preload was established to assure a stable bearing in a zero-g environment.

The ball pivots are made from T-1 tool steel and are accurately centered and retained in a housing bolted to the motor housing. The journal sleeves are also T-1 steel and are shrunk on the shaft and ground in place.

The mounting feature of the journal to the shaft dictated the choice of materials. The shaft material must be magnetic since it is part of the motor flux parts and the coefficient of expansion should be similar to the sleeve. The shaft material was 9M steel with a coefficient of expansion five times more than the most desirable bearing material, tungsten carbide. Therefore T-1 tool steel with a similar coefficient of expansion was chosen. The four-pad tilting-pad journal bearing was selected as a reasonable compromise between high load capacity and minimum shaft-pad motion with rotating unbalance. A length-to-diameter ratio of one was chosen to obtain high load capacities without unduly complicating the fabrication and assembly.

A conventional sleeve journal bearing was considered to be unsuitable because of half-frequency whirl problems associated with this design. Tilting pad bearings are not prone to this problem even in zero-g operation.

5.2.2.4 Recirculation System

The function of the NaK pump recirculation system is to cool the motor and bearings and to provide clean NaK for the hydrodynamic bearings as shown in Figure 5-14. The system shown was designed for ground testing only and employs an oil-to-NaK heat exchanger to cold trap oxide particles, and a 5-micron filter. An economizer is also provided in this circuit to reheat the NaK and assure that the return flow NaK is in the liquid state.

For manned system use, a simpler recirculation system was evaluated. This used a NaK-to-NaK heat exchanger with no filtration or cold trapping. Some preliminary analysis resulted in a compact heat exchanger which was intended to be close-coupled to the pump. Temperatures in the pump are similar for both the NaK-to-NaK and the oil-to-NaK heat exchangers. No hardware was built, however, for the NaK-to-NaK system.

The recirculation pump circulates 1.6 gpm of NaK producing a head rise of 40 ft with a pump speed of 5800 rpm. A radial flow, full-open-vane impeller was selected. Suction pressure is controlled by the main loop pressure. Under the normal operating conditions, the pump will have more suction pressure than the minimum required for a pump of this type. The full-open impeller, by equalizing impeller radial pressure gradients, assures that no impeller axial thrust is present.

The impeller is of conventional design. A large allowance for suction prerotation was made because of the proportionally large suction eye diameter dictated by the diameter of the shaft on which the impeller is mounted. The impeller is keyed to the shaft and located axially with shims.

The pump housing is a close-clearance annular volute with a flow limiting exit diffuser 0.11-inch in diameter. Because of the small flow, only a limited arc near the cutwater of the volute is exposed to high pressures. Consequently, the impeller radial load will be negligible. The annulus is 0.10 inch wide by 0.06 inch deep on a 2.4-inch diameter.

The economizer is used to heat the NaK from the heat exchanger cold trap to prevent possible oxide precipitation at the filter. The simple tube-in-tube counter flow heat exchanger has an effective heat exchange area of 10 square inches. In operation, hot liquid is directed into the shell at 350^{o}F for both fluids.

The cold trap heat exchanger rejects the heat gathered by the NaK as it flows through the pump. The heat transferred is estimated to be 2100 watts. The heat exchanger, being the coldest point in the recirculation system, is also used as a cold trap to remove excess oxide particles which can harm the bearings. The selected design is a counter-flow heat exchanger. In operation, the polyphenyl ether is directed into the outer shell at the top and leaves at the bottom. The fluid side film coefficient though low is sufficient, since

the exposed area is large and the temperature change allowance was 85 to 135°F (a low effectiveness heat exchanger). The NaK is first directed from the bottom upward between an annulus formed by the NaK container and a wire-mesh filled inner can. When the flow reaches the top of the annulus, it is reversed and flows through the inner can and then out of the heat exchanger. The wire mesh inside the inner can presents a large area in which oxides can be collected.

5.2.2.5 Rotor Dynamics

Using the conventional Dunkerly approach, the analysis of the rotor critical speed based on the stiffness of the rotor alone indicated that it was approximately 25,000 rpm.

The minimum calculated bearing stiffness was 19,000 lb/inch based on running the bearings unloaded and with maximum clearance at 6000 rpm. A bearing stiffness of 19,000 lb/inch yields a critical speed of 9000 rpm, thus providing ample margin.

5.2.2.6 Material Selection

The following materials are used in the major parts of the pump:

Part	Material
Motor housing	9Cr-1Mo
Pump housing	304 SS
Journal bearings	
Sleeves and ball	Tungsten T-1
Pads	Moly-Tung M-2
Thrust bearing	Carboloy 44A
Impeller	410 SS
Impeller bolt	Hastelloy B
Shaft	9Cr-1Mo
Rotor and stator cans	Inconel 600

5.2.2.7 Thermal Analysis

The thermal expansion of the NaK pump established the allowable axial clearances used on the main and recirculation pump impellers. Later in development, back vane clearance was increased to a nominal 0.040 inch leaving the front vane clearance as designed to retain good efficiency. This was required due to an unforeseen 1160-to-350°F thermal gradient alternating on the impeller back shroud which causes the impeller to bow. This is discussed in the section on gas in motor cavity and/or recirculation loop. The method of mounting the pump housing to the motor housing and the swirl clearance annulus around the shaft between the motor and main pump minimizes primary loop heat leakage into the motor cavity to a calculated 270 watts.

5.2.3 Demonstrated Performance

The NaK pump has been progressively tested first as separate subcomponents and then as a complete unit which was endurance tested in a NaK component test facility and in the SNAP-8 35-kWe ground test system. A total of 56,493 operating hours have been accumulated on eleven (11) NaK pumps with 3362 start cycles in five separate test loop locations. One unit successfully ran for 10,362 hours with 786 start cycles.

5.2.3.1 Overall Test Program

The NaK pump test program followed a line of tests to determine the subcomponent and overall performance of the unit, as described in the following paragraphs.

5.2.3.2 Subcomponent Testing

a. Bearing Hydrodynamic Design.- The journal and thrust bearing tests (Reference 41) were conducted in individual test rigs using silicone oil to verify the load-carrying capacities and stability of the bearings.

b. Bearing Pivot Fretting Tests.- The bearing pivot-point tests (Reference 41) concerned with c ntact point fatigue and Hertz stresses were conducted separately from the bearing hydrodynamic tests.

c. Motor Tests.- The motor in-air testing using a dynamometer established the torque capabilities, stator and rotor losses, and core and stray losses.

5.2.3.3 Testing of Pump Components

a. Motor Test with Water.- The NaK pump motor (the unit less the main pump) was tested in water which is hydraulically similar to NaK, to determine further motor data such as can loss, total motor, bearing, and recirculation pump power requirements, preliminary starting voltage requirements, recirculation pump performance, motor gap and filter differential pressure characteristics, and the motor NPSH values.

b. Starting Torque Tests with Water.- Using the in-air rotor test data with a canned stator, the locked rotor (or starting torque), input power, and current were established at variable frequencies and input voltages. Later, canned rotor tests during acceptance and inverter tests confirmed the negligible effect of the rotor can on these locked-rotor test values.

c. Starting Torque using SNAP-8 Static Inverter.- The use of the SNAP-8 inverter for NaK pump startup resulted in a different performance than when using a sinusoidal alternator power source. The inverter output was a quasi-square wave form. Test results showed from 15 to 80% higher voltage and 5 to 50% greater power for locked-rotor when a static inverter was used as the pump startup power source.

5.2.3.4 Full Assembly Tests

a. Development Tests.- By using the motor as a calibrated device, the segregation of losses in the unit was continued by establishing overall hydraulic performance and speed versus torque and load performance. The axial thrust due to the main pump and motor rotor, and the impeller radial load on the shaft were estimated by making a pressure survey of the pump volute. Since most losses were established separately and related to theory, the performance of the pump in NaK could be accurately projected.

b. Component Facility Tests.- The projected performance curves from the water tests were confirmed by later tests of the NaK pump in liquid NaK. The NaK eddy current and motor hydraulic loss changes were established, and the reliability of the unit was demonstrated in a 10,000-hour endurance test at the primary conditions of 1170°F.

c. SNAP-8 System Tests.- In parallel with the NaK pump loop tests, NaK pumps were operated in the SNAP-8 35-kWe system ground test systems at Aerojet and NASA-LeRC. The 35-kWe test loops at Aerojet and NASA-LeRC are facilities where operational tests were conducted primarily on the boiler and turbine-alternator while test endurance life data and experience were gathered on the pumps and other SNAP-8 components. The NaK pumps were installed in both the primary and heat rejection loops of these facilities.

d. Acceptance Tests.- Each NaK pump was acceptance tested in water to determine its starting torque, 400-Hz pullout torque, recirculation, hydraulic, and overall pump performance.

5.2.3.5 Overall NaK Pump Performance

The NaK pump overall test results in water were later confirmed by the actual NaK testing. By using water initially as the pump fluid, a more convenient test program could be accomplished than when using NaK. These test results established the motor, pump, and recirculation system component characteristics and hydraulic performance. The NaK eddy currents in the motor and the effect on the motor cylinder hydraulic losses could not, of course, be determined in water, but were deduced from later tests in NaK.

a. Loss Breakdown and Performance Data - 400 Hz.- The NaK pump loss breakdown and performance data for the heat rejection and primary loop conditions are shown in Table 5-V. The pump met performance requirements throughout its development history with only slight deviations.

The 35-kWe system flow rate was increased to 49,000 lb/hr from the original design of 40,200 lb/hr which necessitates using the full head available from the NaK pump. Allowing however for line losses due to ground test piping and a standby electromagnetic pump in series, the pump still has head margin for the 35-kWe and 90-kWe systems.

b. Performance Curves.- Using the performance data from water tests and motor tests, the performance in 495°F NaK was calculated for the heat rejection

loop condition. The value of 0.009 to 0.011-inch front-vane axial clearance was used in the calculation. The pump in the heat rejection loop is expected to attain 37.5% efficiency using 4.56 kWe, and produce 112-ft head at 98.7 gpm (40,200 lb/hr at 495°F).

The NaK pump performance (Figure 5-16) was substantiated by tests in NaK at 495°F, and by tests at 1170°F (Figure 5-17). A slight increase of impeller front vane clearance due to the additional thermal expansion explains the tendency for lower head and power values at the higher temperature. Significantly, the data did not change before and at the end of the 10,000-hour NaK pump endurance test at over 1100°F. As seen from Figures 5-16 and 5-17, the NaK pump shows a performance margin above the requirements for the 90-kWe system.

c. Low Head Performance.- The head-capacity performance of the pump has, at times, been lower than that presented in Figures 5-16 and 5-17, particularly for pumps operating in the primary loop. The data for these figures obtained from pump loop tests were generally confirmed in 35-kWe system tests. Later tests indicated low head values fairly consistently in the primary loop and occasionally in the heat rejection loop. None of the disassembled NaK pump hardware has shown any wear or head-producing fault. No testing abnormalities existed to justify this. The head variations (by as much as 30 feet) as a function of time minimizes the likelihood of misassembly. Consequently, the low head is believed to be a pump-system problem due to either gas in the system, a leaky bypass valve, flow-meter inaccuracy, or a combination of these.

5.2.3.6 Pump NPSH

The net positive suction head (NPSH) required to avoid cavitation damage or low performance is established by considerations of the main pump impeller and the elements in the flooded motor cavity. Both have different NPSH values.

a. Main pump.- The main pump NPSH is determined by a cavitation test in which the suction pressure is reduced while all other parameters are held constant. When the pump head decreases, the impeller performance is being affected by the vapor bubbles formed at its eye.

The conventional 2% head decay was used as the definition of the start of cavitation since no significant damage or loss of performance should occur at this level. At the design capacity of 98.7 gpm, the 2% head decay occurred at 16.6 ft NPSH, well within the SNAP-8 system requirements.

b. Motor Cavity.- In the present configuration, the motor cavity pressure requirements more significantly define the net positive suction pressure required for the NaK pump. The low pressure point of the NaK pump is at the motor rotor retaining nut, next to the recirculation pump end radial bearing or at the recirculation pump eye. Figure 5-18 presents the net positive suction pressure requirements versus capacity for the temperatures that were used in the 35-kWe system tests.

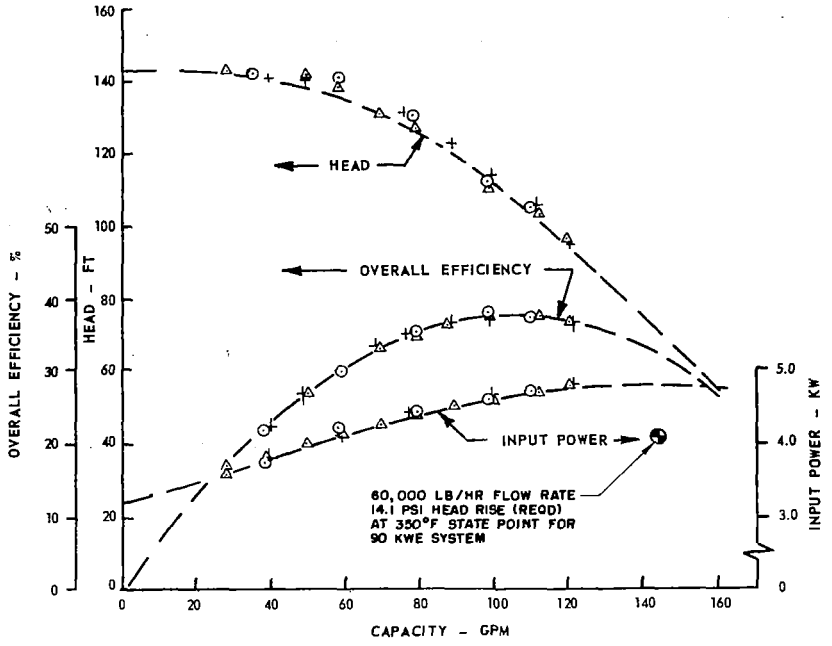

Figure 5-16 NaK Pump Performance in 495°F

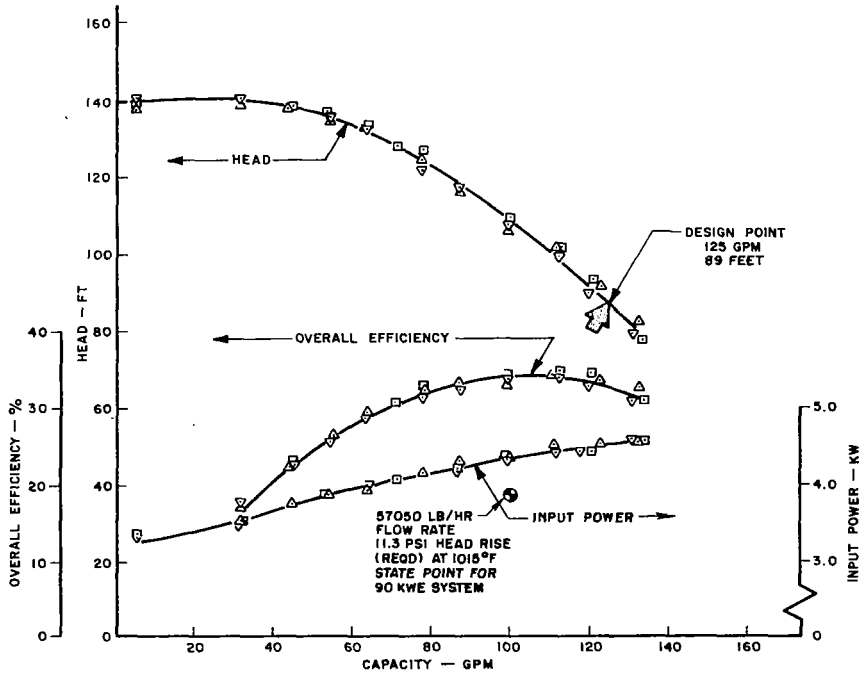

Figure 5-17 NaK Pump Performance in 1170°F NaK
(Input Power: 400 Hz, 208 V, L-L)

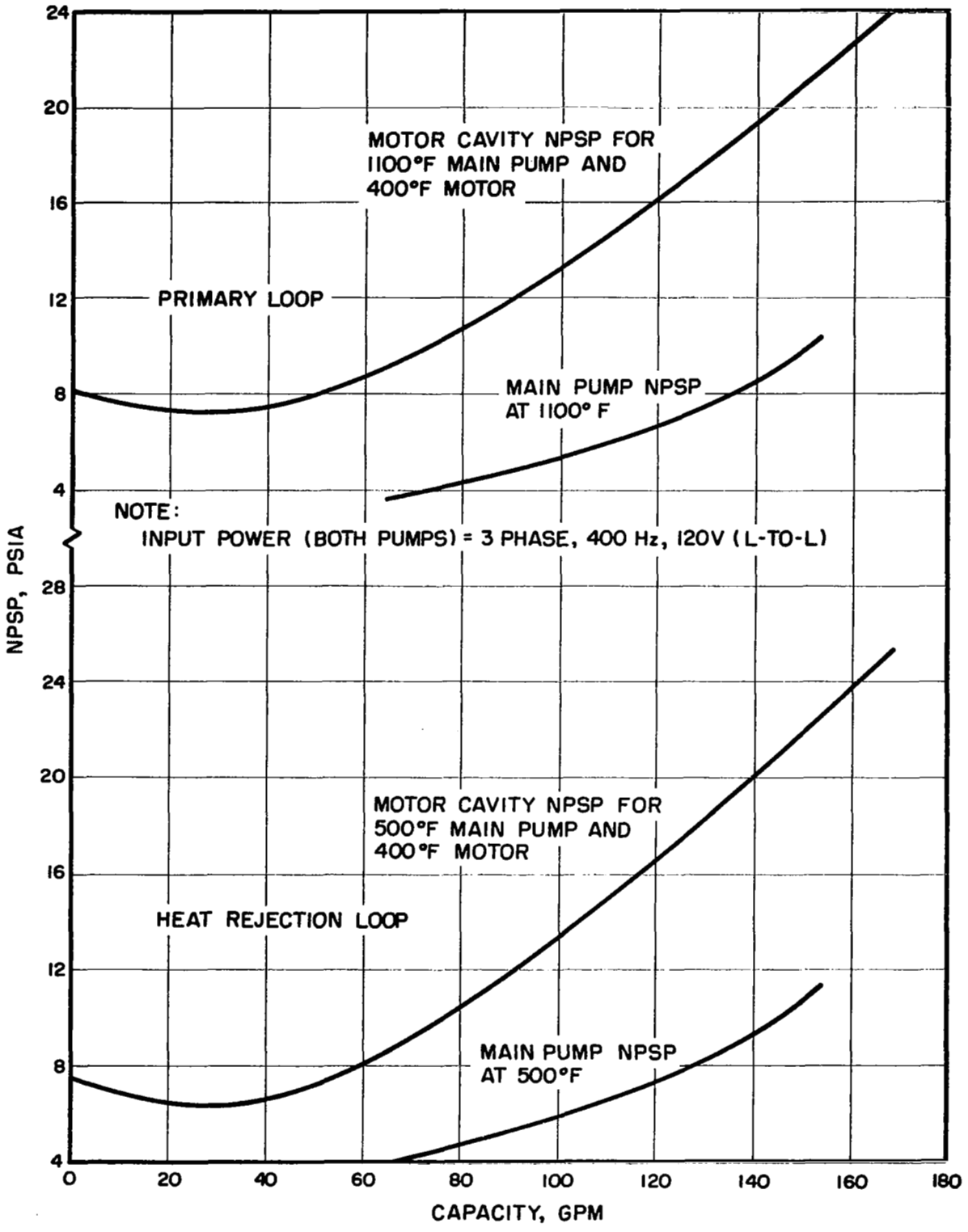

Figure 5-18 Net Positive Suction Pressure as a Function of Capacity - NaK Pump

5.2.3.7 Performance at 95 and 220 Hz

The performance of the unit at 95 and 220 Hz was established in the water test loop and from the motor "in air" test data. NaK pump testing confirmed the data. The performance is shown in Figure 5-19 and 5-20.

5.2.3.8 Motor Performance

a. Motor-Pump Speed Torque Curves.- The motor speed-torque characteristics shown in Figure 5-21 at 400 Hz established during the "in air" motor test provides an operating torque margin of at least 15% using the minimum input voltage (i.e., at the low end of the tolerance band.) By correcting this tested pullout torque value of 72.5 pound-inches for the effects of the rotor and stator cans, and with NaK in the motor air gap, the anticipated maximum torque point in NaK became 78.6 pound-inches providing slightly more margin. This calculated torque value has not been confirmed by test.

In the 35-kWe system startup sequence, the NaK pump starts with 95 Hz and 38 V, or more, with a switchover to 19 V for a 4 to 6-hour run for reactor conditioning. Then the NaK pump is switched to 220 Hz at 88 V for 4 to 6 minutes before ramping up to full speed directly connected to the accelerating SNAP-8 alternator from 220 to 400 Hz. In this way a large continuous excessive motor torque is available for acceleration throughout the NaK pump startup cycle.

b. Motor Starting Torque.- The delivered starting torque (or locked-rotor torque) characteristics of the motor were extensively tested at 60 Hz. These data established the torque supplied to the rotor for a given input voltage at the motor terminals. In this way, the starting torque values for the NaK pump were determined. At some voltage over 50 V (L-L), the motor iron will reach its maximum magnetic-flux carrying capacity or saturation point at which no additional torque is produced with increasing voltage. Unfortunately, this value has not been found by test; however, from nonstart to start experiences with NaK pumps, the torque still increases up to 55 or 60 V. The 60-Hz starting frequency is being considered for the 90-kWe system.

c. NaK Pump Motor 95 and 220 Hz Operation.- During the startup cycle, the NaK pump operates for 4 to 5 hours at 95 Hz and 4 to 6 minutes at 220 Hz. Since, in this space application, the pump power will be supplied by a battery-powered inverter, the energy and current expenditures are very important. To establish the most economical voltage at these frequencies, these operating points were simulated in the water test loop, producing Figure 5-22 for 95 Hz and Figure 5-23 for 220 Hz operation. At 95 Hz the system 19 V (L-L) (11 V, L-N) proved to be virtually at the lowest power and current values, however seemingly close to the knee of the speed-torque curve. However, the NaK pump will operate safely to as low as 12 V (L-L) or 7 V (L-N) since the slip reduces the load.

At 220 Hz, Figure 5-23 shows that the system established 99 V (L-L) (50.8 V, L-N) is at the lowest current and near the lowest power and still provides a suitable margin to the motor torque pullout voltage.

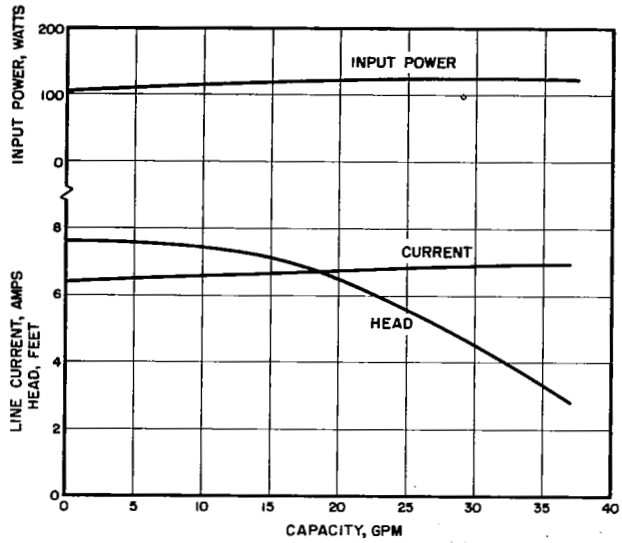

Figure 5-19 NaK Pump Performance with 95-Hz Input Power

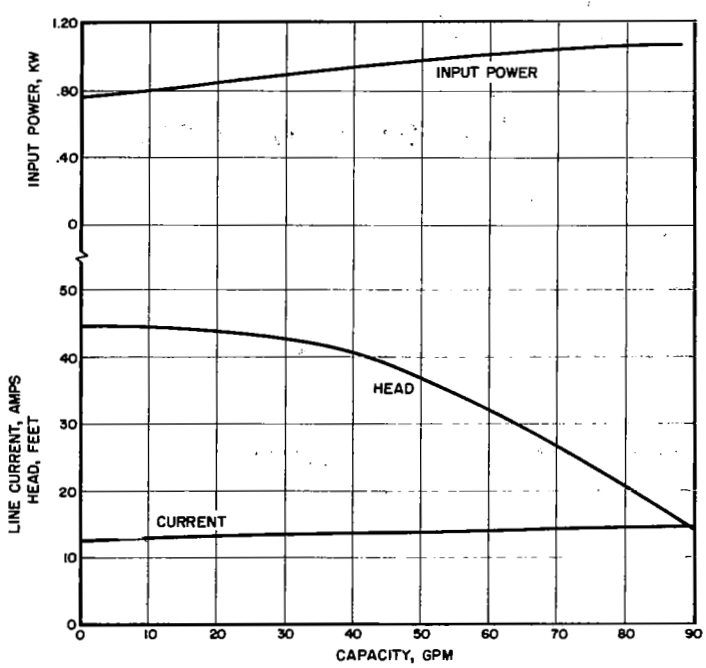

Figure 5-20 NaK Pump Performance with 220 Hz Input Power

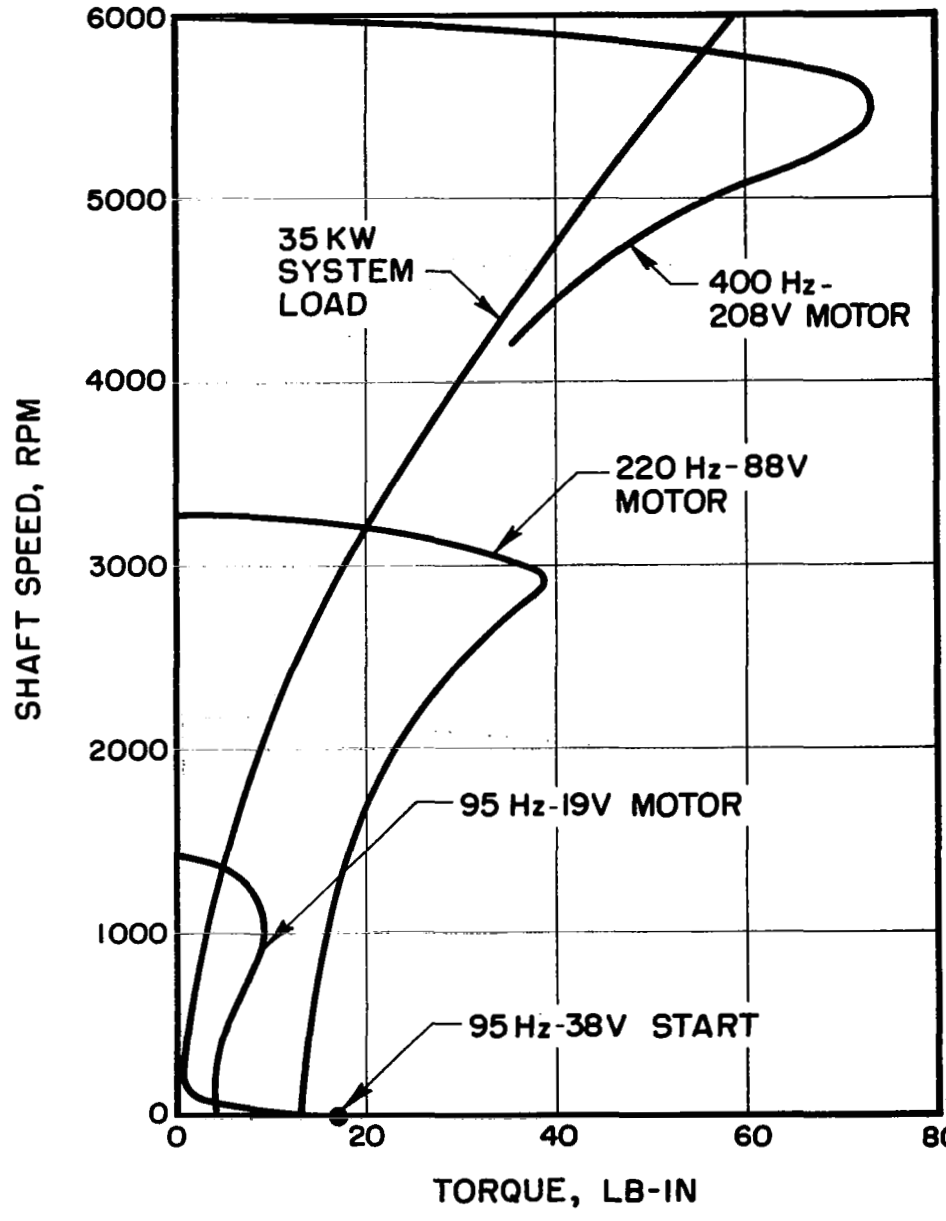

Figure 5-21 NaK-Pump Motor Speed-Torque Characteristics

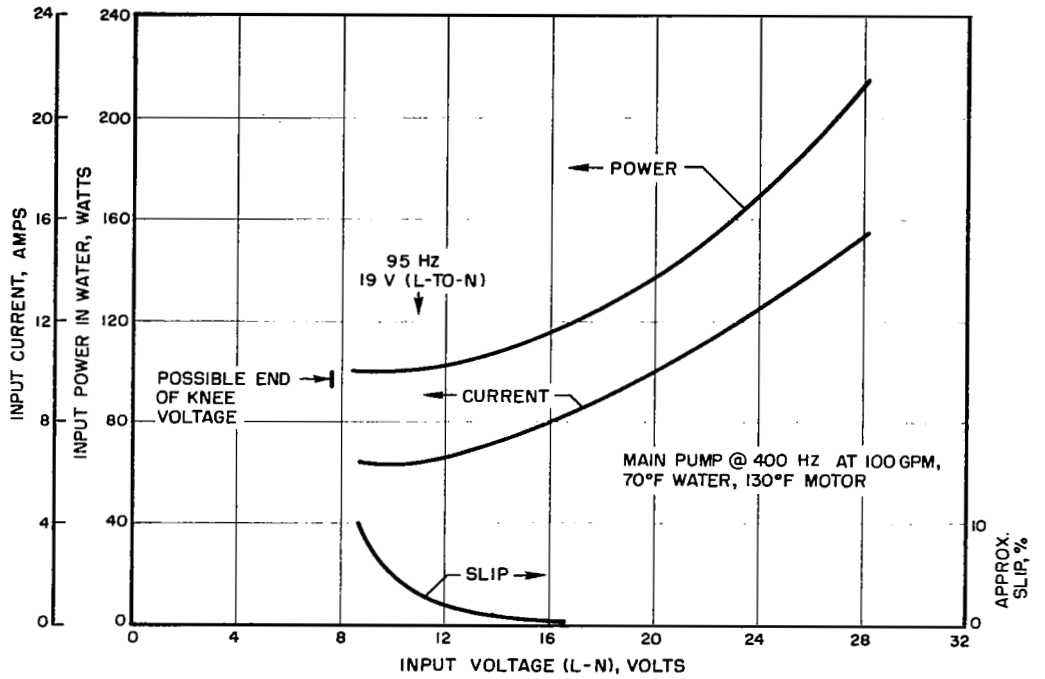

Figure 5-22 NaK Pump Performance at 95 Hz in Water Tests

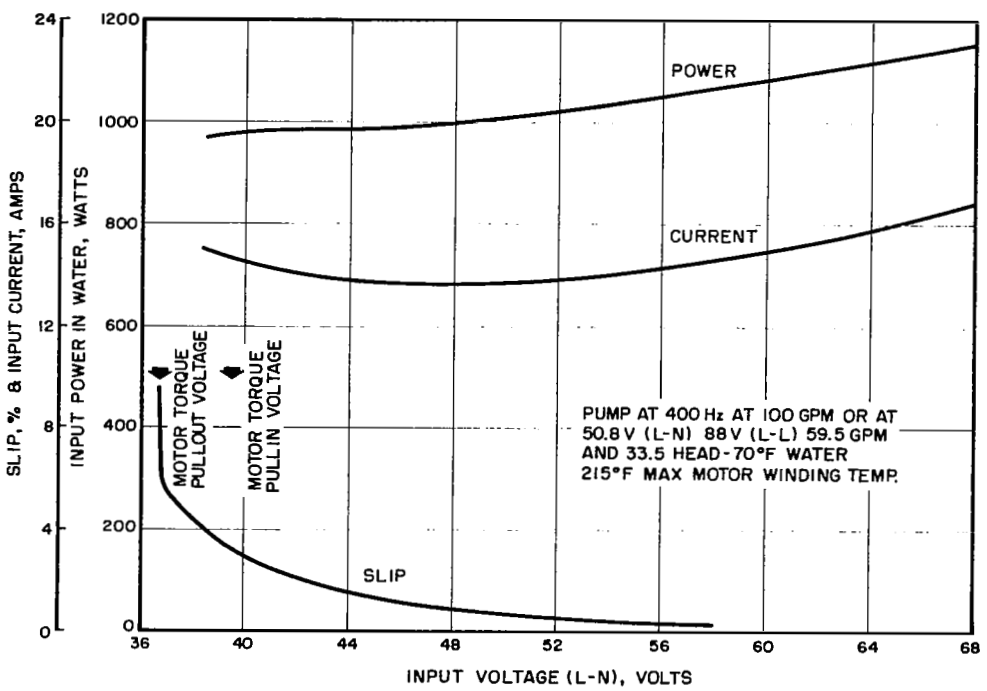

Figure 5-23 NaK Pump Performance at 220 Hz in Water Tests

d. Motor Summary.- In general, the motor development met design goals. However, the hydraulic losses were higher than expected. Therefore, in order to keep the other motor losses down, only a small design speed torque margin was selected.

5.2.3.9 NaK Pump 400-Hz Peripheral Performance

Confirmation of the design loads, temperatures, and accomplished functions for the pump were made as follows:

a. Pump Axial Thrust.- To determine the axial thrust of the NaK pump, pressure values obtained throughout the unit, such as shaft end pressure across the motor rotor, and front and back impeller pressure profiles, were plotted so as to derive a graphical resolution of the axial forces. The results of this calculation, shown versus capacity (corrected for NaK at 495°F) on Figure 5-24 establishes the impeller axial thrust as 95 lb acting toward the pump at shutoff, passing through zero-pound thrust at 95 gpm; to 43 lb acting away from the pump at 150 gpm. Because of the necessity of subtracting large numbers, the expected error is ± 20 lb. The original design value of 0.011 to 0.013-inch back vane clearance was increased to 0.035 to 0.040 inch to prevent back vane rub caused by the thermal growth differential between the pump shaft and housing. As shown in Figure 5-24, this change caused only a small thrust load change of less than 15 lb at any capacity.

Trimming the impeller back vanes will increase the thrust toward the main pump, thereby increasing the shutoff thrust load but decreasing the high-capacity load. It is desirable to avoid operating at the zero-load point for desired thrust bearing operation. The pump head is likely to shift 1.5 to 3 ft in this area with the change of front vane clearance, but otherwise no ill effect will occur.

b. Motor Rotor Axial Thrust.- The main rotor differential pressure in the motor cavity NPSH section produces an axial thrust load on the NaK pump shaft. With a piston area of 10.2 square inches, the 3.18 psi differential at the rated recirculation flow of 1.6 gpm produces an axial thrust of 32.8 lb acting away from the main pump. This results in net thrust load in horizontal ground testing as shown in Figure 5-24. The motor thrust varies with recirculation flow rate maximizing at 41.2 lb at 1.8 gpm maximum flow.

c. Net Shaft Axial Thrust.- The NaK pump may be used vertically (either end up) in ground testing or be exposed to a 1-g load axially in space since the bearings are adequate to support the rotor weight. The summary of axial bearing loads is provided in Figure 5-25.

d. Shaft Radial Loads.- Through the use of four radial pressure taps, located every 90 degrees in the volute just above the impeller tip diameter, an approximation of the impeller radial load was made. This calculation is based on test data and assumes that the velocities or dynamic forces around the impeller periphery are equal. With this assumption, the derived values represent only a good approximation.

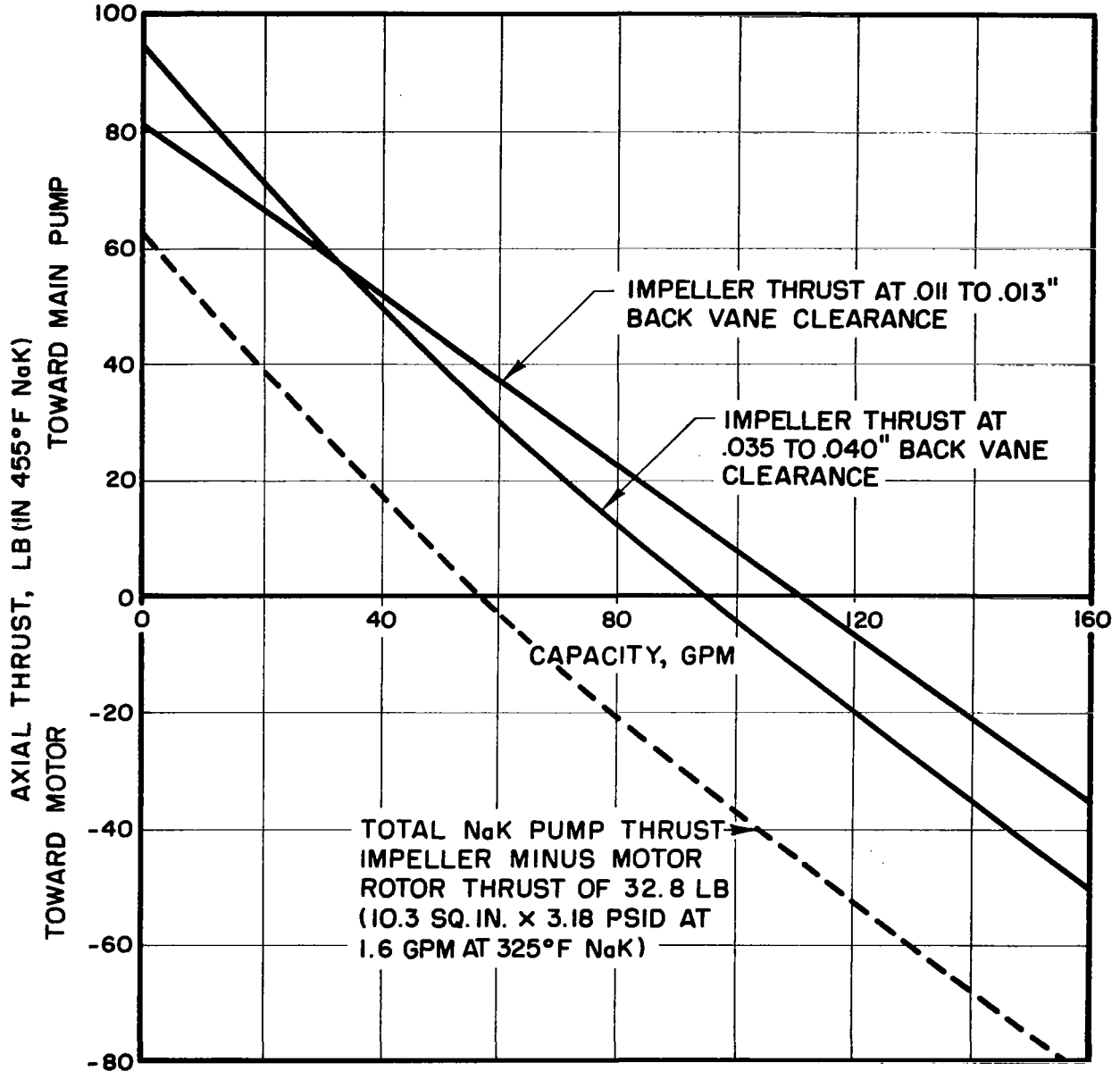

Figure 5-24 NaK Pump Axial Thrust vs Capacity

MOTOR ROTOR THRUST

MAIN AXIAL GPM	PUMP THRUST LB	RECIRC. FLOW GPM	DIFF. PRESS PSI	AXIAL THRUST LB	
0	-95	.8 (Min.)	1.6	16.5	RECIRCULATION PUMP
99	+ 3	1.6 (Norm)	3.18	32.8	AXIAL THRUST = 0 LB
150	+43	1.8 (Max.)	4.0	41.2	OPEN IMPELLER

ROTATING ASSEMBLY WEIGHT = 10.3 LB

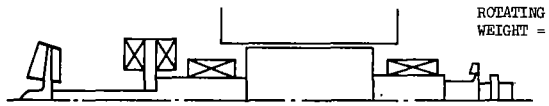

MAIN PUMP | THRUST BEARING | RADIAL BEARING | MOTOR | RADIAL BEARING | RECIRC. PUMP

MAGNETIC LOAD AND BEARING CAUSED LOADS = 0 LB

OPERATING "G" LOADS 0 NORMAL, 1G, MAXIMUM

AXIAL THRUST LOADS - MAXIMUMS

GPM	OG	IG
0	-78.5	-96.8
99	44.2	62.5
150	84.2	102.5

NORMAL AXIAL THRUST LOADS - OG IN SPACE MOUNTED HORIZONTALLY FOR GROUND SYSTEM

GPM	NORMAL - LB
0	-62.2
99	35.8
130	60.3
150	75.8

Figure 5-25 NaK Pump Axial Bearing Loads

GRAVITY ORIENTED MAIN PUMP RADIAL FORCE		ROTATING ASSEMBLY WEIGHT	MOTORS MAGNETIC LOAD	RECIRC. PUMP RADIAL FORCE
GPM	LB	18.3 LB	15 LB MAX	-2.5 LB MAX
0	-9.4		5 LB NORM	
99	-1.6			
150	16.8			

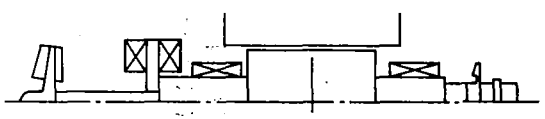

MAIN PUMP | THRUST BEARING | RADIAL BEARING A | MOTOR | RADIAL BEARING B | RECIRCULATION PUMP

MAXIMUM RADIAL LOADS WITH A LINED FORCES - LB

"G" LOAD	BEARING "A"	BEARING "B"
0	39.5	25.2
1	51.6	31.4
3.5	81.7	47.2

NORMAL RADIAL LOADS - IG AS USED IN GROUND SYSTEMS
OG FOR SPACE APPLICATION

"G" LOAD	MAIN PUMP CAPACITY - GPM	BEARING "A" LB	BEARING "B" LB
1	0	-2.1	13.5
1	99	12.4	6.8
1	130	32.9	- 2.5
1	150	46.5	- 7.3
0	0	20.2	7.9
0	99	13.6	7.6
0	130	21.8	9.1
0	150	34.5	15.1

Figure 5-26 NaK Pump Radial Bearing Loads

The radial loads on the NaK pump are summarized on Figure 5-26. The normal motor magnetic load of 5 lb and the recirculation pump radial load of 2.5 lb are insignificant with the major bearing loads caused by the main pump radial force and the rotating assembly weight. The rotor weight is 18.3 lb and, being almost centered between the radial bearings, imposes significant bearing loads only during the 10-minute 3.5-g acceleration period for space applications. Otherwise, the main bearing loads are derived from the main pump radial forces. In ground test systems, this results in maximum radial loads of 46.5 lb on the pump-end bearing and 13.5 lb on the motor-end bearing while operating from 0 to 150 gpm capacity. For space application (zero-g), these change to 34.5 and 15.1 lb, respectively. The design and test bearing load of 50 lb is exceeded only on the pump end bearing at 3.5-g conditions (81.7 lb) or with maximum individual loads aligned for maximum effect (51.6 lb).

e. Thermal Map.- Composite thermal maps of multiple thermal data runs are shown for a 1160°F pump housing in Figure 5-27 and for a 500°F pump housing in Figure 5-28. The temperature differences from calculated values are seen to be small.

5.2.3.10 Bearing Performance

As discussed in the previous sections, the axial and radial bearing loads were semiqualitatively established. With these loads during the long operating history of the unit, the thrust bearings have operated as designed. Some operational and starting difficulties with the radial bearings have been encountered.

The bearings were tested separately to establish their dynamic capabilities using a silicone oil for simplicity to approximate the NaK hydraulic characteristics. However, the oil does not approximate NaK in lubricity nor is there similarity in removing the metal oxide coating in service. Both of these parameters affect startup operation.

a. Radial Bearing Hydrodynamic Tests.- In the silicone oil test, the calculated film thickness for a given load for 0.65 centistoke silicone test oil and the test results compare very closely. Correcting the experimental data for the viscosity of NaK at the highest operating temperature of 600°F shows more than 0.0002-inch minimum clearance at 50 lb load. In the normal pump operating configuration and operating range of 99 to 150 gpm, the loads vary from zero to 46.5 lb (Figure 5-26). However, since the bearings are at 350°F with resulting higher NaK viscosity, the maximum normal operating bearing load produces a film thickness of about 0.0004 inch.

b. Thrust Bearing Hydrodynamic Tests.- The thrust bearing hydrodynamic characteristics were also confirmed using a silicone oil substituted for the NaK. For equally loaded pads, the minimum film thickness was calculated to be 0.0004 inch. With maximum tolerances and deflections causing maximum load differences between the pads, the most heavily loaded pair of pads would have a calculated minimum film thickness of 0.00031 inch which is adequate for

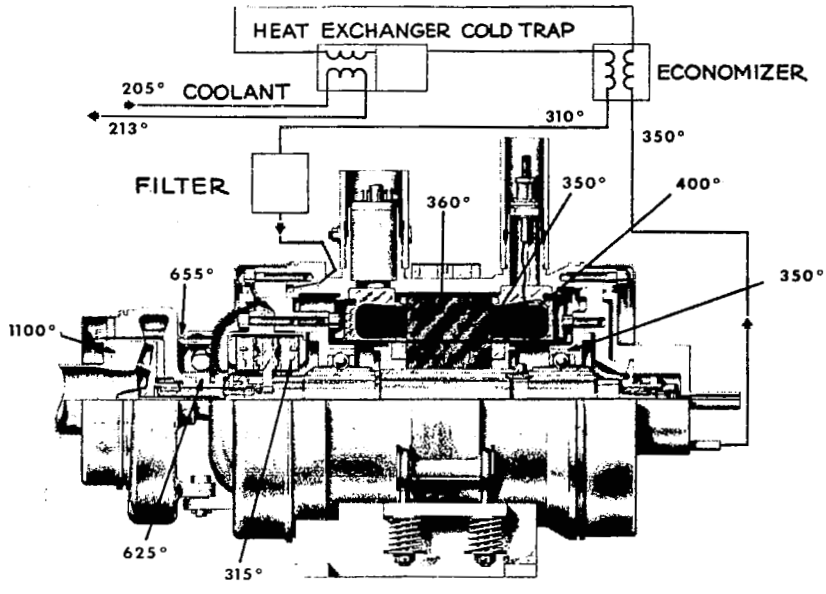

Figure 5-27 NaK Pump Thermal Map at 1160°F Operating Temperature (Calculated Values in Parentheses)

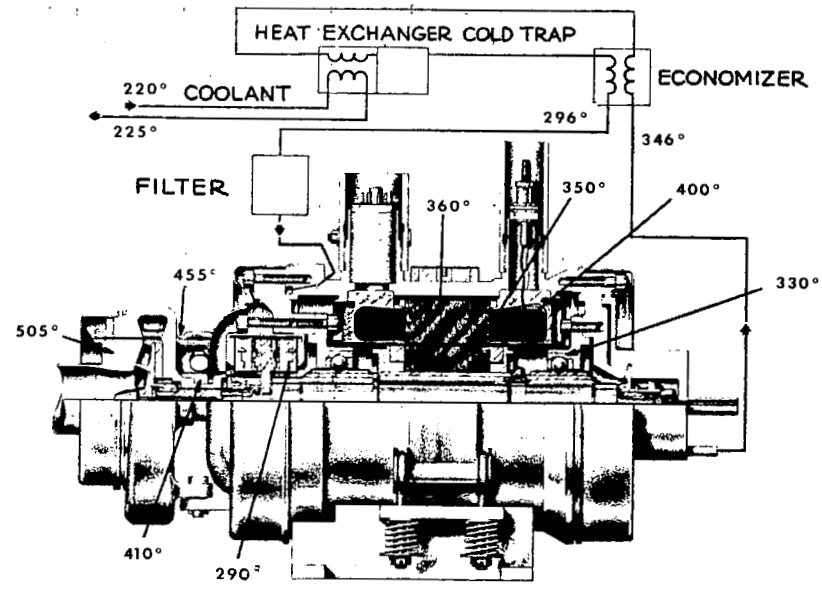

Figure 5-28 NaK Pump Thermal Map at 500°F Operating Temperature (Calculated Values in Parentheses)

this application. The viscosity corrected test results established that the rated load of 80 lb at 6000 rpm results in a minimum film thickness close to the calculated value within the resolution of the instrumentation.

The normal NaK pump operating range of 99 to 150 gpm produces thrust loads of from 35.8 to 75.8 lb.

c. Bearing Pivot Fretting Testing.- A short test program was conducted on a vibrating table using first oil, and then NaK at 600°F. The test results showed that the ball pivots were not significantly damaged in 100 hours. The bearing pivots in one NaK pump were run in NaK for 10,362 hours without sign of wear or deterioration.

5.2.3.11 Recirculation System Performance

a. NaK Side.- Hydraulic performance data were obtained from the water testing establishing the filter differential head requirement with flow shown in Figure 5-29 and the recirculation pump performance as shown in Figure 5-30. The recirculation pump performance, as seen by the system external to the NaK pump, is shown in Figure 5-30 which also shows the system loss curve. This low specific speed pump is flow limited at 1.8 gpm by the discharge diffuser to prevent high axial thrust values across the motor rotor, explaining the negative slope of the curve at the low capacity pump values.

b. Coolant Side.- The NaK pump design considered that the unit would be totally insulated from its environment with the only cooling provided at the heat exchanger cold trap. Polyphenyl ether is used for the coolant, but the motor and heat exchanger design allows use of the heat rejection loop NaK. Because of a low coolant temperature differential (8 to 10°F), the test data instrument error and environment heat losses provide only a rough check. The flow path pressure loss is basically cold trap heat exchanger entrance and exit velocity change effect with a laminar flow channel.

5.2.4 Vibration and Shock Testing

A complete NaK pump was tested in the vibration test facility at NASA-LeRC in accordance with NASA Specification 417-2, Revision C. This included sinusoidal sweep vibration, random vibration, and multiple shocks of 15-g peak in three directions. The post test examination and hydraulic performance results are described in detail in Reference 43 which also gives test times and input power levels.

The pump was tested for hydraulic performance before and after the shock and vibration testing and no measurable change was observed. The pump was filled with a kerosene type of oil to simulate the effects of NaK during the test. Some slight damage occurred to the thrust bearing gimbal sockets and the locking pins, and some minor changes are recommended to alleviate these problems.

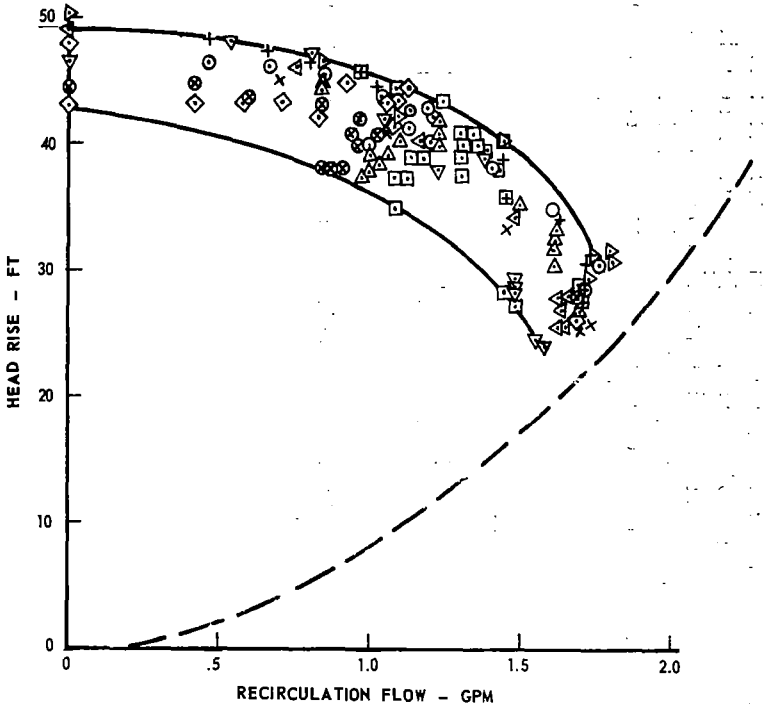

Figure 5-29 NaK Pump Recirculation System Filter Head Drop vs Capacity

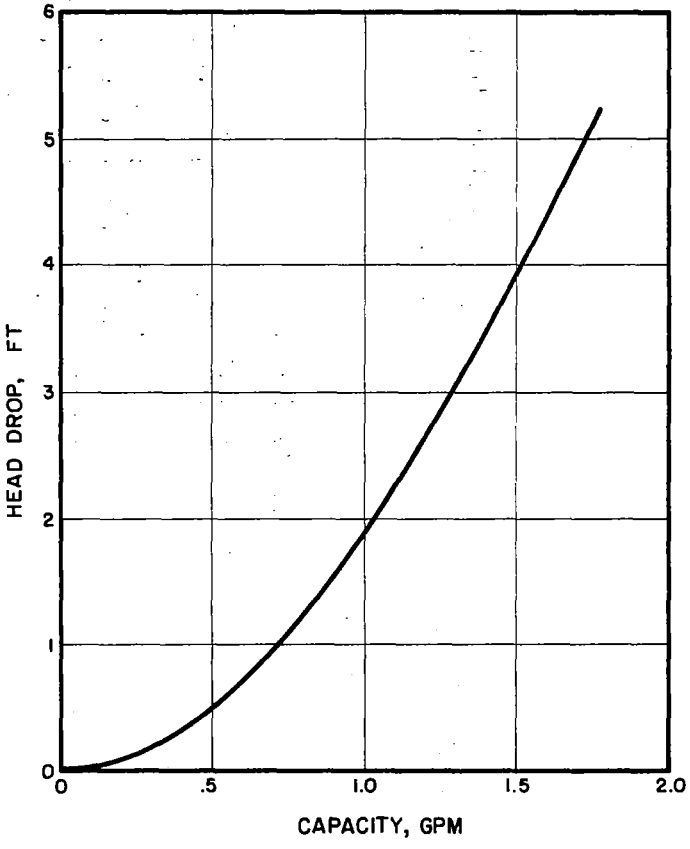

Figure 5-30 Recirculation Pump Performance

5.2.5 Operations

The NaK pump was extensively tested accumulating 56,493 operating hours with 3362 start cycles on 11 NaK pumps. During this period, the NaK pump problems mainly concerned bearing damage/starting difficulties.

The NaK pump has been successfully endurance tested on a single buildup to 10,362 operating hours with 786 start cycles. One hard start occurred on this test using 36 V at the terminals on the 772nd start cycle after 6696 hours operation. At 80 V, the pump started. The radial bearings showed a slight scratch pattern at disassembly.

5.2.5.1 Bearing Problems

In the first water test, the bearings had wedging and wringing problems. These have been resolved to a major extent by design modification; however, some further changes are necessary for maximum reliability. Testing has shown that a reliable bearing system can be made. To better understand the different causes and effects of the bearing problems, they are examined individually in the following paragraphs. Above complete story of bearing design and performance is found in Reference 41.

a. Wringing.- Wringing is the expression used to describe the physical attraction exhibited when two very smooth and flat items, like measuring blocks, are squeezed together. The result is a tight locking of the parts held together by atmospheric pressure. Relapping to four rms finish reduced but did not eliminate the wringing effect. The bearings as originally manufactured had a 1 to 2 rms finish. This resulted in wringing which dragged the pads along a long radius ball contact which made an effective low-angle wedge to totally lock the NaK pump shaft. Roughening the finish decreased the action on the radial bearings, but on the thrust bearings further rework was necessary. The thrust pads were finished with a flat surface matching the flat surface of the running ring or thrust plate. To provide a line contact, the running ring was coned to avoid the flat plate wringing effect. Wringing was then eliminated.

b. Wedging - Gimbal Plates.- The thrust bearing with modifications as above still tended to lock the NaK pump shaft during preliminary testing in the water loop. This was determined to be from the action of the cylindrical gimbal plate pivots whose relatively long radius provides a shallow angle wedge with slight rotation of the gimbal plate.

The thrust bearing had to be assembled with a small clearance (0.004 inch) to limit the shaft end play and for pad no-load stability. Consequently, a small force, or drag, from the pads could be compounded into a locked shaft. In a horizontal plane, the pads fell to a minimum clearance condition. The effect was eliminated by providing centrally located drive pins which prevent sliding movement in the gimbal pivots.

c. Wedging - Journal Pad Ball Pivots.- A wedging action is created when the radial bearing pads are swiveled by the ball operating in the shallow socket in the pad. The resulting wedging action can be severe if the clearance allowance is sufficient or if the ball to pad friction is large. The resultant

large loads either lock the shaft or cause damage to the bearings in startup. The thrust bearing material has not shown any sign of damage, but the radial bearings have been galled and scratched in some instances. The clearance may be limited on the thrust bearing by misassembly, debris behind ball segments or at pads, gravitational dropping of pads and gimbal plates in the assembly, and unusually high-temperature (compared to the housing) bearing parts. With the material coefficient of expansions involved, it is more likely that the thrust bearing clearances would increase with temperature effects. On the radial bearings, the clearance is set by manufacturing, checked, and rechecked for debris behind balls or on the pad. Hydrodynamic film, gravitational location of the pads (located at 45-degree points from center line), the act of galling, and a hot shaft or bearing parts in comparison to the housing, may provide the small clearance condition.

d. NaK Cleaning of Metal Oxides.- Metal oxides on bearing surfaces normally provide the hard surface to reduce friction and tendency to gall for metal-to-metal contact. NaK removes this oxide, cleaning the metal surfaces. The metal sliding friction factor in NaK has been tested as approximately 1.0 to 1.5. When a NaK pump is put into service, the first start has always been successful. It is presumed that no system or assembly debris is present and the bearing probably still has an oxide-coated surface.

e. Debris.- Debris may be in two forms: hard particles or soft materials. The recirculation loop is designed to remove both the relatively soft NaK oxide and soft or hard material particles. The thrust bearings have not been scratched in service, although burnishing on the surfaces shows the passage of some hard debris. The radial bearing frequently carries scratches showing that a few hard particles may produce more debris from the radial pads to compound the scratching effect. NaK oxide particles are not sufficiently hard to scratch the pad material; but, with the wedging effect, a soft material thickness reduces the bearing clearance for a low wedge angle and then the resistance created in passing the pad surface will, in turn, produce large bearing loads. In startups after some running time, this forces the pad and journal surface together under load, creating the conditions most likely to cause welding or galling.

f. Bearing Damage Due to Gas.- The lowest pressure point of the operating NaK pump surrounds the recirculation-pump-end radial bearing. Gas in this area reduces or eliminates the bearing liquid lubrication causing more power losses and a possible direct contact between the sleeve and pad. At the same time, the bearing is deprived of liquid cooling allowing the bearing parts to heat up. A compounding effect results with the internal metal expanding while the housing is unaffected, thus decreasing the clearance and wedge angle. As a result, the load increases causing more heat to be generated. The damage to the radial bearings from gas has been noted in some cases generally ending in scratched or galled motor-end radial-bearing surfaces and a nonstarting unit. The main pump-end radial bearing (and thrust bearing also) operates at about 3 psi higher due to the pressure drop across the motor rotor, and is therefore less likely to be damaged. The thrust bearing, because of harder materials, location and construction, avoiding adverse thermal gradients and growth, does not have this problem.

5.2.5.2 Stator Problems

The second most frequent problem with the NaK pump has been with the motor stator housing. Usually the windings have shorted out because of faults or because of the intrusion of NaK from a can leak. Usually the initial fault is in doubt since the end condition appears the same; that is electrical arc burns through the can with NaK flooded and shorted windings.

a. Winding Short - End-Turn Area.- The apparent winding short has has usually occurred in the stator end-turn area where the wires move during manufacture and from thermal expansion in use. The motor winding air or space gap is maintained during hand winding by a glass-cloth covering impregnated with a resin. The resin is burned off before the entire stator windings are impregnated with a ceramic fill to retain the installation gap. The ceramic then has to hold the wires in position. If a wire is indented or moved into an adjacent wire during manufacture or by use, a hot spot will occur which in heating the wires may compound into a full failure.

The motor stator used in later units after some modifications appears to be much more reliable than the earlier units. Two of the modified design stators operated for 9748 hours and 318 starts and 9116 hours with 207 starts, with no malfunction.

b. Leaks Through Motor Cans.- NaK leaks through the motor cans appear to be similar to winding faults since the motor stator is flooded with NaK from an arc burn through the can. The short to ground follows the NaK conductor through the leak point if NaK has shorted the windings. However, in at least one case, the evidence distinctly pointed toward a can imperfection as being the failure cause. Leaks have occurred only on the motor end cans, not on the cylinders or welds. Early end cans were machined from a solid Inconel plate to a 0.030-inch thickness. As such, machining defects and material inclusions become very important because NaK will dissolve or wash out the non-metal or oxide inclusion to allow a path for leakage. Later pumps have been fabricated utilizing spun sheet Inconel stator end covers which eliminated the can leakage problem.

5.2.6 Recommendations for Future Use

Extensive testing has shown the NaK pump to be generally reliable. This is evidenced by the conditions of pumps after endurance tests. A detailed description of one pump after testing is contained in Reference 44. Some changes to the design are recommended to improve the reliability particularly when some adverse conditions prevail are as follows:

5.2.5.1 Bearings

Indications are that the tungsten carbide material, if applied to the radial bearings, would alleviate most of the scratching problems. Redesign of the ball pivot on the radial bearings to incorporate pins and also reduce clearances to limit pad rotation should be considered.

5.2.6.2 Recirculation System

The original recirculation system was based on ground testing criteria which could include a relatively crude system using polyphenyl ether as the coolant. A long test run on a pump at higher than 500°F winding temperature, confirmed that the use of the heat rejection loop NaK for motor and bearing cooling is satisfactory. As a result, a new recirculation system was designed but not built.

5.2.6.3 Lower NPSH Required

In late 1967, a reduction in maximum primary loop pressure was recommended by the reactor contractor for the purpose of increasing the creep life of the reactor fuel elements. The pump NPSH requirements would be lowered to accomplish this by trimming the main impeller back vane. This provides higher relative pressures in the motor cavity allowing the NPSH of the NaK pump to correspond to the NPSH required by the main impeller.

5.3 MERCURY PUMP

The mercury pump located in the Rankine-cycle loop (Figure 5-31) circulates mercury through the loop and acts as the boiler feed pump. Cutaway and exterior views of the pump are shown in Figures 5-32 and 5-33. The main pump is a single-stage centrifugal pump with a jet pump driven by bypass mercury flow, providing adequate suction conditions to the main pump, particularly during the system startup cycle. Suction conditions for the overall pump are established by the condenser pressure and by the degree of subcooling provided by the condenser. The centrifugal pump is driven by a 400-Hz, 208 V (line-to-line), three-phase electric motor at a speed of approximately 7800 rpm. The pump shaft is supported by ball bearings located between the motor and pump. The bearings are lubricated and cooled by an organic polyphenyl ehter. The same fluid is used to cool the motor and space seal. Mixing of the lubricant and mercury is prevented by a dynamic-static seal-to-space system. The design and development of the SNAP-8 mercury pump is described in more detail in Reference 45.

5.3.1 Development Background

The mercury pump was designed primarily for component reliability and development simplicity and to meet the unique requirements imposed by a vacuum environment. Design flexibility and ease of development were necessary to permit the following:

- Modification of one element of the pump assembly without affecting the design of the whole assembly.
- Minimization of the number of interacting variables to allow more accurate analysis and design procedures.
- Accessibility of elements for assembly and disassembly.
- Installation of instrumentation for acquisition of data.

5.3.1.1 Pump

A centrifugal pump was chosen over a positive-displacement unit since pumping low-viscosity mercury at relatively high pressures would have imposed severe life-limiting wear on a positive-displacement pump. Furthermore, a centrifugal pump is more adaptable to changes in performance requirements. For the pump startup suction conditions, the jet-pump booster was selected instead of an inducer for the following reasons:

- Jet-pump hardware may be easily modified to attain better suction performance while an inducer design change would probably be extensive, if required.
- A jet pump can be made more rugged to withstand cavitation damage.
- In an extreme cavitation mode, the jet-centrifugal pump will produce some flow with available NPSH nearly zero.

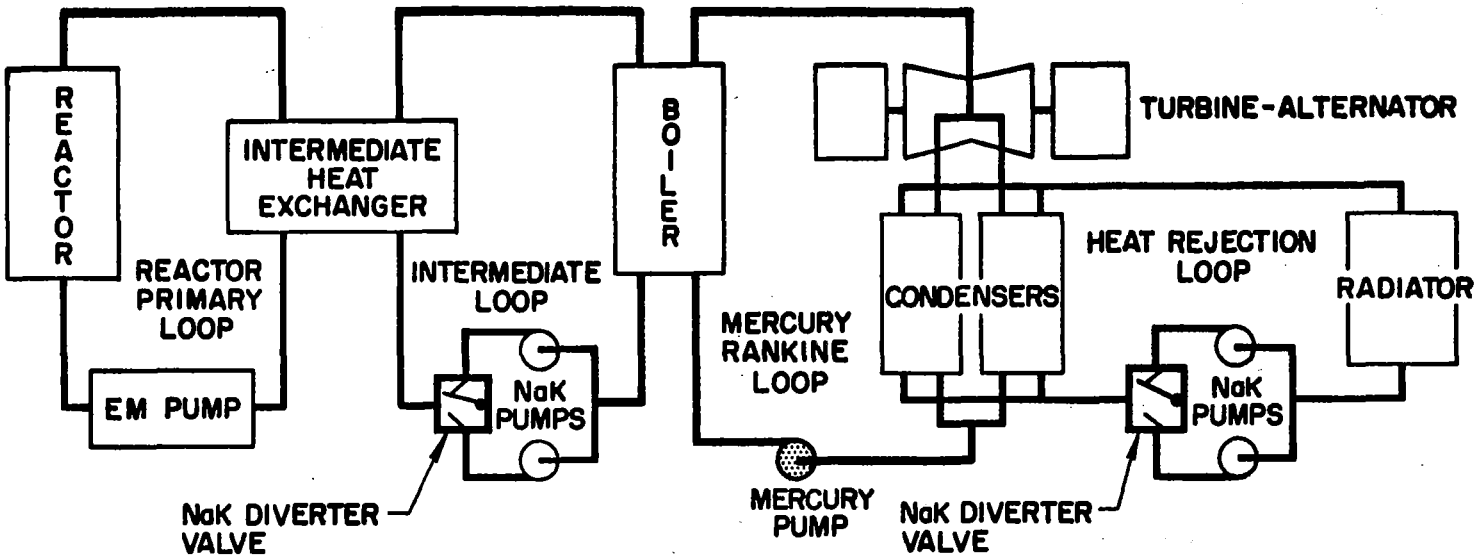

Figure 5-31 Mercury Rankine-Cycle Loop Showing Location of Mercury Pump

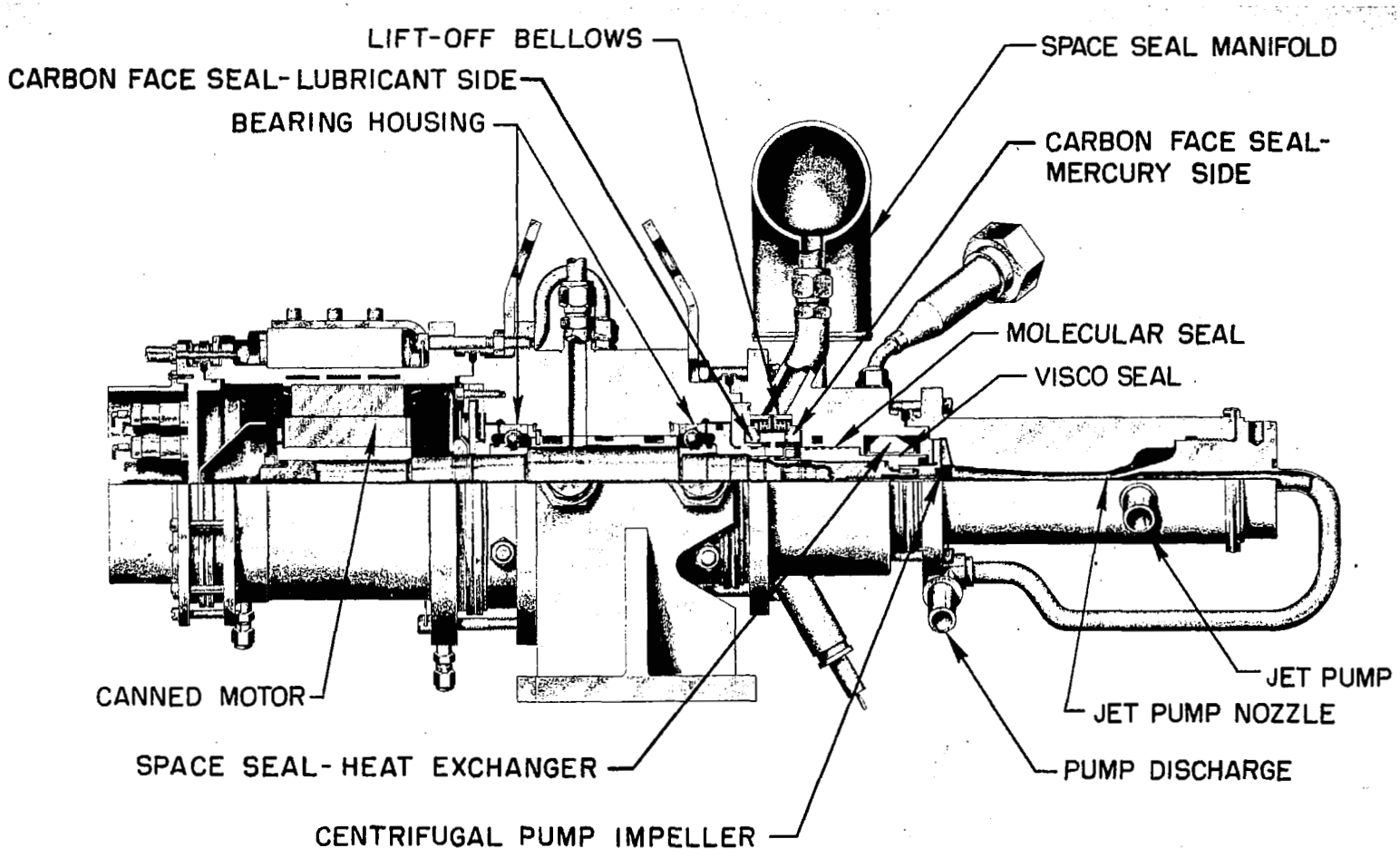

Figure 5-32 Mercury Pump Cutaway View

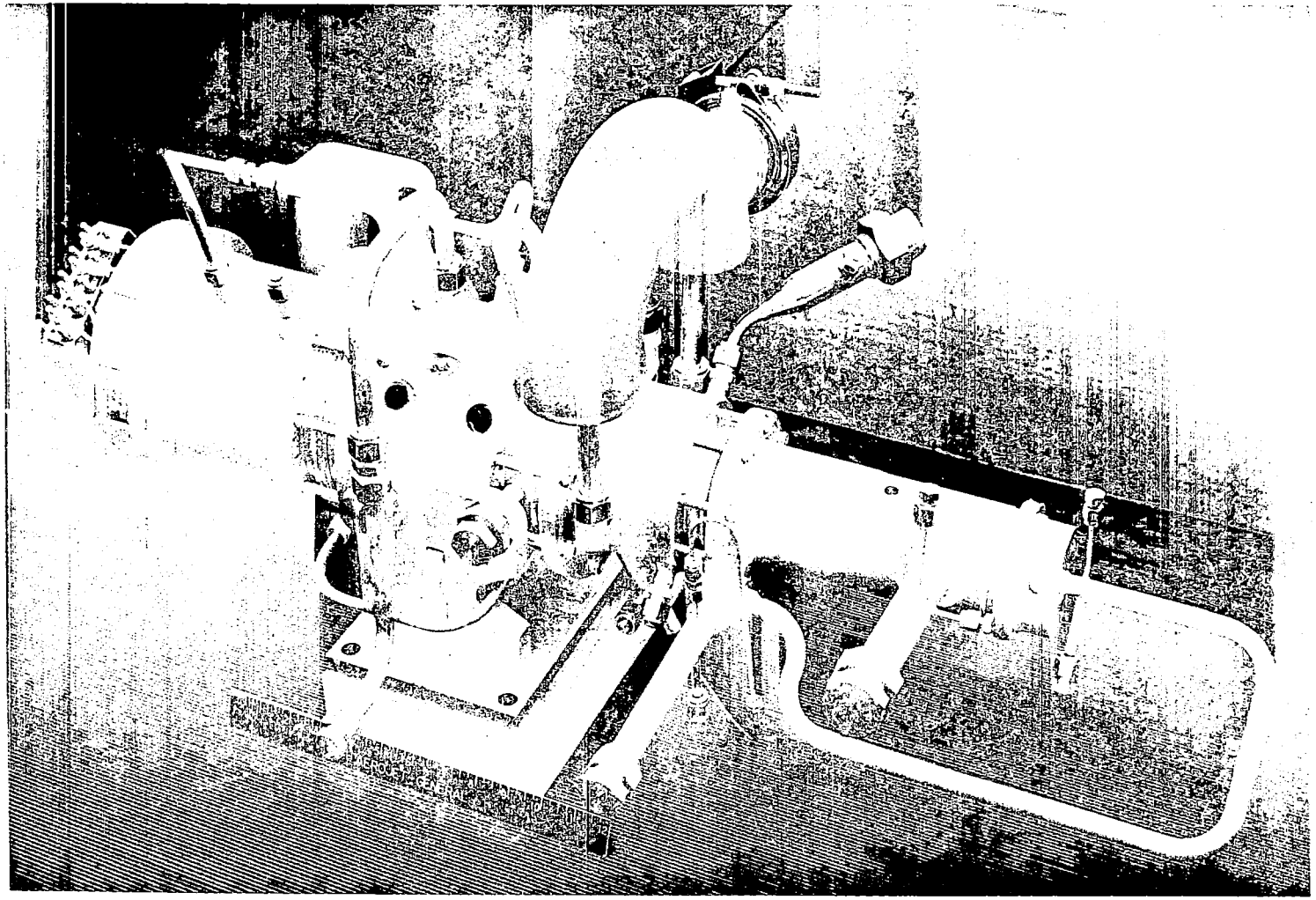

Figure 5-33 Mercury Pump

5.3.1.2 Motor

A standard induction 400-Hz, three-phase motor was selected to provide high reliability, simplicity of construction, and good starting torque capability. The selection of a lubricant-coolant vapor-filled cavity was based on the design technology similarities with the turbine-alternator.

5.3.1.3 Bearings

The SNAP-8 turbine-alternator and mercury pump designs both incorporated the use of polyphenyl-ether lubricated and cooled ball bearings with a space seal system separating the mercury and the bearing lubricant. Bearing selection was based on simplicity, initial reliability, critical shaft speed, and shaft deflection. A detailed description of the design and development of the ball bearings for the mercury pump and turbine-alternator is contained in Reference 30.

Angular contact bearings of basic 207 size (35-mm bore) were selected with the bearings mounted with a 55-lb axial preload to assure positive rolling contact at all times. The ball and rings were made from M-50 consumable electrode triple vacuum melt tool steel, and the separators from silicon iron bronze. Calculations indicated that life limitations would not be due to stress or fatigue but more probably due to wear which is a function of bearing alignment, fits and clearances, material selection, and the removal of wear debris.

5.3.1.4 Shaft Seals

The mercury seal-to-space consists of the main impeller back face (a vaned slinger), a visco pump, a molecular pump, and a face seal in series, similar to that in the turbine-alternator. The visco pump, in pumping against the main pump pressure regime, forms a liquid plug which is cooled by a small heat exchanger incorporated in the seal housing.

The lubricant seal-to-space functions in a manner similar to that of the mercury seal except that a smooth radial slinger is used in place of the vaned slinger and visco pump. The main function of the face seal is to prevent leakage of liquid during startup when the dynamic seals are not effective. The design of the dynamic shaft sealing system is based on the technology described in References 31 and 32.

5.3.1.5 Lubricant in Motor Cavity

The motor-winding insulation selected was compatible with the polyphenyl ether used for bearing lubrication and component cooling. This permitted the use of open stator windings with a conventional organic insulation design. To minimize hydraulic losses, the design incorporated a scavenging slinger so that the motor would operate in lubricant vapor rather than in a liquid-flooded cavity. With a liquid-flooded cavity, the motor power required would produce excessive winding temperatures.

5.3.2 Physical Description, Design Parameters and Requirements

The mercury pump is shown in cross section in Figure 5-32. The design parameters and requirements are shown in Table 5-VI and compared with tested performance. The principle features of the mercury pump are described below.

5.3.2.1 Pump

The pump section includes a centrifugal main pump (an end-suction, single-stage, semi-open centrifugal type) and a jet pump mounted on the end of the unit (Figure 5-32) the driving flow is provided by bypassed flow from the main pump feeding to the eye of the main impeller.

Since the flow was relatively low, a partial-emission 1/3 flowing section volute was chosen. The centrifugal pump was designed to standard criteria. Impeller shroud back vanes were used to assist the operation of the dynamic seals and to reduce the axial load on the bearings. The centrifugal pump was optimized with respect to the motor and bearing designs. A 7800-rpm pump speed was selected on the basis of the 400-Hz motor input frequency.

The specific speed for the centrifugal pump portion, $N_s = \frac{N(\text{rpm}) \cdot Q(\text{gpm})^{1/2}}{H(\text{feet})^{3/4}}$, was calculated to be 522 as designed. Based on test results, a specific speed of 550 was calculated.

Hydraulic design and manufacturing considerations determined the configuration of the impeller passage. Flow transitions were selected which minimized friction losses and maintained maximum fluid control. On the basis of empirical data, an impeller having four front vanes was selected. The front-vane parameters were as follows:

Impeller diameter	1.94 inches
Impeller vane height at discharge	0.1 inch
Impeller inlet diameter	0.75 inch
Impeller vane height at inlet	0.22 inch
Front-vane inlet angle	15 degrees
Front-vane discharge angle	25 degrees

TABLE 5-VI MERCURY PUMP PERFORMANCE DATA

Components and Parameters	Calculated Design Point, Final Design	Tested Performance
Pump, Jet-Centrifugal		
Flow, lb/hr (gpm)	11,600 (1.78)	11,500 (1.78)
Speed, rpm	7,800	7,870
Inlet temperature, ^{o}F	505	505
Density, lb/ft^3	807.5	807.5
Inlet pressure, psia	10.5	10.5
Pressure rise (ΔP), psi	397	458
Head, ft	70.9	81.6
Outlet pressure, psia	407.5	468.5
Hydraulic power, hp	.415	.477
Hydraulic power, kW	.31	.356
Efficiency, %	22.0	23.4
Shaft input power, hp	1.89	2.04
Shaft input power, kW	1.41	1.52
Motor, Induction Type		
Shaft power, kW	2.41	2.41
Electrical efficiency, %	86.8	87.6
Bearing seal system efficiency, % (all less pump)	50.7	55.3
Input power, hp	3.73	3.69
Input power, kW	2.78	2.75
Input amps @ 208 V	10.5	11.6
Overall unit efficiency, %	11.16	12.95
Summary of Losses		
Total electrical, (watts)	368	340
Total hydraulic, (watts)	1002	890
Total heat to lubricant-coolant fluid (watts)	1370	1230

- Electrical-power source: 400-Hz, 3-phase, 208 V (line-to-line)
- Space seal leakage: 2 lb (maximum) of mercury and 3 lb (maximum) of lubricant-coolant fluid in 10,000 hours of operation.
- Starting NPSH: 1/16 ft NPSH available at 1/4 rated mercury flow.
- Lubricant-coolant conditions: (1) Inlet 25 psia maximum at $210^{o}F$ with 2600 lb/hr flow to mercury space seal heat exchanger, (2) 200 lb/hr flow to the motor stator coolant passages and 250 lb/hr flow to the ball bearings.

Using empirical data, the back-vane parameters were as follows:

	Original Impellers	Modified* Impellers
Number of back vanes	32	8
Back-vane height, in.	0.10	0.10
Back-vane clearance, in.	0.10	0.10
Back-vane inside diameter, in.	0.9	1.05

*This modification was applied as a result of operational experience described later.

The height-to-front-vane clearance relationship required that the impeller vane height be at least 0.1 inch at the impeller discharge. To accommodate this vane height, the volute housing was designed for partial emission. The volute housing characteristics are as follows:

Emission	120 degrees
Inlet angle	8.9 degrees
Inlet velocity	29.1 fps

The radial loading on the impeller was determined by analyzing the pressure distribution around the impeller periphery. The following radial and axial impeller loads were calculated.

Flow (% Design)	Radial Load (lb)	Axial Load (lb)
0	29	55
50	13	53
100	7.5	50
130	12	45

The axial load on the impeller was neutralized to a large extent by the use of back vanes.

The purpose of the jet pump was to provide adequate suction pressure to the centrifugal pump to prevent cavitation in the centrifugal pump during startup and extended operation. Since cavitation damage was a critical factor in the performance of the pump during startup and for long-term operation, more emphasis was placed upon producing a noncavitating pump than a high-performance pump. The jet pump was designed to produce sufficient head so that the centrifugal pump would not be required to operate at suction specific speeds of greater than 6000 under any startup or steady-state conditions. The optimum design for the jet pump required a relatively small discharge nozzle area for the jet. Since, however, the optimum small nozzle discharge area would be susceptible to clogging, the nozzle was sized for maximum reliability with a resulting compromise in jet-pump performance.

The hydraulic and physical design parameters for the jet pump are as follows:

Ratio of drive head to suction head	200
Ratio of through-flow to jet-flow	1.29
Ratio of jet-pump head to centrifugal-pump head	0.11
Suction flow velocity	4.73 fps
Jet discharge velocity	64.7 fps
Jet pump discharge head	6.6 ft
Reynold's Number for drive jet	6.5×10^5
Jet nozzle diameter	0.093 in.
Mixing section diameter	0.404 in.

5.3.2.2 Motor

The mercury-pump motor is a conventional 400-Hz, 3-phase, 6-pole, squirrel cage induction motor. A Dupont polyimide ML insulation system was selected which allowed operation to 400°F maximum hot-spot winding temperature for the required life. The 3-phase power leads and the "Y" connected neutral lead are brought out of the motor end bell through individual ceramic terminals. Five Chromel-Alumel thermocouples for winding temperature measurements were embedded in the stator windings and passed through the motor end bell by a separate multiple pin connector.

The stator is cooled by a 200 lb/hr flow of polyphenyl ether through a heat exchanger in the stator housing.

5.3.2.3 Shaft Seals

A dynamic sealing system retards fluid leakage and mixing of the mercury and the polyphenyl ether. A vent is provided so that the small leakages are ported to space.

a. Mercury Shaft Seal.- The mercury shaft seal consists of a visco pump, a molecular pump, and a carbon face seal in series. The visco pump is basically a screw pump, with the helical channel in the rotating element. This generates a pressure differential balancing the back-vane hub pressure of the centrifugal pump impeller. This pressure balance produces a liquid plug. Molecules evaporating from the interface are restricted from flowing to space by the adjacent molecular pump. The molecular pump, similar in appearance to the visco pump, returns the molecules to the liquid interface following contact with the rotating helix and the housing.

A small heat exchanger using polyphenyl ether as the cooling medium is incorporated in the housing adjacent to the liquid plug. This limits the temperature and therefore vapor pressure at the liquid/vapor interface which controls the amount of boil-off from the interface.

The mercury molecular pump was designed to keep the mercury vapor leakage below five pounds in 10,000 hours with the liquid/vapor interface temperature established at 300°F maximum.

The carbon face seal prevents fluid leakage when the pump is not rotating or is operating at low speeds. Tests showed that the carbon contact face wears to a light contact load point in a 10-hour period of continuous contact with a maximum power consumption of less than 400 watts when engaged. To extend the life of this seal for system restart capability a bellows actuator device was incorporated to lift the seal away from the contacting surface when the pump speed exceeds 6000 rpm. The lift-off device is actuated by a separate gas supply with an actuating pressure of 100 psia.

b. Lubricant Seal.- The lubricant seal consists of a slinger and a molecular pump in series as the dynamic seal, and a static carbon face seal. The slinger develops a stable liquid-vapor interface, and the molecular pump restricts molecule leakage. The carbon face seal functions when the dynamic seal is inoperative, as for the mercury seal.

The slinger is a smooth disk with a discharge hole in the housing at the periphery for returning the lubricant to the system. The molecular pump retards leakage of the lubricant vapor, the expected leakage rate being about 0.08 lb in 10,000 hours.

5.3.2.4 Bearing Lubrication System

The lubrication system included a filter, an injection system, and a scavenging device. A 5-micron filter is physically attached to the mercury pump. An injection system supplies the lubricant, and a scavenging device prevents flooding of the bearing cavities.

The lubricant injector to the bearings provides a total lubricant flow of 200 lb/hr. This rate of flow keeps the bearing temperature below 250°F. The design consists of an injection ring with six equally spaced 0.04-inch diameter holes which direct lubricant toward the inner race of the bearings. Two lubricant slingers scavenge the bearing cavities. Each slinger is designed to pump against a 5 psia discharge pressure.

A thermal analysis under flooded motor conditions indicated that the winding temperature would increase by approximately 100°F due to the added power consumption of 0.5 hp and viscous drag. This temperature increase was undesirable from an insulation life standpoint and also because the heat conducted through the rotor must travel through the shaft into the ball bearing area with subsequent detrimental effects on bearing clearances. A motor cavity scavenge slinger was, therefore, incorporated to purge the rotor air gap of fluid and return the fluid to the system. The maximum power loss for a flooded rotor and slinger was calculated to be 0.9 hp, but this falls off rapidly as scavenging is accomplished.

The mercury pump is fitted with lubricant-coolant fluid isolation valves on the inlet and outlet lines to and from the bearing cavity. These two-position 28-Vdc solenoid isolation valves are closed before pump shutdown and opened after the pump reaches full speed. This removes lubricant pressure from the bearing cavities, prevents flooding of the bearings and motor cavities, and reduces leakage through the face seals during startup and shutdown.

5.3.2.5 Bearing System

Single row, angular-contact ball bearings with a low shoulder in the inner ring are used with an outer-ring-piloted one-piece ball separator. The design goal was to obtain the minimum life of 10,000 hours with 99.5% reliability.

Angular-contact bearings were selected for their high load capacity and good radial stiffness. With axial preload, there is no internal looseness under operating conditions, and rolling contact with optimum dynamic balance is maintained at all times. A one-piece iron-silicon bronze cage, selected for maximum strength and light weight, was designed for good lubricant flow.

The loads on the ball bearings are shown in Figure 5-34. The bearings are preloaded using wavy springs. Axial thrust load is produced by pump pressure acting on the end of the shaft and the visco pump sleeve.

The radial bearing loads are developed from the pump, the shaft rotating mass, and the motor magnetic forces. The magnetic force is minimized by maintaining good machine concentricity. The average value for the motor magnetic pull was 10 lb with 30 lb, maximum. With a bearing spring rate of 5×10^5 lb/inch included in the analysis, the critical speed was calculated as 17,300 rpm, a more-than-ample margin over the 7800 rpm nominal operating speed.

5.3.3 Demonstrated Performance

The mercury pump has been tested extensively in component loops simulating system conditions and in the SNAP-8 system test loops. Most of the performance and endurance data were derived from component loop testing while operating experience was derived mainly from the system testing. The mercury pump successfully met design performance requirements. This judgment is based on the evaluation of 689 start cycles and 30,423 operating hours on six pumps. During an endurance run on one unit, 109 start cycles and 12,227 operating hours were logged. A detailed report containing an evaluation of the pump following this endurance test is contained in Reference 46.

The individual mercury pump components and the complete mercury pump motor assembly were evaluated in a progressive test program. The motor, the jet pump, the lubrication system, the sealing system, and motor were first tested independently. After individual component performance was established, the performance of the complete unit was evaluated in two mercury component loops which simulated the SNAP-8 environmental and operational requirements in space.

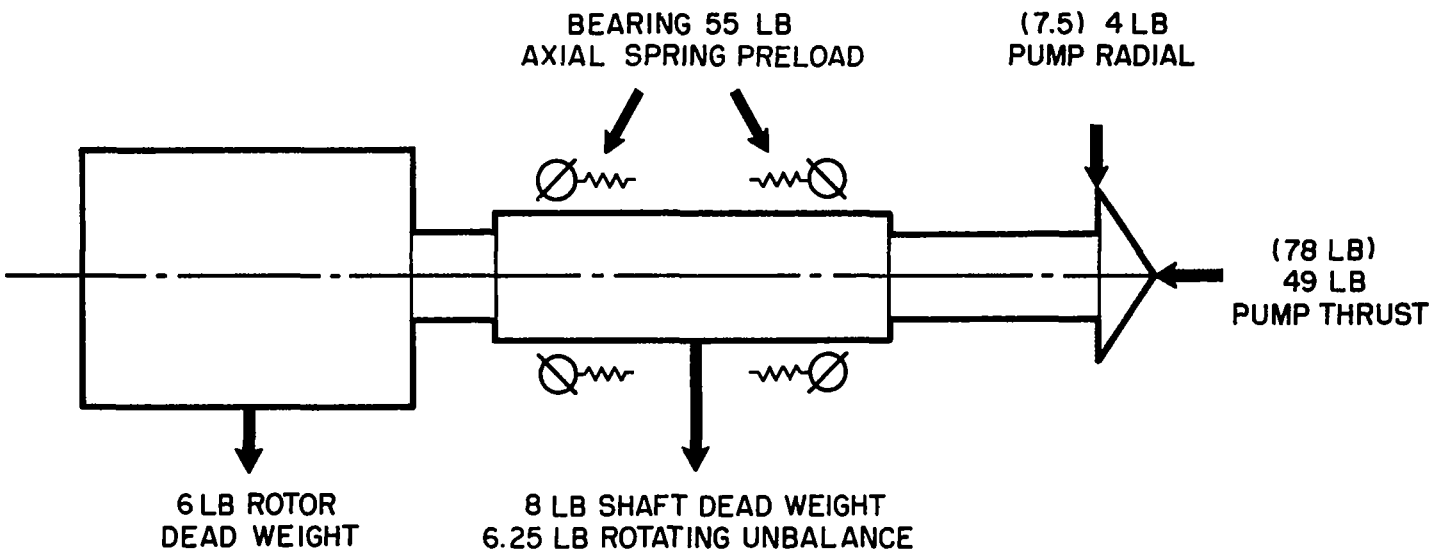

PUMP LOADS ARE COMPUTED FROM TESTED PRESSURE PROFILES
(VALUES IN PARENTHESIS ARE ANALYTICAL)

Figure 5-34 Mercury Pump Bearing Loads

The short-term and endurance capabilities of the unit were also evaluated in the mercury test loops. The hydraulic and electrical performance was determined including head-capacity characteristics, temperature and pressure distributions, and jet-pump and mercury-pump efficiencies. The mercury pump was incorporated into power conversion systems at Aerojet and NASA-LeRC and tested to evaluate the compatibility and effect on performance while operating under actual service conditions. System testing also allowed a more thorough analysis of transient system effects on the mercury pump during system startup and shutdown.

5.3.3.1 Overall Performance

a. Hydraulic Performance at 400 Hz.- The overall head-capacity performance of the pump has not been completely consistent. A reference curve was established in early tests; but, as development progressed, the performance was adjusted to a slightly lower head-capacity curve. The reason for this was that the head varied on a given unit from the values at startup to the slightly reduced values after one to six hours of operation. The performance would remain low, or almost recover to full head following a shutdown and restart cycle. In one case, a long-endurance pump operated for about 6000 hours at full head, then went through a period of low-head operation and finally, following a power-supply shutdown, resumed operation at full head to the completion of the test run. This phenomenon was investigated, but no explanation was reached which can be supported by test data. A possible cause is a low specific speed recirculation effect induced by system loop operating conditions. Analysis of the available test data confirms that the mercury pump performance in in accordance with the lower curves as shown in Figure 5-35.

This provides relatively conservative head values and results in an adequate pump performance margin for the system requirements. Note that the system statepoint in Figure 5-35 is different from the pump design conditions as shown in Table 5-VI. The latter values were based on statepoint conditions established earlier in the program. The reason that the tested head rise is greater than the calculated value is thought to be due to the selection of a conservative head coefficient in the design.

b. Shutoff or Low Flow Operation.- Because of the visco pump heat exchanger, the mercury pump can operate after the rest of the SNAP-8 system has been shut down for long periods of time and has been tested for more than 30 minutes without deleterious temperature rise. The jet pump bypass flow equalizes the fluid temperature, and the space seal heat exchanger effectively limits the maximum temperature.

c. 220-Hz Operation.- At 220 Hz, the mercury pump must operate in the system at either 50 or 66 V (line-to-neutral) power depending on whether or not power is supplied by the alternator. Pump performance at these voltages is shown in Figure 5-36. The head-capacity curve is directly related to the 400-Hz data, as expected.

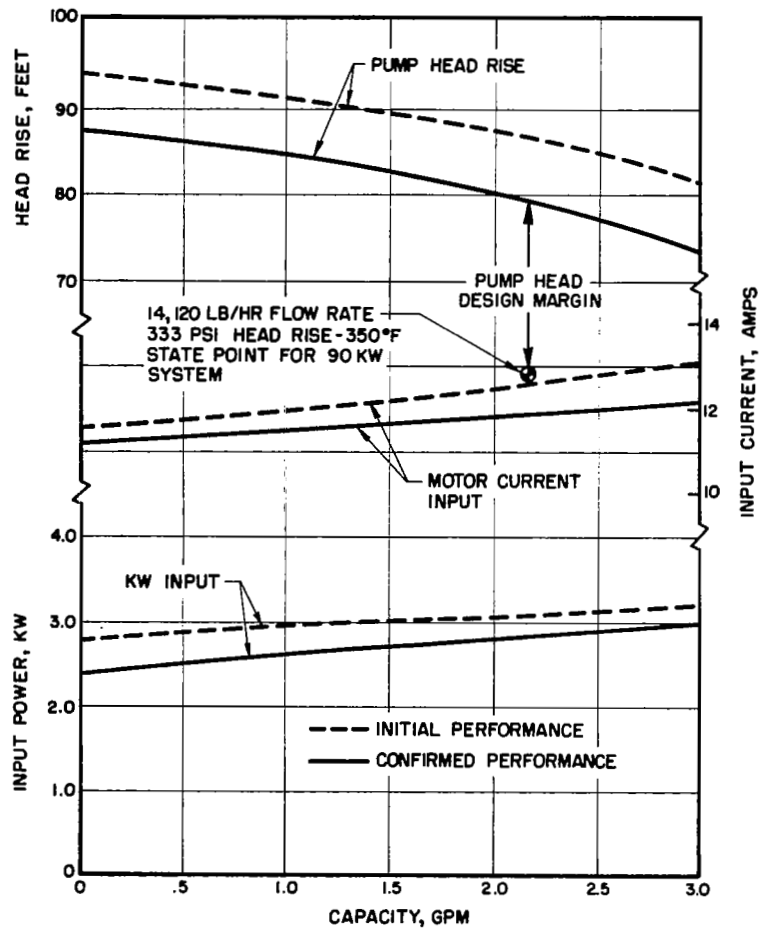

Figure 5-35 Mercury Pump Performance at 500°F (Input Power, 400-Hz, 208 V, L-L)

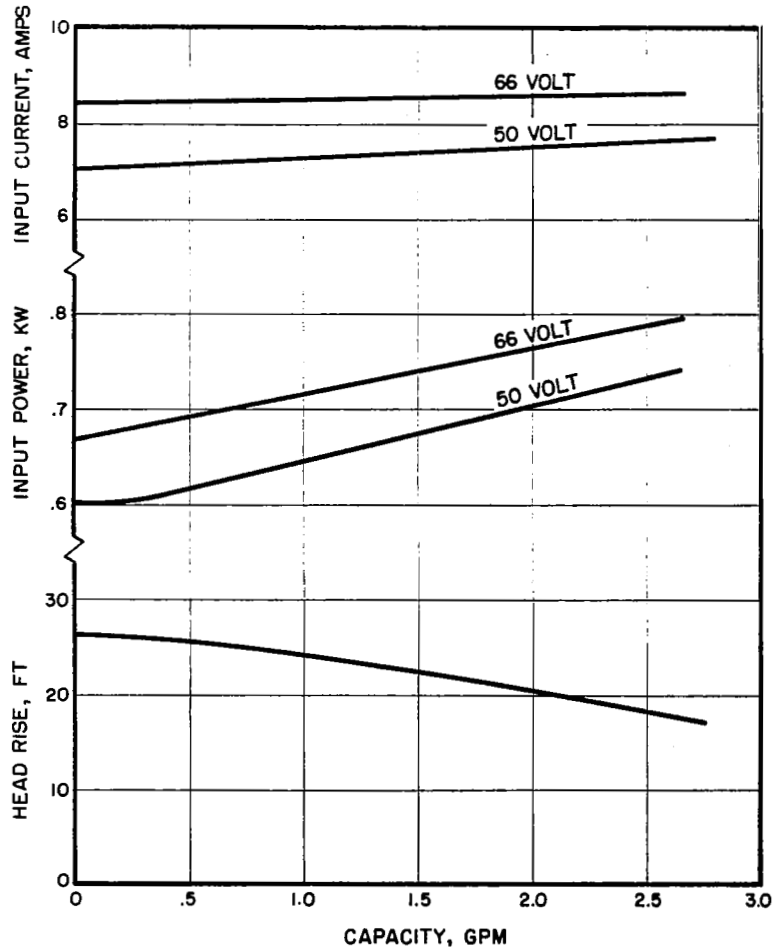

Figure 5-36 Mercury Pump Performance with 220-Hz Input Power (500°F)

5.3.3.2 Jet-Centrifugal Pump Performance at 400-Hz

a. Jet Pump.- Development tests of the jet pump were conducted first using water and later mercury to determine jet pump performance in relation to orifice size, and to establish the location of jet nozzle relative to the centrifugal impeller. The water and mercury tests showed satisfactory correlation, but the jet pump head was low with a resulting low efficiency of approximately 12.5%. This slightly low test efficiency was compensated by the ability to supply an NPSH of seven feet to the centrifugal pump inlet. The jet-pump NPSH was sufficient to suppress centrifugal pump cavitation under normal system starting and operating conditions.

The performance of the jet-centrifugal pump combination was tested by reducing the NPSH supplied to the jet pump as shown in Figure 5-37. At 1.82 gpm, which is near mercury pump rated conditions, the jet pump head is reduced by about 12% when supplied with an NPSH equivalent to 1.5 ft. However, the overall head does not show a corresponding decrease. This, together with pressure profiles along the jet-pump length while in cavitation, indicated that the jet mixing section was too short for this operating point. The jet-to-suction flow mixing had not been completed at the end of the jet pump, but (from the overall head value) mixing may have been completed before reaching the impeller. With the NPSH reduced further, the overall pump head decreases and, shortly after the 2% overall head loss level, the jet pump head becomes so low that the centrifugal eye is completely cavitating.

Figure 5-38 shows the NPSH available at the centrifugal pump inlet as a function of through-flow-capacity for 10% jet pump head loss, 2% overall pump head loss, and minimum NPSH values. The minimum NPSH curve indicates operation within 20% of the rated head but with the pump incurring cavitation damage. The pump has operated with virtually zero NPSH while still producing 10 to 80% of normal head values. A study of this type of operation was made when severe cavitation damage was found on a mercury pump impeller used during tests in the 35-kWe system facility. The jet pump has never shown cavitation damage.

b. Centrifugal Pump.- The centrifugal pump produces greater head than was expected from the design calculations. This was attributed to the use of a conservative head coefficient. The pump produced an established head rise of 81.6 ft. with 23.4% efficiency instead of the original calculated value of 69.5 ft with 22% efficiency.

c. Impeller Back Vane Damage.- Impeller back hub cavitation damage was observed during an endurance test, but the damage was not great enough to hinder performance during 12,227 hours of operation. The impeller used for this test was made from 9M steel. However, the damage was judged to be a life-limiting factor for a goal of 5 years. The back vane pressure is related to pump suction pressure, jet pump differential, centrifugal pump differential pressure, and back vane differential pressure. With pressure and liquid velocity gradients present circumferentially around the impeller hub, cavitation damage is likely to occur if the hub pressure level is near the mercury vapor pressure.

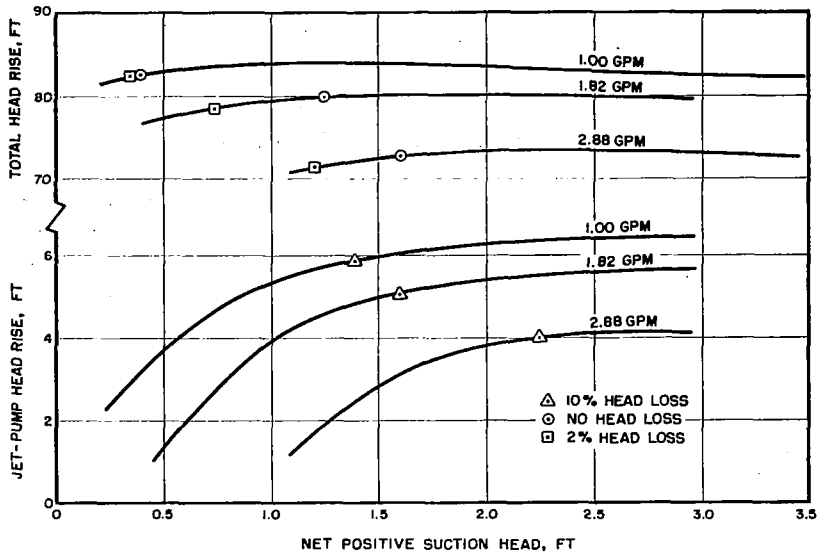

Figure 5-37 Jet-Centrifugal Pump NPSH Performance

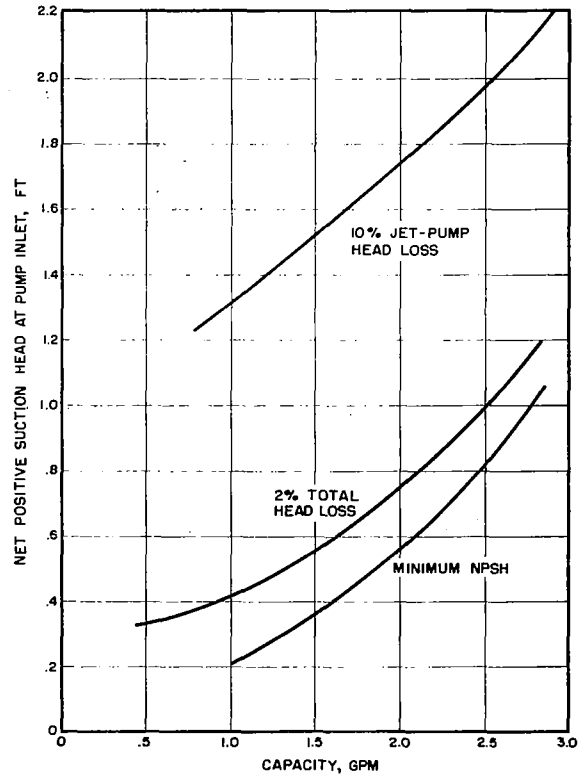

Figure 5-38 Summary of Mercury Pump NPSH Tests

Some modified impellers were fabricated from Stellite 6B for improved cavitation characteristics, and with an increased impeller hub diameter to raise the pressure at the hub. Also the number of back vanes was a contributing factor. Limited testing was later conducted with these impellers. The extent of the testing however was insufficient to indicate whether or not this material and the impeller design changes would totally alleviate the cavitation damage.

d. Impeller Radial and Axial Forces.- The impeller radial and axial forces shown in Figure 5-39 were obtained from pumps operating with full head characteristics. Force measurements were calculated by equating pressure gradients defining the impeller front and back profiles. Similarly, the impeller peripheral pressure profile established the force and direction of the impeller radial load with the assumption that the unmeasured dynamic or velocity forces were balanced.

5.3.3.3 Motor Performance

The motor for the mercury pump has been fully developed and has met the design requirements as proven by the results of the tests described below.

a. Motor Insulation Tests.- A polyimide-insulated motor was submerged in polyphenyl ether and operated at temperatures of 250 and 300°F for 20,000 hours to determine the compatibility of the insulation with the lubricant-coolant. No measurable insulation degradation was observed.

b. Motor "In-Air" Tests.- The motor supplier (Westinghouse) conducted an "in air" test on the pump motor. The test results have been plotted as a speed-torque curve in Figure 5-40 with a predicted computer-developed performance curve shown in Figure 5-41. Test results indicate that the motor performance is adequate, attaining 87.6% efficiency.

c. Motor Input Power.- Figure 5-42 shows the input current and voltage obtained from testing. The pump was operated at rated conditions with motor input voltage as a variable. Figure 5-42 shows that, at the rated 208 V (line-to-line), or 120 V (line-to-neutral), voltage, the lowest current is required. At lower voltage, the power decreases as the load decreases due to the lower operating speeds.

d. Motor Startup Characteristics at 400 Hz.- Because of the low-temperature viscosity of the lubricant-coolant fluid, an acceleration problem can exist (see Figure 5-43). At 400 Hz and 208 V (line-to-line) to the motor terminals, the motor will accelerate to full speed if the motor cavity is not flooded and the lubricant is at least 100°F. If the lubricant temperature or input voltage is lower, the acceleration time will be longer, or full speed may not be attained. If the motor cavity is flooded, the unit will not attain full speed but will stabilize at about 5000 rpm. The motor cavity and ball-bearing lubricant slingers must be at speeds of at least 6000 rpm to overcome the normal 5 psia back pressure before the lubricant flow is initiated. At speeds below 6000 rpm, the unit remains flooded. At a lubricant and pump temperature of 125°F, the unit can reach 5000 rpm in the flooded condition. With a slight temperature increase, the pump can accelerate to 6000 rpm for full purging of the pump motor cavity. Therefore, preheating the unit to 125°F for starting was specified.

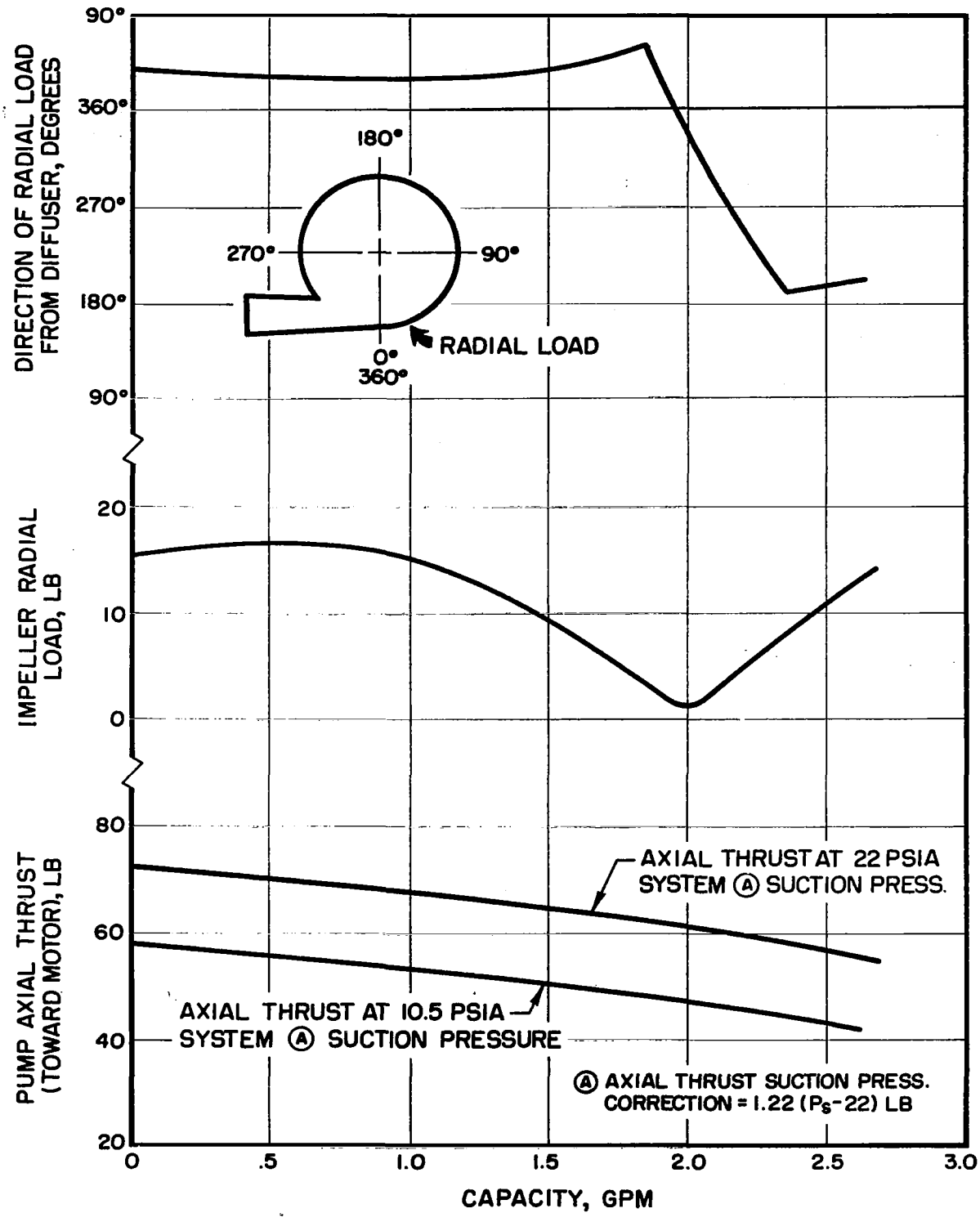

Figure 5-39 Mercury Pump Impeller Radial and Axial Forces

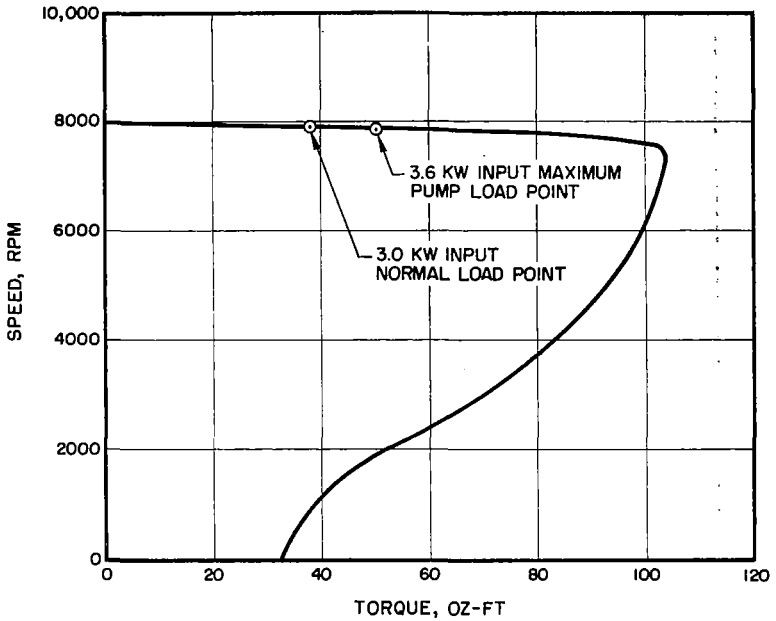

Figure 5-40 Mercury Pump Speed-Torque In-Air Tests (Motor Only)

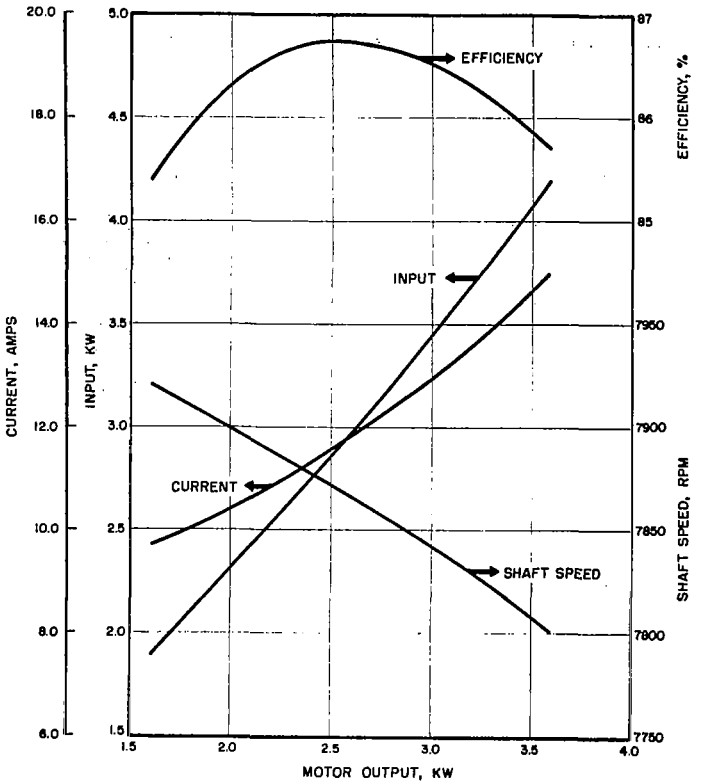

Figure 5-41 Mercury Pump Performance Based on In-Air Tests (Motor Only)

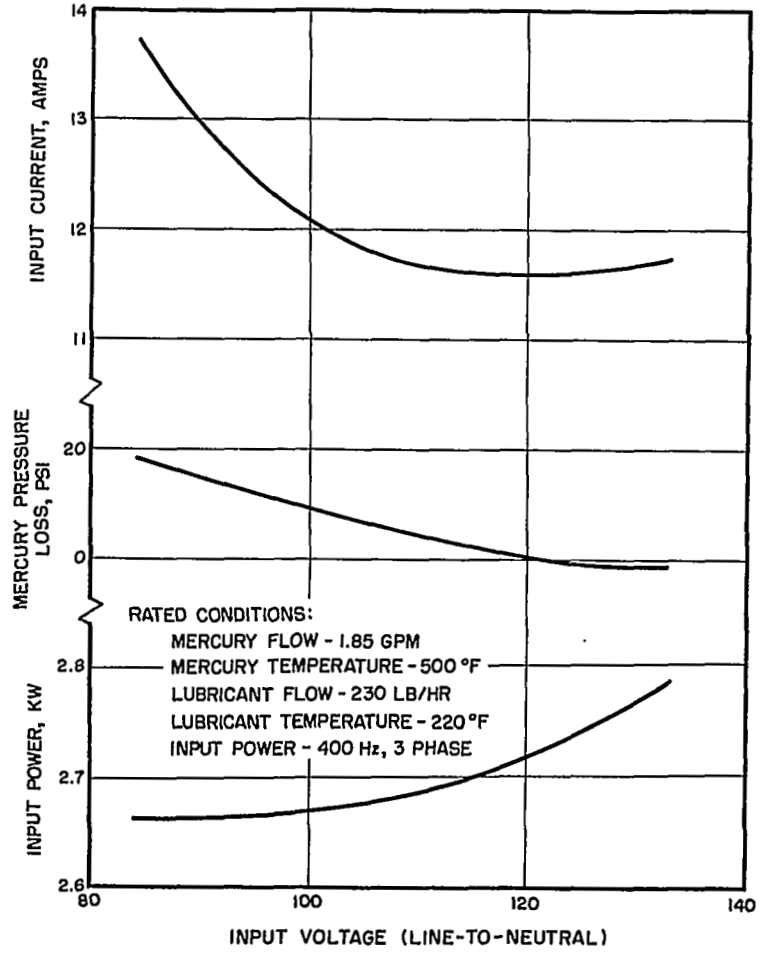

Figure 5-42 Mercury Pump Performance with Varying Voltage

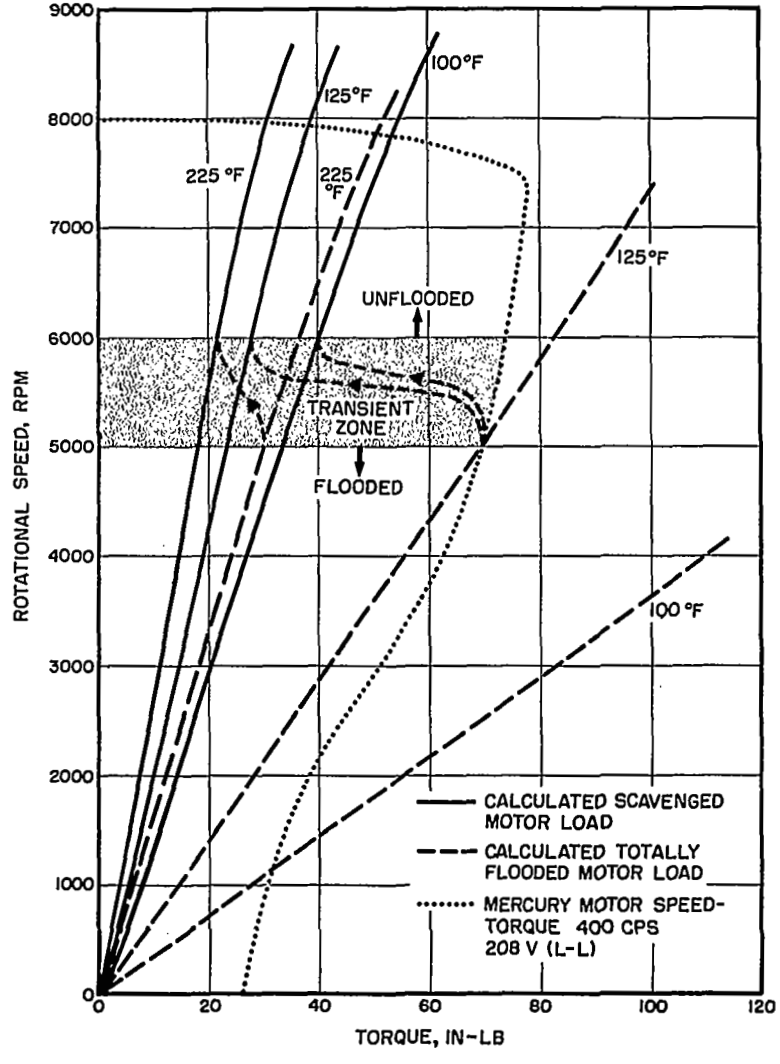

Figure 5-43 Mercury Pump Acceleration Tests

5.3.3.4 Dynamic Seals

The optimum dynamic mercury seal design was derived by individually testing the visco pump, slinger, and molecular pump as separate components. Various screw-type seals, slinger designs, and running clearances were evaluated. The dynamic elements that performed best were then combined into the mercury pump design. An important feature verified during the development was the attainment of the stable liquid-vapor interfaces necessary for good sealing. These interfaces were visually verified at the lubricant slinger and the mercury visco pump.

The tests were not specifically set up to determine long-term operating leakage. Consequently, no precise long-term leakage measurements were made, but a careful recording of fluids in various test systems indicated that the leakage was low, and probably well below the maximum allowable leakage.

Some minor cavitation damage has occurred to the rotating and stationary elements of the visco pump, seemingly at the location of the liquid-vapor interface. The materials used for these parts were 9Cr-1Mo steel for the stationary seal housing and AISI 4340 for the rotating sleeve.

Some design changes were made to fabricate these parts from Stellite 6B which is considered to be at least on order of magnitude improvement in cavitation resistance. Limitations of further testing precluded the judgment as to the extent of the improvement.

a. Mercury Dynamic Seal Pressure.- Figure 5-44 illustrates data from tests conducted to establish the pumping pressure capabilities of the visco and molecular seal pumps. The input power curve step at 81 psia impeller back-hub pressure signifies the pressure limit of the visco pump. The step shows the disk power increase for the larger molecular pump. The increasing power slope at pressures greater than 81 psia shows the molecular pump capabilities for handling liquid until gross mercury leakage occurs at 116 psia. Data from Figure 5-44 and from tests conducted at various pump speeds were used to establish the curves shown in Figure 5-45 which illustrate individual and overall seal component limitations. The visco pump pressure limits the pressure on the impeller back vane and keeps the molecular pump liquid-free. The maximum limit of the mercury visco-molecular pump combination defines the point of gross liquid leakage of the dynamic seal system.

b. Lubricant Dynamic-Seal Pressures.- The lubricant dynamic seal is a smooth disk slinger backed by a molecular pump. The outside diameter of the slinger is at the discharge of the ball-bearing scavenging slinger located on the other side of the slinger disk. The sealing pressure limit related to the bearing outlet pressures is not defined by a step function in that, as the pressure increases, power increases from a combination of the slinger disk, ball bearing turbulence, and the motor rotor cylinder and disk hydraulic losses. As seen in Figure 5-46, these actions result in a gradual power increase with an increase in slope when the motor rotor starts to flood and stabilizing before the gross liquid leakage occurs. Since the power level of

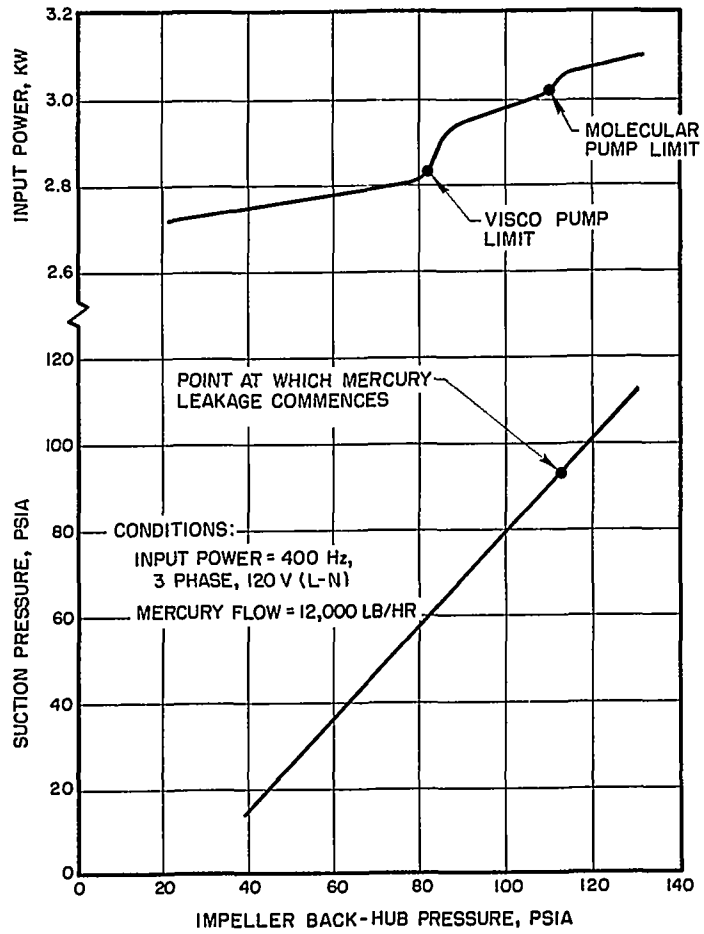

Figure 5-44 Mercury Dynamic Seal Pumping Pressure - Mercury Pump

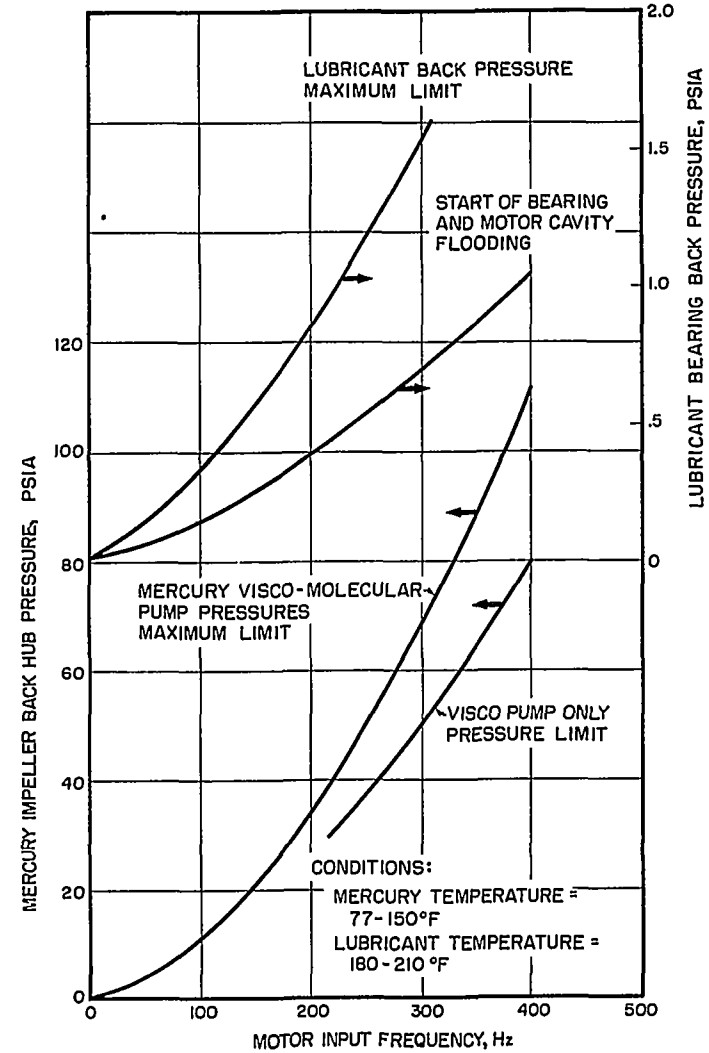

Figure 5-45 Dynamic Seal Component Performance - Mercury Pump

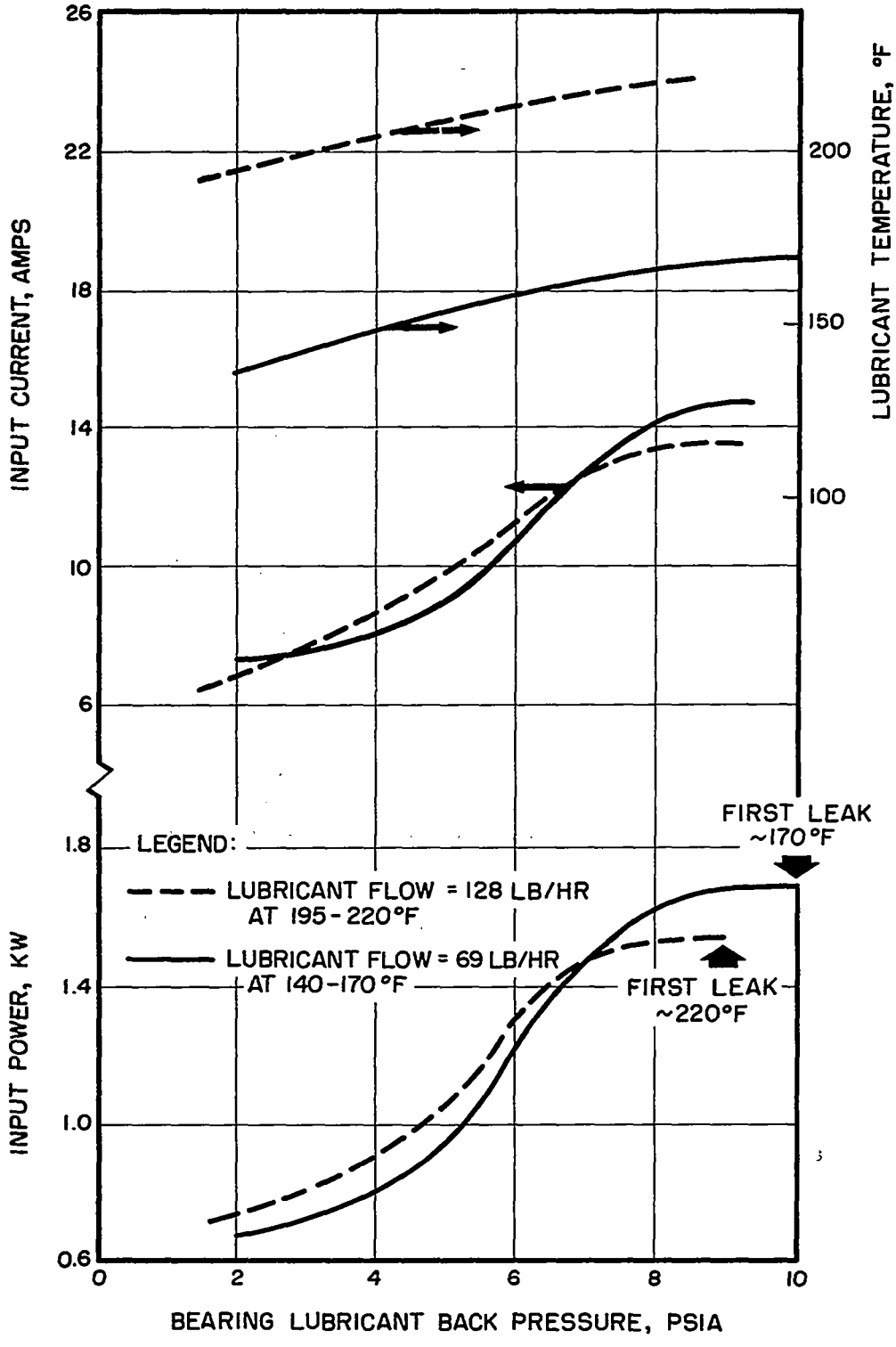

Figure 5-46 Lubricant Pumping Pressure - Mercury Pump Dynamic Seal

the flooded molecular pump is small, no data to indicate when it is filled with liquid is available. However, when the motor cavity becomes flooded, the motor input power noticeably increases. In figure 5-45, beginning of motor-cavity flooding and the gross leakage bearing outlet pressure points are given as a function of frequency.

5.3.3.5 Shaft Static Seal

The lift-off device as shown in Figure 5-32 for the static seals consists of a bellows actuated by 200-psia nitrogen. Although one of these parts operated successfully during the 12,227-hour endurance test, others have shown a tendency to leak at the bellows weld point. Modified designs were tested where a differential bellows was incorporated directly in the face seals. With these changes, the seals were tested for 50 hours without failure.

Some static leakage rate tests were conducted with these seals with variable results. Carbon seals, when new, sealed to 30 and 33 psi on two separate units before mercury leakage occurred. After operation for a short time, leakage occurred between 4 to 12 psi and, after 50 hours of operation with seals in contact, the seals leaked at less than 1 psi. In system operation, the differential pressure would approach zero psi with the seal in contact when the unit is not operating or at a lower speed; therefore, these values are satisfactory. Operating time and experience however is inadequate to judge whether the latest lift-off seals are reliable.

5.3.3.6 Ball Bearings

The ball bearings have operated satisfactorily in all units operated to date. This includes 30,423 operating hours on six pumps with 12,277 hours on the longest run. The following observations were based on examination of ball bearings from the endurance test units:

- The lubrication was good. Both rolling contact elements and the ball separator showed practically no wear.
- The mounting system is satisfactory. No rotating unbalance load was observed, and the ball tracking was good.
- There was no sign of fatigue.
- Contamination control was acceptable. No serious foreign particle damage occurred.
- Varnish (due to heat) deposition of the lubricant on the bearing was judged to be of no consequence.

It is concluded that based on the experience to date a bearing life of five years, or greater, can be expected.

5.3.3.7 Bearing Lubrication and Cooling

The polyphenyl ether lubricant-coolant fluid circulates through the mercury pump to lubricate and cool the ball bearings and to cool the motor and mercury visco pump. No problems have occurred in any of these functions.

a. Bearing Inlet Flow.- The effect of different lubricant flows to the ball-bearing inlet has been tested for flows ranging from 50 to 550 lb/hr. Flows below 150 lb/hr are not recommended since high bearing temperatures are likely to occur. Most mercury pump testing has been at flows of 200 to 300 lb/hr.

b. Bearing Inlet Temperature.- The inlet temperature has little effect on the inlet pressure since the Reynolds number change is small and the pressure loss is almost totally that of the orifice. The inlet temperature does, however, affect the pump power and bearing temperatures directly as shown in Figure 5-47. With a maximum allowable bearing outer-race temperature of 300°F, inlet oil temperatures above 270°F are not advisable. Temperatures lower than 200°F require higher input power. Therefore 215°F ± 5°F is the recommended inlet temperature. Figure 5-47 shows test data of the effect of lubricant inlet temperature on bearing temperature, input current, and power.

c. Bearing Lubricant Back Pressure - 400 Hz.- Figure 5-48 shows the effects of operation at different lubricant pressures. Operation is desirable at back pressures ranging between 2.9 and 8.7 psia, but the power increases about 75 watts per psia within this range.

d. Bearing Lubricant Back Pressure - 220 Hz.- Data from tests at 220-Hz input power indicate that the pump operates unflooded at back pressures up to 2.8 psia. At higher pressures up to 5.6 psia, power increases only gradually. The bearing and motor temperature rise indicates that the unit could operate at steady state with a 5.6-psia bearing lubricant back pressure, and at lubricant inlet temperatures up to 200°F.

e. Motor Housing Heat Exchanger.- The motor housing heat exchanger passages are large for the amount of flow involved, and laminar flow conditions exist. The design value of 0.6 psi pressure drop at 400 lb/hr is confirmed by test data.

f. Mercury Space-Seal Heat Exchanger.- This heat exchanger maintains the visco pump liquid-vapor interface at 300°F, maximum, which controls the vapor pressure at the liquid-vapor seal interface. From an examination of the thermal mapping obtained from testing the seal housing, outside temperature registered 253°F instead of the calculated 326°F (Figure 5-49). Therefore it may be presumed that the liquid-vapor interface temperature is considerably less than 300°F, and consequently the seal leakages would be much less than the allowable rates.

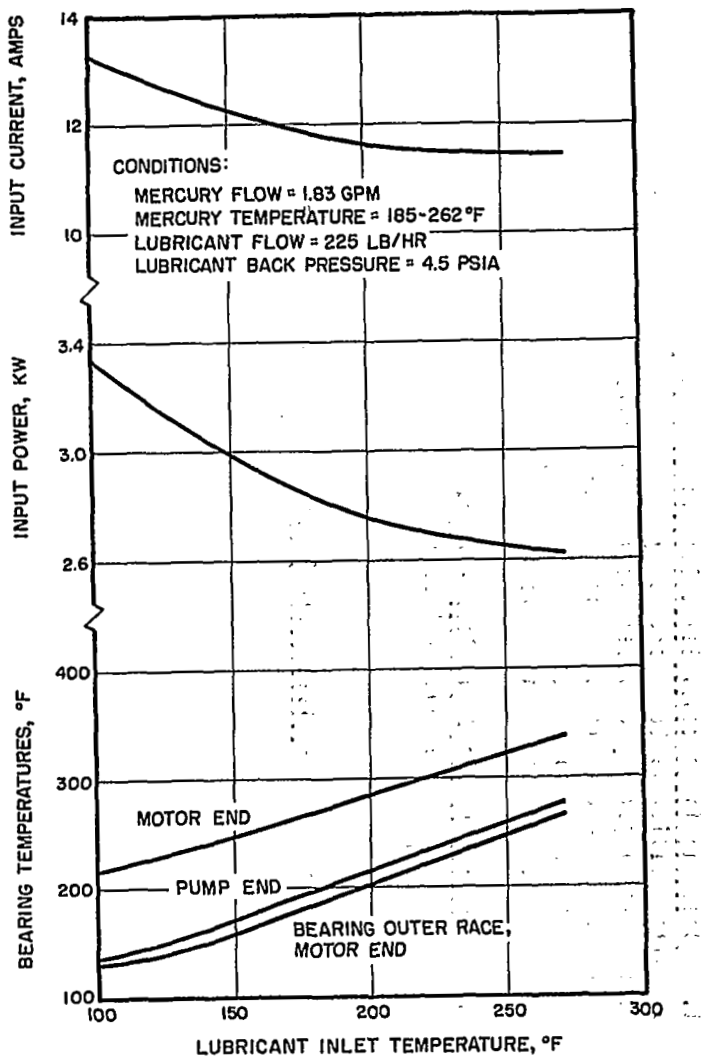

Figure 5-47 Effect of Lubricant Inlet Temperature on Bearing Temperature, Input Power, and Input Current - Mercury Pump

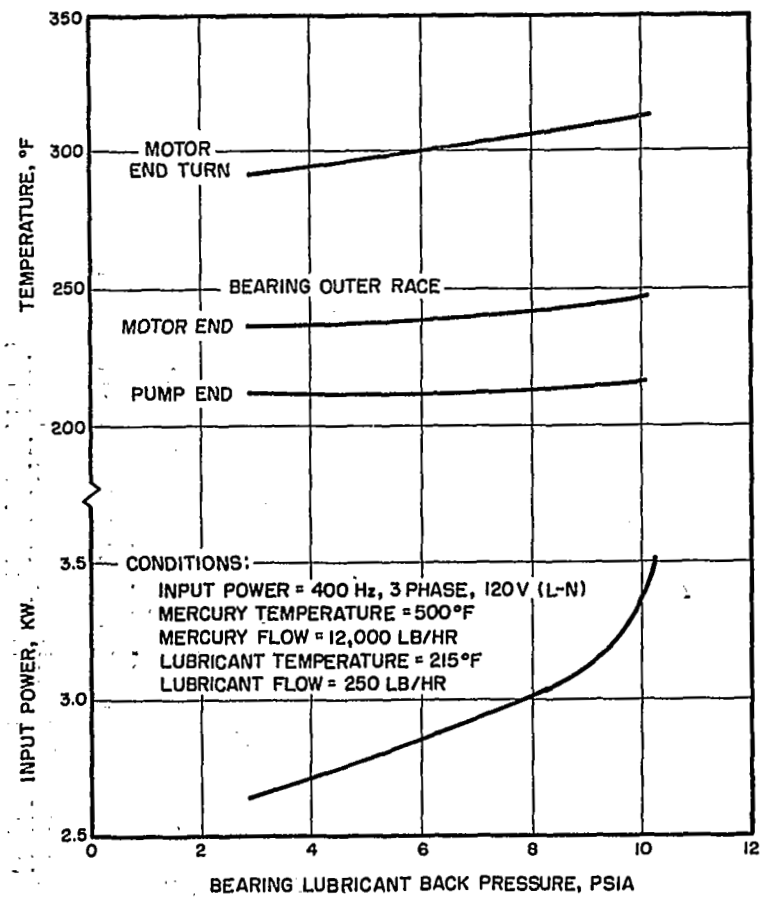

Figure 5-48 Effect of Lubricant Back Pressure on Input Power, Bearing Temperature, and Motor Winding Temperature - Mercury Pump

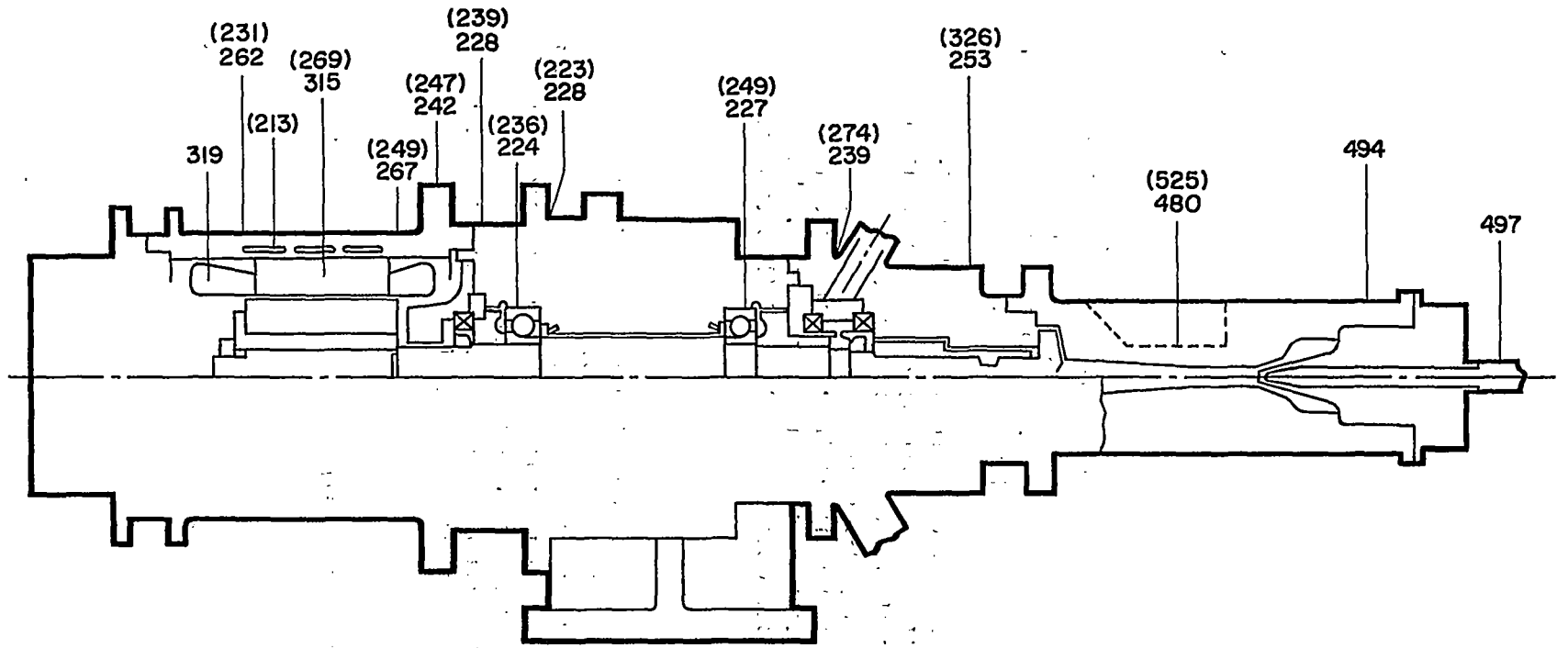

SPACE SEAL COOLANT FLOW 2000-2300 LB/HR AT 210°F INLET TEMPERATURE
MOTOR AND BEARING LUBRICANT/COOLANT FLOW 290-300 LB/HR AT 210°F INLET TEMPERATURE
MERCURY FLOW 13,500 LB/HR AT 500°F SUCTION TEMPERATURE
REF. TEST 06 P32

Figure 5-49 Mercury Pump Thermal Map (Calculated Temperatures in Parenthesis)

5.3.3.8 Temperature Distribution

Temperature distribution in the mercury pump was obtained by operating a pump in a simulated space environment with insulation wrapped around the entire unit to prevent radiation heat losses. All temperatures were lower than calculated with the exception of the motor stator iron temperature and the motor housing temperature (Figure 5-49). The slightly higher stator-iron temperature was caused by an unexpectedly high rate of heat transfer from the winding coil to the stator iron. The higher temperatures of the stator iron and the motor housing were not considered detrimental.

5.3.4 Vibration and Shock Testing

A complete mercury pump was tested in the vibration test facility at NASA-LeRC in accordance with NASA Specification 417-2, Rev. C. This included sinusoidal sweep vibration, random vibration, and multiple shocks of 15-g peak in three directions. The test program and post-test examination of the mercury pump is described in detail in Reference 47.

The test times and input-power levels are shown in Table 5-VII. The only detrimental condition observed after testing was an apparent loss of bearing preload caused by galling of one of the bearing outer races in the housing. The housing is made from 9Cr-1Mo alloy which is susceptible to galling and therefore a recommendation to either "hard-chrome" the housing surface or employ a hardened steel liner in the housing was made. These changes had not been implemented at the conclusion of the SNAP-8 Program effort.

5.3.5 Operational Interfaces

The mercury pump nominal operating conditions are shown in Table 5-VIII for 400-Hz and 220-Hz operation. These values represent the expected operating point for the SNAP-8 system. With the exception of mercury suction pressure, the majority of the mercury pump test time was accumulated under these nominal conditions. However, for operation in a ground test system, the pump suction pressure was greater than the value shown in Table 5-VIII because of the mercury elevation pressure occurring in a 1-g environment. During operation in the 35-kWe test system, pump suction pressures were 30 to 33 psia.

Table 5-IX lists the operational alarm and shutdown limits for 400-Hz operation. The overspeed limit could occur only with over-frequency resulting from a runaway turbine. The shutdown limits signal immediate failure, whereas the alarm limits signal various conditions that will harm the equipment and perhaps eventually cause a failure. Exceeding the shutdown limits of various parameters should be cause for an automatic shutdown.

TABLE 5-VII SUMMARY OF MERCURY PUMP VIBRATION TESTS

Type Test	Run Number	Axis Test	G Level Input	Frequency Input, (Hz)	Sweep Speed	Running Time
Sine	1	X	1	5-2000	1 oct/min	8.4 min
Sine	9	Y	1	5-2000	1 oct/min	8.4 min
Sine	10	Z	1	5-2000	1 oct/min	8.4 min
Random	2	X	3 db/oct 0.4 g^2/Hz -6 db/oct	20-100 100-600 600-2000	20 g's overall	3 min
Random	18	Y	"	"	"	"
Random	11	Z	"	"	"	"
Shock	3, 4, 5	+X	15			11 ms
Shock	6, 7, 8	-X	15			11 ms
Shock	19, 20, 21	+Y	15			8 ms
Shock	22, 23, 24	-Y	15			8 ms
Shock	12, 13, 14	+Z	15			8 ms
Shock	15, 16, 17	-Z	15			8 ms

TABLE 5-VIII MERCURY PUMP NOMINAL OPERATING CONDITIONS

Mercury flow	=	12,000 $\pm$ 500 lb/hr (1.85 gpm)
Suction pressure and temperature	=	10 $\pm$ 1 psia at 500°F
Bearing lubricant-coolant flow	=	200 to 250 lb/hr
Bearing lubricant-coolant inlet temperature	=	215 $\pm$ 5°F
Bearing lubricant-coolant back pressure	=	4.5 to 5.0 psia
Space seal coolant flow	=	2600 $\pm \begin{matrix} 200 \\ 800 \end{matrix}$ lb/hr
Motor coolant flow	=	150 to 250 lb/hr
Voltage (L-L)	=	208 $\pm$ 4 V, 3 phase
Frequency	=	400 $\pm$ 2 Hz

Static seals lifted during operation at rated speed

220-Hz (5 to 10-minute SNAP-8 Standby Condition)

Mercury flow	=	450 lb/hr
Suction pressure and temperature	=	10 $\pm$ 1 psia at 100 to 140°F
Bearing lubricant-coolant flow	=	110 to 140 lb/hr
Bearing lubricant-coolant inlet temperature	=	200 $\pm$ 5°F
Bearing lubricant-coolant back pressure	=	2.8 psia (with seals lifted)
Space seal coolant flow	=	1400 $\begin{matrix} + 100 \\ -450 \end{matrix}$ lb/hr
Motor coolant flow	=	80 to 140 lb/hr
Voltage (L-L)	=	88 $\pm$ 2 V, 3 phase
Frequency	=	220 $\pm$ 2 Hz

TABLE 5-IX MERCURY PUMP OPERATIONAL ALARM AND SHUTDOWN LIMITS - 400 Hz OPERATION

Maximum Speed	=	9000 rpm (S)[+]
Maximum Motor Current (3 phases)	=	16 amps (A)
Maximum Motor Winding Temperature	=	400°F (A)
Maximum Bearing Temperature	=	300°F (S)
Maximum Slinger Discharge Pressure	=	10 psia (A)
Maximum Mercury Inlet Temperature	=	600°F (A)
Low Bearing Flow	=	75 lb/hr (S)
Low Mercury Suction Pressure	=	7 psia (A)

[+](S) = Shutdown
(A) = Alarm

The physical piping connections to the mercury pump are a 1-inch OD mercury suction line, a 3/4-inch OD mercury discharge line, lubricant-coolant inlet and outlet lines to and from the motor and bearings in series at the outboard isolation valves, and an inlet and outlet line to and from the space seal heat exchanger. The space manifold vacuum connection to the toroidal manifold on top of the pump in Figure 5-32 must be flexible to avoid damage to the unit due to pressure differentials caused by forces due to the internal vacuum.

5.3.6 Recommendations for Improvements

Recommendations for improving the reliability of the SNAP-8 mercury pump based on experience gained in the development are as follows:

a. Ball Bearing Lubricant Jets.- The present bearing lubricant system uses six jets (0.040-inch nozzles) per bearing to provide lubricant at a 1-psia inlet pressure. This low pressure has caused control problems in testing, since the velocity of the lubricant is relatively low (only 11.5 fps), and it is predictable that maximum cooling is not achieved. An improved method would use three jets (0.030-inch nozzles) to provide lubricant at a 9-psia inlet pressure and a velocity of 33 fps. This would provide better control of inner race lubrication and improved cooling of the bearings.

b. Static Seals.- The present static carbon face seals run on a tungsten carbide face which wears out the carbon face in a relatively short time when in continuous contact. An investigation of self lubricating face material with better wear characteristics should be made.

c. Mercury Jet Pump.- The length of the mixing section in the jet pump is too short to develop maximum head under cavitation conditions. The throat section (0.44-inch diameter) of the jet pump should be lengthened to, perhaps, 18 diameters instead of six. At the same time, the jet pump could be modified to suit the NPSH requirement of the system in which it will be used. Also, the jet pump (and centrifugal pump) should be relocated closer to the mercury supply source to improve the inlet available NPSH.

d. Space Seals.- Development of Stellite 6B for the space seal elements should be continued, and various configurations that may improve cavitation resistance should be investigated.

System operation should be defined to restrict extent and time of mercury pump allowable operation during low NPSH conditions. The jet pump should be modified to handle the lowest NPSH, lengthened accordingly, and confirmed by testing.

e. Lift-off Seals.- Since the lift-off actuator has proven unreliable in operation, some further development testing on the modified design should be made or alternate designs, such as a centrifugally operated device, should be considered.

f. Bearing Housing.- To eliminate the galling experienced between the housing bore and bearing outer ring, the possibility of either hard chrome plating the housing bore or incorporating a hardened steel liner should be investigated.

g. Centrifugal Pump Impeller.- Tests on the modified design, i.e. Stellite 6B, 8 back vanes, and increased hub diameter should be completed to verify correction of back hub cavitation damage.

5.4 LUBRICANT-COOLANT PUMP

The SNAP-8 system utilizes an organic fluid to lubricate bearings and to cool system components. This fluid, a radiation resistant polyphenyl ether, is circulated through the system by a centrifugal pump driven by an electric motor. The entire pump-motor unit is hermetically sealed. Lubrication and cooling of the motor is accomplished by a small flow of the pumped fluid through the motor and down the hollow shaft which returns the flow to the inlet of the main pump.

5.4.1 Development Background

The development of this pump was subcontracted to the Tapco Division of Thompson Ramo Wooldridge, Inc. The design was made for the SNAP-8 35-kWe system, and all operating experience described in this report is related to the 35-kWe system. However the pump is capable of providing the required flow and head for the 90-kWe SNAP-8 system.

The performance data listed in Table 5-X show the pump development through to the latest test results. The unit met or exceeded all performance requirements. Seven pumps used as test support equipment in six systems accumulated 60,578 operating hours, and more than 1200 start-stop cycles. Three of the units ran for 14,521, 15,345 and 24,862 hours, respectively. One pump was operated at approximately 1/3 rated capacity for 24,862 hours. To date, the lubricant-coolant pump has not had an operational failure.

5.4.2 Physical Description

The lubricant-coolant pump (Figures 5-50 and 5-51) is a hermetically sealed centrifugal pump and squirrel cage 400-Hz motor combination, self-cooled and lubricated. The pumped fluid is circulated through the carbon bearings and open-winding submerged motor to provide the necessary cooling and lubrication. An electrical connector is used for input power to the motor. The design of the unit is covered in detail in Reference 48.

The design and construction of the unit employed conventional technology used extensively on similar equipment. The motor and bearing design and materials are similar to those used in aircraft fuel pumps, and the pump configuration was based on a previously developed and tested design. The unit is comprised of four parts: pump, motor, bearings, and shaft. The weight of the contained oil is 1.7 lb at 70°F, and the weight of the pump 25.7 lb.

5.4.2.1 Pump

The unit is an end suction semi-open centrifugal pump with a single volute. Hydraulic axial thrust is controlled by reducing the impeller back hub pressure to the level of the impeller eye pressure by providing large bypass holes through the impeller shroud. The impeller is keyed, and secured against a shaft shoulder with a lock nut. The seven vanes are swept back and are thin

TABLE 5-X LUBRICANT-COOLANT PUMP DESIGN AND PERFORMANCE DATA

Components and Parameters	Design Point	Design Point Tested Values
Pump, Centrifugal		
Flow, lb/hr	9,400	9,400
Flow, gpm	17	17
Inlet temperature, °F	220-250°F	250°F
Density, lb/ft^3	68.5	68.5
Inlet pressure, psia	3	1.6
Pressure rise, psi	55	63.5
Head, ft	115.7	133.6
Outlet pressure, psia	58	65.1 at 1.6 psia inlet
Hydraulic power, hp	0.58	0.626
Hydraulic power, kW	0.430	0.468
Efficiency, %	43.25	--
Shaft input power, hp	1.34	--
Shaft input power, kW	1.0	--
Motor*, Induction		
Electrical Efficiency, %	77.5	--
Overall Efficiency, %	50.5	--
Input power, hp	2.127	2.185
Input power, kW	1.587	1.63
Power factor, %	66	66.5
Overall pump-motor efficiency, %	27.2	28.7
Summary of Losses		
Total Electrical Losses, watts	266	
Total Mechanical Losses, watts	321	

*A 6-pole motor was selected to provide 7820 rpm at rated conditions with 400-Hz input.

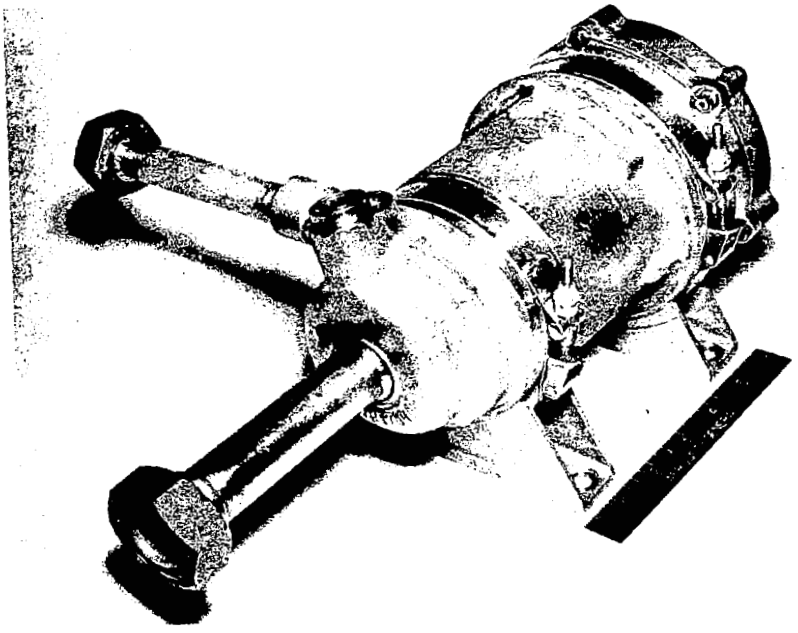

Figure 5-50 Lubricant-Coolant Pump

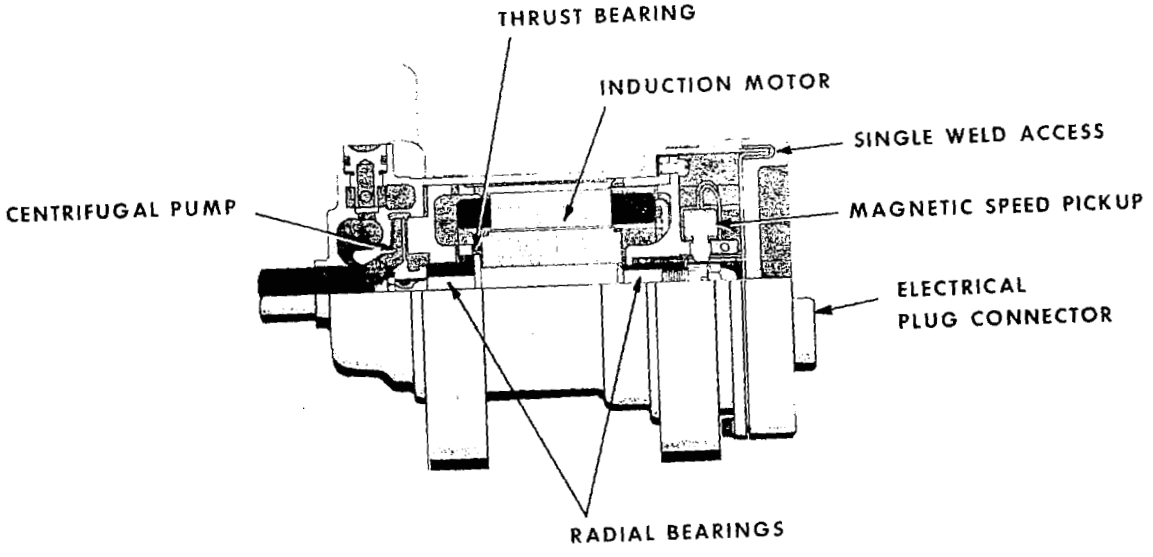

Figure 5-51 Lubricant-Coolant Pump Cutaway View

and sharply pointed at the entrance (Figure 5-52). The volute casing is part of the overall unit housing, and is a single-volute design of normal proportions.

Since it is desirable to keep the back pressure on the turbine-alternator and mercury pump bearings as low as possible to reduce power losses, SNAP-8 system specifications required the lubricant-coolant pump to operate at low suction pressures. The existing pump adequately met this requirement without modification.

5.4.2.2 Motor

The motor is a 1.5 hp, 6-pole, 400-Hz, 3-phase, squirrel-cage induction motor with an ML electrical insulation system. The motor cavity is flooded with the lubricant-coolant fluid and the ML-insulated copper stator wires are fully exposed to the fluid. The motor construction is typical of an open winding in that no cans are employed for the stator and rotor. The rotor (Figure 5-53) uses silver conductor bars and end rings. The rotor laminated stack is 29-gage AISI Type M-15. The stator has 36 slots, and the rotor 47. The stator uses 21 gauge wire with 20 turns per coil and 2 parallel paths.

The motor is cooled by the process fluid which flows from the pump volute through the motor. The fluid returns to the pump impeller eye through the hollow shaft.

5.4.2.3 Bearings and Shaft

The bearings and shaft were adapted from components previously used in an aircraft jet-fuel pump. The radial bearings are straight sleeve journal carbon bushings running against a 410 CRES chrome-plated shaft. The nominal shaft diameter is 0.5 inch with a bearing length of 0.438 inch. The diametrical clearances are 0.001 to 0.003 inch. Positive lubricant flow to the pump-end bearing is through two drilled holes in the housing on the motor side. The motor-end bearing is lubricated by an integral screw pump (Figure 5-53), which moves liquid through the bearing toward the motor rotor. The motor rotor end disk surface acts as a smooth slinger to pump the fluid out.

The axial bearings are simple flat-plate thrust bearings. The main thrust bearing has a carbon bushing operating against a chrome-plated 410 CRES plate shrunk on to the shaft. The smaller, reverse-thrust bearing uses the impeller back hub against the radial bearing end as the bearing surface. The reverse thrust bearing is loaded only momentarily at startup.

The main thrust bearing is made with two radial lubrication feed grooves in the carbon bushing. Positive lubrication through the bearing occurs with centrifugal action outflow past the bearing surfaces and feeder grooves.

The impeller front vane clearance (.005 inch) is set by shimming.

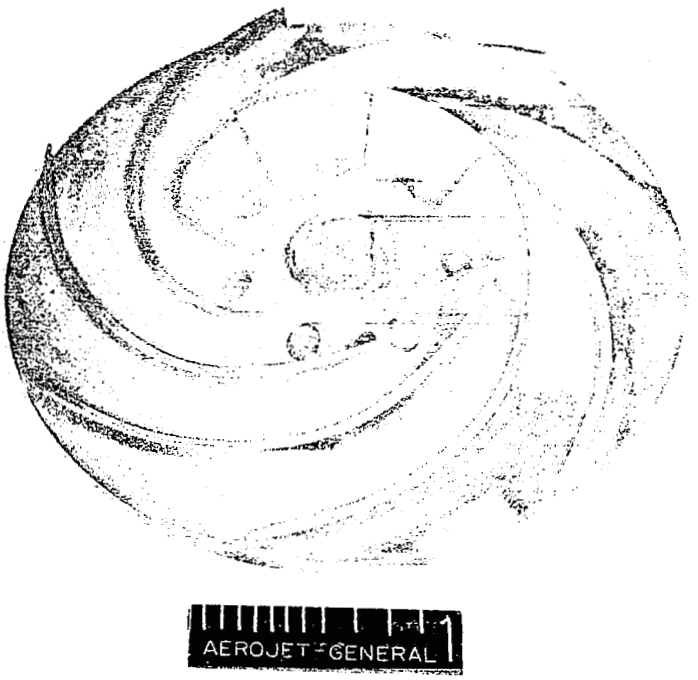

Figure 5-52 Lubricant-Coolant Pump Impeller

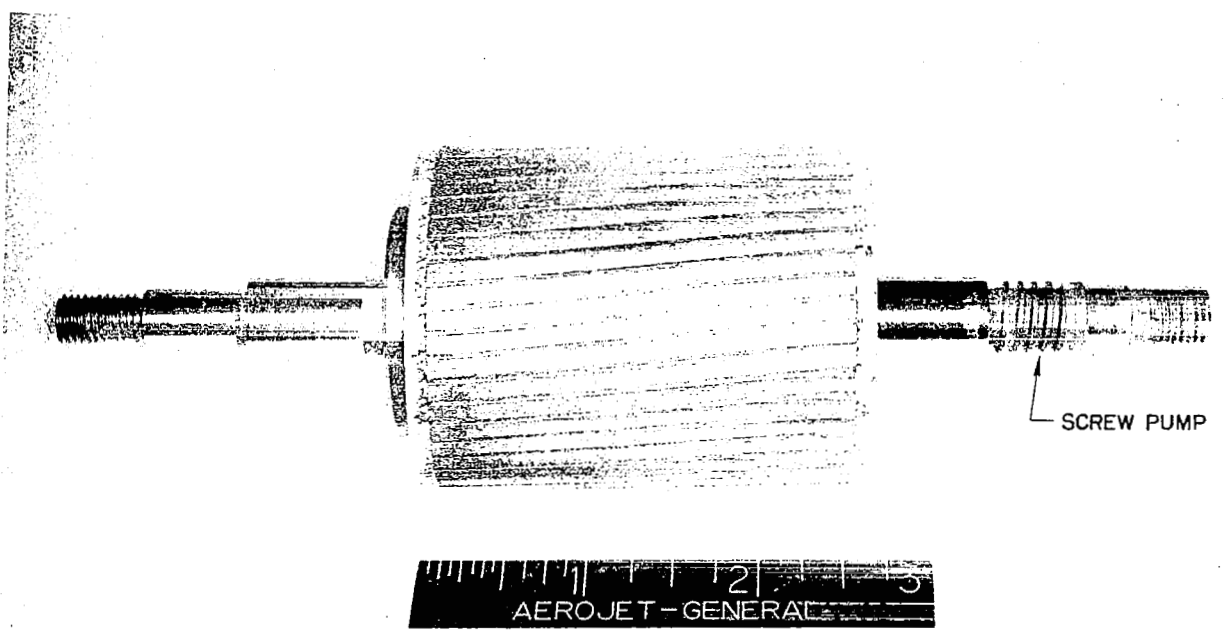

Figure 5-53 Lubricant-Coolant Pump Rotor

The shaft first lateral critical speed is over 100,000 rpm, making the bearing deflection rate the major influence. In calculations using the nominal maximum clearance with the lightest load, the bearing critical speed was 12,000 rpm. Since smaller clearance and heavier loads greatly stiffen the bearing, this was judged an adequate margin over the 7800 rpm operating speed.

5.4.2.4 Miscellaneous

As seen in Figure 5-54, the pump is made in a two-housing form. The one aligning the rotating parts slips into the outer shell. After the motor end seal weld is made, the backup plate protects and supports this weld and end plate. The pump auxiliary instrumentation includes a speed pickup and motor thermocouples.

The unit is mounted on two cradles; straps lock the pump to these cradles and allow the unit to be orientated to any desired position. Furthermore, the construction also allows operation in horizontal, vertical, or any other position in ground testing.

5.4.3 Demonstrated Performance

The lubricant-coolant pump has met all performance requirements, and has exceeded the 10,000-hour endurance goal on three separate units. To date, seven units have accumulated 60,578 hours with more than 1200 start-stop cycles. The longest-term unit logged 24,862 operating hours operation with more 570 start-stop cycles at TRW and at Aerojet.

5.4.3.1 Overall Performance

Tests of three units produced hydraulic performance curves as shown in Figure 5-55. The testing defined the pump input power at rated capacity of 17 gpm as 1.58 to 1.64 kW. The tabulated data are shown in Table 5-X. As can be seen from Figure 5-55, the pump is able to deliver the required capacity and head for a 90-kWe system.

5.4.3.2 Variable Operation

As discussed previously, the pump NPSH is important to the SNAP-8 system because it reduces the back pressure on the bearing slingers which saves power in the turbine and mercury pump. On Figure 5-55, the NPSP (pressure) derived from testing is shown. With polyphenyl ether as the lubricant, the pump starts satisfactorily using the lowest SNAP-8 system applied voltage of 19 V, line-to-line, at a temperature of 70°F. Tests at 125°F demonstrated that the pump will start at 5.5 V, line-to-line, an equivalent one pound-inch of torque.

The pumped polyphenyl ether viscosity increases considerably at lower temperatures which greatly modifies the pump performance. Since the motor is flooded, the motor rotor, the pump, and bearings all contribute to the requirement for more electrical power at lower temperatures. A series of tests was conducted from an 80°F, 220-Hz start through to a 250°F, 400-Hz

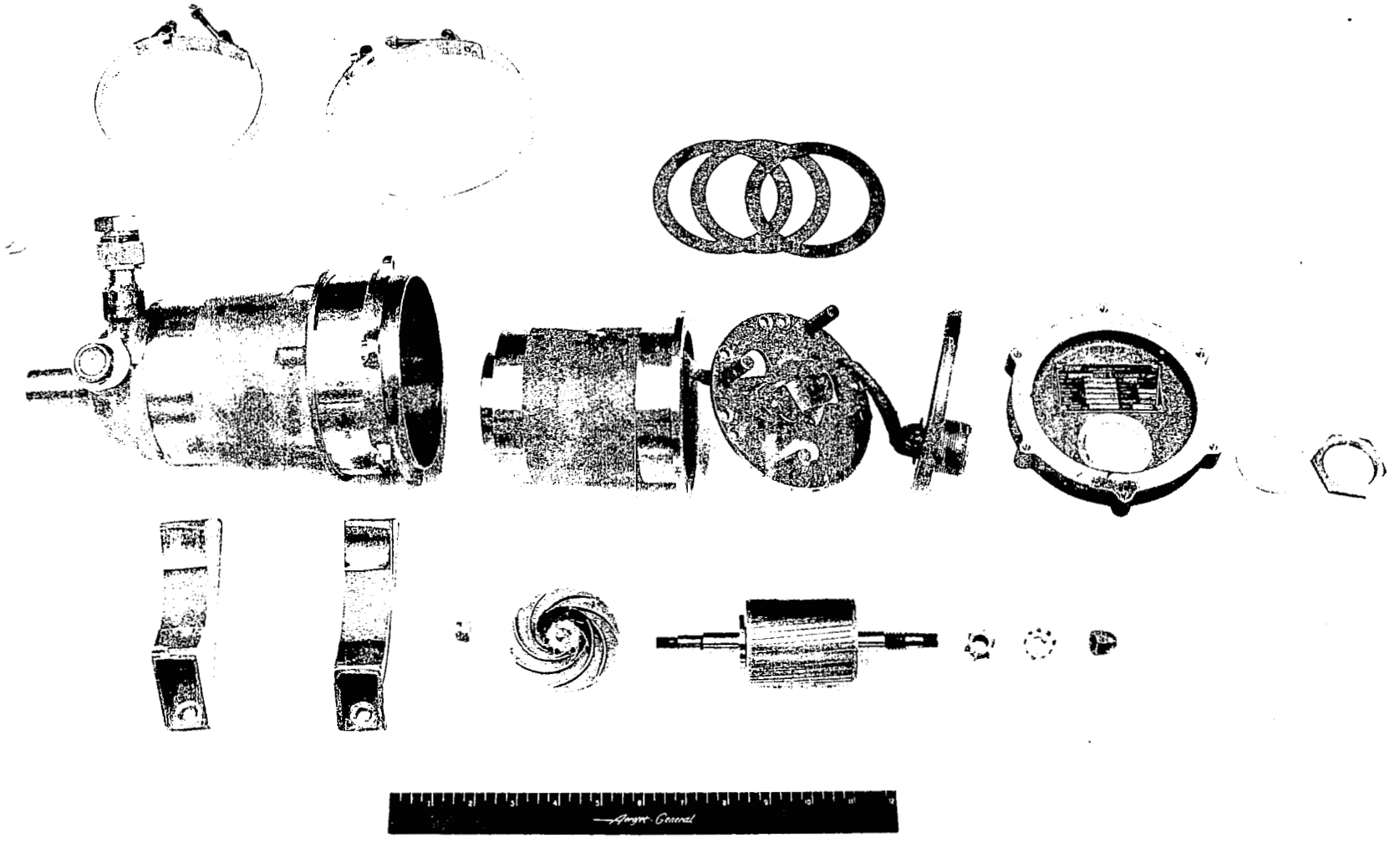

Figure 5-54 Disassembled Lubricant-Coolant Pump

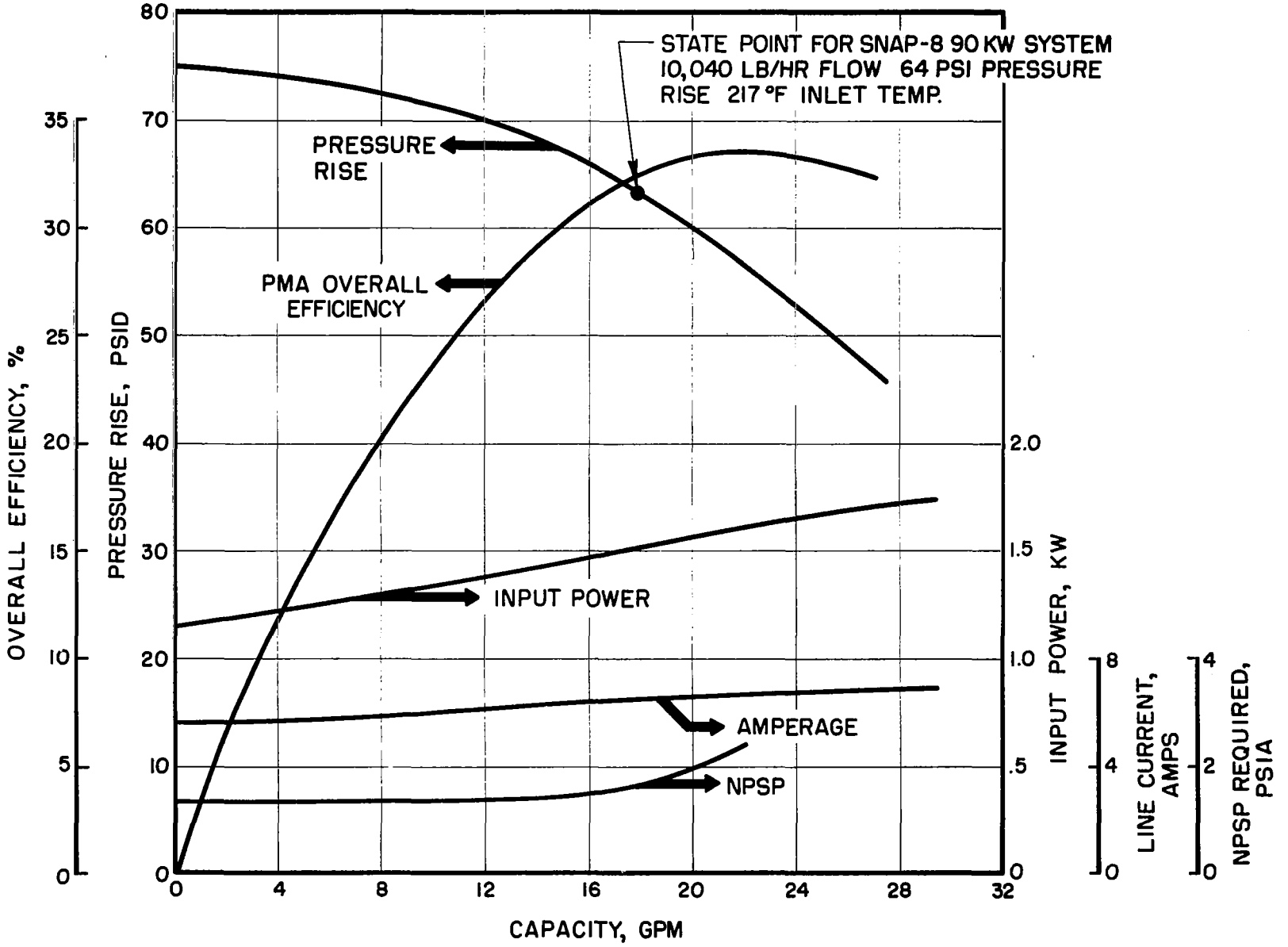

Figure 5-55 Lubricant-Coolant Pump Performance (Input Power: 400 Hz, 208 V, 3 Phase; Fluid Temperature: 250°F)

run with variable capacity. Using the 400-Hz data shown in Figure 5-56 as an example, cold polyphenyl ether increases the input power and amperage, but changes the pressure only slightly at a given lower capacity. Of course, the system losses limit the maximum flow level as illustrated by the last system-limited test points on the curve which increase with increasing temperature. The 220-Hz data provide overall steady-state performance information up to 181°F.

Figure 5-57 shows the pump performance variation with varying voltage while operating at 400 Hz. The curves show that the motor is designed for minimum current at 120 V (L-N or 208 V, L-L). If the unit is operated at 10% low voltage, only a small current change will take place. The input power and pressure rise will decrease with the higher motor slip (lower unit speed).

5.4.3.3 Miscellaneous Performance

a. ML Insulation.- To confirm the ability of the ML insulation system to operate submerged in polyphenyl ether, a 20,088-hour endurance test was made. A rewound commercial motor running submerged was used. A total of 14,000 hours was accumulated at temperatures similar to the pump winding temperature of 260 to 280°F with the last 6000 hours at temperatures of 340 to 360°F. No significant change in insulation ground resistance took place.

5.4.3.4 Environmental Testing

A SNAP-8 lubricant-coolant pump was vibration and shock tested at the NASA LeRC test facility to specification NAS 417-2, Revision C. The pump showed only slight damage in that the exterior housing-to-base surfaces were galled. This was considered to be insignificant. Hydraulic performance tests, before and after the vibration and shock testing, were conducted. These indicated no change in pump performance. The details of this testing are described in Reference 49.

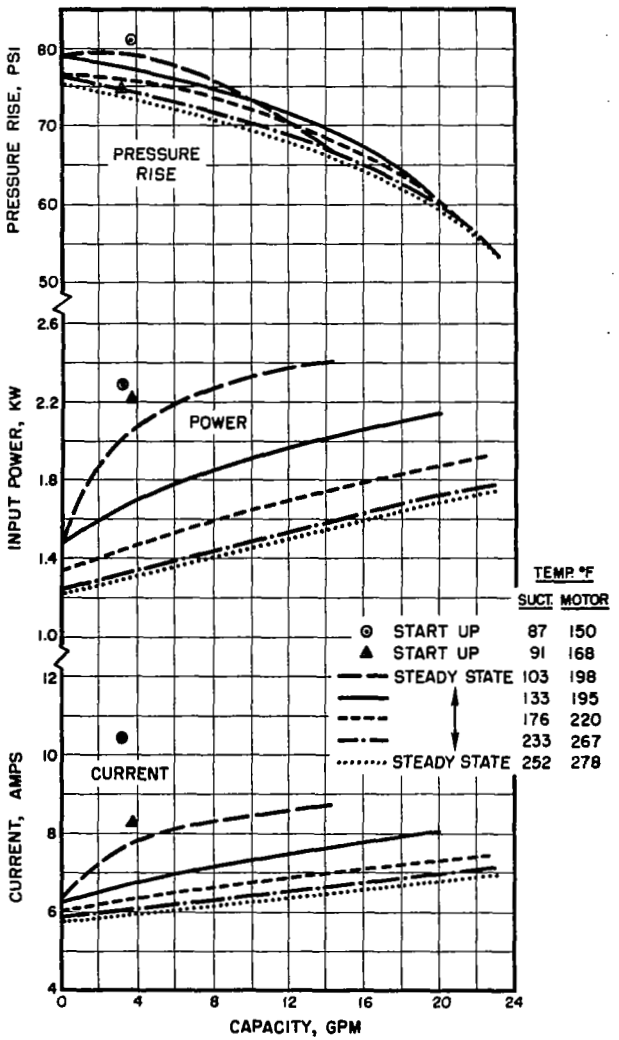

Figure 5-56 Lubricant-Coolant Pump Performance Variation with Varying Temperature (Input Power: 220 Hz, 3 Phase)

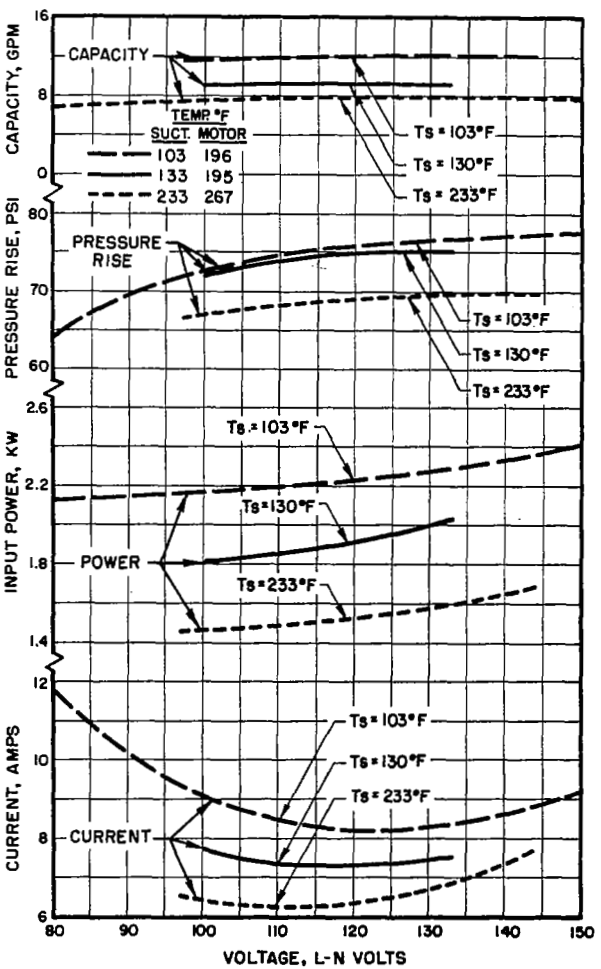

Figure 5-57 Lubricant-Coolant Pump Performance Variation with Varying Input Voltage (Input Power: 400 Hz, 3 Phase)

5.5 BOILER

5.5.1 Development Background

In the SNAP-8 system, the NaK-to-mercury heat exchanger, or boiler, is the interface between the heating fluid, NaK, and the working fluid, mercury. Figure 5-58 shows schematically the relationship of the boiler to the other major power conversion system components in the 90-kWe system. Figure 5-59 shows it in relation to the 35-kWe system.

During the evolution of the SNAP-8 boilers, three major design improvements separate the initial design from the final boiler concept. This evolution is shown in Figure 5-60. The first improvement was a change from a tube-in-shell, cross-counterflow design to a tube-in-tube with pure counterflow. As a result, heat transfer improved with the increased NaK and mercury flow. The change also provided accurate diagnostic data in terms of boiler tube length. Along with the change from tube-in-shell to tube-in-tube, was a decrease in the tubing ID from 0.902 to 0.652 inch, and in increase in the number of tubes from 4 to 7 which resulted in a decrease of mercury flow area from 2.56 to 2.34 square inches.

The second major change was in the mercury containment material from 9% chromium - 1% molybdenum steel (9M) and Haynes 25 steel to the refractory metal, tantalum. References 50 and 51 detail the results of using 9M and tantalum as mercury containment materials. The ramifications of this change were fourfold.

(1) Since 9M or Haynes 25 was wetted only intermittently by liquid mercury, the "dry-wall" boiling correlations based on SNAP-1 and SNAP-2 experience were applied. However, mercury does wet tantalum above 1000°F. The heat transfer is improved in the vapor-quality region of the boiler and is less sensitive to contaminated, mercury-side surfaces.

(2) The 9M and Haynes 25 alloys were susceptible to NaK-side embrittlement (carburization) and mercury-side corrosion/erosion. Tantalum proved to be resistant to mercury corrosion and erosion. These conclusions were reached during extensive metallurgical programs using scale models of boiler configurations with NaK and mercury at simulated operating conditions for long periods of time.

(3) The use of tantalum created a need for a transition joint between it and the Type 316 stainless steel since the two materials cannot be joined by the standard welding methods.

(4) Due to the large differences in thermal expansion between tantalum and Type 316 stainless steel ($\alpha_{ss}/\alpha_{ta} = 2.5$), a means of accommodating the differential growth had to be devised.

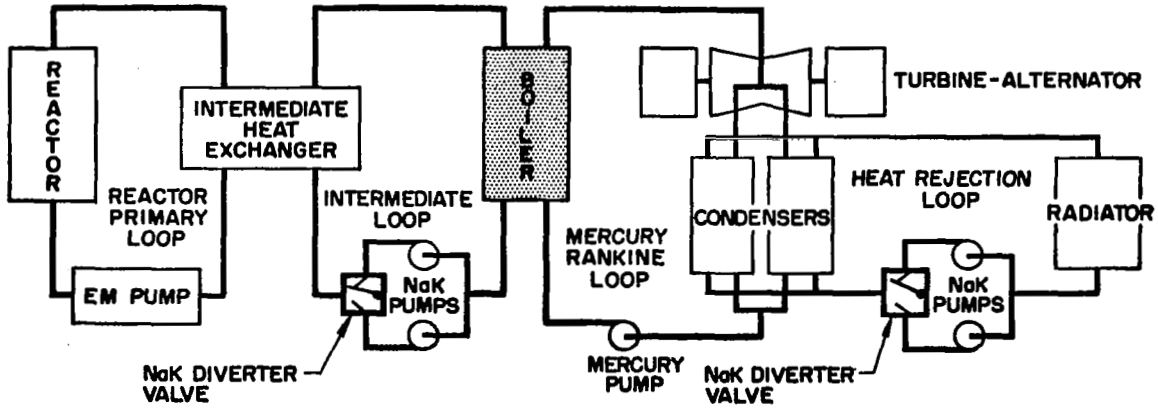

Figure 5-58 90-kWe System Schematic Showing Location of Boiler

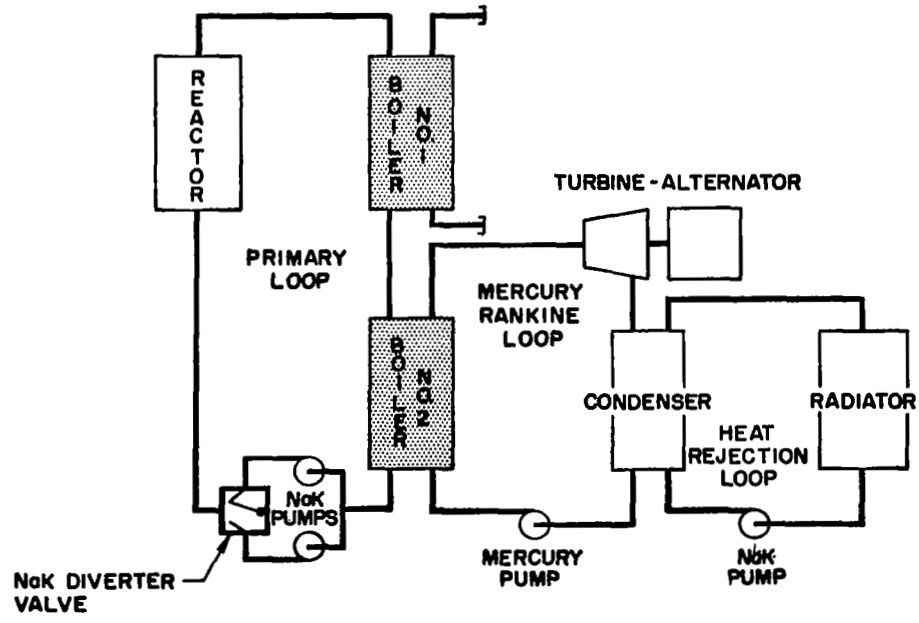

Figure 5-59 35-kWe System Schematic Showing Location of Boiler

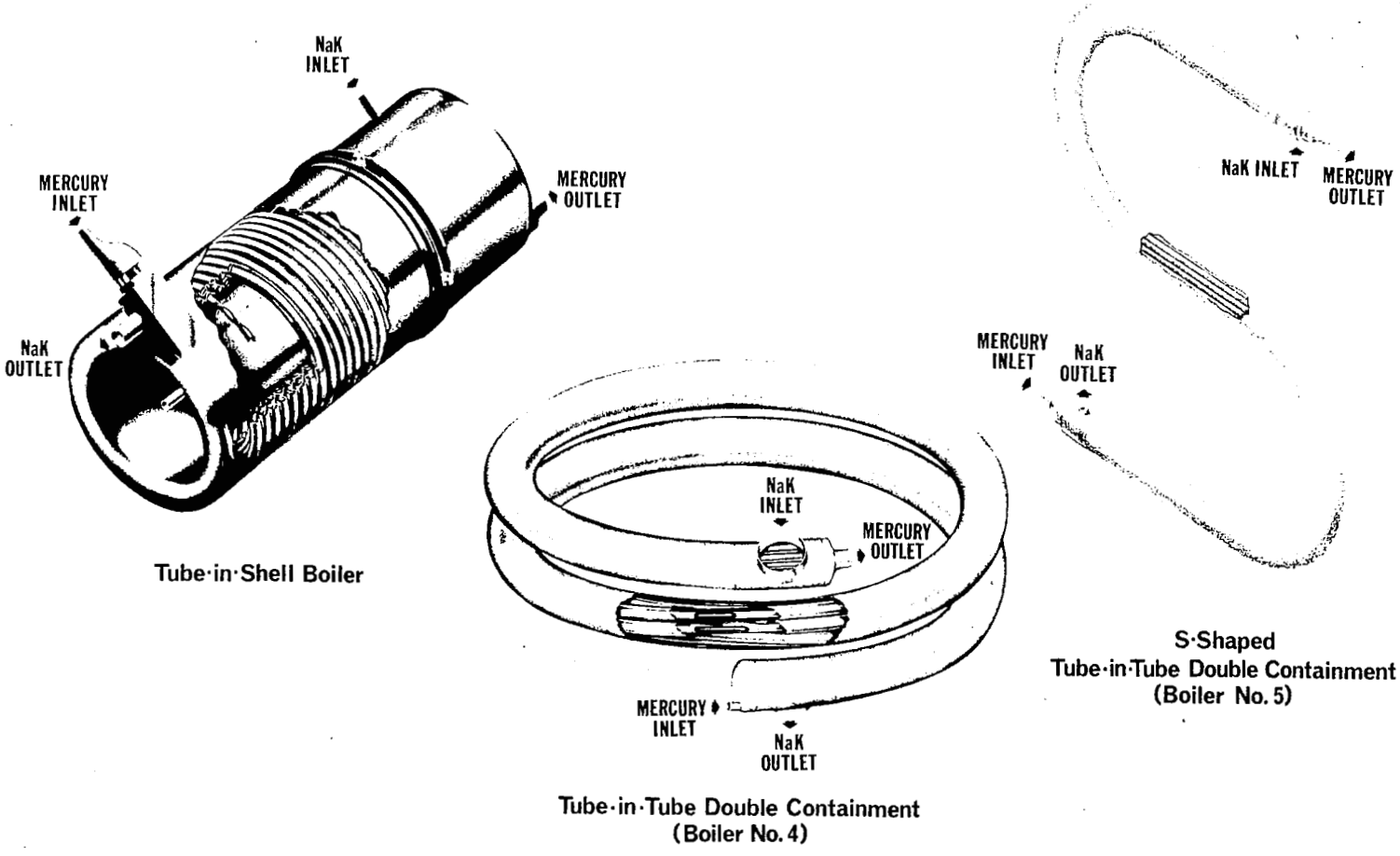

Figure 5-60 Evolution of SNAP-8 Boiler Concepts

A bimetal boiler was designed using a stainless steel tube coextruded with a tantalum inner liner for mercury containment. The purpose of the tantalum was to improve wetting by the mercury which improves "conditioning"* of the boiler. An experimental 1/7th-scale, single-tube bimetal boiler was designed and tested to investigate the bimetal tube and bimetal tube joint structural reliability, and the single-fluted helix configuration for heat and momentum transfer performance characteristics. A 1200-hour test showed that the design had excellent and immediate performance throughout its operation. This meant that clean mercury flow-passage surfaces were provided and maintained in the leak-tight mercury loop. A full-scale boiler design was completed, and one was fabricated. However, this boiler was not used because the double-containment design was preferred over the coextruded, bi-metal design.

The third design change was from single-wall mercury containment to double-wall containment (Figure 5-61). This concept meets the requirements of a man-rated system which specifies double isolation between the radioactive primary loop NaK and the mercury loop. Each tantalum tube is placed inside a Type 321 stainless steel tube, with the volume between the two tubes filled with static (nonflowing) NaK. Seven of these double tubes are placed within an outer tube which contains the flowing NaK. This design is termed the bare-refractory, double-containment (BRDC) boiler.

Tests were made using an experimental tantalum/stainless steel, double-containment, single-tube boiler indicated that the two most important requirements for proper conditioning of the boiler were cleanliness of the boiler tubes, and the assurance of a vacuum-tight system to preclude surface oxidation.

During the design period of the bimetallic boilers, NASA-LeRC designed and fabricated an all tantalum tube-and-header configuration for the mercury with a double-containment feature utilizing static NaK as the heat transfer fluid between the flowing NaK in the primary loop and the mercury. The bimetal tube boiler was designed as a 30-ft long assembly; however, the NASA-LeRC bare-refractory, double-containment boiler was fabricated as a 37-ft long assembly to coincide with the mercury and NaK interfaces of the 35-kWe ground test system.

---

*The term "conditioned," when used in reference to SNAP-8 mercury boilers, really describes how well heat is transferred from the inner surface of the mercury containment tube to the mercury. When the liquid mercury "wets" the tube surface, heat transfer is rapid and efficient. A boiler operating at the optimum level of heat transfer is termed "conditioned." A number of things can inhibit the ability of the mercury to "wet" the mercury containment material - various contaminants, the rate of mercury flow, and the method by which the flow is directed through the containment tube. Tantalum wets as a function of time-temperature and surface cleanliness. If the surface is clean, tantalum will wet immediately. When wetting is poor, heat transfer is less than optimum, and a boiler is said to be "deconditioned." Heat transfer to the mercury results in a decrease in NaK temperature. Hence, the slope of a NaK temperature profile corrected for heat loss is directly proportional to the local heat flux. A decrease in the slope of the temperature profile in the boiling section is a typical indication of boiler performance degradation or deconditioning.

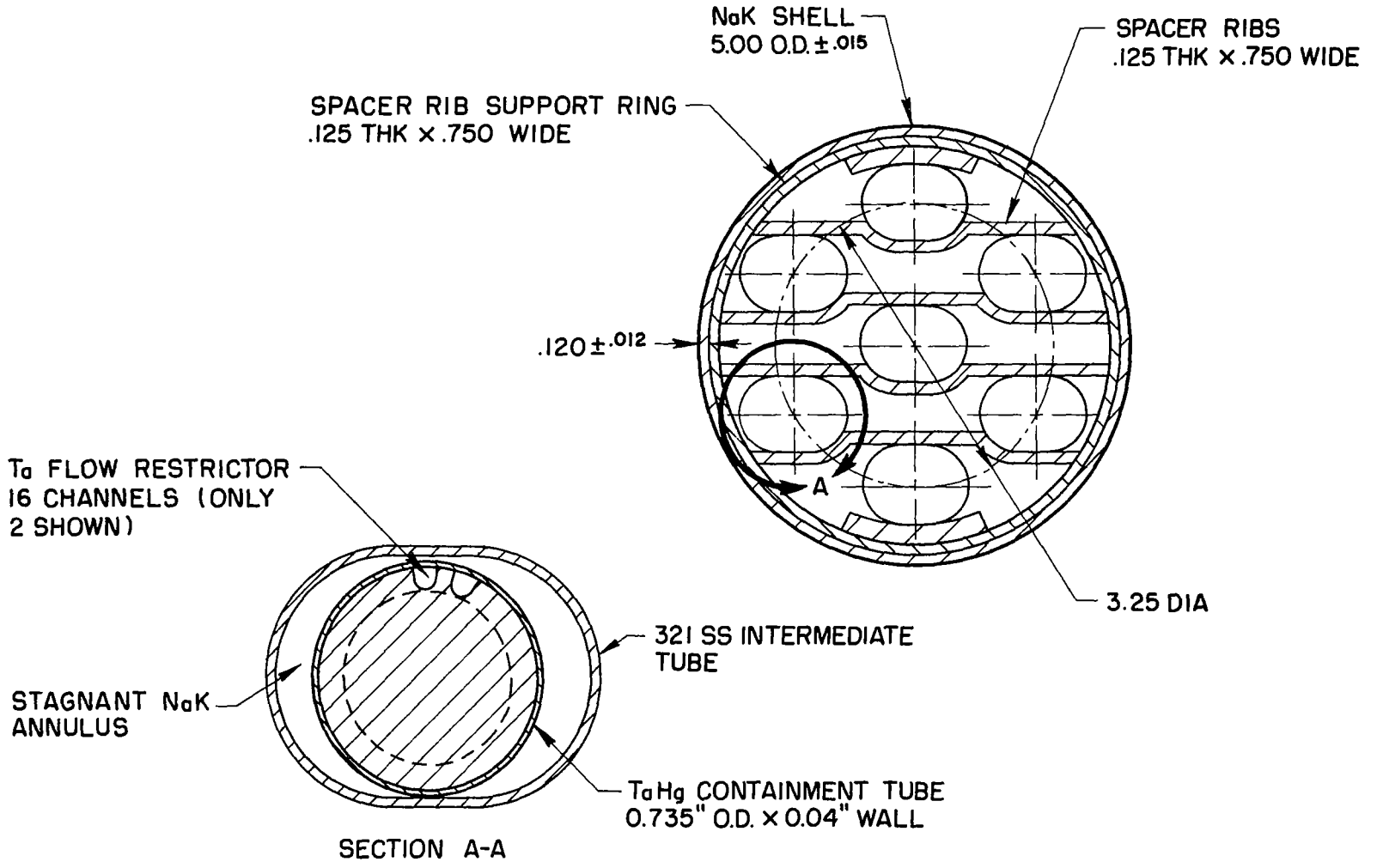

Figure 5-61 BRDC Boiler Cross Section Showing Double Containment Concept

The first three BRDC boilers were designed and fabricated by NASA-LeRC. BRDC Boiler No. 1 was tested in the LeRC W-1 and General Electric test facilities. BRDC Boiler No. 2 was tested exclusively in the Aerojet 35-kWe facility, and BRDC Boiler No. 3 was tested at the LeRC W-1 test loop.

Boiler No. 4 was designed at Aerojet, fabricated at NASA-LeRC, and tested in the Aerojet 35-kWe system facility for 1620 hours and 28 cycles from March through June, 1970. Some deconditioning occurred during the initial runs due to system contaminants. However, as testing progressed, the boiler became conditioned and its performance met all design criteria. No instability was observed over the extreme range of off-design testing, and no failures or incipient failures occurred. One area of concern was a high circumferential thermal gradient ($\sim 500^{\circ}F$) in the shell between the mercury inlet and the NaK outlet collector ring. The measured thermal map was similar to the one for BRDC No. 2. It was deduced at the time of BRDC No. 4 design that the thermal gradient in BRDC No. 2 was due to forced convection of the flowing NaK past the baffles. BRDC No. 4 employed a very low-leakage baffle as well as evacuated annular tubes surrounding the mercury containment tantalum tubes in this area to reduce heat transfer from the NaK to the colder mercury. Further analysis indicated that natural convection was the predominant mechanism for nonsymetrical circumferential thermal gradients, resulting in stratification of the NaK (the colder, more dense fluid gravitating to the bottom).

With the changes in system configuration and performance criteria that accompanied the development of the 90-kWe system, BRDC Boiler No. 4 became obsolete. The design of the new BRDC Boiler No. 5, which will meet the new system requirements, has been completed. The number of tubes was increased from seven to twelve and was designed in an "S" configuration rather than being helically coiled, as the previous boilers had been. The design is shown in Figure 5-60.

The remaining portion of this boiler report will concentrate on the mechanical design, thermal design, interfaces, and predicted performance on BRDC Boiler No. 5. Boiler No. 5 will be compared to Boilers No. 1 through No. 4 for purposes of referencing design changes and presenting calculated performance. The philosophies and criteria used for the design of boilers are covered in detail in Reference 52.

5.5.2 Design Description

Common to all bare-refractory, double-containment boilers is a header arrangement for both the tantalum and stainless steel tubing with the tantalum headers outboard of the Type 316 stainless steel headers. All of the BRDC boilers utilize transition joints at both the mercury inlet and outlet. These transition joints provide the means of connecting the tantalum tube/header system to the stainless steel outer NaK containment tube. The tubing which forms the second wall between the mercury and the primary NaK is of Type 321 stainless steel to form the barrier between the primary NaK and the static NaK systems. In all the BRDC boilers, the primary-loop NaK enters and exits perpendicular to the mercury flow axis or boiler tube axis and is unbaffled throughout the boiler length. Boilers No. 4 and No. 5 were designed with NaK helical turbulator coils rather than baffles, in the high heat flux (liquid and low quality mercury) section to preclude NaK stratification.

The mercury-side geometry in the boilers consists of an inlet flow restrictor, a 16-groove multipassage plug insert, and swirl wire extending from the plug insert end to the mercury outlet. Pictorial representations of BRDC Boiler No. 1, 3, 4 and 5 shown in Figures 5-62, 5-63, and 5-64 (since No. 1, No. 2, and No. 3 are similar, only No. 2 is shown). A comparison of design features of the various boilers is given in Table 5-XI.

All mercury-side components such as headers, concentric reducers, plug inserts, tubing, and mercury inlet orifices, are of pure tantalum. The exceptions are the swirl wire which is made of 90% Ta/10% W and the TA/316SS bimetal joints. The components and subassemblies, that comprise the BRDC Boiler No. 1 through No. 5, have consistently been fabricated with the same type of materials.

Comparing the overall configuration of BRDC Boiler No. 2 and No. 4, all of Boiler No. 4 lies within the envelope generated by the coiled shell while Boiler No. 2 does not. This difference represents a move from the pre-prototypic to a prototypic design. BRDC Boiler No. 5 design is the prototype design planned for the 90-kWe SNAP-8 system.

5.5.3 Design Requirements and Criteria

As system requirements for the boiler were amended and the results of boiler technology programs became available, new operating requirements, design criteria, and interfaces were established which had to be met by the boiler design. Table 5-XII lists the nominal design parameters and requirements for BRDC Boiler No. 1 through No. 5 as dictated by revisions in the state-point operation of the power conversion system. The values of Boiler No. 1 through No. 4 are similar in almost all instances with the exception of mercury vapor pressure drop, inlet pressure, and pinch-point temperature difference. The decrease in vapor pressure drop from 85 to 65 psia was primarily due to a decrease in plug-insert length from 4.0 to 3.5 ft. The attendant decrease in inlet pressure and pinch-point temperature difference from 395 to 375 psia and 57 to 43°F are directly attributable to the decrease in plug-insert length. The relationship of vapor pressure drop and pinch-point temperature differences is discussed in the section on thermal design.

Differences in the operating conditions between Boiler No. 4 and No. 5 resulted from a reduced reactor operating temperature and an improved cycle efficiency. The reduction of the mercury-side pressure drop by a factor of two while maintaining boiler stability and a tube ID of 0.652 inch necessitated a change in the number of tubes from seven to twelve. Other operating criteria for BRDC Boiler No. 4 and No. 5 which itemize emergency, maximum, and minimum conditions are listed in Tables 5-XIII and 5-XIV.

Mechanical design criteria used for BRDC Boiler No. 4 and No. 5 were as follows:

- The boiler envelope and interfaces shall be as described by the power conversion system requirements.

Figure 5-62 BRDC Boiler No. 2 with Mercury Inlet Section Removed

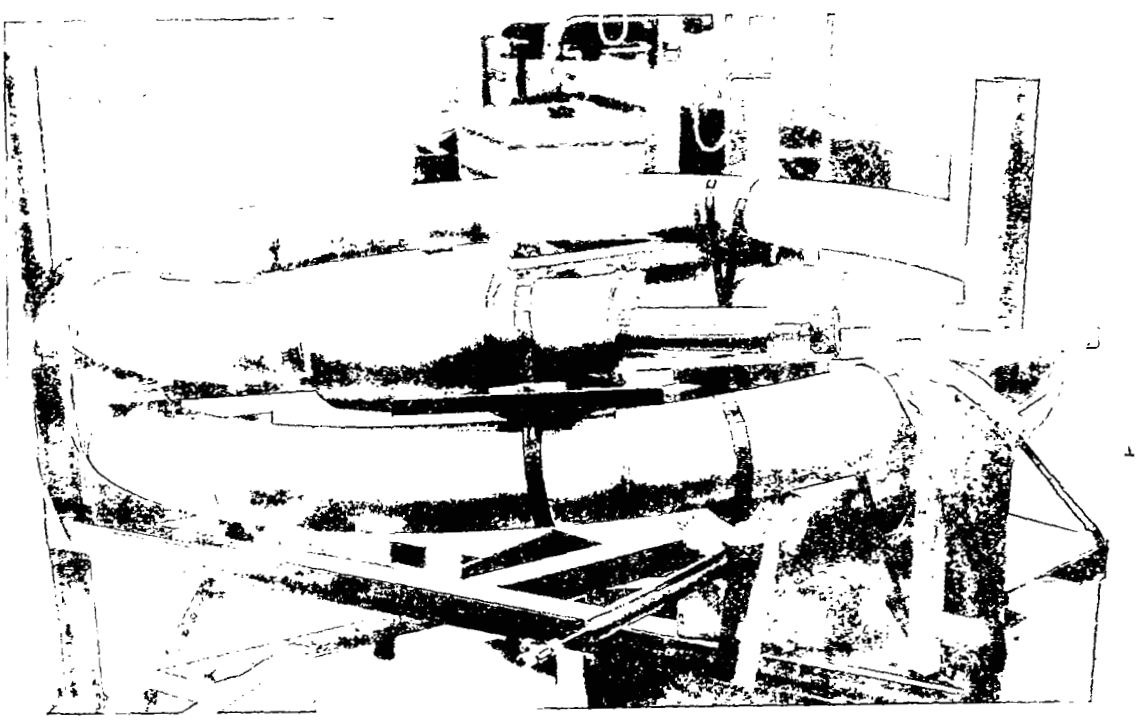

Figure 5-63 BRDC Boiler No. 4 Prior to Installation in 35-kWe System

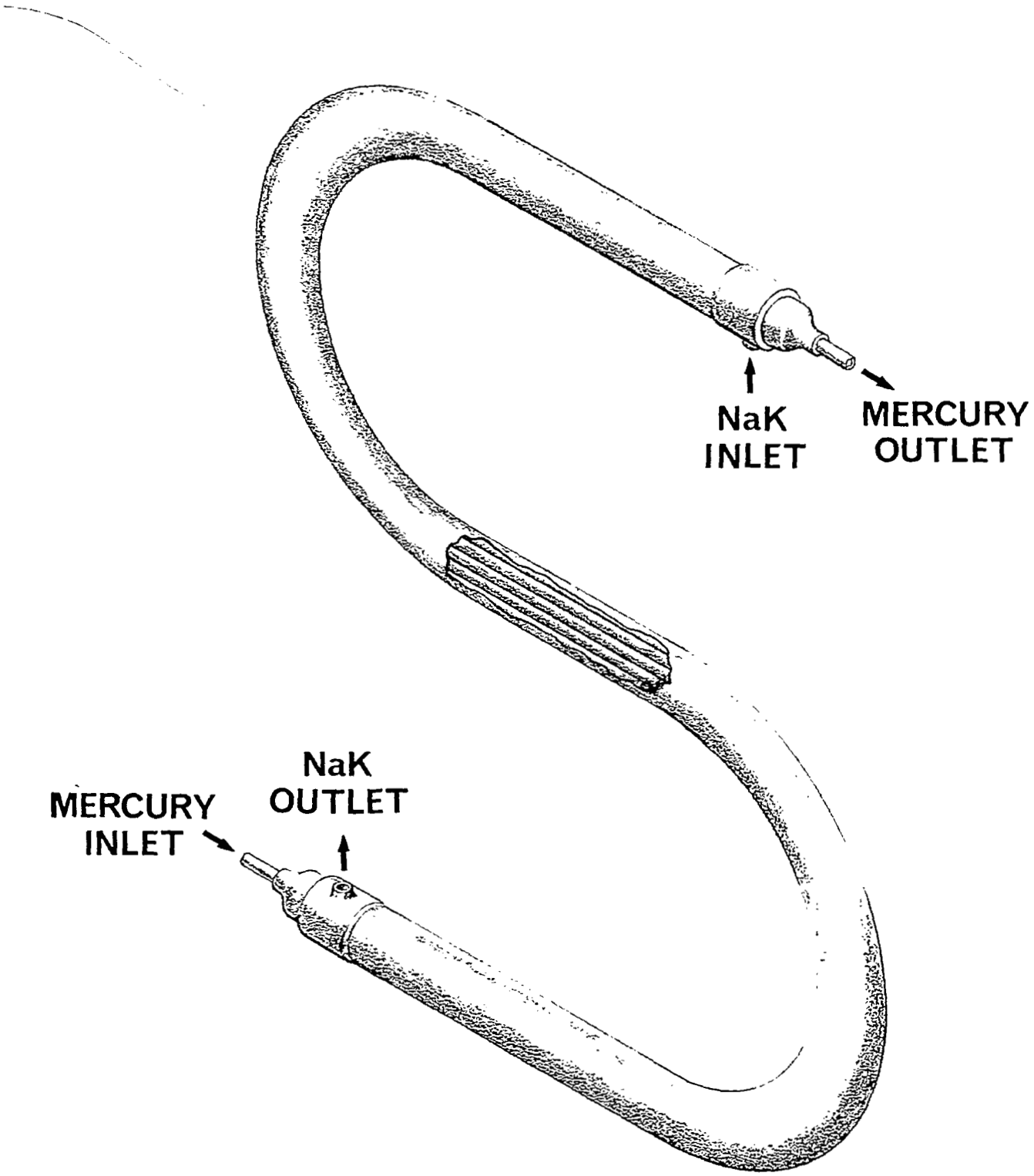

Figure 5-64 BRDC Boiler No. 5, Cutaway View

TABLE 5-XI COMPARISON OF BARE-REFRACTORY DOUBLE-CONTAINMENT BOILER GEOMETRY

Design Items	BRDC Boiler No. 1, 2, 3	4	5
Number of tubes	7	7	12
Boiler length, ft.	37.0	25.0	21.0
MPP length, ft.	4.0	3.5	2.7
NaK tube OD, in.	5.0	5.0	7.62
Tube spacing, in.	1.56 (1)	1.62 (1)	annular
Swirl wire diameter, in.	0.062	0.062	0.062
Swirl wire pitch, in.	2.0	2.0	2.0
NaK turbulator coil diameter, in.	none	0.125	0.125
NaK turbulator coil pitch, in.	none	6.0	6.0
Tantalum tube OD, in.	0.750	0.750	0.750
Tantalum tube ID, in.	0.652	0.652	0.652
Oval tube minor OD, in.	0.88	0.88	0.88
Oval tube major OD, in.	1.098 (2)	1.265 (3)	1.465 (4)
Oval tube wall thickness, in.	0.040	0.049	0.049
Transition joint type	brazed and coextruded	coextruded sleeve	coextruded sleeve
Bellows material	Type 304 SS	none used	none used
Static NaK O_2 getter material	Zr foil	Zr foil	Zr foil
Boiler dry weight, lb.	845	572	833
Boiler wet weight, lb.	1110	742	1030
Boiler shape	Helix straight ends	Helix-fully coiled	S
Boiler coil diameter, in.	48	54.25	25- radius
Boiler coil pitch, in.	10	6.0	none
Primary NaK volume, $in.^3$	5486	3697	4649
Static NaK volume, $in.^3$	1155	923	1510
Hg volume, $in.^3$	1235	835	1203
Hg inlet orifice diameter, in.	0.075	0.070	0.050
No. of tube bundle supports	16	10	7

(1) Dimension shown is on an equilateral triangular array

(2) Made from 1.0 in. OD x 0.040 in. wall Type 321 SS

(3) Made from 1.125 in. OD x 0.049 in. wall Type 321 SS

(4) Made from 1.250 in. OD x 0.049 in. wall Type 321 SS

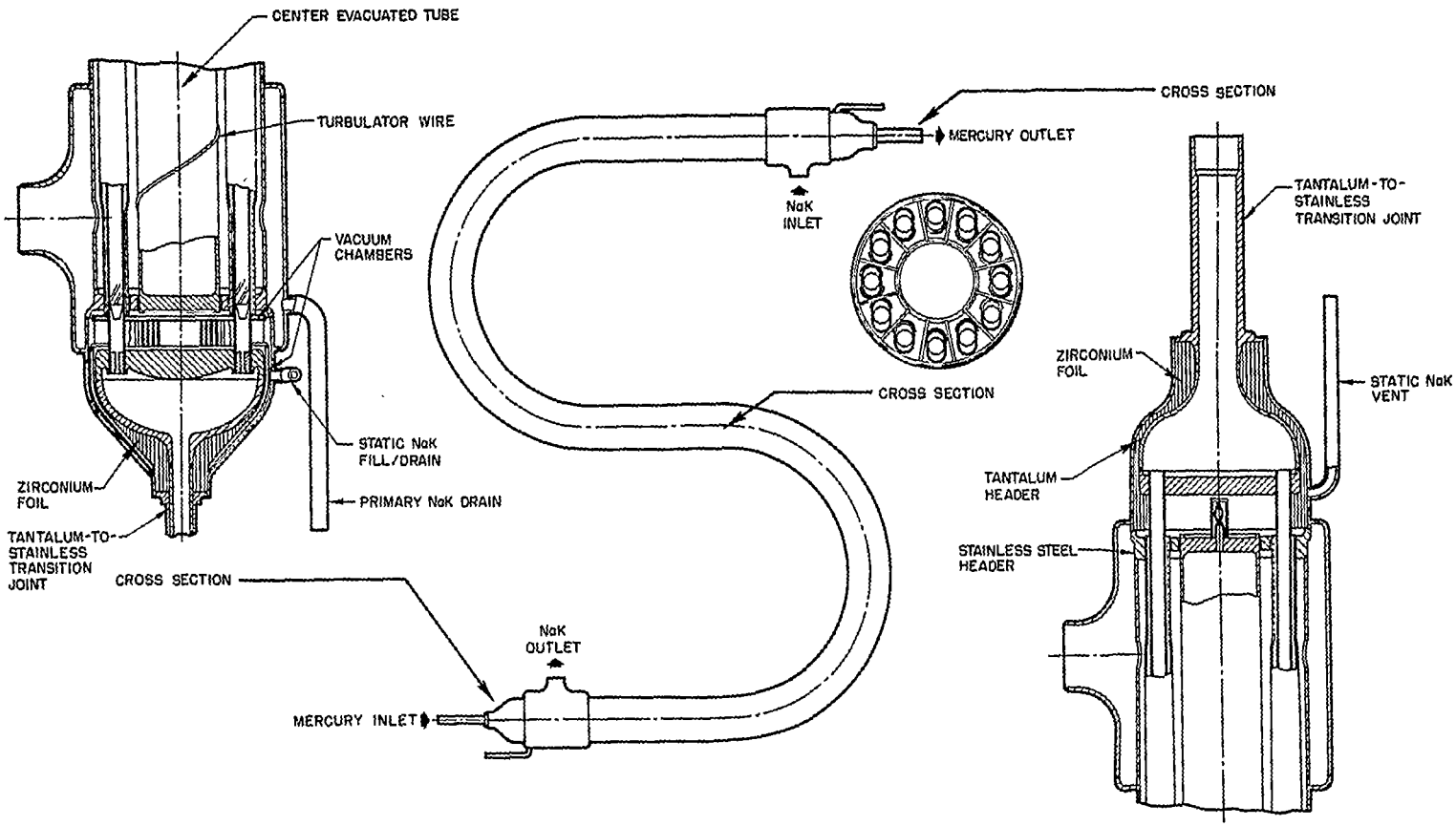

Figure 5-65 BRDC Boiler No. 5

TABLE 5-XII NOMINAL DESIGN OPERATING PARAMETERS - BRDC BOILERS

Parameter	Boiler No. 1, 2, 3	Boiler No. 4	Boiler No. 5
NaK flow, lb/hr	48500	48500	57148
NaK inlet temperature, °F minimum	1280	1280	1185
NaK temperature drop, °F	170	170	170
Maximum NaK ΔP, psid	3	3	3
Mercury (vapor) flow, lb/hr	11800	12300	13775
Mercury (vapor) exit pressure, psia	265	255	148
Mercury (vapor) exit temperature, °F	1250	1250	1165
Mercury (liquid) inlet temperature, °F	500	500	350
Mercury (vapor) ΔP, psid	85	65	32
Mercury (liquid) orifice ΔP, psid	55	55	143
Mercury inlet pressure, psia	395	375	323
Maximum total mercury ΔP, psid	141	141	175
Pinch-point ΔT, °F	57	43	38
Boiler terminal ΔT, °F	30	30	20
Mercury vapor superheat, °F	190	190	197
Thermal power, kW	517	517	600
Stability ΔP/P, %	± 2.0	± 2.0	± 2.0

TABLE 5-XIII BRDC BOILER NO. 4 OPERATING CRITERIA

Mercury Inlet	Mercury Outlet	NaK Inlet	NaK Outlet	Static NaK
Low Schedule Inlet press.= zero to 400 psia Inlet temp. = 70 to 500°F Flow = 0-5400 lb/hr in 60 sec Flow = 11800 lb/hr @ steady state	Outlet press.= zero to 259 psia Outlet temp.= 70 to 1250°F	Inlet press.= zero to 30 psia Inlet temp. = 70 to 1280°F Flow = 48500 lb/hr	Outlet press.= zero to 27 psia Outlet temp. = 70 to 1110°F	Press. = 30 psia Temp. = 70 to 1280°F
High Schedule Inlet press.= zero to 400 psia Inlet temp. = 70 to 500°F Flow = 11800 lb/hr @ steady state	Outlet press. = zero to 259 psia Outlet temp. = 70 to 1300°F	Inlet press. = zero to 30 psia Inlet temp.= 70 to 1330°F Flow = 48500 lb/hr	Outlet press. = zero to 27 psia Outlet temp.= 70 to 1160°F	Press. = 30 psia Temp. = 70 to 1300°F
Emergency Conditions Press.=600 psia Temp.= 600°F	Press.= 330 psia Temp.= 1375°F	Press.= 75 psia Temp. = 1450°F	Press.= 75 psia Temp. = 1450°F	Press. = 75 psia Temp. = 1450°F

TABLE 5-XIV BRDC BOILER NO. 5 OPERATING CRITERIA

Mercury Inlet	Mercury Outlet	NaK Inlet	NaK Outlet	Static NaK
Low Schedule Inlet Press.= Zero to 323 psia Inlet Temp. = 70 to 350°F Flow = 0-7740 lb/hr in 75 sec. 13,775 lb/hr @ steady state	Outlet Press. = zero to 148 psia Outlet Temp. = 70 to 1185 to 1165°F	Inlet Press. = zero to 60 psia Inlet Temp. = 70 to 1185°F Flow = 57148 lb/hr.	Outlet Press. = zero to 57 psia Outlet Temp. = 70 to 1015°F	Press. = 30 psia Temp. = 70 to 1185°F
High Schedule Inlet Press. = zero to 333 psia Inlet Temp. = 70 to 350°F Flow = 7740 lb/hr in 75 sec. 13600 lb/hr steady state	Outlet Press.= zero to 147 psia Outlet Temp. = 70 to 1211 to to 1190°F	Inlet Press.= zero to 60 psia Inlet Temp. = 70 to 1211°F Flow = 57148 lb/hr.	Outlet Press. = zero to 57 psia Outlet Temp. = 70 to 1044°F	Press. = 30 psia Temp. 70 to 1211°F
Maximum Conditions Press. = 500 psia Temp. = 600°F	Press. = 222 psia Temp. = 1375°F	Press. = 90 psia Temp. = 1485°F	Press. = 90 psia Temp. = 1485°F	Press. = 90 psia Temp. = 1485°F

- No bellows shall be used to accommodate the differential thermal expansion between the tantalum and stainless steel.
- The mercury lines at the inlet and outlet shall incorporate a coextruded tantalum-to-stainless steel transition joint.
- The boiler shall utilize multipassage plug inserts and swirl wire turbulators in the tantalum tube.
- Double containment, utilizing stagnant (nonflowing) NaK as the heat transfer fluid between the tantalum tube OD and the Type 321 stainless steel oval tube ID, shall be employed.
- The tantalum tube shall be placed in the Type 321 stainless steel tube such that the clearance will accommodate the differential thermal expansion.
- NaK flow in and out of the boiler shall be manifolded through tee's or collector rings to uniformly distribute the fluid and to lessen the system piping loads at the shell.
- The boiler design shall be capable of continuous steady-state operation for 5 years and a maximum of 100 cycles. A cycle is defined as cold mercury injection with the boiler at the operating temperature to shutdown with the boiler cooling to 100°F.
- The boiler design for stress shall include 1% creep in 5 years and low cycle fatigue.

5.5.4 Mechanical Design

Boiler No. 5 was designed for an effective boiler length of 21.0 ft from the flowing NaK inlet port to the NaK outlet port, as shown in Figure 5-65. The two radii of the S-shaped boiler are identical at 25.0 inches. The NaK containment tube, or shell, is 7.625 inches outside diameter with a 0.120-inch wall of Type 316 stainless steel. The NaK shell was designed to be first coiled, then split in two halves and welded along the centerline perpendicular to the plane of the curvature. The NaK inlet and outlet tees, or manifolds, are also designed in two halves, welded along their centerline parallel to the plane of the 3-inch inlet and outlet ports.

The 12-tube bundle is spaced in an annular array, co-axial with a central tube which has a 3.5-inch outside diameter and a 0.090-inch wall. This central tube, which is evacuated and sealed, decreases the flowing NaK inventory, and helps to support the tube bundle. Seven tube bundle supports are placed throughout the boiler tube length - two in each 180-degree bend section and one in each of the three straight sections.

NaK-side turbulator wires are wound on the 3.5-inch central tube and around the tube bundle. The wire diameter is 0.125 inch, the helix pitch is 6 inches, and the material is Type 316 stainless steel. The wires are wound with opposite helixes to more effectively turbulate the NaK flow. The turbulator coils extend from the NaK outlet tee for a distance of 10.0 ft along the boiler.

The overall design described above and the detailed descriptions to follow have incorporated the best design features of Boilers No. 1 through No. 4 plus design considerations to minimize circumferential and axial thermal gradients at the mercury inlet end of the boiler.

5.5.4.1 Mercury Inlet Section

The inlet header is shown in Figure 5-65 as a centrally located, axial entry configuration. A coextruded, tantalum-to-Type 316 stainless steel transition joint is shown identical in size and length to the joint successfully used in Boiler No. 4 for 1600 hours and 28 starts. The tube is 1.25 inches OD by 0.750-inch ID which includes a 0.150-inch wall of Type 316 stainless steel and a 0.100-inch wall of tantalum. The tube is electron-beam welded to the stainless steel end cap. The total length of the bonded area of the transition joint is 8.0 inches. The tantalum concentric reducer is also electron-beam welded to the transition joint.

The evacuated annular insulator between the tantalum dome and the shell reducer is designed for thermal management. The phenomenon of induced convective patterns, wherein the colder and heavier NaK surrounding the tantalum tubes sinks, has been a persistent problem in all boilers tested. The design minimizes this effect by the use of the axial honeycomb structure in the area between the stainless steel header and the tantalum header.

The oval static NaK tubes surrounding the 12 tantalum tubes are spaced on a 5.625-inch diameter circle (Figure 5-65); the spacing provides for more evenly distributed NaK flow. The 0.050-inch diameter orifices at the entrance of the tantalum tubes were calculated to produce a pressure drop of 143 psid at full flow conditions. The pressure drop versus flow for the orifice, added to the pressure drop versus flow for the remainder of the boiler was calculated to ensure a positive slope throughout all phases of the startup and steady-state operation of the boiler. This was a requirement of the SNAP-8 system to preclude problems in control and reactor operation.

The tantalum plugs placed in the tantalum tubes downstream of the orifices are 2.7-ft long. Sixteen equally spaced helical grooves are cut along the length of each plug at a 6-inch pitch. Circumferential annuli are cut at 10-inch intervals to ensure a redistribution of mercury flow, should a helical groove become blocked or not perform properly. The tantalum tube is swaged onto the tantalum plug. The swaged plug assemblies and the orifices were planned to be tested with water to determine the actual pressure drop through each.

A coiled 0.062-inch diameter wire (90% tantalum - 10% tungsten) with a 2-inch pitch was placed downstream of the plug for the remaining length of the tantalum tubes to maintain a centrifugal field for mercury droplets in the vapor so that the droplets would contact the hot tantalum tube walls and vaporize.

Zirconium foil is shown in the tantalum dome area and the space between the tantalum header and the stainless steel header (Figure 5-65). Zirconium was found to be an excellent hot getter for dissolved gases in the static NaK as evidenced by the post-test analysis of Boiler No. 1 and No. 2.

The boiler shell is shown expanded radially in the area between the stainless steel header and the tantalum header to allow for the annular vacuum chamber within the shell. The purpose of this vacuum insulator is discussed later in this report.

5.5.4.2 NaK Inlet and Outlet Manifolds

The NaK inlet and outlet manifolds are designed as collector rings which surround twelve 1.25-inch diameter holes spaced between mercury tubes and drilled into the 7.625-inch OD flowing NaK shell. The headers are forged in two parts and welded in the plane of the 3-inch port.

The predominant reasons for the manifold design are (1) better distribution of heat in the critical zones where shell failures had previously occurred on earlier boiler designs, and (2) the uniform distribution of the NaK entering and leaving the boiler. The acceptability of the design was borne out by plastic model tests with water as well as by the results of Boiler No. 4 tests. Mixing of the NaK leaving the boiler results in better measurement of the NaK mixed-mean temperature which is essential if good thermal performance data are to be obtained.

5.5.4.3 Tantalum Tube Bundle and Static NaK Tubes

The 12 tantalum tubes are of equal 21-ft lengths. They are not coiled along their lengths as in Boilers No. 1, 2 and 3 which were coiled to obtain equal length tubes in a coiled boiler. Boiler No. 4 was not coiled however (resulting in unequal lengths), and its performance met all design criteria. The tantalum tubes are 0.75-inch OD by 0.049-inch wall (the same as Boiler No. 4).

Each tantalum tube is placed in a Type 321 stainless steel oval tube which contains static NaK. The tantalum tube must then be held against the side of the oval tube so that it is at the greatest radius in both halves of the S-shape. This means that the tantalum tube must cross over in the straight mid-section of the S (see Figure 5-65). Since the coefficient of thermal expansion for the stainless steel oval tube is more than twice that of the tantalum tube, the oval tube will grow outward (or to a larger diameter) relative to the tantalum tube. Consequently, no loading will be experienced between the two metals as the boiler is heated or cooled. Seven lattice-type spacers hold the tubes in the proper positions relative to the evacuated center tube and the NaK shell.

A 0.125-inch diameter wire with a pitch of 6 inches is wound on the center tube for 10 ft, starting at the mercury inlet, prior to installation of the 12 tantalum tubes and stainless steel static NaK tubes. Another wire of the same diameter, pitch, and length is wound on the outside of the 12 tubes counter-rotational to the wire on the center tube. The purpose of these wires is to promote mixing of the flowing NaK in the section of the boiler where the greatest amount of heat transfer occurs. The adequacy of this configuration was vividly demonstrated in a full-scale plastic model of the boiler through which dye was injected in flowing water. The test also confirmed the calculations of the flowing NaK-side pressure drop.

5.5.4.4 Evacuated Center Tube

The center tube runs the full length of the boiler and is attached to the stainless steel headers. It is formed to shape, evacuated to 10^{-4} torr, and seal-welded. This tube was placed in the center of the tube bundle coaxial with the shell. The main purpose of the tube is to decrease the NaK-side free flow area which results in a NaK velocity of 3.4 fps. With this velocity, the Reynolds number is 110,000 and assures turbulent flow and good heat transfer.

5.5.4.5 Mercury Outlet Section

The mercury vapor outlet, like the liquid mercury inlet, is a concentrically located, axial discharge configuration. A coextruded tantalum-to-Type 316 stainless steel transition joint, identical in diameter, length and wall thicknesses to that successfully used in Boiler No. 4 for 1620 hours and 28 starts, is shown in Figure 5-65. The outlet tube is 2.26-inch OD by 1.76-inch ID with a 0.150-inch wall of Type 316 stainless steel. The total length of the bonded area of the joint is 8.0 inches, the same as the mercury inlet joint. Zirconium foil is used in the static NaK area surrounding the bimetal joint-to-dome weld for hot gettering interstitials in the NaK.

5.5.4.6 Stress Analysis

Table 5-XIV itemizes the operating criteria used for the stress analysis of Boiler No. 5. The criteria define the transient, steady-state, and maximum conditions for the flowing NaK side, mercury side, and the static NaK side. Table 5-IX defines the expected boiler-to-system interface loads. The stress computation methods, detailed hand calculations, results, and conclusions appear in Reference 53. Particular emphasis was placed on the mercury inlet section where the most severe pressure and thermal transients occur.

The following areas were stress analyzed in detail using the criteria for pressure and temperatures noted above with design safety factors of 1.25 against creep and yield strength, 1.50 for ultimate strength, and 1.50 for fatigue strength.

- NaK shell
- Static NaK tube

TABLE 5-XV NAK AND MERCURY INLET AND OUTLET INTERFACE LOADS - BRDC BOILER NO. 5

Interface Description	Force (lb)			Moment (in.-lb)			Load Type
	Fx	Fy	Fz	Mx	My	Mz	
	-15.1	-10.1	39.4	433	414	283	Thermal, T = 1190°F
Boiler Mercury Outlet	-12	-9	28.5	333	267	235.5	Weight
	-27.1	-19.1	67.9	766	681	518.5	Total
	-2.1	0	0	0	19.1	-4.25	Thermal, T = 417°F
Boiler Mercury Inlet	2	-8	0	-49	-20	-250	Weight
	-.1	-8	0	-49	-.9	-254.25	Total
	+17.7	-67	+26.6	-434	-276	-504	Thermal, 1185°F, ΔT = 1110°F
Boiler No. 1 NaK Inlet	-1.4	+85	+4	-659	-259	+347	Weight
3-in. OD x 0.085-in. wall, 316 SS	16.3	18	30.6	-1093	-535	-157	Total
	-1	2	11	388	-234	102	Thermal, 1185°F, ΔT = 1110°F
Boiler No. 1 NaK Outlet	-95	-29	-10	494	-2010	1545	Weight
3-in. OD x 0.083 in. wall, 316 SS	-96	-27	1	882	-2244	1647	Total
	-1	2	11	-513	440	-183	Thermal, 1185°F, ΔT= 1110°F
Boiler No. 2 Inlet	-95	-123	-10	402	90	-1024	Weight
3-in. OD x 0.083-in. wall, 316SS	-96	-121	1	-111	530	-1207	Total
	49	11	3	331	-830	-94	Thermal, 1015°F, ΔT = 940°F
Boiler No. 2 Outlet	39	2	-31	132	-248	-134	Weight
3-in. OD x 0.83-in. wall, 316 SS	88	13	-28	463	-1078	-228	Total

- Center evacuated tube
- Stainless steel mercury inlet header
- Stainless steel mainfold sections
- Stainless steel vacuum insulators
- Mercury inlet section
- Mercury outlet section
- Overall boiler stresses with recommended system mountings

The mercury inlet and outlet sections were analyzed with the use of the thermal data discussed in the next sections in conjunction with a finite element computer program (References 52 and 53). These sections have axisymetrical geometry and pressure/temperature distribution directly suited to the application of this computer program. The shell, tubing, stainless steel headers, stainless steel manifolds and the vacuum insulators were calculated by hand. Low-cycle fatigue analyses employed the Manson equation and the finite element computer program, where applicable. Thermal ratcheting was also considered.

The bimetal coextruded transition joints were stress analyzed and the results compared to those values obtained from the Boiler No. 4 analyses since the joints in Boiler No. 5 have the same dimensions as those in Boiler No. 4.

Analysis of the boiler shell stress levels was made for the mounting scheme shown in Figure 5-66 using a piping flexibility computer code. Here the boiler cross-section was transformed into a pipe with an equivalent section modulus. It should be noted that the boiler is shown "cold sprung" so that the boiler shell stresses remain below the allowable during steady-state hot operation. The stresses in the boiler shell are also below the allowable limits at room temperature when the cold springing is performed. The results of the analysis showed that this was an acceptable method of mounting the boiler (Reference 53).

5.5.5 Thermal and Dynamic Design

5.5.5.1 Mercury-Side Heat Transfer, Dynamics and Performance Evaluation

Boiler No. 5 was designed, from the heat-transfer viewpoint, with the same approach used for Boiler No. 4. The heat and momentum transfer correlations for the mercury side of the boiler were for a two-phase, helical-flow regime with wetted tube walls. The correlations developed for the boiler heat transfer design were formulated into the BOiler DEsign and PErformance (BODEPE) analysis computer code (References 52 and 54). This computer code was used to evaluate 1/7-scale and full-scale boiler actual performance data with the predicted performance. The results of the 1/7-scale boiler evaluation were applicable to the Boiler No. 4 design, and provided the basis for

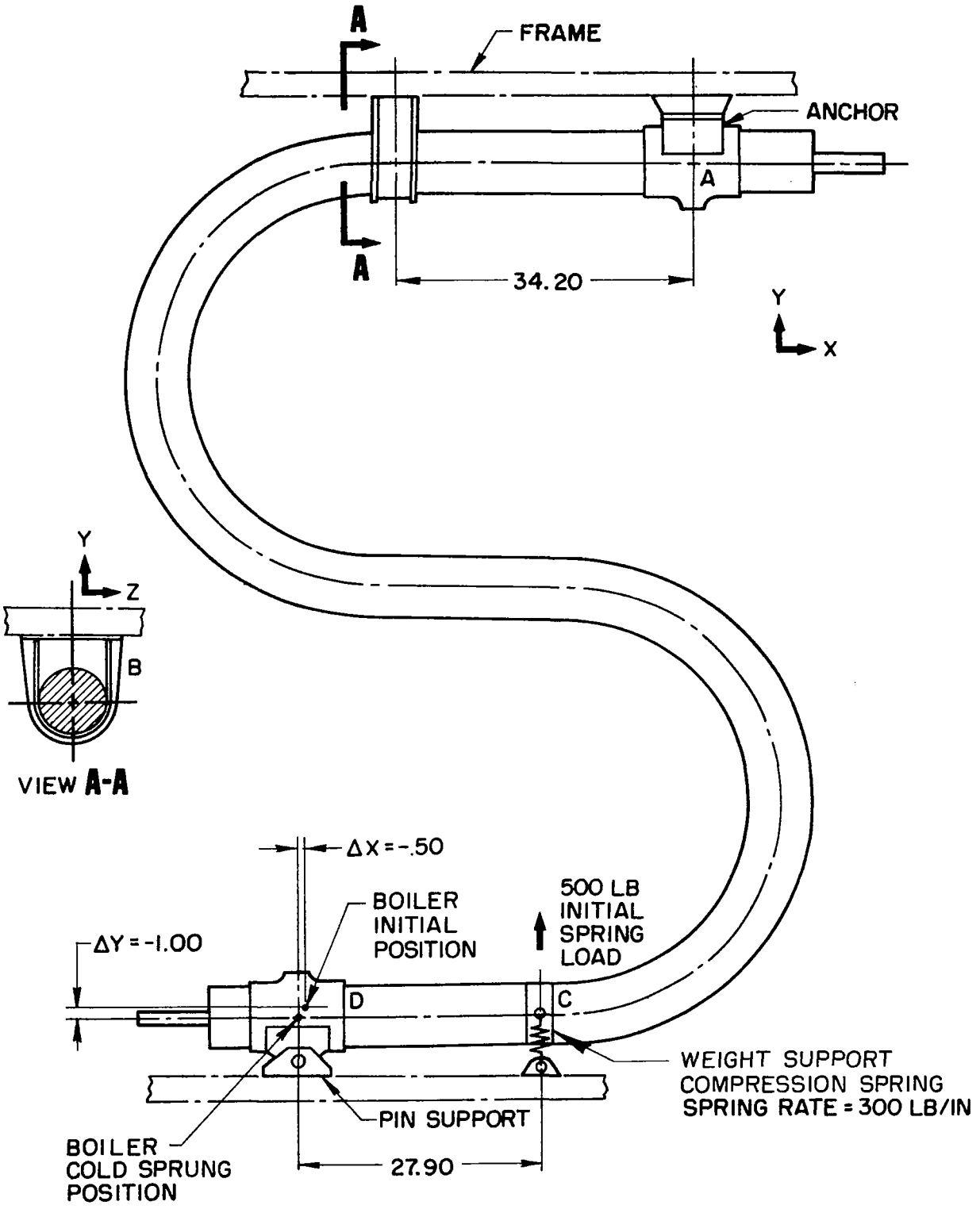

Figure 5-66 BRDC Boiler No. 5 Mounting Scheme

determining many of the performance-related aspects of the boiler design. The soundness of the mercury-side correlation and the 1/7-scale analysis were borne out by the excellent performance of Boiler No. 4 during tests in the 35-kWe system over a wide range of operating conditions.

Predicted performance of Boiler No. 5 at steady-state is shown in Figure 5-67. In Boiler No. 5, there is no excess superheat length which was normally added to the previous boiler designs as further margin to assure complete vaporization of the mercury. This was not done for two reasons: (1) the added length did not improve the performance in the tests of Boiler No. 4 which had excess length, and (2) the envelope restrictions of the power conversion system package precluded the addition of the extra length. Boiler pressure variations are not expected to exceed the ± 2% (the ratio of the vapor) outlet pressure deviation to the vapor outlet pressure) that was experienced with Boiler No. 4 (which was the most stable boiler tested in the SNAP-8 program). Table 5-XVI summarizes the thermal computation for Boiler No. 5 and corresponds to the performance predictions of Figure 5-67.

Comparative design data plots of plug insert pressure drop and plug exit vapor quality versus pinch-point temperature difference of BRDC Boiler No. 4 and No. 5 is shown in Figure 5-68. Reduction of the plug insert length and the NaK temperature band while maintaining a specified pinch-point temperature difference decreases the plug insert pressure drop and the plug insert vapor quality. This behavior is inherent to this plug configuration and test results have shown the optimum pinch-point range is from 30 to 70°F for a given plug insert length. For less than 30°F difference, the plug exit vapor quality is too low and boiler pressure variations become excessive. A difference greater than 70°F means that the plug insert pressure drop is too high, thus reducing cycle efficiency.

Test data from BRDC boilers with plug lengths of 4.0 ft, 3.5 ft, and 3 ft showed that the boiler pressure drop versus mercury flow increases with flow to a maximum value then decreases as the flow is increased to the rated value. It has been concluded that this behavior is characteristic of this mercury-side geometry (a multipassage plug insert and a bare tube with a swirl wire). Whether this effect is detrimental when the system is tested with a reactor is not known, although system analyses indicate that thermal shock of the reactor can occur as a result. However, it is desirable to have a boiler that would have, at all conditions, an increasing pressure drop with increasing flow. Figure 5-69 compares the mercury side pressure drop versus liquid mercury flow for Boilers No. 2, No. 4, and the 1/7-scale boiler.

The pressure drop through the short tube orifices upstream of the plug inserts rises as a square function of the increased flow. Therefore, by choosing an orifice of the proper size, a positive slope of total boiler pressure drop (the sum of the boiler tubes and the orifices pressure drops) is attained for any flow rate. The orifice size was calculated to be 0.050 inch in diameter with a square edge and 0.052-inch diameter orifice with a well rounded entry radius. A plot of orifice ΔP, and total pressure drop using an 0.052 inch square edge orifice is shown in Figure 5-70 for BRDC

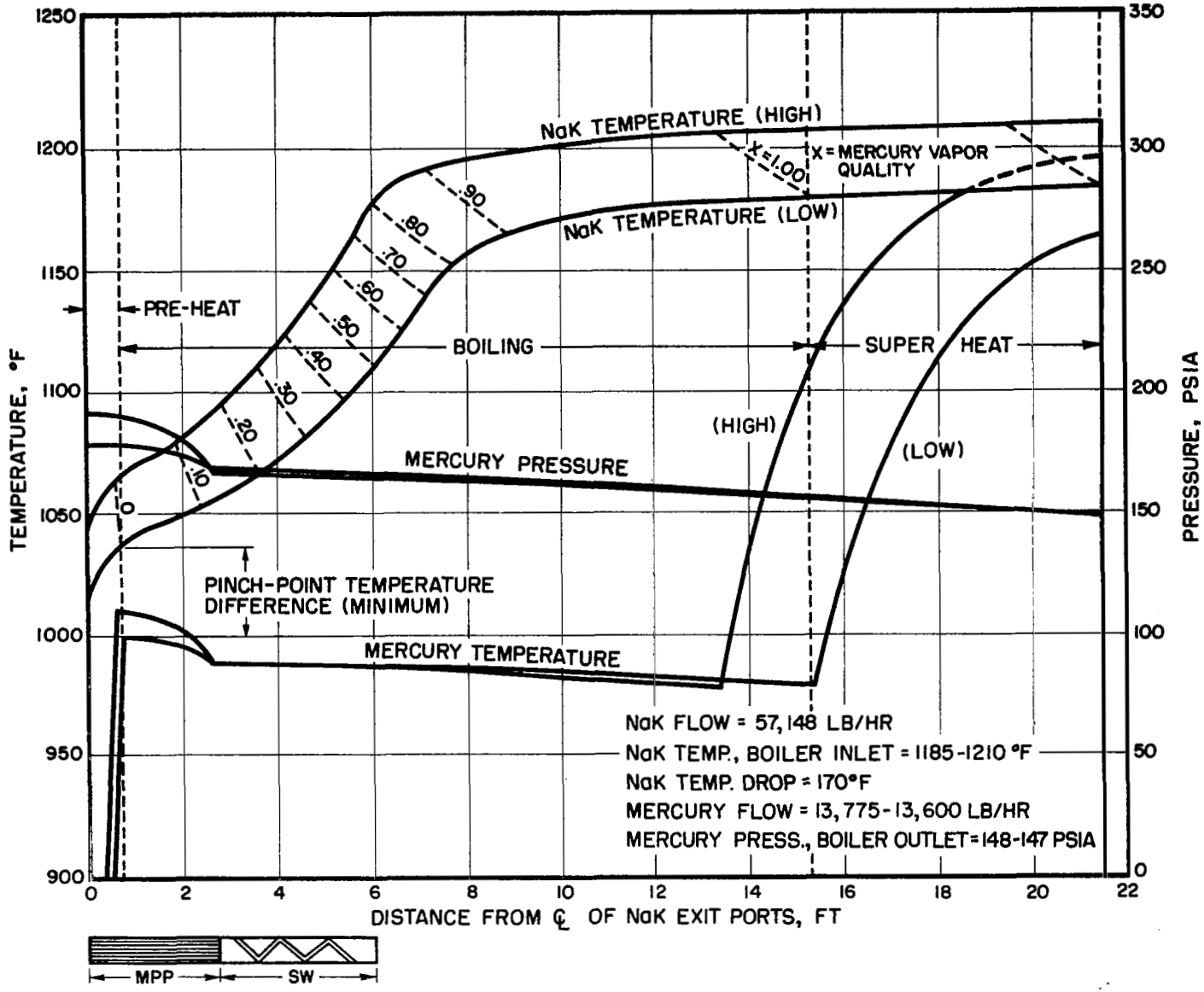

Figure 5-67 Predicted Performance of BRDC Boiler No. 5

TABLE 5-XVI BRDC BOILER NO. 5 - PREDICTED THERMAL DESIGN CHARACTERISTICS AND OPERATING PARAMETERS

Parameter	Dimension	NaK Inlet Temperature Schedule	
		Low	High
NaK Flow Rate	lb/hr	57148	57148
NaK inlet Temperature	°F	1185	1211
NaK Temperature Drop	°F	170	167
NaK pressure Drop	psid	~3	~3
Hg Flow	lb/hr	13775	13600
Hg Exit Pressure	psia	148	147
Hg Exit Temperature	°F	1165	1190
Hg Inlet Temperature	°F	420	420
Hg Vapor Region Pressure Drop	psid	32	46
Hg Flow Restrictor Pressure Drop	psid	143	140
Hg Inlet Pressure	psia	323	333
Pinch-Point Temperature Difference	°F	38	54
Terminal NaK-to-Hg Temperature	°F	20	22
Vapor Superheat	°F	197	224
Mean Preheat Flux	$Btu/hr\text{-}ft^2$	118465	215553
Mean Multipassage Plug Boiling Flux	$Btu/hr\text{-}ft^2$	49237	71292
Mean Swirl Wire Boiling Flux	$Btu/hr\text{-}ft^2$	57921	63338
Mean Superheat Flux	$Btu/hr\text{-}ft^2$	5176	5707
Boiling Termination Point	ft	15.4	13.4
Multipassage Plug Vapor Exit Quality	percent	12	18
Thermal Power Required	kW	600	598
External Power Loss (Assumed)	kW	5	5

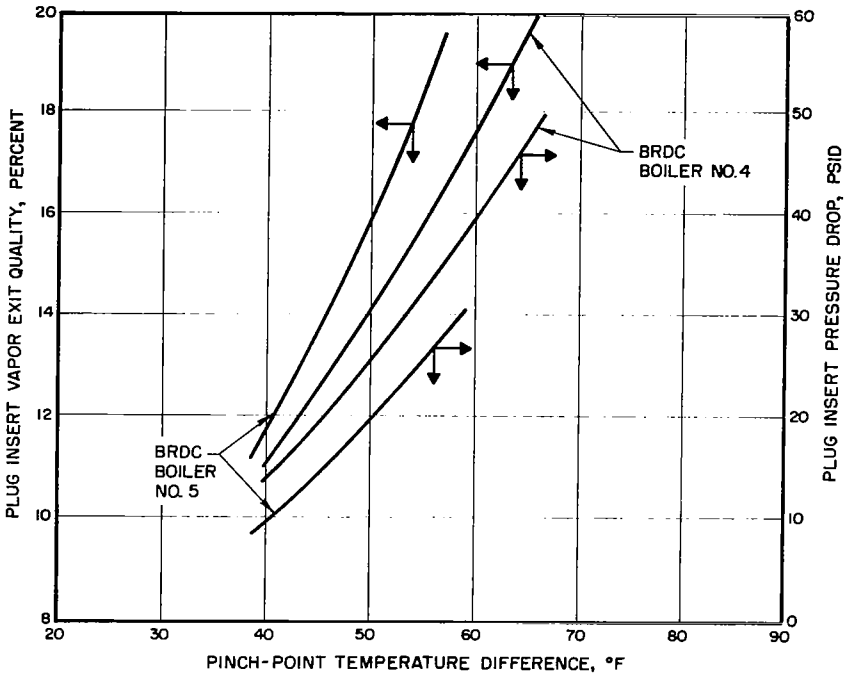

Figure 5-68 BRDC Boilers No. 4 and No. 5 - Performance Comparisons (Design Data)

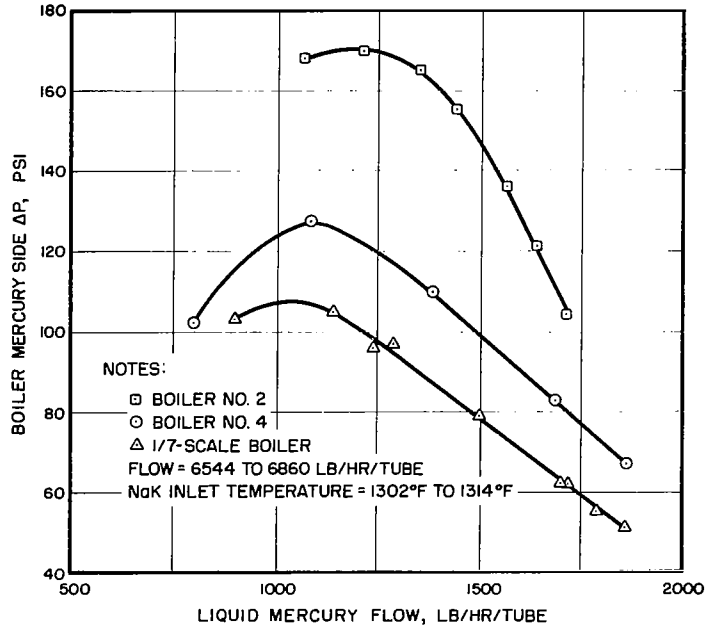

Figure 5-69 BRDC Boilers No. 2, 4, and 1/7 Scale - Mercury Pressure Drop vs Liquid Mercury Flow

Boiler No. 5. The orifice pressure drop was determined to be 128 psid at 100% mercury flow. The pressure drop using the 0.050-inch diameter orifice was determined to be 143 psid which is in agreement with the value noted in Table 5-XVI. The degree of positive slope for the total boiler pressure drop would be greater using the smaller orifice as discussed in Reference 50.

5.5.5.2 NaK-Side Pressure Drop

The power conversion system requirement allows for a boiler NaK-side pressure loss of 3.0 psid, maximum. Preliminary calculations for Boiler No. 5 indicated a total pressure drop of 1.50 psid at 57,500 lb/hr. Water tests of a 10-ft long plastic model of the boiler corroborated the calculations (as did similar tests for Boiler No. 4), the value being 1.70 psid. The predicted NaK pressure drop data for Boiler No. 5, based on the water tests, are plotted in Figure 5-71.

Dye injection tests were employed to observe the effectiveness of the NaK turbulator coils in Boilers No. 4 and No. 5. The tests were conducted on the basis of equal velocities (i.e., the water velocity = NaK velocity) at 2.5, 3.0, 4.0, and 5.0 fps. The Reynolds numbers for water at these velocities were much lower than the NaK Reynolds numbers for the same velocities. From test observations, good mixing occurred at velocities from 3.0 to 5.0 fps within 1.0 to 1.5 feet from the point of injection. At 2.5 fps, the mixing was slower and took about 2.5 ft to develop. The tests described above were run for the tube bundle. Dye tests in the NaK manifolds were made at the same water velocities noted above. At all velocities the dye was distributed evenly throughout the manifolds almost immediately. The flow model was full-scale in cross section with respect to internal dimensions.

The vacuum chamber between the stainless steel header and the tantalum header (see Figure 5-65) is necessary to reduce the thermal gradient across the stainless steel header. The vacuum chamber between the tantalum dome and the NaK shell is required to reduce the thermal gradient in the shell and in the area adjacent to the end of the NaK outlet manifold. The static NaK volume in this area is minimized to decrease the available heat to the cold mercury during startup; this reduces the thermal gradient in the axial direction.

The compartmentalization (axially oriented honeycomb) of the area around each tantalum tube between the stainless steel and tantalum headers is an approach designed to minimize the natural convection of the static NaK as the colder mercury flows through the tantalum tubes. The NaK outlet manifold is placed around this area to further reduce the natural convection by supplying heat over the entire circumference. These approaches were not employed in the Boiler No. 2, although the method of manifolding was successfully demonstrated with Boiler No. 4.

An analysis of the natural convection phenomenon in liquid metals can be seen in Reference 50. It should be pointed out that there is very little information available on the natural convection of liquid metals with the tubes-in-shell configuration described herein, operating in a horizontal attitude.

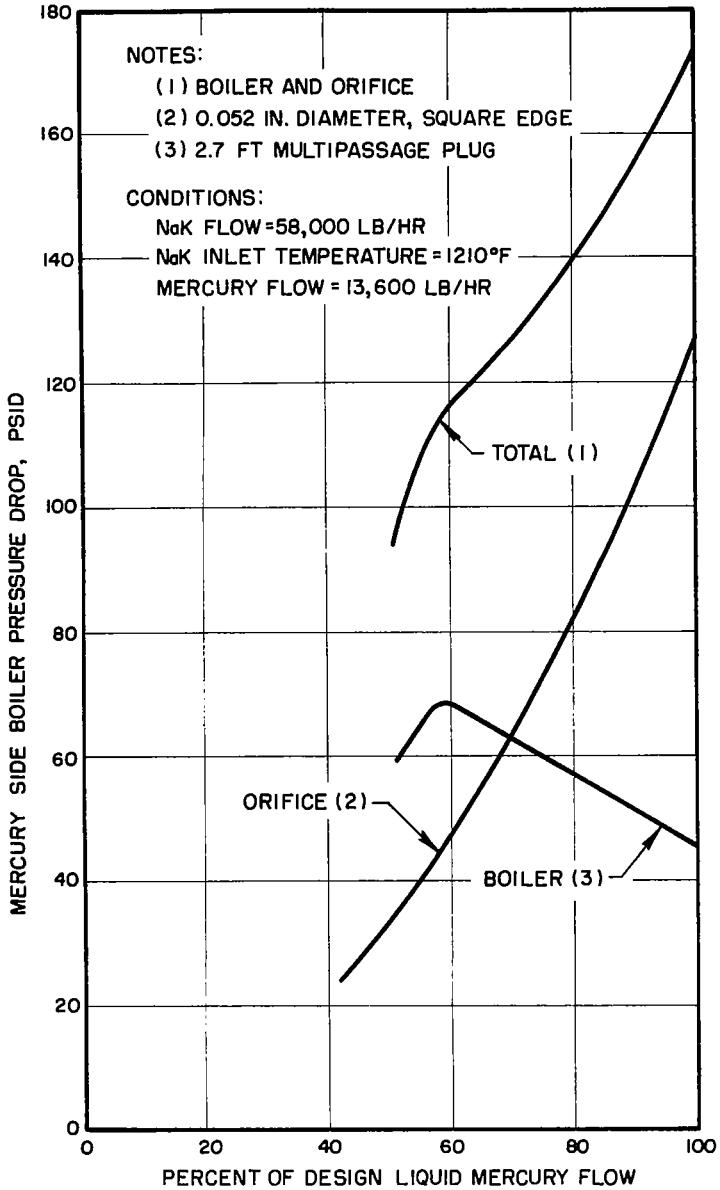

Figure 5-70 BRDC Boiler No. 5 - Mercury Pressure Drop vs Liquid Mercury Flow

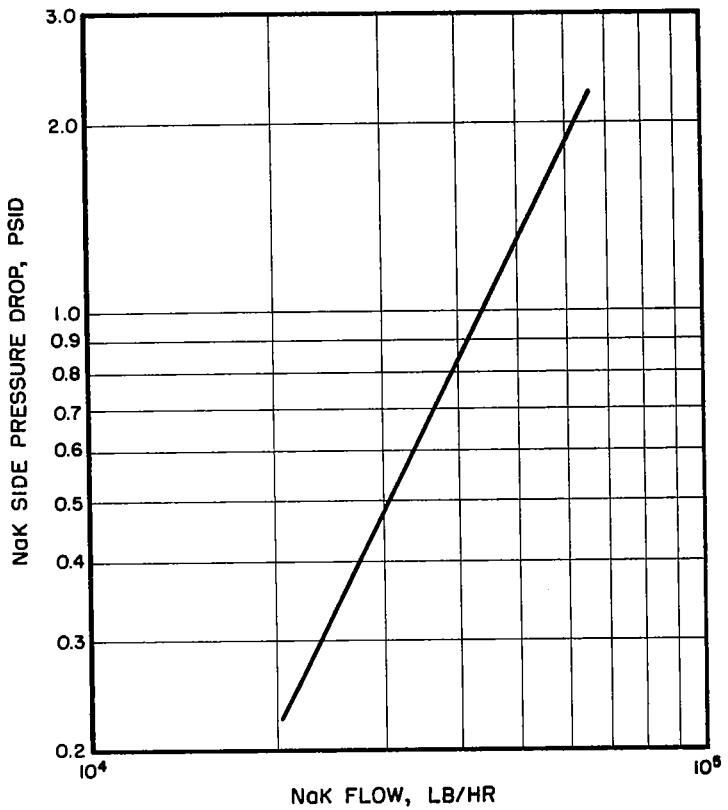

Figure 5-71 BRDC Boiler No. 5 - NaK-Side Pressure Drop vs Liquid Mercury Flow

5.5.5.3 Boiler Thermal Analysis

The analyses and results of the various design approaches for an acceptable mercury inlet section that would meet the startup transient and steady-state conditions are summarized below. The analyses were concerned with the following criteria:

- The inlet dome mercury volume should be as small as possible to minimize the time to fill during startup, yet not be so small that mercury boiling and flashing in the dome causes such a high back pressure (due to the small orifices) on the mercury pump that startup becomes impossible. This can occur since the boiler is preheated to the NaK inlet temperature prior to mercury injection.

- No thermal gradients in any of the materials should be so high as to cause thermal stresses which exceed the allowable strength of the materials during the transient and steady-state operating conditions.

However, it became evident as the design evolved, that the thermal gradients in the dome were too severe for a thick, flat dome which held the mercury volume to a minimum. A thinner, fairly flat dome was unacceptable from a pressure-stress standpoint. It was determined that a hemispherical head was the least stressed but it also resulted in an unacceptably large mercury volume. An elliposoidal dome proved to be the most acceptable as to stress, size and mercury volume. This configuration was analyzed for the transient and steady-state conditions. At the same time, the mercury inlet steady-state temperature was decreased from 420 to 350°F, in keeping with the latest change dictated by the change from the four-stage turbine to the dual multistage reaction turbine concept (90 kWe system).

5.5.6 System Interfaces

Earlier in this section, the system requirements were outlined and discussed with regard to the boiler. The following discussion deals with the constraints the boiler places on the system.

The S-shape of the latest boiler design requires that it be supported in a manner that will minimize excessive loads transmitted to the turbine inlet and to prevent excessive stresses in the boiler shell. The loads transmitted to the turbine inlet are due to the thermal growth of the boiler and turbine in two planes. Minimization of these loads to the required values was done by looping the piping between the turbine inlet and boiler outlet and anchoring the mercury outlet end of the boiler rigidly. To prevent over-stress in the boiler shell, the boiler is coldsprung so that, as it heats up, the thermal growth will return the boiler to the as-fabricated shape. This mounting scheme was shown in Figure 5-66. The spring mount is used since there will be some rotation of the boiler straight section and requires that the mount have some resiliency.

Other constraints on the system that result from placing the looped piping between the boiler and turbine inlet are the allowable line pressure drop and allowable stress.

Liquid mercury inventory in the boiler inlet area affects system startup rates and the attempt was made to keep this volume or weight to a minimum (about 25 lb). From the standpoint of boiler thermal gradients and stress, the minimum weight that was attained was 35.6 lb. From the system viewpoint, this may require an increase in the initial mercury flow ramp with time in order to compensate for the increase in inventory before flow through the orifices and boiler tubes begins.

The double-containment feature of the boiler requires a volume compensator (metal bellows expansion reservoir) to accommodate the static NaK thermal expansion as the boiler is heated to operating temperatures. This means that the system needs additional piping, increased system weight and must provide space for mounting the expansion reservoir.

5.5.7 Performance

5.5.7.1 Steady-State Performance Mapping

The Boiler design was completed in October 1970. However, this unit was not fabricated. Therefore, Boiler No. 5 performance will be discussed in terms of Boilers No. 4 and No. 2 data by comparing steady-state operating parameters such as liquid carryover, NaK temperature profiles, stability, mercury-side pressure drop, terminal temperature difference, and NaK-side pressure drop. Discussion of operating problems is presented in the form of structural failures, contamination of the boiler mercury flow path, and material analyses of Boilers No. 2 and No. 4, and how these results are related to Boiler No. 5.

The purpose of the steady-state performance mapping was to observe the boiler performance over a wide-range of off-design conditions. The ranges covered in the Boiler No. 4 mapping were:

- Mercury flow 3,000 - 12,000 lb/hr
- NaK flow 25,000 - 49,000 lb/hr
- NaK inlet temperature 1,150 - 1,300°F

These ranges of parameters extend from the design point to lower flows and temperatures which simulated Boiler No. 5 operation at the 1200°F power conversion system state-point (see Table 5-XII).

Figure 5-72 is a carpet plot of the mercury vapor pressure drop associated with the preheat boiling and superheat regions of Boiler No. 4. The magnitude of the pressure drop corresponds to predicted values. As was described earlier, each of the curves has an inflection point and negative slope of pressure drop with increasing mercury flow. Note that the inflection point of the curves is a function of the NaK flow, NaK inlet temperature

and plug insert length. These curves are characteristic of the mercury vapor pressure drop behavior of Boiler No. 5 also; only the magnitude of the values would be reduced for Boiler No. 5. During test, this negative slope phenomenon gave rise to some system instability (i.e., the NaK heater response) and would be an undesirable condition to have in a reactor system. Figure 5-70 shows that the slope can be kept positive by simply sizing the orifice; this was done on the Boiler No. 5 design.

Variation of the pinch-point temperature difference* with NaK flow, mercury flow, and NaK inlet temperature is shown in Figure 5-73 for Boiler No. 4. These data show the pinch-point temperature differences at which the boiler operated for the various test conditions. The plot is representative of how Boiler No. 5 pinch-points will vary with lower ranges of operating conditions.

The stability of Boiler No. 4, as measured by fluctuations of the mercury outlet pressure, was less than $\pm$ 1% at 1300°F and less than $\pm$ 2.0% at conditions simulating Boiler No. 5 design conditions. The maximum instability measured on Boiler No. 4 was $\pm$ 4.0% and occurred at a pinch-point temperature difference of about 8.0°F. The Boiler No. 5 design is expected to be within $\pm$ 2%.

Vapor outlet end terminal temperature difference (NaK inlet at the mercury outlet) is shown in Figure 5-74 for Boiler No. 4 plotted as a function of NaK flow, mercury flow and NaK inlet temperature. The terminal temperature difference corresponds to the design prediction, at a value between 40 and 50°F. Boiler No. 5 terminal temperature differences are expected to be about the same magnitude at design conditions and will vary with changes in flows and NaK inlet temperatures in the same manner as did Boiler No. 4. It should be added that Boiler No. 4 test data are all measured with surface-reading thermocouples, as opposed to immersion types. From previous boiler test experience, the immersion thermocouple when in the vapor stream reads about 30°F higher than the surface type. Therefore, adding 30°F to the mercury vapor temperature with the NaK temperature remaining the same, a "true" terminal temperature difference becomes 10 to 20°F, which gives a better comparison with the design expectations.

Also of interest is the observation that the terminal temperature difference reaches a minimum for a given NaK flow and inlet temperature as the mercury flow is increased. Then, as the mercury flow is increased further, the terminal temperature difference also increases. These reversals in the terminal temperature difference occur at pinch-point temperature differences of between 8 to 20°F. The phenomenon is explained by the fact that, at low pinch-point temperature differences, the plug exit quality of the mercury is reduced. Also, the plug-insert is becoming flooded with liquid mercury with most of the mercury boiling occurring in the unplugged tube region (swirl wire only). With the boiling length increased, the superheat length is decreased, more liquid droplets are presented in the vapor stream, and the vapor superheat temperature is reduced.

*The pinch-point temperature difference is defined as the difference between the bulk temperatures of the mercury and NaK at the mercury vapor-to-liquid interface. This point lies in the plug insert at the liquid mercury inlet.

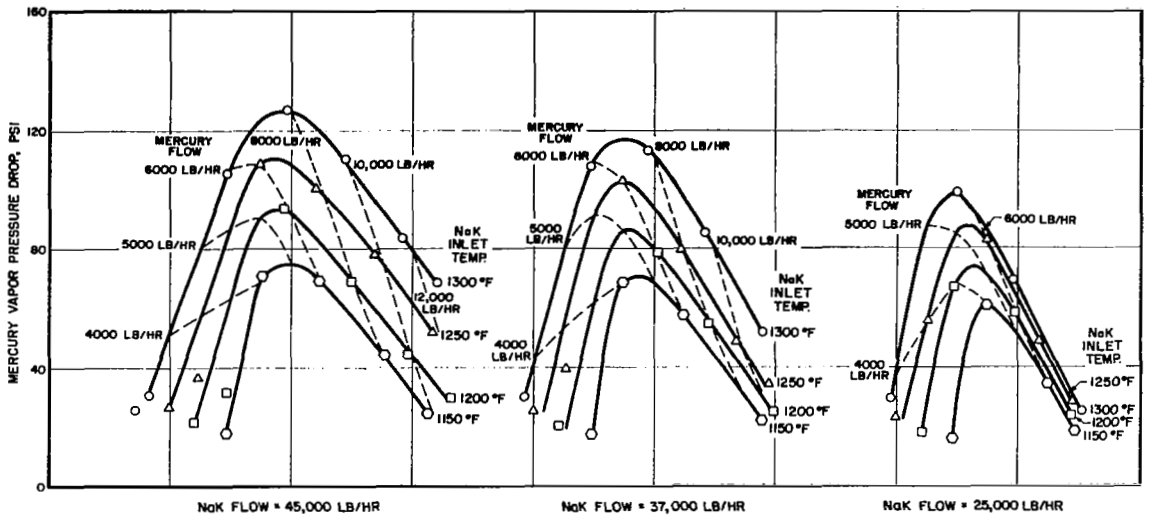

Figure 5-72 BRDC Boiler No. 4 - Performance Carpet Plot
(Mercury Vapor Pressure Drop)

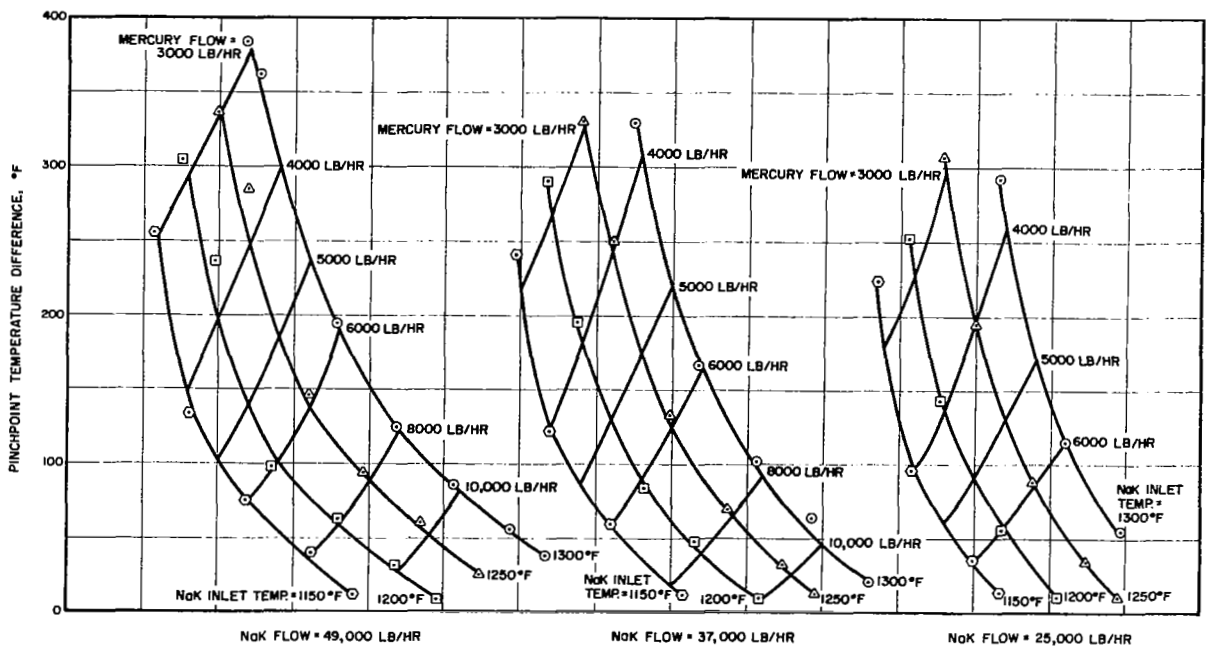

Figure 5-73 BRDC Boiler No. 4 - Performance Carpet Plot
(Pinch-Point Temperature Difference)

With the increase in terminal temperature difference, there was evidence that the boiler became less stable. This effect, however, would not significantly affect Boiler No. 5 operation at these low pinch-point temperature differences would not be encountered over the reactor dead band or at the system state point. Figure 5-75 is a plot of Boiler No. 4 terminal temperature differences at conditions simulating Boiler No. 5 operation at the system state-point.

A test was conducted to evaluate the boiler response to the normal variation of the boiler NaK inlet temperature or reactor temperature deadband. The responses of key boiler parameters over a range of 1170 to 1235°F is shown in Figure 5-76 together with the predicted responses. The results were in accordance with the expectations. The fact that the boiler pressure drop test data are higher in magnitude than the predicted is due to the difference in plug insert lengths of Boilers No. 4 and No. 5.

Although boiler performance is primarily gaged in terms of the mercury-side parameters, another important boiler parameter which relates to system operation is NaK-side pressure drop. Figure 5-77 presents the predicted and actual Boiler No. 4 NaK pressure drop as well as the predicted Boiler No. 5 NaK pressure drop. The predictions for both Boiler No. 4 and Boiler No. 5 were based on water flow tests of cross-sectional, full-scale plastic flow models discussed earlier. In view of the good agreement between the actual and predicted pressure drop for Boiler No. 4, it is expected that Boiler No. 5 NaK-side pressure drop will be as shown. Variations of the NaK temperatures are not sufficient to cause any measurable discrepancies between the calculated and actual values since the NaK density changes by only 2% over a range of temperature from 1150 to 1300°F.

5.5.7.2 Boiler Performance Degradation

During testing, thermal and dynamic performance declined in Boilers No. 2, No. 3 and No. 4. The loss in performance was observed by noting a change in mercury vapor pressure drop, a decrease in the NaK temperature profile in the plug insert and boiling sections, and an increased terminal temperature difference. The times when boiler performance degradation occurred were different for Boilers No. 4 and No. 2, or No. 3; however, Boiler No. 4 deconditioned within four minutes after initial startup, remained that way for four days, and then returned to conditioned operation for the remainder of the 1620 hours of operation. Boilers No. 2 and No. 3 conditioned initially and their performance declined gradually over a period of operation. Figure 5-78 graphically illustrates the difference between a conditioned and a deconditioned boiler and represents a degradation of plug insert effectiveness (i.e., lessening of heat transfer) for Boiler No. 4. The loss of plug insert effectiveness could be caused by enlargement of the plug grooves by corrosion, erosion, by a film of surface oxides and contaminants, or by a combination of all these. Corrosion and erosion have been eliminated as the causes since post-test examination of the Boiler No. 2 tantalum surfaces revealed that these conditions did not occur. Boiler No. 1 was operated in excess of 15,000 hours without pressure drop or plug insert heat transfer degradation. Since the test facility did not contain sources of oil contaminants, Boiler No. 1 was not expected to degrade. Examination of Boiler No. 1 pressure drop versus mercury liquid flow showed it to behave in the identical manner as curve No. 1 of Figure 5-79 for Boiler No. 2.

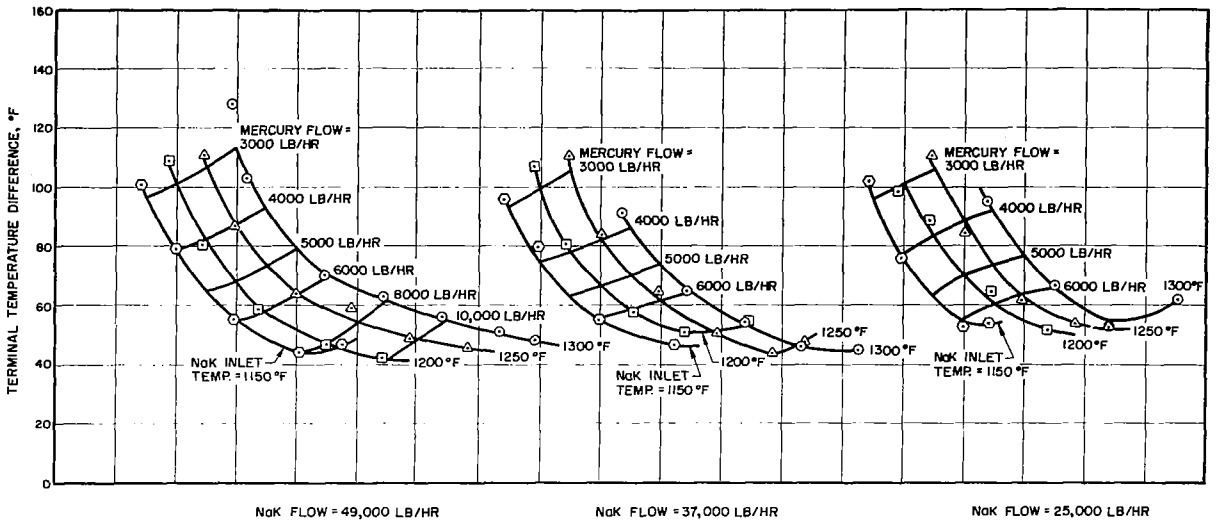

Figure 5-74 BRDC Boiler No. 4 - Performance Carpet Plot (Terminal Temperature Difference)

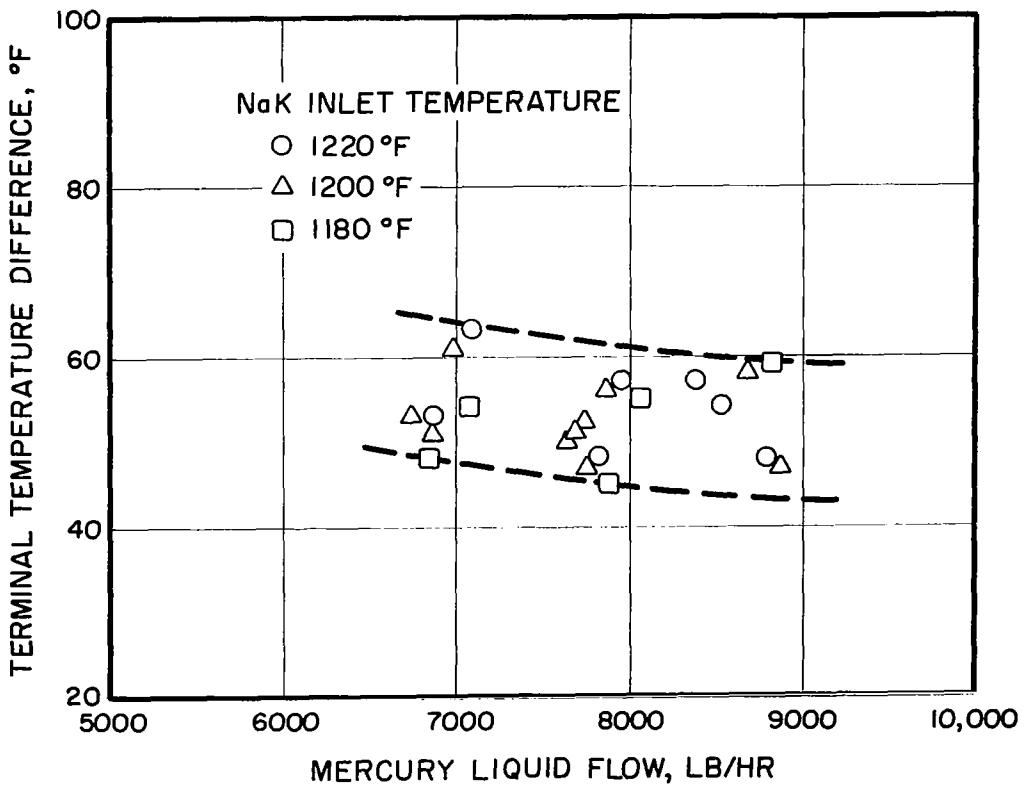

Figure 5-75 BRDC Boiler No. 4 - Terminal Temperature Difference vs Liquid Mercury Flow at Various NaK Inlet Temperatures

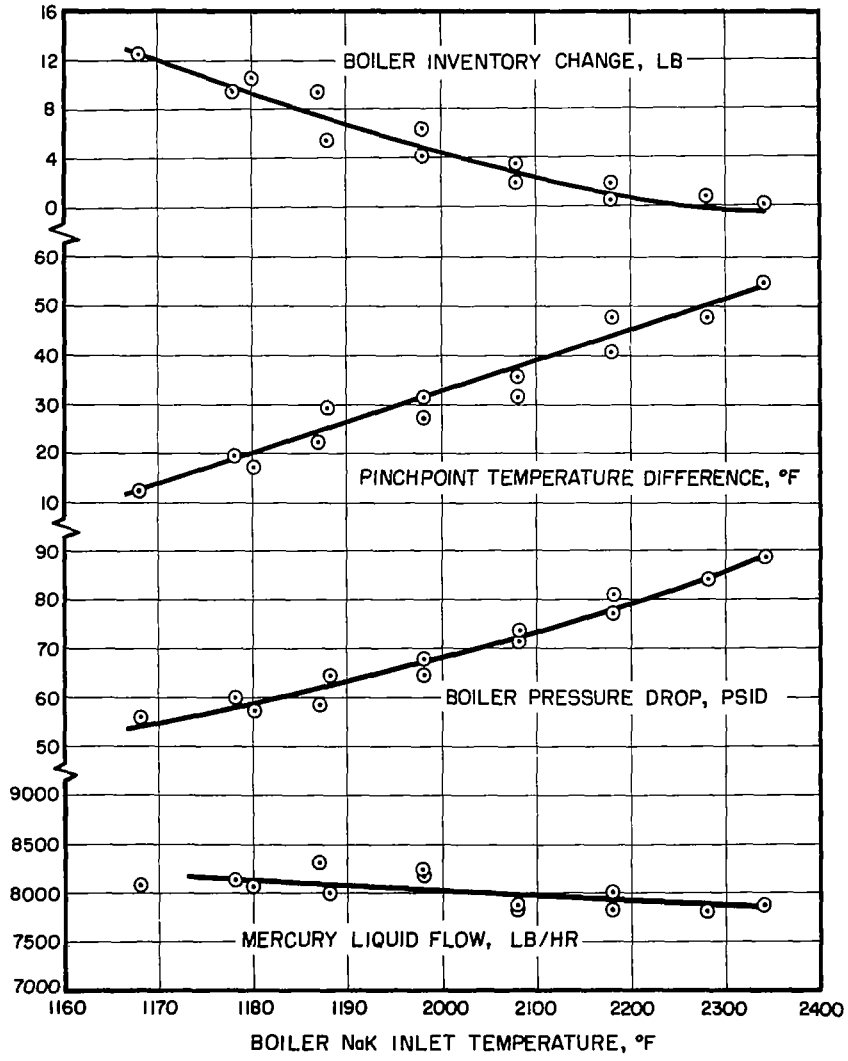

Figure 5-76 BRDC Boiler No. 4 - Performance Results over Reactor Temperature Deadband

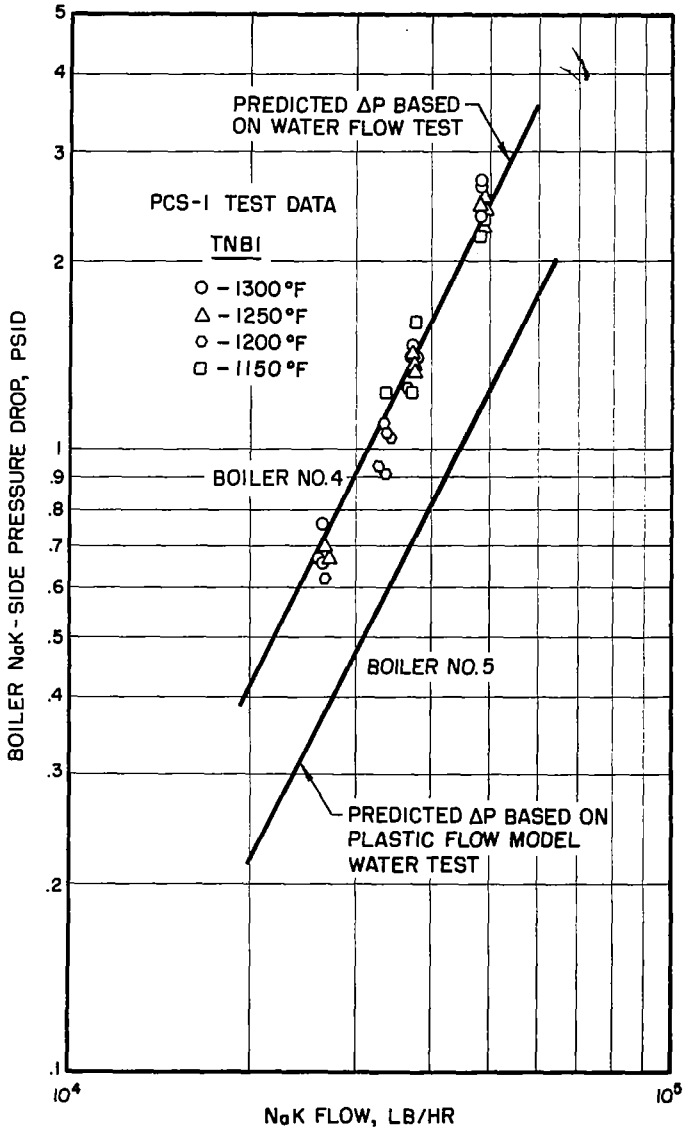

Figure 5-77 BRDC Boilers No. 4 and No. 5 - NaK-Side Pressure Drop vs NaK Flow

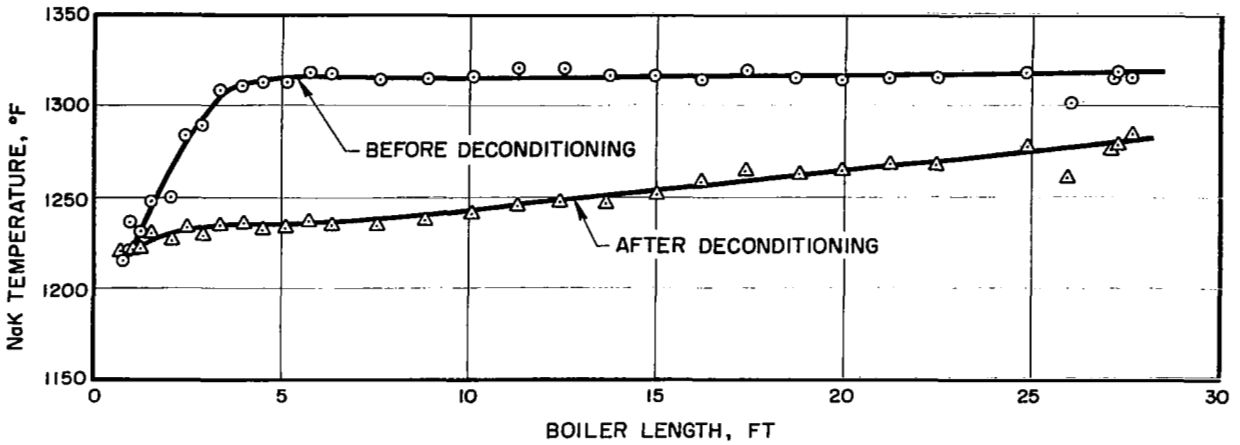

⊙ - TIME 1542		△ - TIME 1544	
MERCURY FLOW	6685 LB/HR	MERCURY FLOW	5410 LB/HR
NaK FLOW	51000 LB/HR	NaK FLOW	51000 LB/HR
NaK TEMPERATURE, IN	1320 °F	NaK TEMPERATURE, IN	1286 °F
PRESSURE DROP	167.4 PSI	PRESSURE DROP	35.3 PSI

Figure 5-78 BRDC Boiler No. 4 - Boiler Deconditioning During Test in 35-kWe System

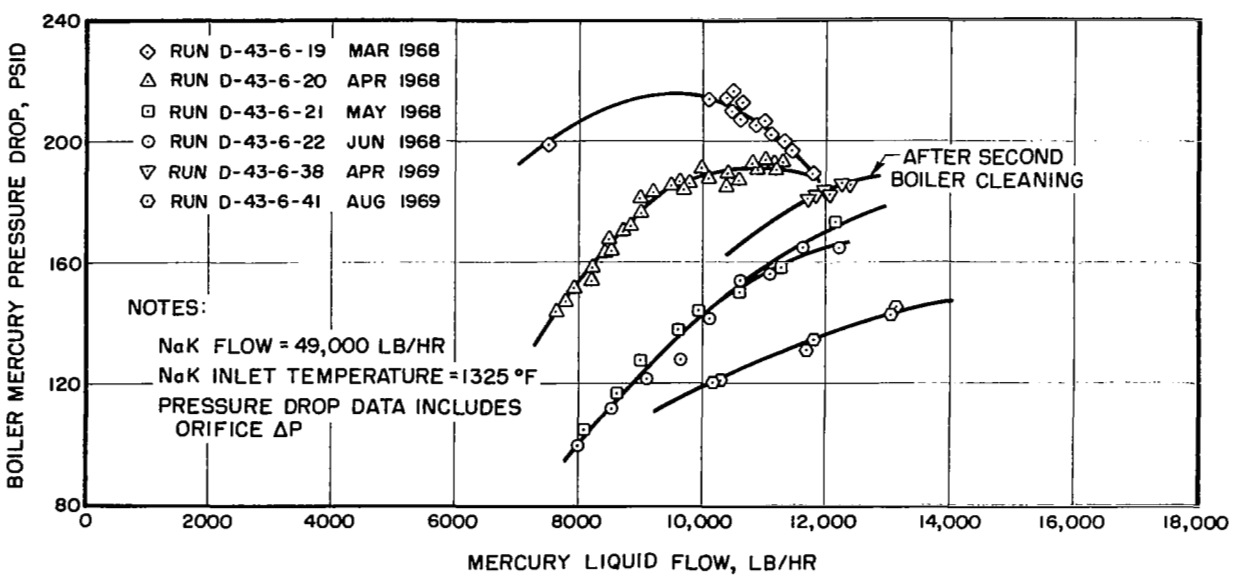

Figure 5-79 BRDC Boiler No. 2 - Performance Degradation Due to Oil Contamination of the Mercury

After the initial conditioned run, Boiler No. 2 never returned to a fully conditioned state. The fact that the unplugged tube length was overdesigned, allowed the boiler to behave in a stable manner and still produce the required superheat and vapor quality.

Boiler No. 4 eventually returned to its predicted performance level and remained conditioned. While the boiler was in the process of conditioning, each shutdown resulted in a partial loss of performance. This cycle reconditioning persisted only until the boiler became fully conditioned and future shutdowns (28 in all) had no effect on the boiler performance. This improvement over Boiler No. 2 was the direct result of minimizing oil contamination (from the mercury pump and the turbine-alternator) and from a tighter control of air in-leakage to the mercury loop.

5.5.7.3 Materials Analysis

Many materials studies were conducted during the course of the SNAP-8 program to fully evaluate various metals in contact with NaK and mercury. Tests were conducted in a 1/19th-scale (based on SNAP-8 liquid mercury flow) loop designated as Corrosion Loop No. 4 (CL-4). Materials tested were 9% chromium - 1% molybdenum steel (9M), columbium, tantalum and Type 316 stainless steel. The degree of mercury wetting, mass transfer deposition, corrosion and erosion were primary concerns. The significant results of the tests were:

- The magnitude of mercury corrosion was as predicted by the corrosion analysis for the test section, however the pattern of corrosion was not as predicted.
- Corrosion product buildup (mass transfer) at the liquid-vapor interface of the entrance plug section was greater than anticipated.
- The corrosion rate in the test section preheat region was less than predicted for this test section but the pattern of corrosion was as predicted.
- Immediate conditioning and good heat transfer performance at initial startup indicated good mercury wetting of the metals when the surfaces were clean.
- Mercury velocity has a significant effect on mercury corrosion rate. Reduced velocities result in a reduction of the mercury corrosion rate.

A 4400-hour corrosion test of 9M was conducted at the same time in a Corrosion Loop No. 3 (CL-3) facility. Mercury and NaK corrosion potential for a long period of time was evaluated, with the following results:

- Tube cracking was observed on the mercury-exposed side of the 9M tube and pitting of the 9M inlet plug was observed. The greatest amount of pitting was noted where the heat transfer from the NaK to the mercury was the greatest.

- Decarburization of the 316 SS shell exposed to NaK was noted in the hottest section of the facility (1310°F) but there was no evidence of corrosion.

- The NaK-side of the 9M tubing exhibited decarburization as well as surface cracking. No decarburization was observed in tube sections where the NaK temperature was below 1270°F.

These tests made it apparent that 9M would not provide sufficient mercury corrosion resistance to meet the SNAP-8 operating life requirements. The CL-4 facility was modified to evaluate tantalum as the mercury containment material. Both explosively-bonded and hot coextruded tantalum inner liner to 316 SS outer tubing samples were tested. The hot coextruded tubing was determined to be superior to the explosively-bonded tubing. The most important results of the investigations of tantalum as a mercury containment material were:

- Tantalum has excellent wetting characteristics and good heat transfer is attained as a result.

- Air in-leakage and/or oil contamination deconditions the tantalum wall, degrades the heat transfer and can eventually destroy the tantalum liner.

- Chemical cleaning of the tantalum surfaces can be successfully used on contaminated tubes to achieve rated heat transfer performance.

A 1/7th-scale (based on SNAP-8 liquid mercury flow) test facility was built to more closely simulate an actual boiler relative to mercury containment tube size and length. The test boiler (SB-1) construction was of a bare tantalum tube in a double-containment 321 SS tube, with both being contained in a 316 SS outer shell. The objectives of testing were:

- Evaluate the heat transfer performance of a bare-refractory, double-containment boiler design.

- Evaluate the ability of the materials of construction to withstand long-term exposure to SNAP-8 environments.

The principal conclusions of the testing were:

- A tantalum, double-containment design will meet the heat transfer requirements of the SNAP-8 system.

- A tantalum boiler is sensitive to deconditioning by surface oxidation and/or contamination but will recondition over a period of time, depending on the degree of surface oxidization or contamination.

- The NaK and mercury at temperatures up to 1300°F did not degrade the strength or ductility of the tantalum tube and welds.

- The mechanical properties of Type 316 SS and 321 SS can be degraded by sigma formation after long-term exposure to NaK at temperatures up to 1300°F.

Another test section (SF-1), similar to SB-1 section, was fabricated to evaluate a metallurgically bonded (explosively bonded) bimetal tube of 316 SS on a tantalum liner. The principal objectives of the testing were to determine the following:

- The structural reliability of the bimetal tube concept for mercury containment in the SNAP-8 boiler; specifically, the tantalum liner, the tantalum-to-stainless steel bond, and the bimetal weld joint.

- The mercury corrosion/erosion effects on the tantalum and 316 stainless steel.

- The potential for a 5 year life of an explosively bonded bimetal tube.

The principal conclusions ascertained from the testing were:

- Explosively bonded bimetal tubing is suitable as a mercury containment material if proper care is exercised during the explosive bonding process to ensure that intimate contact between the two metals is attained over the full surface of the tubes.

- Tantalum has excellent resistance to corrosion from liquid mercury.

- The use of Type 316 SS at temperatures above 500°F and exposed to a mercury vapor quality of 88% or less is unacceptable due to excessive corrosion. Microstructural changes resulting from extended exposure (greater than 2500 hours) at 1300°F can cause degradation of mechanical properties in Type 316 SS.

Test section SB-2 was fabricated which included reduced tube and plug lengths to simulate Boiler No. 4 for test evaluations prior to fabrication of the full-scale boiler. Test results indicated that the shorter plug and tube length did not cause a decrease in the performance of the boiler. The excess superheat length incorporated in previous boilers was deleted in this design, yet the quality of the superheat was not degraded.

Many other peripheral test programs were conducted to ensure materials compatibility with NaK and mercury including such studies as mercury droplet vaporization, tantalum-mercury wetting experiments and thermal contact resistances of surface deposits. These are noted in Reference 52.

Other materials investigations related directly to full-scale boiler designs and post-test analyses are discussed below.

a. Results of Tantalum/316 Stainless Steel Transition Joint Thermal Cycling Tests.- Evaluation of low-cycle fatigue effects by thermal cycling was performed on representative Ta/316 SS coextruded tube specimens after 5353 hours exposure at 1350°F, and 275 thermal cycles between 250 and 1350°F. The results and conclusions from the tests are summarized below:

The specimens did not debond, nor was there any evidence of a tendency to debond. The tantalum liner was ultrasonically inspected without detection of defects.

Tantalum hardness increased from Rockwell B (RB) 78 before testing to RB 85 after 4864 hours at 1350°F measured within 0.010 inch of the bond interface. This effect was attributed to interstitial element diffusion from the 316 SS to the tantalum. The 316 SS hardness increased from a pre-test value of RB 86 to RB 90 after 4864 hours at 1350°F

A 7% decrease in inside diameter of the specimens occurred after 3043 hours. It is concluded that the wide difference in the expansion coefficient of the tantalum (4.1×10^{-6} inch/inch) and the 316 SS (10.7×10^{-6} inch/inch), the difference in their yield strengths, and the relaxation of the residual fabrication stresses caused the decrease in diameter. This change will not significantly affect boiler performance (i.e., pressure drop).

No cracking occurred in either the 316 SS or tantalum after flattening tests (opposite ID surfaces in contact) in the pre-thermal cycle test specimen. However, after 4095 and 4864 hours at 1350°F, the 316 SS cracked on the OD surface when the specimen was flattened to a 0.10-inch ID separation.

Microscopic examination revealed that no change in the diffusion zone width between the 316 SS and tantalum had occurred from exposure at 1350°F.

b. Results of Material Analysis of Previous Boilers.- Boilers No. 1 through No. 5 were designed to use the same materials, namely:

- Type 316 stainless steel for the flowing NaK containment tube, headers, turbulators, tube bundle supports, and evacuated center tube.
- Zirconium foil for the getter material placed at the mercury inlet and outlet transition joints in the static NaK.

- Tantalum for the mercury containment tubes, headers, plug inserts, and orifices.

- 90% tantalum - 10% tungsten mercury-side swirl wire.

The materials analyses of BRDC Boiler No. 1 (performed by the General Electric Company after the unit was tested for 15,250 hours at steady-state operation) and of BRDC Boiler No. 2 (performed by Aerojet) are summarized as follows:

Type 316 stainless steel is less prone to form sigma phase than is Type 321 stainless steel. From the 1300°F operating area of Boiler No. 2, the percentages of sigma phase in 321 SS and 316 SS were 3.8 and 1.5, respectively. From the 1150°F operating area (mercury inlet end) the amounts were 1.2% sigma in 321 SS and none detectable in the 316 SS by optical methods. It was concluded that these amounts of sigma phase formation did not present a problem.

The zirconium foil placed at the mercury inlet and outlet transition joints served its intended purpose which was to absorb dissolved gases (oxygen, nitrogen, hydrogen and carbon), thus maintaining a relatively pure static NaK.

Swaging the tantalum tubes over the plug inserts to prevent crossover flow between the plug grooves was successful. This operation produced a near zero-clearance contact between the tube wall and the land area of the grooves that was maintained during the boiler operation.

There appeared to be no life-limiting problems associated with the use of tantalum. Corrosion or erosion was not detectable in either Boiler No. 1 (15,250 hours operation) or Boiler No. 2 (8,700 hours operation). It is expected that no appreciable corrosion/erosion of tantalum would be present after 5 years.

Static NaK corrosion of the tantalum surfaces, in general, did not occur except at two TIG welds (performed in the field under less than ideal conditions) where it was evident that the NaK had removed oxides from the heat-affected zone with resultant voids. It was postulated that the oxide was present due to an insufficiently pure inert atmosphere when welding. It is concluded that NaK corrosion of tantalum is not a life-limiting factor.

Metallic deposits were observed on the tantalum tubing inner surface from the plug insert exit end to the end of the tubing at the mercury vapor outlet. These deposits (i.e., mass-transfer products) generated in other parts of the mercury loop, were carried by the mercury stream in elemental form and in solution and deposited on the walls of the boiler during evaporation of the mercury. The metallic elements were nickel, iron, chromium, and cobalt, and were deposited in various quantities depending on the quality of the mercury vapor. Figure 5-80 compares mercury vapor quality, mercury temperature, percent of element, and percent tantalum plotted versus the boiler length.

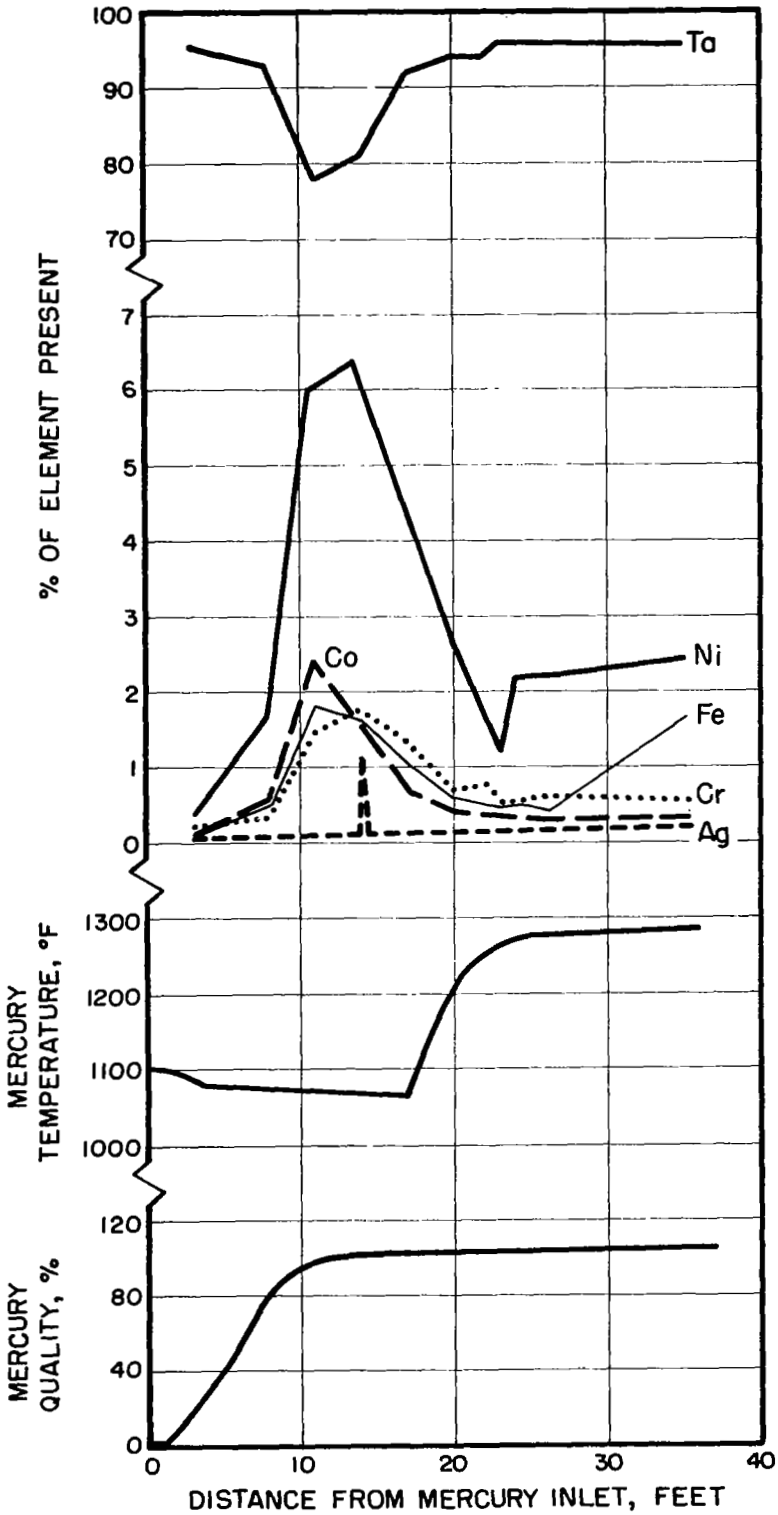

Figure 5-80 BRDC Boiler No. 2 - Metallurgical Analysis of Tantalum Tube ID Determined by X-Ray Fluorescence

These results show that maximum deposition occurred at about 15 ft from the mercury inlet where the vapor quality was a maximum of 98% and superheating begins. These mass-transfer elements, once deposited, form intermetallic compounds of CR_2Ta, $TaNi_3$, and Fe_7Ta_3 with the tantalum. They did not diffuse into the tantalum to any extent nor did they affect the mechanical properties of the tantalum. The deposits were as much as 0.002-inch thick in some locations; however, the effects on heat transfer rates would be minimal. It was concluded that the mass-transfer deposits will not inhibit boiler operation for 5 years.

The boiler design is good from a metallurgical standpoint and tantalum, 90% Ta-10% W, 316 SS, 321 SS, and zirconium as boiler materials are acceptable for 5 years of operation.

5.5.8 Technical Summary

SNAP-8 boiler design and development has demonstrated that:

- Tantalum is a satisfactory mercury containment material for 5 years of operation.
- Correlations are available to accurately predict NaK-side and mercury-side pressure losses and heat transfer values.
- Care must be exercised to preclude mercury-side air and oil contamination for immediate and continued boiler conditioning.

5.6 CONDENSER

The SNAP-8 condenser, shown in the mercury loop schematic (Figure 5-81 for the 90-kWe system and 5-82 for the latest, 35-kWe system), is a heat exchanger that condenses the saturated mercury vapor entering from the turbine exhaust. NaK, the coolant, is pumped through the condenser to a radiator where the heat it absorbs from the condensing mercury is rejected to space. In addition, the condenser must also maintain a back pressure on the turbine as required by the system, and subcool the mercury to maintain an acceptable net positive suction head (NPSH) for the mercury pump.

5.6.1 Development Background

Two major problems were confronted in the design and development of the condenser: (1) the lack of a generalized correlation for condensing mercury heat-transfer coefficients, and (2) the absence of a rational set of design criteria for application to zero-gravity condenser operation. Therefore, the condenser development included detailed analytical investigations of heat-transfer modes and single-tube tests. The condenser size and number of tubes was found to be influenced by the mercury inlet velocity, condensing mercury heat-transfer coefficient, and the diameter and spacing of the tubes.

The resulting SNAP-8 condenser is a counter-flow tube-in-shell heat exchanger (Figure 5-83). It consists of 73 tapered tubes for mercury. Containment surrounded by a tapered shell containing the flowing NaK coolant. Tapered tubes were used to maintain vapor velocity through the condenser length. This provides a continual movement of condensing droplets and results in a stable liquid-vapor interface in a very low or zero-gravity environment.

Concurrent with the condenser analysis and design, NASA-LeRC conducted the Mercury Evaporation and Condensation Analysis (MECA) project on both a straight and tapered tube. The tests determined local overall heat transfer coefficients, local NaK-side heat transfer coefficients, local mercury-condensing heat transfer coefficients, and mercury-side flow and pressure characteristics. The results of these single-tube tests led to the conclusion that the tapered tube design was best suited to the SNAP-8 application. A limitation of approximately 8 psia inlet pressure and a condensing length of 40 inches were set for the multitube condenser design. In addition, these data also indicated that the proposed design was conservative from a comparison of the design overall heat transfer coefficient of 960 Btu/hr-ft^2-^{o}F to the test value of 1900 Btu/hr-ft^2-^{o}F.

Four units were fabricated to the reference configuration shown in Figure 5-83. The tapered mercury containment tube material selected was 9% Chromium - 1% Molybdenum Steel (9M) which was acceptable for the NaK and mercury temperatures at which the condenser operates. This material was also utilized for the mercury outlet reducer and for the mercury headers. Type 410 stainless steel was selected for the tapered shell, NaK manifolds, and mercury inlet transition section. Type 410 SS was chosen based on its comparable coefficient of linear thermal expansion to the tube-side-material, 9M.

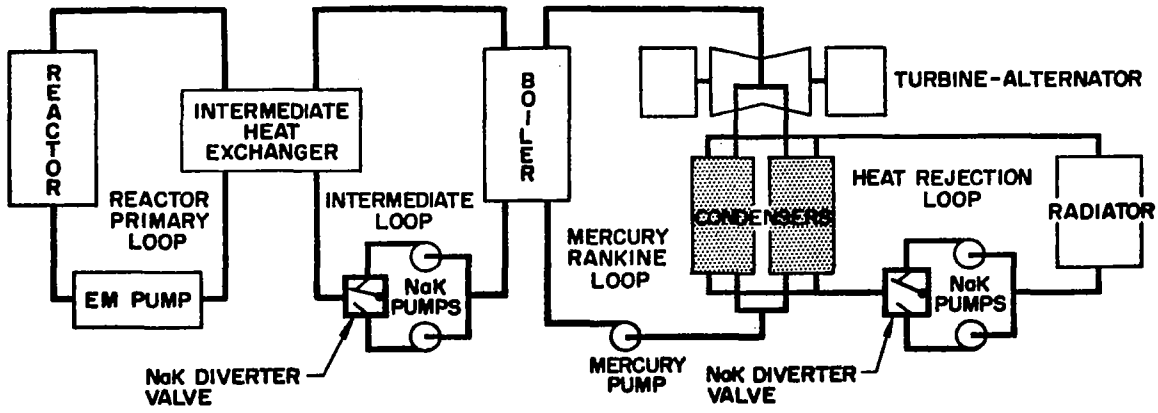

Figure 5-81 90-kWe System Diagram Showing Location of Condensers

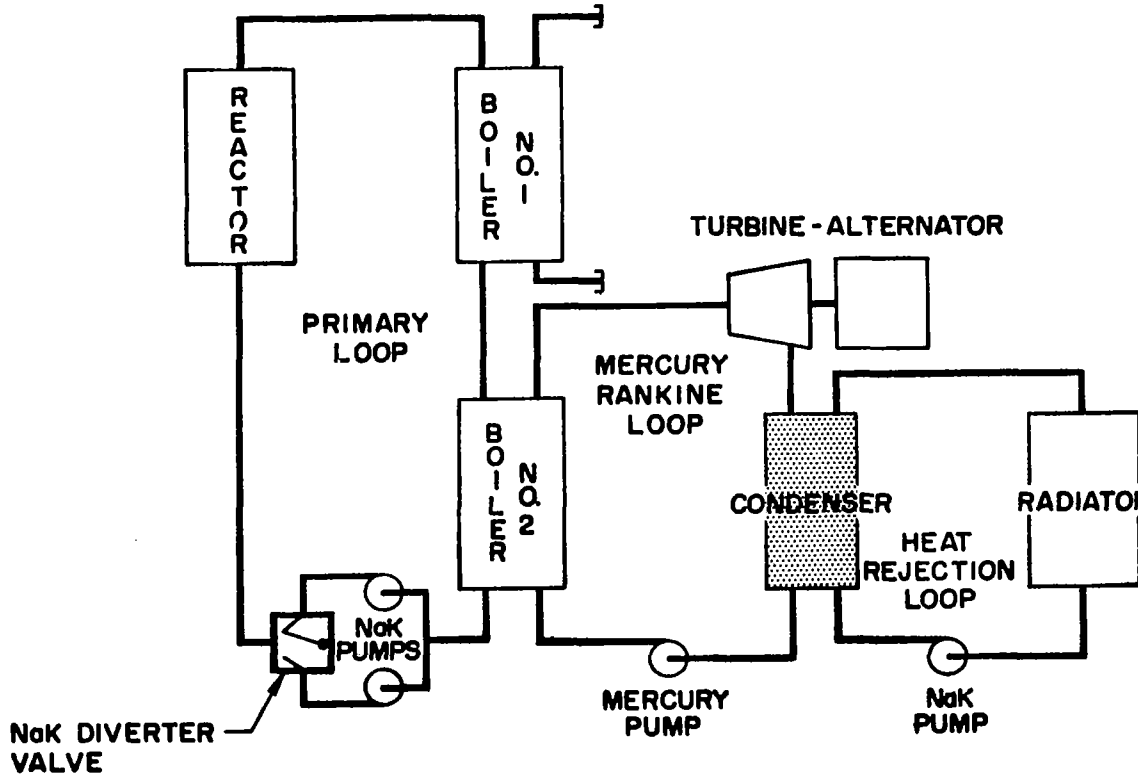

Figure 5-82 35-kWe System Diagram Showing Location of Condensers

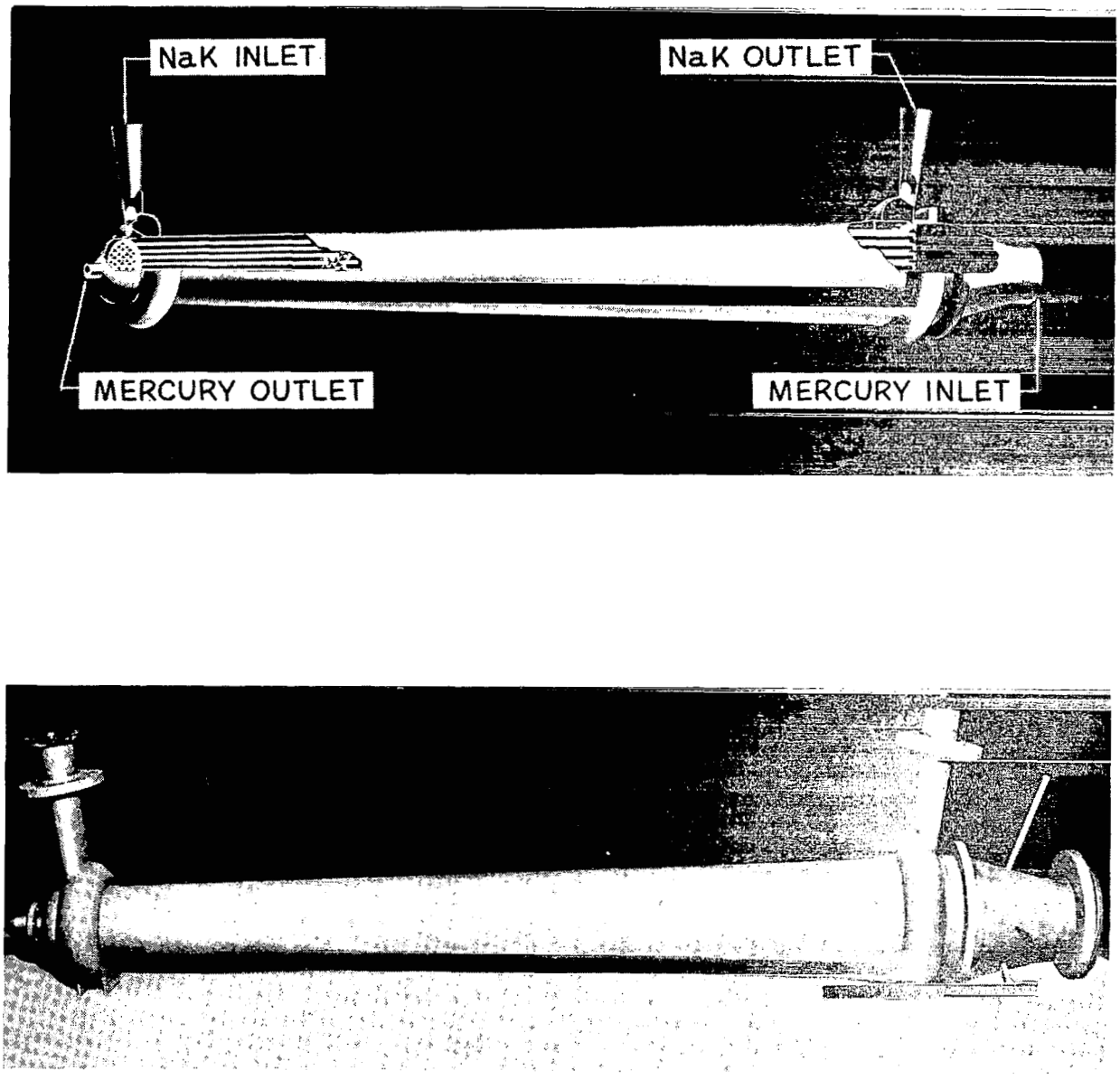

Figure 5-83 SNAP-8 Condenser Cutaway View (Top) and Actual Hardware (Bottom)

The header configuration was the main mechanical design problem because of the number and close proximity of the tube joints. Two approaches used were a welded-and-back-brazed technique and a rolled-and-welded technique. The first two condensers built used the welded-and-back-brazed method. The remainder of the mechanical design made use of the available industrial heat exchanger fabrication techniques, i.e. rolled-and-welded.

Three condensers were tested at Aerojet and at NASA-LeRC. The first unit fabricated was tested at Aerojet under conditions identical to its space application with the exception of zero gravity. The test objectives were to investigate the relationships between flow rates, temperatures, condenser inventory, and condensing pressure. These tests showed that the condenser complied with the power conversion system requirements. The total test time on this unit was 2000 hours with no structural failures encountered.

The second unit fabricated was tested at Aerojet in 35-kWe test system for 16,274 hours with no structural failures and has the longest operating time for any single component tested in the 35-kWe system. Much of the information to follow is based on the data taken from tests of this condenser.

A third unit was held as a spare. The fourth was shipped to NASA-LeRC for installation in the W-1 loop (which was similar to the Aerojet 35-kWe loop) where it was tested for 2568 hours and 144 startup-shutdown cycles. Here again, performance was as expected with no structural failures.

Since the testing of these condensers, the power conversion system state point was changed which created a need for the condenser to operate at higher mercury flows, lower condensing pressures, increased interface loads at the NaK manifolds, and lower NaK-side pressure drop. Prediction of the operation at higher mercury flows and lower condensing pressure was undertaken by defining the limits of the condenser with a complete performance map. The next step was to correlate the test performance data with a mathematical model which analyzed the effects of both pressure drop and heat transfer. The criteria, analysis, and the resultant mathematical model developed to accurately evaluate condenser performance at any set of conditions appears in Reference 4.

A redesign of the condenser was completed which reduced NaK-side pressure drop and strengthened the NaK and mercury inlet and outlet ports to accommodate interface loads. These modifications were based on structural and NaK-side pressure drop requirements only and did not affect the mercury-side geometry or thermal behavior of the condenser. The two condensers chosen for the modifications have the rolled-and-welded header design. Reference 55 documents the changes.

5.6.2 Design Description

The SNAP-8 condenser is a counter-flow, tube-in-shell heat exchanger with the condensing fluid, mercury, flowing through the tubes and the coolant fluid, NaK, flowing through the shell. The mercury inlet and outlet are concentric and parallel to the tube bundle while the NaK entry and exit flow directions are perpendicular to the tube bundle (see Figure 5-83). There are 73 tapered, 9M mercury condensing tubes rolled-and-welded to the fixed 9M headers in a triangular pitch array and are 51.50 inches long. Figure 5-84 shows one of these tapered tubes.

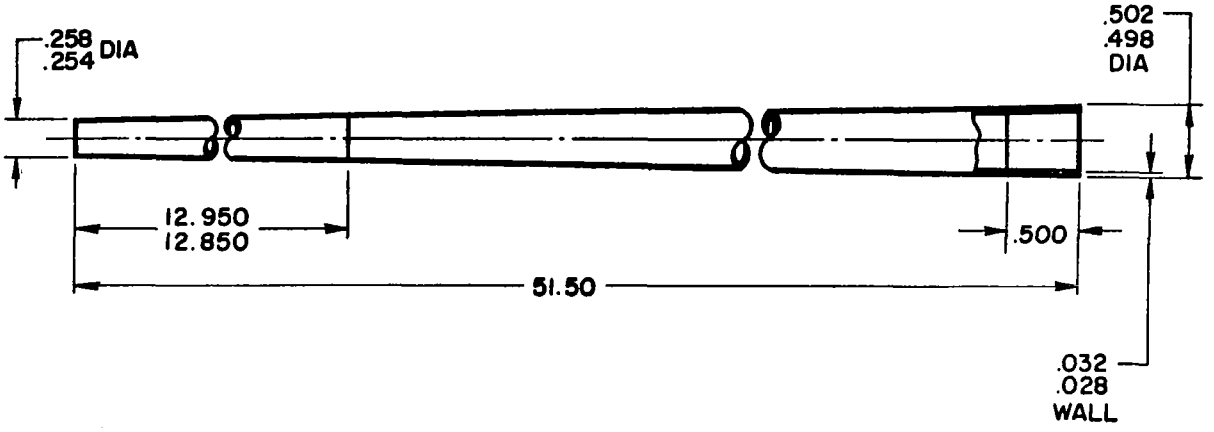

Figure 5-84 Mercury Condenser Tapered-Tube Configuration

The tapered shell is made of Type 410 stainless steel with a 0.083-inch wall thickness which encloses the tube bundle and a Type 410 SS skirt assembly. The annular space between the skirt and the shell is blanked off at the NaK outlet end only, so that NaK is trapped preventing flow bypass external to the outer tubes; whereas, the space between the skirt and the tube bundle forms the flow path. There are two tube-bundle spacers made of 410 SS placed at 28 and 13 inches from the mercury outlet header. These spacers add stiffness to the tube bundle and prevent contact between adjacent tubes.

Cold NaK from the radiator enters the condenser through a 410 SS toroidal manifold and twelve 0.750-inch diameter holes drilled in the shell and leaves the condenser at the NaK outlet with the same arrangement. The NaK inlet and outlet is 3.00-inch OD with a 0.083-inch wall thickness. The NaK flow through the tube bundle is unbaffled, other than the two tube-bundle spacers noted above.

Condensed liquid mercury leaves the condenser through a 316 stainless steel concentric reducer. Mercury vapor enters the condenser through a conically shaped transition section made of 0.083-inch thick

410 SS which incorporates four instrumentation ports spaced 90 degrees apart. A 1.50-inch OD by 0.095-inch wall thickness mild steel port was also provided in the transition section to evacuate the condenser and mercury loop after installation in the test loop or power conversion system.

The condenser dry weight is 94.5 lb. The wet weight of the condenser is 144.7 lb. which includes the dry weight, 32.6 lb of NaK, and 17.6 lb. of mercury. The overall length is 61.2 inches with a maximum diametral envelope of 12.0 inches (located at the NaK outlet manifold).

5.6.3 Design Requirements and Criteria

Operational design requirements set forth for the initial condenser design for the 35-kWe system are given in Table 5-XVII. The stability criterion used to determine the critical tube diameter was a Bond number of 15.3 maximum. A Bond number less than or equal to 15.3 yielded the critical tube dimension at the vapor-liquid interface of 0.24-inch ID. Second, for stable operation in zero gravity, slug flow in the condensing tube must be prevented. This established the minimum vapor velocity of 100 fps at the condenser inlet.

Table 5-XVIII lists the most recent operating requirements as specified by the new power conversion system state point for the 90-kWe system. The condensing pressure requirement of 2.5 psia is not attainable with the use of one condenser unless the number of tubes were increased from 73 to 120 (zero-gravity operation only).

Condenser operating transients during the power conversion system startup and shutdown are listed in Tables 5-XIX and 5-XX. The condenser must be capable of operating for 100 startup and shutdown sequences as a minimum, within an operating life of 5 years.

The mechanical design criteria emphasized the following:

- Condenser fluid connections shall withstand any combination of radial and axial forces and bending and torsional moments at the maximum operating temperatures (910°F) and pressures (120 psia) that the connecting system tubing is capable of withstanding. Interface loads shall not cause the loss of fluid containment, excess deformation, or any condition which would prevent the condenser from meeting the operating life (5 years) and performance requirements.

- The design proof pressure is 275 psia at room temperature (70°F) which includes a 1.25 load uncertainty factor, a factor of 1.5 for ultimate strength, and a factor of 1.15 for 0.2% yield strength.

- All welds shall be dye-penetrant and radiographically inspected for surface and internal defects. Propagating defects are not allowed.

TABLE 5-XVII CONDENSER DESIGN REQUIREMENTS FOR THE 35-kWe SYSTEM

Configuration

1. Counterflow, tube-and-shell, unbaffled
2. Tapered tubes 0.45-inch ID at inlet, and 0.125 ID at outlet
3. Shell tapered to maintain constant clearance (0.060 inch) between tubes except between center tube and adjacent tubes, where clearance is 0.090 inch.
4. Constant tube wall thickness of 0.020 inch
5. Equilateral triangular tube arrangement

Design Data

Mercury flow rate	11,000 lb/hr
NaK flow rate	38,400 lb/hr
Mercury inlet temperature	680°F
Mercury exit temperature	520°F
NaK inlet temperature	495°F
NaK outlet temperature	662°F
Mercury inlet pressure	15.5 psia
Mercury outlet pressure	11.5 psia
NaK inlet pressure	45 psia
NaK outlet pressure	40 psia
Mercury inlet quality	96% vapor
Heat transferred (condenser)	1,330,000 Btu/hr
Heat transferred (subcooler)	47,800 Btu/hr
Mercury vapor inlet velocity	150 ft/sec
Condensing mercury film coefficient	2,000 Btu/hr°F-Ft^2

TABLE 5-XVIII CONDENSER OPERATING REQUIREMENTS FOR THE 90-kWe SYSTEM (For two condensers operating in parallel)

Parameter	Quantity per Condenser
Mercury outlet temperature, °F	NaK Inlet Temp. $^{+4^{\circ}}_{-0^{\circ}}$
Mercury liquid flow at outlet, lb/hr	7,060
NaK-side pressure drop, psid	4 ± 2 at 40,000 lb/hr
Mercury-side pressure drop, psid	0.5 (max.)
Heat removal capability, kWe	465
Mercury inventory within condenser heat exchange passages (0 to 1g), lb	10 to 40
Condensing pressure fluctuations, psia	± 0.28
Minimum mercury outlet pressure (0g), psia	2.0
Mercury inventory excluding heat exchanger passages, lb	8 ± 2
Initial mercury inventory within condenser (0 to 1g), lb	≥ 10
NaK inlet temperature, °F	350
NaK inlet pressure, psia	60 to 85
NaK flow, lb/hr	56,000
Mercury vapor flow at inlet, lb/hr	6,778
Mercury vapor inlet pressure, psia	2.5
Mercury vapor inlet quality, %	96
Mercury vapor inlet temperature, °F	520

TABLE 5-XIX CONDENSER OPERATING CONDITIONS DURING 35-kWe SYSTEM STARTUP

Parameter / Duration of Phase	Phase / Units	Conditions During Each Phase of Start Sequence(1)						
		I	II	III	IV	V	VI	VII
	As Noted	5 Hours	1 Min (min.)	5-10 Min	50-100 Sec	50-__* Sec	7-10 Min	Steady-State
NaK Flow								
Initial	lb/hr	≈1960	≈1960	≈4540	≈4540	7000-21800	7000-21800	40000
Final	lb/hr	≈1960	≈4540	≈4540	7000-21800	7000-21800	≈40000	40000
Max Rate of Change	lb/hr/sec	0	41.3	0	410	0	45	0
NaK Inlet Temperature	°F	50-450	50-450	150-450	150-450	150-460	460	460
NaK Inlet Pressure								
Initial	psia	18-50	18-50	33-65	33-65	60-85	60-85	60-85
Final	psia	18-50	33-65	33-65	60-85	60-85	60-85	60-85
Max Rate of Change	psi/sec	0	.25	0	5	0	0	0
Mercury Vapor Flow								
Initial	lb/hr				0	6400	6400	11800
Final	lb/hr	N/A	N/A	N/A	6400	6400	11800	11800
Max Rate of Change	lb/hr/sec				264	0	17	0
Mercury Vapor-Liquid Interface Pressure - Initial, Min	psia	N/A	N/A	N/A	0	3-14	3-14	14
Final, Max					3-14	3-14	14	14
Mercury Vapor Inlet Quality								
Initial	%	N/A	N/A	N/A	0	≥98	≥98	96
Final					≥98	≥98	96	96
Condensing Phase Pressure Drop, Max	psia	N/A	N/A	N/A	.2	.2	.5	.5
Mercury Inlet Temperature								
Initial	°F	N/A	N/A	N/A	70-1300	535-670	535-670	670
Final					535-670	535-670	670	670
Other Requirements and Remarks	-	(2)	(2)	(2)	(3)	(4)	-	-

* To be added at a later date.

(1) Phase Description:
- I. 95-Hz inverter output, reactor outlet temperature, increased to 1300°F.
- II. NaK and lubricant-coolant pumps accelerate to 220 Hz.
- III. 220-Hz operation, system stabilizing.
- IV. Mercury injection, flow (vapor) reaches 54% of rated (vapor) flow.
- V. Mercury flow holds at 54% of rated; alternator output is 400 Hz.
- VI. Mercury flow increases to rated.
- VII. System is producing rated power (35 kWe).

(2) The mercury vapor pressure at startup is in the range of 0-0.9 psia. Noncondensible gases (for temp ≥50°F) in the condenser, prior to startup, will be at 10 microns Hg initially.

(3) a. Mercury flow from condenser = 0 lb/hr.
b. Mercury inventory accumulated ≥10 lb.
c. Maximum vapor pressure, mercury at exit: 1 psia.

(4) a. Condensing pressure - vapor pressure of subcooled mercury at exit ≥2-1/2 psid.
b. 70 lb ≥ mercury inventory ≥10 lb.

TABLE 5-XX CONDENSER OPERATING CONDITIONS DURING 35-kWe SYSTEM SHUTDOWN

Barameter / Phase	Units	Conditions During Each Phase of Shutdown Sequence(1)						
		I	II	III	IV	V	VI	VII
Duration of Phase	As Noted	Steady State	7-10 min	50 - * __ sec	300 sec	400-600 sec	60 sec (min)	5 hours
NaK Flow								
Initial	lb/hr	40000	≈40000	7000-21800	7000-21800	≈4540	≈4540	≈1960
Final	lb/hr	40000	7000-21800	7000-21800	4540	≈4540	≈1960	≈1960
Max Rate of Change	lb/hr/sec	0	-45	0	-410	0	-41.3	0
NaK Inlet Temperature	°F	460	460	150-460	150-450	150-450	50-450	50-450
NaK Inlet Pressure								
Initial	psia	60-85	60-85	60-85	33-65	33-65	33-65	18-50
Final	psia	60-85	60-85	60-85	60-85	33-65	18-50	18-50
Max Rate of Change	psi/sec	0	0	0	-5	0	-.25	0
Mercury Vapor Flow								
Initial	lb/hr	11800	11800	6400	6400			
Final	lb/hr	11800	6400	6400	0	N/A	N/A	N/A
Max Rate of Change	lb/hr/sec	0	-17	0	-264			
Mercury Vapor-Liquid Interface Pressure - Initial, Min	psia	14	14	3-14	14	14	N/A	N/A
Final, Max		14	3-14	3-14	14	14		
Mercury Vapor Inlet Quality								
Initial	%	96	96	≥98	≥98	N/A	N/A	N/A
Final		96	≥98	≥98	0			
Condensing Phase Pressure Drop, Max	psia	.5	.5	.2	.2	N/A	N/A	N/A
Mercury Inlet Temperature								
Initial	°F	670	670	535-670	535-670	N/A	N/A	N/A
Final		670	535-670	535-670	70-1300			
Other Requirements and Remarks	-	-	-	(4)	(3)	(2)	(2)	(2)

* To be added at a later date.

(1) Phase Description

I. System is producing rated power (35 kWe).

II. Mercury flow decreases to 54% of rated.

III. Mercury flow holds at 54% rated; alternator output is 400 Hz.

IV. Mercury injection, flow (vapor) reaches 54% of rated (vapor) flow.

V. 220-Hz operation, system stabilizing.

VI. NaK and decelerate to 200 Hz.

VII. 95-Hz inverter output, reactor outlet temperature, decreased to 100°F.

(2) The mercury vapor pressure at startup is in the range of 0-0.9 psia. Noncondensible gases (for temp ≥50°F) in the condenser, prior to startup, will be at 10 microns mercury initially.

(3) a. Mercury flow from condenser = 0 lb/hr.

b. Mercury inventory accumulated ≥10 lb.

c. Max vapor pressure, mercury at exit: 1 psia.

(4) a. Condensing pressure - vapor pressure of subcooled mercury at exit ≥2-1/2 psid.

b. 70 lb ≥ mercury inventory ≥ 10 lb.

- Acceptance tests of the condenser include water flow tests of both the NaK and mercury circuits, proof pressure tests, and helium leak tests.

- The condenser was designed with a reliability goal of .995 in 10,000 hours of continuous rated operation in the induced environments. This reliability goal was not re-calculated for the new life requirement of 5 years.

5.6.4 Mechanical Design

5.6.4.1 Overall Design

To restate briefly, the design incorporates Type 410 stainless steel throughout except for the tube bundle and tube headers (9M steel), the mercury exit plenum (316 SS) and the evacuation port (C-1015 mild steel). Provisions for shell drainage were incorporated by placing six 0.125-inch diameter holes equally spaced in the shell under the NaK outlet manifold. Also, the manifolds have a four degree slant for drainage of NaK ullage since the condenser will be mounted vertically for testing with the mercury flow in the direction of gravity. A mounting collar is provided with six holes of 0.404 to 0.411-inch diameter, equally spaced to accommodate the system installation scheme. The welds specified in the overall assembly are manual tungsten-inert-gas (TIG) welds.

5.6.4.2 Tube-Bundle Subassembly and Tapered Shell

The 73 tapered condensing tubes, tube headers, and tube spacers comprise the condenser tube-bundle subassembly. Two "egg-crate" or latticed tube-bundle spacers maintain the tube spacing and add some stiffness to the bundle to prevent tube contact. Placement of the supports at 13.0 and 29.0 inches from the mercury outlet tube-sheet was determined from an analysis of the vibration characteristics of the condenser tubes under sinusoidal and random vibration. The latticed spacers were fabricated from 0.020-inch thick 410 SS, 0.375-inch wide. A typical cross section of the spacers is shown in Figure 5-85.

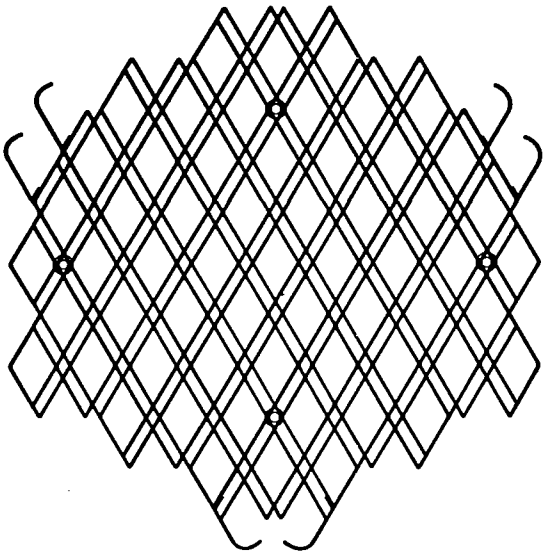

Figure 5-85 Condenser Tube Bundle Lattice Support

The NaK containment shell was designed with a taper to maintain a constant free-flow area and velocity so that the NaK-side heat transfer film coefficient would remain essentially unchanged. The tapered shell also facilitates assembly of the tube bundle and shell. The tubes with headers attached are shown in Figure 5-86. The skirt assembly between the tube bundle and the shell is shown in Figure 5-87.

5.6.4.3 Tube-to-Header Welds

The design approaches for the tube-to-header weld joint configuration were (1) a welded and back-brazed joint, and (2) a rolled-and-welded joint. Both concepts were successful in the SNAP-8 program.

The welded and back-brazed joint utilized a trepanned header, automatic tungsten electrode, inert-gas (TIG) weld, and subsequent back-braze at 1800°F in a hydrogen atmosphere. This weld joint is shown schematically in Figure 5-88. Condensers with these joints have accumulated 18,274 hours of service without a joint failure. Disadvantages to this type of weld joint design, however, were the cost and time involved for the brazing process and the tube distortion due to the 1800°F braze temperature.

The rolled and welded joint eliminated the back-brazing operation, replacing it with a grooved header into which the tube was rolled prior to welding. This type of joint also incorporated a trepanned tube header, with an automatic TIG weld. Figure 5-89 shows this weld joint design. This joint was used in a unit which has been in service for 2658 hours and 144 startup/shutdown cycles without a joint failure. Two advantages of this design concept are (1) the portion of the tube material rolled into the tube header will act as the load-carrying member leaving the weld to function as a seal, and (2) the rolling operation will ensure a controllable fit-up to give the best possible weld. To verify the acceptability of the rolled and welded tube header joint, a development study was made which included manufacture and inspection techniques.

A seven-tube sample header made from 9M which was used in the development program is shown in Figure 5-90. From the results of the tube joint fabrication program, the following conclusions were reached:

- The force required to push an unwelded, rolled tube from the header was 3000 lb. After post-weld stress relief, one of the tubes from which the weld was removed required a force of 2635 lb to push it from the header. It was concluded that the joint tightness and strength is not significantly affected by welding and stress relief.

- The weld quality is improved by the tight fit of the tube after rolling.

- Automatic tungsten-inert-gas (TIG) welding was determined to be the best welding technique for the application.

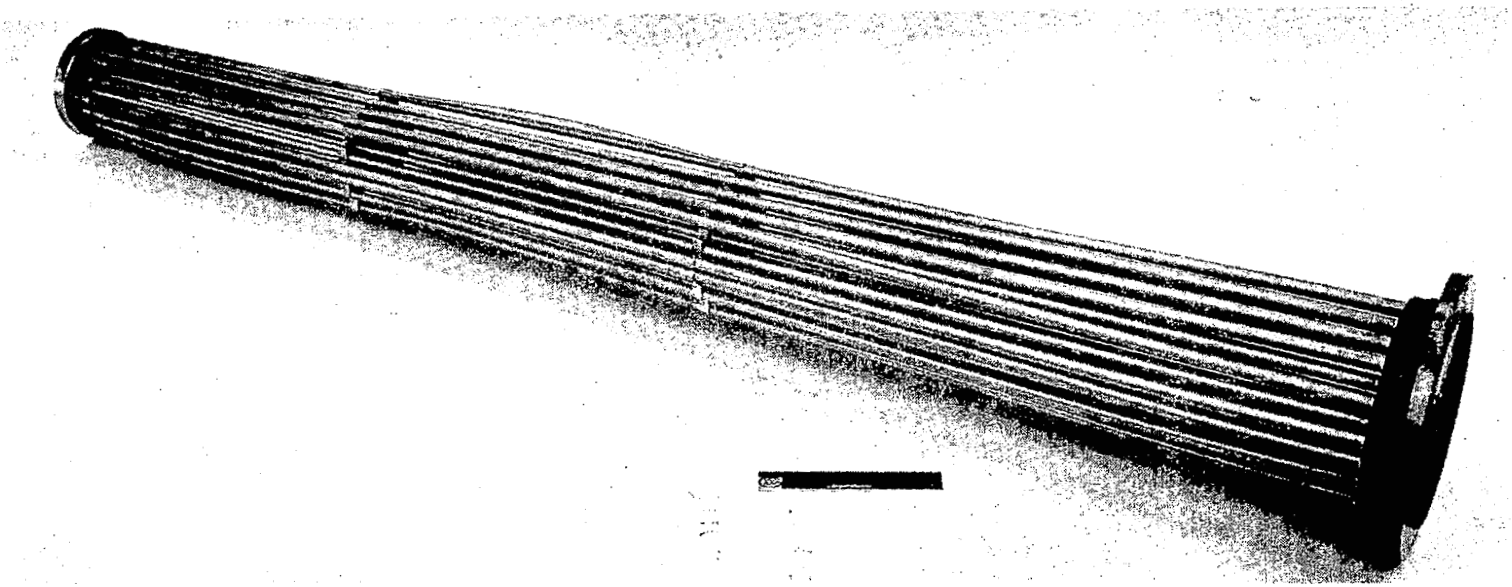

Figure 5-86 Condenser Tube Bundle with Headers Attached

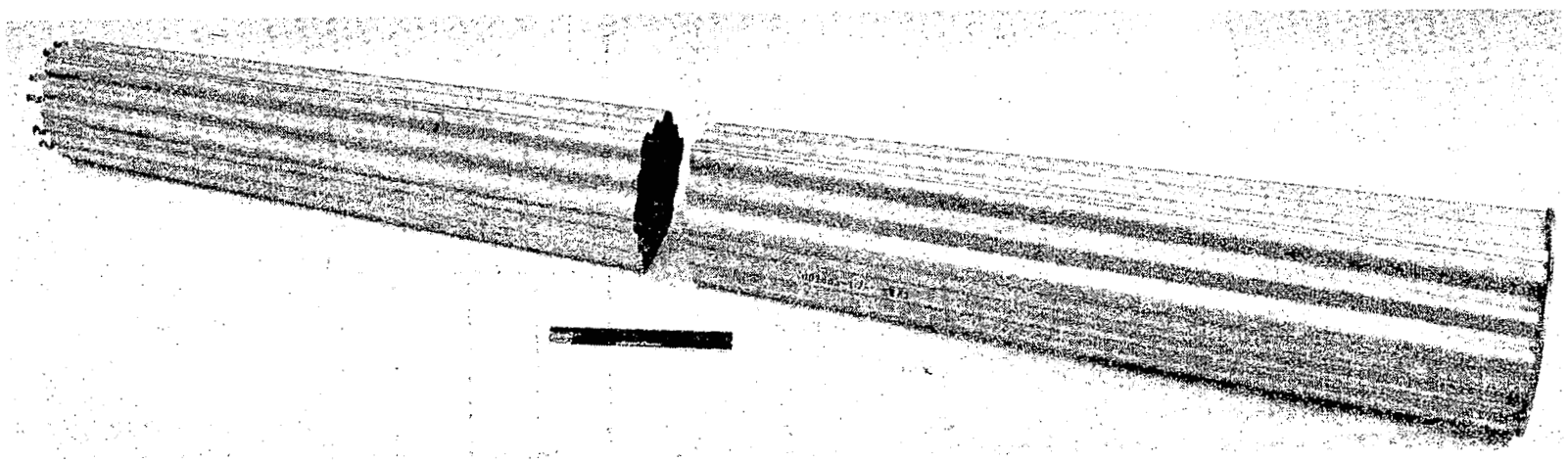

Figure 5-87 Condenser Skirt Assembly

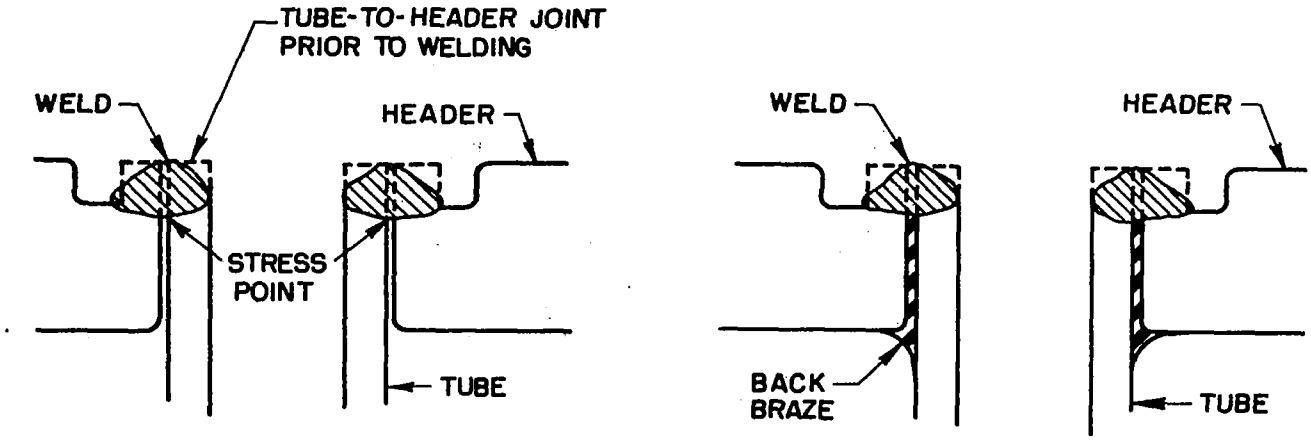

Figure 5-88 Condenser Tube-to-Header Weld and Back Braze Joint

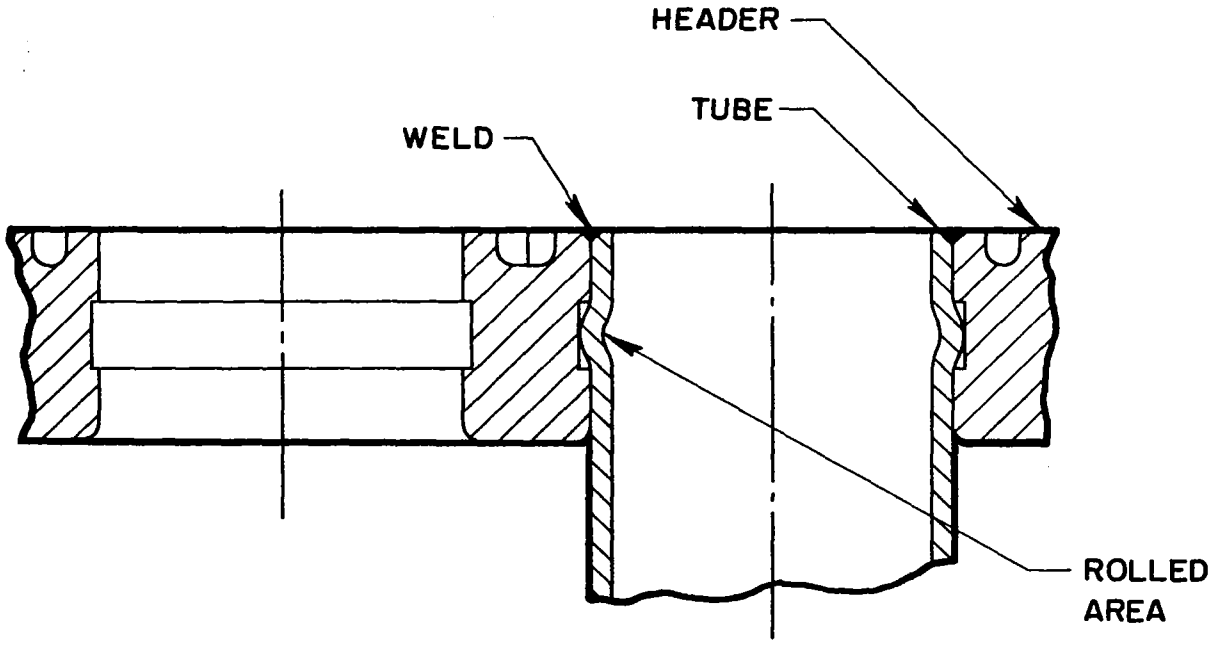

Figure 5-89 Condenser Tube-to-Header Rolled and Welded Joint

A method of gamma radiographic inspection of the tube-to-tube sheet welds, employing radioactive Americium 241, was developed specifically for the inspection of the condenser. A schematic of this inspection technique is shown in Figure 5-91 and uses a source-to-film distance of one-half inch. The method is superior to conventional X-radiography since there is no interference from adjacent tubes to cloud interpretation of the radiograph. Porosity of 0.003-inch diameter was detectable as were cracks in the weld and weld undercutting with representative inspection samples.

Typical, as-fabricated, tube-to-header welds and back-braze of tubes-to-header for the condensers fabricated are shown in Figures 5-92 and 5-93.

5.6.4.4 NaK Inlet and Outlet Manifolds

Both the NaK inlet and outlet manifolds were designed to be fabricated from a two-piece forging joined by a girth weld. They were designed so that they mate with the 3.0-inch OD heat rejection loop piping, and have a four degree slope from the horizontal for drainage of NaK loop fluid. The manifold assembly can be slid over the tapered shell and welded in place. Both manifolds were designed with the same configuration, except that the inlet manifold has a "flow-splitting" vane. The purpose of this vane is to uniformly distribute the entering NaK to the twelve 0.750-inch diameter holes in the shell and thence along the tube bundle.

5.6.4.5 Stress Analysis

Criteria for the stress analysis are given in Table 5-XIX and 5-XX. Maximum values for temperature and pressure were used for the condenser stress analysis and the areas of special consideration are:

- Tube bundle
- Tapered shell
- NaK inlet manifold
- NaK outlet manifold
- Mercury outlet plenum
- Mercury inlet transition

Analyses of the tube bundle and condenser shell natural frequencies for lateral sinusoidal excitation were found to be:

- Tube bundle 110 Hz
- Shell 431 Hz

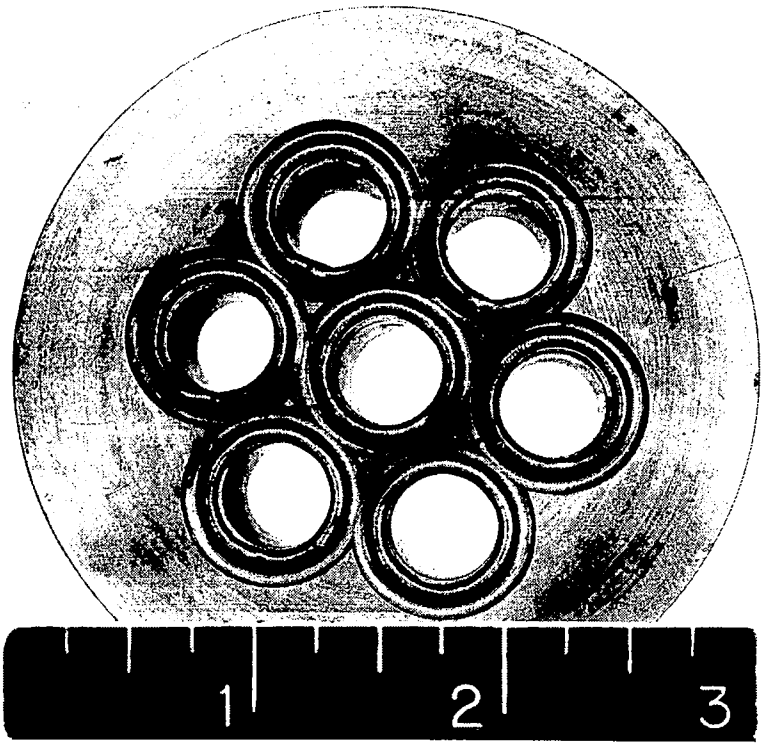

Figure 5-90 Sample Tube-to-Header Welds

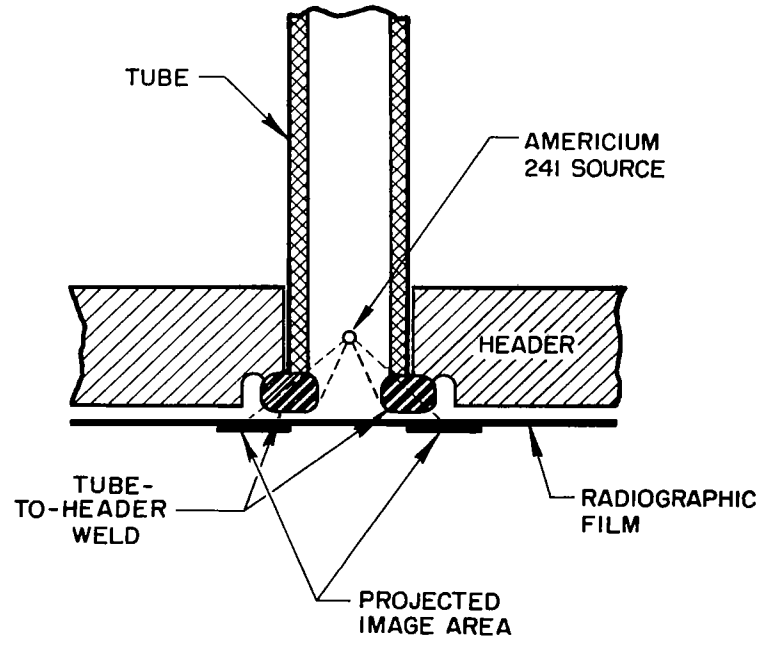

Figure 5-91 Condenser Table-to-Header Weld Inspection Technique

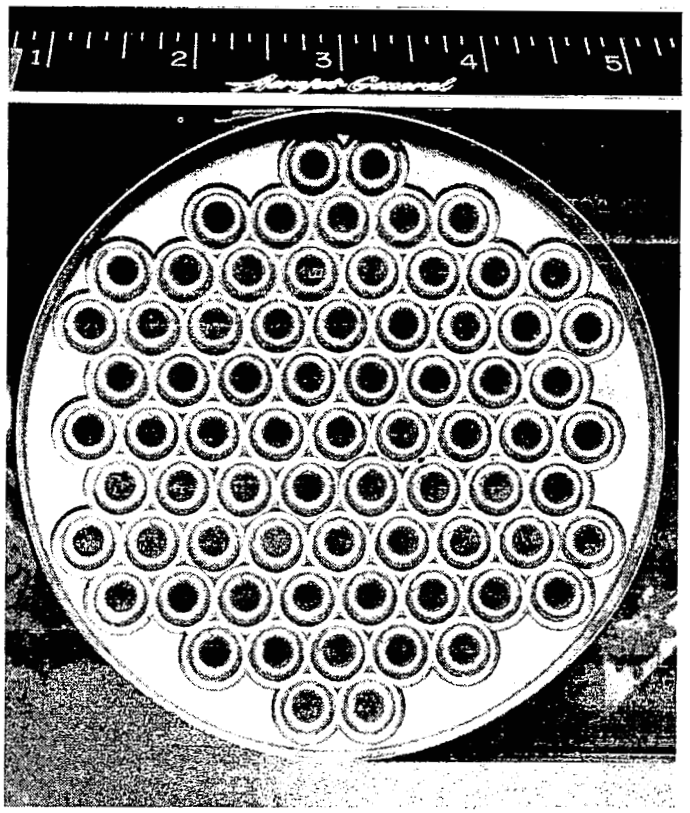

Figure 5-92 Condenser Tube-to-Header Welds

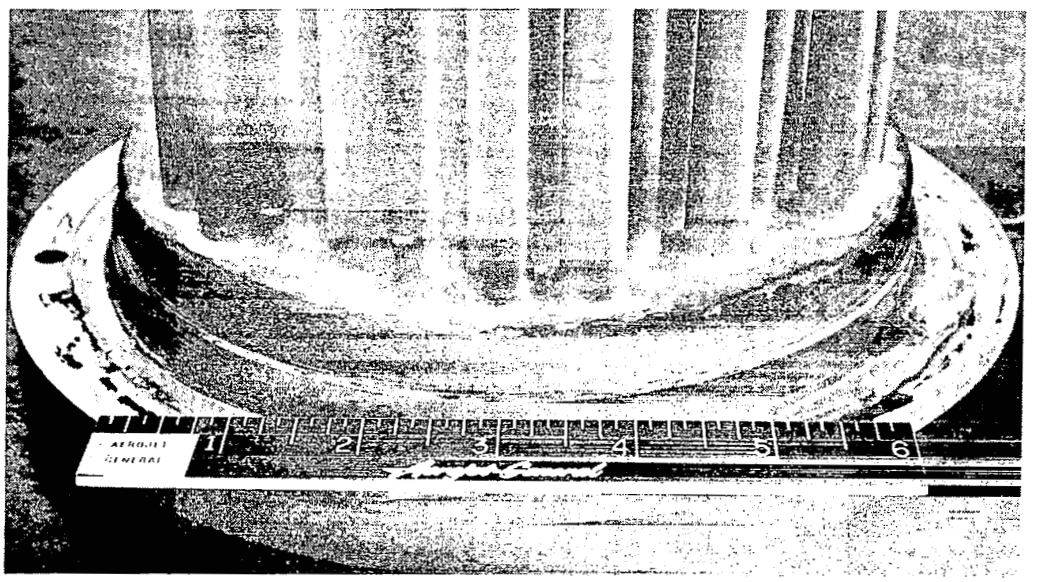

Figure 5-93 Condenser Back-Braze of
Tubes to Header

5.6.5 Thermal and Dynamic Design

5.6.5.1 Preliminary Design Analysis

Selecting a SNAP-8 condenser configuration which would meet the thermal performance requirements of Table 5-XVII required a knowledge of the mercury condensing film coefficient, NaK film coefficient, and stability criteria. A detailed literature review at the initiation of the design effort established the following information.

Based on the data of Reference 56, an average mercury-side heat transfer coefficient of 2000 Btu/hr-ft^2-^{o}F was selected for use in the design analysis. The NaK-side film coefficient for in-line flow through tube bundles was established from Reference 57. Preliminary calculations showed this heat transfer coefficient would vary from about 3000 to 5300 Btu/hr-ft^2-^{o}F.

Two design principles for stability were:

$$B_o = \frac{\rho_\ell g D_t^2}{T} < 15.3$$

where B_o = Bond number

ρ_ℓ = liquid density

g = local acceleration of gravity

T = surface tension

D_t = critical tube internal diameter (at the interface)

From this equation the critical tube internal diameter is $D_t \leq 0.24$ inch. To prevent slug flow, the critical droplet height of the condensate, d, must be less than one-half the local tube diameter, D_t. This condition will be met if the vapor velocity is kept above a minimum value. The relationship between the critical tube diameter and the minimum vapor velocity is:

$$d/D_t = (\text{constant})(We)^{-1} = (\text{constant}) \left[\rho_g v_g^2 D_t/\sigma\right]^{-1} < 1/2$$

where

d = critical droplet height

D_t = local tube diameter

We = Weber number

ρ_g = vapor density

v_g = vapor velocity

σ = surface tension

The constant in the equation is not an exact term and must be determined experimentally, but it is estimated to be between 1.0 and 3.0. However, solving the above equation for the vapor velocity and assuming the constant to have minimum value of 1.0 gives a minimum vapor velicty to prevent slug flow which in turn gives a maximum flow area.

$$v_g > (2.0\ \sigma/\rho_g D_t)^{1/2} = 100 \text{ fps}$$

$$A_g = \dot{W}_g/\rho_g\ v_g, \text{ sq. ft.}$$

The requirement to maintain minimum vapor velocity down the length of the condenser tube to prevent slug flow (and resultant instability) indicated the need to taper the condensing tubes. Figure 5-94 shows the effect on mercury vapor velocity, where the calculated velocity profiles for a straight and tapered tube of equal surface area versus distance from the tube inlet are shown. The tapered tube configuration was selected with the amount of taper being a variable in the configuration selection analysis.

5.6.5.2 Configuration Analysis and Selection

With the basic design information and principles established, a parametric study was made utilizing an IBM 7094 digital computer. The computer program analysis resulted in a number of condenser designs which theoretically met the requirements.

A total of 56 design concepts were analyzed in the computer study, based on the following input data:

Tube inside diameter -

•	at mercury inlet	0.40	0.45	0.50 in. (start of taper)
•	at subcooler inlet	0.125	0.20	0.25 in. (end of taper)
•	at condenser outlet	0.125	0.20	0.25 in.
•	Tube wall thickness	0.020	0.025 in.	
•	Tube pitch*/tube OD at mercury inlet	1.375	1.355 in.	
•	Tube material	Croloy 9M		

* Pitch is defined as the distance between tube centers. The ratio of pitch to tube outside diameter will be noted by P/D ratio.

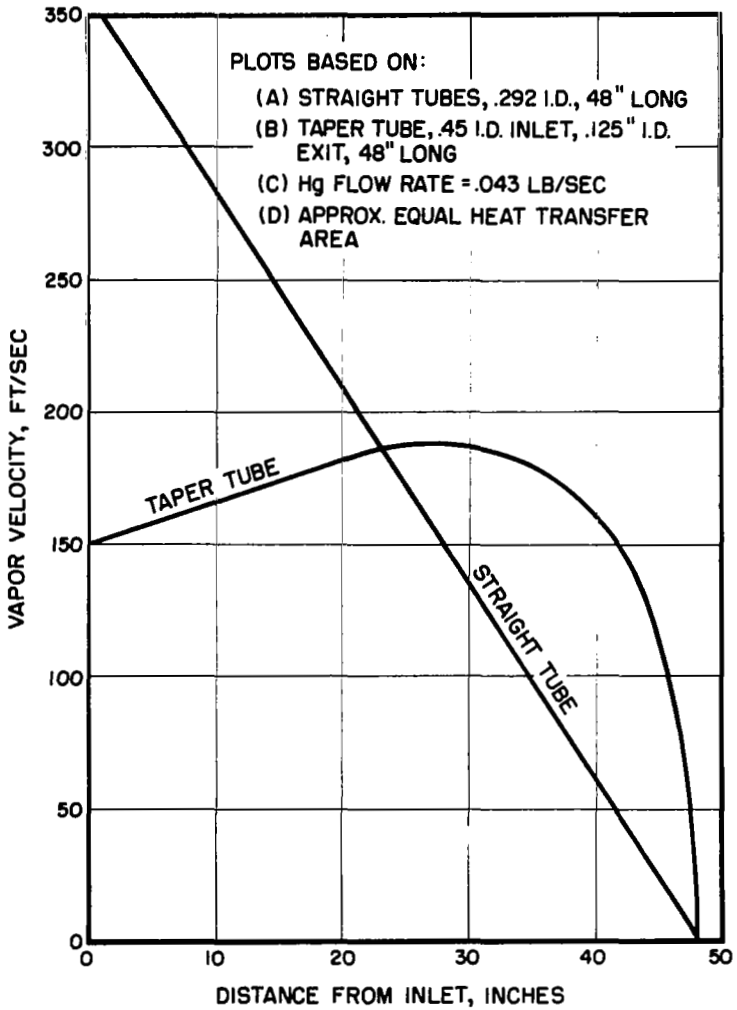

Figure 5-94 Vapor Velocity vs Distance From Inlet for Straight and Tapered Condenser Tubes

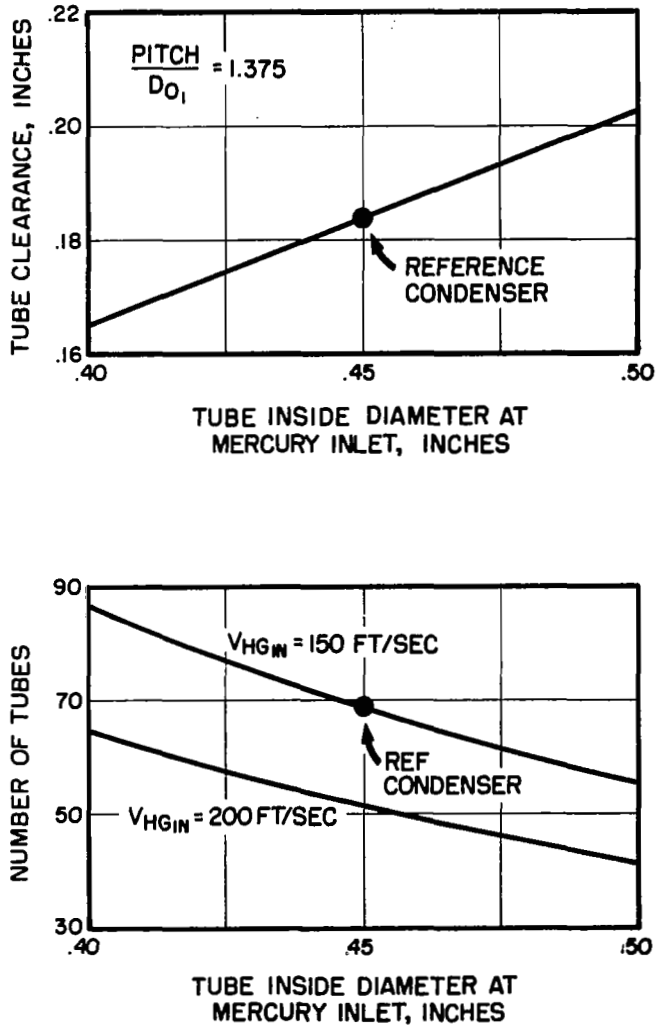

Figure 5-95 Condenser Tube Clearance and Number of Tubes vs Mercury Tube Inlet Inside Diameter

The results of the 56 computer cases are plotted in Figure 5-95 through 5-97 with the selected design point designated in each of the figures.

Figure 5-95 shows the tube clearance, tube diameter and number of tubes as a function of tube inside diameter at the mercury vapor end for inlet velocities of 150 and 200 fps. The number of tubes was increased from the 70 shown to 73 because symmetry was desired with the equilateral triangular array of the tubes in a circular housing. The mercury vapor flow was the nominal design condition of 11500 lb/hr. In Figure 5-96, condenser tapered tube length and pressure drop are plotted versus mercury inlet tube internal diameter for condensing mercury heat-transfer coefficients of 1000, 2000, and 3000 Btu/hr-ft^2-^{o}F, inlet vapor velocities of 150 and 200 fps and subcooler entrance diameters of 0.125, 0.20, and 0.25 inch. Both the tapered condensing length and the mercury pressure drop are strong functions of the condensing film coefficient and the vapor inlet velocity. Condenser heat transfer area (mercury-side) and overall conductance as a function of mercury inlet tube inside diameter are given in Figure 5-97 for an inlet velocity of 150 fps. The graphs show that the condensing heat-transfer has dominance over tube inside diameter in affecting the conductance and heat transfer area. The tapered tube exit diameter had a negligible influence on the condensing area and the overall unit conductance in the condenser.

In summary, the final condenser geometry that was selected is given below:

No. of condensing tubes:	73
Tapered tube length, in.	38.6
Subcooler tube cylindrical length, in.	12.9
Total tube length, in.	51.5
Tube wall thickness, in.	0.030
Tube clearance, in.	0.185
Tube pitch/diameter ratio	1.375
Tube inlet inside diameter, in.	0.450
Tube outlet inside diameter, in. (<0.24 for conservatism)	0.200
Condenser heat transfer area, ft^2	19.8

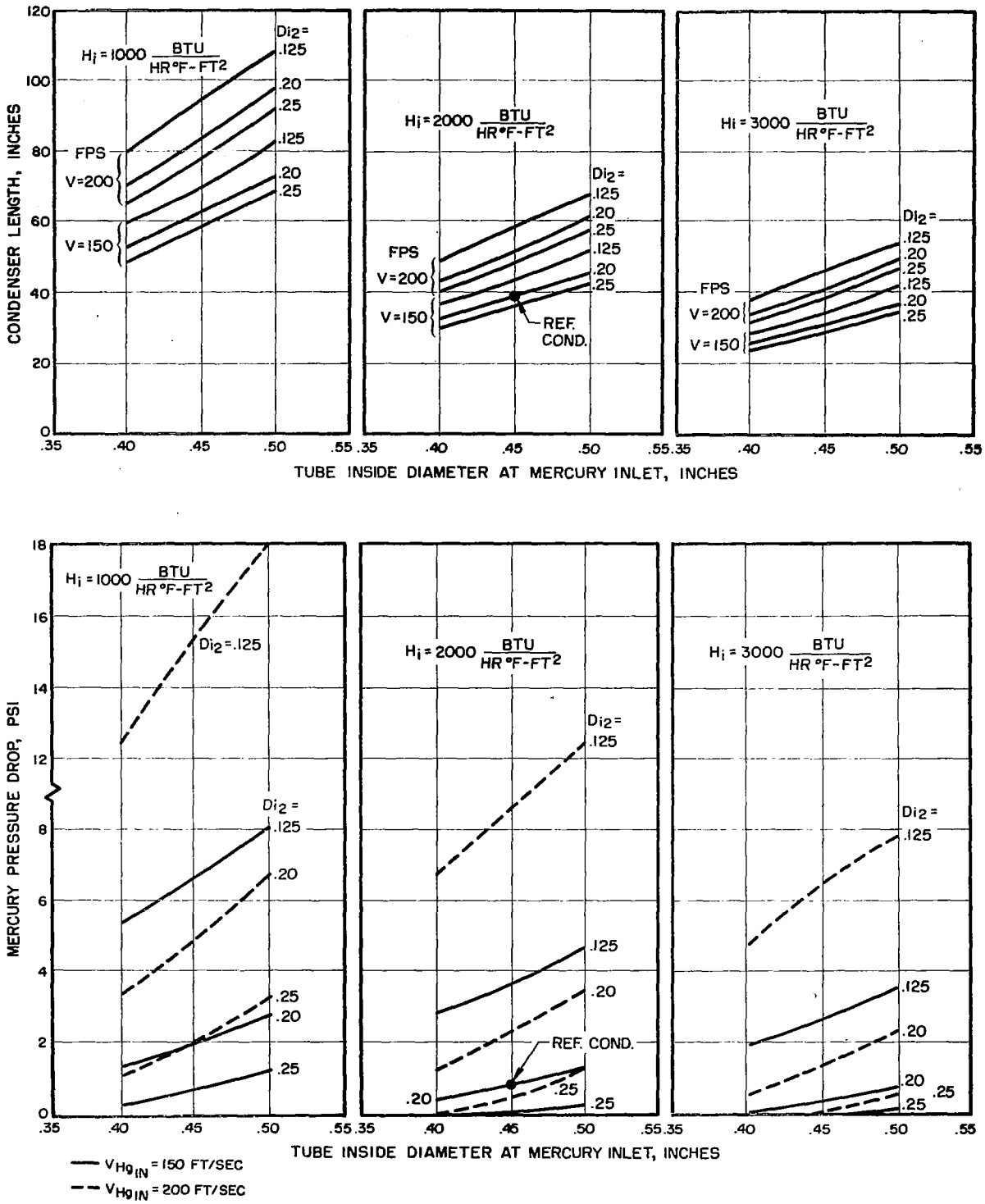

Figure 5-96 Condenser Length and Mercury Pressure Drop Vs Mercury Tube Inside Diameter

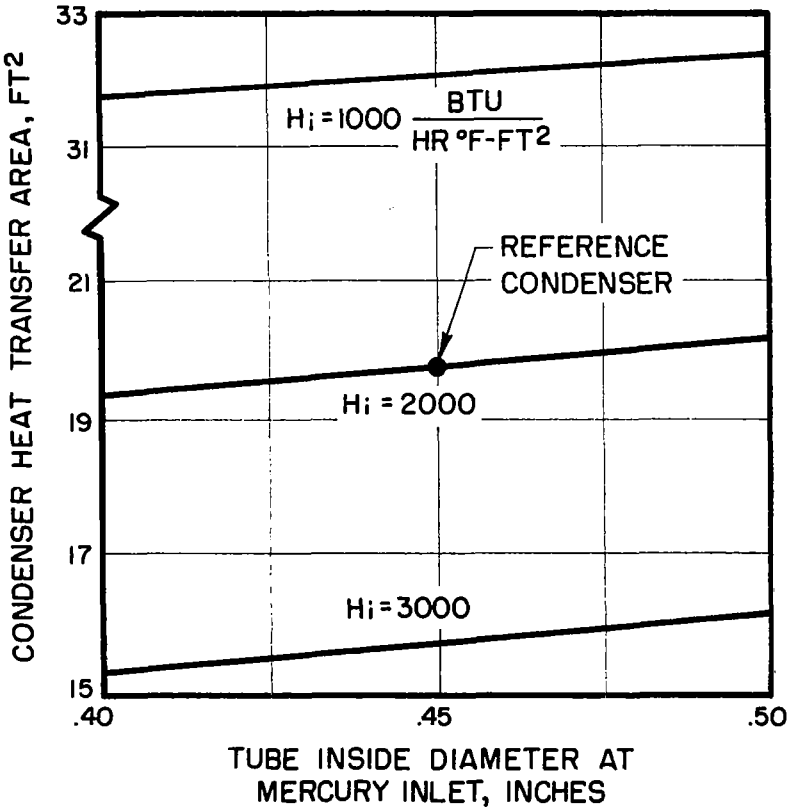

REFERENCE

$V_{HG_{IN}}$ = 150 FT/SEC

D_{O_2} = .20 INCHES

NOTE: HEAT TRANSFER AREA NOT A STRONG FUNCTION OF V_{HG} OR D_{O_2}

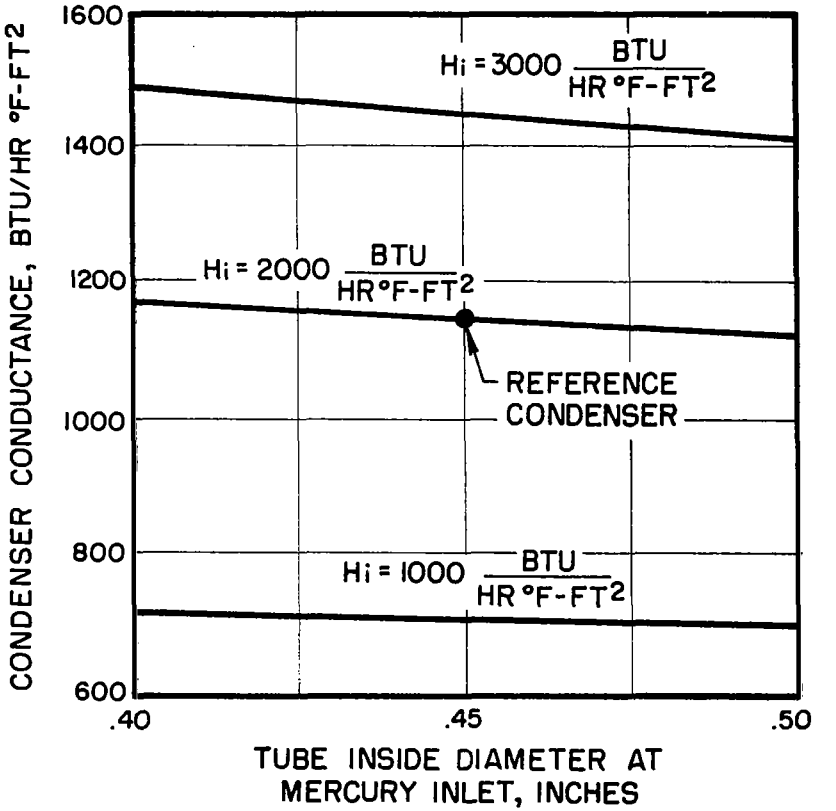

REFERENCE

$V_{HG_{IN}}$ = 150 FT/SEC

D_{O_2} = .20 INCHES

NOTE = CONDUCTANCE NOT A STRONG FUNCTION OF V_{HG} OR D_{O_2}

Figure 5-97 Condenser Heat Transfer Area vs Mercury Tube Inlet Inside Diameter

The heat transfer and dynamic values at design conditions are:

Mercury condensing film coefficient, Btu/hr-ft^2-^{o}F	2000
NaK film coefficient, Btu/hr-ft^2-^{o}F	3000
Overall unit conductance, Btu/hr-ft^2-^{o}F	1044
NaK-side pressure drop, psid	7.0
Mercury side pressure drop, psid	3.0

5.6.5.3 Results of Single-Tube Tests (MECA)

Data were obtained from the NASA-conducted MECA (Mercury Evaporating and Condensing Analysis) program where a single tapered condenser tube of the selected geometry was tested in 1-g and zero-g environments and its performance compared with a condenser tube of constant diameter. The details and results of these tests are reported in Reference 56 and 58. The heat transfer results are summarized and presented below.

The overall heat transfer coefficients or conductances varied from 500 to 1200 Btu/hr-ft^2-^{o}F for the constant diameter tube, compared to values of 1250 to 3700 Btu/hr-ft^2-^{o}F for the tapered tube configuration. Increasing the NaK mass flow and decreasing the condensing length brought about an increase in the overall heat transfer coefficients for both configurations.

The local mercury condensing film coefficients were calculated to be in the range from 1200 to 22,000 Btu/hr-ft^2-^{o}F for the constant diameter tube. The condensing coefficients for the tapered tube were not computed.

Over a condensing length range of 8 to 40 inches, the overall mercury-side static pressure loss went from a 0.5 psi pressure rise to a pressure loss of 3.0 psi, respectively, for the tapered tube configuration. For condensing lengths greater than 40 inches, a choked flow condition was observed in the tapered condensing tube.

When the NaK flow, NaK inlet temperatures and mercury flow were kept constant, the mercury inlet static pressure decreased rapidly as the condensing length was increased to about 25 inches, and then leveled off as the condensing length was increased further. Depending upon the combination of test variables used, the inlet static pressure varied from 8 to 24 psia.

The results of this test program for the tapered tube were extrapolated to the 73-tube condenser design and gave an overall unit conductance of 1900 Btu/hr-ft^2-^{o}F compared to a design value of 1044 Btu/hr-ft^2-^{o}F. The large difference between the two values was attributed

to the value used for the local condensing coefficient in the design calculations which was 2000 Btu/hr-ft^2-^{o}F. Extrapolation of the MECA condensing coefficients of a straight tube to the tapered tube gave an average mercury condensing film coefficient of 147,000 Btu/hr-ft^2-^{o}F. Consequently, the condensing film offers relatively no thermal resistance and the total heat transfer conductance is governed mainly by the Nak-side film coefficient and the wall resistance.

5.6.6 Interfaces

The SNAP-8 system is expected to experience the effects of several types of tolerance variations which include the particular component performance tolerances. The purpose of the condenser in the SNAP-8 system, other than to condense mercury vapor, is to provide a back pressure on the turbine and an adequate net positive suction head (NPSH) for the mercury pump. An excessively low condensing pressure and corresponding temperature will result in an NPSH value below the 1.0-ft limit and cause mercury pump cavitation. A condensing pressure higher than the system requires will result in a turbine power output reduction. This condition can be caused by noncondensible gas buildup in the condenser, by variation of condensing length due to condenser heat transfer degradation, and by shifts of mercury inventory to or from the condenser. Noncondensible gases from other parts of the system collect in the condenser since the vapor-liquid interface separates the gas from the vapor; because of the low pressure, the gas occupies a significant volume. This can cause an increase of the condenser inlet pressure and a degradation of turbine efficiency.

5.6.7 Demonstrated Performance

5.6.7.1 One-g Performance

An extensive performance mapping of the condenser was conducted at design and off-design conditions which defined the condenser operating limits with the tapered tube configuration (Reference 26). The ranges of variables tested are listed below:

Range of Test Variables	
Mercury flow, lb/hr	8000 - 12000
NaK flow, lb/hr	30000 - 50000
NaK inlet temperature, ^{o}F	200 - 500
Condensing Pressure, psia	2.5 - 18.0
Mercury inlet quality, %	90 - 98

Of particular interest were condensing pressure, heat transfer, mercury pressure drop and stability, specifically at certain off-design conditions extending to choked-flow. During the data analysis, it became apparent that an improvement in the previous mathematical equations used to define condenser performance was necessary especially at far off-design conditions of choked-flow. Reference contains the details of the new correlations which simultaneously evaluate changes in mercury pressure, temperature, quality, pressure drop, NaK temperature, and NaK flow. The two correlating equations that define the condenser operation for any condition are presented below:

$$T_{SAT} = \frac{\dot{W}_L \lambda X}{(C_{PN}\dot{W}_N - C_{PH}\dot{W}_L} \left[\frac{1.0}{1 - e^{-UA/C_{PN}\dot{W}_N}}\right] + T_{Ni} \quad {}^{o}F$$

and

$$UA = 4.26\dot{W}_L \left[1.0 - \frac{2.81\dot{W}_N}{10^5} + \frac{2.89\dot{W}_N^2}{10^{10}}\right] \left[1.0 - \frac{7.04\ T_{Ni}}{10^3} + \frac{1.76\ T_{Ni}^2}{10^5}\right] \left[1.0 + \frac{10^6}{4.17\ T_{Ni}^3}\right]$$

where

T_{SAT} = Condensing temperature, ^{o}F

T_{Ni} = NaK inlet temperature, ^{o}F

$\dot{W}_L$ = Liquid mercury flow, lb/hr

$\dot{W}_N$ = NaK flow, lb/hr

λ = Mercury latent heat of vaporization, Btu/lb

X = Mercury vapor quality

C_{PN} = NaK specific heat, Btu/lb-^{o}F

C_{PH} = Mercury specific heat, Btu/lb-^{o}F

UA = Heat transfer coefficient, Btu/hr-^{o}F

The effects of choked-flow and/or temperature potential loss are contained in the equation for UA. It is significant to note that regardless of the heat transfer variation caused by chocked-flow and temperature potential loss, the product UA remains essentially a constant.

A carpet plot of condensing pressure variation with NaK flow, mercury flow and NaK inlet temperature is shown in Figure 5-98. The test data are also shown (indicated by open circles) and demonstrate good agreement with the correlating equations shown by the dashed lines. An interesting feature of the plot is that, for each mercury flow, a minimum condensing pressure is reached as the NaK temperature is lowered, regardless of NaK flow. Also shown in the figure is the predicted condenser performance at the most recent power system state point. Theory predicts that the condenser will operate with a 5-psia condensing pressure (the requirement is 8 psia) and, therefore, is satisfactory.

The NaK-side temperatures measured at five different NaK inlet temperatures with constant NaK flow and mercury flow are plotted versus condenser length in Figure 5-99. Each lower NaK-inlet temperature represents condenser conditions approaching choked flow where the condensing length is something less than ten inches. It is apparent that a point is reached where the available condensing length cannot be used and the condensing regime is confined to a small length of the condenser.

Figure 5-100 presents the derived data for the mercury-side pressure drop with condenser outlet pressure (mercury pump suction pressure) as a function of condensing pressure, condensing length and mercury flow. The curves are corrected for the liquid mercury head and represent zero-gravity operation. The condenser model, defined by the above equations, was used to derive the absolute vapor pressure drop data in conjunction with the observed changes in vapor pressure drop during the tests (see Reference). In determining the absolute pressure drop values, liquid hold-up on the tube walls due to choked-flow was considered and found to increase as operating conditions approached choked-flow conditions.

Condenser instability is attributable to choked-flow operation and the resultant liquid holdup that occurs above the vapor-liquid interface. Velocities in this area are inadequate to move the condensed liquid film to the interface. Therefore, accumulations of liquid above the interface would result in slug-flow which would cause interface instability, especially in zero gravity.

5.6.7.2 Predicted Zero-Gravity Performance

The aforementioned test results and observations are now applied to the operation of the SNAP-8 condenser at different power conversion system state points. These state-points are:

State Point	Hg Flow (lb/hr	Condenser Pressure (psia)	NaK Flow (lb/hr)	Hg Temp. (in) (°F)	NaK Temp. (in) (°F)
1*	11,000	15.5	35,000	680	495
2	12,300	14.0	40,000	669	457
3	14,000	8.0	47,500	616	417
4*	7,000/ cond.	2.5	28,000/ cond.	520	350

At each of these state points, general aspects of expected zero-gravity performance is compared to the one-g operation.

a. State-Points 1 and 2.- The thermal performance was excellent as demonstrated over 16,274 hours of operation. Figure 5-98 shows that the 15.5-psia condensing pressure at a NaK flow of about 35,000 lb/hr can be achieved and that the design criteria used for predicting heat transfer were good. The mercury-side pressure drop is shown in Figure 5-100 and it shows that, for a range of condensing length (15 to 35 inches), the outlet pressure ranges from 12.0 to 15.0 psia. Therefore, the mercury-side pressure drop ranges from a pressure loss of 1.5 psi to a pressure recovery of about 0.3 psi which is adequate for either one-g or zero-g operation. These values of pressure drop indicate that the condenser has no excess liquid holdup and the interface is stable in either gravity of zero-gravity environments.

For state-point 2, good thermal performance was again demonstrated by the condenser. The mercury-side pressure drop range was a pressure loss of 1.7 psi to a pressure recovery of 0.5 psi which is acceptable for both a one- and zero-gravity operational environment. Operation at this state point indicated that the vapor-liquid interface was stable.

b. State-Point 3.- A major change was made in the power conversion system state point in order to obtain a net usable electrical output greater than the 35-kWe at the old state point. This change required the condenser to operate with a condensing pressure of 8.0 psia with a mercury flow of 14,000 lb/hr. The thermal performance of the condenser, shown in Figure 5-101 indicates that the condenser is adequate for operation at this new set of conditions. A considerable loss of mercury temperature (due to pressure drop) is quite evident from the mercury temperature profile, however there is some recovery of temperature and pressure. From the heat transfer viewpoint the condenser is satisfactory for both one-g and zero-g environments.

---

* Condenser design point
** 2 condensers in parallel (90-kWe SNAP-8 system)

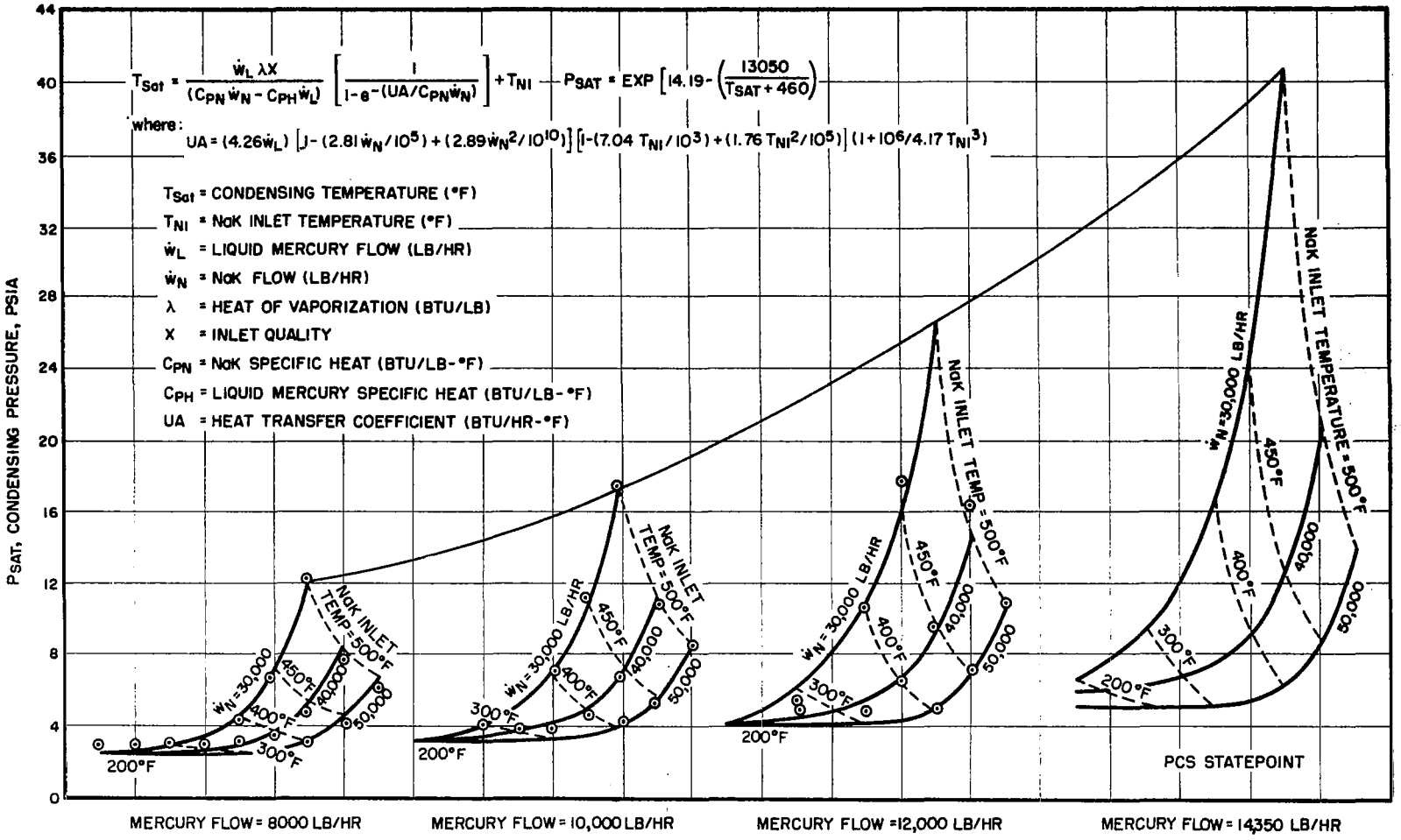

Figure 5-98 Condenser Carpet Plot - Condensing Pressure Variation with NaK Flow, Mercury Flow, and NaK Inlet Temperature

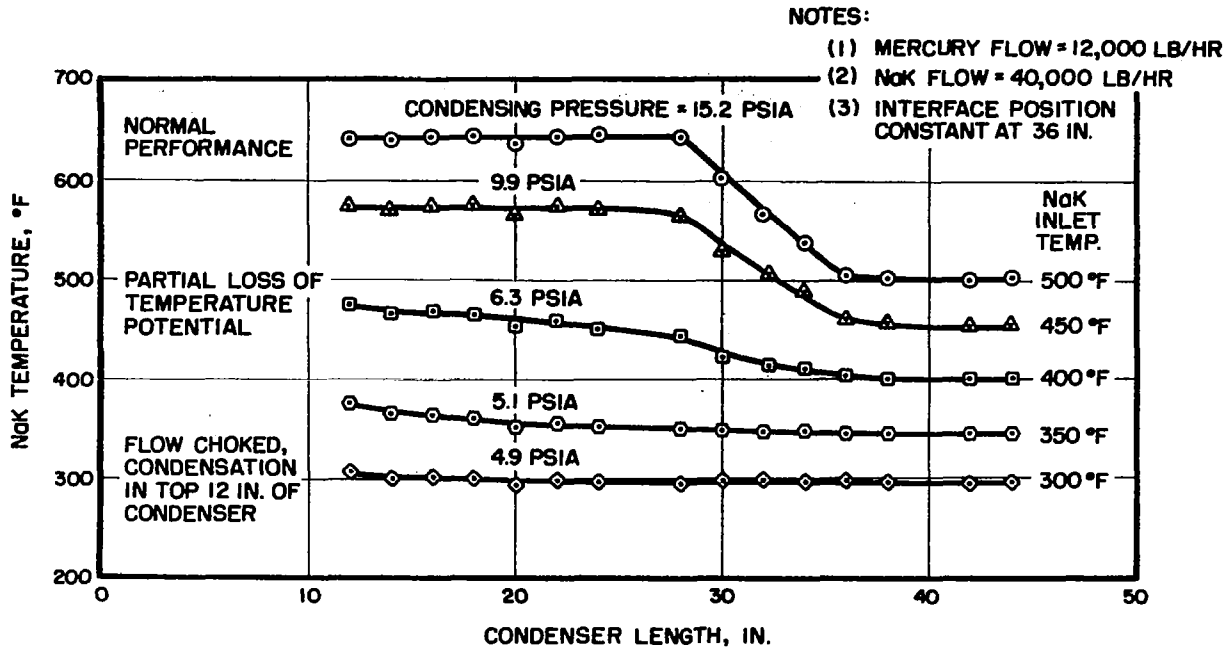

Figure 5-99 Condenser NaK-Side Temperature vs Condenser Length (Mercury and NaK Flow Constant)

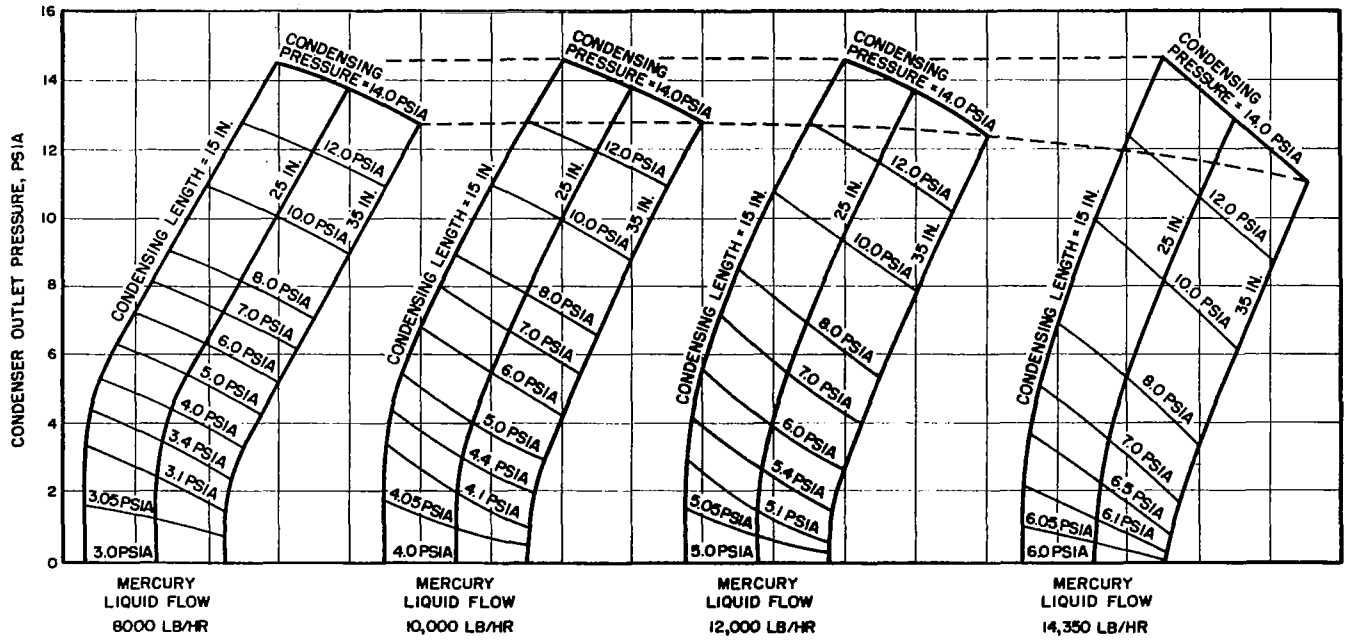

Figure 5-100 Condenser Carpet Plot - Mercury Outlet Pressure vs Mercury Flow at Various Condensing Lengths and Condensing Pressures

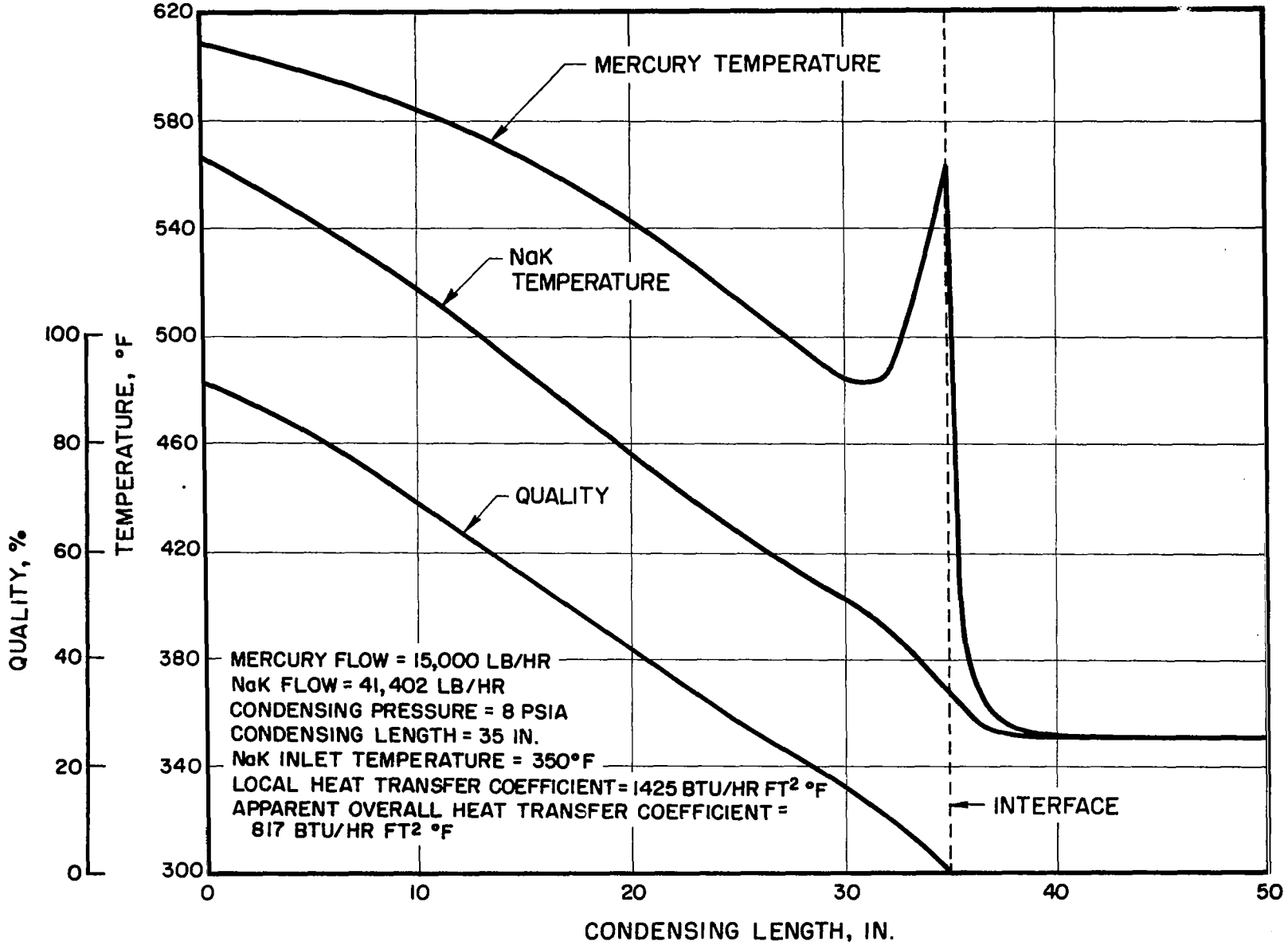

Figure 5-101 Condenser Mercury Quality and Temperature vs Condensing Length

The condenser mercury-side pressure drop at this operating point was 1.0 psi to 4.5 psi for condensing lengths of 15 and 35 inches, respectively. This is a limitation of zero-g operation since the condenser cannot provide the minimum mercury pump suction pressure of 6.5 psia unless the condensing length is kept below 18 inches. However, the condenser is acceptable for one-g operation over the condensing lengths specified. No indications of choked flow were observed during one-g operation at the 8.0-psia condensing pressure. Stability also becomes a problem due to the necessity of maintaining a short condensing length in zero-g operation. At about 18 inches from the inlet tube sheet, the tube internal diameter is 0.35 inch which violates the stability criterion of a maximum diameter of 0.24 inch. It is concluded that the condenser would be unstable in zero-gravity at the 8 psia condition.

c. State-Point 4.- There are no test data from the 35-kWe test system to indicate that the condenser can operate at 2.5 psia with a 7000 lb/hr mercury flow. This operating condition coincides with the 90-kWe system design point wherein two condensers were planned to be placed in parallel (see Figure 5-82). The closest approach in testing was a mercury flow of 8000 lb/hr which permitted a minimum condensing pressure of about 8.0 psia. All predictions had to be based on the mathematical model. The model predicts that the 2.5-psia condensing pressure is possible with the existing condenser (slight modification to reduce entrance losses) with a NaK inlet temperature of 350°F and a NaK flow of about 28,000 lb/hr. These NaK conditions are somewhat arbitrary. The condenser is so choked that lowering the NaK temperature or raising the NaK flow would have basically negligible effect on the condensing pressure; they represent minimum requirements necessary to achieve the 2.5 psia. Thermally, the condenser is capable of 2.5 psia in either one-g or zero-g environments.

The condenser pressure drop is excessive because of the choked-flow condition. In one-g operation, it does not matter because of the liquid head available; but in zero-g operation, the condenser is unsatisfactory; unless, of course, the liquid level is again raised to the point that condensation is restricted to the top few inches of the condenser. There are no test data with which to predict what this liquid-level would have to be. The 35-kWe system data do indicate, however, that the condensing length might have to be less than 10 to 15 inches, which was the limiting value of testing. For a more typical condensing length, the entire 2.5-psia condensing pressure would most likely be lost in pressure drop.

Because of the choked flow, the interface is assumed to be unstable. Data at 3.0 psia and 8000 lb/hr showed inventory holdup, which is assumed to be a symptom of possible interface instability. Therefore, the condenser would be satisfactory in one-g operation, but not in zero-g operation. Because of the pressure drop, the condensing length would have to be small which would violate the basic stability criterion of maximum tube diameter.

The following items summarize the thermal and dynamic capabilities of the condenser for one-g and zero-g operation:

- At the 15-psia design condition, the condenser is satisfactory with respect to thermal performance, pressure drop, and interface stability. It is satisfactory for both one-g and zero-g operation. It is capable of condensing pressure adjustment by inventory control.

- At the 8 psia operating condition, the condenser is thermally acceptable in both one-g and zero-g. The pressure drop is unacceptable in zero-g unless very high inventory levels are used. In one-g operation, it is acceptable. The necessary short condensing length to control pressure drop would cause interface instability in zero-g use. Condensing pressure control by means of inventory control would be poor in both one-g and zero-g operation.

5.6.7.3 Shock and Vibration Test Results

The purpose of the environmental shock and vibration tests (performed at NASA-LeRC) was to evaluate the condenser structural design at the levels that are expected during system launch, and maneuvering modes in space. NASA specification 417-2, Rev. C, was used as a guide in performing the tests on the condenser. Sinusoidal, random and shock tests were conducted along the three mutually perpendicular axes. Reference 59 describes the test procedures and results pertaining to the pre- and post-test quality conformance, mounting, instrumentation and the dynamic responses of the condenser structure.

Prior to the environmental tests, the condenser was inspected to establish a reference as to its structural integrity, configuration and hydraulic performance. The following procedures were used in their listed order.

- Hydraulic flow test of both NaK and mercury circuits with water.

- Proof pressure test at 275 psia

- Helium leak check per MIL-STD-271

- Dye penetrant inspection of the external welds per MIL-I-6866

- Radiographic inspection of the tube bundle position per MIL-I-6866

During the shock and vibration tests, the condenser would be in a nonoperating state simulating launch conditions, i.e. the mercury-side would be void of fluid, while the NaK-side would be filled. The fluid used to simulate NaK in the condenser was an oil whose density at 70°F is 47.1

compared to 50.1 for NaK at 600°F. The condenser was mounted on an all-aluminum support fixture as shown in Figure 5-102 and instrumented with 10 uniaxial accelerometers, also shown. Accelerometers 9 and 10 cannot be seen as they are located in two central tubes about 13.0 inches in from the mercury inlet header. Also indicated in the figure are the axis designations for the system to which all inputs and responses are referenced.

a. Sinusoidal Vibration.- The condenser was excited with frequencies ranging from 20 to 2000 Hz with a 1.0-g peak acceleration amplitude and a sweep of one octave per minute along each of the three orthogonal axes. Resonant response of the condenser shell occurred at 145, 280, 440, and 900 Hz for the Y-axis and 100, 230, 470, and 800 Hz for the Z-axis. The maximum amplification occurred at the two lowest frequencies with a value of 9.0 acting at a point 27 inches from the support at the small end of the condenser. The tube bundle had the same resonant frequencies as the shell with maximum amplification factors of 9.0 for the Y-axis and 10.0 for the Z-axis at frequencies of 150 and 95 Hz, respectively. The values given above are for responses measured in the same direction as the excitation.

System damping was estimated from the response at the lowest frequencies of 100 to 145 Hz. The fraction of critical damping was between 0.044 and 0.050 inches at the half-power point. It was also observed that the condenser behaves as a fixed-fixed beam or a fixed-hinged beam.

b. Shock.- Shock loading was applied to the condenser (along the three axes in both directions) in the form of a half-sine pulse with a 12-g peak acceleration amplitude and an eleven millisecond duration. The maximum shell response was 20-g in the same axis as the input for both the Y and Z axes (for both directions) at a point 10 inches from the support at the large end of the condenser. The tube bundle responses were equal to those measured on the shell with values of 19 to 20 g for the Y and Z axes.

The calculated dynamic load factors for the shell and tube bundle were 1.67 and 1.58, respectively, for the data given above. The relative displacements of the shell and tapered tubes were computed from the peak responses and the first mode natural frequencies. The resultant values were 0.0176 inch for the Z-axis and 0.010 inch for the Y-axis (response in the same direction as the shock load) for the shell, and 0.010 inch for the tapered tubes. The value obtained for the tapered tubes is approximately 1/20 of the tube spacing; therefore, it is concluded that there is no danger of the 9M tubes hitting one another.

c. Random Vibration.- Responses of the condenser were to be determined over a frequency range of 20 to 2000 Hz to random vibration having an overall level of 20-g root mean squared (rms). The acceleration density was distributed over the frequency range as follows:

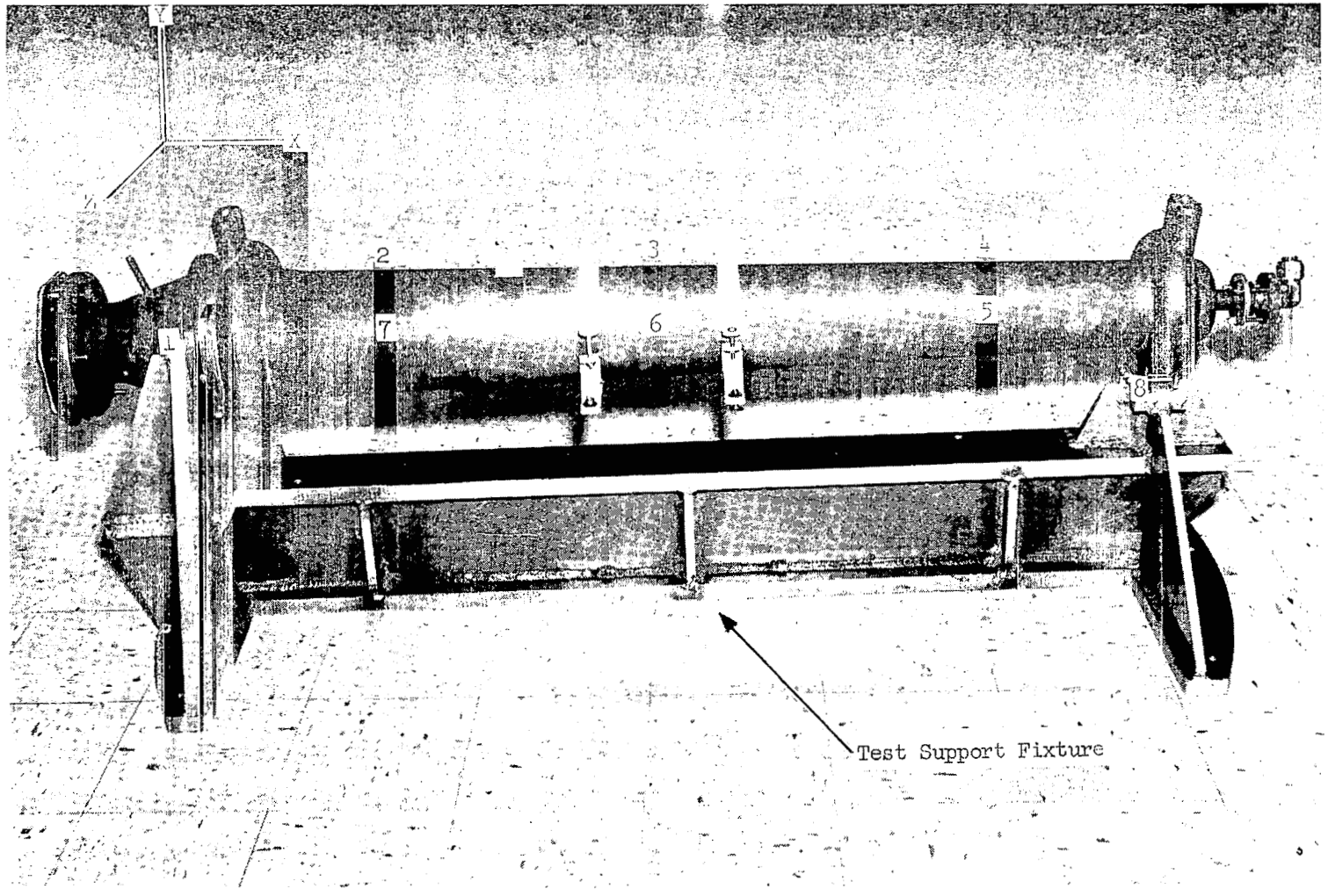

Figure 5-102 Condenser Mounted in Vibration Test Fixture

20 to 100 Hz - 3.0 dB/octave, increase

100 to 600 Hz - 0.4 g^2/Hz, constant

600 to 2000 Hz - 6.0 dB/octave, decrease

This procedure was followed for each perpendicular axis. The tolerances for acceleration density were +100 and -50% for the 0.4g^2/Hz level. The frequency analyzers used had a bandwidth of 25 Hz.

Most of the maximum responses occurred between 100 and 150 Hz with the remaining responses scattered between 160 and 195 Hz. Values of the shell acceleration density responses in the same axis as the input varied from 0.8 to 1.70 g^2/Hz for the Y-axis and 1.3 to 2.20 g^2/Hz for the Z axis at frequencies of 100 to 120 Hz. Responses recorded for the 9M tubing were 1.0 to 1.20 g^2/Hz for the Y and Z axes and at 100 to 105 Hz, respectively.

The computed relative-mean squared (Yms) displacement value in the Y direction for the maximum response of the tube bundle was 0.023 inch at 105 Hz, if it is assumed that the instantaneous acceleration of the input is Gaussian. That is, 0.3% of the time the instantaneous peak acceleration is greater or equal to three times the rms value. Then the maximum relative displacement would be 3 (0.023) = 0.069 inch. If the tube clearance is 0.192 inch as specified, then the minimum clearance for a condition where any two adjacent tubes were displaced in opposite directions would be:

$$\text{minimum clearance} = 0.192 - 2.0(.069) = 0.054 \text{ inch}$$

Hence, it is predicted that, unless the tubes were bent during fabrication to the point where the clearance is reduced to less than 0.138 inch, the possibility of two adjacent tubes colliding is remote.

Subsequent to the shock and vibration tests, the condenser was again subjected to the quality conformance inspection outlined previously. The results of this inspection verified that the condenser had withstood the imposed environmental conditions without detrimental effects. Other conclusions that were reached from the results of these tests were:

- The present condenser design is acceptable for use in a system and is capable of withstanding the vibrational loading specified.
- From a structural aspect, the materials and fabrication procedures are adequate for the application.
- The fluid dynamics of the condenser would not be appreciably changed by vibrations and shocks imposed on it during launch conditions.

- Maximum responses of the condenser, both shell and tube bundle, are experienced between 100 and 150 Hz.

- Filling the NaK-side of the condenser prior to launch and/or maneuver phases of the system adds to the inherent structural damping and serves to reduce the condenser responses.

5.7 OTHER MECHANICAL COMPONENTS

The mechanical components described in this section of the report were in various stages of development when the SNAP-8 program was terminated. The components and development status are summarized below.

(1) Intermediate Loop Heat Exchanger.- A conceptual design was prepared and design requirements were formulated. No hardware was built or tested.

(2) Auxiliary Heat Exchanger.- A heat exchanger was designed, built, and tested for the 35-kWe system. However, failures in the shell and the new requirement for a dual heat rejection loop and double-containment dictated a new heat exchanger design which was built but never tested. No concept or design parameters were formulated for the 90-kWe system.

(3) Mercury Flow Control Valve.- A valve was designed, built and tested for the 35-kWe system. This valve operated throughout the program, from 1966 through midyear 1970. The basic design is considered acceptable for the 90-kWe system with some modifications to the valve orifice shape and changes in the speed of opening and closing.

(4) Heat Rejection Flow Control Valve.- Conceptual designs and design parameters were formulated, but no units were built or tested for the 90-kWe system. A design used in the single start 35-kWe system was controlled by temperature and not flow, so its test experience was not applicable to the new concept.

(5) NaK Diverter Valves.- This valve was designed and built for the 35-kWe system but was never tested. The valve for the 90-kWe system would have been of the same design except slightly larger to accommodate the higher NaK flows.

(6) Solenoid Valves.- The valves designed, built, and tested during the SNAP-8 35-kWe system development program were similar to the valves planned for the 90-kWe system except that the method of latching was slightly different and the size of the solenoids was greater for the latter valves. The design requirements and conceptual designs of the valves for the 90-kWe system were formulated but no hardware was built or tested.

(7) Expansion Reservoirs.- Conceptual designs and design parameters for three of the eight expansion reservoirs required for the 90-kWe system were completed. However, no hardware was built or tested.

(8) Mercury Injection System.- A system was designed, built and tested for the 35-kWe single-start SNAP-8 system. This test experience was applied to the conceptual design and formulation of the design parameters for the 90-kWe system. The mercury injection system for the 90-kWe system was not built or tested.

The above components are considered undeveloped only in the sense that they were never built for or tested in a 90-kWe system. As can be seen, components (2), (3), (6) and (8) above were tested in the 35-kWe system and the results were applicable to later designs for the 90-kWe system to varying degrees.

5.7.1 Intermediate and Auxiliary Heat Exchangers

5.7.1.1 Intermediate Heat Exchanger

The function of the intermediate heat exchanger (IHX) in the 90-kWe system, as shown in Figure 5-103, is to provide the capability of separating the power conversion system from the reactor primary loop, yet transfer heat from the reactor to the boiler with the minimum heat loss. The IHX also serves the function of separating the radioactive NaK in the reactor primary loop from the NaK in the intermediate loop which allows the development testing of the power conversion system and replacing of power conversion system components without the need for radioactive decontamination.

a. Preliminary Design Concepts.- Initial design analyses were conducted to determine the feasibility of fitting a tube-in-shell configuration IHX in the gallery section of the 90-kWe system. Reactor primary loop NaK flows through the shell of the heat exchanger and intermediate loop NaK flows through the tubes. Design maps were generated for tube pitch-to-diameter ratios (and an equilateral triangular array of tubes) of 1.20, 1.35, and 1.50. These ratios were chosen because they compared with a pitch-to-diameter of 1.375 for the SNAP-8 condenser. A typical design map is shown in Figure 5-104 which presents minimum shell diameter as a function of the number of tubes with the tube ID as an independent variable. Lines of constant tube length and constant tube-side pressure drop are also cross-plotted. The maps permitted the selection of a heat exchanger size that would "best-fit" in the 90-kWe system gallery. The requirement for a $10^{\circ}F$ terminal temperature difference dictated a heat exchanger with an effectiveness of 0.95. The required UA was 1.95×10^5 Btu/hr $^{\circ}F$.

Consideration was also given to compact heat exchanger concepts and to separable heat exchangers. Separable heat exchangers are desirable for incorporation in long-term space mission applications where hardware replacement can extend mission life. A typical design concept of a separable heat exchanger is shown in Figure 5-105. A tradeoff study was performed to permit a selection between a compact and a tube-in-shell IHX. A preliminary design for each concept was prepared and, based on this effort, the tube-in-shell approach was recommended. The reasons for selecting the tube-in-shell approach were as follows:

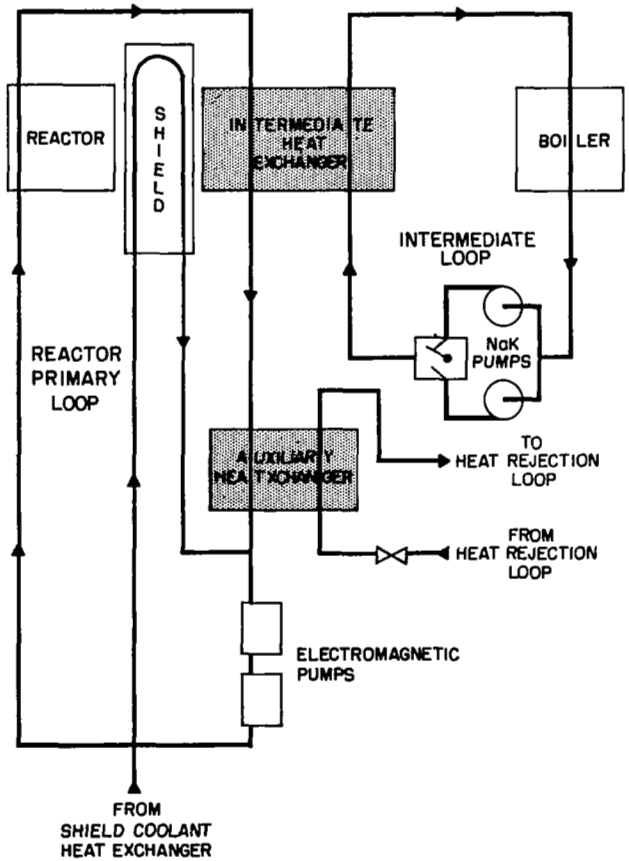

Figure 5-103 90-kWe System Schematic Showing Location of Intermediate Heat Exchanger and Auxiliary Heat Exchanger

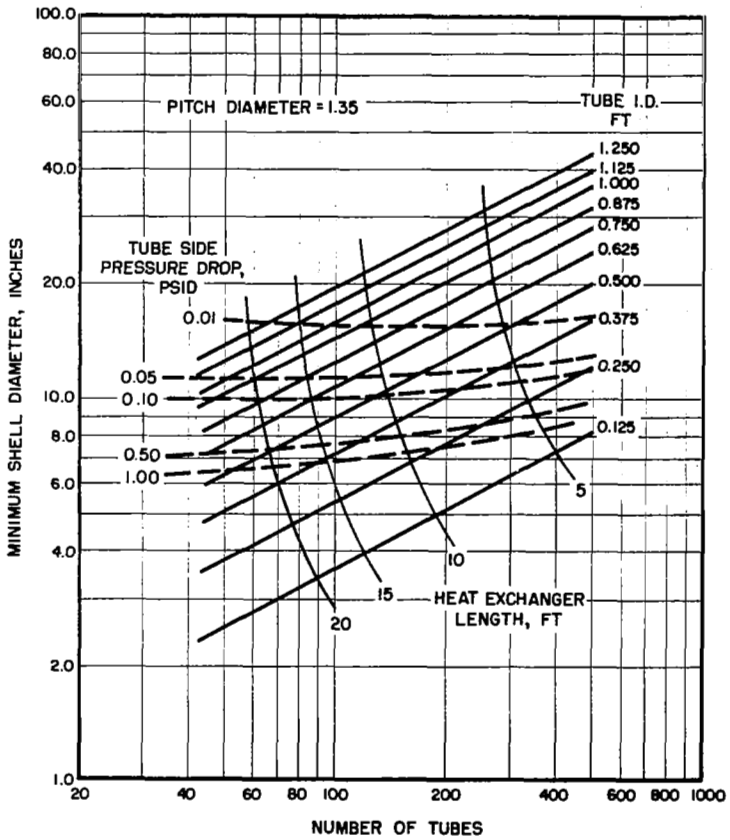

Figure 5-104 Intermediate Heat Exchanger - Minimum Shell Diameter vs Number of Tubes (Pitch-to-Diameter Ratio = 1.35)

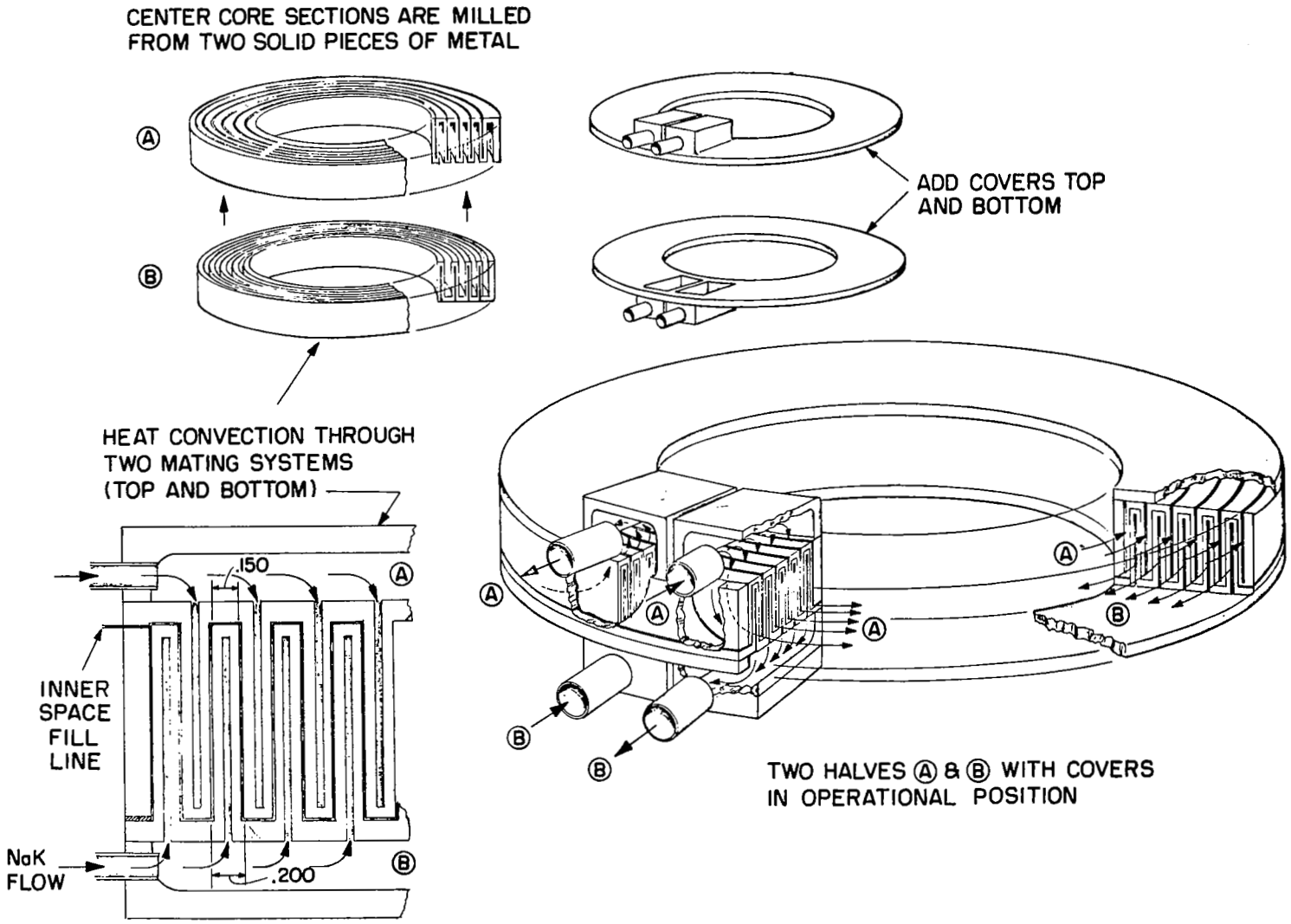

Figure 5-105 Separable Intermediate Heat Exchanger Concept

- Tube-in-shell heat exchanger technology is state of the art. The compact (intermeshing panels) design required a separate development effort. The advantages of a compact unit were not sufficiently compelling to justify the required R&D effort.

- The compact design was nonseparable. Since a separable design was considered to be a requirement for mission applications, the development of this configuration was not justified.

- The compact unit had to be fabricated from high strength nickel alloy (because of design stresses) which had long lead times and were expensive.

- Fabrication of the intermeshing panels associated with the compact heat exchanger design was judged to be not feasible.

Further design effort was conducted for the tube-in-shell configuration and a preliminary component specification was written. However, the SNAP-8 program was terminated before any further work could be done on this component.

b. Physical Description.- The development of the intermediate heat exchanger progressed to the point where feasibility and tradeoff studies and a conceptual design were completed. The recommended tube-in-shell configuration resulting from these efforts is shown in Figures 5-106 and 5-107. The heat exchanger is a double contained, tube-in-shell, 600-kWt design. An eccentric toroidal manifold is used to provide equal flow radially into the shell from the reactor power loop inlet line and outlet line. The manifold design is similar to that used on the mercury condenser. The intermediate loop inlet and outlet manifolds are also similar in configuration to the condenser manifold which never experienced a failure in test. The static NaK tubes separating the reactor loop from the intermediate loop are brazed to an inner static NaK header. The basic design is similar to the configuration used for the SNAP-8 NaK-to-mercury boiler.

A total of 121 intermediate loop tubes (1/2-inch OD) are encased in a toroidal 9.88-inch OD shell. The material used throughout the heat exchanger is Type 316 stainless steel. Further details of the conceptual design configuration are shown in Table 5-XXI.

c. Design Parameters.- The design parameters for the intermediate heat exchanger are presented in Table 5-XXII.

5.7.1.2 Auxiliary Heat Exchanger

a. Functional Description.- The function of the auxiliary loop heat exchanger is to transfer heat from the reactor primary loop to the heat rejection loop of the 90-kWe system, as shown in Figure 5-103, to preheat the condenser and radiator. The heat rejection loop flow is started and maintained by the heat rejection loop NaK pump. The reactor primary loop flow is started and maintained by the electromagnetic (EM) pumps.

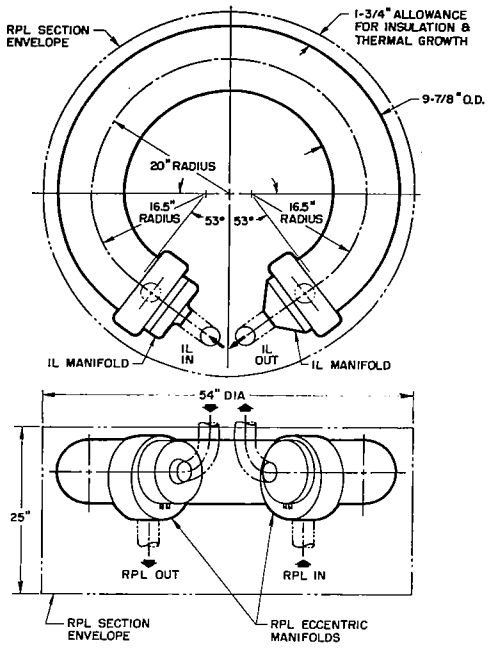

Figure 5-106 Recommended Tube-in-Shell Configuration for Intermediate Heat Exchanger

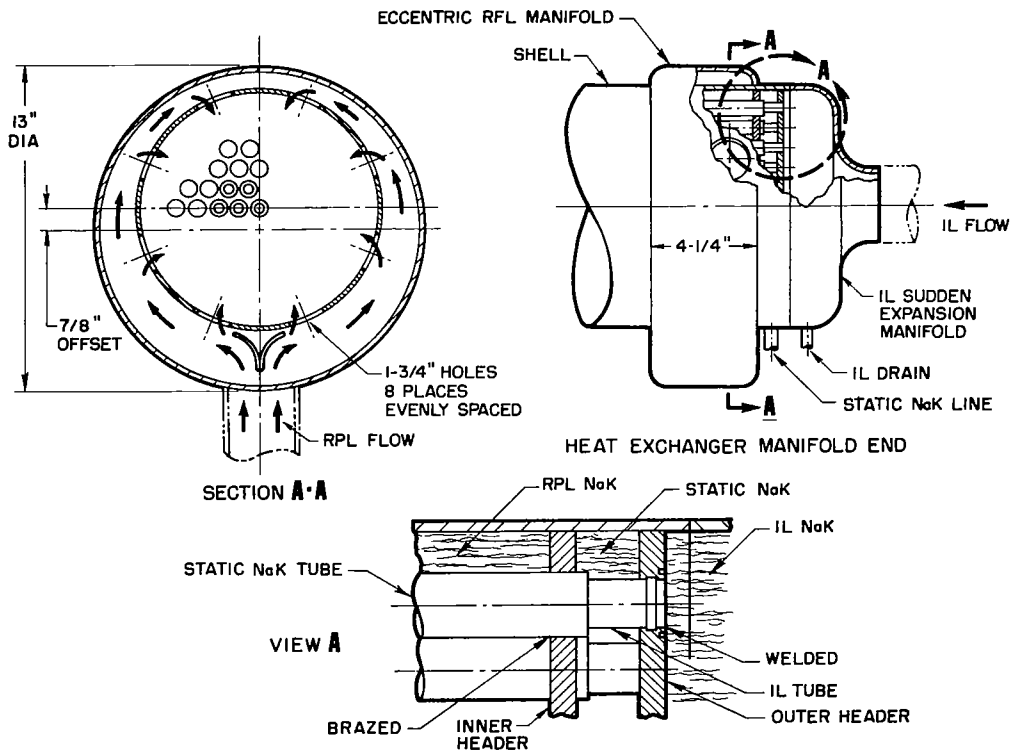

Figure 5-107 Recommended Manifold Configuration for Intermediate Heat Exchanger

TABLE 5-XXI INTERMEDIATE HEAT EXCHANGER CONCEPTUAL DESIGN RESULTS SUMMARY

Shell	9.88 in. OD x 0.188 in. wall
Number of Tubes	121
IL Tube (Inner)	1/2 in. x 0.035 in. wall
Static NaK Tube (Outer)	5/8 in. x 0.35 in. wall
Pitch/Diameter Ratio	1.252
Tube Length (Heat Transfer)	103.5 in.
Velocity in Tubes	3.43 fps
Velocity in Shell	1.70 fps
Tube-Side Pressure Drop	0.286 psid
Shell Side Pressure Drop	0.0066 psid
IL Inlet (Sudden Expansion)	K = 0.04 ΔP = 0.355 psid
IL Outlet (Gradual Contraction)	K = 0.04 ΔP = 0.018 psid
Weight of Empty IHX	635.19 lb
Weight of RPL NaK @ 1125°F	102.70 lb
Weight of RPL NaK @ 75°F	122.45 lb
Weight of IL NaK @ 1125°F	56.13 lb
Weight of IL NaK @ 75°F	67.01 lb
Weight of Static NaK @ 1125°F	17.29 lb
Weight of Static NaK @ 75°F	19.84 lb
Total Weight of Full IHX @ 1125°F	811.36 lb
Total Weight of Full IHX @ 75°F	844.49 lb
Volume of RPL NaK	3914.00 in^3
Volume of IL NaK	2145.48 in^3
Volume of Static NaK	633.90 in^3

NOTE: The above results do not include pressure drop through the RPL eccentric manifolds and holes into the shell or pressure drop through the IL manifolds into the tubes. Also not included are the design configurations for the internal tube supports and shell baffles and their corresponding weights.

TABLE 5-XXII INTERMEDIATE HEAT EXCHANGER CONCEPTUAL DESIGN REQUIREMENTS

Heat Load	600 kW
Flow (RPL and IL)	65,000 lb/hr
Reactor Primary Loop (RPL) Fluid	NaK
Intermediate Loop (IL) Fluid	NaK
Static Fluid	NaK
RPL Inlet Temperature	1200°F
Log Mean Temperature Difference	20°F
Material	316 stainless steel
Inlet and Outlet Lines (RPL and IL)	3 in. x 0.120 in. wall tubing
Structural Design Temperature	1400°F
Structural Design Pressure	75 psi
Shell Side Maximum Pressure Drop (max.)	1 psid
Tube Side Maximum Pressure Drop (max.)	3 psid

Flow through the heat rejection loop side of the auxiliary heat exchanger is maintained during reactor primary loop heatup prior to mercury injection. When the proper temperature in the heat rejection loop is reached and the SNAP-8 is started (by injecting mercury into the boiler), the "on-off" valve in the auxiliary heat exchanger line is shut, thus isolating the reactor primary loop from the heat rejection loop for the remainder of the steady-state operation.

The auxiliary heat exchanger performs two major functions during the startup and shutdown phases of the SNAP-8 nuclear power systems operation. First, during system startup the auxiliary heat exchanger provides an initial heat load for the reactor so that the reactor can more readily follow the transients imposed during the mercury injection phase of the Rankine-cycle loop startup. The NaK leaving the auxiliary heat exchanger on the auxiliary loop side preheats the boiler-to-turbine vapor line and must be maintained above some minimum temperature. Second, during system shutdown, the auxiliary heat exchanger removes heat from the primary loop during reactor shutdown and decay heat removal periods, ensuring that the reactor is not subjected to high temperatures for long periods of time.

Although the auxiliary heat exchanger functions during several phases of startup and shutdown, the significant operating point, as far as heat exchanger design is concerned, occurs during the startup phase just prior to mercury injection when the NaK pumps are operating at the 220-Hz plateau.

Three units were fabricated by the General Electric Co. to the configuration shown in Figure 5-108 for the 35-kWe system. No units were designed or built for the 90-kWe system.

The design parameters for the 35-kWe system are listed in Tables 5-XXIII through 5-XXVII for various operating conditions.

TABLE 5-XXIII AUXILIARY HEAT EXCHANGER DESIGN OPERATING CONDITIONS

Parameter	Quantity
Thermal Energy Transfer Capability, kWt	70 - 100
*Primary Loop Side Pressure Loss (Maximum), psid	0.15
*Auxiliary Loop Side Pressure Loss (Maximum), psid	1.0
NaK Outlet Temperature, Auxiliary Loop Side (Minimum), $^{\circ}$F	1100

* Measured between inlet and outlet system/component interface.

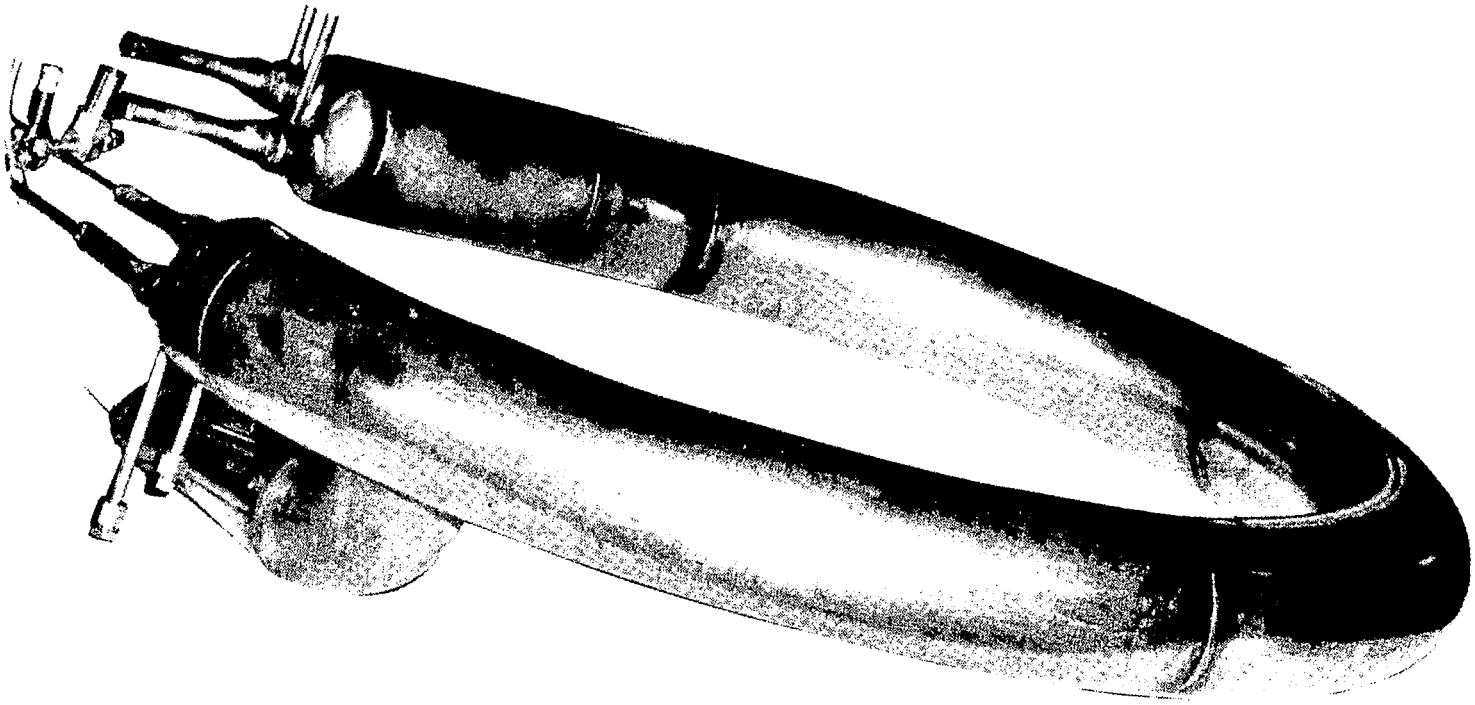

Figure 5-108 Auxiliary Heat Exchanger for 35-kWe System

TABLE 5-XXIV SYSTEM CONDITIONS AT AUXILIARY HEAT EXCHANGER INTERFACE

Parameter	Quantity
Flow Rate, Primary Loop Side, lb/hr	27,000
Flow Rate, Auxiliary Loop Side, lb/hr	1,150
NaK Inlet Temperature, Primary Loop Side, ^{o}F	1,300
NaK Inlet Temperature, Auxiliary Loop Side, ^{o}F	110

TABLE 5-XXV AUXILIARY HEAT EXCHANGER LONG-TERM NONOPERATING CONDITIONS

Parameter	Value
Flow Rate, Primary Loop Side	49,000 lb/hr
Flow Rate, Auxiliary Loop Side	0
NaK Inlet Temperature, Primary Loop Side	1160^{o}F

b. Physical Description.- The following describes the heat exchanger shown in Figure 5-108:

- Shell: 5.00-inch OD x 0.120-inch wall, Type 316 SS, formed in helix with a 6.00-inch pitch and approximately 44-inch coil diameter.
- Heat rejection tubes: Two in parallel, 1.25-inch OD x 0.049-inch wall, Type 316 SS running the length of and within the shell.
- Double-containment tubes: Two, one each surrounding the heat rejection tubes, 1.50-inch OD x 0.049-inch wall, Type 316 SS running the length of the heat exchanger.
- Heat rejection inlet baffle tubes: Two, one each inside HR tubes for 10.0-inch distance, 0.625-inch OD x 0.035-inch wall, Type 316 SS. Their purpose is to reduce the high thermal gradient between the heat rejection loop inlet NaK and the primary outlet NaK.
- Swirl wire: On inside surface of outer shell to mix primary NaK flowing through auxiliary heat exchanger.

TABLE 5-XXVI AUXILIARY HEAT EXCHANGER CONDITIONS DURING STARTUP FOR 35 KWE SYSTEM

	Phase / Units	Conditions During Each Phase of Startup Sequence (1)						
		I	II	III	IV	V	VI	VII
Duration of Phase	As Noted	5 hours	2 min.	5-10 min.	50-100 sec	50 sec(min)	7-10 min	Long-Term Steady-State
NaK Flow, Primary Loop Side								
Initial	lb/hr	0	11600	27000	27000	49000	49000	49000
Final	lb/hr	11600	27000	27000	49000	49000	49000	49000
Max. Rate of Change	lb/hr/sec	11600	180	0	2455	0	0	N/A*
NaK Inlet Temperature, Primary Loop Side								
Initial	°F	50-1100	1330	1330	1330	1130 (min)	1200-1250	1110-1160
Final	°F	1330	1330	1330	1130(min)	1200-1250	1110-1160	1110-1160
Max. Rate of Change	°F/sec	0.1(2)(3)	2	negligible	5	5	1	N/A
NaK Pressure, Primary Loop Side								
Initial	psia	5 -35	35	35	35.	30	30	30
Final	psia	35	35	35	30.	30	30	30
Max. Rate of Change	psia/sec	0.004	negligible	negligible	-0.18	0	0	N/A
NaK Flow, Auxiliary Loop Side								
Initial	lb/hr	0	500	1150	1150	2100		
Final	lb/hr	500	1150	1150	2100	2100	N/A	N/A
Max. Rate of Change	lb/hr/sec	500	7.5	0	~100	0		
NaK Inlet Temperature, Auxiliary Loop Side								
Initial	°F	50	50	110	110	125	N/A	N/A
Final	°F	50	110	110	125	125		
Max. Rate of Change	°F/sec	0	1	0	0.5	0		
NaK Outlet Temperature, Auxiliary Loop Side								
Initial	°F	50	1250	1100	1100	760	N/A	N/A
Final	°F	1250	1100	1100	760	760		
Max. Rate of Change	°F/sec	0.3(3)	3	0	8.	0		
NaK Pressure, Auxiliary Loop Side								
Initial	psia	18-25	18-25	33-50	33-50	50-75	60-85	60-85
Final	psia	18-25	33-50	33-50	50-75	60-85	60-85	60-85
Max. Rate of Change	psia/sec	0	0.25	0	5	0	0	N/A

(1) Phase Description

I. 0- to 95-Hz inverter output, reactor outlet temperature increased to 1300°F.

II. NaK pumps accelerated from 95- to 220-Hz operation.

III. NaK pumps at 220-Hz operation, system transient stabilization period.

IV. Mercury injection, turbine and pump acceleration to rated speed.

V. Mercury flow at approximately 54% rated, tubrine and pumps at rated speed.

VI. Mercury flow increased to rated condition.

VII. System at rated condition.

(2) During Phase I, the temperature rate of change will be approximately 1°F/sec for approximately a 6-minute period.

(3) Transients occur after flow reaches final value.

* Not applicable.

TABLE 5-XXVII AUXILIARY HEAT EXCHANGER CONDITIONS DURING SHUTDOWN FOR 35 KWE SYSTEM

	Phase / Units	Conditions During Shutdown Sequence(1)			
		I	II	III	IV
Duration of Phase	As Noted	30 sec.	~200 sec	~200 sec	~5 hour
NaK Flow, Primary Loop Side					
Initial	lb/hr	49000	49000	27000	27000
Final	lb/hr	49000	27000	27000	11600
Max. Rate of Change	lb/hr/sec	0	-2455	0	-180
NaK Inlet Temperature, Primary Loop Side					
Initial	°F	1200-1250	1200-1250	1180-1220	1130-1170
Final	°F	1200-1250	1180-1220	1130-1170	1100-1150
Max. Rate of Change	°F /sec	0	-4	-0.5	N/A
NaK Flow, Auxiliary Loop Side					
Initial	lb/hr	0	~2100	1150	1150
Final	lb/hr	~2100	1150	1150	500
Max. Rate of Change	lb/hr/sec	2000	50	0	7.5
NaK Inlet Temperature, Auxiliary Loop Side					
Initial	°F	300	325	250	200
Final	°F	325	250	200	50(min)
Max. Rate of Change	°F/sec	1	-1	-0.3	-0.2
NaK Outlet Temperature, Auxiliary Loop Side					
Initial	°F	-	840	1020	970
Final	°F	840	1020	970	1080
Max. Rate of Change	°F/sec	~8	~3	0.3	0.5

(1) Phase Description

I. Mercury flow at approximately 54% rated, turbine and pumps at rated speed (time period to permit stabilization of the condition).

II. Mercury flow reduced to zero, turbine decelerated, pumps switched to inverter at 220-Hz, reactor power reduced by fast setback.

III. NaK pumps at 220-Hz operation. The period for system stabilization.

IV. Decay heat removal period. NaK pumps decelerated to and remain at 95-Hz operation.

5.7.2 Mercury Flow Control Valve

The mercury flow control valve is located in the Rankine-cycle loop between the mercury pump discharge and boiler inlet (Figure 5-109). This valve meters the flow of mercury to the boiler during system startup and shutdown cycles. The valve and drive motor assembly are shown in Figure 5-110. During startup and shutdown, flow is metered to the boiler according to prescribed rates of increase or decrease by the movement of a shear plate at constant speed over a shaped orifice plate for set periods of time. The rate of travel of the shear plate, and therefore rate of change of flow, can be varied by changing the voltage supplied to the valve drive motor. A secondary function of the valve is to provide a means for trimming system power output by adjusting mercury flow.

Tests in the Aerojet 35-kWe test facility and the NASA-LeRC W-1 facility were conducted from 1966 through midyear of 1970 using these valves.

Changes in valve requirements as a result of SNAP-8 system state-point changes for the 90-kWe system, including the low-pressure mercury injection startup, necessitated modifications to the currently existing valves. The modifications included changes in flow rate, pressure drop, and speed of opening and closing the valve. However, the existing valve can meet the requirements by merely changing the shaped orifice to meet the new requirements. Speed changes can be obtained by increasing or decreasing the voltage input to the valve motor.

5.7.2.1 Physical Description

The design employs the sliding-gate valve principle. The actuating arm is pivoted in a ball and socket which is driven through a screw mechanism and gearing by a dc electric motor. The motor is a standard commercial unit. Bellows provide the primary seal between the valve body cavity and the ball pivot, while the ball and socket act as a secondary seal to preclude the escape of mercury to the environment. Seal disks are forced against the valve seat with a spring which effectively minimizes leakage and ensures that the sealing surfaces are wiped clean as the valve opens and closes.

The orifice plate was cut in a shape to result in a mercury flow ramp rate prescribed for producing acceptable system startup transients.

Two microswitches are provided, one to stop the motor when the valve approaches the full-open position, and one to stop the motor when the valve is fully closed.

A position-sensing potentiometer was attached to the screw mechanism at the top of the valve. The measurements of valve position versus flow at various motor voltage settings were obtained during valve and system testing to determine the best valve opening rates and required motor input voltages to produce the flow ramp required for the power conversion system startup. Table 5-XXVIII lists the requirements and parameters for the valve used in the 35-kWe system.

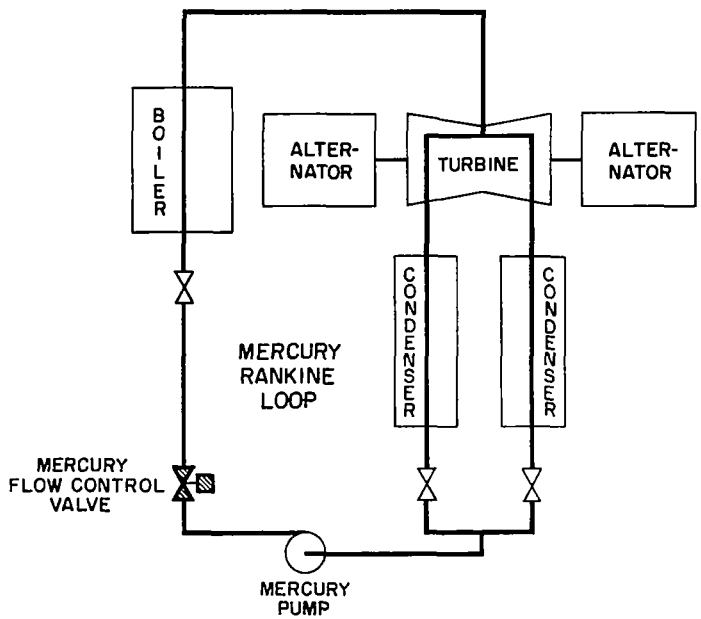

Figure 5-109 Schematic Showing Location of Mercury Flow Control Valve

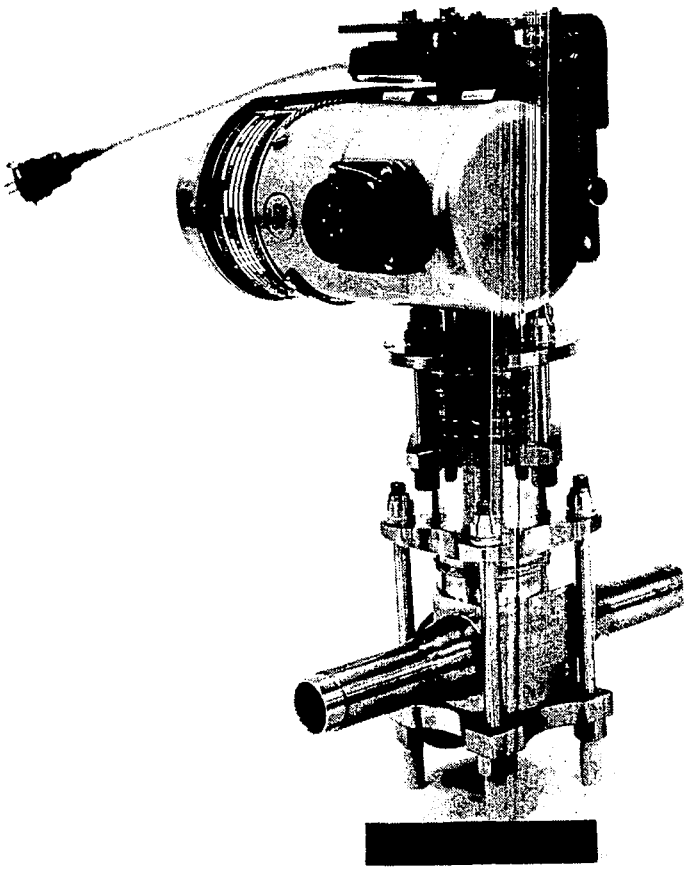

Figure 5-110 Mercury Flow Control Valve

TABLE 5-XXVIII DESIGN PARAMETERS FOR THE MERCURY FLOW CONTROL VALVE

Description of Requirements	Design Parameters
Motor	
Motor type	Permanent magnet
Nominal voltage, Vdc	27
Rated current, amp	0.10
Wattage	2.70
Rated torque, lb-in.	25.0
Output shaft speed, rpm	1.0
Operating temperature range, °F	-65 to +250 (continuous), +400 (intermit.)
Motor gear reduction	3763 to 1 (Gear Train Eff. = 50%)
Gearing	
Number of teeth (driven gear)	66
Number of teeth (driving gear)	30
Gear ratio	2.2:1
Worm Gear	
Total linear travel, in.	0.437
Pitch of gear, in.	0.0416
Linear speed, in./minute	0.0916
Valve	
Operating pressure, psia	500
Operating temperature, °F	515
Flow rate, lb/hr	0 to 11,200
Full flow pressure drop, psid	10
Total time to open valve	286 sec. @ Nominal Voltage
External leakage	zero
Internal leakage	100 cc/hr max.
Lubrication	Self Lubricating
Power required to maintain valve in open or closed position	None
Valve type	Throttling, power operated

The materials of construction are listed in Table 5-XXIX. No basic materials problems were encountered during tests. However, on occasion, mass transfer from the mercury loop deposited in the valve and caused leakage in excess of design requirements.

5.7.2.2 Demonstrated Performance

The demonstrated performance characteristics of the flow control valve for the 35-kWe system are shown in Figures 5-111 and 5-112. Included are valve resistance coefficients and valve actuator characteristics. Travel time varies linearly with the valve opening for any constant power input. The plots were based on experimental data utilizing mercury as the working fluid.

An evaluation of the mercury flow control valve performance during 35-kWe system tests resulted in the generation of startup transients shown in Figure 5-113.

Testing of the valve during the 35-kWe system test program was concerned with the relationship between pressure drop and flow rate as a function of valve position. These data are shown in Figure 5-114. The data are not correlated as a function of valve percentage-open, but rather as a function of the position of the valve travel mechanism between the valve limit switches. This method was used because the valve limit switches were not necessarily at the full-closed or full-open positions and the calibration of the valve position indicator was made between the limit switches. The data of Figure 5-114, therefore, pertained to the specific limit switch settings.

The mercury flow control valve was operated over a wide variety of conditions as shown in Table 5-XXX. Listed are the approximate hours of operation within various temperature ranges, the number of temperature changes and the number of valve position changes. The valve performance was good and no problems were experienced.

Other tests, conducted as part of the 35-kWe system operation, established the capability of the valve under many conditions and operational modes. The basic valve design is considered to be capable of meeting the requirements for properly controlling mercury flow during startup and shutdown for the 90-kWe system with modifications to the shape of the orifice and changes in the speed of opening and closing the valve.

5.7.3 Heat Rejection Flow Control Valve

The restart system for the 90-kWe SNAP-8 system requires the use of a flow control valve for the heat rejection loop flow through the condenser. Its location in the SNAP-8 90-kWe system is shown in Figure 5-115. The positions and movement of the valve are controlled by electrical signals from the programmer.

TABLE 5-XXIX MATERIALS OF CONSTRUCTION, MERCURY FLOW CONTROL VALVE

Item Description	Material
Valve Body	Haynes 25 Alloy (AMS-5759B)
Seal Seat	Stellite 6B
Seal Disk	Stellite 6B
Guide Disk	Stellite 6B
Spring, Seal Disk	Type 302 SS (AMS-5688)
Bellows	Type 321 SS
Ball Socket	Type 347 SS
Valve Stem and Ball	Stellite 6B
Screw - Actuating	Stellite 6B
Nut - Actuating	Type 410 SS
Thrust Race	Torrington Co. P/N TBR-815
Thrust Bearing	Torrington Co. P/N NTA-815
Roller Bearing	Torrington Co. P/N J-88
Roller Bearing	Thompson Co. P/N A-61014-SS
Gear, Motor	Type 303 SS
Gear, Valve	Brass
Actuator, Electric Motor	Barber-Colman, EYLC 9353-1
Switch, High-Temp., Subminiature	Minark Electric Co., Unimax Type FC-2
Potentiometer	Bourns Inc, Model 157, 1.000" Travel, SK± 5%, Type 5, P/N 15725-9-1.00-502
Receptacle, Electric	MS-3102A-16S-8P

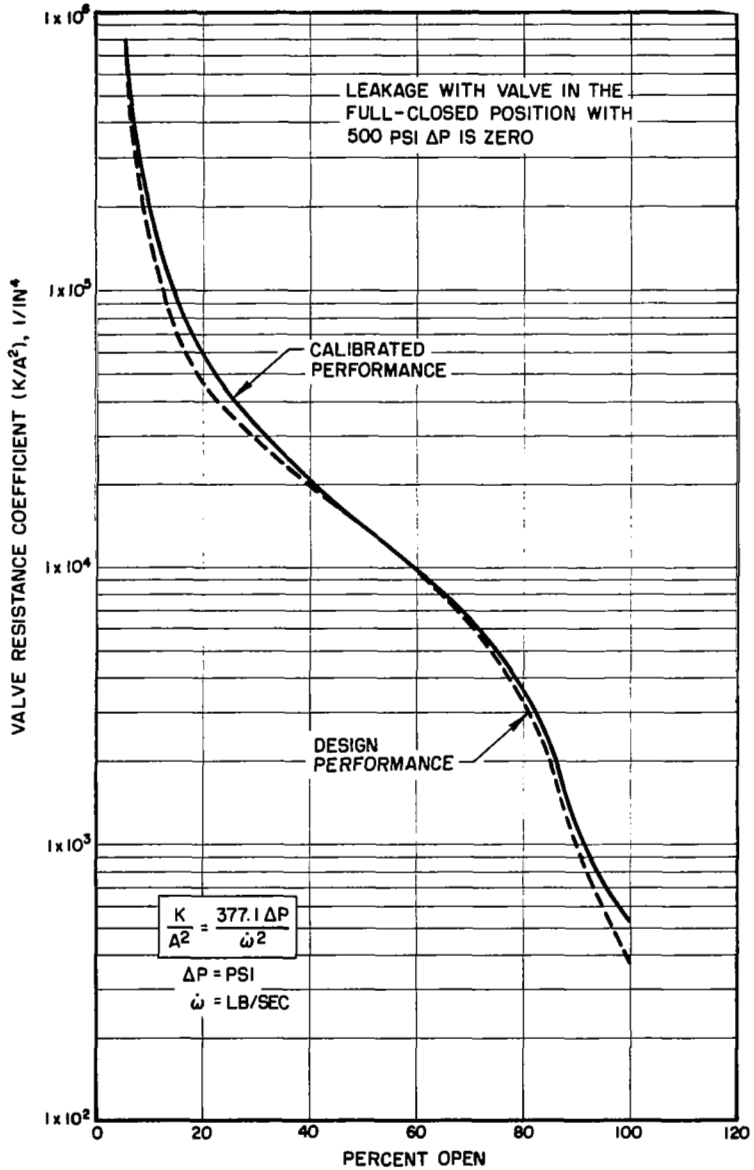

Figure 5-111 Flow Characteristics - Mercury Flow Control Valve

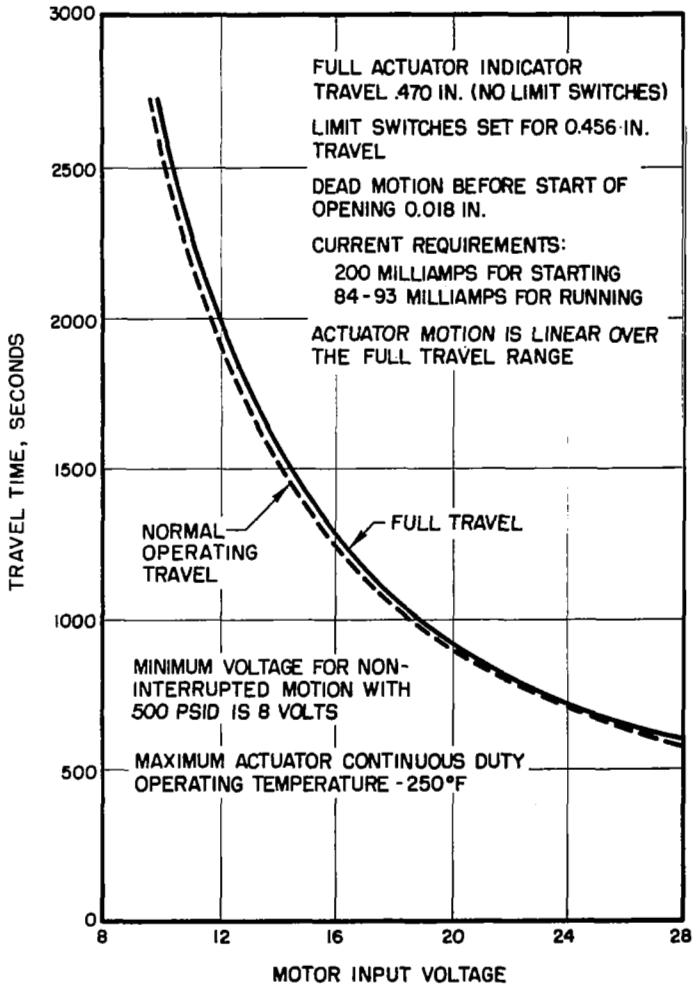

Figure 5-112 Voltage vs Travel Time - Mercury Flow Control Valve

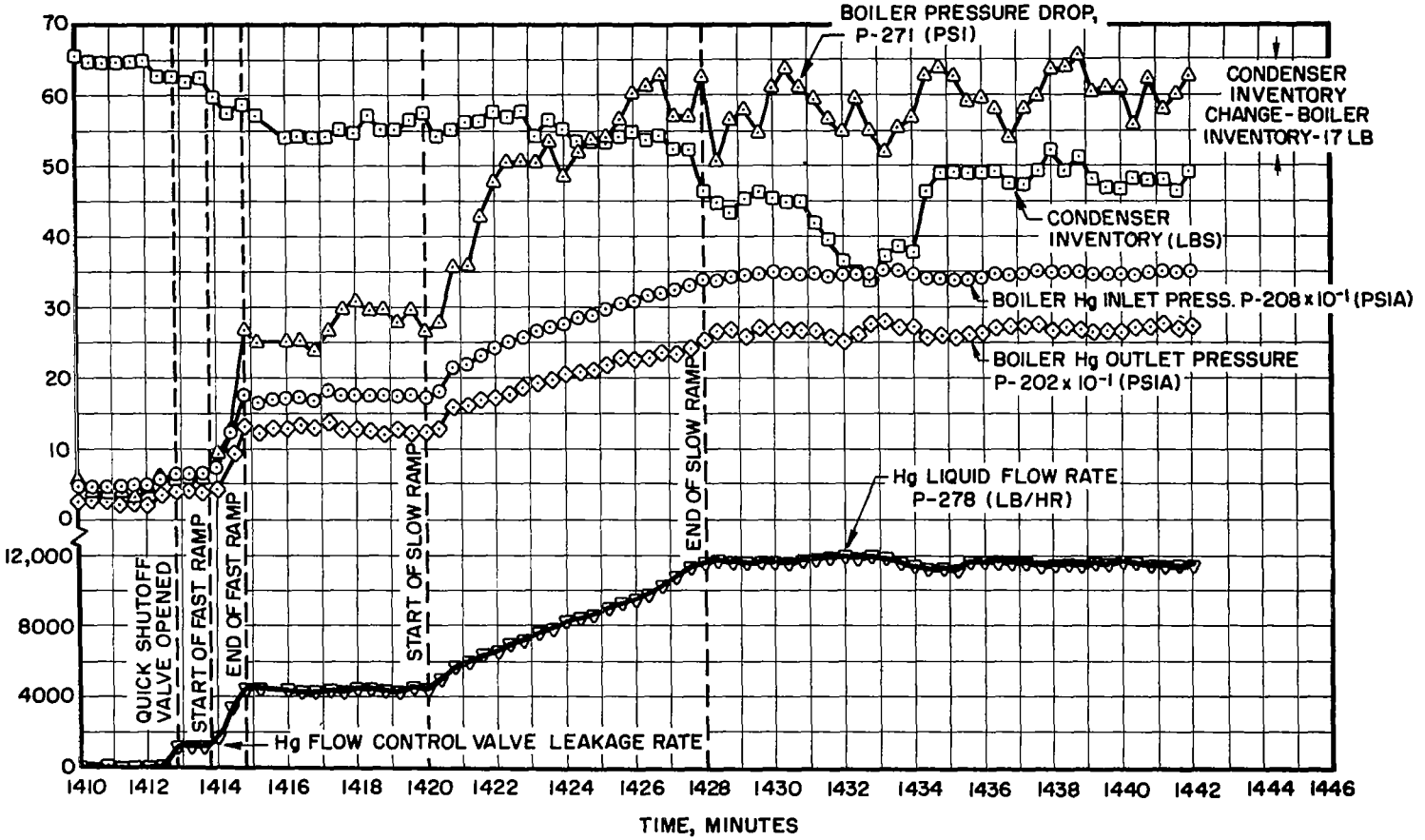

Figure 5-113 Startup Transients - Mercury Flow Control Valve

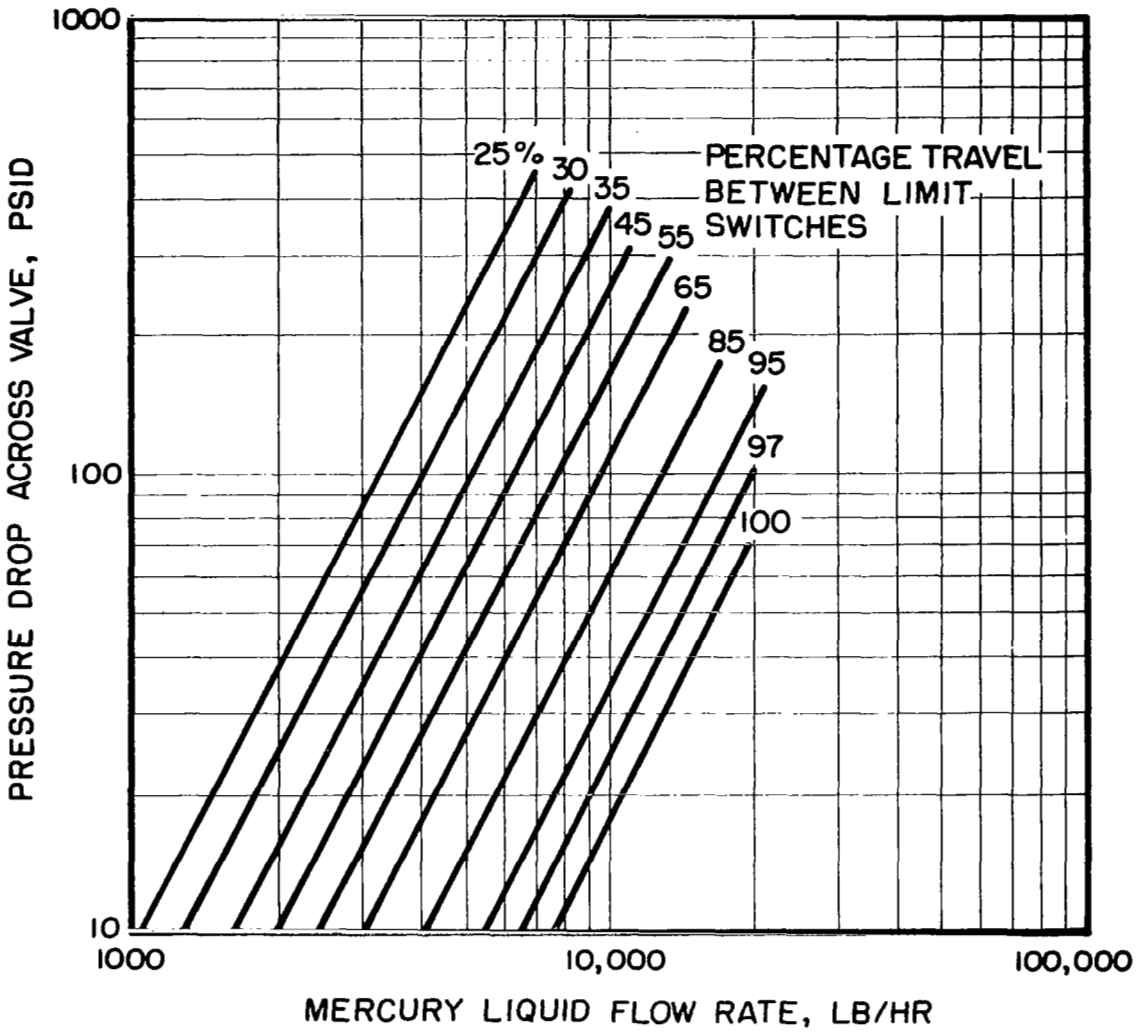

Figure 5-114 Pressure Drop vs Flow Rate and Valve Position - Mercury Flow Control Valve

Prior to the SNAP-8 system startup, the heat rejection flow control valve is signalled to move to the zero percent open (closed) position. The valve remains in this position throughout the reactor startup and mercury injection periods until the condenser pressure reaches a predetermined upper limit value. At this time the valve is signalled to move, at a constant rate, (1) in a direction to increase the flow through the condenser if the condensing pressure exceeds the predetermined upper limit value, (2) in a direction to decrease the flow through the condenser if the condensing pressure is below a predetermined lower limit value, or (3) to remain stationary if the condenser pressure stays within the upper and lower limit values.

After the startup has proceeded to the point where rated mercury flow is attained, the valve is signalled to move to a predetermined position which will establish rated flow in the heat rejection loop.

During shutdown, the valve will be signalled to move in a manner to maintain condensing pressure at a predetermined level. Generally, the valve will be signalled to move in a direction to decrease the flow through the condenser.

The valve design parameters are listed in Table 5-XXXI.

5.7.3.1 Physical Description

The three conceptual designs proposed to meet the requirements of the 90-kWe system all employed the use of a dc motor to drive each respective valve. One design was for a plug valve set at a 145 degree angle to the flow path and driven by the motor through a ball-screw. Another design included a spring-loaded shear plate driven by the motor through a screw. The third design included a spring-loaded shear plate on a pivoted shaft and driven by the motor through spur gears and screws. This design was almost identical to the mercury flow control valve.

5.7.3.2 Design Parameters

The design parameters for the heat rejection flow control valve planned for the 90-kWe system are listed in Table 5-XXXI. Many changes to the requirements were considered, one of which was the bypass flow of NaK through the valve when the valve was fully closed. This was incorporated in the three conceptual designs described above, as was a requirement that the dc motor be capable of operation in a 600°F environment. The latest revisions to the system however, deleted the need for bypass flow and reduced the motor temperature from 600 to 450°F.

Figure 5-116 is a plot of pressure drop and flow rate versus percent valve opening for the new valve, and Figure 5-117 is a plot of orifice effective area versus percent valve opening. These plots and the design parameters of Table 5-XXXI essentially describe the basic requirements of the valve.

TABLE 5-XXXI DESIGN PARAMETERS - HEAT REJECTION FLOW CONTROL VALVE

Description of Requirement	Design Parameters
Operating Temperature, ^{o}F	50 - 450
Flow Rate, lb/hr	0 - 59,000
Working Pressure, psig	0 - 85
Valve Response	Start Open Within 100 milliseconds. Open or Close at 0.35% of Full Travel per Second.
Leakage, Internal	Shall not Exceed 1000 cc/hr.
Pressure Drop, Full Open, psid	3
Operating Life, hours	1000 Cycle, 40,000
Power Requirements	28 $\pm$ 2 Vdc, 10 amps max.

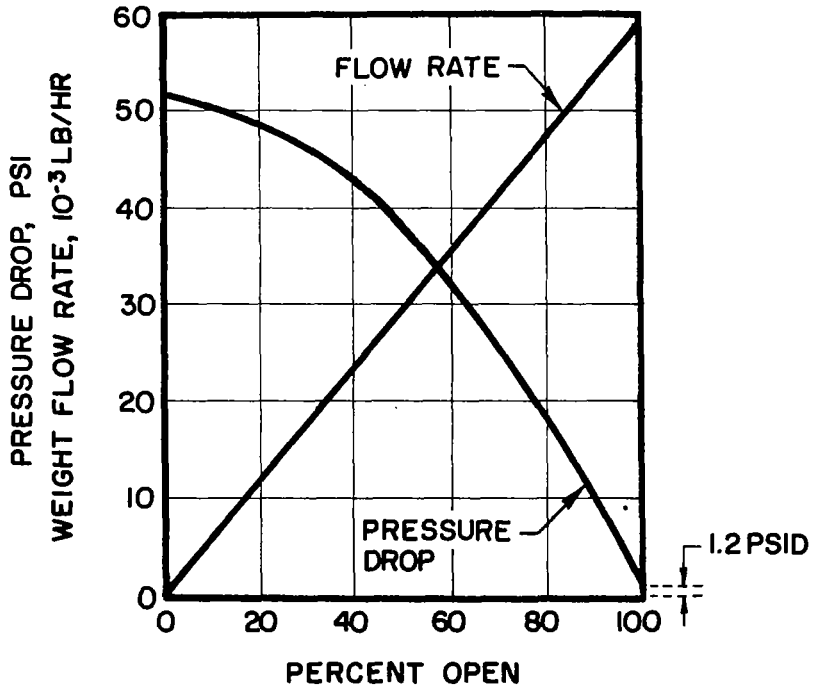

Figure 5-116 Pressure Drop and Flow Rate vs Percent Valve Opening - Heat Rejection Flow Control Valve

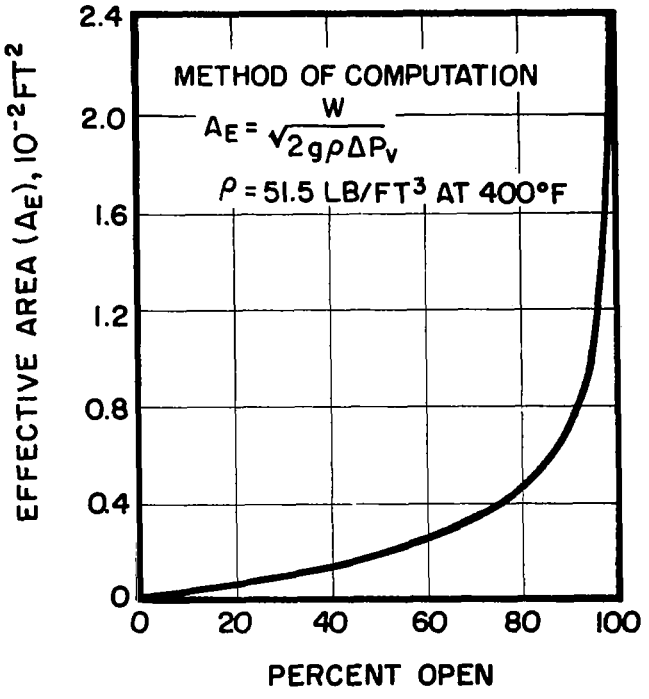

Figure 5-117 Orifice Effective Area vs Percent Valve Opening - Heat Rejection Flow Control Valve

5.7.4 NaK Diverter Valves

The need for a NaK diverter valve became apparent with the decision that two primary-loop NaK pump assemblies should be used in parallel with the 35-kWe system. This was based on the redundant-system concept wherein one NaK pump would operate and, in the event of failure, the second pump could be put on line. In such an operational mode, it was evident that flow from discharge to suction of the nonoperating pump should be reduced to a point where only preheating of the nonoperating pump should be allowed.

NaK diverter valves are required at the outlet of the redundant NaK pumps in the intermediate loop and heat rejection loop of the 90-kWe system, as shown in Figure 5-118, and at the outlet of the redundant NaK pumps in the primary loop of the 35-kWe system as shown in Figure 5-119.

5.7.4.1 Physical Description

The cross-sectional drawing of the valve can be seen in Figure 5-120. The valve is in a "Y" configuration with all three ports having a 2.5-inch outside diameter and a 0.083-inch wall thickness.

There are two inlet ports and one outlet port. Each inlet is connected to its respective NaK pump discharge line. The outlet port is common to both inlets. The hinged poppet assembly is situated in the valve body such that it will swing away from the flowing NaK port and into the other port. This effectively allows flow to proceed from the active port, through the valve, and out the valve discharge port. Recirculatory flow from the active pump, through the inactive pump, and back to the active pump suction is thus prevented. However, an orifice placed in the poppet plate is designed to allow 200 lb/hr of NaK to flow through the idle pump to maintain it at proper standby temperature.

The bracket shown between the two inlets was added to prevent the transmittal of any system line loads into the valve proper.

5.7.4.2 Design Parameters

The operational mode design parameters for the delivered valve are summarized in Table 5-XXXII. The other design parameters are summarized in Table 5-XXXIII. These were based on the 35-kWe system. The value would have to be increased in size from a 2.5-inch port diameter to 3.0 inches to accommodate the increase in NaK flow from 49,000 lb/hr to 58,000 lb/hr for the 90-kWe system. This change was not incorporated however, due to the termination of the SNAP-8 program.

5.7.4.3 Mechanical and Thermal Design

A flexure joint was chosen over a pivoted joint because of the poor lubricity of NaK and the possible galling of the pivot. Materials had to be selected carefully because of the high NaK temperature and the susceptibility

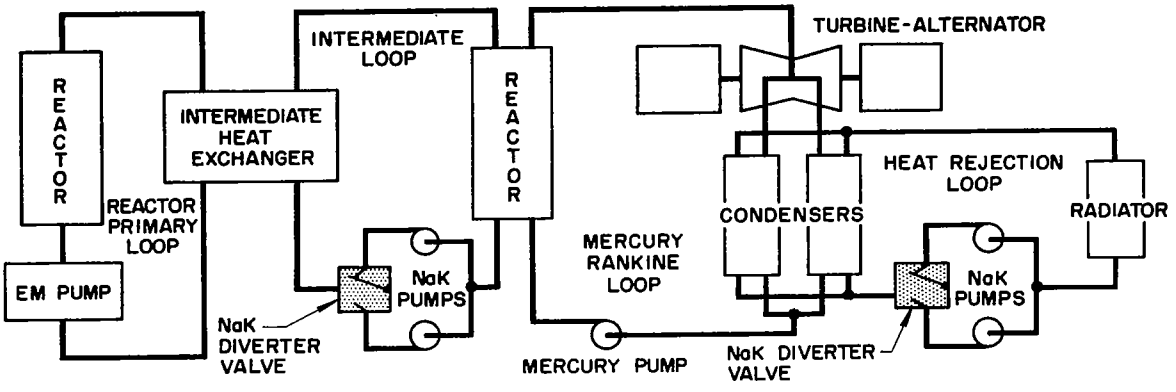

Figure 5-118 90-kWe System Schematic Showing Location of NaK Diverter Valves

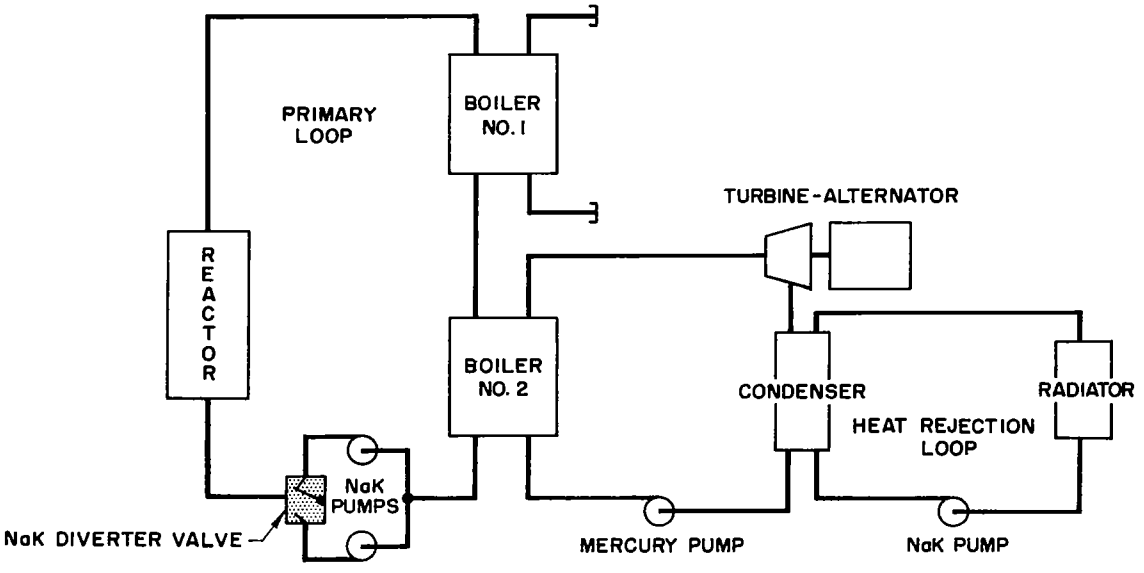

Figure 5-119 35-kWe System Schematic Showing Location of NaK Diverter Valve

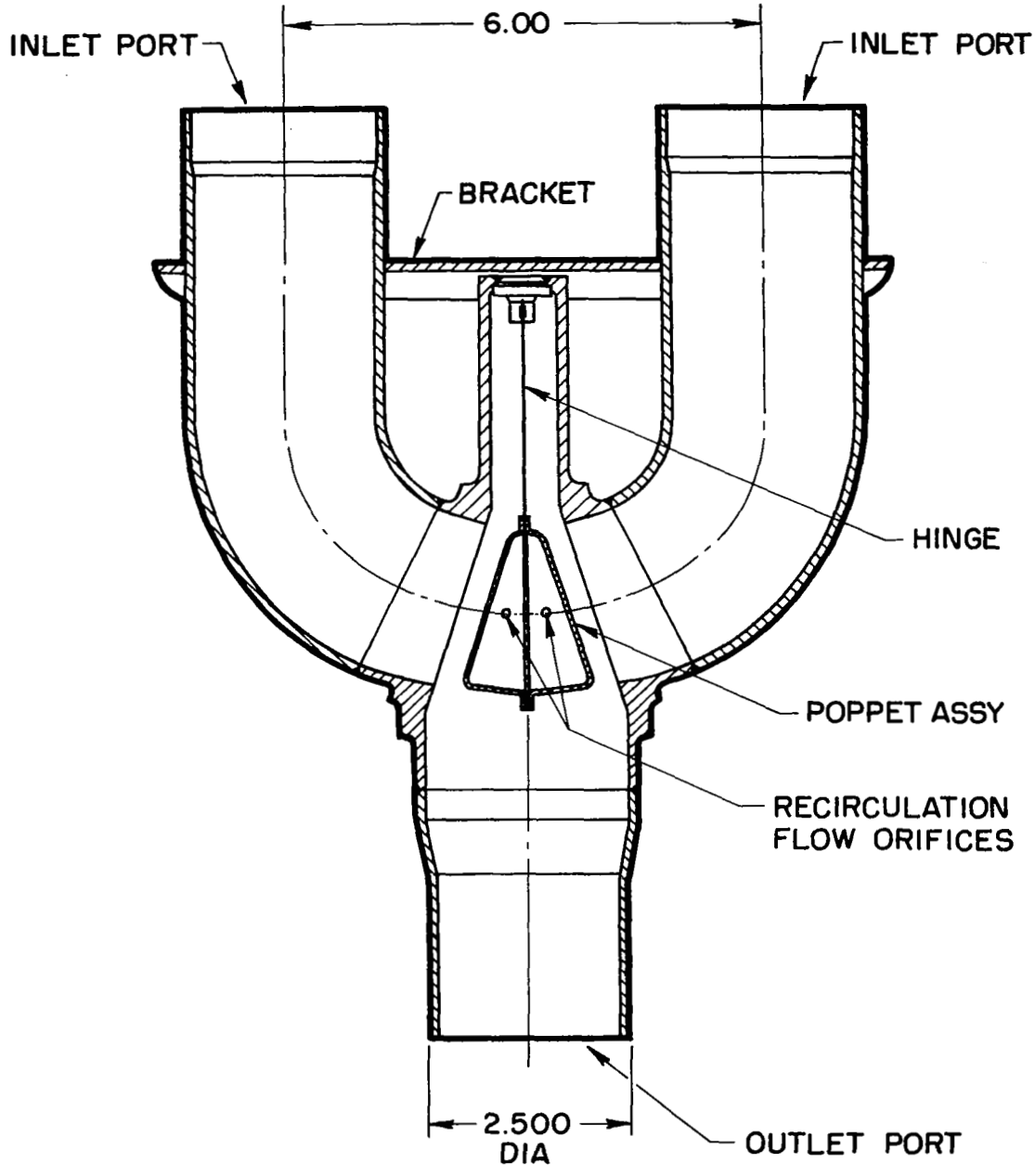

Figure 5-120 Cross Section of NaK Diverter Valve

TABLE 5-XXXII NaK DIVERTER VALVE OPERATIONAL DESIGN PARAMETERS

Operational Mode	NaK Flow Rate (lb/hr)	NaK Temp. °F	Pump Suction Pressure, Min. (psia)	Pump Discharge Pressure, Min. (psia)	Valve Inlet Pressure, Min. (psia)
Startup and Shutdown	9,800 - 12,200	50 - 1300	25.0	~ 26.6	~ 26.2
Startup and Shutdown	27,000	~ 1250	21.3	~ 28.1	~ 26.2
Steady State	49,000	1110 - 1160	10.3	~ 33.4	~ 27.2

TABLE XXXIII NaK DIVERTER VALVE DESIGN PARAMETERS

	Description	Design Parameter
1.	Pressure Drop (Inlet Port to Outlet Port)	0.1 psid at 12,000 lb/hr NaK at 1200°F 1.0 psid at 29,000 lb/hr NaK at 1200°F
2.	Backflow (Inlet Port to Inlet Port)	Backflow Orifice - Size Equivalent to a flow of 200 lb/hr NaK at 1110-1160°F and a ΔP of 25 psid. Seal Leakage - 10% of backflow max.
3.	Flowrate	49,000 lb/hr of 1200°F NaK at an inlet pressure of 50 psia.
4.	Temperature	Operating: +50°F to 1350°F Nonoperating: -65°F to +165°F.
5.	Pressure	Operating: 75 psia (Max.) Proof: 122 psia (Min.) at Room Temp. Burst: 530 psia (Min.) at Room Temp.
6.	External Leakage	1×10^{-7} standard cubic centimeters per second (SCCS) Helium (Max.) at 15 psid
7.	Operating Life	5 years unattended at a fluid temperature of 1200°F including a minimum of 1000 full operating cycles during the service period.
8.	Reversals in Direction of Movement	10,000 minimum
9.	Valve Position, Nonoperating	Normally open
10.	Transient Temperatures	50°F to 1300°F at an average rate of 150°F/minute and a maximum rate of 600°F in 15 seconds.

of many materials to NaK corrosion. Table 5-XXXIV lists the materials chosen. The Stellite 6-B valve seat was incorporated to resist corrosion and erosion as well as to minimize the possibility of "cold welding" between the poppet and seat.

TABLE 5-XXXIV NaK DIVERTER VALVE MATERIALS OF CONSTRUCTION

Description	Material
1. Valve Body	Type 316 Stainless Steel
2. Bracket	Type 316 Stainless Steel
3. Poppet Shell	Type 304 Stainless Steel
4. Poppet Seal Ring	Inconel 718
5. Poppet Orifice Plate	Inconel 718
6. Hinge	Inconel 718
7. Hinge Retainer	Inconel 600
8. Poppet & Hinge Assy Braze Material	AMS 4778 and AMS 2675
9. Valve Seat	Stellite 6B

The poppet was shaped in the manner shown in Figure 5-120 to assure quick closing and a minimal resistance to flow. As it moves toward the closed position, the side of the poppet begins to block the port, thus increasing the pressure differential across the poppet, which in turn causes it to move more rapidly to the full-closed position.

An extensive and detailed stress analysis was performed by the supplier and reviewed by Aerojet. The stress levels were well within the yield strength of the materials used, and in most cases they were well below the proportional limit of the materials.

5.7.4.4 Demonstrated Performance

A prototype valve acceptance test was performed with water as the test fluid; the valve responded well under all conditions. Test results agreed with the analytical predictions. The tests represented the minimum checkout testing conducted to verify correct fabrication and assembly of the valve, and were not intended as a complete development test program. The unit successfully completed the development checkout tests with results that were within specified requirements.

5.7.5 Solenoid Valves

Two-position, latching, double-solenoid valves are used throughout the SNAP-8 system with polyphenyl ether, mercury, and NaK as service fluids. The valves are used primarily to allow or prevent flow of the particular service fluid in a given portion of the system. All but one of the valves are two-way valves of the same basic design with the remaining one a four-way valve. The location of each valve in the 90-kWe SNAP-8 system is shown schematically in Figure 5-121. Operation of the valves is controlled by the programmer during startup and shutdown cycles. During steady-state system operation, all valves remain in a fixed position.

A total of thirteen solenoid valves are required in the 90-kWe system in the following locations:

- Turbine-Alternator.- One at the inlet and one at the outlet of the bearing lubricant circuits for each side of the dual path turbine-alternator; a total of four valves. The purpose of the valves is to prevent the flow of the lubricant fluid into the bearing cavities when the turbine-alternator is not operating, or when operating at reduced speeds during startup and shutdown transients. Flooding of the bearing cavities prior to a startup can result in excessive resistance to rotation and long acceleration periods during the startup transient.

- Mercury Pump.- One at the inlet and one at the outlet of the bearing lubricant circuit. The purpose of these valves is the same as stated for the turbine-alternator.

- Auxiliary NaK Coolant Loop.- One in the auxiliary NaK loop line between the branch point from the heat rejection loop and the inlet to the auxiliary heat exchanger. Flow through this branch circuit is required only during startup and shutdown cycles. If flow were permitted through this branch circuit during normal system operation, a large loss of reactor heat would occur resulting in poor system performance.

- Mercury Injection System.- Six solenoid valves are associated with the operation of the mercury injection system during startup and shutdown cycles. Five of the valves have mercury as the service fluid and the sixth valve is located in the lubricant-coolant loop with polyphenyl ether as the service fluid. The location and function of the individual valves is as follows:

  - Mercury condenser isolation valve.- One of these valves is located in the mercury line at the outlet of each condenser; a total of two valves. The purpose of these valves is to prevent the back-flow of mercury into the condenser during startup when mercury is being injected into the Rankine-cycle loop. When the injection cycle is completed, the valves are opened and remain open during normal steady-state system operation.

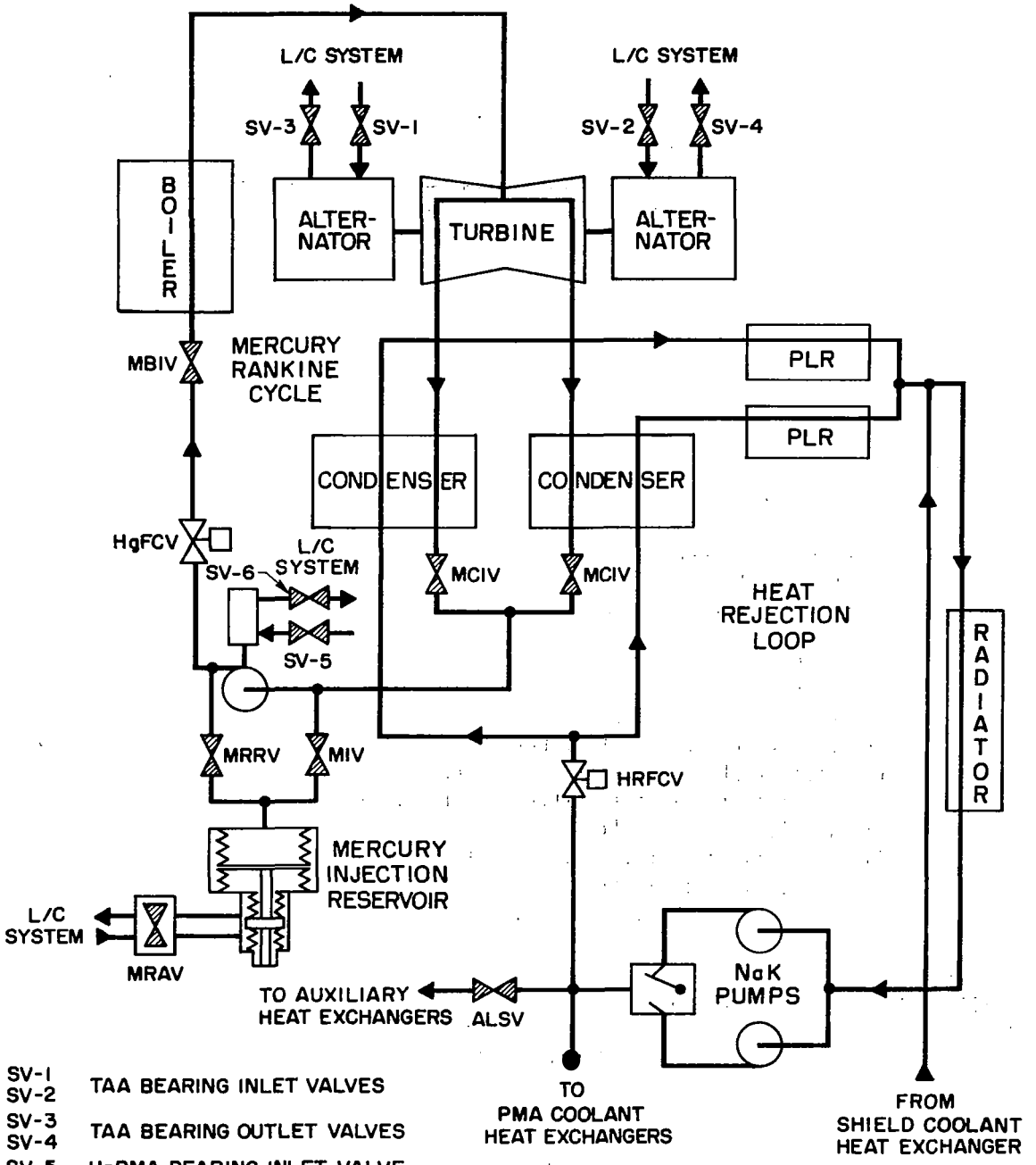

SV-1 SV-2	TAA BEARING INLET VALVES
SV-3 SV-4	TAA BEARING OUTLET VALVES
SV-5	HgPMA BEARING INLET VALVE
SV-6	HgPMA BEARING OUTLET VALVE
ALSV	AUXILIARY LOOP SHUTOFF VALVE
HgFCV	MERCURY FLOW CONTROL VALVE
HRFCV	HEAT REJECTION LOOP FLOW CONTROL VALVE
MBIV	MERCURY BOILER ISOLATION VALVE
MCIV	MERCURY CONDENSER ISOLATION VALVE
MIV	MERCURY INJECTION VALVE
MRAV	MERCURY RESERVOIR ACTUATOR VALVE
MRRV	MERCURY RESERVOIR RECHARGE VALVE

Figure 5-121 90-kWe System Schematic Showing Location of Solenoid Valves

- Mercury boiler isolation valve.- One of these valves is located in the mercury line at the inlet to the boiler. The purpose of this valve is twofold; first, to permit a solid fill of liquid mercury in the loop as close to the boiler inlet as possible prior to injection of mercury into the boiler during startup; and, second, to rapidly stop the flow of mercury to the boiler during an emergency shutdown.

- Mercury injection valve.- One of these valves is located at the outlet of the mercury reservoir to permit the flow of mercury into the Rankine-cycle loop during system startup; it will also permit mercury to flow into or out of the loop during mercury inventory trim periods.

- Mercury reservoir recharge valve.- One of these valves is located in a line between the mercury pump discharge and the mercury reservoir outlet port. During system shutdown with the mercury pump continuing to operate, this valve is opened to permit the mercury loop inventory to be pumped back into the mercury reservoir.

- Mercury reservoir actuator valve.- A four-way valve is located in the lubricant-coolant loop to act as a flow-direction device for operating the mercury reservoir actuating piston. When the valve is in the "inject" position, pressure and flow from the lubricant coolant pump is directed through the valve to one side of the mercury reservoir actuator to inject fluid in the mercury loop. When the valve is moved to the "dump" position, the mercury reservoir actuator moves to permit the rapid return of mercury from the loop to the reservoir.

A total of ten solenoid valves are required in the 35-kWe system. All of the types and functions described for the 90-kWe system are required; but, since only one condenser is used in the 35-kWe system, only one mercury condenser isolation valve is required and, since a single-path turbine-alternator is used in the 35-kWe system, only one inlet and one outlet valve are required in the bearing lubricant circuit.

A photograph of the latching double-solenoid valve is shown in Figure 5-122. Each valve has an opening and a closing solenoid. The valve is held open or closed by ball detents on the valve plunger, so that no electrical power is required to hold the valve in either position.

Figure 5-123 shows the typical current required to attain a pull force in the solenoid for various plunger-to-solenoid gaps. Curves of pressure drop vs. flow through the valve and differential pressure across the valve versus minimum volts to actuate the valve open or closed at various solenoid temperatures are shown in Figure 5-124 for a typical valve.

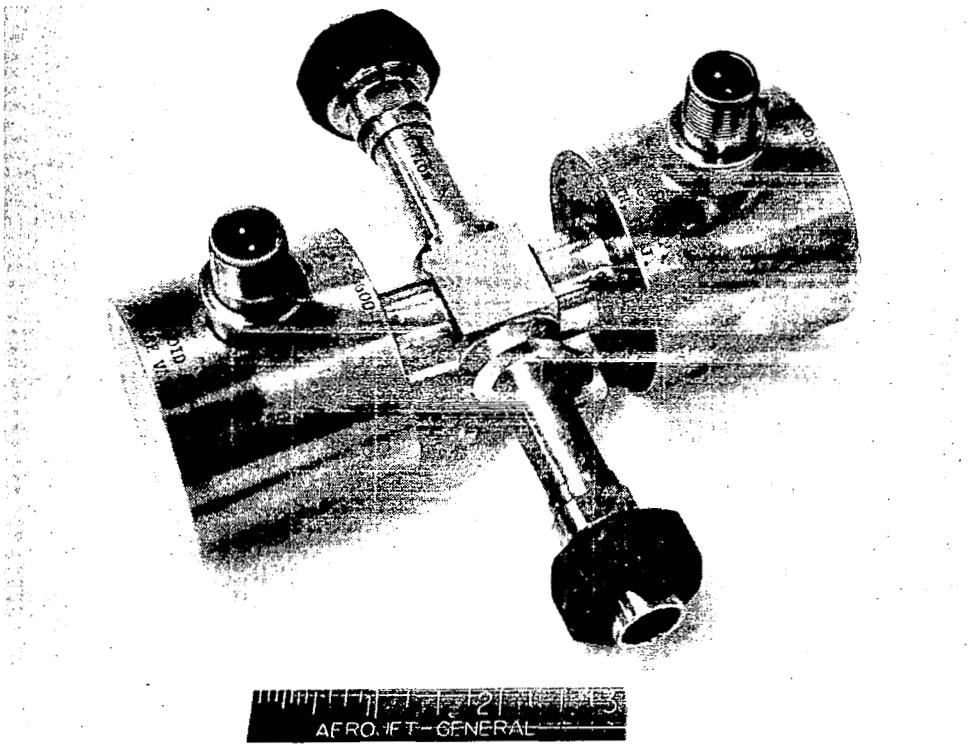

Figure 5-122 Two-Position, Latching, Double-Solenoid Valve

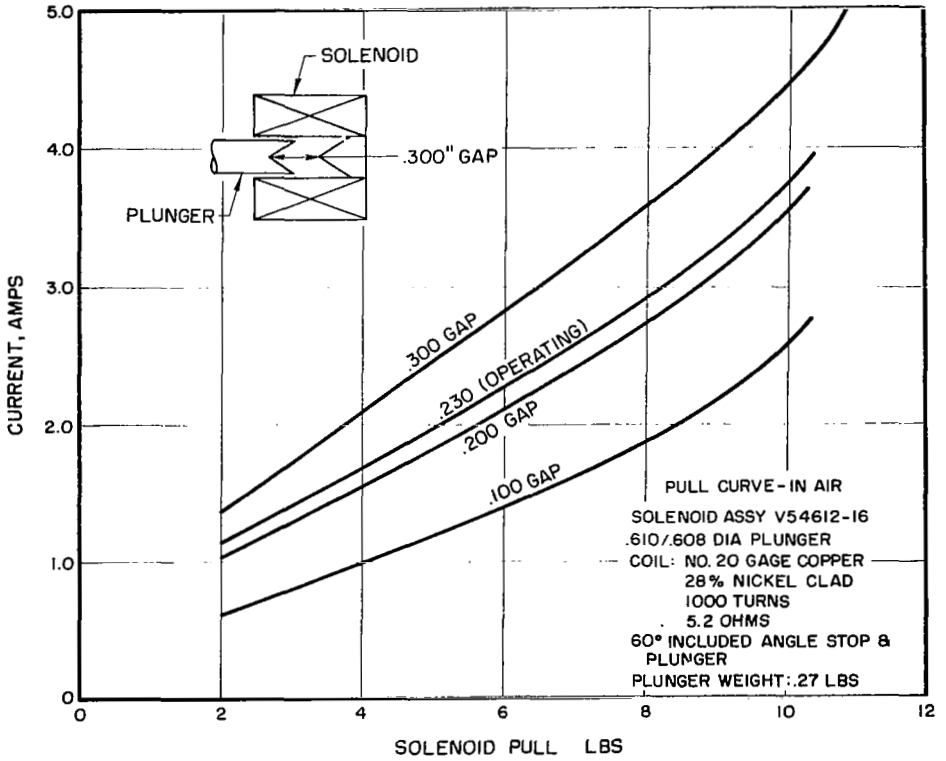

Figure 5-123 Solenoid "Pull" Curves - Various Plunger-to-Solenoid Gaps (Typical)

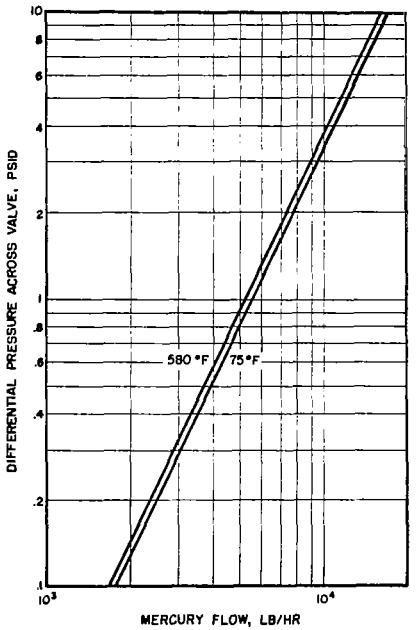

Pressure Drop vs Mercury Flow

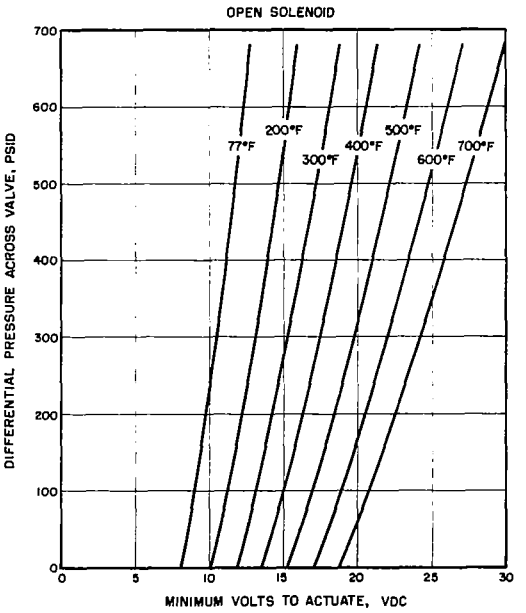

Differential Pressure vs Minimum Volts to Actuate at Various Temperatures - Open Solenoid

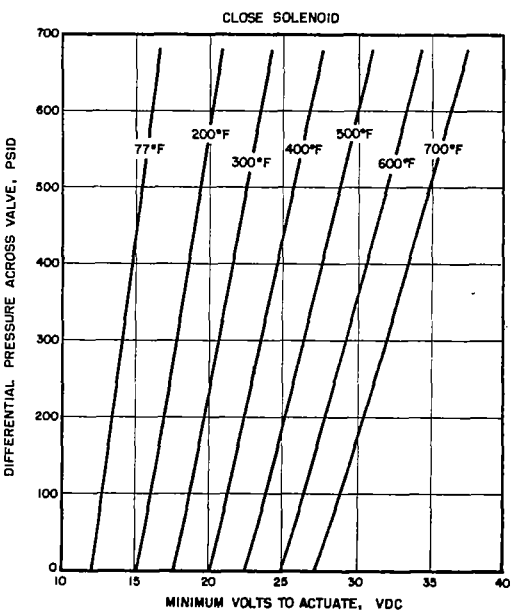

Differential Pressure vs Minimum Volts to Actuate at Various Temperatures - Closed Solenoid

Figure 5-124 Solenoid Valve Typical Performance Curve

5.7.6 Expansion Reservoirs

Eight expansion reservoirs were required in the 90-kWe system;

- Intermediate loop reservoir.- located in the NaK loop between the intermediate loop heat exchanger and the boiler. Its purposes are to maintain a void-free loop, compensate for a loop volume increase due to a temperature increase, and to ensure a net positive suction head for the pump.

- Heat rejection loop reservoir.- located in the heat rejection loop between the condenser and the radiator. Its purposes are the same as those for the intermediate loop reservoir.

- Boiler reservoir.- part of the static NaK system of the boiler. Its purposes are to maintain a void-free static NaK system to assure good heat transfer, especially in zero-gravity, and to compensate for a volume increase due to a temperature increase.

- Lubricant-coolant reservoir.- located in the lubricant-coolant loop. Its purposes are the same as those for the intermediate loop reservoir.

- Reactor power loop reservoir.- located in the NaK loop between the reactor and the intermediate loop heat exchanger. Its purposes are the same as those for the intermediate loop reservoir.

- Intermediate heat exchanger reservoir.- part of the static NaK system of the heat exchanger. Its purposes are the same as those for the boiler reservoir.

- Shield coolant heat exchanger reservoir.- part of the static NaK system of the heat exchanger. Its purposes are the same as those for the boiler reservoir.

- Auxiliary heat exchanger reservoir.- part of the static NaK system of the heat exchanger. Its purposes are the same as those for the boiler reservoir.

Figure 5-125 is a schematic of the 90-kWe system, showing the location of the expansion reservoirs described above.

Analyses were performed to size the reservoirs for the 90-kWe system configuration using S-shaped boilers, an intermediate loop, and a parallelepiped frame. A review of the reservoir specifications and design criteria was conducted.

As a result, new or revised specifications, incorporating all the changes required to meet conditions for the 90-kWe system, were prepared for the intermediate, heat rejection, and lubricant-coolant loop expansion reservoirs and for the boiler expansion reservoir.

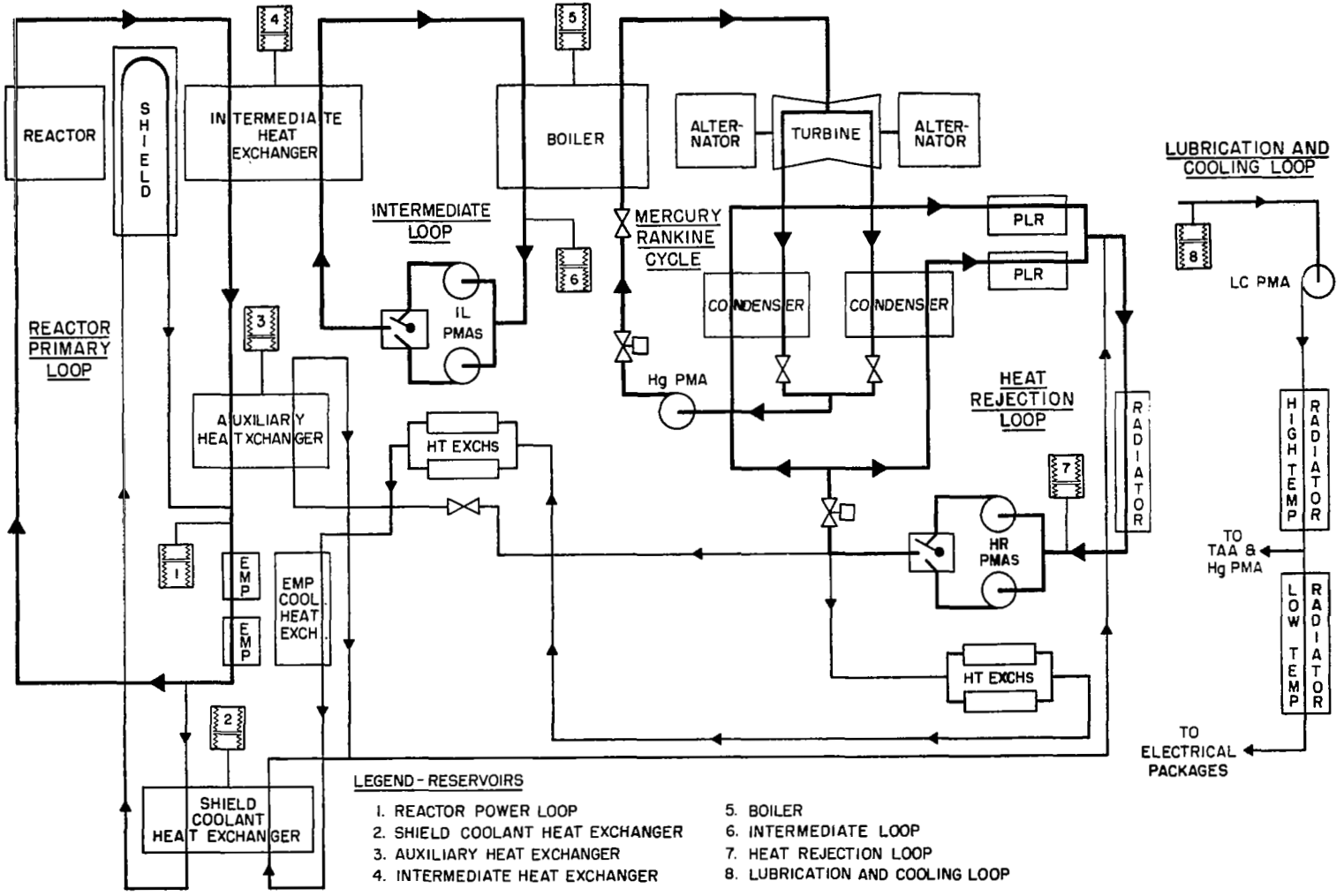

Figure 5-125 90-kWe System Schematic Showing Location of Expansion Reservoirs

Other specifications planned for the 90-kWe system, but not written due to program termination, were for the reactor power loop, the intermediate heat exchanger, and the auxiliary heat exchanger. It was planned to make the intermediate loop and the heat rejection loop reservoirs identical in diameter (18.5 inches) and length (34 inches). The lubricant-coolant reservoir was planned to be the same diameter, but shorter (26 inches). This would permit the three reservoirs to be made from the same bellows forming dies and tooling, permitting a substantial cost saving.

All reservoirs were planned to be of the same design, namely:

- A tandem-bellows configuration with encapsulated service fluid between the outside of the bellows and the inside of the reservoir shell to reduce the pressure differential across the bellows to a reasonable value for long life.

- A captured diatomic gas as the pressurant to be precharged and contained within one of the bellows.

- A small gas vent line in the bellows containing the service fluid to remove any gases trapped or generated in the particular loop that the reservoir services.

- The bellows configuration was to be of the "nesting ripple" design, welded at each convolute outside and inside diameter. The "nesting ripple" design would allow for the maximum bellows stroke for the minimum overall length. This was an important factor in the 90-kWe system.

A sketch of the basic expansion reservoir design can be seen in Figure 5-126. The split plate shown between the two bellows was designed to compensate for volume changes in the encapsulated service fluid as the temperature increased. In this way the bellows convolutes would not be subjected to stresses resulting from the expanding encapsulated service fluid.

Inconels and stainless steels were used as materials of construction. The Inconels were chosen for the high-temperature applications, whereas the Type 300 stainless steels were chosen for the lower-temperature applications.

All reservoirs were cylindrical with the intermediate loop, reactor loop, heat rejection loop, and lubricant-coolant loop reservoirs being of the same diameter.

Table 5-XXXV shows a typical list of expansion reservoir design parameters when a welded bellows is used for a 1400°F NaK application.

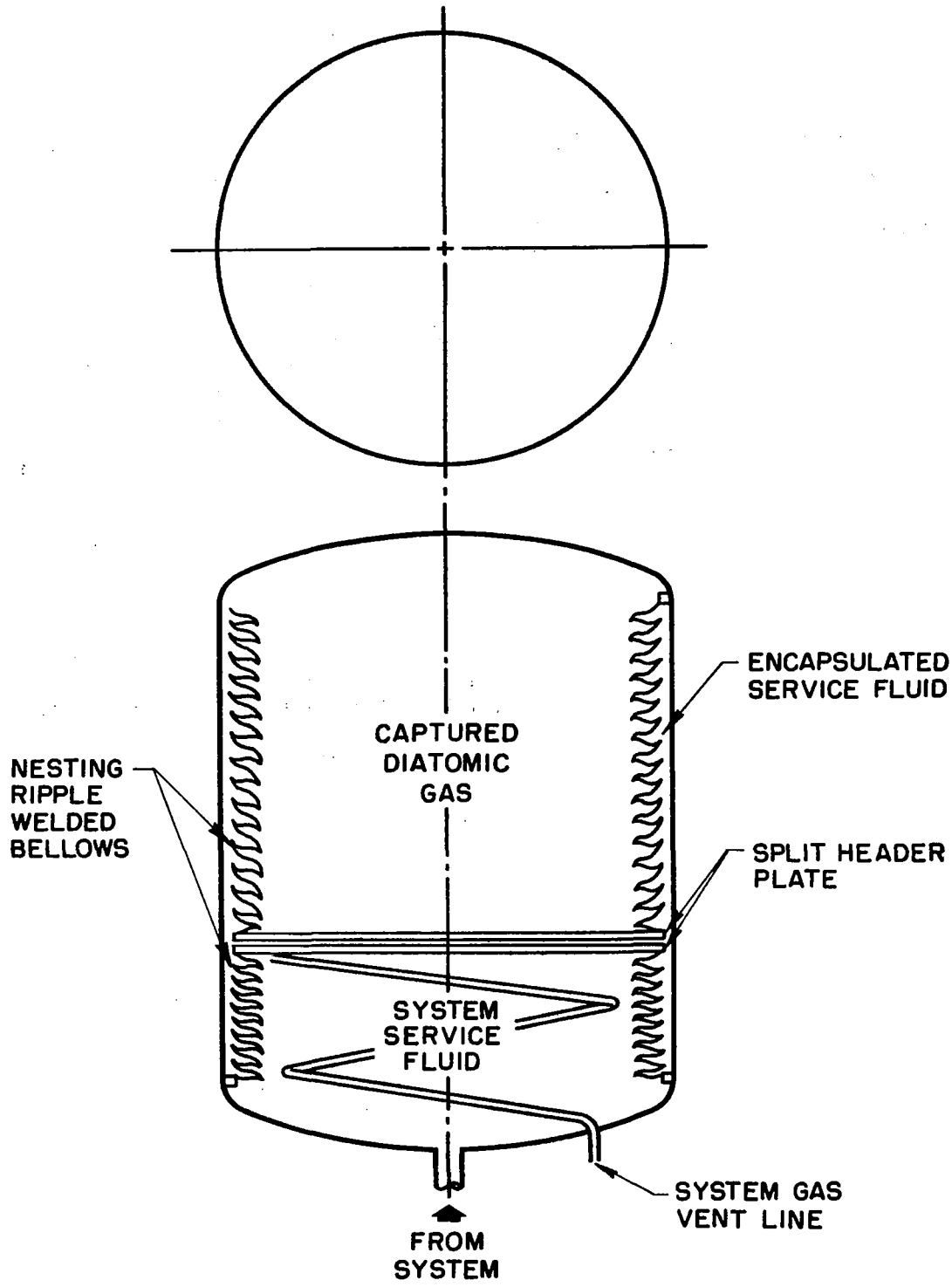

Figure 5-126 Basic Expansion Reservoir Design

TABLE 5-XXXV TYPICAL DESIGN PARAMETERS - PRIMARY NAK LOOP EXPANSION RESERVOIR

Design Parameter	Value
1. Bellows OD and ID, in.	21.0 x 19.0
2. Bellows effective area, $in.^2$	314
3. Maximum volume, $in.^3$	NaK = 4715, Gas = 8200
4. Bellows materials	Inconel 625
5. Material thickness, in.	0.010
6. Number of convolutes	NaK = 56, Gas = 56
7. Bellows free length	16.79 in. at 0.300 in. pitch
8. Active bellows stroke, in.	15.0
9. Stroke per convolute, in.	0.27
10. Bellows spring rate, lb/in.	NaK = 22.5, Gas = 22.5
11. Pressure to stroke, psid	1.10 for 15.0 in. stroke
12. Bellows nested length, in.	1.79
13. ΔP allowable - bellows, psid	23.7 internal to external at $70^{\circ}F$
14. Allowable stress, $lb/in.^2$	17,300 at $1400^{\circ}F$
15. Expulsion efficiency, %	Greater than 98
16. Shell material	Inconel 718
17. Pitch, in.	0.300 max., 0.032 min.
18. Pitch-to-span ratio	0.3 max.
19. Total estimated dry weight, lb.	212
20. Proof pressure, psid	200 for shell
21. Burst pressure, psid	450 for shell
22. Life cycles - min. at $1170^{\circ}F$	Infinite

5.7.7 Mercury Injection System

The functions of the mercury injection system are:

- Store liquid mercury during launch and system heatup prior to power conversion system.
- Inject mercury into the low pressure (suction) side of the mercury pump at a programmed rate to assure a smooth startup without subjecting the reactor to thermal shock.
- Control mercury loop inventory at the best level for efficient system operation. Mercury would be removed or added to the mercury loop as required.
- Add mercury to the loop to make up any losses through pump or turbine seals-to-space.
- Accept the mercury inventory pumped into the mercury reservoir by the mercury pump during a system shutdown such that a restart can be initiated with no external assistance.

The location of the mercury injection system in the SNAP-8 90-kWe system is shown schematically in Figure 5-127, and a photograph of the mercury injection system for a single start 35-kWe system shipped to NASA-LeRC is shown in Figure 5-128. This unit contains a single bellows and is pressure actuated using a nitrogen gas bottle, regulator, and valves as shown. However, the design planned for the 90-kWe system at the termination of the program can be seen in Figure 5-129. This design incorporated redundant bellows, an actuator piston, and a four-way valve with the lubricant-coolant fluid supplying the actuating force. No units were procured nor was the design developed beyond the conceptual stage.

Ten concepts analyzed were all low-pressure systems. All concepts were analyzed, based on the following operational requirements and limitations:

- Operate in a zero to one gravity.
- Perform a minimum of 20 startups and shutdowns without adjustment or servicing.
- Multiple startup attempts (at least two).
- Trim the inventory in the mercury loop to establish valid steady-state conditions in the condenser.
- Accept mercury inventory during a normal shutdown.
- Accept mercury inventory during an emergency shutdown.
- Respond to an emergency shutdown signal any time after initiation of injection.

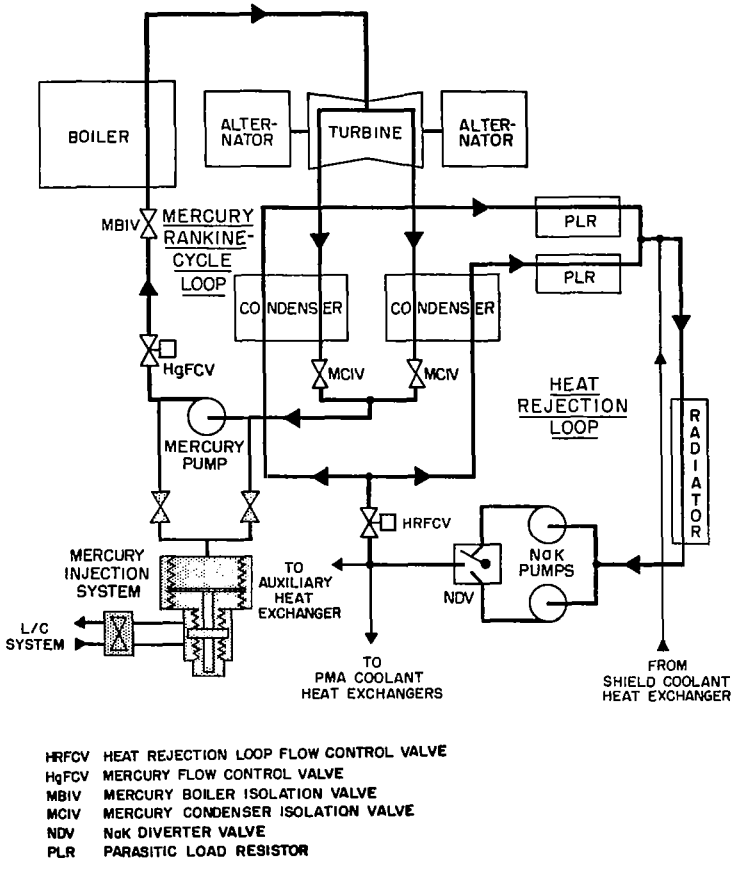

Figure 5-127 Portion of 90-kWe System Schematic Showing Location of Mercury Injection System

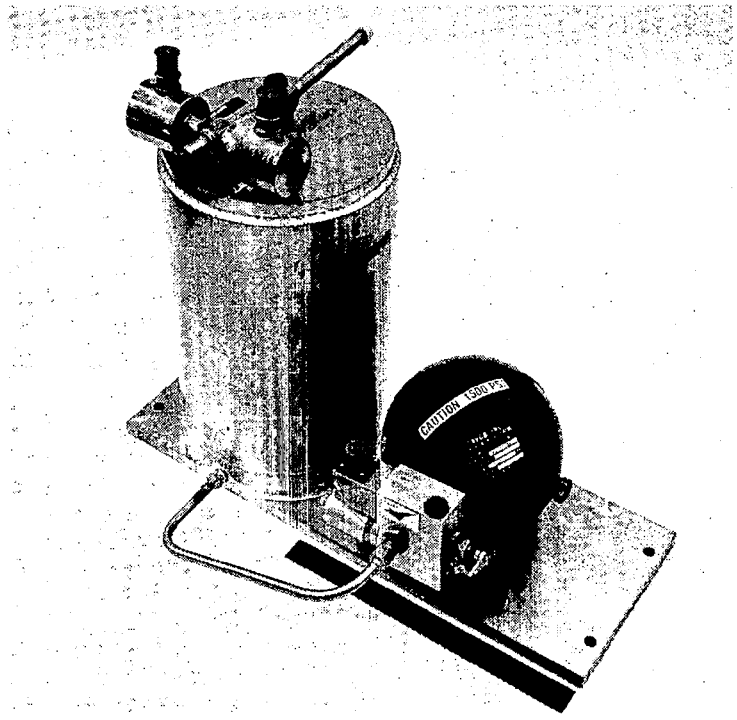

Figure 5-128 Mercury Injection System for SNAP-8 35-kWe Power Conversion System

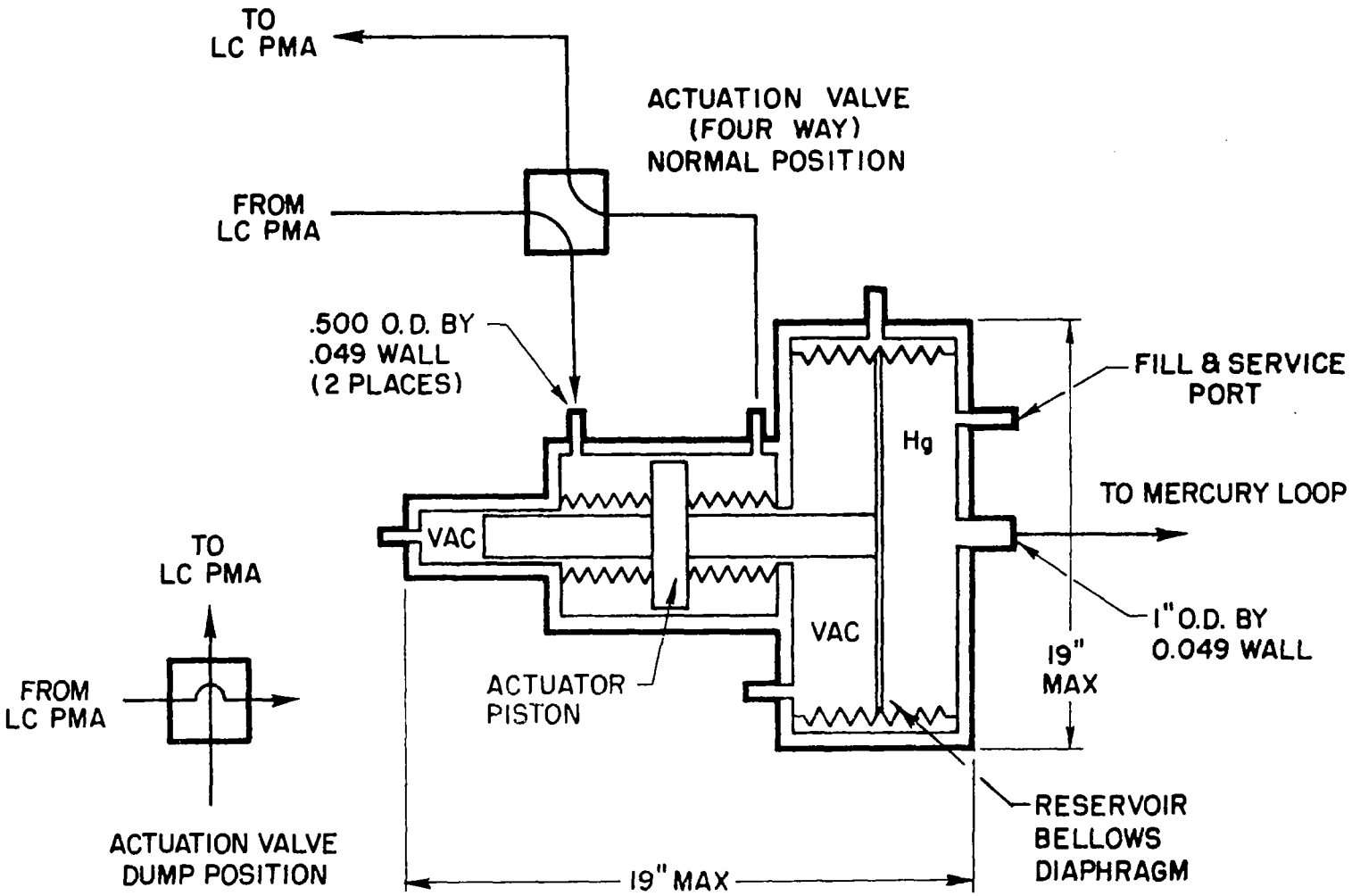

Figure 5-129 Schematic of Mercury Injection System for SNAP-8 90-kWe Power Conversion System

- Stop injecting mercury when a specific minimum quantity has been injected and a minimum pressure in the condenser has been reached.

- When the mercury pump is operating, the pump inlet conditions must be maintained above minimum NPSH for the particular speed and flow, and below the pressure capability of the visco seal.

- Maintain predictable and repetitive pressure-versus-time profile at the mercury flow control valve inlet during the injection phase.

- Make up for nominal leakage past the turbine-alternator and mercury pump seals.

- Not required to overcome loss of mercury loop integrity.

The system selected for the 90-kWe system was a low-pressure injection reservoir with redundant bellows, powered by a piston which was moved by the pumped lubricant-coolant fluid. Porting to inject or extract mercury to or from the main loop was controlled by a four-way valve in the lubricant-coolant loop such that discharge pressure from the lubricant-coolant pump could be directed to either side of the actuating piston.

A preliminary specification was prepared and vendors were being contacted to formulate a workable, fabricable design of the mercury injection reservoir at program termination.

A mercury injection system for a single-start 35-kWe system include a mercury injection reservoir which consists of a 120 convolute, nesting ripple, 0.012-inch thick, Type 347 SS bellows, a ball-end safety shutoff valve, a hold-down bolt, a pressure gate, and a canister. The shutoff valve is a double solenoid, latching, spring-loaded shear plate design. The nitrogen pressurization system consists of a 3000-psig pressure vessel, a two-way solenoid valve, a pressure regulator, a charge valve and a check valve. This system is mounted on a plate that is welded to the bottom of the reservoir.

The design parameters of the existing mercury injection systems for a single-start 35-kWe system are itemized in Table 5-XXXVI. The design parameters for the low-pressure mercury injection system for the 90-kWe system utilizing the lubricant-coolant pump discharge pressure for actuation are itemized in Table 5-XXXVII.

TABLE 5-XXXVI DESIGN PARAMETERS - MERCURY INJECTION SYSTEM FOR SINGLE-START SNAP-8 35-kWe SYSTEM

Parameter	Design Description
Reservoir Assembly	
Number of convolutes	120
Diaphragm thickness & type	0.012 in., nesting ripple
Material	Type 347 SS
Bellows OD & ID	8.00 x 6.50 in.
Effective area	41.4 $in.^2$
Spring rate	20 lb/in.
Volume displacement	335 $in.^3$ min. with 10 psid max.
Operating pressure	
Internal to bellows	600 psi max. with ΔP internal to external 10 psi max.
External to bellows	600 psi max. with ΔP external to internal 30 psi max.
Bellows & top plate weight	19.27 lb
Stresses (includes pressure stress at 10 psi ΔP and deflection stress)	
ID joint (room temp.)	
Mean stress	23,000 $lb/in.^2$
Alternating stress	16,000 $lb/in.^2$
Life	Infinite
OD joint (room temp.)	
Mean stress	21,000 $lb/in.^2$
	16,500 $lb/in.^2$
	Infinite
Stroke	8.75 in.
Fundamental longitudinal accordion vibration mode	10 Hz
Shell requirements	
Operating pressure	1800 psig
Proof	2250 psig
Burst	2500 psig
Bellows acceptance test fluid	Freon TF-22
Shell material	Type 410 SS

TABLE 5-XXXXVI (continued)

Parameter	Design Description
Nitrogen Pressurization System	
Pressure vessel volume	150 $in.^3$ min.
Solenoid valve	
Operating pressure	3000 psig
Proof pressure	4500 psig
Burst pressure	6660 psig
Flow rating	With inlet press. range of 3000 psig to 700 psig & an increasing flow from zero to 5 SCFM, the outlet pressure is to be maintained at 600 $\pm$ 15 psig.
Current drain	1.4 amps max. at 18 - 30 Vdc, Continuous duty
Pressure regulator	
Outlet pressure	600 $\pm$ 15 psig
Flow rating	Zero to 5 SCFM (increasing flow only) at 600 $\pm$ 15 psig.
Lockup	650 psig (Max.) regulated pressure
Startup & Shutoff Double-Solenoid Valve	
Current Drain	3.0 amps max. at 28 Vdc., intermittent duty.
Minimum pull voltage at 72°F.	15 Vdc at zero psid, 28 Vdc at 350 psid
Normal operating pressure	350 psid
Maximum solenoid temperature	400°F (soak), 275°F (operating)
Flow capacity	600 lb/hr (polyphenyl ether) at 0.25 psid and 250°F.

TABLE 5-XXXVII DESIGN PARAMETERS - MERCURY INJECTION SYSTEM FOR SNAP-8 90-kWe SYSTEM

Parameter	Design Description
Reservoir Assembly	
Large Bellows OD & ID	17.00 in. OD x 16.00 in. ID
No. convolutes (large bellows)	15
Small bellows OD & ID	1.062 in. OD x 0.562 in. ID
No. convolutes (small bellows)	68
Diaphragm thickness & type (large bellows)	0.008 in. thick, AMS 5507 (316 L)
Diaphragm thickness & type (small bellows)	0.005 in. thick, AMS 5507 (316 L)
Stroke (large bellows)	3.360 in.
Nested height (large bellows)	0.390 in.
Effective area (large bellows)	213.8 $in.^2$
Total volume (large bellows)	690 $in.^3$
Press. req'ts (large bellows)	
Operating	80 psia max.
Proof	150 psia
Burst	250 psia
Temp. Req'ts (large bellows)	
Operating	$50^{\circ}F$ to $463^{\circ}F$
Maximum	$600^{\circ}F$
Press. req'ts (small bellows)	
Operating	100 psia max.
Proof	188 psia
Burst	313 psia
Temp. req'ts. (small bellows)	
Operating	$50^{\circ}F$ to $250^{\circ}F$
Service life	5 years
Weight	130 lb
Shell & plates mat'l.	AMS 5507 (316 L)

6.0 ELECTRICAL CONTROL SYSTEM

6.1 CONTROL SYSTEM DESIGN

6.1.1 Introduction

The SNAP-8 eletrical control system provides the control and regulating functions necessary for startup, steady-state operation, and shutdown of the power plant. These functions include:

- Regulation of the turbine-alternator speed to provide constant output power frequency to the load.
- Regulation of the alternator output voltage.
- Control of the startup and shutdown sequencing.
- Providing startup and shutdown power.
- Protection of the power system and connected load.

The components which perform these functions and their interconnections are shown diagrmatically on Figure 6-1. The major control system components are:

6.1.1.1 Voltage Regulator-Exciter.- The alternator output voltage is controlled by controlling its field excitation power. The voltage regulator-exciter supplies field excitation power to the alternator as required to maintain constant output voltage.

6.1.1.2 Speed Control System.- The speed of the turbine-alternator is regulated by matching the output power to the available turbine power. This is accomplished by means of a parasitic load which absorbs any power in excess of the vehicle load requirements. The speed control module regulates the output power frequency by controlling the power flow through the saturable reactor to the parasitic load.

- Parasitic Load Resistor.- Absorbs the power output from the speed control saturable reactor.
- Programmer.- Controls all functions of the power conversion system including sequencing at startup and shutdown, and provides internal and external fault protection in conjunction with the protective system.
- Protective System.- Detects internal and external faults in the electrical system and initiates the necessary corrective action.
- Inverter.- Converts dc battery power to adjustable frequency, adjustable voltage ac power as required to operate the pump motors during startup and shutdown of the power conversion system.

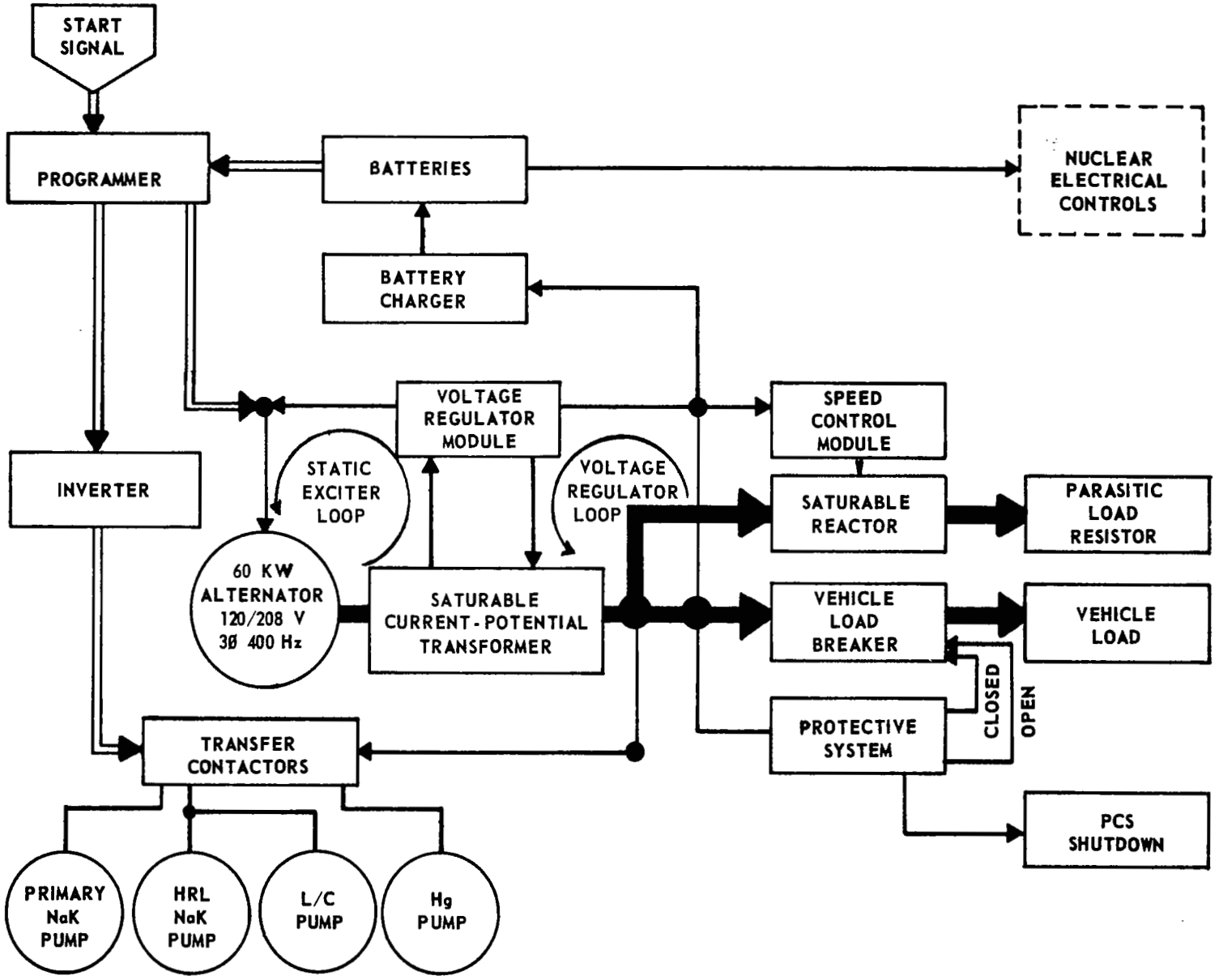

Figure 6-1 Electrical Control System Block Diagram - 35-kWe SNAP-8 System

- Direct-Current Power Supply.- Provides a power source for startup and shutdown of the power conversion system. It includes means of recharging and maintaining the batteries during periods which the power conversion system is operating.

- Vehicle Load Breaker.- Connects the vehicle load to the power conversion system.

- Motor Transfer Contactors.- Transfer the pump motors from start-up and shutdown inverter power to alternator power for steady state operation.

6.1.2 90-kWe System

The electrical system block diagram for the 90 kWe system is shown in Figure 6-2. The system design utilizes existing SNAP-8 components with a minimum of modifications.

Two SNAP-8 alternators are required to generate 120-kW of electrical power to supply 90-kW of useful output in addition to the power system auxiliaries. They will be driven by a single turbine assembly and operate in parallel. The sharing of the electrical power (kW) will be accomplished by proper alignment of the stators and rotors of the two alternators. Once the relationship between the two machines is set the load sharing is established by the machine electrical characteristics. The power output of an alternator is a function of the angle between the internal voltage and the terminal voltage commonly referred to as the displacement angle, or power angle.

The terminal voltage of two alternators connected in parallel is identical; therefore, the load division is a function of the power angle of each machine. When machines are coupled mechanically to a common prime mover, the power angle is determined by the alignment between the two machines. To determine the effect of angular differences between the two machines on their load sharing, the kW output vs power angle was calculated for the SNAP-8 alternator. Figure 6-3 shows that, for 60 kW output at 1.0 PF, the power angle is 28.3 degrees. Allowing a maximum unbalance load of 10% between two paralleled alternators, the maximum angular alignment error may be determined from the power vs power angle curve. If one alternator is supplying 57 kW while the other is supplying 63 kW, the power angles are 26.6 degrees and 30.2 degrees, respectively. The difference of 3.6 electrical degrees or 1.8 mechanical degrees is the angular tolerance allowed between alternators to divide the load within 10% of each other.

The angular deflection of the alternator quill shaft will have little effect on the load sharing between machines. The calculated deflection at 60 kW load is only 0.21 degrees. Inasmuch as the load sharing is affected by the difference between the two quill shafts, the net effect will be negligible.

Proper alignment between machines can be accomplished by control of winding placement and by proper indexing of the assemblies. As an alternative the alternators may be adjusted on test by incorporating a means of adjusting the stator angular position.

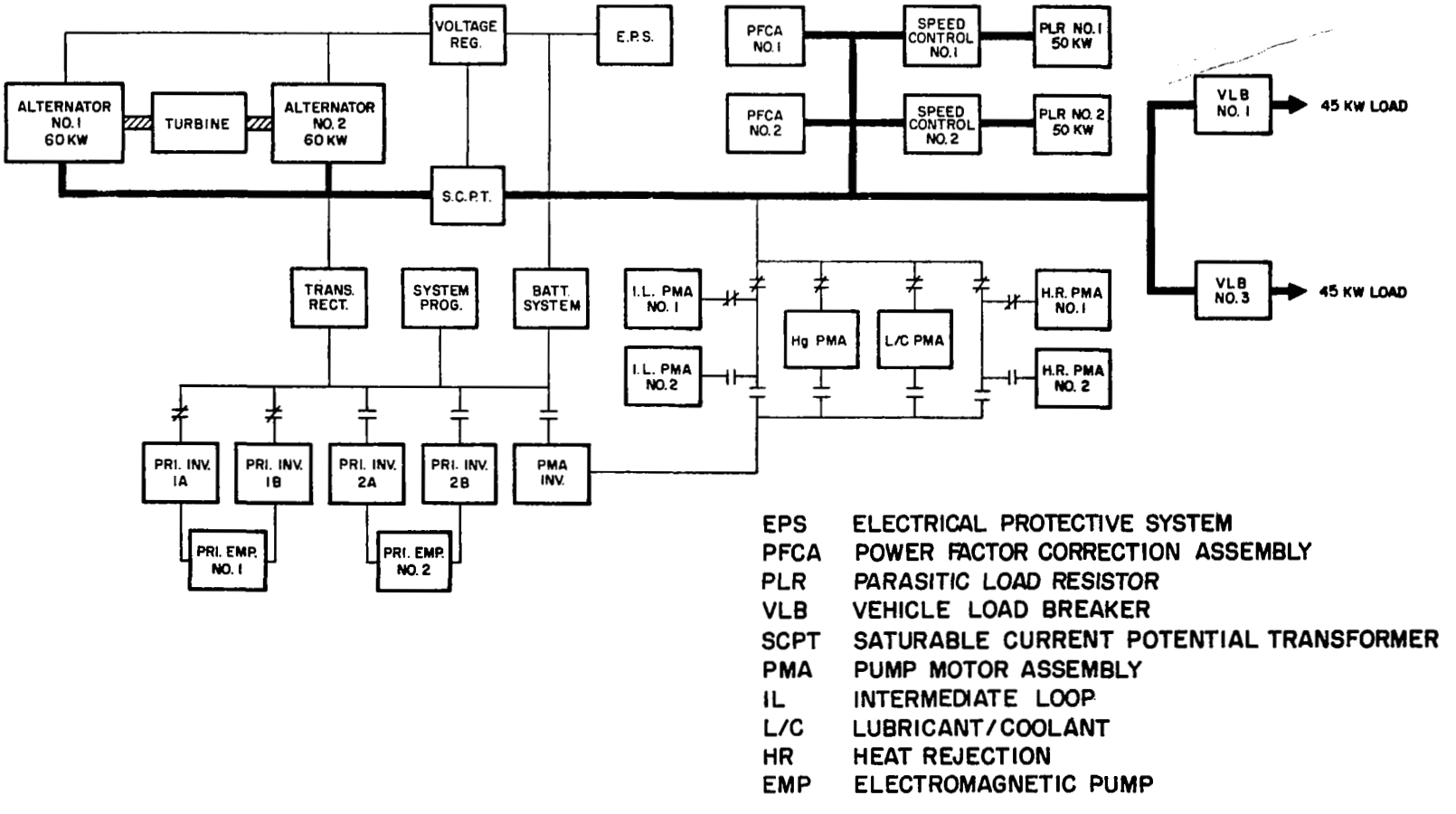

Figure 6-2 Electrical System Block Diagram for 90-kWe SNAP-8 System

The reactive load division between alternators may be accomplished by supplying the same field excitation to each machine. For a particular machine operating at a constant output voltage the field current, power output (kW) and power factors are interrelated. Therefore, if the power output and field current are predetermined then the power factor is also predetermined. For example, if the field current of the two alternators is made identical by connecting the two field coils in series, and the power is divided equally by proper alignment as previously discussed, then the power factor of each machine will be the same within the limitations imposed by machine manufacturing variations. Figure 6-4 shows the relationship between power factor, field current and power output of the SNAP-8 alternator. For a power factor change from 1.0 to 0.95 lagging at 60 kW output, the field current change is from 12.2 to 14.3 amperes. This difference is an indication of the strong influence of the power factor upon the field current of the alternator. Considering that the variation in rated load field current of the five prototype alternators was less than one ampere, it can be expected that the power factor difference between paralleled alternators would be less than 0.05 units.

A single voltage regulator-exciter will supply excitation and control the voltage of two alternators. The saturating current potential transformer (SCPT) will require modification to meet the modified requirements of the higher rated system. The total excitation power of the two alternators each operating at 60 kW, 1.0 PF, is lower than one alternator operating at its original design rating of 60 kW, 0.75 PF, as shown by the following table.

Alternator Excitation Required

	35-kWe System	90-kWe System
Alternator rating, kW	60	60 (2 Req'd)
Alternator PF	0.75 lag	0.975 lag
Alternator field current, amp	19	13 (each)
Alternator field voltage	48	31 (each)
Alternator field power, watts	912	403 (each)
Alternator output current, amp	222	171 (each)
SCPT current, amp	222	342 (total)
Excitation power required, watts	912	806 (total)

The primary winding of the static exciter would require fewer turns capable of a higher current capacity while the output winding would need more turns of a lower current capacity to meet the requirements of the combined alternator system. The overall size of the unit should be the same since the power output is similar.

As an alternative to supplying equal excitation to both alternators from a single voltage regulator-exciter, two voltage regulator-exciters may be used with cross-current compensation. This would force equal divisions of

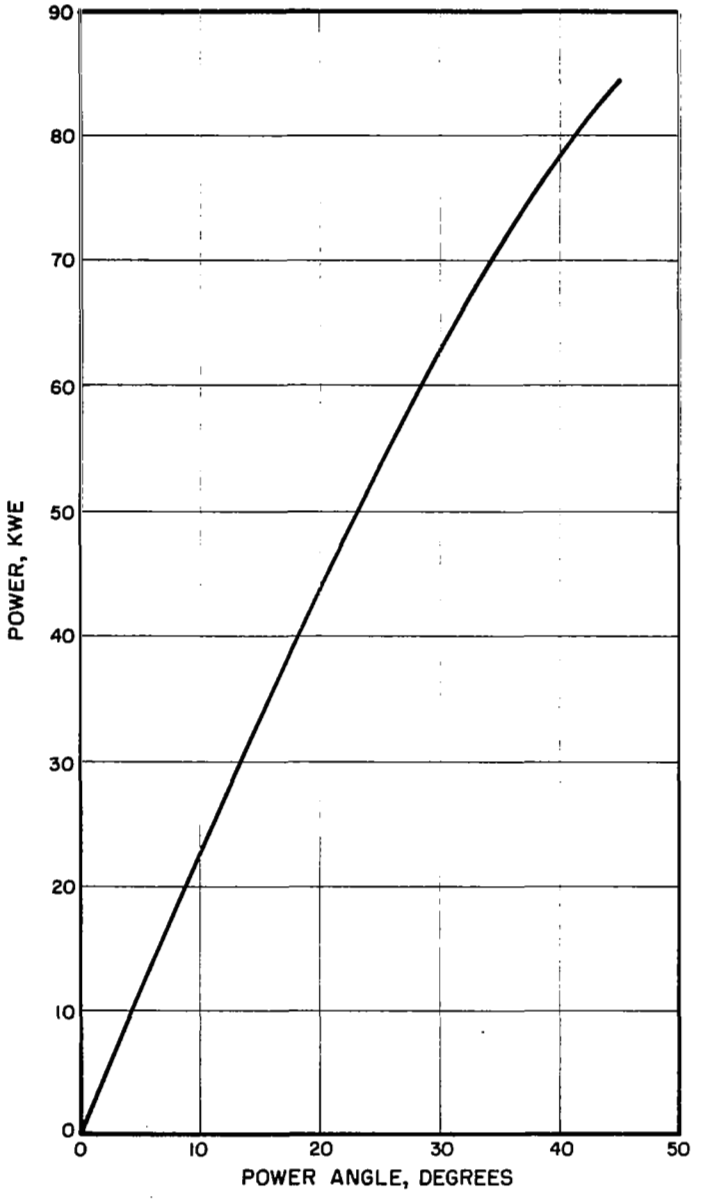

Figure 6-3 Alternator Output Power vs Power Angle

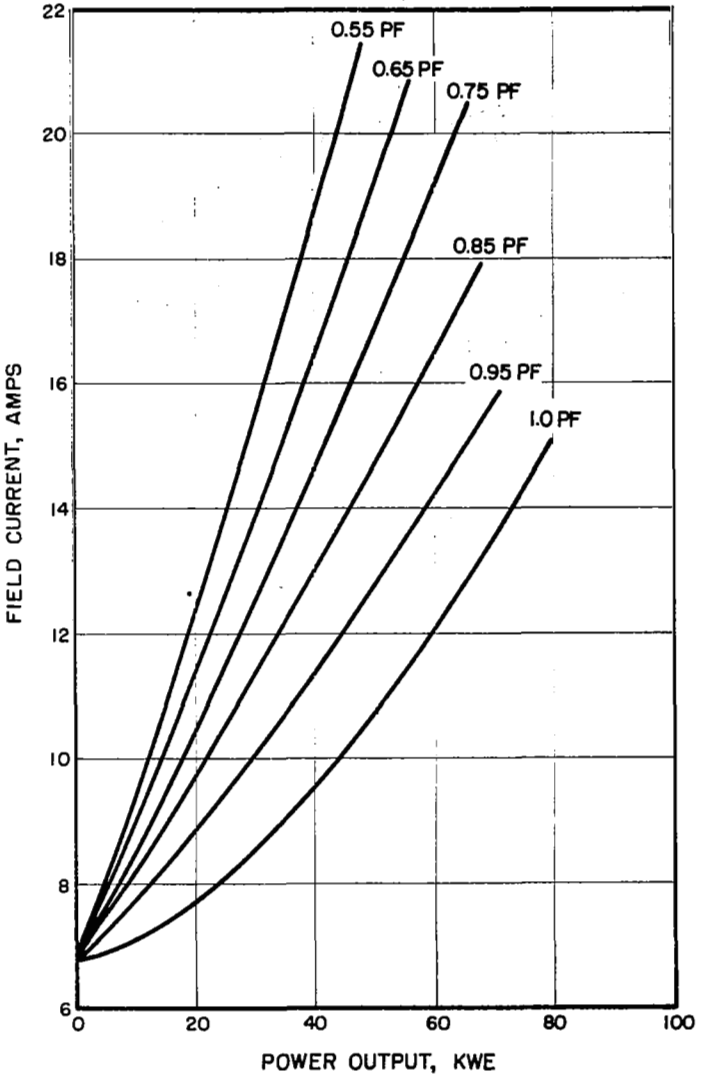

Figure 6-4 Alternator Field Current vs Load

reactive kVa by sensing current of each alternator and adjusting the field excitation to minimize the circulating currents.

The speed control for the 90-kWe system would require a capability of dissipating approximately 100 kW of electrical power. This can be accomplished by using two of the present SNAP-8 speed control units and parasitic load resistors rated 50 kW each. For best results, the frequency settings should be staggered so that the power to one unit will approach minimum before the second unit is unloaded. This will decrease the speed regulation accuracy slightly but will result in less system voltage distortion due to nonlinear currents to the speed control.

The third consideration for parallel operation of alternators is stability. Instability can result from variation in driving torque, load, and field excitation. The relationship between torque and power angle along with the mechanical inertia of the rotating parts and the damping torque resulting from the rate of change of the power angle could provide the elements of an oscillatory system.

The conditions imposed by the proposed parallel operation of alternators eliminate most of the variables that could cause instability. Variations in field excitation may be eliminated by series connection of the alternator fields and the relationship between torque and power angle is the same for both alternators since they are driven from a common prime mover.

The power factor correction requirements of the 90-kWe system are approximately double that of the 35-kWe system as shown on the following table.

Power Factor Correction Requirements

	35-kWe System	90-kWe System
Pump-motor	18.4	18.4
Speed control	16.1	32.2
Vehicle load	21.6	55
Total	56.1	105.6

This requirement may be met by use of two power factor correction assemblies.

The vehicle load is 90-kWe at 0.85 PF resulting in a load current of 294 amperes. The present vehicle load breaker is rated 175 amperes. To use available hardware, the vehicle load may be divided into two 45 kW sections, each controlled by a separate vehicle load breaker.

The requirements for other electrical system components are expected to be applicable to the 90-kWe system with little or no change. These include:

- System programmer
- Electrical protective system
- Pump-motor
- Motor transfer contactors

6.1.3 35-kWe System

The 35-kWe system electrical system is shown in the block diagram Figure 6-1. The major components shown were developed and tested as part of the overall power conversion system. A brief description of their functions is given in the introduction of this section followed by detailed discussion of each major component in the following sections. A major effort of the SNAP-8 Program was devoted to the development of these components. Many of the components developed are suitable with little or no change for higher-power systems, including the 90-kWe system.

6.1.4 Design Approach for Electrical Control Components

The major design objective of the SNAP-8 electrical control system is to provide a system with good performance and the highest possible reliability. At the time of the electrical system development, the reliability goal of the SNAP-8 power conversion system was 99.9% for 10,000 hours of continuous operation in a space and nuclear radiation environment. Whereas an increase in component weight could be tolerated to improve reliability, a failure would render the total system useless.

The design techniques employed to assure reliable performance were:

- Use of components of proven reliability
- Circuit simplicity
- Electrical connections of positive reliability
- Redundancy of vulnerable components
- Component derating
- Isolation of circuit elements from environmental hazards
- Performance testing

The selection of components was strongly influenced by their reliability under the imposed environmental conditions. Magnetic control components were favored over semiconductors since they are less susceptable to nuclear

radiation damage. Similarly, silicon diodes were favored over transistors and silicon controlled rectifiers.

Where rectifiers are required, the diodes were connected in series-parallel combinations (quads). By use of this redundant configuration, a single diode failure may be tolerated without affecting the function of the rectifier. The use of the quad also effectively derates each diode 50% in both voltage and current, under normal operation. Figure 6-5 illustrates how the failure rate is reduced by redundancy. For example, a single diode failure rate of 0.01% is decreased to 0.00001 % when the diode is replaced by a quad.

Resistors are selected for their resistance to failure by short circuiting and then connected in parallel combinations to minimize the effect of a single open-circuit failure.

Major emphasis has been placed on the integrity of electrical connections to minimize this common cause of electrical failure. Welded connections are used wherever possible throughout the electrical equipment. Electrical connections which depend upon spring pressure to maintain contact are avoided.

The electrical components are designed for operation in a space environment and high nuclear radiation in addition to environments of terrestrial origin resulting from packaging, handling, transportation, and storage. Factors such as operation in hard vacuum have resulted in the use of conduction as the major means of component cooling. Heat generated within the component is removed by conduction to cooled heat sinks upon which the components are mounted. Component placement was in many cases governed by the availability of good heat conduction paths to the cooled surfaces.

The nuclear radiation level to which the electrical components were to be exposed was an important factor in determining the component selection. The electrical components are required to withstand the following total integrated radiation dose:

1×10^{11} NVT fast neutrons

1×10^{6} rads (c) gamma

6.2 VOLTAGE REGULATOR-EXCITER

6.2.1 Introduction

The voltage regulator-exciter provides ± 3% regulation over a load range of 3.5 to 35 kW at a power factor of 0.85 lagging under all specified environmental conditions. Required reliability was 99.9% for 10,000 hours of continuous operation.

To meet these system requirements the voltage regulator-exciter was designed to regulate the alternator voltage to the following requirements:

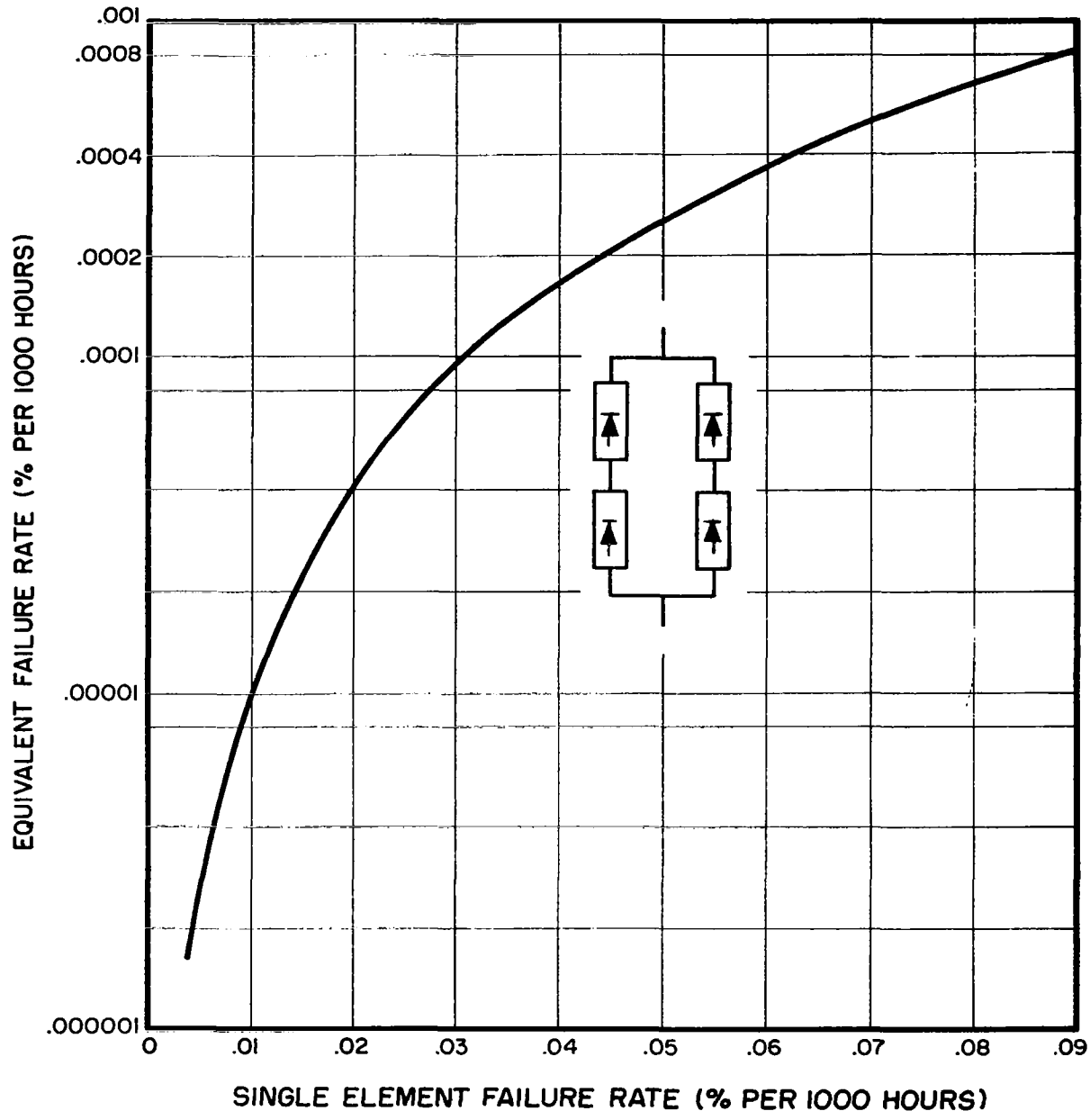

Figure 6-5 Failure Rate for Rectifier Quad - 10,000-Hour Mission

- 208 volts line-to-line ± 3%
- 0 to 60 kW alternator load
- 0.75 lagging to 1.0 power factor
- 400 Hz ± 1% frequency range

If the alternator frequency deviates from 400 Hz, the voltage is maintained proportional to frequency to avoid saturation of magnetic devices. The regulator is designed to supply specified currents under short circuit conditions to allow protective devices in the load to function, and to recover to normal operating conditions when the fault is removed.

The alternator voltage is regulated by automatically adjusting the alternator field current to compensate for changes in load and field-coil temperature. Regulation is provided by the voltage regulator and the saturable current potential transformer. The voltage regulator module reuses the alternator output voltage and compares it to a reference which is proportional to frequency. The output of the voltage regulator controls the saturation level of the saturable current potential transformer which supplies the required field current to maintain the alternator voltage within specified limits.

As in all SNAP-8 components, the primary design considerations are reliability and performance. The voltage regulator-exciter is a sealed unit designed for conduction cooling to the heat sinks upon which it is mounted.

It is designed to avoid multiple amplifier stages, regulated power supplies, and other complicating circuits. A schematic of the unit is shown in Figure 6-6. To reduce complication and eliminate a failure mode, an external voltage adjustment is omitted. Circuits requiring the semiconductors and no capacitors are used because of the vulnerability of these components to nuclear radiation and high temperature. A basic circuit was chosen which uses magnetically active components and excludes the use of transistors and silicon controlled rectifiers. The system is stabilized by means of a damping transformer in preference to a resistance-capacitance network.

The diodes are controlled avalanche silicon types. Only wire-wound or film-type resistors are used because the possibility of short circuit failure of these types is very low. The cores of the magnetic components are built up of laminations, and coils are layer wound to minimize the possibility of turn-to-turn shorts. To minimize breakage, no wire smaller than Number 30 is used in any of the wire-wound components.

During operation at no load, all the alternator field excitation is supplied by the voltage winding of the saturable current potential transformer. When load is applied to the alternator, the load current passing through the current winding of the saturable current potential transformer supplies additional excitation to the alternator field to compensate for the additional voltage drop in the alternator produced by such a load current. Lagging power factor current produces more excitation than in-phase or leading current, and

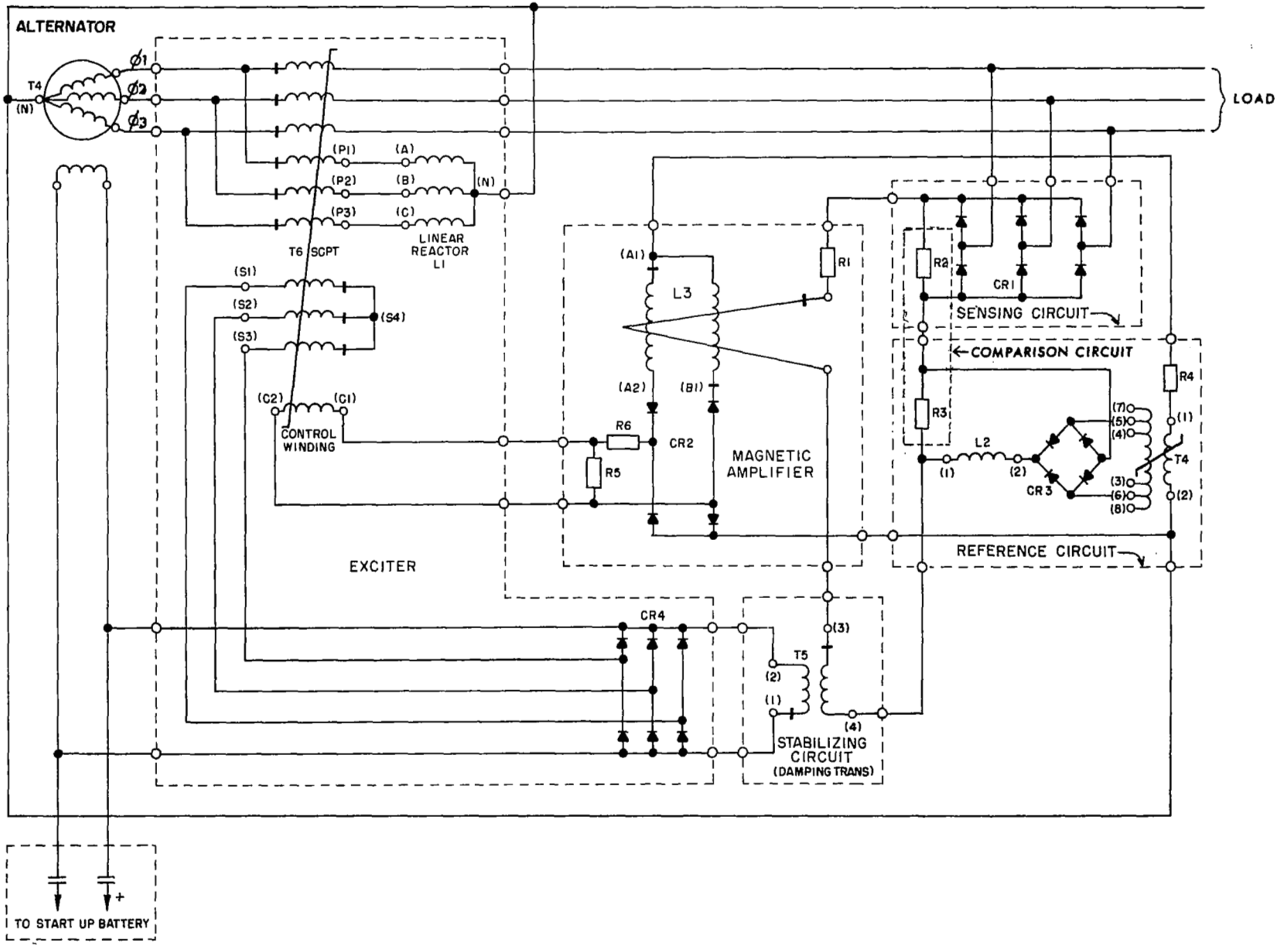

Figure 6-6 Voltage Regulator-Exciter Schematic

since lagging power factor loads require more excitation than in-phase or leading loads, the increased excitation supplied by the load current tends to compensate for changing power-factor loads. Compensation is not precise, so a regulator control-circuit is provided to adjust the output of the saturable current potential transformer. When a load change occurs, and the compensation is too great or too little, the voltage output of the alternator rises or falls accordingly. The voltage regulator senses this change and supplies control current from the magnetic amplifier to the saturable current potential transformer. This changes the output of the saturable current potential transformer in the correct direction to return the alternator voltage to the rated level.

The voltage regulator-exciter is capable of regulating the output voltage of the SNAP-8 alternator from 0 to 80 kVa over a power factor range from less than 0.75 lagging to 0.9 leading. The minimum lagging power factor is determined by the field current requirements of the alternator. The maximum continuous field current capability of the voltage regulator-exciter is 24 amperes. The alternator field current requirement at 80 kVa 0.75 power factor lagging is approximately 20 amperes.

The voltage regulator-exciter will provide excitation under fault conditions to deliver the following fault currents.

- Three-Phase Short Circuit - 2.8 Pu
- Single-Phase L-N Short Circuit - 4.2 Pu
- Single-Phase L-L Short Circuit - 3.0 Pu

The voltage regulator-exciter and alternator must be protected from overheating which would result from short circuits of extended duration (greater than 15 seconds). This protection is provided by the electrical protection system which will open the vehicle load breaker and/or shut down the power conversion system in the event of the resulting low or unbalanced voltages.

The rating summary of the voltage regulator-exciter is as follows:

Rated voltage	120/208, ± 3%
Rated frequency, Hz	400, ± 1%
Rated current, amp	200
Power Factor	0.75* Lag to 0.9 Lead
Rated output, kVa	80

* Will operate at lower lagging power factor until field current limit of 24 amperes is exceeded.

Maximum continuous current, amp	222
Maximum continuous field current, amp	24
Voltage regulator heat sink temperature, ^{o}F	170
Reactor-transformer heat sink temperature, ^{o}F	240
Voltage regulator loss, watts	110
Reactor-transformer loss, watts	80
Voltage regulator weight, lb	72
Reactor-transformer weight, lb	72

6.2.2 Physical Descriptions

The voltage regulator module and saturable current potential transformer module are hermetically sealed packages to protect the components, wiring, and insulation from earth and space environments. The enclosures are so constructed the heat developed within the module is transferred through the base to a liquid-cooled heat sink. Electrical connections are made into the modules through hermetically sealed feed-through terminals with ceramic insulators. The voltage regulator module is shown in Figure 6-7, and the saturable current potential transformer module is shown in Figure 6-8.

Included in the voltage regulator module are the saturating transformer reference, the voltage sensing and comparison circuit, the magnetic amplifier, and the damping transformer. The exciter unit includes the saturating current potential transformer, and the linear reactor.

6.2.3 Demonstrated Performance

During acceptance tests with the SNAP-8 alternator, four voltage regulator-exciters were tested. The load was varied from no load to full load, 60 kW at 0.75 PF with the frequency held in constant at 400 ± 1 Hz. All four units held the voltage within ± 0.6%. The recovery time of the four units on sudden load application (60 kW at 0.75 PF) varied from 0.35 to 0.27 seconds; on removal of the same load, the recovery time varied from 0.27 to 0.20 seconds. All systems were stable during these tests and showed no tendency to oscillate. On sudden application and removal of two-per-unit impedance load, the voltage dip and rise was approximately 15%; when various short-circuit tests were conducted, the minimum current value was demonstrated to be 2.85 per unit on a three-phase line-to-line short circuit.

One voltage regulator-exciter was operated in an endurance test regulating the voltage of an alternator driven by the turbine. The unit performed successfully in this test for 12,996 hours without failure and with no adjustments.

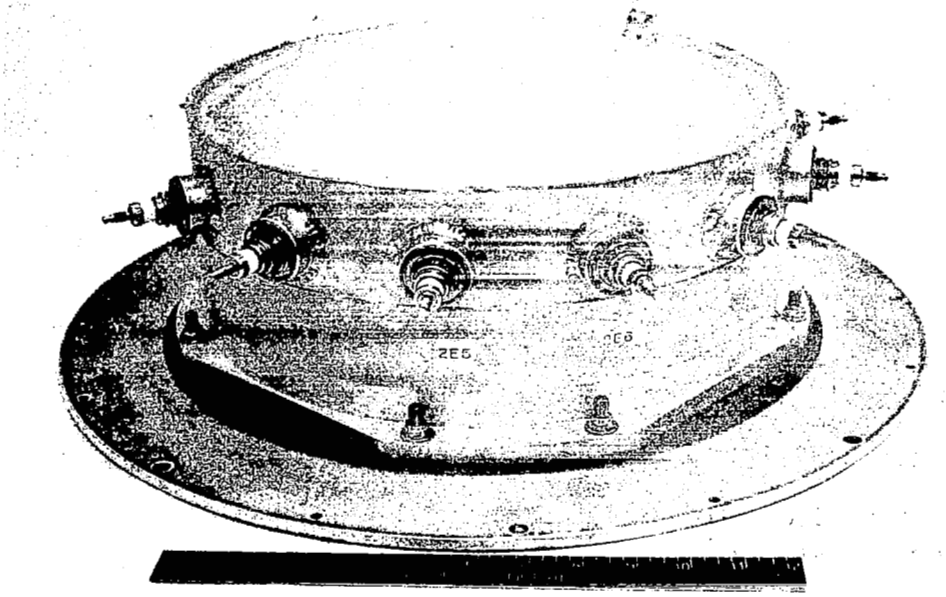

Figure 6-7 Voltage Regulator Module

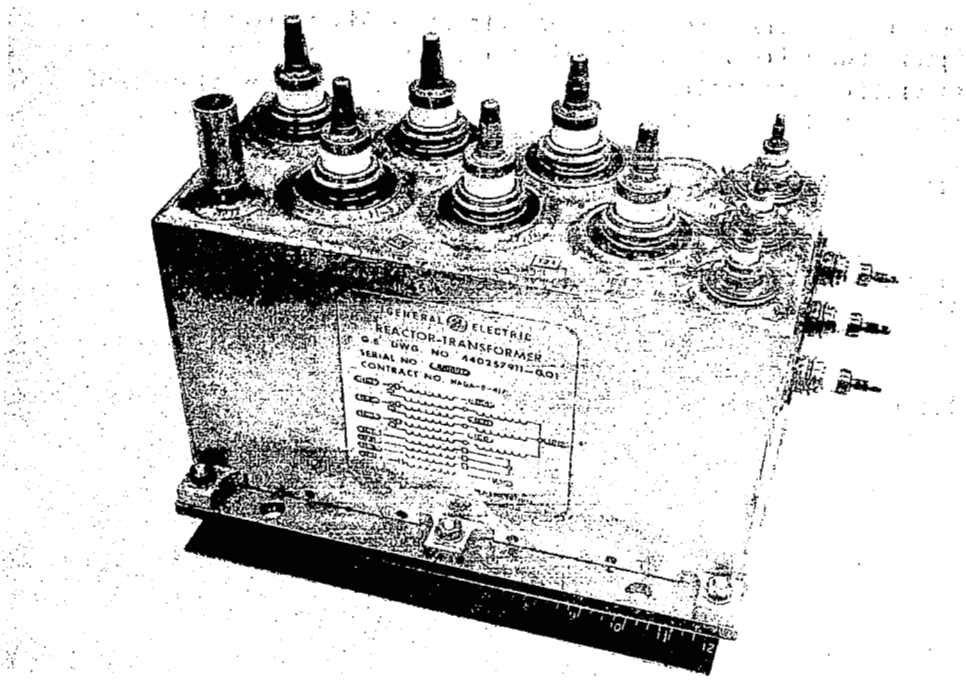

Figure 6-8 Saturable Current Potential Transformer Module

Another unit operated successfully in the electrical test facility, during an endurance test, for 23,130 hours. During these tests, the voltage regulator module was mounted on a heat sink which was maintained at a temperature of 170 to 180°F to simulate the expected temperature of the low-temperature liquid-cooled heat sink. The saturable current potential transformer was mounted on a heat sink held at approximately 240°F, the expected temperature of the high-temperature heat sink. During this period of operation, the voltage held within ± 2.5% of the set point including the effects of load, temperature, and time changes.

Suddenly applied and removed load tests were conducted during the turbine-alternator tests with the speed control system regulating the turbine-alternator speed and the voltage regulator-exciter regulating the alternator voltage. When a load of 36 kW at 0.83 lagging power factor was suddenly applied, the initial voltage dip was 14% and the recovery to 5% occurred in 0.2 seconds. When the same load was suddenly removed, the initial voltage rise was 9.3% and the recovery to ± 5% occurred in 0.15 seconds (see Figure 6-9).

Detailed information on the design and performance of the voltage regulator-exciter may be found in Reference 60.

6.3 SPEED CONTROL

6.3.1 Introduction

The speed control regulates the speed of the turbine-alternator to maintain the frequency of the output electrical power within specified limits of 400 Hz ± 1%. The speed of the turbine-alternator is controlled by matching the output power to the available turbine power. This is accomplished by means of a parasitic load which absorbs any surplus power over the requirements of the vehicle load. The speed control system accomplishes this function by sensing the alternator output frequency and controlling the current flow through an adjustable impedance saturable reactor to the parasitic load.

The selection of the saturable reactor as the power control element of the speed control system was based on reliability. Compared to silicon controlled rectifiers and self-saturating magnetic amplifiers, the saturable reactor was considered the most reliable and least susceptable to damage or degradation due to nuclear radiation. It also provided less distortion to the alternator output and lower radio frequency interference because of its slower turn-on characteristic. Its disadvantages of increased size and weight and higher control power requirements were considered of lesser consequence in view of the reliability goal of the system.

6.3.2 Design and Development

The simplicity of the speed control basic circuitry is shown in the schematic diagram, Figure 6-10. Seven rectifiers are required, although the redundancy of parts used to improve reliability results in the use of 28 diodes. No bias supply, regulated or unregulated, is necessary for normal steady-state operation of the system. The active components are wound magnetic

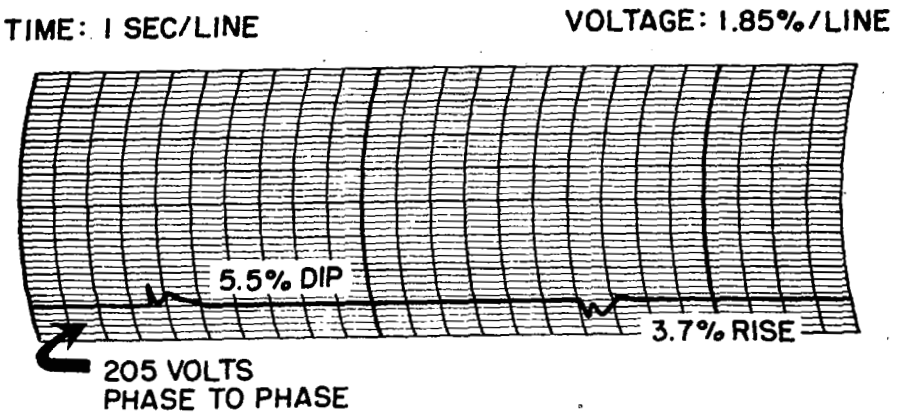

Load, 36 kw, 1.0 PF Suddenly Applied and Removed

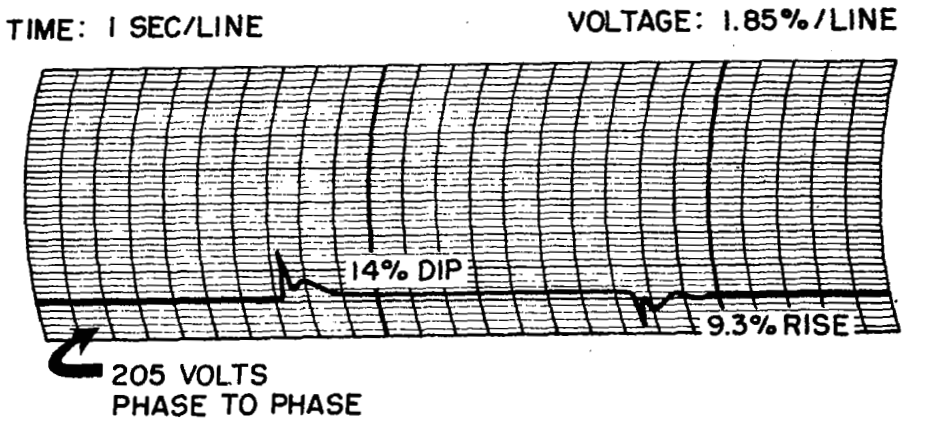

Load, 36 kw, .83 PF Suddenly Applied and Removed

Figure 6-9 Voltage Regulator Exciter Response to Suddenly Applied and Removed Loads

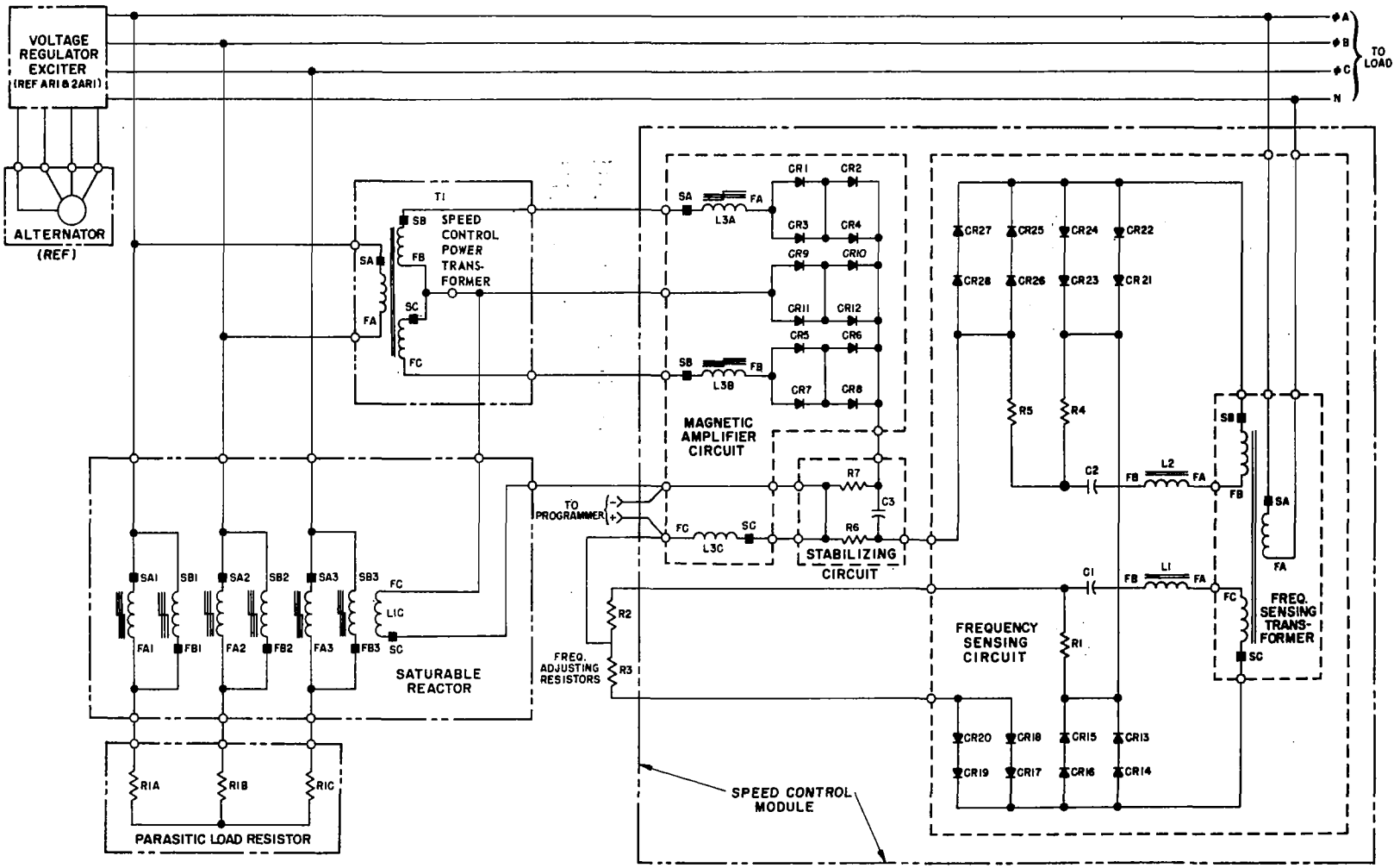

Figure 6-10 Speed Control System Schematic

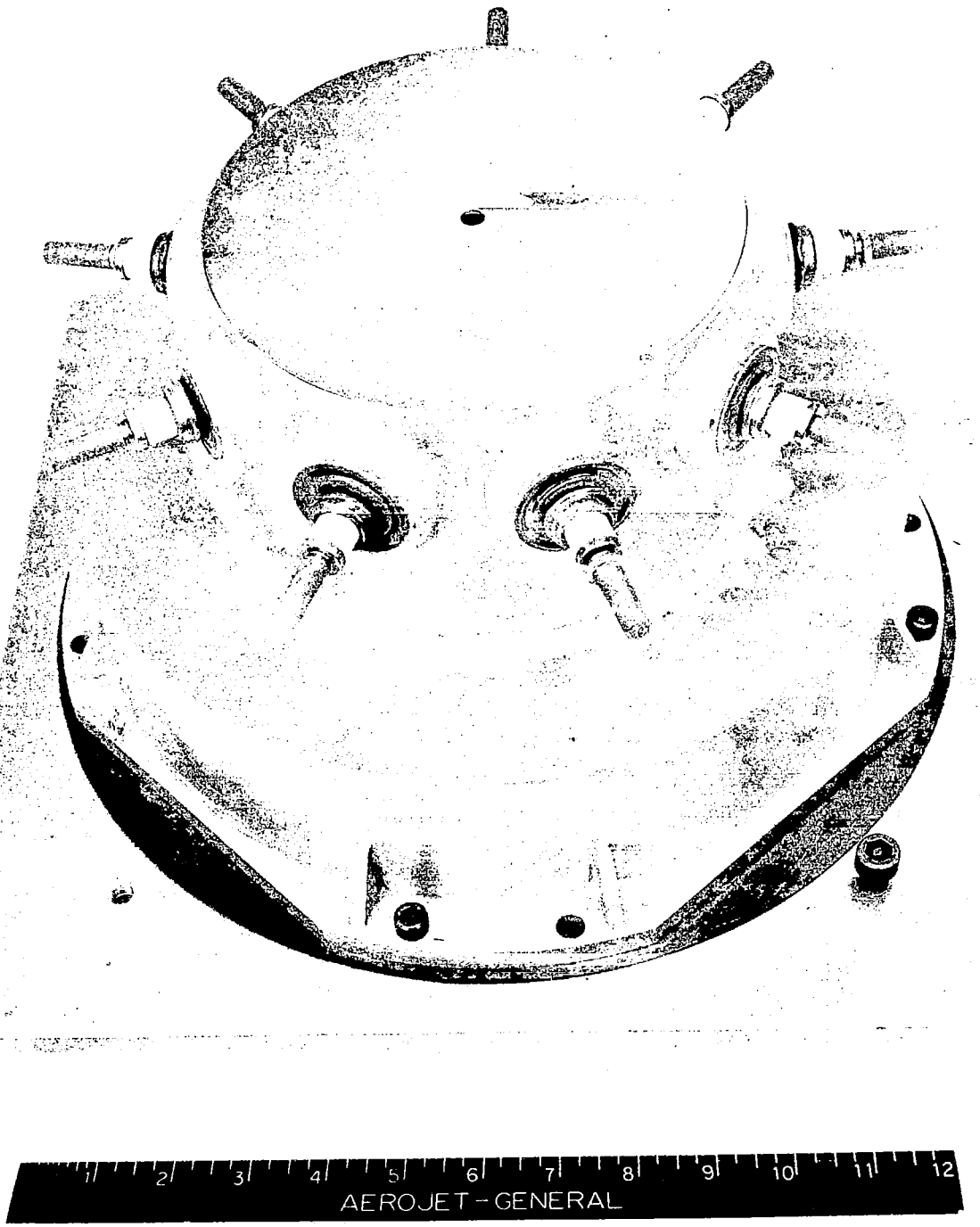

Figure 6-11 Speed Control Module

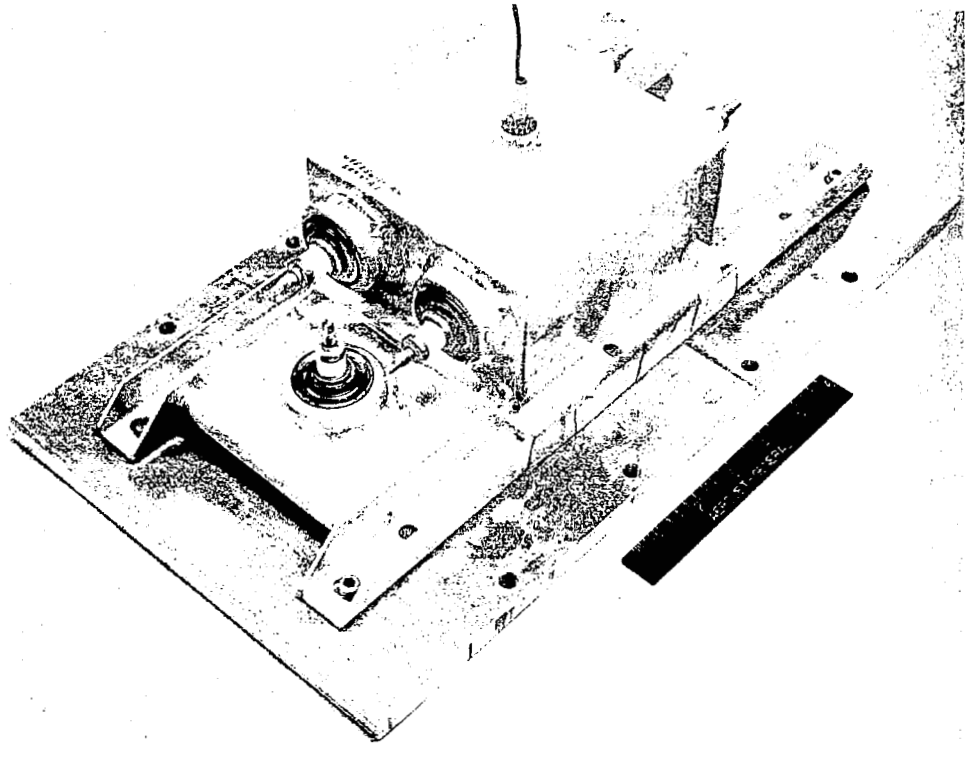

Figure 6-12 Speed Control Power Transformer

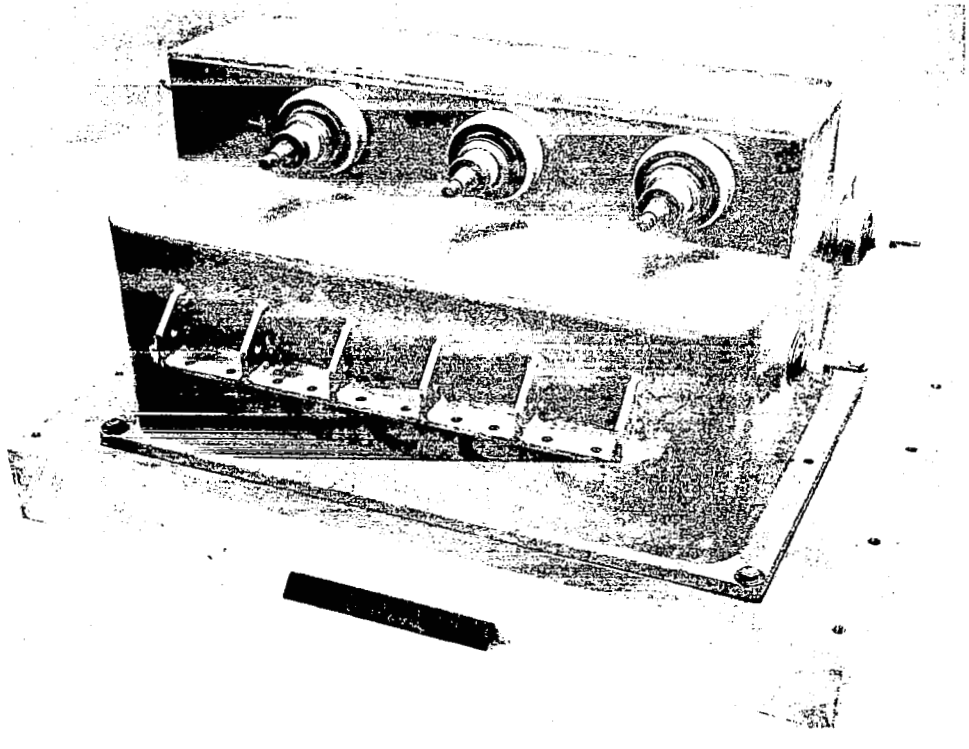

Figure 6-13 Saturable Reactor

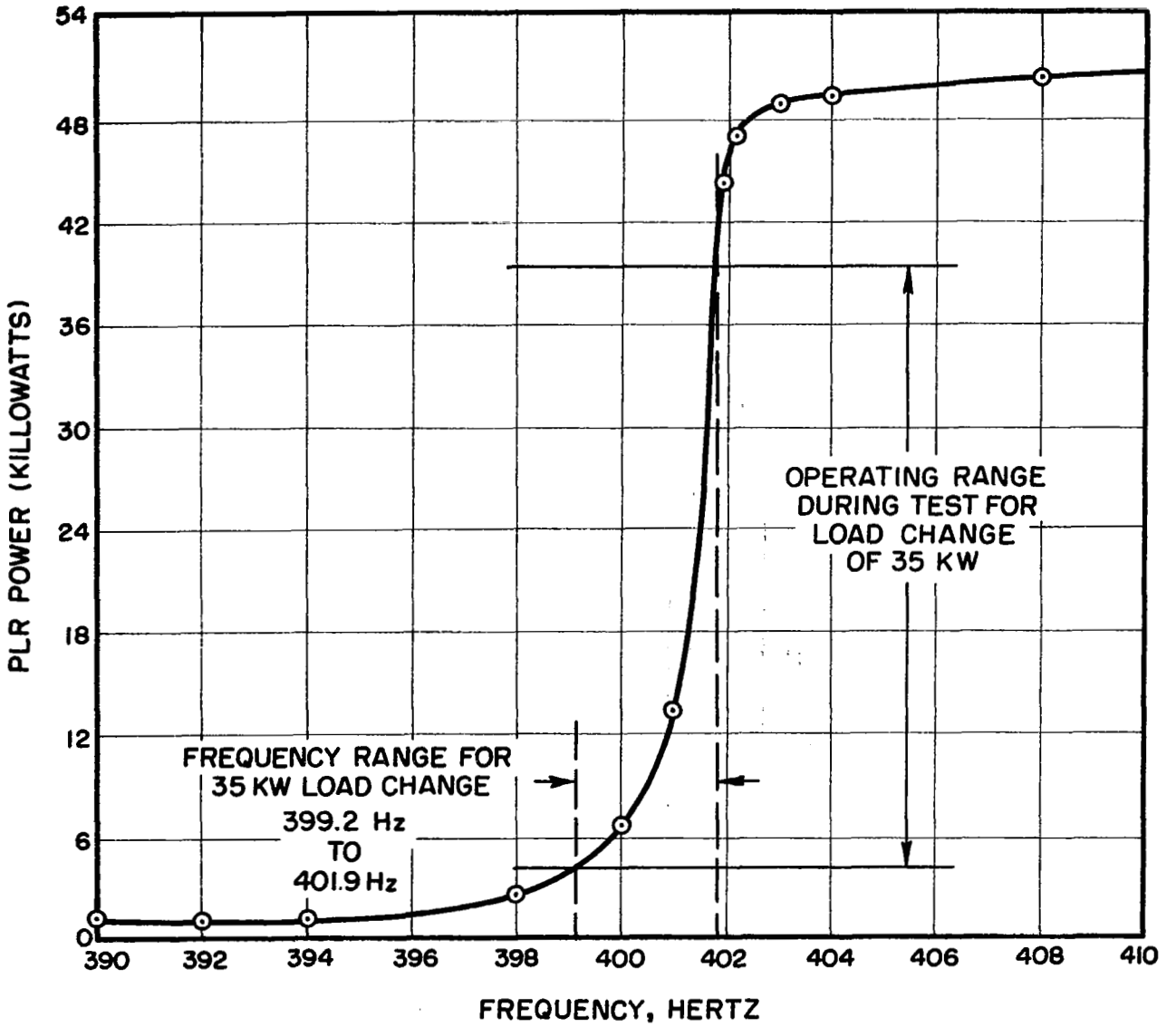

Figure 6-14 Alternator Frequency vs Parasitic Load Power

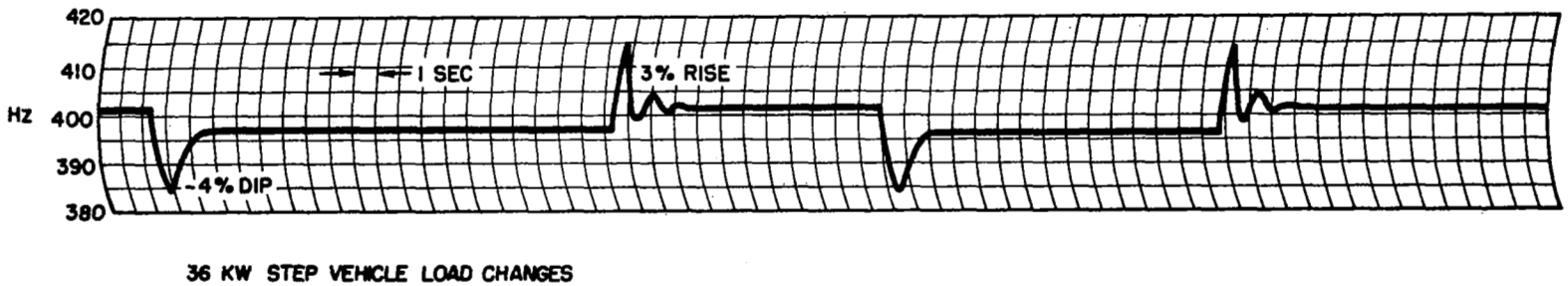

Figure 6-15 Speed Control Load Change Transients

In the power conversion system tests, the stability of the speed control system has been completely satisfactory for all the load and test loop conditions experienced. No instability has been experienced since the stabilizing circuit was optimized and installed.

The speed control has demonstrated long-life capability by operating for nearly 13,000 hours in the 35 kWe system tests and for over 23,000 hours in the electrical component test facility with no failures experienced and no adjustments required.

Detailed information on the design and performance of the speed control system may be found in Reference 61.

6.4 PARASITIC LOAD RESISTOR

6.4.1 Introduction

The parasitic load resistor is a component of the speed control system. Its purpose is to absorb alternator power in the amount necessary to control the speed of the turbine-alternator. The speed of the turbine is controlled by maintaining a load on the power conversion system equal to the system load capability. The speed control accomplishes this by sensing the alternator frequency and controlling the power delivered to the parasitic load resistor. The parasitic load resistor converts the surplus electrical power developed by the power conversion system into heat and dissipates this energy into the heat rejection NaK system, from which it is finally dissipated into space by the radiator.

Detail design information on the Parasitic Load Resistor may be found in Reference 62.

6.4.2 Design and Development

The design is shown in Figure 6-16 and consists of eighteen straight tubular resistance heater elements, six per phase, installed in a Type 316 stainless steel cylindrical tank.

The terminals are protected by extensions of the cylindrical structure; the heater elements are connected in wye, and three terminals are provided for connection to the three-phase output of the saturable reactor.

The heater elements are made up of two coils of Nichrome V resistance wire wound in parallel and embedded in compressed magnesium oxide with a sealed terminal on each end. There are no bends in the heater tube so the possibility of cracks and voids in the magnesium oxide is minimized making the possibility of failure due to hot-spot burnout minimal. The diameter of the heater wire is 0.030 inch, large enough so the possibility of breakage is minimized. The eighteen-heater elements are connected in wye, six units per phase. The three-phase connections are made at one end of the unit (Figure 6-17), and all of the units are connected together at the opposite end to form the neutral of the wye (Figure 6-17). All of the electrical connections to the parasitic load resistor are welded to eliminate the possibility of failure due to the loose-connection oxidation syndrome.

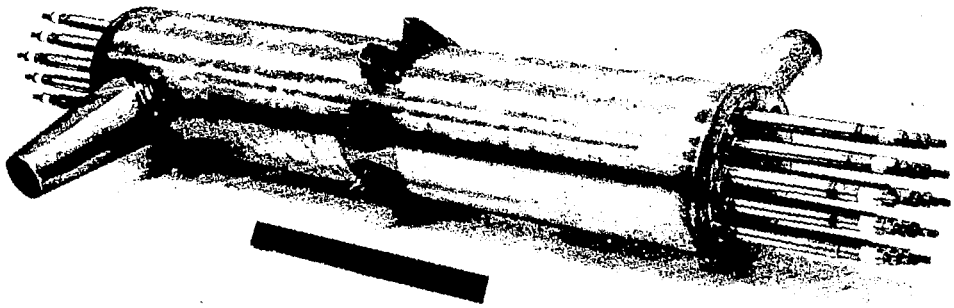

Figure 6-16 Parasitic Load Resistor

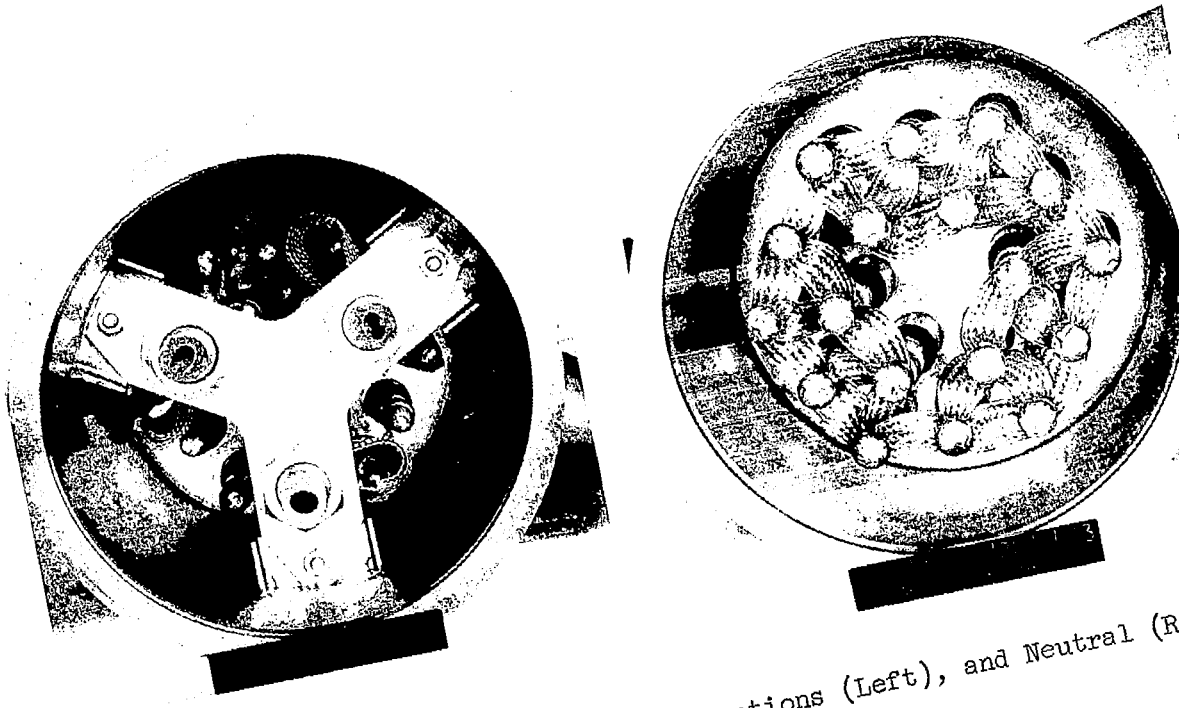

Three-Phase Input Connections (Left), and Neutral (R

In the cylindrical housing of the parasitic load resistor, the NaK flows in one end, around the heater elements, and out the other end. The operating temperature of the Nichrome V wire in the heater elements is the most important factor in determining the operating life of the unit. Figure 6-18 shows the wire temperature as a function of sheath power density.

Data obtained from industry sources indicate that the resistance elements will have a life of hundreds of thousands of hours at a temperature of 1500°F, and a much longer life at the temperature expected when the parasitic load resistor operates in the heat rejection NaK loop where the wire temperature will be 1000 to 1200°F.

The connection of the heater elements into the enclosure end plate is shown in Figure 6-19. This was done using a brazed and welded double seal to ensure positive NaK containment. The tubular extensions of the end plate and heater elements were made in two lengths to allow clearance for X-ray inspection of all weld joints.

All fabrication procedures and inspection tests for the heater units were satisfactorily completed except for the insulation resistance tests. The magnesium oxide insulation is hygroscopic and absorbs moisture from the atmosphere which results in the formation of hydrates and consequent low insulation resistance. The hydrates must be removed by heating to a temperature above the hydrate decomposition temperature of about 800°F. Heating of the elements in this manner raised the insulation resistance and eliminated the problem.

The rating of the parasitic load resistor is as follows:

Power rating	47 kW
Voltage at full power, L-L	182 volts
Current	150 amps
Power factor	0.99 minimum
Power density (heater element)	75 watts/in.^{2}
NaK flow rate	40,000 lb/hr
NaK inlet temperature	650°F
NaK inlet pressure	72 psi

6.4.3 Physical Description

The parasitic load resistor is shown in Figure 6-16. The connections to the saturable reactor are made to the three insulated terminals shown in Figure 6-17.

The connection to the heat rejection NaK system is made at the cones shown in Figure 6-16. The maximum tubing loads allowed at the PLR-tubing interface are:

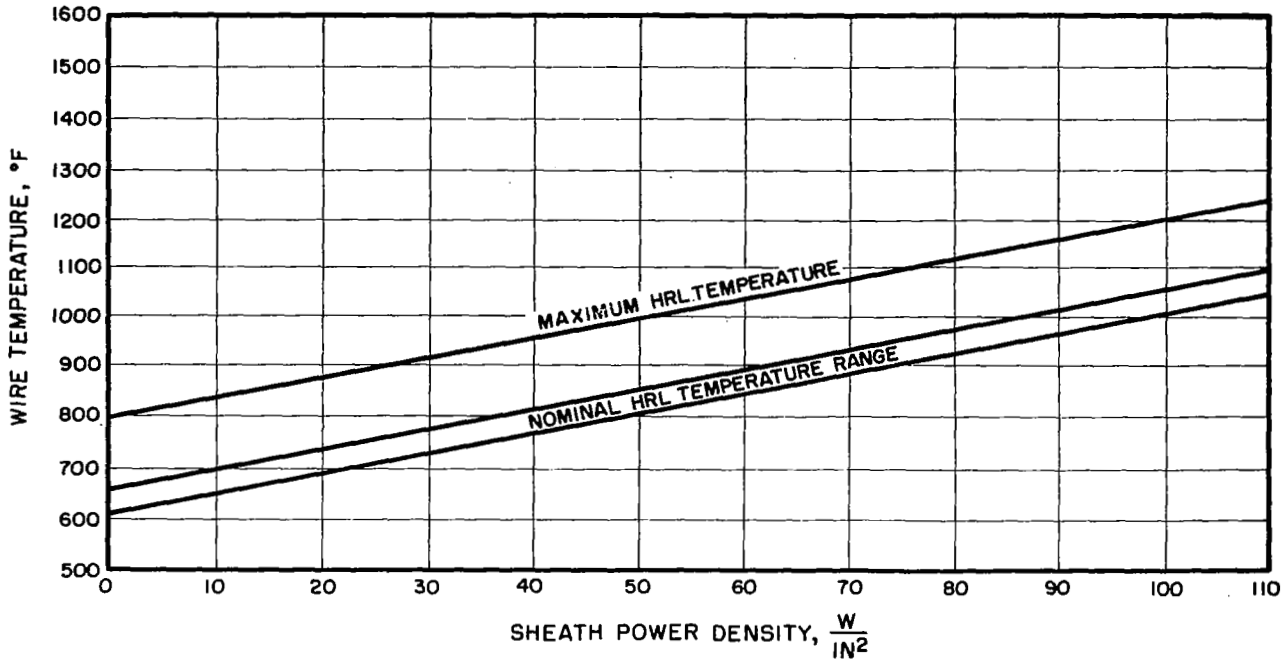

Figure 6-18 Heater Wire Temperature vs Sheath Power Density - Parasitic Load Resistor

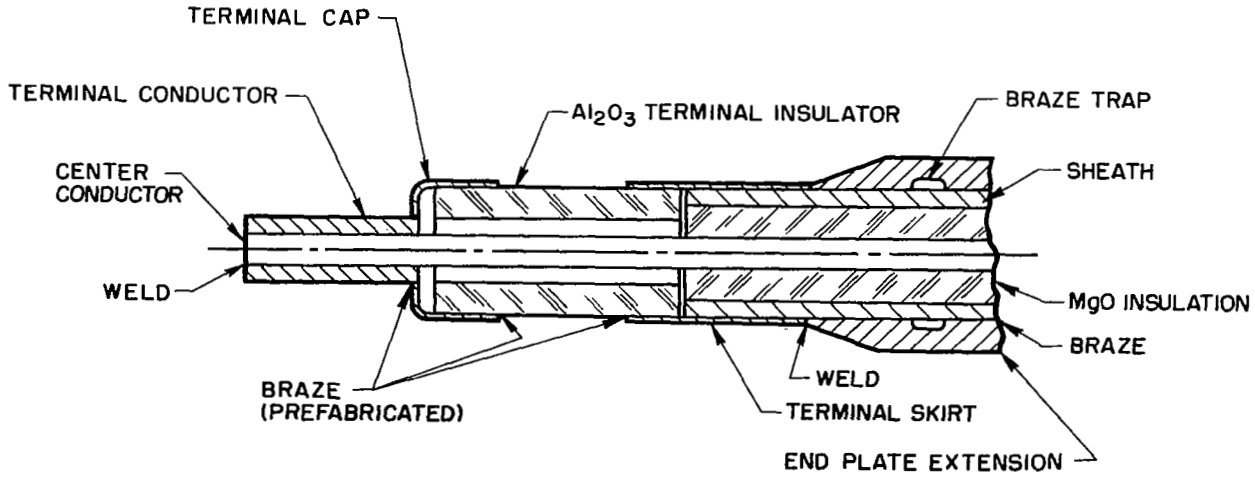

Figure 6-19 Heater Element-to-Case Seal - Parasitic Load Resistor

Force axial to NaK tubing	100 lb
Force radial to NaK tubing	141 lb
Torsional moment	100 ft-lb
Bending moment	141 ft-lb

6.4.4 Demonstrated Performance

Three units of the original design were tested. One unit failed after operating at partial load for about 600 hours and after being in a loop for more than 3500 hours. The failure was caused by a defective circumferential weld between the heater element and the end-plate assembly. As a result of the weld failure, NaK seeped into the heater element, saturated the magnesium oxide, and shorted the heater element to the case. Examination of the defective weld joint showed that a complete burn-through in the element sheath had occurred during fabrication, and that two weld passes had been used to circumferentially weld the end of the outer doubler tube to the sheath. The second weld pass formed a thin metal bubble over the void. The thin section failed during test in the NaK loop and allowed the NaK to short the element.

A second unit failed after 297 hours of operation. It was established that the basic cause of the failure was a defect in the weld, the result of a burn-through of the weld and formation of a bubble very similar to the defect which caused the earlier failure. The third unit was originally installed in the primary NaK loop operating at 1200°F. It functioned in this location for 302 hours and was then moved to the heat rejection loop operating at 605°F. In this location, it operated for 12,993 hours until the loop was shut down. No failures occurred in any of the welds of this unit and no problems were experienced with it.

Two failures were caused by defects in the doubler tube-to-sheath weld. This defect would have been detected if the welds had been X-rayed after fabrication of the resistance elements. This failure mode was eliminated from new units by requiring that all welds be X-rayed.

The present design reflects this improvement in which all welds may be X-rayed. Since there is a double seal at this point - a welded seal which can be X-rayed and a brazed seal - the possibility of NaK leaks into the magnesium oxide is very unlikely.

6.5 PROGRAMMER

6.5.1 Introduction

The purpose of the SNAP-8 programmer is to provide the signals in the required sequence to perform the starting and shutdown functions of the power conversion system. Initially, the SNAP-8 system was conceived as an instrument-rated system which would be started once, then shut down only as the result of the failure of a vital part. Later, the concept of a man-rated system required that the programmer be able to start the system, shut it down in a controlled manner, and restart it as required.

The programmer for the startup only application was built and tested. The programmer for the man-rated system was only partially fabricated when the SNAP-8 program was terminated.

6.5.2 Design

The functions which were provided by the start programmer include the following:

- Start the pump inverter
- Start pumps on inverter at 95 Hz
- Accelerate the pumps from 95 Hz to 220 Hz
- Inject mercury
- Open mercury flow control valve along prescribed ramps
- Transfer pumps from inverter power to alternator power at 220 Hz
- Activate lubricant-coolant valves and startup seals on the turbine-alternator and mercury pump
- Flash alternator field
- Apply and remove speed control bias power
- Close vehicle load breaker

The start programmer electrical components consist of: relays, diodes, resistors, timers, frequency sensing circuits, and silicon controlled rectifiers.

The timers are capable of satisfactory operation at an input voltage of 28 ± 4 Vdc and the contacts are capable of handling two amperes inductive load at 28 Vdc. The timers reset immediately at the end of their timing cycle. Upon removal of dc power, the timer returns to its starting condition.

Flexibility was built into the start programmer so that changes can be easily made in the operation of the system as required. The timers are designed to allow for adjustment of operating time over a wide range; spare contacts are provided on the relays to accommodate additional functions, and provision was made for adjustment of the pickup frequency of the frequency detecting circuits. It was designed with spare relays, diodes, and terminal boards installed so that changes can be made. The unit would be fully accessible as mounted in the test control console for power conversion system tests, so required changes can be made.

The frequency sensing assemblies which operate the motor transfer contactors, the lubricant-coolant valves, and the bias circuits have been completed and tested. The alternator speed protective assembly has also been completed and tested. This assembly senses the alternator voltage buildup during startup. If voltage has not started to rise when the turbine-alternator reaches a predetermined speed, the programmer then terminates the startup sequence and shuts down the system.

6.5.3 Physical Description

The start programmer is designed for ground system testing only, and requires air cooling. All controls are accessible for easy adjustments. The unit requires input power at 28 $\pm$ 4 Vdc and one-phase input from the alternator, 120 volt line-to-neutral, 400 Hz.

6.5.4 Demonstrated Performance

The programmer designed for starting only, was successfully used to start both the 35-kWe system at Aerojet, and to perform a series of startup tests in the SNAP-8 ground test facility at NASA-LeRC.

The automatic system startup was successful and proceeded through all of the startup sequences as referenced in section 6.5.2.

6.6 ELECTRICAL PROTECTIVE SYSTEM

6.6.1 Introduction

In an electrical power system, the most common electrical hazard for which protection is required is the short circuit. Other possible faults include open circuits, overvoltage, undervoltage, overfrequency, underfrequency, overload, and unbalanced voltages.

The SNAP-8 system is basically different from most power systems because speed is regulated by maintaining a controlled load on the system and the voltage is regulated to a value proportional to frequency rather than being independent of frequency. These unique characteristics have an important influence on the protective system requirements.

For example, an overload beyond the ability of the system will result in a drop in speed and voltage, so that overloads need not be sensed directly but can be detected by an undervoltage sensor.

Also, a substantial loss of load caused by an open circuit, or for other reasons, will result in overspeed of the turbine-alternator, so a means must be provided for sensing overspeed and shutting down the system. Since voltage output is proportional to speed, the voltage rises when overspeed occurs; so, overspeed may be detected as overvoltage.

The SNAP-8 alternator and excitation system are capable of producing a short-circuit current as high as four times rated. The temperature produced by such overcurrents will damage the alternator insulation in a short time, if protection is not provided. Short circuits also produce voltage disturbance; so that an over-under voltage sensing system will detect short-circuit faults.

The current concept of the SNAP-8 power conversion system is that of a man-rated system having personnel available to monitor performance, make adjustments, diagnose troubles, and make repairs. The purpose of a protective system for such a manned space power system is two-fold: (1) the equipment that is repairable or replaceable in space must be protected so that it sustains only minimum damage when a fault or failure occurs, (2) the power conversion system must be maintained in operation as long as possible with no false opening of the vehicle load breaker and no false shutdowns.

Faults in the vehicle load which are not cleared by local protective equipment must be sensed and the vehicle load breaker opened. Power conversion system faults cannot be cleared by opening a protective breaker to isolate the failure from the rest of the system, because if this is done a vital function will be lost and the system will stop operating, with the possibility that damage will result. When an electrical fault within the system is detected, the only action that can be taken is to shut the system down in a way that will minimize damage.

6.6.2 Design

The electrical protective system module has the primary function of protecting the electrical generating system from damage caused by:

- Short circuits in the electrical power distribution system
- Badly unbalanced vehicle loads
- Excessively high turbine-alternator speeds.

The protective system has a secondary function of minimizing possible damage to other electrical generating system components by shutting down the system as safely as possible should any of the above listed malfunction conditions be detected within the electrical generating system.

To meet these requirements the functions performed by the electrical protective system module are as follows:

(1) Open the Vehicle Load Breaker prior to mercury injection.

(2) Sense line-to-neutral voltage of each phase of the alternator voltage, and once two or more of these voltages reach a predetermined minimum value, provide a signal to enable the programmer to close the vehicle load breaker at the proper time during the startup sequence.

(3) After the alternator voltages reach the predetermined minimum value, provide a signal if two or more phases of the voltage vary below 108 V or above 132 V. This signal shall immediately do two things.

   a. Open the vehicle load breaker

   b. Start a 0.5-second timer.

With the vehicle load breaker open, if the fault is on the load side of the breaker, the alternator voltages will return to normal in less than 0.5 seconds. If this occurs the electrical protective system will stop the timer, reset it, and reclose the load breaker. If the fault still exists, the alternator voltages will again vary outside the normal band, and the electrical protective system will re-open the breaker and restart the timer. This cycling of the vehicle load breaker and timer will continue until one of the following events occur:

(1) The load fault corrects itself by burning open or by tripping its own individual protective device. If the fault corrects itself, the alternator voltage will return to normal, the vehicle load breaker will reclose and remain closed, and the 0.5-second timer will be reset.

(2) The 0.5-second timer times out sending a signal to the programmer to start an automatic shutdown of the power conversion system.

(3) An external command signal is sent to hold the vehicle load breaker open and stop the cycling. With the breaker held open, the alternator voltage will return to normal and the 0.5-second timer will be reset.

If the fault is in the power conversion system, the alternator voltages will not return to normal when the breaker is opened, the 0.5-second timer will time out and start an automatic shutdown of the power conversion system.

The electrical protective system consists of three identical circuits, one monitoring the line to neutral voltage in each of the three phases of the alternator output voltage as shown in Figure 6-20. Each circuit consists of a single-phase bistable magnetic amplifier whose output

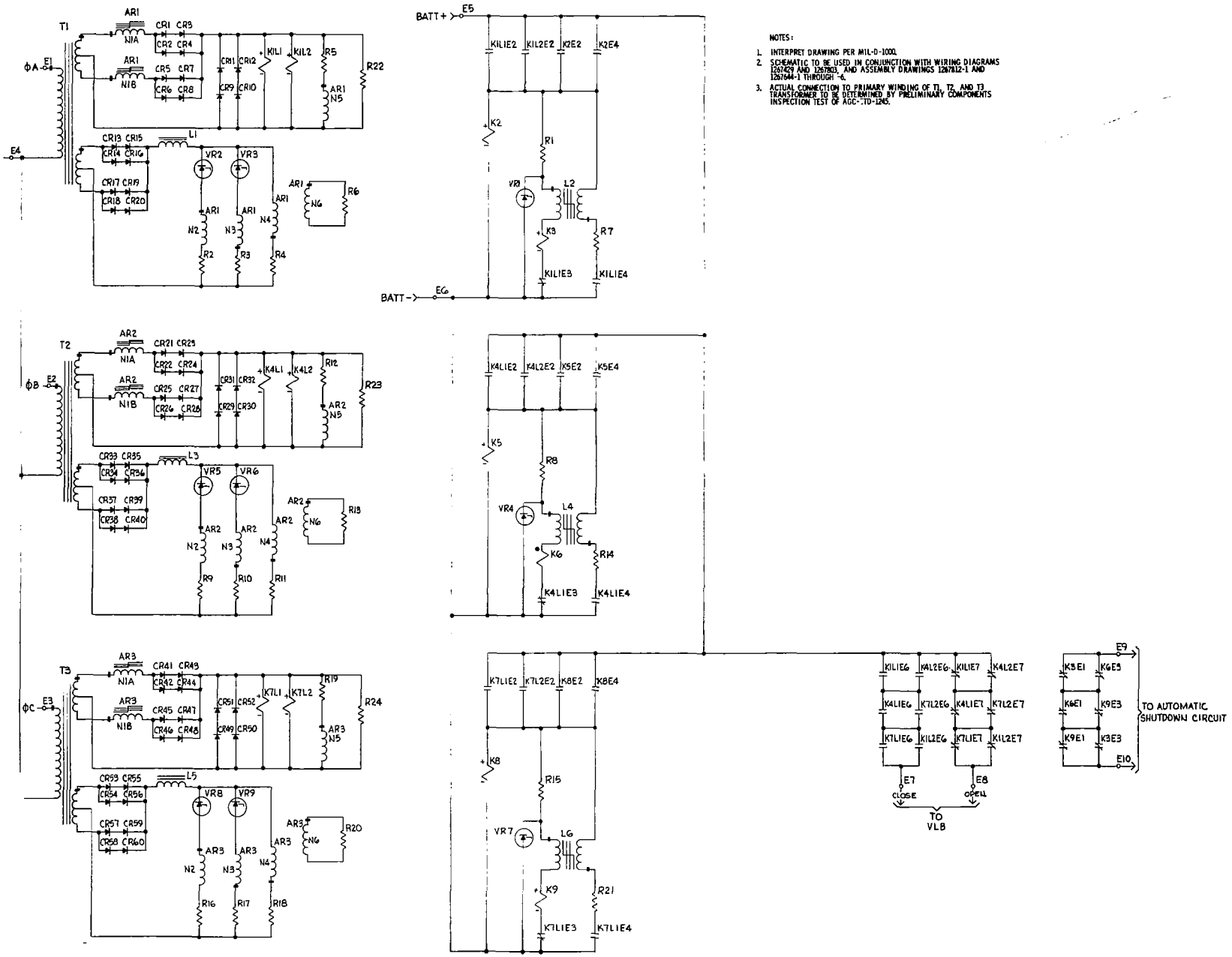

Figure 6-20 Electrical Protective System Schematic Diagram

energizes two four-pole double-throw relays, a preset dual-voltage sensing circuit, a timing circuit, and relay logic output circuitry. Two high-reliability 10-watt silicon zener diodes in each circuit are the basic reference standards, one for the under-voltage limit and the second for the over-voltage limit.

All heat is considered to be transferred only by conduction to an actively cooled heat sink, none by radiation or convection. The protective system housing is cast from aluminum which eliminates possible thermal interface barriers where the walls of the housing join the base plate.

The electrical protective system design achieves high reliability by simplicity of concept and circuitry, derating of components, redundancy of the most vulnerable parts, use of highly reliable components, special consideration and design of all electrical connections, protection of parts from environmental hazards, and a thermal design which assures that each component will operate well below its rated temperature.

The protective system is composed of wound components, resistors, relays and diodes; no transistors, controlled rectifiers, or capacitors are required assuring that this system can operate in a relatively high-temperature and nuclear-radiation environment.

All electrical connections are welded assuring that high temperature, vibration, and shock cannot cause failure of the protective system because of loss of an electrical connection. To prevent failures due to dust, moisture, salt, etc., the complete assembly is potted in a high-temperature resin which isolates all the parts, connections and connecting wires from environmental hazards.

Two-out-of-three logic circuitry is used to minimize the possibility of a false shutdown signal causing shutdown of the power conversion system. Operation of at least two of the three under-over voltage sensors are required to produce protective action.

Detail design information on the electrical protective system may be found in Reference 63.

6.6.3 Physical Description

Fabrication of the electrical protective system was partially completed at the time the program was terminated.

All of the components of this design are mounted on the cast aluminum housing to facilitate heat transfer into the aluminum base from which the heat is transferred to a liquid-cooled heat sink. This unit is designed for operation in a space environment.

This unit requires a three-phase and neutral input from the alternator and an uninterrupted source of 28 $\pm$ 4 Vdc. Its output must be connected to the close and open circuits of the vehicle load breaker and to the automatic shutdown circuit of the power conversion system programmer.

6.7 POWER FACTOR CORRECTION ASSEMBLY

6.7.1 Introduction

There are several benefits which may be derived from increasing the operating power factor of the SNAP-8 alternator. These include:

- Increased alternator efficiency. At rated vehicle load of 35 kW 0.85 lagging power factor the alternator power factor is 0.7 lagging. By increasing the alternator power factor from 0.7 to 1.0, its efficiency is increased from 87.1 to 91%.

- Increased alternator life and reliability. An increase in alternator power factor reduces the winding currents and consequently winding temperatures which increase the insulation system life.

- Increased alternator power capacity. An increase in alternator power factor from 0.7 to 1.0 would allow an increase in alternator power rating of 43% while maintaining the same output current.

Power factor correction may be accomplished by several means; improving the power factor of the connected loads, the use of leading power factor devices such as synchronous motors, or the use of power factor correction equipment such as synchronous condenser or static capacitors. The use of static capacitors was selected as being the most reliable, having the least effect on the system design, and the easiest to implement.

Capacitors using Kapton (polyimide) film dielectric were selected as offering the best combination of features suitable for the SNAP-8 application. These include:

- Low dissipation

- High dielectric strength

- High-temperature capability

- High nuclear radiation tolerance

Among the other dielectric materials considered in making the selection for the SNAP-8 application were:

- Glass ceramic and mica materials.- Rejected because of the large volume required.

- Electrolytic capacitors.- Rejected because of high losses and low reliability.

- Impregnated paper.- These are commonly used for commercial power factor correction service but rejected for SNAP-8 because of higher losses, larger size, and lower nuclear radiation tolerance.

- Teflon Film.- Rejected because of low nuclear radiation tolerance.

- Mylar film.- Rejected because of high dissipation factor.

- Polycarbonate film.- This film has low losses and good nuclear radiation resistance making it second choice only to the polyimide film finally selected.

At the time of the power factor correction capacitor development, no suitable capacitors were available using polyimide film requiring that such a capacitor be developed for the application.

Detail information on the design of the Power Factor Correction Assembly is included in Reference 64.

6.7.2 Design and Development

The rating of the power factor correction assembly was selected to increase the alternator power factor to unity at rated system load. At this operating point, the alternator will operate at minimum current and near maximum efficiency. A maximum variation in reactive load may be tolerated with a minimum effect on alternator efficiency.

The capacitors are connected line to line at 208 V to allow the use of minimum capacitance for the required kvar. A total capacitance of 175 microfarads per phase was required to correct the power factor to unity. A unit capacitor of 17.5 microfarads was selected as providing a convenient size for the assembly. It was small enough that a single failure per phase would be acceptable without badly unbalancing the load and would not decrease the system power factor to a significant degree.

Because of the unique requirements of the SNAP-8 system and recent availability of polyimide film, it was necessary to develop special capacitors. Some of the special features incorporated into the design of the SNAP-8 power factor correction capacitors to enhance their reliability were:

- Hermetically sealed welded enclosures

- High-temperature radiation resistant polyimide film dielectric

- Sulfur hexafluoride gas fill

- Helium trace for leak detection

The capacitor specifications include a burn-in test at 270 V, 415 Hz, for 168 hours, and require that the voids in the capacitor be filled with a mixture of sulfur hexafluoride and 10% helium. The sulfur hexafluoride has a dielectric constant about 2.3 times that of air, increasing corona start voltage substantially. The small amount of helium was added for the purpose of detecting leaks in the sealed cans.

The use of a fuse to remove a failed capacitor from the circuit was necessary to prevent damage to other capacitors and to the power system. Figure 6-21 is a photograph of the fuse developed and the components which make up the fuse. The fuse wire is 20-gage copper welded to the base and to the terminal at the opposite end. Two 12-gage insulation lead wires welded to the terminal provide connections to two capacitors. The fuse wire is supported and protected by the fiberglass reinforced epoxy tube cemented to the metal ends of the fuse.

To prevent failures due to connections, all electrical connections are welded. The assembly is designed to transfer the capacitor heat through the bottom of the can into a liquid-cooled heat sink. A stress analysis performed on this configuration indicated positive margins of safety for all components of the assembly.

A thermal analysis shows a temperature rise within the capacitors of approximately 50°F. The resulting hot-spot temperature within the capacitors does not exceed approximately 220°F. The polyimide dielectric film used in the capacitor is able to operate at temperatures above 500°F. The solder within the capacitor has the lowest operating temperature capability of all the materials being limited to approximately 400°F. The large temperature difference between the actual and permissible temperature values and the low-temperature gradients within the components contributes to high reliability and long life.

6.7.3 Physical Description

The capacitor developed is shown in Figure 6-22. Its envelope is 3 x 2.75 x 5.5 inches over the terminals. It is rated at 17.5 microfarads, 208 V, 400 Hz, nominal. Each capacitor when connected to a 208 V, 400 Hz source will supply a leading load of 1.9 kvar. Thirty of these capacitors (10 per phase) are used to provide the 57 kvar required to correct the alternator power factor to 1.0.

The assembly is shown in Figure 6-23. The capacitors are mounted on an aluminum base with a silicone heat-transfer compound applied between the bottom of each capacitor and the base. The capacitors are connected to three overhead bus bars through special high-reliability protective fuses.

The power factor correction assembly, is designed to be mounted on a liquid-cooled heat sink with a surface temperature of 170°F or lower. The unit is capable of operating in a vacuum environment with conduction to the heat sink as the only means of heat transfer.

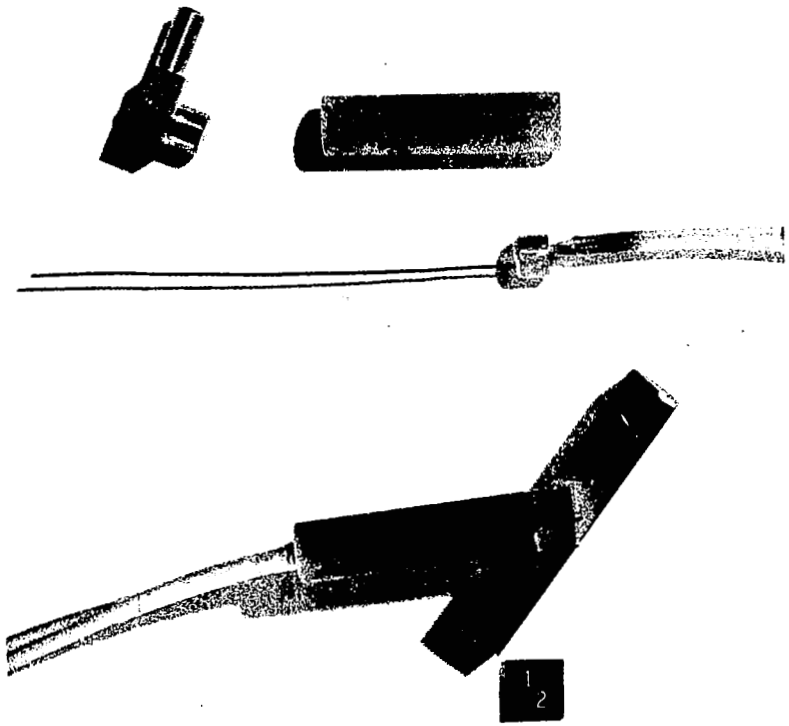

Figure 6-21 Fuse Components and Weld Sample

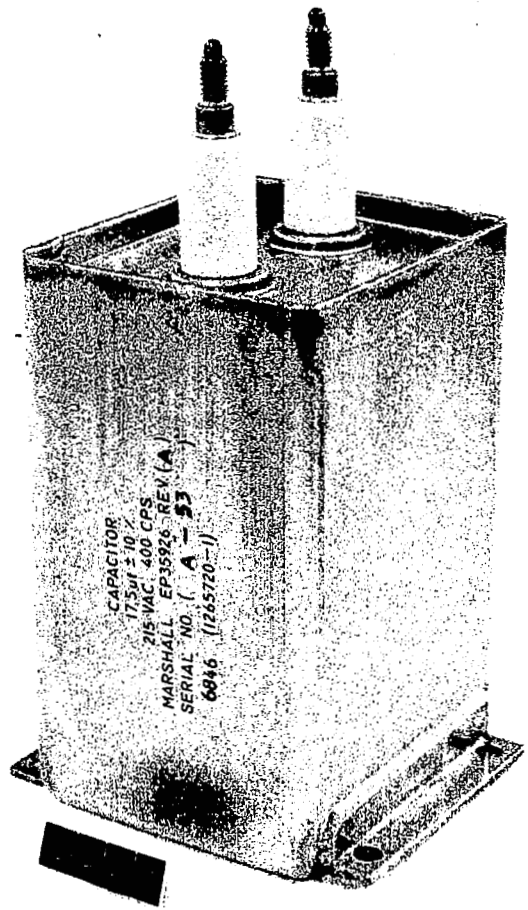

Figure 6-22 Power Factor Correction Capacitor

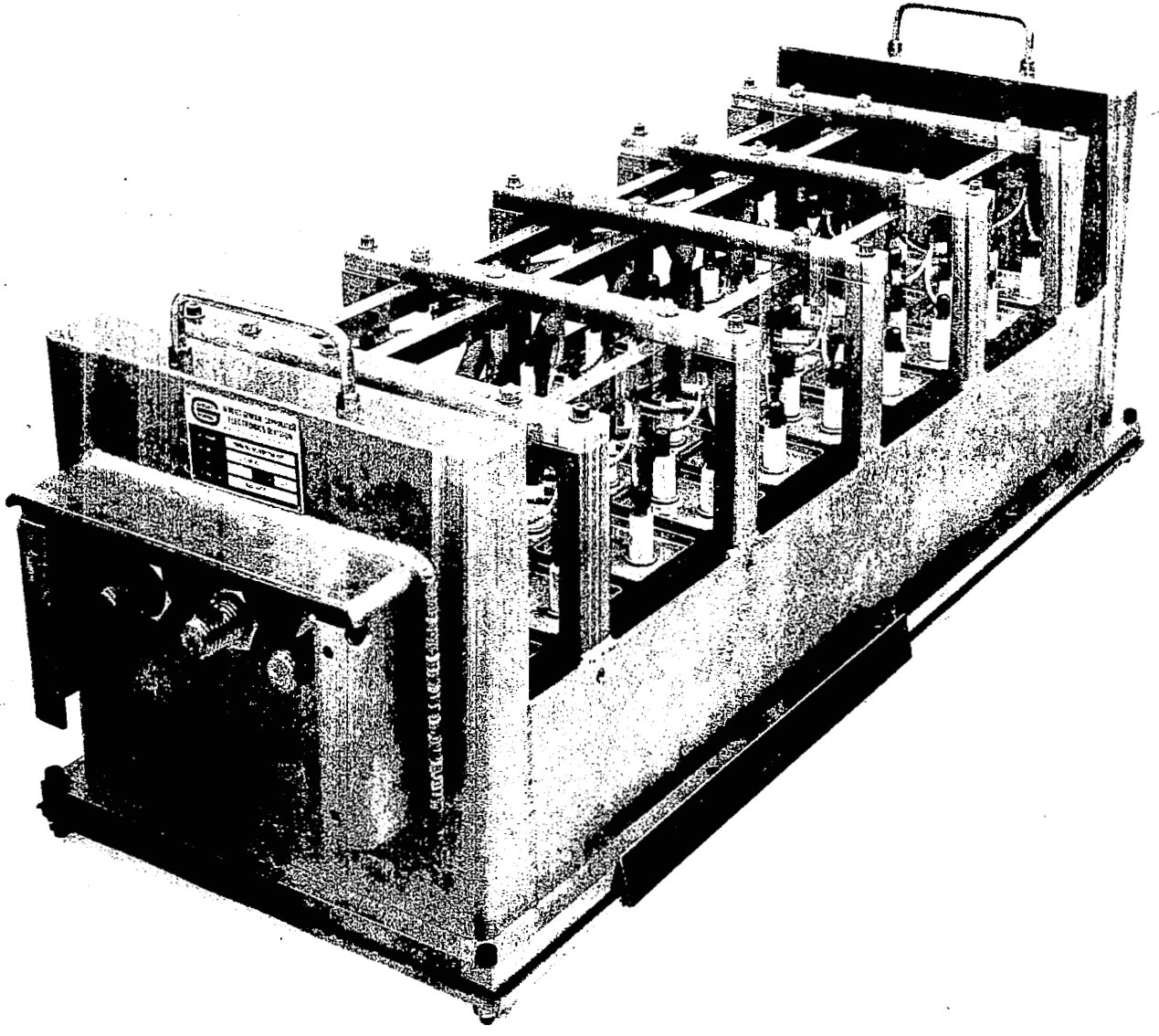

Figure 6-23 Power Factor Correction Assembly

6.7.4 Demonstrated Performance

Endurance testing of a preprototype power factor correction assembly containing 21 capacitors was conducted in the electrical component test facility along with other SNAP-8 electrical components. Power was supplied by the SNAP-8 alternator operating at 60 kW load and controlled by the SNAP-8 speed control and voltage regulator-exciter.

During 12,329 hours of test operation, two capacitors failed after 223 hours of test time. A third unit failed at 4843 hours due to a test facility malfunction which resulted in abnormally high voltage being applied to the capacitor assembly. The remaining capacitors were operating satisfactorily at the time the facility was shut down. During the endurance testing, the capacitor assembly was maintained at 120°F for 4843 hours and then increased to 170°F for the remaining 7486 hours.

Whenever capacitor failures occurred during testing, the failed units were isolated by the protective fuses so that there was no disturbance on the power system operation and the remaining capacitors in the assembly continued to function.

Following the early capacitor failures during the endurance testing, a burn-in test was added to the capacitor acceptance test procedure to eliminate substandard units with random defects. It was also determined during the failure investigation that the normal corona start voltage of the capacitor was 290 V in air. This appears to be adequate margin above the maximum operating voltage of 218 V. The use of sulfur hexafluoride fill with its high dielectric constant further increases this safety margin.

6.8 INVERTER

6.8.1 Introduction

The SNAP-8 power conversion system requires a source of adjustable-frequency ac power to drive the pump motors during system startup and shutdown while the alternator is not operational. This power is provided by a dc-to-ac inverter which converts battery power to adjustable-frequency ac power to control the speed of the pump motors. The voltage is adjusted with respect to frequency to provide the motor torque requirements during startup and various running speeds.

During the SNAP-8 startup sequence, the inverter supplies power to operate the pump motors at reduced speed while the system is being heated. After heatup is accomplished, the pump speed is increased to approximately 70% of rated and held until the alternator is started. When the alternator frequency matches that of the inverter the pumps are transferred to the alternator power and the inverter is shut down. Similarly, during shutdown the pump motors are transferred to inverter power when the alternator frequency decreases to approximately 70% of rated.

6.8.2 Developed Hardware

A rotary dc-to-ac inverter was developed to meet the requirements of an early version of the SNAP-8 system. This unit consisted of a hermetically sealed dc motor driven permanent magnet alternator built on a single shaft in a common enclosure. This unit is shown in Figure 6-24. It requires no external cooling means as all its losses over an operating cycle are absorbed by a built-in heat sink. The SNAP-8 system concept at the time of the inverter development required system startup only. The startup cycle required the inverter to operate for 5 hours at 95 Hz followed by 8.5 minutes at 220 Hz. Its rating is in accordance with the following table.

Inverter Rating

Output		
Frequency, Hz	95	220
Power, kW	0.37	1.70
Voltage, L-L	19	88
Power Factor, Lagging	0.30	0.28
Phases	3	3
Operating time, minutes	300	8.5
Input		
Voltage, Vdc	27-33	27-33
Current, amps	24	172
Size	15.9 inches diam x 24.85 inches long	
Weight	318.5 lb	

The output winding of the inverter is tapped to provide the specified output voltage at the two frequencies. A contactor is included within the inverter housing to switch output voltage taps.

Two inverters were built to the requirements listed above and were performance tested. One unit was incorporated into the power conversion system and used to perform its function as part of the system startup.

Detailed information on the design of this unit is included in Reference 65.

6.8.3 90 kWe System Requirements

Changes in the SNAP-8 system and component requirements resulted in new requirements for the inverter. These changes included:

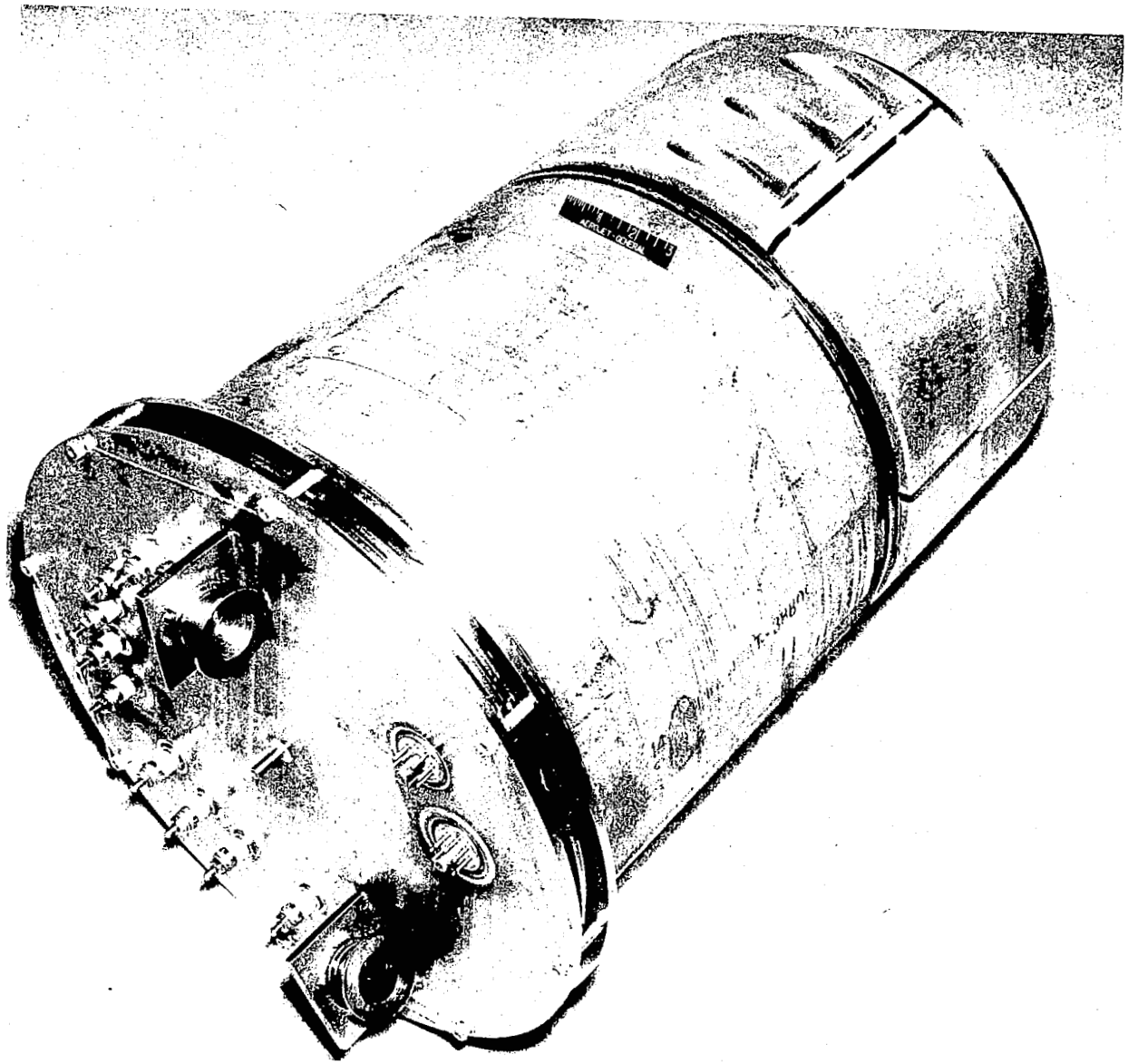

Figure 6-24 Inverter

- Addition of system shutdown and restart capabilities with the capability for 100 startup-shutdown cycles.
- Increased pump motor power requirements.
- Provision for high pump motor starting torque capability

While the basic functions of the inverter remained the same, its capability requirements were significantly modified requiring a new inverter design. The modified requirements are summarized in the following table:

Time (Min.)	Function	Freq. (Hz)	Volts (L-L)	Power (kW)	PF
0-10	Run lubricant pump*	60	15	0.05	0.5
10-10.5	Start	60	65	5.5	0.5
10.5-300	Run L/C, HRL	60	15	0.15	0.5
300-300.5	Start IL	60	65	7.5	0.5
300.5-310	Run L/C, HRL, IL	60	15	0.25	0.5
310-312	Ramp 60 to 280 Hz	60/280	31/145	-	-
312-315	Run L/C, HRL, IL	280	145	4.2	0.5
315-315.5	Start Hg	280	145	8.8	0.4
315.5-318	Run L/C, HRL, IL, Hg	280	145	5.7	0.5

The input voltage to the inverter was increased from 28 Vdc to 56 Vdc reflecting the increased battery voltage. Cooling was added to provide for the shutdown and restart capability.

The inverter requirements may be met using either a rotary inverter, as was previously developed, or by a static inverter using solid-state switching devices. The tradeoff between a static inverter and a rotary inverter involved evaluating their relative merits including complexity, reliability, service life, and efficiency. A key factor in evaluating a rotary inverter was brush life of a hermetically sealed unit in a space environment.

To evaluate this factor, a test program was undertaken to determine if inverter brushes would provide satisfactory life for 100 startup and shutdown operating cycles. Previous investigations indicated that helium and carbon dioxide atmospheres possessed desirable characteristics. Endurance tests were performed under controlled conditions in a brush test rig designed to simulate the inverter brush and commutator system. The brushes used were designed for high-altitude aircraft where limited atmosphere was available. The brushes were tested in wet helium, dry helium, and dry carbon dioxide atmospheres.

---

* L/C: lubricant-coolant pump; HRL: heat rejection loop NaK pump; IL: intermediate loop NaK pump; Hg: mercury pump.

The brush wear rate during the endurance tests indicated that the brush life of a rotary inverter would substantially exceed requirements for 100 startup and shutdown cycles. The maximum wear using a carbon dioxide atmosphere during the full-term endurance test was 0.015 inch as compared with a typical allowable wear of 0.30 inch.

Brush performance in helium and carbon dioxide was substantially different than performance in air. This was particularly true of voltage drop between the brush and commutator which is a factor affecting commutation. This indicates that inverter performance testing must be made with the final atmosphere in the rotor cavity.

The effects of the square wave output of a static inverter on pump motor performance was evaluated by testing a NaK pump motor with a static inverter power supply and comparing the results with those using a sinusoidal power source. The inverter output was a typical quasi-square wave characteristic of an unfiltered three-phase inverter. Voltage control was achieved by use of a pulse-width modulator at the input of the inverter bridge. The pulse-width modulator frequency of approximately 2000 Hz was superimposed upon the quasi-square wave output of the inverter. The test results indicated that to produce equal motor locked rotor torque, 15 to 80% higher voltage was required using the static inverter. The higher increase being at the lower voltage where the effect of the pulse-width modulator was greatest. For equal motor output 5 to 50% greater power was required, the higher value again being at the low voltage where the pulse-width modulator caused the greatest wave shape distortion.

It appears that either a static or rotary inverter could be designed to meet the revised pump inverter requirements. The selection should be based on the current state of the art at the time of development. Consideration should be given to the following items in making the selection:

- Reliability
- System weight - inverter plus batteries
- System efficiency - inverter plus motor
- Radiation tolerance
- Adaptability to changing requirements

6.9 OTHER ELECTRICAL COMPONENTS

The following electrical components are considered undeveloped insofar as no prototype hardware has been developed which is applicable to the present concept of the SNAP-8 system.

- Reactor power loop electromagnetic pumps and inverter system
- Direct-current power supply

- Switchgear
- Electrical distribution and harness system

6.9.1 RPL EM Pump and Inverter System

The SNAP-8 90-kWe system design incorporates electromagnetic pumps to circulate NaK through the reactor power loop to transfer heat from the reactor to the intermediate heat exchanger. The electromagnetic pumps must operate continuously while the reactor is supplying power and after system shutdown during system cooling. To perform this function, the electromagnetic pump system must be capable of operating from battery power during startup and shutdown, and alternator power during long-term system operation. This power is provided by a pump inverter which is capable of operating both from the battery and a transformer-rectifier unit.

6.9.1.1 Electromagnetic Pumps

The electromagnetic pumps are tentatively selected as flat linear polyphase induction pumps with two redundant pumps in series, each capable of full system pumping requirements. The advantages of the flat linear induction pump are:

- A totally sealed liquid metal system using no mechanical seals
- No electric current conducted into the liquid metal from an external source.
- Winding assemblies may be installed or removed without cutting the fluid ducting.
- Dual windings on each pump allow operation at reduced performance with a failed stator winding.

The pumps provide controlled variable flow during system startup and shutdown, and constant flow during steady-state operation. Variable flow will be accomplished by variable frequency and voltage supplied by the pump inverters.

6.9.1.2 Electromagnetic Pump Inverters

Variable voltage and frequency power is supplied to the electromagnetic pumps by the electromagnetic pump inverters. A separate inverter is used for each pump stator. The inverter is designed to accept power from the battery source during system startup and shutdown, and from the transformer-rectifier unit during system steady-state operation. The output of the inverter is three-phase ac power. The tentative inverter output power profile is shown in the following table:

Electromagnetic Pump Inverter Power Requirements

Time (min)	Input Voltage	Frequency (Hz)	Voltage (L/L)	Power (kW)	Power Factor
10-300	56*	10	15	0.25	0.5
310-312	56	10/40	15/75	0.25/1.0	0.5
312-318	56	40	75	1.0	0.5
318-320	56	40/60	75/120	1.0/3.5	0.5
320-323	56	60	120	3.5	0.5
323-	150**	60	120	3.5	0.5

6.9.2 Direct-Current Power Supply

A direct current power supply is required as part of the SNAP-8 system to provide power during startup and shutdown of the power plant and power to the controls and electromagnetic pump inverters during steady-state operation. The direct-current power supply consists of a battery system and a transformer rectifier unit.

The SNAP-8 power conversion system requires direct-current power at 28, 56 and 150 V; 28 Vdc power is used for electrical controls of the power conversion system and nuclear system controls; 56 Vdc power is used to operate the pump inverter and the electromagnetic pump inverter during system startup and shutdown; and 150 Vdc power is used for the electromagnetic pump inverters during steady-state operation. Startup and shutdown power requirements are supplied by the battery system while steady state power requirements are provided by a transformer-rectifier unit which converts the alternator 400-Hz output to direct current.

The battery system includes the battery, a battery charger, and the necessary controls to maintain the battery in a charged condition. The battery output is plus and minus 28 Vdc with a common connection, the 28 V to common being used for the power conversion system controls while the 56 Vdc from the plus to minus terminals is used to power the inverters during system startup and shutdown. The battery is sized to provide for two system startups and one system shutdown without recharging, plus an ample reserve.

The transformer-rectifier unit converts the alternator 400-Hz output to direct current to meet the power conversion system steady-state dc requirements. In addition, 28 Vdc is required for system controls and 150 Vdc is used to power the electromagnetic pump inverters.

---

* Battery voltage

** Transformer-Rectifier Voltage

6.9.3 Switchgear

The SNAP-8 power conversion system requires the following items of switchgear to perform the necessary power switching operations:

- Vehicle load breaker to connect the vehicle load to the power conversion system.
- Motor transfer contactors to transfer the pump motors from inverter power during startup and shutdown, to alternator power for steady state operation.
- Inverter dc contactor to connect the inverters to the dc power supply.

6.9.3.1 Vehicle Load Breaker

The vehicle load breaker is a three-pole, single-throw, 175-amp hermetically sealed relay. It has two operating coils, a closing coil and a trip coil which operate on a current pulse to latch in either open or closed position. A set of single-pole double-throw auxiliary contacts are rated at 5 amps.

An available, hermetically sealed aircraft contactor was selected for use as the vehicle load breaker. A rating summary of this unit is shown on the following table.

Vehicle Load Breaker Rating Summary

Main Contacts

175 amps Three-pole single throw
120/208 V
60/400 Hz
Continuous Duty
Interrupting Capacity: 2000 amps

Auxiliary Contacts

5 amps Single-pole double throw

Coil operating voltage	28 Vdc
Pickup voltage	18 Vdc
Coil current (latched-pulsed)	5.5 amps
Minimum operating pulse time	0.035 sec
Ambient temperature	-65°C (-85°F) to +125°C (+257°F)
Weight	5.5 lb
Size	4.3 x 4.3 x 5.5 in.

6.9.3.2 Motor Transfer Contactors

The motor transfer contactors are three-pole double-throw power relays rated 50 amps. The relay is designed to be held in the energized position by an electromagnetic coil and in the de-energized position by a permanent magnet. The motor transfer contactors are installed in the SNAP-8 system so that the long-term operation is with the relay de-energized and the pump motors connected to the 400-Hz alternator power source. The pump motors are connected to the inverter power source when the relay coil is energized. By operating the relay in the de-energized position during long-term operation of the power conversion system, the reliability of the relays are enhanced.

An available, hermetically sealed aircraft power relay was selected for use as the motor transfer contactor. A rating summary of this unit is given in the following table.

Motor Transfer Contactor Rating Summary

Type: Three-pole double-throw

Contact Rating:

- 50 amps continuous duty
- 120/208 V
- 400 Hz
- 500 amps interrupting capacity
- 200 amps motor starting capacity

Coil Operating voltage - 28 Vdc

Pickup voltage - 18 Vdc

Ambient temperature - $70^{\circ}C$ to $+120^{\circ}C$

Weight - 1.7 lb

6.9.3.3 Inverter DC Contactor

The inverter dc contactors are required to connect the inverters to the dc power supply. They are single-pole, single-throw, hermetically sealed units, designed to the same general requirements as the other SNAP-8 system switchgear.

The specification and selection of the inverter dc contactor is dependent upon the power requirements of the inverters which they control. This work was not completed at the time of the program termination.

6.9.4 Electrical Distribution and Harness System

The function of the SNAP-8 electrical distribution and harness system is to distribute control and output power among the various electrical components. It consists of the electrical wiring between the electrical components and includes the following power networks:

- 400-Hz alternator power system
- 56 Vdc inverter input power
- 28 Vdc control power
- Adjustable frequency inverter output power

Various concepts of electrical distribution and harness systems have been studied during the evolution of the SNAP-8 power conversion system. These have included:

- Open bus system for high current using round tabular anodized aluminum conductors.
- Hermetically sealed wiring system using insulated conductors in a conduit filled with inert gas.
- Unsealed cables made from high-temperature insulated wire cooled by conduction and radiation.

All harness systems featured welded connections and avoidance of splices to provide maximum reliability.

The final selection of the electrical harness and distribution system must consider the requirements of the exact application for which it is to be used. Factors to be considered include:

- Mechanical environment such as shock and vibration requirements
- Insulation requirements such as temperature, atmospheric pressure and presence of contaminants such as mercury, NaK, lubricants, moisture, and salt spray
- Shielding for electromagnetic interference.

7.0 INSTRUMENTATION

During the SNAP-8 development program, many component and system tests were performed. These tests were conducted in loops containing the SNAP-8 working fluids - NaK, mercury, and polyphenyl ether. To operate and control the test loops, and to obtain performance data, a variety of instrumentation was used. This section of the report describes the various unique instrumentation designs and applications that were used in these test loops. A number of instrumentation sensing devices were also tested, and results of these tests are discussed.

The largest and most significant SNAP-8 test loop was designed for testing the 35-kWe system. In this loop, more than 800 measurements were made:

Type	Quantity
Current (transmittal signal)	25
Current (visual)	20
Frequency (transmitted signal)	4
Frequency (visual)	2
Flow	20
Fluid Level	20
Position	10
Pressure (transmitted signal)	69
Pressure (visual)	69
Pressure (switches)	6
Rotational speed	5
Temperature	440
Vacuum	15
Vibration	9
Volts (transmitted signal)	26
Volts (visual)	41
Watts (transmitted signal)	21
Watts (visual)	19
Total:	821

Approximately 320 of the transmitted signals were recorded on a digital data acquisition system. A variety of conventional indicators and recorders were used to indicate and record the other transmitted signals. Various conditioners and amplifiers were employed to convert signals from the test-loop sensors and transducers to signals suitable for recording.

The instrumentation components that were mounted in the test loop were an integral part of the SNAP-8 system, since they came in intimate contact with liquid metals and had to operate at relatively high temperatures. Each measurement variable (such as pressure, temperature, and flow) will be discussed separately; and where appropriate within each measurement type, the application to NaK service will be separated from that of mercury service.

7.1 PRESSURE MEASUREMENTS - TRANSDUCERS

Pressure transducers were employed for two reasons. First, it was desirable to ascertain the capabilities of these transducers so that they could be proven for eventual use in space missions. Second, the millivolt output signal of aerospace-type pressure transducers is compatible with the digital data acquisition system and recorders that were used in SNAP-8 component and system tests. (Industrial-type pressure transmitters have either a 3-to-15 psig pneumatic output signal or a 4-to-20 milliampere electrical output signal.)

Three types of commercially available pressure transducers were evaluated during the SNAP-8 test program. These transducers operate on variable-reluctance, potentiometer, and strain-gage principles. After a considerable amount of testing, strain gage transducers were adopted as the standard and used exclusively.

The variable-reluctance transducer system proved to be unreliable (poor transducer operation, signal conditioner drifting, or both). Also, the variable reluctance circuit cannot be checked out electrically after the transducer is installed in the test loop and while the loop is actually operating. This can be done with strain-gage and potentiometer instruments, using shunt calibration methods. Therefore, confidence in the accuracy and reliability of the variable-reluctance pressure transducers was further reduced.

The potentiometer pressure transducers are easily damaged by overpressure surges, particularly in the mercury loop, and wiper arms wore out occasionally because the pressure medium fluctuated slightly over one point for long periods of time.

7.1.1 NaK Service

In the selection, specification, and installation of pressure transducers for NaK service on the SNAP-8 system, the following potential problems must be considered since they affect instrumentation design:

- Pressure measurements are made at locations where the NaK fluid temperature can be as high as 1350°F. Since pressure transducers cannot operate at this temperature, some form of cooling mechanism must be provided.

- NaK is highly corrosive, therefore, transducer materials must be carefully selected and specified.

- Dissolved sodium oxide is present in NaK and will precipitate out rapidly at temperatures below 300°F; this precipitate can plug pressure taps and transducer ports. Judicious installation designs are needed to overcome this problem.

- Prior to filling the loop with NaK, the piping system is evacuated for long periods of time to detect any leaks. This means that the transducer must be able to withstand a vacuum without suffering changes in calibration or zero shifts.

The methods used to eliminate or minimize these problems are described in the following paragraphs.

7.1.1.1 Cooling and Sodium Oxide Plugging

Since the upper limit of temperature compensation for strain-gage pressure transducers is 600°F for absolute pressure transducers, and 400°F for differential pressure transducers, these transducers must be kept at or below the above-mentioned temperatures when they are used to measure the pressure of a medium at 1350°F. The easiest method of cooling a pressure transducer is to connect it to the process piping with a "stand-off tube". In NaK service, the length of this tube is critical. A long stand-off tube will reduce the temperature of the NaK that comes in contact with the transducer to such an extent that the sodium oxide present in the NaK will precipitate out in this "cold trap." Eventually, a solid sodium oxide plug will form between the transducer and process line and prevent the pressure transducer from sensing the actual pressure in the process piping. Since operating conditions will vary with each application, the following rule of thumb is useful: Make the stand-off tube long enough so that the temperature of the NaK contacting the pressure transducer is within the compensated temperature range of the transducer, and make the tube short enough so that the temperature of the NaK contacting the transducer is above 300°F, the approximate cold-trap temperature.

7.1.1.2 Specifications

Detailed specifications were written to meet the transducer design requirements. The significant information from these specifications is summarized below.

a. Absolute Pressure Transducers for NaK Service.- Unbonded strain-gage pressure transducers with a compensated temperature range to 600°F can operate at temperatures up to 700°F, but can withstand an over-range pressure of only two times their rated range. A 3/8 in. OD x 0.049 in. wall, Type 316 stainless steel stand-off tube is used with mounting stubs welded to the

transducer body. The space inside the transducer between the diaphragm and pressure port is in the shape of a truncated cone to allow for drainage of precipitated sodium oxide out of the transducer.

b. Differential Pressure Transducers for NaK Service.- Unbonded strain-gage pressure transducers with a compensated temperature range to 400°F are prepared. These transducers provide high operating temperature capability at the sacrifice of over-range protection. The pressure ports are located in a vertical position to provide maximum draining.

7.1.1.3 Installation Design and Testing

Pressure transducers in NaK service should always be mounted above the process piping to aid the draining of precipitated sodium oxide back into the test loop. To prevent plugging of the transducer or the stand-off tube, a secondary installation "crutch" can be employed. A sketch of this installation method is shown on Figure 7-1.

To ascertain the optimum length of the stand-off tube between the pressure transducer and the process piping, a thermal profile of the tube and the transducer was established by mounting thermocouples on the tube and transducer. Test variables were (1) the NaK temperature in the process piping, and (2) thickness of insulation surrounding the process piping.

The conclusions from this test program are summarized in Figure 7-2. The length of transducer stand-off tube required to maintain a temperature of 300°F at the transducer diaphragm is shown as a function of the process NaK temperature for two process pipe insulation thicknesses.

7.1.2 Mercury Service

The design considerations for the selection, specification, and installation of pressure transducers for mercury service are different than those for NaK service. The following are the most important factors influencing design.

- Process temperatures up to 1300°F are encountered in the system.
- Mercury tends to dissolve containment materials. Alloys susceptable to mercury attack can erode rapidly.
- Fast-acting valves in the mercury loop can cause high pressure surges (water hammer).
- Vacuum conditions exist in the mercury loop for long periods of time prior to mercury injection.

The effect of these factors on the design of mercury pressure transducers is explained in the following paragraphs.

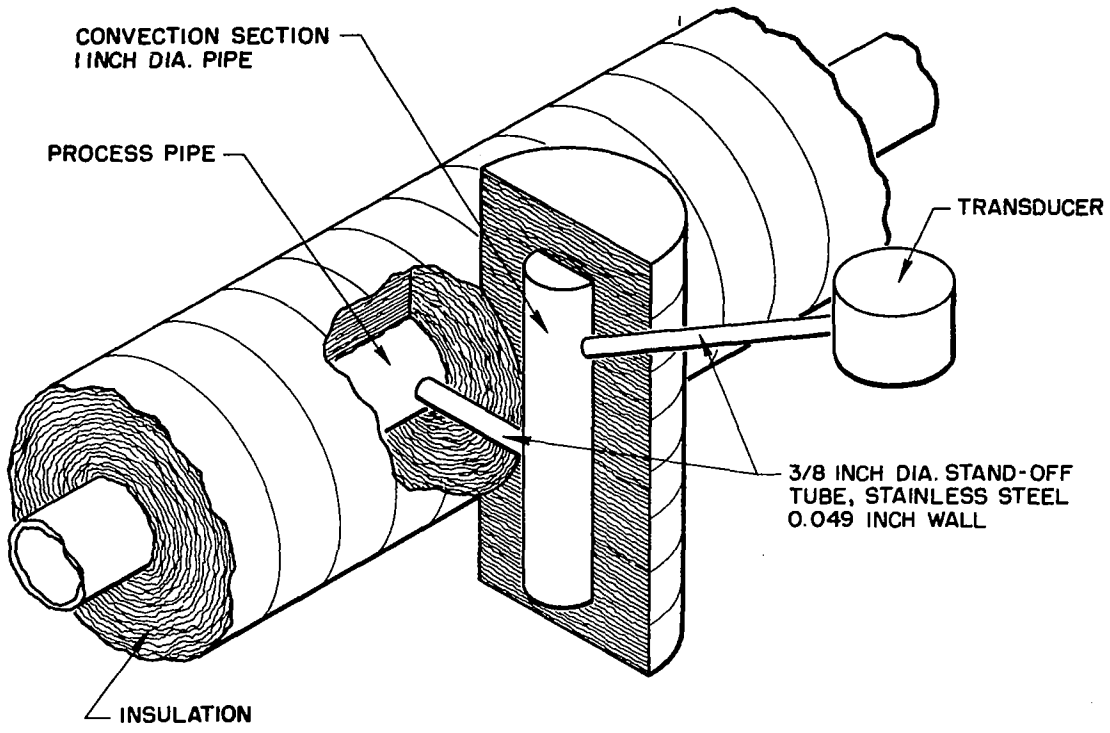

Figure 7-1 Installation of NaK Pressure Transducer Showing Stand-Off Tube Used to Protect Transducer

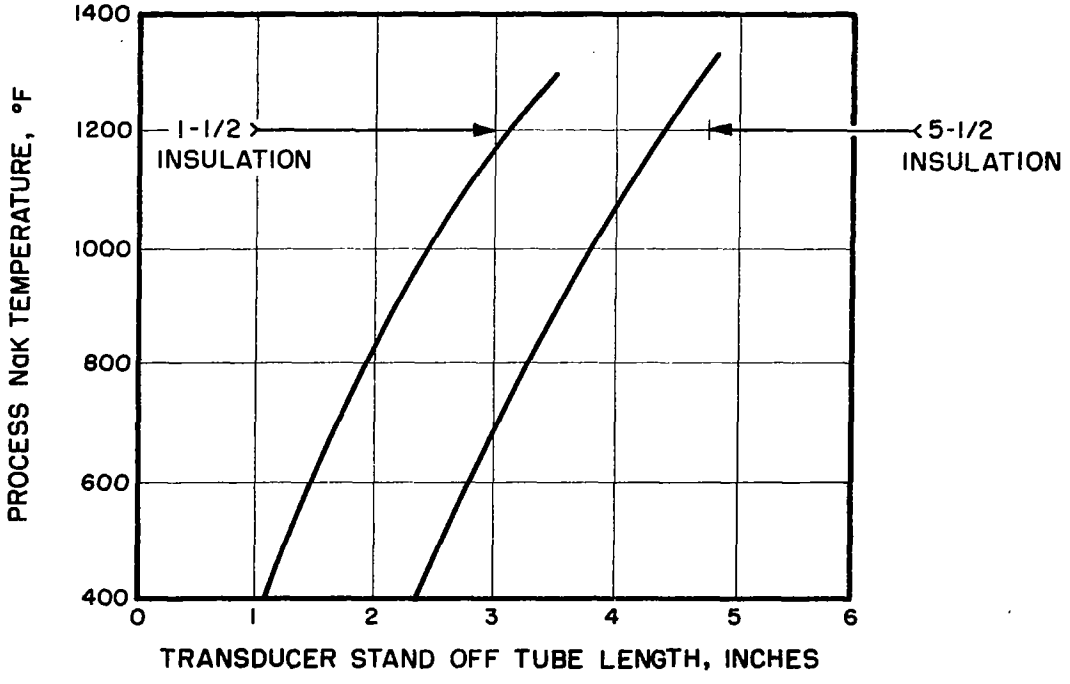

Figure 7-2 Transducer Stand-Off Tube Length Required to Maintain 300°F at Transducer as a Function of NaK Temperature and Process Pipe Insulation Thickness

7.1.2.1 Transducer Cooling

In mercury service, stand-off tubes are used to cool transducers. Since no plugging problems exist as with NaK service, the length of this tube is not critical; it must only be long enough to cool the transducer to well within its compensated temperature range.

7.1.2.2 Installation for Mercury Liquid Service

In mercury liquid service, the transducer should be installed in a slightly downward position from the process piping. A good rule of thumb is to install it so that an angle of approximately 7-1/2 degrees is created between an imaginary horizontal plane passing through the center of the process pipe and the transducer stand-off tube. This allows a layer of cool mercury liquid to permanently come in contact with the transducer diaphragm.

7.1.2.3 Installation for Mercury Vapor Service

In mercury vapor service, the transducer must be installed in a position below the process line to obtain the cooling protection of the condensed mercury that will permanently stay in the stand-off tube between the transducer diaphragm and the loop piping. If the transducer is installed above the piping, mercury vapor at 1200°F will continually reach the pressure transducer and cause permanent damage.

When the transducer is installed below the process line, a condensing process continuously takes place in that part of the stand-off tube closest to the mercury vapor piping. This poses a special problem as follows: When mercury condenses, it contains no elements in solution. Therefore, it tends to dissolve the metals with which it comes in contact until it is saturated with the elemental metals present in the containment alloys. If this containment alloy is positioned in such a manner that the condensed mercury continually flows away and vapor continues to condense, a condition termed "condensing reflux" exists. Under these conditions alloys susceptible to mercury corrosion can erode very rapidly.

This phenomenon was noted in the Type 316 stainless steel pressure transducer stand-off tubes that were first used in SNAP-8 mercury vapor service. A corrosion rate of 0.01 inch per 1000 hours of operation at 1250°F and 275 psia was observed. Therefore, in subsequent installations, short stubs of 9Cr-1Mo steel were used to connect the mercury vapor process piping to the Type 316 stainless steel stand-off tube of the pressure transducer. A typical installation of this type is shown in Figure 7-3.

7.1.2.4 Over-Range Protection

During early phases of the SNAP-8 program, a considerable number of pressure transducers, especially differential pressure transducers, were damaged in the mercury loop by water hammer effects which cause momentary high over-pressures in the process piping. These overpressures permanently deform the transducer diaphragm which results in an erroneous output signal. Water hammer is generated in the mercury loop by fast opening and closing valves

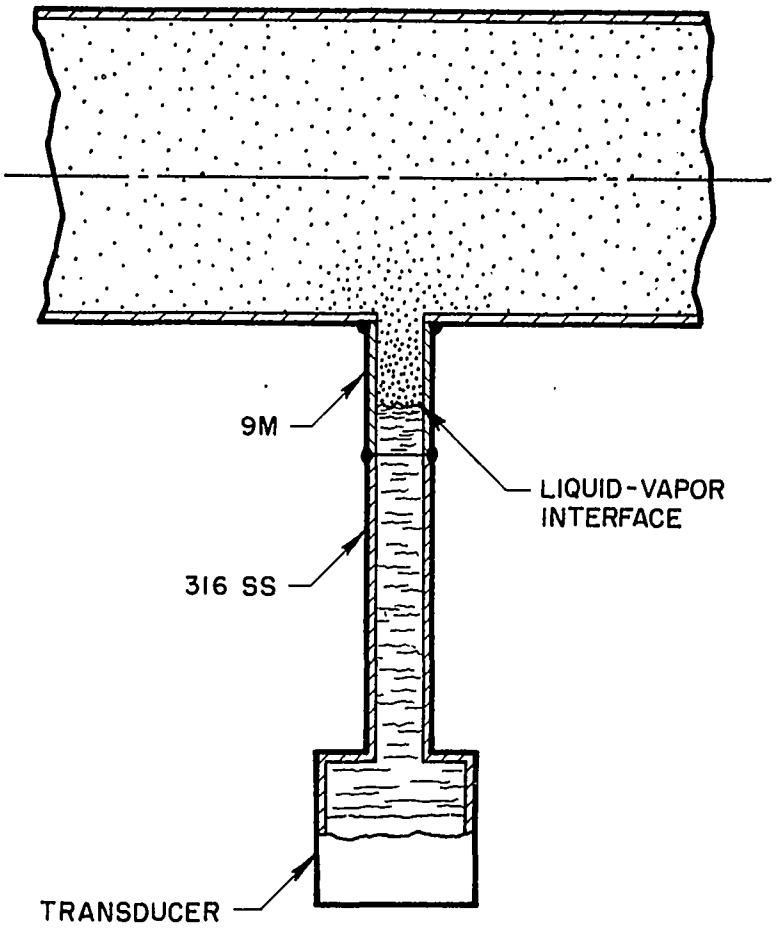

Figure 7-3 Pressure Transducer Installation for Mercury Vapor Service

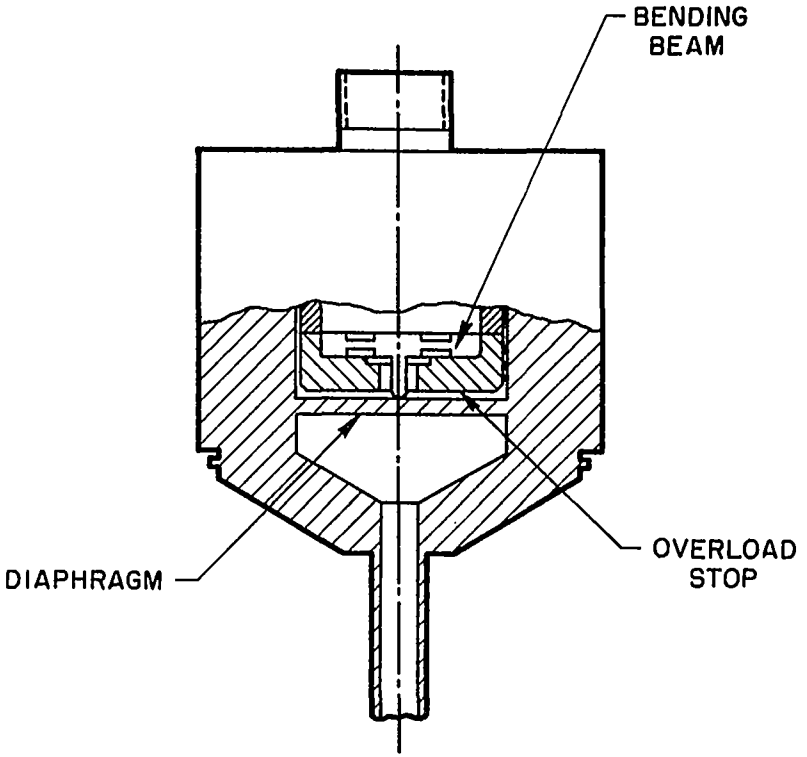

Figure 7-4 Pressure Transducer with Overhead Stop to Prevent Diaphragm Damage

which protect important pieces of equipment. No experimental data are available regarding the actual value of these surges. However, using conservative methods of calculating water hammer, a calculated value of 528 lb/in.^{2} above ambient pressure is obtained for a typical situation in the SNAP-8 mercury liquid piping.

For absolute pressure measurements the damage due to over-ranging of pressure transducers was eliminated by the use of bonded strain-gage pressure transducers that employ an overload stop to prevent the deformation of the transducer diaphragm. The construction of this type of transducer is shown in Figure 7-4. Early versions of this instrument provided 10:1 overload protection. Subsequent models were built and used that have a 15:1 overload protection range.

In the case of differential pressure measurements, the water hammer problem is more severe. For example, flow in the liquid mercury loop is measured with a venturi that creates a pressure drop of 15 psid at nominal flow. A 0-30 psid range differential pressure transducer used to measure this pressure drop would only survive a 300 psi (ten-times rated range) pressure surge. This problem was solved by the use of two protection methods. First, small orifices were made in the lines from the venturi to the transducer to dampen the shock waves. Secondly, a 0-100 psid differential pressure is used, but it is calibrated in the signal conditioner-recorded system only from 0-30 psid. Thus, a 1000 psid (ten-times rated range) over-range protection is obtained.

7.1.2.5 Specifications

Several specifications for both absolute and differential mercury service pressure transducers were written. Although these specifications primarily concern mercury service, they also incorporate features useful in NaK loops. Salient features of these specifications are described below.

a. Absolute Pressure Transducers.- Bonded strain-gage pressure transducers are specified but with a cleaning port and an external shunt to provide calibration capability. Other interesting features are the requirements for operation at 5×10^{-3} mm mercury vacuum, high overload protection, and thorough helium leak and dye penetrant inspections.

b. Differential Pressure Transducers.- Bonded strain-gage differential pressure transducers are specified but with high over-range protection and external shunt calibration capability. It does not permit the use of a fluorinated compound as a filling fluid. Fluorinated hydrocarbons, normally used by transducers manufacturers to fill the space created between the two diaphragms of a differential pressure transducer are not permitted. If a differential pressure transducer filled with a fluorinated compound should be damaged, this fluid could come in contact with NaK and a small explosion could occur.

7.2 PRESSURE MEASUREMENTS - VISUAL GAGES

Visual pressure gages were used in the SNAP-8 test loops as a backup for pressure transducers and to make noncritical pressure measurements. Both absolute (or gage) and differential pressure gages were utilized. They were installed according to the same general rules that were described previously for pressure transducers.

7.2.1 Absolute Pressure Gages

Bourdon tube gages were used for visual absolute pressure measurements. All pressure gages were purchased with Type 316 stainless steel bourdon tube, socket, and tip.

These pressure gages do not incorporate temperature compensation, therefore, tests were conducted to determine the thermal shift of these pressure gages with test cell temperatures of from 70 to 160°F. From these tests it was concluded that, above 50% of full-scale reading, the thermal shift error is reasonably constant and equal to approximately ± 1% of the reading for every 40°F step above ambient temperature.

7.2.2 Differential Pressure Gages

Pneumatic, bellows diaphragm differential pressure gages with mechanical linkages were used on the SNAP-8 test program. These gages were tested to ascertain their accuracy at elevated test-cell temperatures. They were calibrated and then thermally cycled from room temperature (78°F) to 175°F. It was determined that, within this temperature range, a thermal zero shift of +0.15 to -0.5% (full scale) occurred and a thermal sensitivity shift of +2.5 to -3.0% (full scale) occurred. Special correction curves were drawn to compensate for these errors.

7.3 TEMPERATURE MEASUREMENTS

The two most common devices for measuring temperatures that must be recorded are thermocouples and resistance thermometers. During early phases of the SNAP-8 program, both of these temperature sensing devices were used. The use of platinum resistance thermometers, however, was discontinued, and Chromel-Alumel (ISA Type "K") thermocouples were used exclusively for the following reasons:

- Standardization on Chromel-Alumel thermocouples simplified calibration, check-out, and data reduction procedures.
- The advantage of platinum resistance thermometers over thermocouples (especially at 1300°F where most of the important temperatures are measured) is doubtful. Chromel-Alumel is very stable at 1300°F (no long-term history at this temperature for platinum resistance thermometers exists). Also, the application error is just as large for a resistance thermometer as it is with a thermocouple.

- Signal conditioners required for use with resistance thermometers are more difficult to use than thermocouple reference junctions.

- Since not all platinum resistance thermometers have the same (identical) calibration curve, many channels must be checked out separately and individual calibration curves must be obtained and incorporated into the data reduction programs.

Two types of thermocouples were used on the SNAP-8 test program: probes with thermowells and surface thermocouples.

7.3.1 Thermocouple Probes

Thermocouple probes were installed in the SNAP-8 system test loop at locations where highly accurate measurements were required (for example, NaK and mercury boiler outlet temperatures). These thermocouple probes were installed with thermowells; a photo of both thermocouple and well is shown on Figure 7-5.

7.3.2 Surface Thermocouples

Most temperature measurements in the test loops were made with surface thermocouples. A typical thermocouple installation (before insulation) is shown on Figure 7-6 which shows the ceramic insulators and welding strap that make this instrument so reliable. This type of thermocouple is highly accurate in liquid metal service because of the very high film coefficients associated with liquid metals and because of the thick layers of insulation used to cover the thermocouple and the piping.

7.4 FLOW MEASUREMENTS

Three types of flow measuring devices were successfully employed in the test loops: venturi flow tubes, magnetic flowmeters, and turbine-type flow transducers. Design, calibration, and test experience with these instruments is described below.

7.4.1 Venturi Flow Tubes

Venturi flowmeters were used in conjunction with differential pressure measuring devices in both NaK and mercury test loops. Figure 7-7 shows the design for the Type 316 stainless steel venturi used to measure the mercury vapor flow at the boiler outlet 35-kWe system. The annular sections shown in Figure 7-7 permit the circumferential averaging of the upstream and throat pressure measurements.

7.4.1.1 Liquid Service

Venturi flow tubes for NaK and liquid mercury service were calibrated with water at Reynold's numbers equivalent to the SNAP-8 system flow requirements. The water calibration data were converted to give a curve of Reynold's

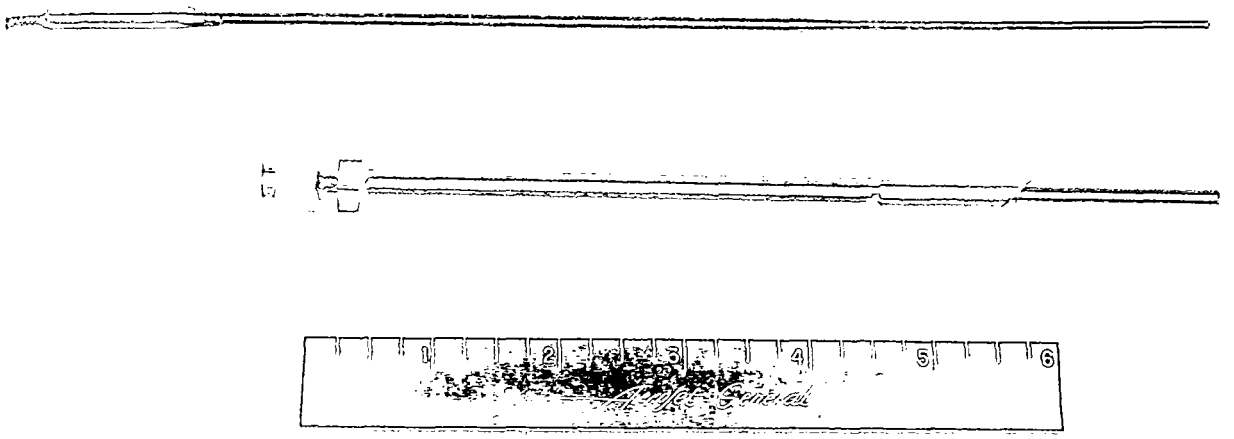

Figure 7-5 Immersion Thermocouple and Well

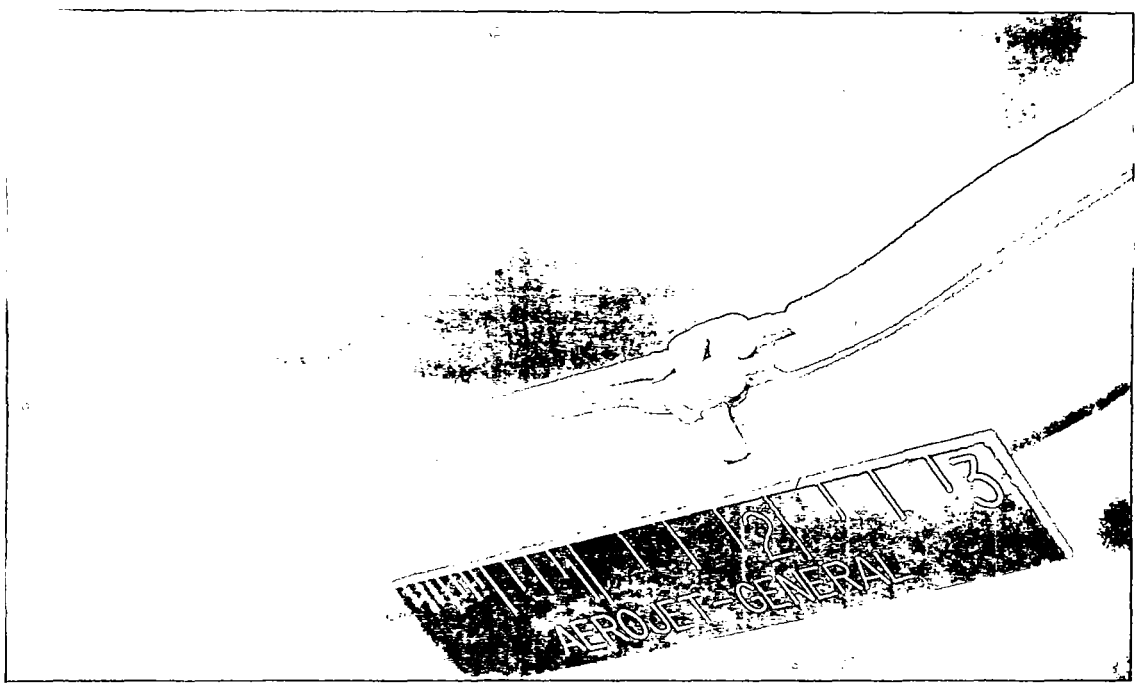

Figure 7-6 Typical Surface Thermocouple Installation

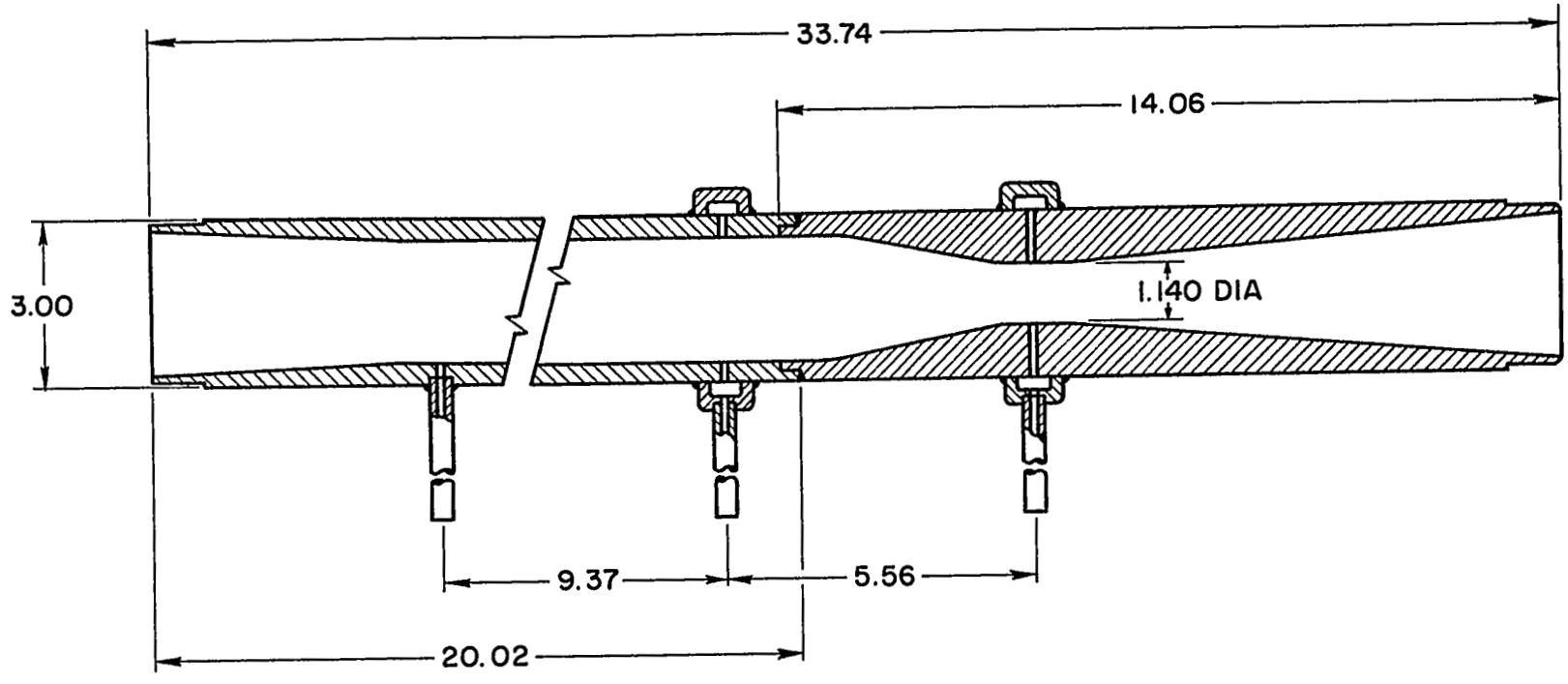

Figure 7-7 Mercury Vapor Venturi Flow Meter

number vs discharge coefficient of the venturi flow tube. Data from this curve were then used to calculate the values required to plot a curve of flow vs differential pressure for the venturi.

7.4.1.2 Vapor Service

The mercury vapor venturi shown in Figure 7-7 was designed and fabricated at Aerojet. After construction, it was shipped for calibration to the Colorado Engineering Experiment Station in Boulder, Colorado, an organization specializing in gas flow research and flowmeter calibrations. The calibration results showed a venturi discharge coefficient of 0.98 at a Reynold's number of 100,000, exactly as predicted by ASME published data.

7.4.2 Magnetic Flowmeters

Magnetic flowmeters for NaK service were used as backup instruments to the venturi tubes and where flow measurement with a venturi was impractical (for example, where flows are low and differential pressure measurements are difficult). They also serve as excellent flow measuring devices in NaK purification loops where they are used in conjunction with cold-trapping systems.

The magnetic flowmeters used proved to be very reliable instruments. While they were not flow calibrated, flows were obtained by theoretical equations (see below). Flowmeters installed in series with venturi tubes gave data that agreed within $\pm 5\%$ of venturi results.

Electromagnetic flowmeters cannot be calibrated with water in a conventional hydraulic laboratory because water is a nonconductive fluid. However, a calibration curve can be calculated. The method and equations used in calculating the flowmeter calibration curves are defined in Reference 66.

7.4.3 Turbine-Type Flow Transducers

All SNAP-8 rotating machinery (pumps, turbine, alternator) are cooled and lubricated with an organic fluid. Turbine-type flow transducers are used to measure the flow of this fluid. For flow in the 1500-2500 lb/hr range, transducers with conventional magnetic pickups which sense the rotational speed of the rotors are used. In applications where very low flows have to be measured (100-150 lb/hr), turbine flowmeters are used which include an oscillator-preamplifier system to sense the rotor rotational speed. This eliminates the need for a magnetic pickup and its accompanying drag on the rotor, an undesirable feature which results in inaccuracies at low flows.

All turbine-type flow transducers were periodically recalibrated. Meters with magnetic pickups never indicated any changes in calibration factors. However, the extremely small transducers with the oscillator-preamplifier system have a tendency to wear out after approximately 2500 hours.

Turbine-type flow transducers were calibrated by the instrument manufacturers with water and with oil having the same kinetic viscosity as the lubricant-coolant fluid.

7.5 LEVEL MEASUREMENTS

During early phases of the SNAP-8 test program, all level measurements were made with contact probes using an electrical insulator between the probe and the tank, as shown in Figure 7-8. These instruments operate on the principle that, when NaK comes in contact with the probe, the electrical circuit is completed causing current to flow which lights a lamp or actuates some type of indicating device. These probes proved to be unreliable. Most failures were caused by electrical shorts of the probe to the tank due to wetting and/or sodium oxide buildup between the probe and the tank.

Since level measurements are of vital importance during startup, shutdown, and steady-state operation, it became evident that the level measuring devices had to be improved. An extensive design and development effort was launched to obtain more reliable methods of level measurement. A detailed description of the types of level probes investigated during the development effort and the designs employed in the test loops is contained in Reference 67. A brief description of each of the basic level probes which were developed is presented below:

7.5.1 Digital Level Probe - Welded Installation

This design, shown in Figure 7-9, operates in the following manner: When the NaK level is below the tip of the probe, electrical current flows up through the sheath and the voltage drop across the sheath is relatively high. As the level in the tank rises, NaK contacts the probe tip causing current to flow through the NaK to ground which decreases the sheath voltage drop. This step change in voltage drop is detected as a digital level measurement.

7.5.2 Analog Straight Level Probe - Top Entry

Originally, NaK analog level measurements were primarily made with top-entry "J" probes. However, the bent sections often failed due to thinning, the probes were difficult to install and remove, and their sensitivity was low. Bottom entry probes were often inaccessible and they introduced the possibility of dangerous NaK leaks. Therefore, an analog straight-level probe with top entry (shown schematically on Figure 7-10) was developed. The probe was made by adding an extension piece to a digital probe. In operation, when NaK touches this extension, a second electrical parallel path is created. The voltage drop across the parallel paths is measured to obtain a signal which is proportional to the tank level. This system also provides a digital check point when NaK first touches the extension since an abrupt change in voltage drop occurs.

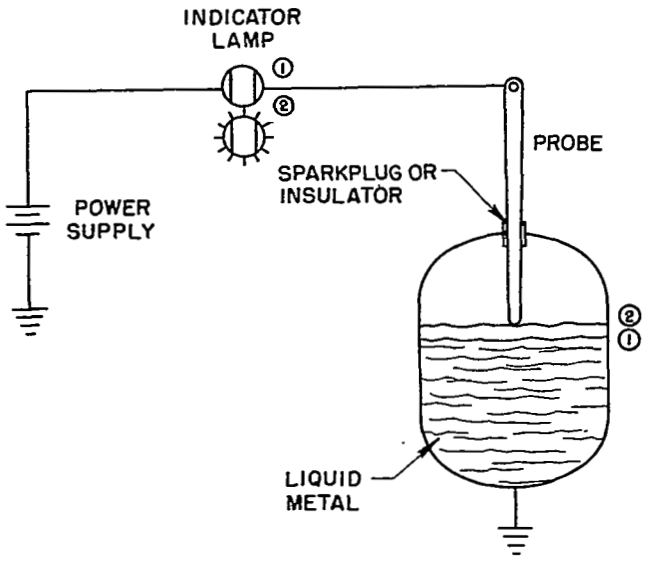

Figure 7-8 Contact Probe Installation and Electrical Circuit

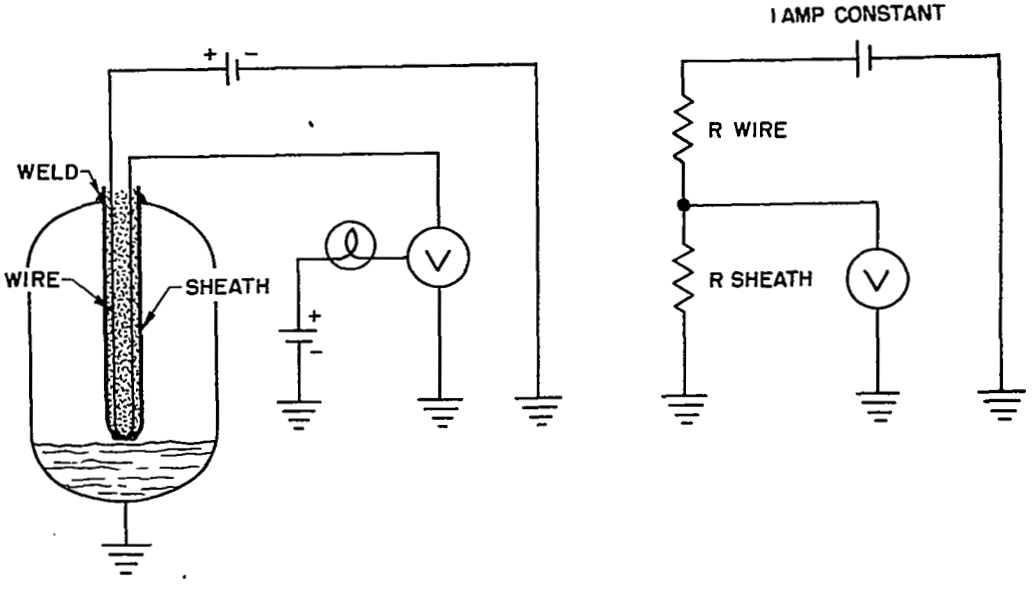

Figure 7-9 Digital Level Probe Installation and Electrical Circuit

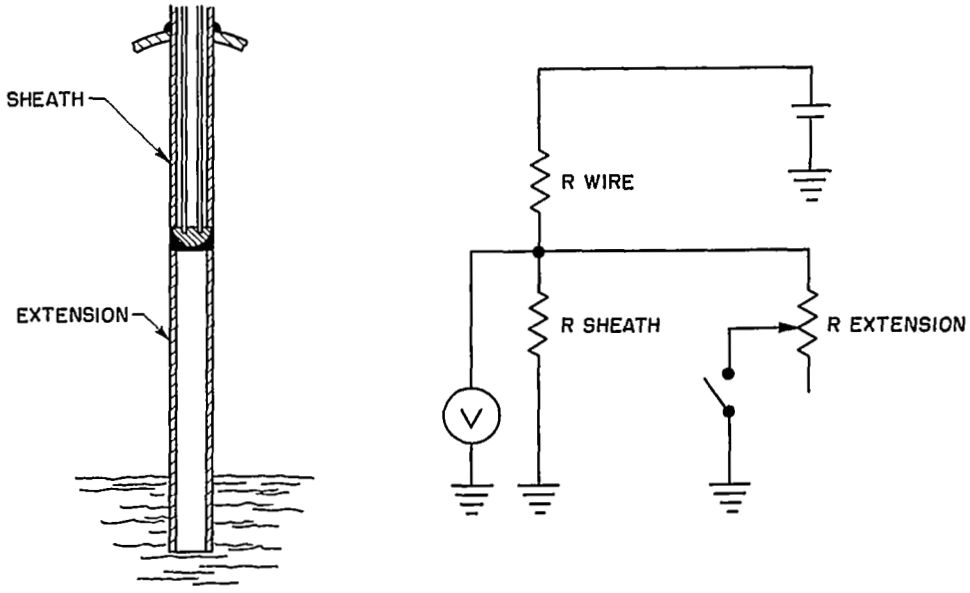

Figure 7-10 Analog Straight Level Probe and Electrical Circuit

Figure 7-11 Combined Analog-Digital Probe

7.5.3 Combined Analog-Digital Probe

To provide added confidence in the accuracy and reliability of level measurements, the combined analog-digital probe shown in Figure 7-11 was designed. It utilizes a multiconductor material in which two conductors are used for the analog system and others with digital circuitry to provide digital check points on the analog measurements.

7.5.4 Analog Level System - Top Entry "J" Probe

This method is shown in Figure 7-12. Changes in level are detected by the varying voltage drop across the vertical upward portion of the "J".

7.6 VIBRATION MEASUREMENTS

The SNAP-8 vibration measurements cannot be considered part of liquid metal instrumentation, as such. However, the vibration measurement system used during the 35-kWe system tests is worthy of a brief summary.

The vibration sensors are piezoelectric accelerometers connected to charge amplifiers. The noteworthy features of this vibration measurement system are its versatility and capability to record continuously.

A block diagram of the entire vibration measurement system is shown in Figure 7-13. It consists of twelve channels that can be monitored in several ways. All twelve channels are wired to a high-speed tape recorder. This recorder is turned on manually for short periods of time at "data points" and during startup and planned shutdown periods. The recorder will also turn on automatically when an unscheduled emergency shutdown occurs.

Four critical channels are also recorded on two separate tape recorders that operate continuously. These recorders always have one hour of previous data stored on their tapes, thus providing a record of any malfunction or failure. A sonic analyzer graphically displays frequency versus acceleration information, and an audio system provides sounds that are proportional to acceleration. Selector switches permit the display of any accelerometer output signal on the sonic analyzer or its audible presentation through the audio system. Playback of any channel from any recorder on the sonic analyzer or the audio system is also possible.

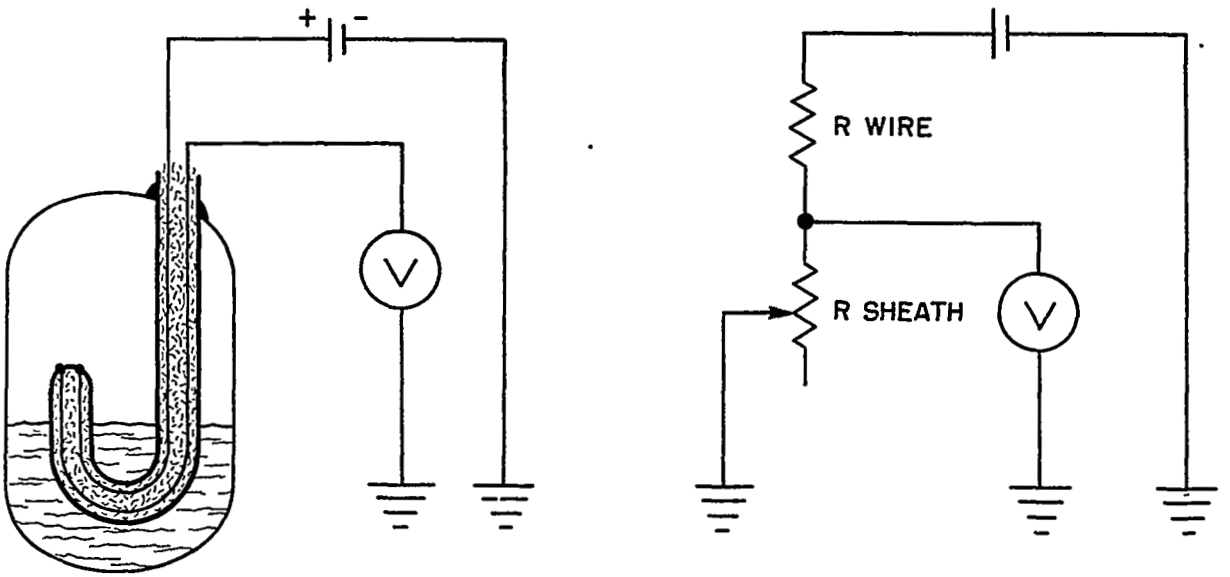

Figure 7-12 Analog Top Entry "J" Level Probe and Electrical Circuit

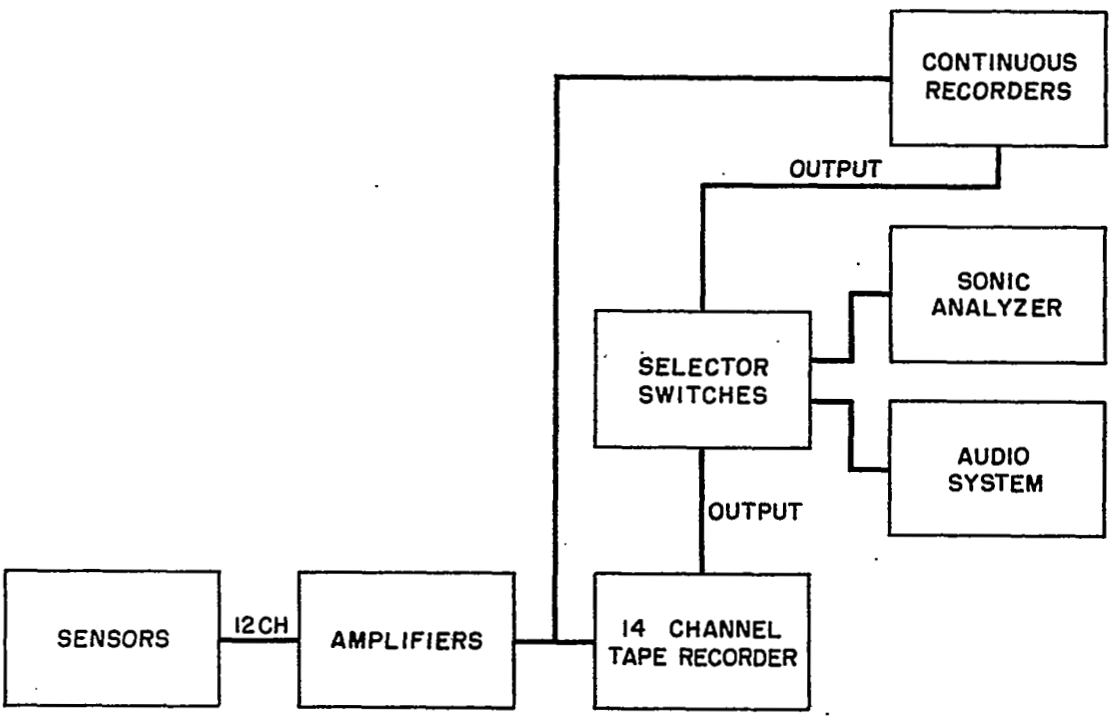

Figure 7-13 Vibration Measurement System Block Diagram

8.0 CONCLUSIONS

8.1 GENERAL SNAP-8 DESCRIPTION AND PROGRAM RESULTS

The objective of the SNAP-8 program was to establish the technological base for the subsequent development of mission-capable multikilowatt mercury Rankine-cycle space power systems. The SNAP-8 system is designed for a five-year operating life, man-rated operation, and restartability. The deliverable power output capability spans the range from an initial value of 30 kWe to 90 kWe for the final version. Electrical power is generated by a turbine-alternator in a mercury Rankine-cycle loop. Heat is transferred to the mercury loop from the nuclear heat source by means of sodium potassium eutectic alloy (NaK) subsystems. Heat is rejected from the mercury loop to another NaK subsystem which in turn radiates the system waste heat to space. Up to 600 thermal kilowatts are required from the heat source depending upon the system electrical power output.

Specific conclusions associated with the SNAP-8 system technology are presented in the following sections.

8.2 SYSTEM LEVEL

The following conclusions concern system level design, analysis, and testing:

(1) The existing component configurations can be integrated into a system capable of producing 35-kWe net output.

(2) The existing component designs could be combined to provide a system capable of delivering 90 kWe, corresponding to a system efficiency of 15% with a 600-kWt heat source subject to the following considerations:

- The turbine design would be changed from an impulse turbine with a 14-psia vapor exhaust pressure to a reaction turbine with a 2- to 3-psia vapor exhaust pressure. The design of the modified turbine has been completed under this program. The alternators associated with the reaction turbine would be the same configuration as the alternators developed and tested during the SNAP-8 program. The thrust loads associated with a reaction turbine design are eliminated by designing a dual mercury flow path unit with one alternator at each end of the shaft. In addition, the two alternators are required to produce the higher power levels.

- The remaining components are either identical in design to those fully developed during the SNAP-8 program, or represent simple extrapolations from existing design concepts. An example of the former is the condenser of which two are required of the present configuration for a 90-kWe system.

An example of the latter is the boiler which would use the same basic construction as the 35-kWe system boiler, but would require additional mercury flow tubes.

(3) A product improvement program from the 90-kWe system baseline would lead to a SNAP-8 system which would produce 120 kWe with a system efficiency of 20% when provided with a 600-kWt heat source.

(4) The system startup sequence has been demonstrated during test and can be applied without violating power conversion system or nuclear system limits.

(5) A low-volume power conversion system with a 90-kWe output capability has been designed within an envelope 5 x 12 x 10 ft (height).

(6) Material barrier problems have been resolved and system and component materials have been selected; for example, the mercury boiler containment material is tantalum, piping systems are fabricated from Type 316 stainless steel, mercury condenser tubes are high chromium steel (9% chrome, 1% molybdenum, balance iron).

(7) An on-line backup pump with 10 to 20% rated flow capability is required in the reactor primary loop to prevent a reactor overtemperature excursion during a loss-of-flow incident.

(8) System design and fabrication should apply the liquid metal system operational methods and procedures successfully developed and applied during the SNAP-8 testing program; for example:

- Purify liquid metal (sodium-potassium) systems to the 10 ppm (oxygen) range prior to operation, over a period of one or more days.
- Use chloride-free solvents during Type 316 stainless steel cleaning and inspection operations (dye-penetrant inspection).
- Use chloride-ion-free insulation systems as defined by military specifications.
- Protect mercury loop from oil contamination due to backstreaming from the vacuum pumping station through the use of cryopump traps.

8.3 COMPONENT AND SUBSYSTEM LEVEL

The following conclusions concern component design, analysis, and testing:

(1) Mercury boiler and condenser heat exchanger analysis methods and designs have been developed, documented, and verified in test.

(2) Components which have been developed are capable of the long-life operation required for the SNAP-8 system. A summary of achieved operating performance is presented in Table 8-I.

(3) The developed speed control system operates with no indication of instability, even during operations involving full alternator output load changes.

(4) The dynamic shaft seal designs developed for the mercury pump and the turbine-alternator performed successfully and are considered to have advanced the state-of-the-art of dynamic seals.

(5) Stellite 6B exhibits a phase change from face centered cubic to close packed hexagonal crystal structure when exposed to 700°F and greater temperatures for extended time periods.

(6) The parasitic load resistor can be used in applications requiring a highly reliable immersion type of heater which is hermetically sealed and can operate in the 50-kW range.

(7) Techniques for fabricating tantalum/stainless steel bimetallic joints have been developed and successfully tested.

(8) The state-of-the-art for level probe designs for use with liquid metal systems has been advanced.

TABLE 8-I TEST RECORD FOR SNAP-8 POWER CONVERSION SYSTEM COMPONENTS

Component	Cumulative Operating Hours*			Startup Cycles Individual Unit, Maximum
	Total Hours	No. of Units Tested	Individual Unit, Maximum Hours	
Turbine-Alternator	15717	7	12442	135
Mercury Pump	30423	6	12227	109
NaK Pump	56493	11	10362 (1)	786
Lubricant-Coolant Pump	60578	7	24862 (2)	570
Boiler, Tantalum	25601	4	15125 (3)	135
Condenser	20842	3	16274	144
Alternator	42609	5	23130 (4)	135
Parasitic Load Resistor	14234	2	13295	81
Valves:				
Mercury Flow Control	10319	1	10319	59
Double Solenoid	90568	13	12442	135
Electrical System (5)	42066	3	25682 (6)	156
Power Factor Correction Ass'y	12329	1	12329	63
TOTAL	420514			

(1) Second and third units operated 9560 and 7028 hours.

(2) Second and third units operated 15345 and 14521 hours.

(3) Second unit operated 8699 hours.

(4) Second unit operated 12442 hours.

(5) Includes speed control, voltage regulator, and electrical protective system.

(6) Second set operated 12996 hours.

* Operating hours were accumulated in one system test facility, two pump test facilities, one electrical test facility, and represent the achievement of specific test objectives of which endurance was one part.

REFERENCES

3.1 SYSTEM DESCRIPTION

1 H. Derow, B. E. Farwell, SNAP-8 Materials Report for January - June 1964, Vol. II: Development of Component Materials, Aerojet Report 2880, Vol. II, July 1964, NASA-CR-54717

2 H. Derow, B. E. Farwell, SNAP-8 Materials Report for January - June 1965, Aerojet Report 3038, July 1965, NASA-CR-54719

3.2 STATE-POINT DEFINITION

3 W. Waters, Preliminary Design of MK 70 Reaction Turbine for SNAP-8 90 kWe System, Aerojet-General TM 3710:71-651, May 1971, NASA-CR-72919

4 J. N. Hodgson, Mathematical Correlation of Observed Condenser Heat Transfer Variations, Aerojet-General TM 7994:70-621, April 1970, NASA-CR-72911

5 A. B. Burgess, SCAN, A Computer Code for SNAP-8 System Analysis with Influence Coefficient Calculation Option, Aerojet-General TM 4921:66-375, November 1966, NASA-CR-72912

6 R. G. Geimer, Analysis of a SNAP-8 EGS Based on Unmodified -1 Component Performance, Aerojet-General TM 4923:65-1-323, September 1965, NASA-CR-72913

3.3 SYSTEM DESIGN

7 L. P. Lopez, SNAP-8 Power Conversion System Design Review, Aerojet-General Report No. 4017, June 1970, NASA-CR-72945

8 M. Parkman, B. Farwell, D. Whaley, R. Arabian, SNAP-8 Mercury Corrosion and Materials Research, Topical Report 6-60 to 12-62, Aerojet-General Report No. 2517, Vol. III, September 1963, NASA-CR-62349

9 H. Derow, B. Farwell, SNAP-8 Materials Report for July - December 1964, Aerojet-General Report 2989, January 1965, NASA-CR-54718

10 Mercury Corrosion Loop Testing Program, Final Report, Aerojet-General Report 0584F, August 1963, NASA-CR-52725

11 H. Derow, SNAP-8 Power Conversion System Breadboard Assembly - Materials Evaluation After 8700 Hours Operation, Paper presented at Intersociety Energy Conversion Engineering Conference, Las Vegas, Nevada, September 1970

12 S. Birken, Response of the SNAP-8 Reactor During Automatic Startup, Atomics International Report NAA-SR-9646, September 1964 (Confidential)

13 C. Code, Analysis of the Response of the SNAP-8 Nuclear System During Startup of the Power Conversion System, Atomics International Report NAA-SR-9626, June 1964 (Confidential)

14 R. G. Geimer, Preliminary Startup and Shutdown Investigations of SNAP-8 Reference System (Revision 'D'), Aerojet-General TM 4851:65-1-295, March 1965, NASA-CR-72914

15 L. R. Favero, Status Report of the PCS-G System Analysis, Aerojet-General TM 4942:69-601, November 1969, NASA-CR-72915

16 R. A. Lottig, R. H. Soeder, Investigation of Mercury - Flow Ramp Rates for Startup of the SNAP-8 System, NASA-TM X-52689, September 1969

17 F. Boecker, Investigation of Mercury-Flow Ramp Rates for SNAP-8 from Self-Sustaining Flow to Rated Flow, NASA-TM X-52737, December 1969

18 D. E. Knittle, Modified Thermal Analyzer Digital Computer Program, Aerojet-General TM 4942:69-602, November 1969, NASA-CR-72916

19 T. P. Hecker, F. Boecker, R. J. Frye, Shutdown Characteristics of a SNAP-8 Power Conversion System, NASA-TN-D-6172, March 1971

20 P. A. Thollot, H. B. Block, K. S. Jefferies, Experimental Investigation of Reactor Loop Transients During Startup of a Simulated SNAP-8 System, NASA-TN-D-4546, May 1968

21 R. P. Macosko, W. T. Hanna, S. H. Gorland, K. S. Jefferies, Performance of an Experimental SNAP-8 Power Conversion System, NASA-TM-X-1732, March 1969

22 J. L. Albers, R. H. Soeder, P. A. Thollot, Design Point Performance of a Double Containment Tantalum and Stainless Steel Mercury Boiler for SNAP-8, NASA-TN-D-4926, December 1968

23 K. S. Jefferies, Experimental Investigation of Reactor Loop Transients During SNAP-8 Power Conversion System Startup, NASA-TM-X-52735, December 1969

SYSTEM OPERATION (cont.)

24 J. N. Hodgson and R. P. Macosko, A SNAP-8 Breadboard System - Operation Experience, Paper presented at Intersociety Energy Conversion Engineering Conference, Boulder, Colorado, 12-16 August, 1968.

25 J. N. Hodgson, Experimental Investigation of the SNAP-8 Mercury Rankine Cycle Power Conversion System, Aerojet-General Report 3657, December 1969, NASA-CR-72679

26 J. N. Hodgson, PCS-1 Testing of March - May 1970, Aerojet-General TM 7992:70-633, 4 August 1970, NASA-CR-72917

27 D. Yee, DCHT - Double Containment Boiler Hydrogen Transport Computer Program for SNAP-8, Aerojet-General TM 4923:68-512, 22 January 1968, NASA-CR-72940

5.1 TURBINE ALTERNATOR

28 E. Eber, Engineering Support Documentation for the SNAP-8 Turbine-Alternator Assembly, Aerojet-General Report No. 2954, Volume II, November 1965, NASA-CR-72955

29 M. G. Cherry, Design Calculations for the Improved Performance SNAP-8 Turbine, Aerojet-General TM 4932:66-437, August 1966, NASA-CR-72922

30 R. S. Foley, Ball Bearing Design for SNAP-8 Turboalternator and Mercury Pump, Aerojet-General Report No. 3656, June 1971, NASA-CR-72825

31 R. L. Lessley, J. N. Hodgson, Low Leakage Dynamic Seal to Space, ASME Paper 65-GPT-14

32 J. N. Hodgson, Designing a Molecular Pump as a Seal to Space, ASME Paper 65-GPT-15

33 M. S. Hugins, G. Mironenko, L. K. Severud, O. L. Smithers, SNAP-8 Turbine-Alternator Structural Analysis, Aerojet-General TM 4932:67-467, -468, -469, May 1967, NASA-CR-72931

34 A. T. Caffo, H. Efron, Stress Analysis for the SNAP-8 Turbine Inlet Housing, Aerojet-General TM 4932:67-470, May 1967, NASA-CR-72932

35 M. G. Cherry, SNAP-8 Turbine Alternator Assembly (TAA) 5/4 - 7500 Hours of Operation in PCS-1, Phase IV, Step 3, Aerojet-General TM 4932:69-580, May 1969, NASA-CR-72927

36 M. G. Cherry, Mechanical Evaluation of TAA 5/4 After 10,823 Hours of Operation in PCS-1, Aerojet-General TM 7977:70-617, October 1970, NASA-CR-72921

37 A. J. Stromquist, A. L. Hibben (Lewis Research Center), and R. S. Foley (Aerojet-General Corporation), Shock and Vibration Tests of a SNAP-8 Turbo-Alternator, NASA-TM-X-67851, May 1971

38 M. G. Cherry, J. R. Pope, Development of a 60 kW Alternator for SNAP-8, Aerojet-General Report No. 3652, November 1969, NASA-CR-72669

39 R. S. Foley, Evaluation of SNAP-8 Alternator P/N 094069, S/N 481490 After 23,130 Hours of Endurance Testing in the Electrical Component Test Facility (ECTF), Aerojet-General TM 3710:71-650, June 1970, NASA-CR-72920

5.2 NaK PUMP

40 C. P. Colker, C. S. Mah, C. L. Foss, Design and Development of a Canned-Motor Pump for High Temperature NaK Service in SNAP-8, Aerojet-General Report No. 3663, April 1971, NASA-CR-72823

41 J. R. Pope, NaK Lubricated Journal and Thrust Bearings for a Pump-Motor Assembly in SNAP-8, Aerojet-General Report No. 3666, July 1971, NASA-CR-72824

42 R. P. Dillingham, SNAP-8 Materials Report for January-June 1964 Volume I - Electrical Insulation Development, Aerojet-General Report No. 2880, July 1964, NASA-CR-54716

43 R. B. Nelson, Evaluation of SNAP-8 Liquid NaK Pump-Motor (NaK PMA) following Vibration and Shock Testing, Aerojet-General TM 7979:70-636, December 1970, NASA-CR-72926

44 G. B. Bosco, Jr., SNAP-8 Mod-1 NaK Pump-Motor Assembly Buildup 1/4 - 10,000 Hour Endurance Testing, Aerojet-General TM 4932: 69-588, August 1969, NASA-CR-72929

5.3 MERCURY PUMP

45 J. R. Pope, C. S. Mah, C. L. Foss, Design and Development of SNAP-8 Mercury Pump Motor Assembly, Aerojet-General Report No. 3665, November 1969, NASA-CR-72664

46 C. S. Mah, Endurance Testing of the Mercury Pump-Motor Assembly in LML-5 - a Final Test Report, Aerojet-General TM 4932:69-585, August 1969, NASA-CR-72928

47 C. L. O'Dear, R. D. Follet, Shock and Vibration Tests of a SNAP-8 Mercury Pump, NASA-TM-X-52990, March 1971

5.4 LUBRICANT-COOLANT PUMP

48 E. Eber, Engineering Support Documentation for the SNAP-8 Lubricant-Coolant Pump-Motor Assembly, Aerojet-General Report No. 3152, February 1966, NASA-CR-72956

49 A. J. Stromquist (Lewis Research Center), C. L. Foss (Aerojet-General Corporation), Shock,Vibration and Acceleration-Load Tests of a SNAP-8 Motor-Driven Lubricant-Coolant Pump, March 1971, NASA-TM-X-52972

5.5 BOILER

50 E. S. Chalpin, G. L. Lombard, SNAP-8 Tube-in-Tube Mercury Boiler Development Using 9% Chrome, 1% Moly Steel, Aerojet-General Report No. 3662, October 1969, NASA-CR-72531

51 H. Derow, B. E. Farwell, E. B. Johnson, L. A. Kimura, J. C. Whipple, M. K. Wong, D. Yee, Evaluation of Tantalum for Mercury Containment in the SNAP-8 Boiler, Aerojet Report No. 3680, November 1969, NASA-CR-72651

52 A. J. Sellers (Aerojet-General Corporation), Thermal Design of the SNAP-8 Tantalum Stainless Steel Boiler, June 1971, NASA-CR-72760

53 E. S. Chalpin, Design Review of the Bare Refractory Double-Containment (BRDC) Boiler Number 5 for PCS-G, SNAP-8, Aerojet-General TM 7978:70-643, October 1970, NASA-CR-72918

54 A. J. Sellers, BODEPE - IBM 360 Computer Code for the SNAP-8 Boiler Heat and Momentum Transfer Analysis, Aerojet-General TM 4921:68-551A, June 1971, NASA-CR-72907

5.6 CONDENSER

55 E. S. Chalpin, Design Review of PCS-G Condenser, P/N 1268340-1, Redesigned from P/N 093043, Aerojet-General TM 7996:70-629, July 1970, NASA-CR-72946

56 R. A. Lottig, R. W. Vernon, W. D. Kenney, Experimental Heat-Transfer Investigation of Non-Wetting, Condensing Mercury Flow in Horizontal, Sodium-Potassium-Cooled Tubes, May 1967, NASA-TN-D-3998

57 O. E. Dwyer, Eddy Transport in Liquid-Metal Heat Transfer, Brookhaven National Laboratory Report BNL 6046, February 1962

58 R. W. Vernon, R. A. Lottig, W. D. Kenney, Experimental Investigation of the Pressure Characteristics of Non-Wetting, Condensing Flow of Mercury in a Sodium-Potassium-Cooled, Tapered Tube, November 1966, NASA-TN-D-3691

59 E. S. Chalpin, G. L. Lombard, Vibration Tests with the SNAP-8 Condenser P/N 093043-1 S/N A-1, Aerojet-General TM 7996:70-624, April 1970, NASA-CR-72925

6.0 ELECTRICAL CONTROL SYSTEM

60 S. L. Bradley, Design and Development of a Voltage Regulator-Exciter for the SNAP-8 Nuclear-Electrical Power-Conversion System, Aerojet-General Report No. 3658, October 1969, NASA-CR-72645

61 S. L. Bradley, Development of the Speed Control for the SNAP-8 Electrical Generating System, Aerojet-General Report No. 3114, November 1969, NASA-CR-72670

62 S. L. Bradley, R. M. Hill, SNAP-8 Parasitic Load Resistor, Aerojet-General Memo 354:64-176, September 1964, Aerojet-General Report No. 3492, December 1967, and Aerojet-General TM 4936:69-552, January 1969, NASA-CR-72933

63 N. E. Waldschmidt, SNAP-8 Electrical Protective System Module Design Review, Aerojet-General TM 7997:70-607, April 1970, NASA-CR-72938

64 R. M. Hill, SNAP-8 Power Factor Correction Assembly, Aerojet-General TM 4936:69-568, July 1969 and Aerojet-General TM 4968: 70-618, March 1970, NASA-CR-72936

65 S. L. Bradley, Rotary Inverter Design Review, Aerojet-General Memo 354:64-217, December 1964, NASA-CR-72934

7.0 INSTRUMENTATION

66 R. G. Affel, G. H. Burger, C. L. Pearce, Calibration and Testing of 2 and 3 1/2 inch Magnetic Flowmeters for High Temperature NaK Service, ORNL-2793

67 R. C. Jackson, SNAP-8 Liquid Metal Level Measurement, Aerojet-General TM 4937:66-398, December 1966, NASA-CR-72923

· NASA-Langley, 1971 – 28
Coml., Birmingham, Ala.